

UNIVERSITY OF CALIFORNIA,
IRVINE

Total Synthesis of (2*R*)-Hydroxynorneomajucin
and
Development of Strategies for the Assignment of Absolute Stereochemistry

DISSERTATION

submitted in partial satisfaction of the requirements
for the degree of

DOCTOR OF PHILOSOPHY

in Chemistry

by

Charles J. Dooley III

Dissertation Committee:
Professor Scott D. Rychnovsky, Chair
Professor Christopher D. Vanderwal
Professor Vy M. Dong

2022

DEDICATION

To the memory of Uncle Mike Booth and Chris “Uncle” Kehas

TABLE OF CONTENTS

LIST OF TABLES	VII
LIST OF FIGURES	VIII
LIST OF SCHEMES	VIII
LIST OF EQUATIONS	XI
LIST OF ABBREVIATIONS.....	XII
ACKNOWLEDGEMENTS.....	XV
CURRICULUM VITAE.....	XIX
ABSTRACT OF THE DISSERTATION	XXI
CHAPTER 1. A BRIEF INTRODUCTION OF STEREOCHEMISTRY AND HOW TO DEDUCE ABSOLUTE CONFIGURATION.	1
1.1 Abstract.....	1
1.2 Introduction.....	2
1.2.1 Stereochemistry.....	2
1.2.2 Types of Chirality	2
1.3 Determination of Absolute Configuration	3
1.3.1 NMR-Based Methods	4
1.3.2 Methods Based on Optical Spectroscopy	5
1.3.3 X-Ray Crystallography	6
1.4 The Competing Enantioselective Conversion Method	7
1.4.1 Configuration Assignment through Inherent Substrate Reactivity.....	7
1.4.2 The Competing Enantioselective Conversion Method	8
1.4.3 CEC Assignment of Stereogenic Carbinols	9
1.4.4 CEC Assignment of Primary Amines	10
1.5 Summary.....	11
1.6 References.....	11
CHAPTER 2. EFFORTS TOWARD THE DETERMINATION OF ABSOLUTE CONFIGURATION OF 1,3-DIENES BEARING ADJACENT STEREOCENTERS USING CHIRAL 1,2,4-TRIAZOLINE-3,5-DIONES	17
2.1 Abstract.....	17
2.2 Introduction.....	18

2.3	Synthesis of Triazolinediones	22
2.4	Analysis of Diels–Alder Enantioselectivity	25
2.5	Conclusion and Future Outlook	28
2.6	Supporting Information.....	30
2.6.1	General Information.....	30
2.6.2	General Procedure 1: Formation of isocyanates	32
2.6.3	General Procedure 2: Semicarbazide formation	32
2.6.4	General Procedure 3: Cyclization of Semicarbazides ²⁹	32
2.6.5	General Procedure 4: Diels–Alder Protocol	33
2.6.6	General Procedure 5: Kinetic Resolution Protocol.....	34
2.6.7	Compound Synthesis and Characterization	34
2.6.8	Diels–Alder Chemistry with TAD Reagents:	51
2.7	References.....	54
CHAPTER 3. .. USING THE COMPETING ENANTIOSELECTIVE CONVERSION METHOD TO ASSIGN THE ABSOLUTE CONFIGURATION OF CYCLIC AMINES WITH BODE’S ACYLATION REAGENTS		
		59
3.1	Abstract.....	59
3.2	Introduction.....	60
3.2.1	Inspiration from Bode.....	61
3.2.2	Prior work on CEC method for Secondary Amines.....	63
3.3	Results and Discussion	65
3.3.1	Brief Exploration of New Reagents and Mode of Analysis	65
3.3.2	Expansion of Substrate Scope.....	66
3.3.3	Examination of Degrading Selectivity in the CEC Reaction.....	69
3.3.4	Effect of Conformation on the CEC Selectivity	72
3.4	Conclusions.....	74
3.5	Acknowledgements and Contributions	75
3.6	Supporting Information.....	75
3.6.1	General Experimental Details.....	75
3.6.2	Chemicals.....	76
3.7	References.....	82

CHAPTER 4.	CRYSTALLIZATION OF LIQUID ALKENES AND DIOLS AS OSMATE ESTER DERIVATIVES.....	87
4.1	Abstract.....	87
4.2	Introduction.....	88
4.2.1	Motivation.....	88
4.2.2	Background.....	90
4.2.3	Osmylation as a Crystallization Strategy.....	91
4.3	Results and Discussion.....	92
4.3.1	Crystallization of Liquid Alkenes.....	92
4.4	Redox Neutral Crystallization of Diols as TMEDA-Osmate Esters.....	97
4.4.1	Introduction.....	97
4.4.2	Results and Discussion.....	98
4.5	Conclusions and Future Directions.....	101
4.6	Acknowledgements and Contributions.....	102
4.7	Supporting Information.....	102
4.7.1	General Information.....	102
4.7.2	General Procedure 1: Formation of Osmate Esters from Alkenes ^{9b}	103
4.7.3	General Procedure 2: Redox Neutral Formation of Osmate Esters from Diols.....	104
4.7.4	Compound Synthesis and Characterization.....	105
4.8	References.....	114
CHAPTER 5. ...	DEVELOPMENT OF STRATEGIES TOWARD THE TOTAL SYNTHESIS OF (2 <i>R</i>)-HYDROXYNORNEOMAJUCIN AND RELATED <i>ILLICIUM</i> SESQUITERPENES....	118
5.1	Abstract.....	118
5.2	Introduction.....	119
5.2.1	Introduction to the Illicium Sesquiterpenes.....	119
5.2.2	Danishefsky's Total Synthesis of (±)-Jiadifenin.....	121
5.2.3	Theodorakis's Enantioselective Syntheses of (–)-Jiadifenolide and (–)-Jiadifenin....	123
5.2.4	Zhai's Total Synthesis of Jiadifenin.....	127
5.2.5	Sorensen's Total Synthesis of (–)-Jiadifenolide.....	128
5.2.6	Paterson's Total Synthesis of (±)-Jiadifenolide.....	130
5.2.7	Fukuyama's Formal Synthesis of (±)-Jiadifenin.....	131

5.2.8	Shenvi's Gram-Scale Synthesis of (–)-Jiadifenolide	132
5.2.9	Zhang's Protecting Group Free Synthesis of (–)-Jiadifenolide	133
5.2.10	Micalizio's Synthesis of (–)-Jiadifenin and (2S)-hydroxy-3,4-dehydroneomajucin 135	
5.2.11	Maimone's Oxidative Approach to (–)-Majucin and (–)-Jiadifenoxolane A	137
5.2.12	Gademann's Approach to (2R)-hydroxynorneomajucin	139
5.2.13	Introduction to (2R)-hydroxynorneomajucin.....	141
5.3	Initial Efforts Toward the Synthesis of (2R)-hydroxynorneomajucin	142
5.3.1	Retrosynthesis	142
5.3.2	Investigation of Tsuji–Troost Reactivity	143
5.3.3	Optimization of α -Hydroxylation.....	148
5.3.4	Forward Synthesis.....	150
5.3.5	Investigation of Pauson–Khand Reactivity.....	151
5.4	Second Generation Route Toward (2R)-hydroxynorneomajucin	158
5.4.1	Revised Retrosynthesis	158
5.4.2	Synthesis of the Enyne Precursor	160
5.4.3	Constructing the Core	163
5.4.4	End Game Strategy	169
5.5	Summary	175
5.6	Supporting Information.....	177
5.6.1	General Experimental Details	177
5.6.2	Chemicals.....	178
5.6.3	Compound Synthesis and Characterization	179
5.6.4	X-ray Crystallography Data.....	231
5.7	References.....	234
	APPENDIX A: SPECTRAL DATA FOR COMPOUNDS IN CHAPTER 2	244
	APPENDIX B: SPECTRAL DATA FOR COMPOUNDS IN CHAPTER 4	287
	APPENDIX C: SPECTRAL DATA FOR COMPOUNDS IN CHAPTER 5	300

LIST OF TABLES

Table 3-1 Selectivity and conversion data with calculated axial conformation energy. ^a	73
Table 4-1 Alkenes and the Derived Crystalline Osmate-TMEDA Esters. ^a	94
Table 4-2 Unsuccessful substrates.	96
Table 4-3 Optimization of redox neutral osmylation of 1,2-diols.....	99
Table 5-1 Pharmacophore mapping of ODNM analogues.....	127
Table 5-2 Optimization of the Tsuji–Trost.	147
Table 5-3 Optimization of the α -hydroxylation.....	149
Table 5-4 Attempted Pauson–Khand reactions using a variety of enynes.	158
Table 5-5 Comparison of ¹ H NMR spectra of isolated and synthetic 5-8 . ³²	227
Table 5-6 Comparison of ¹³ C NMR spectra of isolated and synthetic 5-8 . ³²	228
Table 5-7 Crystal data and structure refinement for 5-155 (sdr60).....	232

LIST OF FIGURES

Figure 1-1 Examples of the different types of chirality.....	3
Figure 1-2A. Generic scheme describing the CEC method. B. Reaction coordinate diagram, displaying the energy difference leading to stereochemical assignment.....	9
Figure 2-1 Summary of the ambiguity surrounding frondosin B.....	19
Figure 2-2 Representative Diels–Alder reactions with PTAD (2-1).....	20
Figure 2-3A. Kinetic resolution of a racemic diene using Sulfinyl naphthoquinone 2-8 . B. Kinetic resolution of racemic diene using chiral triazolinediones.....	21
Figure 2-4 Novel triazolinediones reagents targeted for application in CEC reactions.....	22
Figure 2-5 Potential new directions for biaryl-based triazolinediones.....	30
Figure 3-1 Enantioenrichment of N-heterocycles using α -hydroxy enones as acyl surrogates. .	62
Figure 3-2 Kinetic resolution of secondary amines using hydroxamic acid 3-7	63
Figure 3-3 Basic CEC strategy for cyclic amines—published work with examples.....	64
Figure 3-4 Acylation reaction and plot of experimental and simulated CEC kinetic data for 3-58	71
Figure 4-1 Determination and revision of the absolute configuration of (–)-illisimonin A. Our published assignment was based on ferrocene ester 4-4 , whose absolute configuration was determined through X-ray crystallography. Osmate ester 4-5 was prepared in fewer steps and retained greasy protecting groups.	89
Figure 5-1 Different carbon skeletons of the Illicium sesquiterpenes.....	119
Figure 5-2 Representative seco-prezizaane sesquiterpenes.....	120
Figure 5-3 Initial SAR mapping of jiadifenin-like compounds.....	123
Figure 5-4 (2R)-hydroxynorneomajucin.....	141
Figure 5-5 Natural products recently synthesized using Pauson–Khand reactions.....	154
Figure 5-6 Initial attempts at the key Pauson–Khand reaction.....	154
Figure 5-7 Calculated conformers for 5-131	155
Figure 5-8 Investigation of potential Tsuji–Trost starting materials.....	162
Figure 5-9 Highlighting the final manipulations necessary for the conversion of 5-189 to 5-8 .169	
Figure 5-10 Overlaid ¹ H NMR Spectra of 5-8 . Top: Isolated. ³² Bottom: Synthetic.....	229
Figure 5-11 Overlaid ¹ H NMR of the F1 domain from the COSY reported in the isolation paper and synthetic 5-8	230

LIST OF SCHEMES

Scheme 1-1 Conversion of secondary alcohol into MTPA esters for Mosher analysis. ^{6d}	4
Scheme 1-2 Example of the Horeau method with a generic enantioenriched secondary alcohol. M = Medium group; L = large group.	7
Scheme 1-3 CEC of stereogenic secondary alcohols with selected published examples.	10
Scheme 1-4 CEC assignment of primary amines using pseudoenantiomers of Mioskowski's reagents.	11
Scheme 2-1 Synthesis of 2-17	23
Scheme 2-2 Failed approach toward 2-18	24
Scheme 2-3 Successful synthesis of 2-30	25
Scheme 2-4 Model system to evaluate NMR-based reaction assay.	26
Scheme 2-5 Kinetic resolution using triazolinedione 2-17	27
Scheme 2-6 Attempted kinetic resolution using 2-18	28
Scheme 3-1 Comparison of the Original and Brominated Acyl Transfer Reagents.	65
Scheme 3-2 CEC Results for Cyclic Secondary Amines.	67
Scheme 3-3 CEC Results with 3-Alkyl Pyrazoles.	68
Scheme 3-4 CEC examples with clinically relevant cyclic amines.	69
Scheme 3-5 Hydroxamic Acid Crossover Experiment.	72
Scheme 4-1 Regioselective osmylation of isopentenyl adenosine.	97
Scheme 4-2 Isolation of a triol-osmate complex by Paquette.	99
Scheme 4-3 Osmylation of 1,3-diols.	100
Scheme 4-4 Osmylation of complex 1,2-diol and amino alcohol substrates.	101
Scheme 5-1 Danishefsky's synthesis of 5-2 and 5-3	122
Scheme 5-2 Theodorakis' Synthesis of key intermediate 5-24	124
Scheme 5-3 Completion of the total synthesis of 5-4	125
Scheme 5-4 Theodorakis's synthesis of 5-3 from common intermediate 5-24	125
Scheme 5-5 Zhai's synthesis of 5-3	128
Scheme 5-6 Sorensen's synthesis of 5-4	129
Scheme 5-7 Paterson's synthesis of 5-4	130
Scheme 5-8 Fukuyama's formal synthesis of 5-3	132
Scheme 5-9 Shenvi's total synthesis of (–)-jiadifenolide.	133
Scheme 5-10 Zhang's total synthesis of 5-4	134
Scheme 5-11 Proposed mechanism of the formal [4+1] annulation.	135
Scheme 5-12 Micalizio's approach to 5-81	136
Scheme 5-13 Divergence of 5-81 to 5-3 and 5-5	137
Scheme 5-14 Maimone's Synthesis of 5-6 and 5-7	138
Scheme 5-15 Gademann's Approach to 5-8	140
Scheme 5-16 Derivatization of 5-8 from 5-100	141
Scheme 5-17 Initial synthetic plan.	143
Scheme 5-18A . Formation of quaternary centers by Pd-catalyzed asymmetric allylic alkylation. B . Cartoon model explaining rationale for regioselectivity.	144
Scheme 5-19 Xie's use of a Tsuji–Trost toward the hyperolactones.	145

Scheme 5-20 Initial attempts to access 5-105 from keto-ester 5-106 .	146
Scheme 5-21 Decagram scale synthesis of 5-122 .	150
Scheme 5-22 Synthesis of enyne 5-131 .	150
Scheme 5-23 Mechanism of the Pauson–Khand reaction.	152
Scheme 5-24 Synthesis of alternate enyne substrates.	156
Scheme 5-25 Revised retrosynthesis of 5-8 .	159
Scheme 5-26 Potential approach to 5-156 .	160
Scheme 5-27 Synthesis of enyne 5-156 through epoxide 5-159 .	161
Scheme 5-28 Synthesis of 5-156 .	163
Scheme 5-29A. Pauson–Khand of the free diol 5-156 . B. Protection of the secondary alcohol as an oxalate. C. Silylation of the secondary alcohol.	164
Scheme 5-30 Attempts to install the final quaternary center.	165
Scheme 5-31A. Divergent results for hydrocyanation of 5-155 . B. Mechanistic pathway proposed by Utimoto.	168
Scheme 5-32 Conversion of 5-155 into desired lactone 5-189 .	168
Scheme 5-33 Efforts toward epimerizing the A-ring methyl stereocenter.	170
Scheme 5-34A. Luche reduction reported by Micalizio. ²⁵ B. Proposed stereochemistry for the Luche reduction reported by Gademann and Daepfen. ³⁰ C. Calculated NMR data for the alcohol diastereomers. D. Precedent from Wicha describing stereochemical divergent results.	172
Scheme 5-35 Completion of the synthesis of 5-8 on small scale.	173
Scheme 5-36 Alternate end-game strategy leading to the 5-8 .	175
Scheme 5-37 The first total synthesis of 5-8 , completed in 17 steps from 5-173 .	177

LIST OF EQUATIONS

Equation 2-1 Selectivity equation based on diastereomeric excess.	25
---	----

LIST OF ABBREVIATIONS

Å	Angstroms
Ac	Acetate
AIBN	2,2'-Azobis(2-methylpropionitrile)
aq.	Aqueous
Atm	Atmosphere
ax	Axial
Boc	tert-Butyloxycarbonyl
Bn	Benzyl
Bu	Butyl
Bz	Benzoate
°C	Degree Celsius
CSA	Camphorsulfonic acid
d	day(s)
δ	Chemical shift
DBU	1,8-Diazabicycloundec-7-ene
DCM	Dichloromethane
DIBAL-H	Diisobutylaluminium hydride
DIPEA	N,N-Diisopropylethylamine
DMP	Dess-Martin periodinane
DMSO	Dimethyl sulfoxide
DMAP	4-Dimethylaminopyridine
DMPU	1,3-Dimethyl-tetrahydropyrimidinone
dppf	1,1'-bis(diphenylphosphino)ferrocene
dr	diastereomeric ratio
ee	enantiomeric excess
eq	equatorial
Et	Ethyl

g gram
h Hour(s)
HF Hydrofluoric acid
HFIP hexafluoro isopropanol
HMPA Hexamethylphosphoramide
HMDS 1,1,1,3,3,3-Hexamethyldisilazane
HRESIMS High-resolution electrospray ionization mass spectrometry
HPLC High pressure liquid chromatography
Hz Hertz
IR Infrared spectrometry
J Coupling constant
L liter
LD Lethal dose
LDA Lithium diisopropylamide
 μ micro
m-CPBA 3-Chloroperoxybenzoic acid
m milli
M Molar
Me methyl
MHz Megahertz
min Minute(s)
MOM Methoxymethyl
MPLC Medium pressure liquid chromatography
MS Molecular sieves
NMP N-Methyl-2-pyrrolidone
NMR Nuclear Magnetic Resonance
NOE Nuclear Overhauser Effect
Ph Phenyl

PMB p-Methoxybenzyl ether
Pr propyl
PPTS Pyridinium p-toluenesulfonate
PTSA p-Toluenesulfonic acid
Py Pyridine
rt Room Temperature
rxn Reaction
SAR Structure Activity Relationship
sec secondary
t tert
TASF Tris(dimethylamino)sulfonium difluorotrimethylsilicate
TBAF Tetra-n-butylammonium fluoride
TBDPS *tert*-Butyldiphenylsilyl
TBS *tert*-Butydimethylsilyl
TES Triethylsilyl
TIPS Triisopropylsilyl
Tf Trifluoromethanesulfonate
TFA Trifluoroacetic acid
THF Tetrahydrofuran
THPO Tetrahydropyranone
TLC Thin-layer chromatography
TMEDA Tetrahmethylethylenediamine
TMS Trimethylsilyl
Ts Tosyl

ACKNOWLEDGEMENTS

There are many people to thank throughout my Ph.D. First and foremost, I'd like to thank Prof. Scott Rychnovsky for being very supportive during my time at UCI. Scott gave me a lot of freedom in the group, and I really appreciate his mentorship. Scott always kept life interesting as well. You are infamous on campus for unicycling to campus when the weather permits, and I'm certainly not going to let you forget the time when you didn't think Sarah was a real person. Truly though, I wouldn't be the scientist and researcher that I am without you, and I really can't thank you enough.

I would also like to thank Professor Chris Vanderwal and Professor Vy Dong for being members of my thesis committee. I really appreciate the advice and ideas that I have gotten through interacting with both of you, and I'm very thankful to have had your mentorship throughout graduate school.

I certainly need to thank Dr. Alex Burtea for mentoring me when I first joined the lab. Alex really taught me how to do chemistry and be efficient in the lab, and I owe a lot of who I am as a scientist to him. He also pulled me onto the amine CEC project when things were bleak with my PTAD work. You may have been loud and clapped constantly and blasted spaceman on loop, but I really enjoyed working with you. And I certainly missed you when you graduated. But I kept your spirit alive through clapping and yelling 'Sah dude' at Paul.

I also need to thank Dr. Sunshine Burns. Sunshine was always motivating (in his own way) and kept you going when you wanted to throw in the towel for the day. His enthusiasm and drive were infectious, and you always knew if you were going to be working late, Sunshine would be around to keep you going. Or talk you into a late-night Taco Bell run. I also learned a lot about how to plan and execute a total synthesis from him, as well as how to plan around failure. A lot of how I think about synthesis comes from Sunshine's mentorship, and I'm very thankful that I got the chance to work with him.

I was blessed to overlap with the last of the Overman postdocs, Dr. Nick Weires, Dr. Prof. Spencer Pitre, and Dr. Tyler Allred. Working one room over, I was always bugging these guys for advice during my first few years in graduate school, probably more often than they would have liked. Not only were they full of knowledge, but they were fun to be around and became great friends of mine. I'm very thankful that they have adopted me into the lab, and included me in their Overman lab happy hours once they had left. Thank you all for always making my time in the lab more enjoyable, and for always listening to my problems. I especially need to thank Tyler, who was here while I struggled through the majority of my synthesis and was full of endless advice.

I also need to thank my current lab mates who have kept me sane during my time here. First and foremost, Leah Sal. Leah and I joined the lab together as first years and went through all the trials and tribulations of our Ph.D.'s together. Leah was my rock in the lab, and was always down to give advice, team up on our molecules-of-the-month, be crusty old fifth years on Saturday mornings, or listen to my many many problems. You're one of the main reasons I was able to vaguely keep my sanity in the last few months here, and I'm going to miss being in the lab with you every day.

“Pistol” Paul “The Wall” “Birdman” Carlson, the man of many names. Bird and I worked in the same lab space since he joined the lab in my second year, when we invaded the empty Overman bay. Bird was the first graduate student I took under my wing (get it?), and I hope that I have been a good mentor to you. I’m certainly proud of how you have matured as a scientist, and I appreciate the methodical and organized way that you pursue your chemistry. And the fact that you know every named reaction known to man. Thank you for dealing with my daily insanity, being my nomenclature wizard (I’m never going to live down ipso), keeping the Burtea-spirit alive, and being the best lab mate to share space and equipment with. I hope that you will shout “sah-dude”, “did it work?”, “recalcitrant”, and clap at whoever takes over my fume hood.

Bryant, you crazy breakdancing dude. Thank you for also being a night-owl in the lab, and for embracing the EDM spirit. I never got a chance to work with you on a project (amazing given the number of projects you had), but you are a great chemist full of ideas and ambition, and it would have been sick getting to team up on a molecule. Good luck in your last year here, and I hope you’ll find your way to Boston after you graduate.

Jess, you are a ray of sunshine in the lab, which is funny since you took over Sunshine’s old hood and desk. Thank you for always being positive and uplifting, checking in on my terrible sleep schedule, and hanging out at my desk with questions (yes, I actually did enjoy that). You are a capable chemist, and I look forward to seeing what you accomplish over the next couple of years. You are the most likely to come to the dark side and move to Boston, and when you do I will be waiting with a “sah dude” and dunkies.

Matt, you are by far one of the smartest people I know. It boggles my mind that you can casually take graduate physics and computer science classes for fun. You absorb information like a sponge, and have an insane passion for learning. Thank you for becoming Chuck Jr., and always being down to debate physical chemistry and toss ideas around. Good luck finishing up the lyconadins and diplopyrone, and I hope that taking all my group jobs won’t be too much of a weight on you.

Jordan and Emily, as the youngest members of the lab you guys were both great additions to the lab. You have both improved so much in the short time that I’ve known you, and I wish you both luck as you tackle candidacy and the rest of your Ph.D.’s.

There are also a lot of people outside of my lab that I also need to specifically thank:

Natalie, I don’t even know where to begin. I want you to know that I stared at this first sentence for several hours before I could even put my thoughts together because there’s just so much I could say. Thank you for always listening to my rants, always being there to commiserate my gripes about chemistry, and just being a great friend all around. We went through everything in this program together, including job interviews and the timing of key stages of our respective syntheses, which is why I relate to you the most out of everyone I’ve known here. I mean I literally did one of my interviews in your dining room when there was construction at my apartment complex. I can’t imagine what my experience would have been like without you here. I don’t know what I’m going to do when we start our jobs and you’re not just across the hall from me anymore. Stalking my location on your phone will be much less satisfying I suppose. I spent so many hours

at your fume hood or desk talking about problems in our respective chemistry or in life, and I hope you know how much your friendship has meant to me.

Scott, thank you for getting me into tennis, being fat and going to Panda Express with me, and for being a great friend. I loved that many days you would drop into my bay and chat for a few minutes before getting to work, even if Natalie didn't like it. You would always come to share a cool result or to ask for advice. Honestly I'm not sure why, because I feel like my advice was never that great. But I did look forward to you dropping in to chat or heckle me or just share funny memes (there were a lot of memes over the years). You're one of the smartest chemists I know, and one of my best friends here, and I'm very thankful that graduate school has brought you into my life. Now if only I could convince you and Natalie that Boston is better than Boulder, and you should both move there instead. I hope you won't go too crazy in your last year once me and Natalie are gone, but I will be sure to bombard you with reels and memes so it feels like I never left.

Nick, thank you for helping me keep my sanity with our daily coffee trips. I'm not sure if the switch from weekly Chick-Fil-A to daily coffee was healthy, but I can't imagine going without it. We not only singlehandedly kept Peet's in business, but also had a daily opportunity to get out of lab for a little while and talk about problems in our syntheses. Obviously, our friendship is much more than daily coffee trips, but I had to write that in. For real, you are one of the most talented chemists I know, and I can't imagine my experience here without you. During the pandemic when we were at home, our daily Warzone sessions were one of the only things keeping me from completely losing my mind. Thank you for being a great friend, for always inviting me to the Pronin lab parties at your place, for getting me hooked on Call of Duty again, and for introducing me to the wonderful world of Nick Cage films. If you ever decide to leave the warm beaches of La Jolla, you're always welcome in Boston.

Kirsten, you are literally one of my day-one friends here and I'm so glad I got to meet you at UCI. I had to single you out among our friend group because we did literally everything together our first two years here. Classes, teaching, orals, shopping, you name it. I'm very sorry for torturing you in classes, especially during exams, by cracking my knuckles and back. I will never forget all the long hours we spent working on mech or synth homework as first years, all the Sunday trips to Walmart to get groceries, all the times you iced me, and I will especially never forget the infamous outing to Dirty Nelly's. I know I have said this a few times now, but you are one of the most talented chemists I know, and you are going to crush it at GSK. Honestly it might have been for the best that we both didn't end up at GSK, because I'm not sure the process department would have been ready for that much energy. But I do want you to know that your friendship has meant the world to me, and I'm stoked that you and Justin will only be a short drive away on the East coast.

Meghen, Justin, Tyler, and Carly, you guys are also all my day-one homies and I'm so happy that grad school brought us all together. Justin and Tyler, our literal day one trip to Eureka to get beers during orientation will forever be legendary (and also will forever make Kirsten jealous she wasn't invited). I don't even know how to express how much my friendship with all of you has meant to me, and I think if I wrote out all the memories I have with all of you, this section

would be longer than Chapter 1. All the parties, all the football Sundays, all the bonfires in Huntington, our friendsgiving feasts. I really am lucky that I stumbled into such a great friend group here, and I'm going to miss you all so much as we all go our separate ways.

All of the members of the Pronin and Vanderwal labs, past and present, thank you all for being amazing friends and coworkers. We all share a love of chemistry, and we have such a great dynamic between all of our groups that I think is incredibly special. The happy hours that we started up recently have been a great way for us all to get together outside of lab, and I hope they will continue for a long time. The synthetic labs will always have a special bond, since we can all relate to the trials and frustration of total synthesis, and I'm so glad that I got to share in this crazy experience with all of you.

I wouldn't be where I am today if it were not for all my undergraduate professors, particularly Dr. Weinreb, Dr. Eyet, and John Tipping. Dr. Weinreb really gave me my start in organic chemistry research, and she was endlessly supportive (and forgiving). Dr. Eyet, I can't count how many hours I spent in your office as an undergrad, and even in the year that I taught labs there. You were such a great mentor, and you helped whip me into shape as an undergrad (where we can definitely agree, I needed it). John, I don't know that you would ever read this, and I don't know if you're even aware, but you are the one who convinced me that I was good at organic chemistry and that I should pursue graduate school. I was all set to take the MCAT, go to medical school, and not look back. But you are the one who opened my eyes to the fact that organic chemistry is what I really wanted to do. You were incredibly influential in my senior year, and I really don't know how to thank you for setting me down this path.

I especially need to thank my Mom, my Dad, my sister Christina, and the rest of my family for being incredibly supportive while I pursued my Ph.D. It definitely was not easy being 3,000 miles away from you guys, especially during the last two years when travelling was hard due to COVID. I love you all, and I'll be so happy to be back in New England.

Sarah, there really are not enough words to express how much your love and support has meant to me. You moved away from your family, and away from a job you loved to come and be here with me and work at a job that was less than ideal (putting it mildly). You always knew what to say to cheer me up after a bad day in the lab, and you were always there for me in my darkest days. You took care of so much for me so that I could focus on getting my chemistry done, and I really don't think I would have been able to function day to day without you, especially not in these last few months. I don't know how to thank you for all that you've done for me over the past 5 years. I love you so much, and I can't wait to start our lives together.

Finally, I need to thank my dogs Tucker and Brenna. They weren't super helpful in terms of chemistry, but they were excellent listeners and great distractions from writing my dissertation.

CURRICULUM VITA

Charles J. Dooley III

Education

Ph.D. University of California, Irvine
Organic Chemistry
Advisor: Prof. Scott D. Rychnovsky

Irvine, CA
Aug 2017 – April 2022

Honors B.A. Saint Anselm College
Chemistry (*summa cum laude*)
Advisor: Prof. Carolyn K. Weinreb

Manchester, NH
Aug 2012 - May 2016

Experience

VHG Reference Materials

Manchester, NH

Production Chemist

December 2016 - July 2017

- Prepared and analyzed ion chromatography standards by classical wet chemistry techniques according to current Good Manufacturing Practices (cGMP).
- Verified performance of lab balances, fume hoods, volumetric glassware, thermometers, and pipettes.
- Assisted in the preparation of standard operating procedures (SOP) for new products being brought to market.

Publications

1. **Dooley, C. J., III**; Burtea, A.; Mitilian C.; Dao, W.; Qu, B.; Salzameda, N.; Rychnovsky, S. D. Using the Competing Enantioselective Conversion Method to Assign the Absolute Configuration of Cyclic Amines with Bode's Acylation Reagents. *J. Org. Chem.* **2020**, *85*, 10750–10759.
2. Burns, A. S.; **Dooley, C., III**; Carlson, P. R.; Ziller, J. W.; Rychnovsky, S. D. Relative and Absolute Structure Assignments of Alkenes Using Crystalline Osmate Derivatives for X-ray Analysis. *Org. Lett.* **2019**, *21*, 10125–10129

Presentations

1. **Dooley, C. J., III**; Rychnovsky, S. D. "Approaches Toward the Total Synthesis of (2*R*)-hydroxynorneomajucin and Related *Illicium* Sesquiterpenes." American Chemical Society Fall Meeting and Exposition, Atlanta, GA. August 22-26, 2021.
2. **Dooley, C. J., III**; Weinreb, C. K. "Synthesis of Alkynes Via N-tosyl Hydrazones." SOAR Student Poster Session, Manchester, NH. April 28, 2016.
3. Muldoon, C. I.; Cassidy, J.; Scafidi, A.; **Dooley, C. J., III**; Moreau, W. M.; Eyet, N. "Saint Anselm College Chemistry Club: We Work Periodically." American Chemical Society 250th National Meeting and Exposition, Boston, MA. August 16-20, 2015.
4. Arcand, C.; **Dooley, C. J., III**; Weinreb, C. K. "Synthesis of Alkynes from Aldehydes and Ketones via α -Substituted N-Tosyl Hydrazones." American Chemical Society 250th National Meeting and Exposition, Boston, MA. August 16-20, 2015.

5. **Dooley, C. J., III**; Weinreb, C. K.; “Synthesis of Alkynes from Aldehydes and Ketones via α -Substituted N-Tosyl Hydrazones.” NH-INBRE Regional Conference, New Castle, NH. August 6, 2015.

Skills

- Experienced in the design and implementation of synthetic strategies toward complex targets.
- Thorough understanding of synthetic organic lab techniques, including air-free reactions, handling pyrophoric reagents, normal and reverse-phase chromatography (Teledyne ISCO and Biotage Isolera).
- Understanding of instrumental protocol necessary for operation of High Performance Liquid Chromatography (HPLC), Mass-Spectrometry, and Liquid Chromatography-Mass Spectrometry (LCMS).
- Experienced in acquisition and interpretation of 1-D and 2-D nuclear magnetic resonance (NMR) experiments.

Honors and Awards

- | | |
|--|-------------------|
| ○ Delta Epsilon Sigma National Honor Society Member | May 2014 |
| ○ Alpha Lambda Delta National Honor Society Member | May 2015 |
| ○ NH-INBRE Undergraduate Research Fellow | June 2015 |
| ○ American Institute of Chemists Foundation Award | May 2016 |
| ○ Saint Anselm College President’s Award | May 2016 |
| ○ American Chemical Society Undergraduate Award in Inorganic Chemistry | May 2016 |
| ○ UCI Allergan Research Fellow | April 2021 |

ABSTRACT OF THE DISSERTATION

Total Synthesis of (2*R*)-hydroxynorneomajucin

and

Development of Strategies for the Assignment of Absolute Stereochemistry

By

Charles J. Dooley III

Doctor of Philosophy in Chemistry

University of California, Irvine, 2022

Professor Scott D. Rychnovsky, Chair

The first chapter serves as a general introduction to the topic of stereochemistry and stereochemical determination in organic chemistry. Stereochemistry is a subject that was first conceived following Pasteur's separation of tartaric acid enantiomers in 1848. The notion of asymmetric carbon atoms is now second nature to organic chemists, however determination of the geometrical configuration about stereogenic carbon atoms is still non-trivial. This chapter provides a general introduction for the work discussed in chapters 2–4.

The second chapter details efforts towards developing a Competing Enantioselective Conversion (CEC) method to determine the absolute configuration of dienes bearing adjacent chiral centers. Chiral analogues of 1,2,4-triazoline-3,5-diones (TAD) were synthesized and used as dienophiles in enantioselective Diels–Alder reactions with dienes bearing adjacent chirality. Kinetic resolution with these new reagents displayed moderate selectivity, but the prohibitive synthesis of the reagents rendered efforts to develop a CEC method fruitless.

The third chapter details an expansion of the competing enantioselective conversion (CEC) method for cyclic secondary amines. Previously, Bode's chiral acylated hydroxamic acids were used to determine the stereochemistry of primary amines, as well as cyclic and acyclic secondary amines. The enantioselective acylation has herein been evaluated for 4-, 5-, and 6-membered cyclic secondary amines, including medicinally relevant compounds. The limitations of the method were studied through computational analysis and experimental results. Control experiments were performed to investigate the cause of degrading selectivity under the CEC reaction conditions. The present study expands the scope of the CEC method for secondary amines and provides a better understanding of the reaction profile.

The fourth chapter details the crystallization of alkenes and diols as osmate ester derivatives. Organic compounds containing alkenes are often challenging to crystallize. We have found that osmium tetroxide and TMEDA form stable crystalline adducts with alkenes, allowing the determination of absolute structure by X-ray crystallography. Osmium, a heavy atom, facilitates the crystallographic analysis and the determination of absolute configuration using common Mo X-ray sources. The utility of this method for determining absolute structure and configuration was demonstrated on several unsaturated substrates. We also investigated a redox-neutral crystallization strategy of 1,2- and 1,3- diols using potassium osmate, and results are reported.

The fifth chapter details the completion of the first total synthesis of (2*R*)-hydroxynorneomajucin. Our synthetic strategy initially hinged on utilizing a Pauson–Khand reaction of an advanced bis-lactone intermediate to construct the core of the natural product which, unfortunately, was not successful. The key features of our revised synthetic strategy include an asymmetric Tsuji–Trost allylic alkylation to set a key quaternary center, a Pauson–Khand to close

the core of the molecule, and a late-stage conjugate addition to install the final quaternary center. This strategy has allowed us to complete the first total synthesis of (2*R*)-hydroxynorneomajucin to date in 17 steps from simple starting materials.

Chapter 1. A Brief Introduction of Stereochemistry and How to Deduce Absolute Configuration.

1.1 Abstract

Stereochemistry is a subject that was first conceived following Pasteur's separation of tartaric acid enantiomers in 1848. The notion of asymmetric carbon atoms is now second nature to organic chemists, however determination of the geometrical configuration about stereogenic carbon atoms is still non-trivial. This chapter serves as a general introduction to how absolute stereochemistry is determined, and provides a general background for the work discussed in chapters 2–4.

1.2 Introduction

1.2.1 Stereochemistry

Every student of the physical sciences is familiar with the concept of stereochemistry. Molecular chirality was first recognized by the French chemist Louis Pasteur in 1848 when he observed that crystals of sodium ammonium tartrate had certain facets which distinguished them.¹ These facets were either inclined to the right or inclined to the left. Based on this recognition, Pasteur was able to separate the crystals by their “handedness”. The term “chirality” was proposed in 1894 by Lord Kelvin, and is now the predominant term used to describe molecular asymmetry.

Following Pasteur’s experiments, in 1874 the asymmetric carbon atom was proposed independently and almost simultaneously by Jacobus Henricus van’t Hoff and Joseph Lebel. They suggested that four different substituents on the same carbon atom would result in two possible geometrical assemblies that were non-superimposable mirror images of one another. They also proposed that the four substituents attached to the carbon atom were arranged in a tetrahedron. In order to classify these asymmetric carbon atoms, the Cahn–Ingold–Prelog (CIP) system was developed. This system assigns either an *R* or *S* designation to a carbon stereocenter resulting from the priority of the substituents attached.² The CIP system serves as a simple and effective descriptor of a single stereocenter, a contrasting feature to other properties such as optical rotation that are characteristic of a whole molecule.

1.2.2 Types of Chirality

The most common type of chirality is the chiral center (point chirality), which is what many imagine when they look at an organic molecule (Figure 1-1A). However, a molecule does not necessarily need to contain a chiral center to be chiral. In addition to point chirality, asymmetry can manifest in axial chirality and planar chirality. A very common example of axial chirality is

1,1'-bi-2-naphthol (BINOL), which does not contain any chiral centers but rather a chiral axis (Figure 1-1B). This occurs when free rotation about a central bond or axis is sterically restricted. Planar chirality is the least commonly encountered but occurs when a chiral molecule contains two non-coplanar rings that are each not symmetric (Figure 1-1C). An example of this is the planar chiral ferrocene derivative developed for the kinetic resolution of secondary alcohols.³

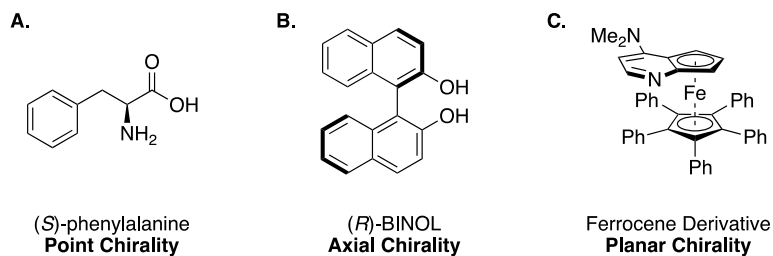


Figure 1-1 Examples of the different types of chirality.

1.3 Determination of Absolute Configuration

The field of asymmetric synthesis has seen tremendous advances over the past few decades. As this field grows, it becomes increasingly important to be able to identify and accurately determine the absolute configuration of the stereocenters of interest. To keep up with this growing need, several useful methodologies and technologies have been developed.⁴

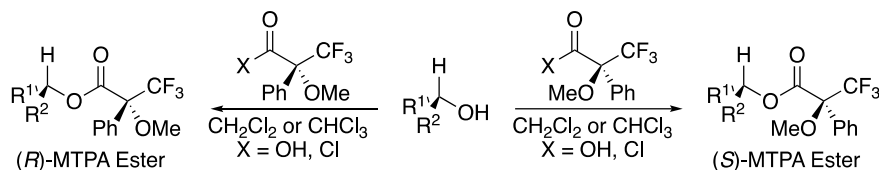
Classically, absolute stereochemistry was determined by degradation of a compound of interest to a compound of known configuration. This allowed for assignments to be made by measurement and comparison of the optical rotation. However, this method is time intensive and relies on the ready availability of large amounts of the compound of interest. In the context of natural product isolation, this is rarely feasible. Fortunately, advances in instrumentation and methodology have allowed for more direct and simpler stereochemical assignments. Many methods now derivatize the compound of interest in various ways to change its spectroscopic or physical properties. These derivatives can often be characterized by NMR or optical techniques to

give information about the spatial arrangement of the stereocenter of interest. The following sections will give more detail on these specific methods.

1.3.1 NMR-Based Methods

The determination of absolute stereochemistry can frequently be done through use of NMR spectroscopy.^{4,5} One of the most common methods for determining the stereochemistry about stereodefined alcohols and amines is the Mosher method.⁶ In this method, the parent chiral alcohol or amine is acylated with (*R*)- and (*S*)- α -methoxy- α -trifluoromethylphenyl acetic acid (MTPA) to afford esters and amides respectively.

Scheme 1-1 Conversion of secondary alcohol into MTPA esters for Mosher analysis.^{6d}



The ¹H NMR of each MTPA ester is then acquired to determine the resulting changes in chemical shift to the protons proximal to the stereocenter in question. The arene of the MTPA ester displays an anisotropic effect on the substituent on the same face of the molecule, providing an identifiable pattern in the change of chemical shift. Through analysis of this pattern in both diastereomeric MTPA esters, the absolute configuration of the alcohol stereocenter can be confidently assigned. The Mosher method is very popular because unlike many other chiroptical and crystallographic methods, it does not require specialized instrumentation or training to determine absolute configuration. However, this method necessitates two separate reactions, purifications, and detailed spectroscopic analyses to confidently assign one stereocenter.

An alternative method was developed which does not require the covalent linkage of a chiral group to the origin stereocenter. This method uses a chiral reagent or solvent, often called a chiral shift reagent, to generate a noticeable change in chemical shift through molecular

interactions in solution.⁷ These interactions can then be analyzed in a similar manner to Mosher's method. Practically, the use of chiral shift reagents is very useful as it does not require a reaction or purification to determine the configuration of a desired compound, but it is often plagued by incomplete separation of peaks in the NMR spectra.

1.3.2 *Methods Based on Optical Spectroscopy*

Complimentary to NMR spectroscopy, other techniques to determine absolute stereochemistry have been developed based on optical characterization techniques. It has long been known that chiral molecules interact with plane polarized light, and in the early 20th century optical rotation was used to establish stereochemistry.¹ Recent advances in DFT computation has allowed optical rotation to become a more powerful tool in absolute structure assignment.⁸ While practically useful, optical rotation has been eclipsed by circular dichroism as the optical method of choice for determination of absolute configuration.

The exciton chirality method for electronic circular dichroism (ECD) spectroscopy has emerged as a powerful tool for the determination of absolute stereochemistry.⁹ In this method, at least two chromophores are attached to the stereocenters of interest, and the interaction of the chromophores in space leads to predictable changes in the Cotton effect, allowing for stereochemical assignments. In many cases, para-substituted benzoates have been used as chromophores for the assignment of asymmetric polyols.^{8d,e} Similar to chiral shift reagents for NMR, advances have been made that allow the use of chromophores that do not need to be covalently linked to the stereocenters of interest. Several reports make use of a zinc porphyrin tweezer complex, which can complex to Lewis basic functional groups and allow for ECD configurational assignments to be made.¹⁰ This not only obviates the need to synthetically

manipulate the compound of interest, but also allows the assignment of a single stereocenter through clever design.

The more common approach to solving absolute stereochemistry using circular dichroism involves performing DFT calculations of either the ECD or VCD spectrum.¹¹ By comparing the calculated spectra with the experimental data, the absolute configuration can be deduced with good confidence. However, as with many methods of absolute structure assignment, errors can occur which obscure stereochemical assignments. Recently, a former lab member completed the synthesis of racemic and enantiopure illisimonin A.¹² The absolute configuration of the isolated natural product was assigned by DFT calculation of the ECD spectrum.¹³ However, through total synthesis, it was found that the absolute configuration had been mis-assigned due to an error in the calculation. This is not to disparage the significant efforts of other groups, but rather to showcase that even with advances in computation and instrumentation, the assignment of stereochemistry remains a significant challenge.

1.3.3 *X-Ray Crystallography*

X-ray crystallography has long been considered the gold standard for absolute structure assignment. The absolute configuration of an enantiomerically pure crystalline substance is found by solving for the Flack parameter.¹⁴ In order to solve the Flack parameter, an organic substance must contain either a chiral center of known absolute configuration or a heavy atom. The installation of a moiety with known chirality functions as an internal reference when solving the crystal structure. The presence of a heavy atom increases the anomalous scattering of the incident X-rays, giving the compound a distinct diffraction pattern. Advances in the Flack method have allowed it to be applied to organic compounds which do not contain a heavy atom, typically through use of Cu X-ray sources.¹⁵

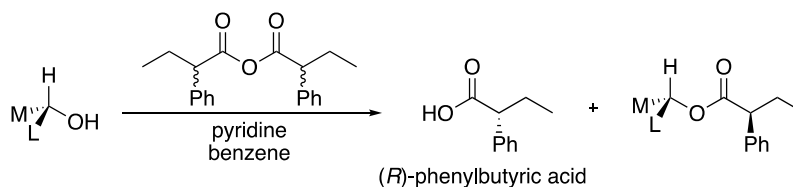
A particular challenge is that many organic compounds tend not to be crystalline. Several derivatization strategies have been developed to increase the crystallinity of organic compounds. One such strategy is to form a salt from amines or carboxylic acids, generally with a chiral counterion. Alcohols and amines have been derivatized with 4-nitrobenzoyl chloride or 4-bromobenzoyl chloride to afford crystalline esters and amides respectively. A promising advance is the use of ferrocene carboxylic acid to form esters.¹⁶ These ferrocene derivatives are generally highly crystalline, and contain a heavy atom to increase anomalous dispersion. Recently, alcohols have also been crystallized as guanidinium salts through reaction with SO₃ in the presence of a guanidine.¹⁷ Ketones and aldehydes have also been transformed into 3,5-(NO₂)₂-phenylhydrazones. Recently, our group has devised a strategy to crystallize enantiomerically pure liquid alkenes by formation of osmate esters.¹⁸ This methodology will be the topic of Chapter 4.

1.4 The Competing Enantioselective Conversion Method

1.4.1 Configuration Assignment through Inherent Substrate Reactivity

A distinct approach to solving absolute stereochemistry involves using the inherent reactivity of a chiral substrate. Horeau developed this method based on the concept of partial resolution (Scheme 1-2).¹⁹

Scheme 1-2 Example of the Horeau method with a generic enantioenriched secondary alcohol.
M = Medium group; L = large group.



The goal was to make use of the chiral environment of the alcohol during the esterification process to achieve a partial resolution of racemic 2-phenylbutyric anhydride. After the reaction, the phenylbutyric acid was recovered and its optical rotation was measured to determine the

enantioenrichment. This gave valuable information on the preferred reactivity of the chiral secondary alcohol substrate. It was found that the reaction occurred in a way which minimized steric interactions during the esterification process. While this method is very useful, the enrichment of the recovered acid byproduct was often very small, and optical rotation was not always a reliable tool. By converting the recovered acid to the methyl ester, König was able to utilize gas chromatography with a chiral stationary phase to determine the enrichment of the recovered product.^{19h} This advancement makes the determination of low levels of enantioenrichment more practical and reliable.

1.4.2 *The Competing Enantioselective Conversion Method*

Inspired by the Horeau method, the Rychnovsky group has developed the Competing Enantioselective Conversion (CEC) method as a quick and reliable means of determining absolute configuration. Rather than perform a partial resolution, the CEC method takes advantage of an enantioselective catalyst/reagent to react with an enantioenriched substrate. The CEC method works as follows: an enantioenriched substrate reacts with both enantiomers of an enantioselective reagent, and both reactions are quenched after the same amount of time. The reaction conversion is then assayed, and the faster reaction is identified (Figure 1-2A). The reactions proceed at different rates due to the energy difference between the diastereomeric transition states (Figure 1-2B). The absolute configuration is then assigned by comparison to an empirical model of the reagent stereoselectivity.

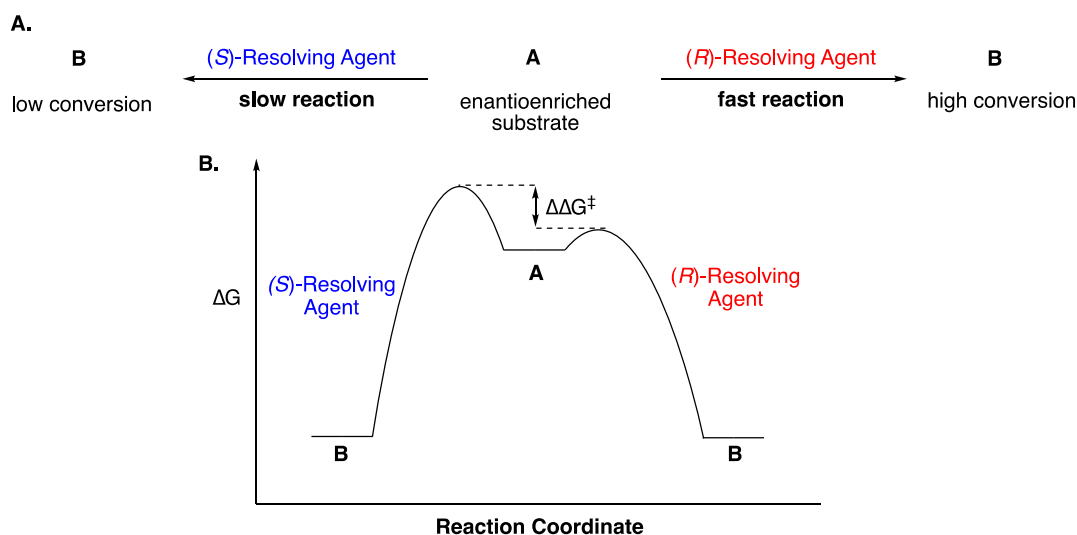
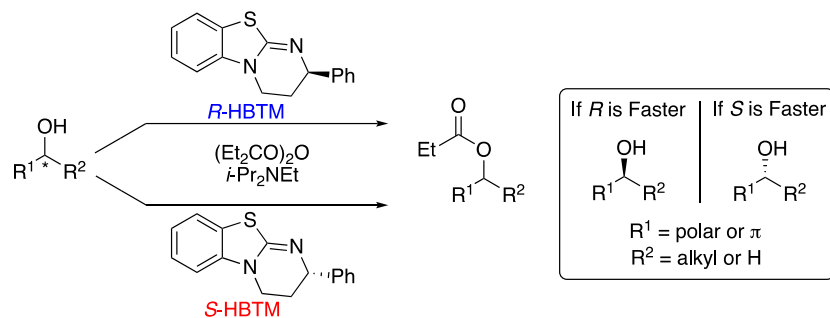


Figure 1-2A. Generic scheme describing the CEC method. **B.** Reaction coordinate diagram displaying the energy difference leading to stereochemical assignment.

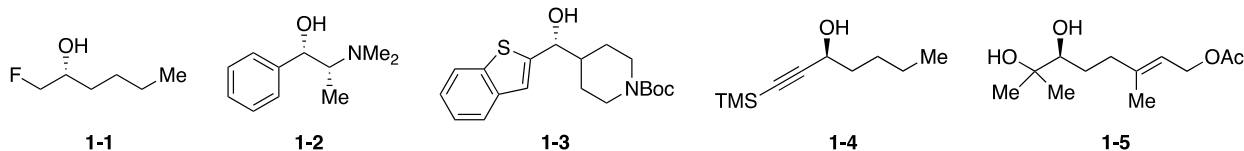
1.4.3 CEC Assignment of Stereogenic Carbinols

Previously, the CEC method has been applied to various classes of chiral alcohols using Birman's homobenzotetramisole (HBTM) acylation catalysts.²⁰ For the assignment of alcohols, the enantioenriched alcohol reacts with propionic anhydride in the presence of each enantiomer of HBTM catalyst in parallel reaction vessels. The two reactions are quenched after the same amount of time, and the conversion is assayed by either TLC or ¹H NMR. This method has proven to be effective for secondary alcohols which bear either a π -group or a heteroatom adjacent to the chiral alcohol (Scheme 1-3).²¹ In addition to this class of substrates, the enantioselective acylation with HBTM has also been applied to β -chiral primary alcohols,²² oxazolidinones and lactams.²³

Scheme 1-3 CEC of stereogenic secondary alcohols with selected published examples.



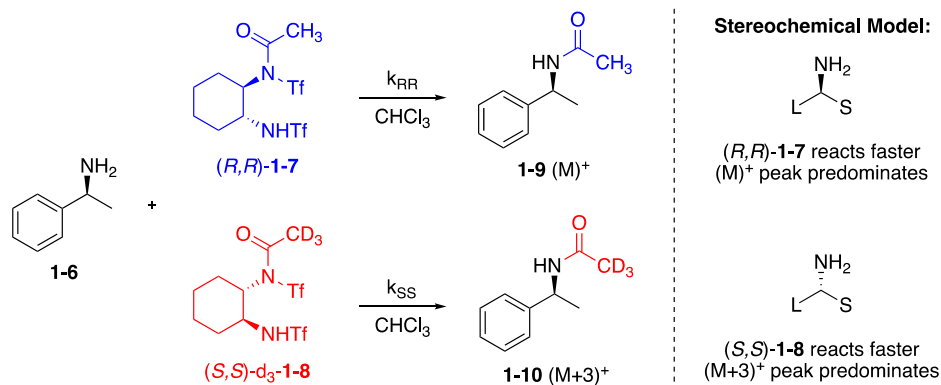
Selected Examples:



1.4.4 CEC Assignment of Primary Amines

An attractive feature of the CEC method is that it can be applied to any functional group for which effective kinetic resolution conditions exist. In 2012, the CEC method was extended to stereogenic primary amines by taking advantage of Mioskowski's enantioselective acylation reagents (Scheme 1-4).²⁴ Rather than conduct two separate reactions and analyses, this CEC method could be performed in one pot by using pseudoenantiomeric acylation reagents **1-7** and **1-8**. Reagent **1-7** bore an acetyl group, and the pseudoenantiomer **1-8** was modified to an acetyl-*d*₃ group. By differentiating the enantioselective reagents by mass, it allowed for the analysis to be performed by ESI-MS, greatly facilitating the speed and simplicity of the method. Though the method was effective for primary amines, it lacked adequate reactivity for secondary amines. In addition to this, the deuterated reagent lost deuterium enrichment over time, complicating the analysis. To address both concerns, a different kinetic resolution system was used and developed into a CEC method, which will be the topic of Chapter 3.

Scheme 1-4 CEC assignment of primary amines using pseudoenantiomers of Mioskowski's reagents.



1.5 Summary

This chapter provided a general overview of the topic of stereochemical assignment. Different instrumental, as well as chemical methods for the assignment of absolute configuration were discussed. The content of this chapter serves as a general introduction to chapters 2, 3 and 4, all of which focus on methodology development toward assigning stereochemistry and structure.

1.6 References

- ¹ Gal, J.; Cintas, P. Biochirality: Origins, Evolution, and Molecular Recognition. *Top. Curr. Chem.* **333**, 1–40.
- ² (a) Cahn, R. S.; Ingold, C.; Prelog, V. Specification of Molecular Chirality. *Angew. Chem. Int. Ed.* **1966**, *5*, 385–415. (b) Prelog, V.; Helmchen, G. Basic Principles of the CIP-System and Proposals for a Revision. *Angew. Chem. Int. Ed.* **1982**, *21*, 567–583.
- ³ Ruble, J. C.; Latham, H. A.; Fu, G. C. Effective Kinetic Resolution of Secondary Alcohols with a Planar-Chiral Analogue of 4-(Dimethylamino)Pyridine. Use of the Fe(C₅Ph₅) Group in Asymmetric Catalysis. *J. Am. Chem. Soc.* **1997**, *119*, 1492–1493.
- ⁴ (a) Wenzel, T. J.; Chisholm, C. D. Assignment of Absolute Configuration Using Chiral Reagents and NMR Spectroscopy. *Chirality* **2011**, *23*, 190–214. (b) Seco, J. M.; Quiñoá, E.; Riguera, R. The Assignment of Absolute Configuration by NMR. *Chem. Rev.* **2004**, *104*, 17–118.

⁵ Eliel, E. L.; Wilen, S. H. *Stereochemistry of Organic Compounds*; John Wiley & Sons, Inc.: Hoboken, NJ, 1994; pp 101–147 and 991–1105.

⁶ (a) Dale, J. A.; Dull, D. L.; Mosher, H. α -Methoxy- α -Trifluoromethylphenylacetic Acid, a Versatile Reagent for the Determination of Enantiomeric Composition of Alcohols and Amines. *J. Org. Chem.* **1969**, *34*, 2543–2549. (b) Dale, J. A.; Mosher, H. S. Nuclear Magnetic Resonance Enantiomer Regents. Configurational Correlations via Nuclear Magnetic Resonance Chemical Shifts of Diastereomeric Mandelate, O-Methylmandelate, and α -Methoxy- α -Trifluoromethylphenylacetate (MTPA) Esters. *J. Am. Chem. Soc.* **1973**, *95*, 512–519. (c) Ohtani, I.; Kusumi, T.; Kashman, Y.; Kakisawa, H. High-Field FT NMR Application of Mosher's Method. The Absolute Configurations of Marine Terpenoids. *J. Am. Chem. Soc.* **1991**, *113*, 4092–4096. (d) Hoye, T. R.; Jeffrey, C. S.; Shao, F. Mosher Ester Analysis for the Determination of Absolute Configuration of Stereogenic (Chiral) Carbinol Carbons. *Nat. Protoc.* **2007**, *2*, 2451–2458.

⁷ For a review, see: (a) Wenzel, T. J.; Wilcox, J. D. Chiral Reagents for the Determination of Enantiomeric Excess and Absolute Configuration Using NMR Spectroscopy. *Chirality* **2003**, *15*, 256–270. For selected examples, see: (b) Kobayashi, Y.; Hayashi, N.; Kishi, Y. Toward the Creation of NMR Databases in Chiral Solvents: Bidentate Chiral NMR Solvents for Assignment of the Absolute Configuration of Acyclic Secondary Alcohols. *Org. Lett.* **2002**, *4*, 411–414. (c) Kobayashi, Y.; Hayashi, N.; Kishi, Y. Application of Chiral Bidentate NMR Solvents for Assignment of the Absolute Configuration of Alcohols: Scope and Limitation. *Tetrahedron Lett.* **2003**, *44*, 7489–7491. (d) Ghosh, I.; Zeng, H.; Kishi, Y. Application of Chiral Lanthanide Shift Regents for Assignment of Absolute Configuration of Alcohols. *Org. Lett.* **2004**, *6*, 4715–4718. (e) Ghosh, I.; Kishi, Y.; Tomoda, H.; Omura, S. Use of a Chiral Praseodymium Shift Reagent in Predicting the Complete Stereostructure of Glisoprenin A. *Org. Lett.* **2004**, *6*, 4719–4722. (f) Bian, G.; Fan, H.; Huang, H.; Yang, S.; Zong, H.; Song, L.; Yang, G. Highly Effective Configurational Assignment Using Bisthioureas as Chiral Solvating Agents in the Presence of DABCO. *Org. Lett.* **2015**, *17*, 1369–1372. (g) Seo, M.-S.; Kim, H. ¹H NMR Chiral Analysis of Charged Molecules via Ion Pairing with Aluminum Complexes. *J. Am. Chem. Soc.* **2015**, *137*, 14190–14195.

⁸ (a) Stephens, P. J.; Devlin, F. J.; Cheeseman, J. R.; Frisch, M. J.; Rosini, C. Determination of Absolute Configuration Using Optical Rotation Calculated Using Density Functional Theory. *Org. Lett.* **2002**, *4*, 4595–4598. (b) Lattanzi, A.; Scettri, A.; Zanasi, R.; Devlin, F. J.; Stephens, P. J. Absolute Configuration Assignment of Norcamphor-Derived Furyl Hydroperoxide Using Density Functional Theory Calculations of Optical Rotation and Vibrational Circular

Dichroism. *J. Org. Chem.* **2010**, *75*, 2179–2188. (c) Stephens, P. J.; Pan, J. J.; Devlin, F. J.; Krohn, K.; Kurtán, T. Determination of the Absolute Configurations of Natural Products via Density Functional Theory Calculations of Vibrational Circular Dichroism, Electronic Circular Dichroism, and Optical Rotation: The Iridoids Plumericin and Isoplumericin. *J. Org. Chem.* **2007**, *72*, 3521–3536.

⁹ For a review on the electronic circular dichroism exciton chirality method, see: (a) Harada, N.; Nakanishi, K.; Berova, N. In *Comprehensive Chiroptical Spectroscopy, Vol. 2: Applications in Stereochemical Analysis of Synthetic Compounds, Natural Products, and Biomolecules*, 1st ed.; Berova, N.; Polavarapu, P. L.; Nakanishi, K.; Woody, R. W., Eds.; John Wiley & Sons, Inc.: Hoboken, NJ, 2012; pp 115–166. For additional selected publications, see: (b) Harada, N.; Nakanishi, K. Exciton Chirality Method and Its Application to Configurational and Conformational Studies of Natural Products. *Acc. Chem. Res.* **1972**, *5*, 257–263. (c) Gargiulo, D.; Cai, G.; Ikemoto, N.; Bozhkova, N.; Odingo, J.; Berova, N.; Nakanishi, K. CD Exciton Chirality Method: New Chromophores for Primary Amino Groups. *Angew. Chem. Int. Ed.* **1993**, *32*, 888–891. (d) Zhou, P.; Zhao, N.; Rele, D. N.; Berova, N.; Nakanishi, K. A Chiroptical/Chemical Strategy for Configurational Assignments of Acyclic 1,3-Skipped Polyols: Model 1,2,4,6-Tetrols. *J. Am. Chem. Soc.* **1993**, *115*, 9313–9314. (e) Mori, Y.; Sawada, T.; Sasaki, N.; Furukawa, H. A Simple Strategy for Determining the Absolute Configurations of Acyclic 1,2,4,6,8-Pentols. *J. Am. Chem. Soc.* **1996**, *118*, 1651–1656.

¹⁰ (a) Huang, X.; Fujioka, N.; Pescitelli, G.; Koehn, F. E.; Williamson, R. T.; Nakanishi, K.; Berova, N. Absolute Configurational Assignments of Secondary Amines by CD-Sensitive Dimeric Zinc Porphyrin Host. *J. Am. Chem. Soc.* **2002**, *124*, 10320–10335. (b) Li, X.; Tanasova, M.; Vasileiou, C.; Borhan, B. Fluorinated Porphyrin Tweezer: A Powerful Reporter of Absolute Configuration for Erythro and Threo Diols, Amino Alcohols, and Diamines. *J. Am. Chem. Soc.* **2008**, *130*, 1885–1893. (c) Li, X.; Borhan, B. Prompt Determination of Absolute Configuration for Epoxy Alcohols via Exciton Chirality Protocol. *J. Am. Chem. Soc.* **2008**, *130*, 16126–16127. (d) You, L.; Pescitelli, G.; Anslyn, E. V.; Di Bari, L. An Exciton-Coupled Circular Dichroism Protocol for the Determination of Identity, Chirality, and Enantiomeric Excess of Chiral Secondary Alcohols. *J. Am. Chem. Soc.* **2012**, *134*, 7117–7125. (e) Zhang, J.; Gholami, H.; Ding, X.; Chun, M.; Vasileiou, C.; Nehira, T.; Borhan, B. Computationally Aided Absolute Stereochemical Determination of Enantioenriched Amines. *Org. Lett.* **2017**, *19*, 1362–1365. (f) Takeda, S.; Hayashi, S.; Noji, M.; Takanami, T. Chiroptical Protocol for the Absolute Configurational Assignment of Alkyl-Substituted Epoxides Using Bis(Zinc Porphyrin) as a CD-Sensitive Bidentate Host. *J. Org. Chem.* **2019**, *84*, 645–652.

- ¹¹ (a) Pescitelli, G.; Bruhn, T. Good Computational Practice in the Assignment of Absolute Configurations by TDDFT Calculations of ECD Spectra. *Chirality* **2016**, *28*, 466–474. (b) Merten, C.; Golub, T. P.; Kreienborg, N. M. Absolute Configurations of Synthetic Molecular Scaffolds from Vibrational CD Spectroscopy. *J. Org. Chem.* **2019**, *84*, 8797–8814.
- ¹² Burns, A. S.; Rychnovsky, S. D. Total Synthesis and Structure Revision of (–)-Illisimonin A, a Neuroprotective Sesquiterpenoid from the Fruits of *Illicium Simonsii*. *J. Am. Chem. Soc.* **2019**, *141*, 13295–13300.
- ¹³ Ma, S.-G.; Li, M.; Lin, M.-B.; Li, L.; Liu, Y.-B.; Qu, J.; Li, Y.; Wang, X.-J.; Wang, R.-B.; Xu, S.; Hou, Q.; Yu, S.-S. Illisimonin A, a Caged Sesquiterpenoid with a Tricyclo[5.2.1.0^{1,6}]Decane Skeleton from the Fruits of *Illicium Simonsii*. *Org. Lett.* **2017**, *19*, 6160–6163.
- ¹⁴ (a) Flack, H. D. On Enantiomorph-Polarity Estimation. *Acta Crystallogr., Sect. A: Found. Crystallogr.* **1983**, *39*, 876–881. (b) Flack, H. D.; Bernardinelli, G. The Use of X-Ray Crystallography to Determine Absolute Configuration. *Chirality* **2008**, *20*, 681–690.
- ¹⁵ (a) Hooft, R. W. W.; Straver, L. H.; Spek, A. L. Determination of Absolute Structure Using Bayesian Statistics on Bijvoet Differences. *J. Appl. Crystallogr.* **2008**, *41*, 96–103. (b) Parsons, S.; Wagner, T.; Presly, O.; Wood, P. A.; Cooper, R. I. Applications of Leverage Analysis in Structure Refinement. *J. Appl. Crystallogr.* **2012**, *45*, 417–429.
- ¹⁶ (a) Holstein, P. M.; Holstein, J. J.; Escudero-Adan, E. C.; Baudoin, O.; Echavarren, A. M. Ferrocene Derivatives of Liquid Chiral Molecules Allow Assignment of Absolute Configuration by X-Ray Crystallography. *Tetrahedron: Asymmetry* **2017**, *28*, 1321–1329. (b) Shibata, T.; Arai, Y.; Takami, K.; Tsuchikama, K.; Fujimoto, T.; Takebayashi, S.; Takagi, K. Iridium-Catalyzed Enantioselective [2 + 2+2] Cycloaddition of Dienes and Monoalkynes for the Generation of Axial Chiralities. *Adv. Synth. Catal.* **2006**, *348*, 2475–2483.
- ¹⁷ Brummel, B. R.; Lee, K. G.; McMillen, C. D.; Kolis, J. W.; Whitehead, D. C. One-Pot Absolute Stereochemical Identification of Alcohols via Guanidinium Sulfate Crystallization. *Org. Lett.* **2019**, *21*, 9622–9627.
- ¹⁸ Burns, A. S.; Dooley, C.; Carlson, P. R.; Ziller, J. W.; Rychnovsky, S. D. Relative and Absolute Structure Assignments of Alkenes Using Crystalline Osmate Derivatives for X-Ray Analysis. *Org. Lett.* **2019**, *21*, 10125–10129.

¹⁹ (a) Horeau, A. Determination of the Configuration of Secondary Alcohols by Partial Resolution. In *Stereochemistry: Fundamentals and Methods*; Fiaud, J., Horeau, A., Kagan, H. B., Eds.; Thieme, Stuttgart, Germany, 1977; Vol. 3; pp 51–94. (b) Horeau, A. Principe et Applications d'une Nouvelle Methode de Determination Des Configurations Dite "Par Dedoublement Partiel." *Tetrahedron Lett.* **1961**, *2*, 506–512. (c) Horeau, A. Determination des configurations par "dedoublement partiel" - II precisions et complements. *Tetrahedron Lett.* **1962**, *3*, 965–969. (d) Horeau, A.; Kagan, H. B. Determination des configurations par "dedoublement partiel"—III: Alcools steroides. *Tetrahedron* **1964**, *20*, 2431–2441. (e) Weidmann, R.; Horeau, A. Determination des configurations d'alcools secondaires par "dedoublement partiel" IX (1). - Semimicromethode non polarimetrique. *Tetrahedron Lett.* **1973**, *14*, 2979–2982. (f) Schoofs, A.; Horeau, A. Nouvelle methode generale de determination de la purete enantiomerique et de la configuration absolue des alcools secondaires chiraux. *Tetrahedron Lett.* **1977**, *18*, 3259–3262. (g) Horeau, A.; Nouaille, A. Micromethode de Determination de La Configuration Des Alcools Secondaires Par Dedoublement Cinetique. Emploi de La Spectrographie de Masse. *Tetrahedron Lett.* **1990**, *31*, 2707–2710. (h) König, W. A.; Gehrcke, B.; Weseloh, G. Determination of the Absolute Configuration of Secondary Alcohols with Horeau's Method Including Enantioselective Gas Chromatography. *Chirality* **1994**, *6*, 141–147.

²⁰ (a) Birman, V. B.; Li, X. Homobenzotetramisole: An Effective Catalyst for Kinetic Resolution of Aryl-Cycloalkanols. *Org. Lett.* **2008**, *10*, 1115–1118. (b) Zhang, Y.; Birman, V. B. Effects of Methyl Substituents on the Activity and Enantioselectivity of Homobenzotetramisole-Based Catalysts in the Kinetic Resolution of Alcohols. *Adv. Synth. Catal.* **2009**, *351*, 2525–2529.

²¹ (a) Wagner, A. J.; David, J. G.; Rychnovsky, S. D. Determination of Absolute Configuration Using Kinetic Resolution Catalysts. *Org. Lett.* **2011**, *13*, 4470–4473. (b) Wagner, A. J.; Rychnovsky, S. D. Determination of Absolute Configuration of Secondary Alcohols Using Thin-Layer Chromatography. *J. Org. Chem.* **2013**, *78*, 4594–4598. (c) Wagner, A. J.; Miller, S. M.; King, R. P.; Rychnovsky, S. D. Nanomole-Scale Assignment and One-Use Kits for Determining the Absolute Configuration of Secondary Alcohols. *J. Org. Chem.* **2016**, *81*, 6253–6265. (d) Brito, G. A.; Della-Felice, F.; Luo, G.; Burns, A. S.; Pilli, R. A.; Rychnovsky, S. D.; Krische, M. J. Catalytic Enantioselective Allylations of Acetylenic Aldehydes via 2-Propanol-Mediated Reductive Coupling. *Org. Lett.* **2018**, *20*, 4144–4147. (e) Burns, A. S.; Ross, C. C.; Rychnovsky, S. D. Heteroatom-Directed Acylation of Secondary Alcohols To Assign Absolute Configuration. *J. Org. Chem.* **2018**, *83*, 2504–2515.

²² Burns, A. S.; Wagner, A. J.; Fulton, J. L.; Young, K.; Zakarian, A.; Rychnovsky, Scott. D. Determination of the Absolute Configuration of β -Chiral Primary Alcohols Using the Competing Enantioselective Conversion Method. *Org. Lett.* **2017**, *19*, 2953–2956.

²³ Perry, M. A.; Trinidad, J. V.; Rychnovsky, S. D. Absolute Configuration of Lactams and Oxazolidinones Using Kinetic Resolution Catalysts. *Org. Lett.* **2013**, *15*, 472–475.

²⁴ Miller, S. M.; Samame, R. A.; Rychnovsky, S. D. Nanomole-Scale Assignment of Configuration for Primary Amines Using a Kinetic Resolution Strategy. *J. Am. Chem. Soc.* **2012**, *134*, 20318–20321.

Chapter 2. Efforts Toward the Determination of Absolute Configuration of 1,3-Dienes Bearing Adjacent Stereocenters Using Chiral 1,2,4-Triazoline-3,5-Diones

2.1 Abstract

Efforts towards developing a Competing Enantioselective Conversion (CEC) method to determine the absolute configuration of dienes bearing adjacent stereocenters are described herein. Chiral analogues of 1,2,4-triazoline-3,5-diones (TAD) were synthesized and used as dienophiles in enantioselective Diels–Alder reactions with dienes bearing adjacent chirality. Kinetic resolution with these new reagents displayed moderate selectivity, but the prohibitive synthesis of the reagents rendered efforts to develop a CEC method fruitless.

2.2 Introduction

The determination of absolute configuration, even with the advent of new technologies and methodologies, is often challenging.¹ Chapter 1 outlined a general introduction to the topic of stereochemical assignment, including the competing enantioselective conversion (CEC) method which was pioneered in our group. Previously, our group had devised CEC methods to assign the configuration of secondary alcohols,² β -chiral primary alcohols,³ oxazolidinones and lactams,⁴ primary amines,⁵ and cyclic secondary amines.⁶ Our lab's continued interest in developing simple methods to assign absolute configuration motivated us to expand the scope of the CEC method to different functional groups (see chapter 1.4 for more details). We were interested in developing a CEC method to assign the stereochemistry of chiral centers adjacent to dienes and alkenes by using enantioselective Diels–Alder and ene reactions respectively.

Dienes and alkenes are common functionalities in natural products and are often intermediates in terpene and steroid total syntheses. Among natural products, the controversial stereochemical assignment of (+)-frondosin B is an excellent example of the potential utility of this method.⁷ This natural product was first synthesized by the Danishefsky lab in 2001 and its optical rotation matched that of the isolated natural product. However, a year later the Trauner group targeted the same enantiomer but found that the optical rotation had the opposite sign (Figure 2-1). This discrepancy between the optical rotations inspired three subsequent total syntheses and a study using ECD and VCD to assign the absolute configuration with certainty.¹⁰ This prominent example, as well as the ubiquity of dienes as synthetic intermediates, inspired our studies towards new methods of assigning the absolute configuration of dienes bearing neighboring chiral centers.

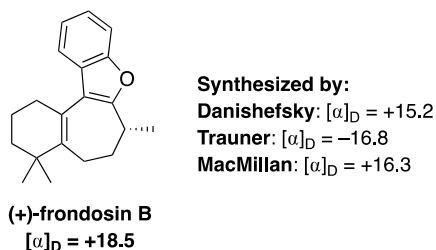


Figure 2-1 Summary of the ambiguity surrounding frondosin B.

There has been significant progress in the field of enantioselective Diels–Alder chemistry in the past 50 years.⁸ Many such examples use chiral Lewis acids to dictate the enantioselectivity of the reaction, or utilize chiral organocatalysts to turn the dienophile into a transient chiral directing group.⁹ While the literature is teeming with different enantioselective variants of the Diels–Alder reaction, several key factors are necessary for its application in CEC reactions. These factors include excellent diastereo- and enantiocontrol dictated by the chiral resolving agent, and, ideally, fast and uniform reaction kinetics. The problem with applying the CEC method towards many catalytic, enantioselective Diels–Alders is that the chiral catalysts complicate the kinetics, making it harder to have controlled reactivity across substrate classes. As such, we sought a stoichiometric chiral dienophile which would have suitable attributes. This attracted us to the potential of 1,2,4-triazoline-3,5-dione (TAD) reagents.

Triazolinediones were first reported in 1894 by Thiele and Stange,¹⁰ but an effective synthesis was not published until 1960 when Cookson first synthesized and isolated 4-phenyl-1,2,4-triazoline-3,5-dione (PTAD, **2-1**, Figure 2-2).¹¹ Triazolinediones are known for their characteristic red color and have been shown to react 1,000-30,000 times faster than azodicarboxylates in Diels–Alder cycloadditions.¹² Computational studies on triazolinediones have concluded that they react *via* concerted-asynchronous transition states and are highly endo-selective.¹³ Several representative Diels–Alder reactions with **2-1** are shown in Figure 2-1. In cyclic systems, such as siloxy diene **2-2**, the reaction with **2-1** forms bridged bicycle **2-3** as a single

diastereomer in 76% yield.¹⁴ The diastereocontrol is often good in semi-cyclic dienes as well, as shown by the reaction with diene **2-4**.¹⁵ Additionally, the reaction with **2-1** has been used on an industrial scale as a method of purifying sterol extracts.^{6c} These reactions typically take place immediately at ambient temperature but are often instantaneous even at low temperature. Due to their high reactivity and general diastereoselectivity, we envisioned synthesizing chiral triazolinediones in hopes of conferring enantioselectivity in Diels–Alder and ene reactions.

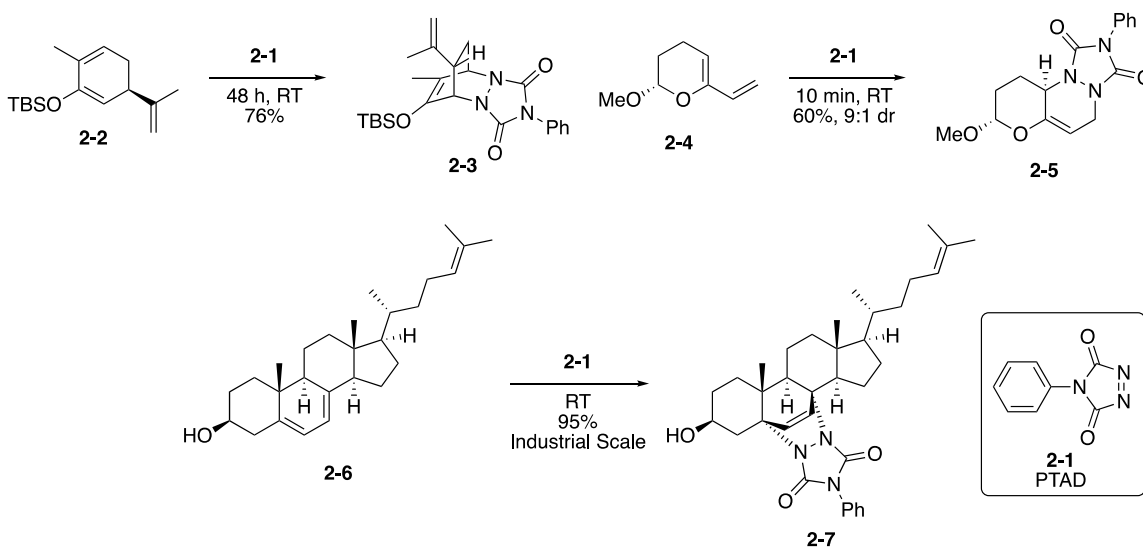


Figure 2-2 Representative Diels–Alder reactions with PTAD (**2-1**).

Kinetic resolutions of dienes bearing adjacent chirality are sparse, but a few key examples exist. The reactivity of quinones in Diels–Alder chemistry is well preceded, and the use of 2-(*p*-tolylsulfonyl)-1,4-benzoquinones and naphthoquinones in asymmetric Diels–Alder chemistry is well documented (Figure 2-3A).¹⁶ Sulfonyl naphthoquinone **2-8** has previously been used to resolve racemic diene **2-9** with a selectivity of 57.1 at 38% conversion (calculated from data presented in their work).^{15e} This astounding selectivity is only hindered by reaction kinetics, taking 3 days to reach 38% conversion. For application in a CEC reaction, this system would need to be rendered more reactive. Paquette and coworkers also disclosed a similar study on kinetic resolutions of racemic dienes **2-11** using chiral scaffolds of triazolinediones (Figure 2-3B).

Paquette evaluated kinetic resolutions with chiral TAD reagents derived from (*S*)-(-)- α -methylbenzylamine (**2-14**), (+)-dehydroabietylamine (**2-15**), and (+)-endobornylamine (**2-16**), but his systems displayed only modest selectivity.¹⁷

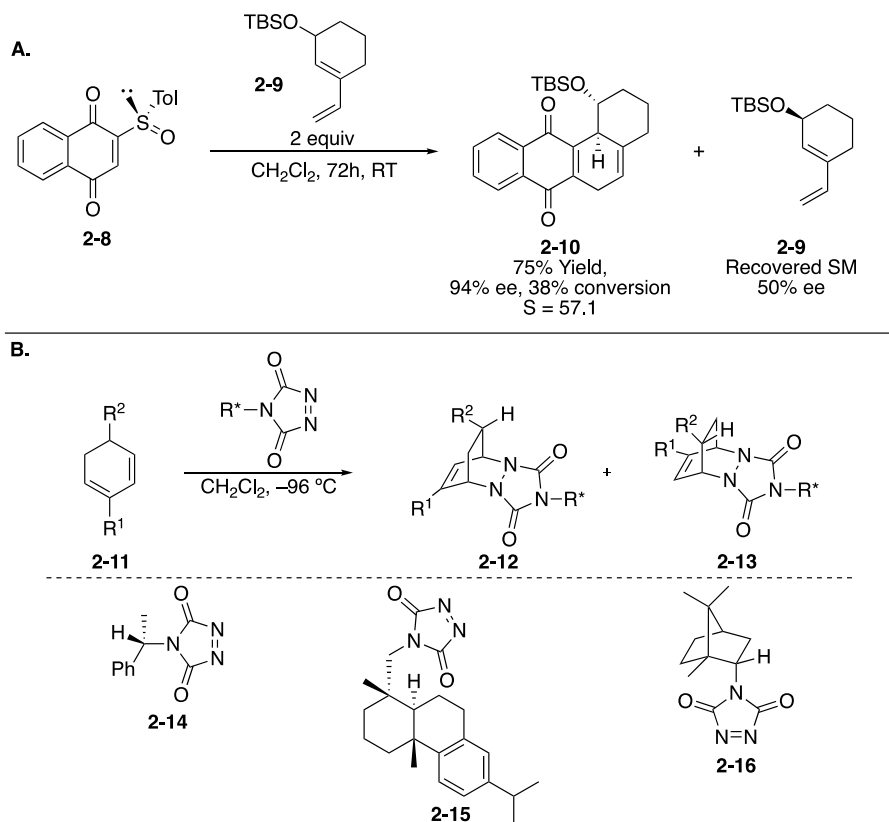


Figure 2-3A. Kinetic resolution of a racemic diene using Sulfinyl naphthoquinone **2-8**. **B.** Kinetic resolution of racemic diene using chiral triazolinediones.

Despite the lack of precedent for chiral triazolinediones, we chose to further evaluate these reagents for asymmetric Diels–Alder reactions because of their high reactivity and their tendency to proceed through highly ordered transition states. Additionally, having one reagent that can resolve stereocenters next to both dienes and alkenes was a very attractive facet of this class of molecules. We hypothesized that by changing the chiral environment of the reagent, we could achieve higher enantioselection than what has been observed in the literature for this class of compounds. Binaphthyl atropisomers are known to convey excellent enantioselectivity in an array

of organometallic transformations,¹⁸ and we sought to develop a TAD reagent with this scaffold (**2-17**). In addition, inspired by recent work by the Ishihara group using chiral iodonium salts to enable enantioselective oxidative dearomatizations (**2-19**, Figure 2-4),¹⁹ we desired to make a triazolinedione with a similar structure (**2-18**). The enantioselectivity of this chemistry is known to be driven by hydrogen-bonding interactions between the acetate ligands and the amide arms,²⁰ and we believed that a triazolinedione could exhibit a similar conformation. In order to examine the utility of these novel reagents in enantioselective Diels–Alder reactions, we needed to develop routes to synthesize them.

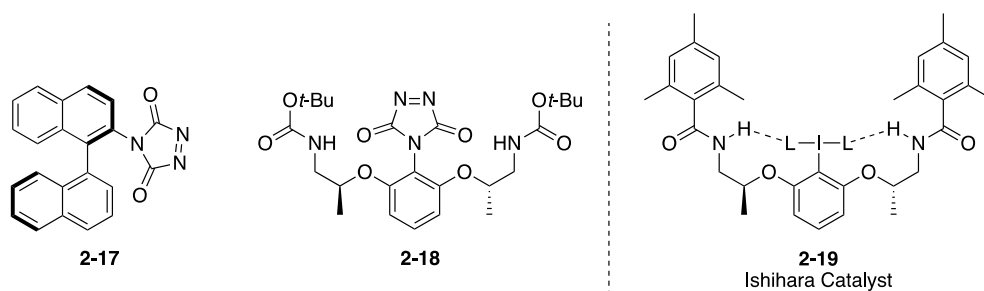


Figure 2-4 Novel triazolinediones reagents targeted for application in CEC reactions.

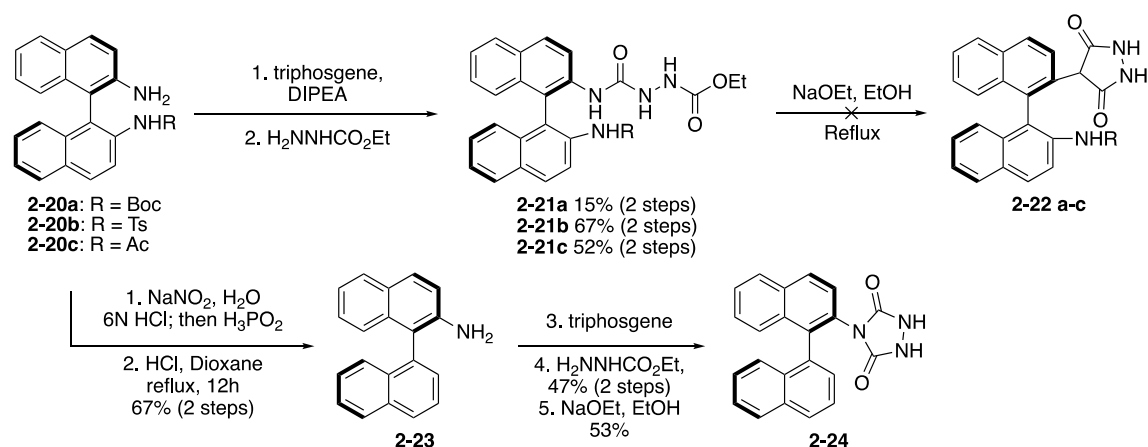
2.3 Synthesis of Triazolinediones

Having devised chiral triazolinediones **2-17** and **2-18** (Figure 2-4), we needed to synthesize these compounds to evaluate their utility. To synthesize **2-17**, we initially attempted to utilize the Cookson method on mono-protected (*R*)-1,1'-bi(2-naphthylamine) ((*R*)-BINAM) derivatives (Scheme 2-1).¹⁰ Protected amines **2-20a-c** were treated with triphosgene to form intermediate isocyanates, which were then treated with ethyl carbazate to form the desired semicarbazides **2-21a-c**. Unfortunately, cyclization of intermediate **2-21a** with sodium ethoxide in refluxing ethanol led to decomposition of the starting material. We initially speculated that the steric bulk of the carbamate protecting group was inhibiting the reaction; however, compounds **2-21b** and **c** also

decomposed under the reaction conditions. It has been noted that urazole synthesis is sensitive to certain functionalities,²¹ and it seemed that the protected amines were causing side reactivity.

Knowing that the second amine was problematic, we elected to remove the additional amine with a Sandmeyer reaction. Treatment of **2-20c** with sodium nitrite under acidic conditions followed by the addition of hypophosphorous acid induced reductive deamination. Removal of the acetamide with hydrochloric acid in dioxane at reflux delivered **2-23** in 67% yield over two steps.²² Unfortunately, it was not discovered until later that the material had partially racemized during the hydrolysis (measured rotation +4.5, reported +91).²³ This intermediate was subsequently reacted with triphosgene, followed by ethyl carbazate to afford the desired semicarbazide in 47% over two steps. Cyclization of this material with refluxing sodium ethoxide provided urazole **2-24** in 53% yield. Triazolinedione **2-17** could be prepared by oxidation of the urazole, however due to the high reactivity and preceded instability of these reagents, we elected to only oxidize the material immediately before use in a Diels–Alder reaction.

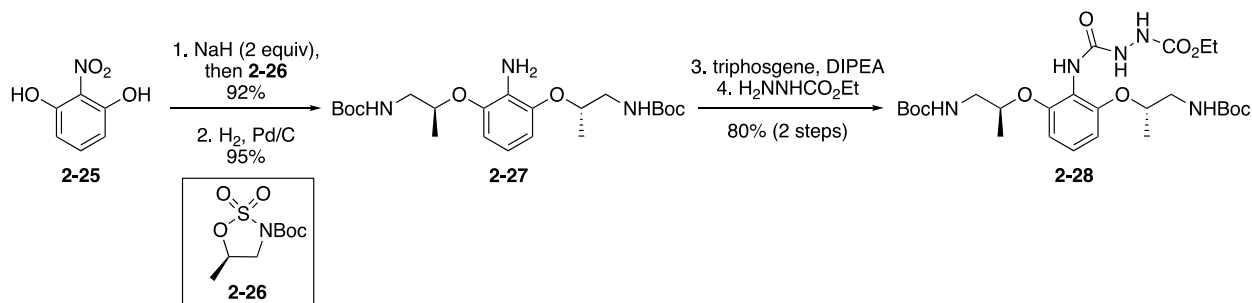
Scheme 2-1 Synthesis of **2-17**.



With access to **2-17**, we shifted our efforts toward synthesizing **2-18** (Scheme 2-2). Taking inspiration from Ishihara's work, we elected to modify their procedures to pursue an amino-derivative. Treatment of nitroresorcinol (**2-25**) with 2 equivalents of sodium hydride, followed by

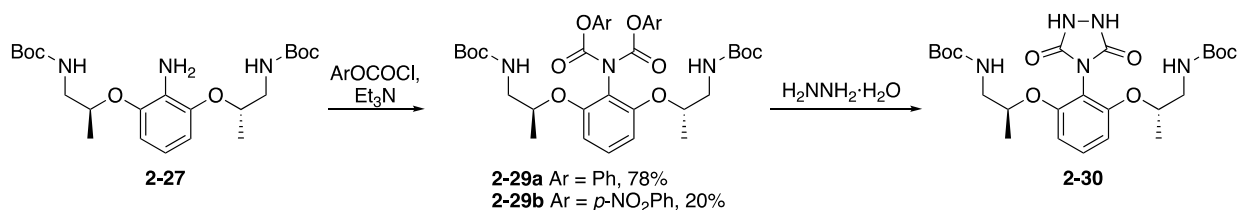
the addition of cyclic sulfamidate **2-26** cleanly afforded a double S_N2 product in 92% isolated yield. Hydrogenation of the nitro group unveiled amine **2-27** in good yield. With this amine, we attempted the Cookson urazole synthesis. Isocyanation enacted by triphosgene, followed by treatment with ethyl carbazate yielded semicarbazide **2-28**. However similar to compounds **2-22a-c** this material decomposed upon treatment with sodium ethoxide. This is likely due once again to problematic reactivity of the carbamates. Unfortunately, in this system the carbamates could not be removed since they are hypothesized to confer enantioselectivity to the system. As such, an alternative route was pursued.

Scheme 2-2 Failed approach toward **2-18**.



There is precedent showing that urazoles can be synthesized by the addition of hydrazine to imidodicarbonates, albeit in lower yields than the Cookson method.²⁴ With this precedent in mind, we synthesized phenyl- and *p*-nitrophenyl imidodicarbonates **2-29a** and **2-29b** through treatment of **2-27** with the respective aryl chloroformate (Scheme 2-3). It is worth mentioning that the major side product formed when **2-27** was treated with *p*-nitrophenyl chloroformate was the isocyanate, likely due to the enhanced leaving group ability of the carbamate. Treatment of **2-29a** with hydrazine led to **2-30**, but the product was contaminated with unreacted starting material. Treatment of **2-29b** with hydrazine led to **2-30**, which was also unfortunately contaminated, albeit with unidentified impurities. We elected to use this impure material in the Diels–Alder to examine selectivity.

Scheme 2-3 Successful synthesis of 2-30.



2.4 Analysis of Diels–Alder Diastereoselectivity

With access to urazoles **2-24** and **2-30**, we were excited to examine the potential diastereoselectivity these reagents would confer on Diels–Alder reactions. To determine the selectivity of our TAD reagent, we needed to synthesize suitable racemic and enantiopure dienes. We looked to the chiral pool, and synthesized alkenyl triflate **2-33** from (*R*)-carvone in one step.²⁵ A racemic vinyl triflate (**2-35**) was also prepared to perform kinetic resolution reactions. In order to have a quick and reliable means of determining the enantioenrichment of recovered starting material, we next attempted to find conditions to separate the enantiomers of **2-35** via HPLC separation on a chiral stationary phase. Unfortunately, after examining every column in the department, as well as the chiral GC system in the Pronin lab, we were unable to find suitable separation conditions. As such, we decided to determine selectivity and conversion through NMR analysis. According to the equations for selectivity in kinetic resolutions, the diastereomeric ratio from the NMR can be used to determine the selectivity of the system in the following way (equation 1, see supporting information for more details).

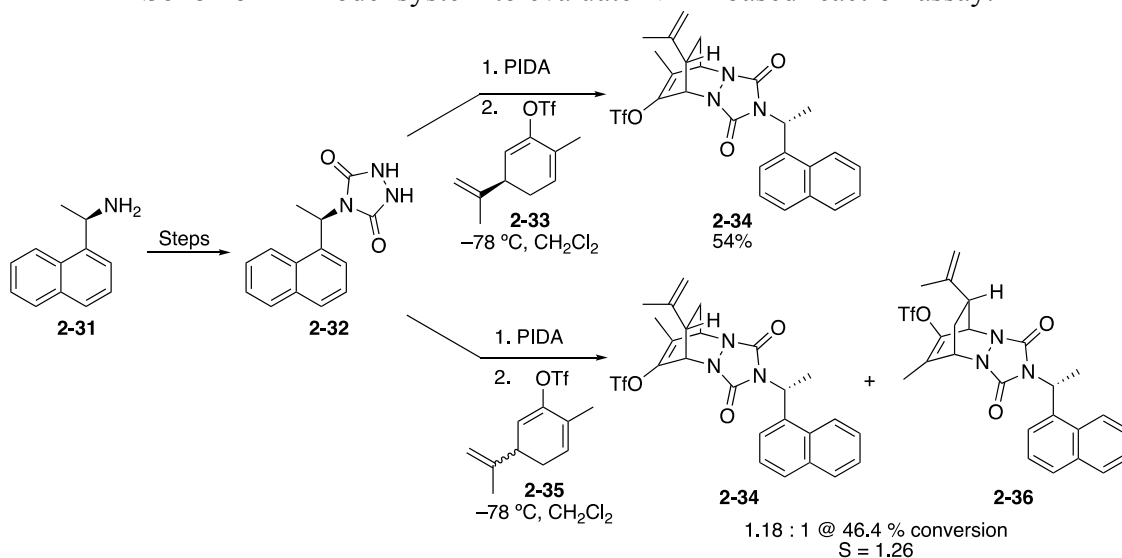
$$\text{Selectivity} = \frac{\text{Log}[1 - \text{conversion} (1 + de)]}{\text{Log}[1 - \text{conversion} (1 - de)]}$$

Equation 2-1 Selectivity equation based on diastereomeric excess.

To familiarize ourselves with this NMR based method of analysis, we synthesized a simple chiral TAD reagent to use as a model system. We chose to use α -(naphthyl)ethylamine **2-31** as our starting material (Scheme 2-4), following Paquette's success with **2-14**.¹⁷ The synthesis was

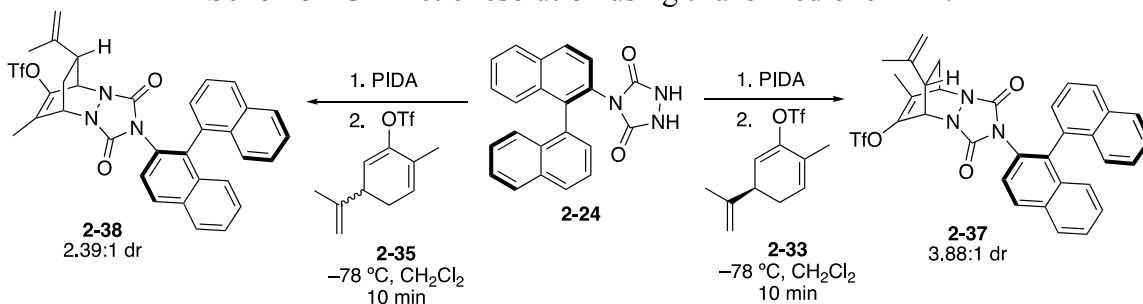
carried out uneventfully using the Cookson method (see SI for details). Triazolinediones are known to be highly sensitive to alcohols and water,²⁰ and as such we were concerned about the long-term stability of our reagents. As discussed earlier, rather than isolate our TAD reagents, we chose to perform Diels–Alder reactions with freshly oxidized urazoles. Treatment of **2-32** with (diacetoxyiodo)benzene (PIDA) in dichloromethane generated a bright red solution of the desired triazolinediones.²⁶ This solution was then immediately added dropwise to a solution of one equivalent of **2-33** at $-78\text{ }^{\circ}\text{C}$. The characteristic red color of the reagent faded almost immediately, and the reaction mixture was warmed to room temperature and was evaporated to dryness to afford **2-34**. NMR analysis of the crude reaction mixture, and subsequent 2D NMR analysis of the purified adduct revealed that the Diels–Alder proceeded with excellent diastereoselectivity. Kinetic resolution of this triazolinedione was carried out by treatment of the triazolinediones with 2 equivalents of **2-35**, which afforded a 1.18:1 ratio of diastereomeric products **2-34** and **2-36** respectively at 46.4% conversion, correlating to a selectivity of 1.26. This selectivity correlated well with the kinetic resolutions performed by Paquette.¹⁶

Scheme 2-4 Model system to evaluate NMR-based reaction assay.



Having established the utility of an NMR-based assay for the kinetic resolution in the model system, we were ready to evaluate our new chiral reagents. We first looked at the reaction with **2-17**. Since urazole **2-24** was racemized during its the synthesis (~5% ee), the reaction with enantiopure diene **2-33** can be viewed as a kinetic resolution. When urazole **2-24** was oxidized to triazolinedione **2-17**, followed by addition to **2-33**, compound **2-37** was observed as a 3.88:1 mixture of diastereomers. Given the high diastereoselectivity observed in the formation of **2-34** (Scheme 2-4), the mixture of diastereomers in **2-37** must be a partial resolution of the biaryl axis. Viewed from this standpoint, the resolution observed was quite exciting. Reaction of the same triazolinediones with **2-35** generated a 2.4:1 mixture of diastereomers favoring **2-38**. It was shown by Heathcock that racemic substrates and racemic resolving agents can undergo mutual kinetic resolution, wherein enantiomeric excess of recovered substrate and resolving agent increase as the reaction proceeds.²⁷ In such a reaction, the selectivity is equal to the diastereomeric ratio, allowing us to tentatively estimate the selectivity to be approximately 2.4 for this reagent. This result is the highest enantioselectivity ever reported with a chiral triazolinedione.¹⁷

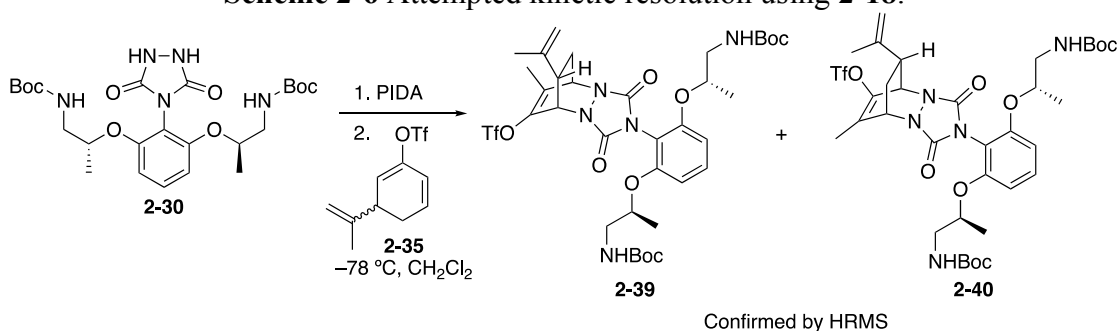
Scheme 2-5 Kinetic resolution using triazolinedione **2-17**.



We next evaluated the potential selectivity of **2-18**. Given the impurities in **2-30**, we elected to simply pursue the kinetic resolution to see if any useful data could be obtained. Oxidation of **2-30** with PIDA, followed by addition of this solution to a cold solution of racemic diene **2-35** led to a mixture of diastereomeric adducts **2-39** and **2-40**. The identity of these compounds were

confirmed by high resolution mass spectrometry (HRMS); however, the relevant region of the crude proton NMR was obscured, and it was challenging to ascertain a reliable dr from the reaction. At this point in my graduate career, I began working on several other projects in the lab, and this work was unfortunately never revisited.

Scheme 2-6 Attempted kinetic resolution using **2-18**.



2.5 Conclusion and Future Outlook

This work lays the groundwork for a potential new CEC method for determining the absolute configuration of dienes bearing adjacent chirality. Two novel triazolinedione reagents **2-17** and **2-18** were synthesized and evaluated in Diels–Alder reactions. An NMR-based assay of the selectivity of kinetic resolutions of racemic diene **2-35** with these reagents was established. While no selectivity could be determined for **2-18**, BINAM-derived **2-17** showed modest enantioselectivity in Diels–Alder reactions. While the selectivity was modest, it was still approximately two-fold higher than any other chiral triazolinedione reported in the literature.

Several other assays could be used to improve the ease of operation and utility of this method. Ideally, a thorough search of the literature may reveal a diene with vicinal chirality that will separate by either HPLC or GC, allowing us to determine enantiomeric excess and conversion directly from the crude reaction mixture. Selectivity can be determined based on optical rotation, but this forces the kinetic resolutions to be run on sufficient scale to re-isolate enantioenriched starting material without any impurity. Iodobenzene is a byproduct in the oxidation/Diels–Alder

reaction, and it is challenging to separate from the greasy dienes used, which can pose problems for polarimetry, especially since optical rotation is notoriously sensitive to impurities. Other ideas include exploring LC-MS analysis of the Diels–Alder adducts. Since the products of the kinetic resolution are diastereomeric, LC-MS could be a useful means of determining conversion and selectivity.

In terms of the chemistry, there is much that can still be done with this project to potentially uncover a highly enantioselective reagent. The use of BINAM derived **2-17** was always meant to be a starting point for further evaluation. Hundreds of other derivatives can be imagined, where other functional groups are installed to potentially increase selectivity. However, these derivatives often come at the cost of step-count in their preparation. One extremely simple modification that can be made comes from the work done by Slaughter, in which the mono-triflate **2-41** was coupled with various Grignards to generate intermediate phenols (Figure 2-5A).²² These phenols were then activated and subjected to Buchwald–Hartwig coupling with benzylamine. By using this same strategy, we could access several derivatives from readily accessible BINOL, and potentially increase the enantioselectivity in the Diels–Alder reactions.

Many ligands based on a biaryl scaffold exhibit greater enantioselectivities from the addition of other aryl substituents around the ring system. Recently, the process group at Amgen disclosed a large-scale synthesis of (*S*)-TRIP, generating intermediate diol **2-44**.²⁸ This derivative can also be subjected to a similar sequence of reactions to access bulkier triazolinediones which might confer greater enantioselectivity to the system (Figure 2-5B).

Another interesting avenue which is unprecedented in the literature is the direct Buchwald–Hartwig coupling of protected urazoles with aryl triflates (Figure 2-5C). This direct coupling reaction would significantly shorten the synthesis of the triazolinediones. The bis-Boc urazole is

not known but could potentially arise from treatment of bis-Boc hydrazine with *p*-nitrophenyl chloroformate, and then heating the intermediate with ammonia. This reaction, if feasible, could provide a convenient means of synthesizing several triazolinediones, potentially leading to a suitable reagent for the desired CEC reaction. This project is filled with opportunity for creativity and novelty, and I hope that another student will revisit this work.

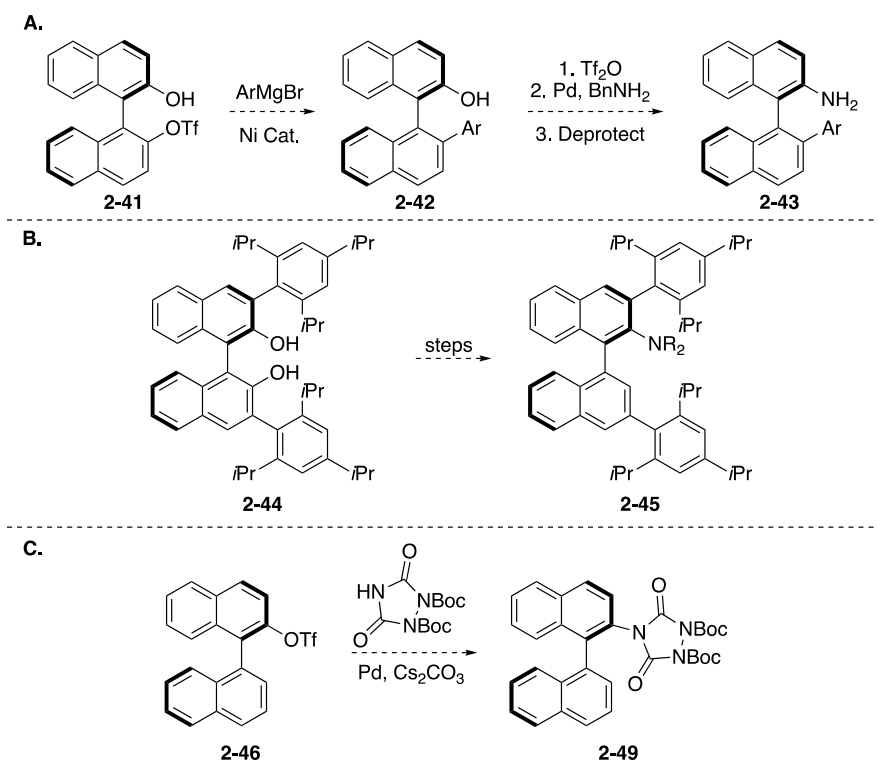


Figure 2-5 Potential new directions for biaryl-based triazolinediones.

2.6 Supporting Information

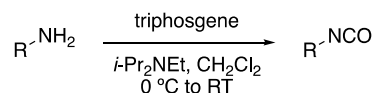
2.6.1 General Information

All chemicals were purchased from Sigma–Aldrich, Acros Organics, Alfa Aesar, TCI, Fisher Scientific, or CombiBlocks and used without further purification. Deuterated solvents were purchased from Cambridge Isotope Laboratories. Solvents were purchased as ACS grade or better and passed through a solvent purification system equipped with activated alumina columns prior

to use. All amine bases were distilled over calcium hydride and stored under argon. Unless otherwise stated, all reactions were performed in flame-dried glassware under an atmosphere of argon. Reactions were monitored by thin layer chromatography (TLC) using glass plates coated with a 250 μm layer of 60 \AA silica gel. TLC plates were visualized with a UV lamp at 254 nm, or by staining with potassium permanganate or cerium molybdate (Hanessian's stain). Column chromatography was performed using forced flow (flash chromatography) on silica gel (SiO_2) columns by standard techniques or with an automated purification system (Teledyne ISCO) on prepacked silica gel columns.

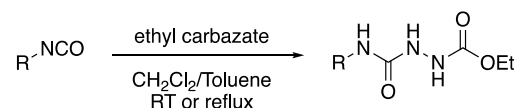
^1H NMR spectra were recorded at 500 MHz or 600 MHz using either a Bruker DRX500 (cryoprobe) or Bruker AVANCE600 (cryoprobe) at 298.0 K. ^{13}C NMR spectra were obtained at 125 MHz or 151 MHz on a Bruker DRX500 (cryoprobe) or Bruker AVANCE600 (cryoprobe) at 298.0 K unless otherwise stated. Chemical shifts (δ) are reported in parts per million (ppm) and referenced to the residual solvent peak. NMR data are reported as follows: chemical shift, multiplicity (s = singlet, d = doublet, t = triplet, q = quartet, m = multiplet, dd = doublet of doublet, ddd = doublet of doublet of doublets, dddd = doublet of doublet of doublet of doublets, dt = doublet of triplets, td = triplet of doublets, dq = doublet of quartets, br = broad, app. = apparent), coupling constants (J) in hertz (Hz), and integration. Infrared (IR) spectroscopy was performed on a Nicolet iS5 spectrometer using a diamond iD5 ATR attachment unless otherwise stated and are reported in terms of frequency of absorption (cm^{-1}). Optical rotations were performed on a JACSO P-1010 spectrometer using a glass 50 mm cell with a D-line at 589 nm. High resolution mass spectrometry (HRMS) was performed using ESI-TOF. Melting points were taken on an Electrothermal® melting point apparatus and are uncorrected.

2.6.2 General Procedure 1: Formation of isocyanates²⁹



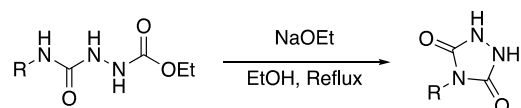
A round bottom flask was charged with triphosgene (0.5 equiv) and dichloromethane (0.05 M) and was cooled to 0 °C in an ice bath. A vent needle connected to a bubbler of saturated sodium bicarbonate was added to quench HCl generated in the reaction. A solution of amine or aniline (1 equiv) was added dropwise, followed by the addition of diisopropylethylamine (3 equiv). The reaction mixture was allowed to stir for 20 min at 0 °C, after which time the bubbler was removed, and the reaction was stirred for 2 hours at RT. The reaction was quenched by the addition of water and was extracted with CH₂Cl₂ (3x). The organic extracts were washed with 10% aq. citric acid, saturated aq. NaHCO₃, dried over Na₂SO₄, and concentrated *in vacuo*. Crude materials were either chromatographed by flash chromatography or taken crude to the next step.

2.6.3 General Procedure 2: Semicarbazide formation³⁰



Isocyanates were dissolved in either dichloromethane or toluene (0.1 M), and ethyl carbazate (1 equiv) was added in one portion. The reaction was allowed to stir either at RT or at reflux until the reaction was deemed finished by TLC. The reaction mixture was concentrated *in vacuo* and was purified by silica gel chromatography.

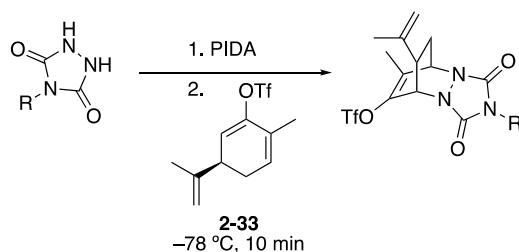
2.6.4 General Procedure 3: Cyclization of Semicarbazides²⁹



Sodium metal in mineral oil was cleaned with hexanes and cut into smaller pieces with a razor blade. The outer layer of oxides was scraped off to reveal the clean metal, which was cleaned of

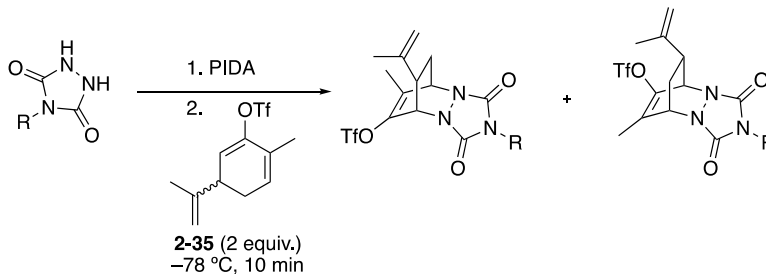
mineral oil with successive hexanes washes. The cleaned sodium metal (6 equiv) was added to a flame dried microwave tube containing absolute ethanol (0.2 M). The mixture was stirred at 35 °C to ensure full consumption of the sodium metal. Subsequently, the semicarbazide (1 equiv) was added as a solution in ethanol, and the reaction was heated to reflux. The reaction was acidified to pH 2 with aq. 2 M HCl and was then extracted with ethyl acetate. The organic extracts were washed with water, dried over Na₂SO₄, and concentrated *in vacuo*. Crude products were purified by silica gel chromatography.

2.6.5 General Procedure 4: Diels–Alder Protocol



To a suspension of urazole (1 equiv) in CH₂Cl₂ (0.1 M) was added (diacetoxyiodo)benzene (PIDA) (1 equiv). This solution was stirred at RT for 30 min, during which time the suspended urazole dissolved and the solution turned deep red in color. Simultaneously, a solution of **2-33** (1 equiv) in CH₂Cl₂ (0.2 M) was cooled to -78 °C. Once the oxidation solution had turned deep red, it was added dropwise to the diene. The solution was stirred at -78 °C for 15 min, during which time the red color faded completely. The solution was then warmed to RT and concentrated *in vacuo*. The crude material was purified by silica gel chromatography.

2.6.6 General Procedure 5: Kinetic Resolution Protocol



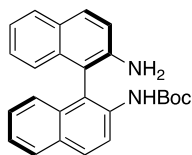
To a suspension of urazole (1 equiv) in CH_2Cl_2 (0.1 M) was added (diacetoxyiodo)benzene (PIDA) (1 equiv). This solution was stirred at RT for 30 min, during which time the suspended urazole dissolved and turned deep red in color. Simultaneously, a solution of **2-35** (2 equiv) in CH_2Cl_2 (0.2 M) was cooled to -78°C . Once the oxidation had turned deep red, the solution was added dropwise to the diene. The solution was stirred at -78°C for 15 min, during which time the red color faded completely. The solution was then warmed to RT and concentrated *in vacuo*. The conversion and selectivity of the chiral TAD reagent were determined based on crude NMR analysis as follows:

$$(1) \text{ Conversion} = \frac{\sum \text{Integration}_{\text{Diastereomers}}}{\text{Integration}_{\text{Diene}} + \sum \text{Integration}_{\text{Diastereomers}}}$$

$$(2) \text{ Diastereomeric excess (de)} = \frac{\text{Integration}_{\text{Diastereomer 1}}}{\sum \text{Integration}_{\text{Diastereomers}}} - \frac{\text{Integration}_{\text{Diastereomer 2}}}{\sum \text{Integration}_{\text{Diastereomers}}}$$

$$(3) \text{ Selectivity} = \frac{\text{Log}[1 - \text{conversion} (1 + \text{de})]}{\text{Log}[1 - \text{conversion} (1 - \text{de})]}$$

2.6.7 Compound Synthesis and Characterization



(R)-tert-butyl-(2'-amino-[1,1'-binaphthalen]-2-yl)carbamate (2-20a):

To a solution of (*R*)-1,1'-binaphthyl-2,2'-diamine (0.203 g, 0.714 mmol) in 1,4-dioxane (3.6 mL) was added di-*tert*-butyl decarbonate (0.283 g, 1.28 mmol), and the solution was heated to reflux overnight. The solution was cooled, diluted with water (3 mL), and extracted with CH_2Cl_2 (3 x 3

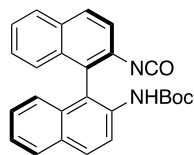
mL). The organic extracts were washed with water (3 x 3 mL), dried over sodium sulfate, and concentrated *in vacuo*. The crude material was purified by silica gel chromatography (4:1 Hex:EtOAc) to afford **3a** as a clear oil (0.132 g) containing 16 wt% ethyl acetate, 7 wt% dichloromethane, and 2 wt% water (36% yield of **2-20a**).

R_f = 0.4 (7:3 Hex:EtOAc) visualized by UV.

$^1\text{H NMR}$ (500 MHz, CDCl_3) δ 8.52 (d, J = 9.1 Hz, 1H), 7.98 (d, J = 9.0 Hz, 1H), 7.87 (dd, J = 12.1, 8.5 Hz, 2H), 7.82 (dd, J = 8.1, 1.3 Hz, 1H), 7.37 (ddd, J = 8.0, 6.7, 1.1 Hz, 1H), 7.31–7.18 (m, 4H), 7.15 (d, J = 8.8 Hz, 1H), 7.09 (d, J = 8.5 Hz, 1H), 6.93 (d, J = 8.4 Hz, 1H), 6.36 (s, 1H), 3.66 (s, 2H), 1.40 (s, 9H);

^{13}C $\{^1\text{H}\}$ NMR (125 MHz, CDCl_3) δ 153.3, 143.0, 135.7, 134.0, 132.8, 130.8, 130.4, 129.3, 128.4, 128.3 (2C), 127.3, 126.9, 125.3, 124.7, 124.0, 122.7, 119.8, 119.2, 118.3, 110.8, 80.8, 28.4.

HRMS (ESI-TOF) m/z calcd for $\text{C}_{25}\text{H}_{24}\text{N}_2\text{O}_2\text{Na}$ ($\text{M} + \text{Na}$) $^+$: 407.1736, found 407.1746.



(*R*)-tert-butyl(2'-isocyanato-[1,1'-binaphthalen]-2-yl)carbamate (S2-1):

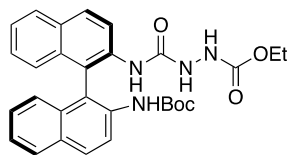
Following general procedure 1, **2-20a** (97 mg, 0.25 mmol) was dissolved in CH_2Cl_2 (1.0 mL) and was added to a solution of triphosgene (37 mg, 0.13 mmol) in CH_2Cl_2 (4.0 mL). Crude material was purified by silica gel chromatography (3:1 Hex:EtOAc) to afford the title compound as a white oily solid (60 mg) containing 8 wt% CH_2Cl_2 and 6 wt% ethyl acetate (50% yield of **S2-1**).

R_f = 0.18 (4:1 Hex:EtOAc) visualized by UV.

$^1\text{H NMR}$ (500 MHz, CDCl_3) δ 8.42 (s, 1H), 7.99–7.88 (m, 4H), 7.68 (m, 1H), 7.45 (m, 4H), 7.31–7.27 (m, 1H), 7.24–7.18 (m, 2H), 1.73 (s, 1H), 1.38 (s, 9H).

^{13}C $\{^1\text{H}\}$ NMR (125 MHz, CDCl_3) δ 158.9, 151.6, 137.7, 135.3, 132.9, 132.3, 131.6, 131.1, 129.8, 129.8, 128.8, 128.4, 128.2, 128.0, 127.7, 126.6, 126.3 (2C), 126.2, 125.6, 124.5, 121.4, 82.9, 28.1.

HRMS (ESI-TOF) m/z calcd for $\text{C}_{26}\text{H}_{22}\text{N}_2\text{O}_3\text{Na}$ ($\text{M} + \text{Na}$) $^+$: 433.1528, found 433.1537.



(R)-ethyl-2-((2'-((tert-butoxycarbonyl)amino)-[1,1'-binaphthalen]-2-yl)carbamoyl)hydrazine-1-carboxylate (2-21a):

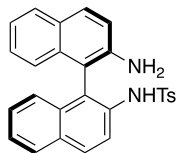
To a solution of triphosgene (22 mg, 0.065 mmol) in CH_2Cl_2 (2.5 mL) cooled to 0 °C was added a solution of **2-20a** (51 mg, 0.13 mmol) in CH_2Cl_2 (1.0 mL), followed by diisopropylethylamine (80. μL , 0.40 mmol). The solution was allowed to warm to RT and was stirred for 3 h. After this time, ethyl carbazate (14 mg, 0.13 mmol) was added in one portion, and the resulting solution was allowed to stir for 24 h prior to the addition of water. The organics were extracted with CH_2Cl_2 , dried (Na_2SO_4), and concentrated *in vacuo*. The crude material was purified by silica gel chromatography (3:2 to 0:1 Hex:EtOAc) and was isolated as a white solid (13 mg) containing 4 wt% CH_2Cl_2 and 2 wt% ethyl acetate (15% yield of **2-21a**).

R_f = 0.08 (7:3 Hex:EtOAc) visualized by UV.

^1H NMR (500 MHz, CDCl_3) δ 8.60 (d, J = 9.1 Hz, 1H), 8.30 (d, J = 9.0 Hz, 1H), 8.01 (t, J = 8.9 Hz, 2H), 7.93 (d, J = 8.2 Hz, 1H), 7.86 (d, J = 8.2 Hz, 1H), 7.41 (dt, J = 12.1, 7.5 Hz, 2H), 7.25 (m, 3H), 7.08 (s, 1H), 7.03 (d, J = 8.5 Hz, 1H), 6.97 (d, J = 8.5 Hz, 1H), 6.47 (s, 1H), 6.35 (s, 1H), 6.15 (s, 1H), 3.91 – 3.69 (m, 2H), 1.69 (s, 3H), 1.38 (s, 9H), 1.07 (t, J = 7.2 Hz, 3H).

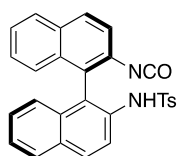
^{13}C $\{^1\text{H}\}$ NMR (125 MHz, CDCl_3) δ 155.3 (2C), 154.0, 135.2, 132.7, 132.6, 130.9, 130.6, 130.2, 130.0, 128.4, 128.2, 127.4, 127.2, 125.42, 125.36, 125.1, 125.0, 121.3, 119.7, 117.9, 81.5, 62.3, 29.9, 28.2, 14.3.

HRMS (ESI-TOF) m/z calcd for $C_{29}H_{30}N_4O_5Na$ ($M + Na$)⁺ : 537.2114, found 537.2125.



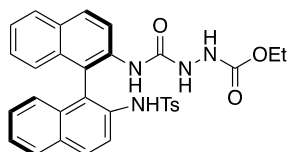
(R)-N-(2'-amino-[1,1'-binaphthalen]-2-yl)-4-methylbenzenesulfonamide (2-20b):

Compound was synthesized using known procedure and spectral data were consistent with those previously reported.³¹



(R)-N-(2'-isocyanato-[1,1'-binaphthalen]-2-yl)-4-methylbenzenesulfonamide (S2-2):

Following general procedure 1, **2-20b** (0.201 g, 0.457 mmol) was reacted with triphosgene (0.080 g, 0.27 mmol) and diisopropylethylamine (0.25 mL, 1.4 mmol) in CH_2Cl_2 (3 mL). The crude material was taken into the following reaction without purification.



(R)-ethyl 2-((2'-((4-methylphenyl)sulfonamido)-[1,1'-binaphthalen]-2-yl)carbamoyl)hydrazine-1-carboxylate (2-21b):

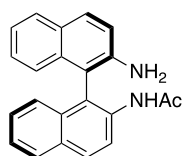
Following general procedure 2, crude **S2-2** (75 mg, 0.16 mmol) was reacted with ethyl carbazate (19 mg, 0.18 mmol) in refluxing toluene (1.5 mL). Crude material was purified by silica gel chromatography (3:2 to 1:9 Hex:EtOAc) to afford **2-21b** as a white foam (68 mg) containing 9 wt% ethyl acetate (67% yield of **2-21b** over two steps).

R_f = 0.2 (3:2 Hex:EtOAc) visualized by UV.

¹H NMR (500 MHz, CDCl₃) δ 8.56 (d, *J* = 9.1 Hz, 1H), 8.04–7.88 (m, 4H), 7.83 (d, *J* = 8.2 Hz, 1H), 7.47 (d, *J* = 8.0 Hz, 2H), 7.42–7.35 (m, 2H), 7.22 (t, *J* = 7.7 Hz, 1H), 7.12 (d, *J* = 8.1 Hz, 2H), 7.11–7.04 (m, 1H), 6.93 (d, *J* = 8.5 Hz, 1H), 6.75 (s, 1H), 6.63 (d, *J* = 8.5 Hz, 1H), 6.44 (s, 1H), 6.33 (s, 1H), 5.87 (s, 1H), 3.87–3.76 (m, 2H), 2.37 (s, 3H), 1.10 (t, *J* = 7.1 Hz, 3H).

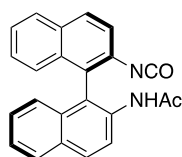
¹³C {¹H} NMR (125 MHz, CDCl₃) δ 155.1, 144.3, 136.5, 135.5, 134.0, 132.6, 132.4, 131.2, 130.6, 130.5, 129.8, 128.5, 128.2, 127.8, 127.44, 127.38, 125.8, 125.4, 125.0, 124.4, 120.6, 119.8, 119.6, 116.9, 62.6, 60.5, 21.7, 21.2, 14.3.

HRMS (ESI-TOF) *m/z* calcd for C₃₁H₂₈N₄O₅SNa (M + Na)⁺ : 591.1678, found 591.1683.



(*R*)-N-(2'-amino-[1,1'-binaphthalen]-2-yl)acetamide (2-20c):

Compound was synthesized using known procedure and spectral data were consistent with those previously reported.³²



(*R*)-N-(2'-isocyanato-[1,1'-binaphthalen]-2-yl)acetamide (S2-3):

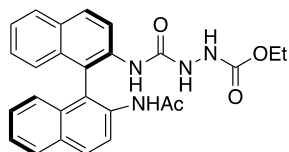
Following general procedure 1, **2-20c** (85 mg, 0.26 mmol) was reacted with triphosgene (39 mg, 0.13 mmol) and diisopropylethylamine (0.14 mL, 0.78 mmol) in CH₂Cl₂ (5.2 mL). The product was characterized without further purification. **S2-3** was isolated as an orange dust (85 mg) containing 9 wt% dichloromethane and minor impurities.

R_f = 0.74 (3:2 Hex:EtOAc) visualized by UV.

¹H NMR (500 MHz, CDCl₃) δ 8.10 (s, 1H), 8.00 (d, *J* = 8.8 Hz, 1H), 7.92 (dd, *J* = 10.8, 8.4 Hz, 3H), 7.60 (d, *J* = 8.8 Hz, 1H), 7.50–7.44 (m, 3H), 7.38 (d, *J* = 8.7 Hz, 1H), 7.28 (ddd, *J* = 8.4, 6.8, 1.3 Hz, 1H), 7.26–7.20 (m, 2H), 2.28 (s, 3H).

¹³C {¹H} NMR (125 MHz, CDCl₃) δ 169.9, 159.9, 137.5, 134.8, 133.1, 132.3, 131.7, 131.3, 130.23, 130.16, 128.8, 128.5, 128.2, 128.0, 127.7, 127.0, 126.6, 126.4, 126.1, 126.0, 124.5, 120.9, 23.5.

HRMS (ESI-TOF) *m/z* calcd for C₂₃H₁₆N₂O₂Na (M + Na)⁺ : 375.1110, found 375.1112.



(*R*)-ethyl-2-((2'-acetamido-[1,1'-binaphthalen]-2-yl)carbamoyl)hydrazine-1-carboxylate (2-21c):

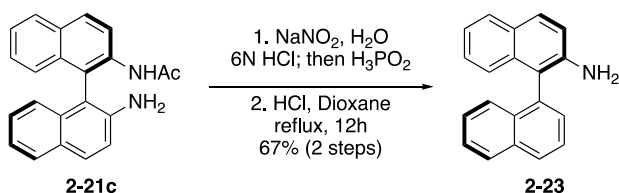
Following general procedure 2, crude **S2-3** (64 mg, 0.19 mmol) was reacted with ethyl carbazate (30 mg, 0.29 mmol) in refluxing toluene (2.0 mL). Crude material was purified by silica gel chromatography (3:2 to 1:9 Hex:EtOAc) to afford **2-21c** as a white solid (59 mg) containing 5 wt% ethyl acetate (63% yield of **2-21c**).

R_f = 0.32 (3:2 Hex:EtOAc) visualized by UV.

¹H NMR (500 MHz, CDCl₃) δ 8.38 (d, *J* = 9.0 Hz, 1H), 8.25 (d, *J* = 9.0 Hz, 1H), 8.01 (dd, *J* = 9.1, 5.4 Hz, 2H), 7.91 (dd, *J* = 10.7, 8.2 Hz, 2H), 7.42 (t, *J* = 7.5 Hz, 2H), 7.28–7.22 (m, 3H), 7.02 (dd, *J* = 17.0, 7.4 Hz, 4H), 6.42 (s, 1H), 3.88–3.78 (m, 1H), 3.76–3.68 (m, 1H), 1.79 (s, 3H), 1.06 (t, *J* = 7.1 Hz, 3H).

¹³C {¹H} NMR (125 MHz, CDCl₃) δ 170.2, 155.8 (2C), 135.2, 134.7, 132.8, 132.7, 131.6, 130.9, 130.1, 129.7, 128.5, 128.3, 127.3, 127.2, 125.81, 125.78, 125.2 (2C), 122.8, 121.9, 121.4, 119.6, 62.3, 24.1, 14.3.

HRMS (ESI-TOF) m/z calcd for $C_{26}H_{24}N_4O_4Na$ ($M + Na$)⁺ : 479.1695, found 479.1702.



(S)-1,1'-binaphthyl-2-amine (2-23):

To an ice cooled solution of **2-20c** (0.625 g, 1.91 mmol) in aq. HCl (6 M, 53 mL) was added sodium nitrite (0.132 g, 1.91 mmol). The resulting diazotized solution was allowed to stir at 0 °C for 30 min and was subsequently poured into a cooled mixture of aq. hypophosphorous acid (125 mL of 50 wt%) and water (63 mL). The mixture was allowed to stir at -78 °C in a Neslab cryobath overnight. The reaction mixture was extracted with benzene (3 x 60 mL), and the organic extracts were washed with aq. 1 M NaOH (2 x 60 mL), aq. 1 M HCl (2 x 60 mL), water (3 x 60 mL), dried over sodium sulfate, and concentrated *in vacuo*.

The crude material was re-dissolved in 1,4-dioxane (20 mL) in a 2-neck round bottom flask equipped with a reflux condenser, and concentrated HCl (aq) (12 M, 10 mL) was added. The resulting mixture was heated to reflux for 7 h. After this time, the reaction mixture was cooled and diluted with water (100 mL). The solution was treated with 2.5 M NaOH (aq) until pH 7–8, and was then extracted with benzene (3 x 60 mL). The combined organic layers were washed with water (3 x 60 mL), dried over sodium sulfate, and concentrated *in vacuo*. The crude material was purified by silica gel chromatography (9:1 to 3:2 Hex:EtOAc) to afford **2-23** as a yellow solid (0.353 g) containing 2.5 wt% dichloromethane (67% yield of **2-23** over two steps).

R_f = 0.83 (3:2 Hex:EtOAc) visualized by UV.

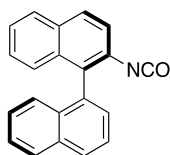
¹H NMR (600 MHz, CDCl₃) δ 8.00–7.96 (m, 1H), 7.82–7.79 (m, 1H), 7.66 (dd, J = 8.3, 6.9 Hz,

1H), 7.51 (td, $J = 7.4, 6.8$ Hz, 1H), 7.43 (dd, $J = 8.4, 1.1$ Hz, 1H), 7.33 (ddd, $J = 8.3, 6.7, 1.3$ Hz, 1H), 7.24 (ddd, $J = 8.1, 6.7, 1.3$ Hz, 1H), 7.18 (ddd, $J = 8.2, 6.7, 1.4$ Hz, 1H), 7.13 (d, $J = 8.8$ Hz, 1H), 7.03 (dd, $J = 8.4, 1.1$ Hz, 1H), 3.45 (s, 2H).

^{13}C { ^1H } NMR (151 MHz, CDCl_3) δ 141.9, 134.8, 134.5, 134.3, 132.6, 129.2, 129.1, 128.5, 128.3, 128.1, 128.0, 126.6, 126.5, 126.3 (2C), 126.0, 124.6, 122.3, 118.3, 117.6.

HRMS (ESI-TOF) m/z calcd for $\text{C}_{20}\text{H}_{15}\text{NH}$ ($\text{M} + \text{H}$) $^+$: 270.1283, found 270.1290.

$[\alpha]^{23}_{\text{D}} = +4.5$ ($c = 0.46$, THF).



(S)-2-isocyanato-1,1'-binaphthalene (S2-4):

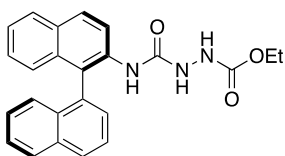
Following general procedure 1, **2-23** (74 mg, 0.28 mmol) was reacted with triphosgene (43 mg, 0.15 mmol) and diisopropylethylamine (0.15 mL, 0.87 mmol) in CH_2Cl_2 (5.6 mL). The material was taken crude into the next step, but a small portion was purified for characterization by silica gel chromatography (9:1 Hex:EtOAc) to afford **S2-4** as a clear oil.

$R_f = 0.8$ (4:1 Hex:EtOAc) visualized by UV.

^1H NMR (500 MHz, CDCl_3) δ 8.07 (d, $J = 8.3$ Hz, 1H), 8.01 (d, $J = 8.2$ Hz, 1H), 7.94 (dd, $J = 8.7, 7.1$ Hz, 2H), 7.68 (dd, $J = 8.3, 6.9$ Hz, 1H), 7.56–7.45 (m, 3H), 7.39–7.25 (m, 5H).

^{13}C { ^1H } NMR (125 MHz, CDCl_3) δ 134.0, 133.9, 133.7, 132.8, 132.5, 131.5, 130.9, 129.4, 129.3, 128.75, 128.71, 128.1, 127.1, 126.8, 126.4, 126.3, 125.8, 125.7, 125.43, 125.35, 123.3.

$[\alpha]^{22}_{\text{D}} = -1.0$ ($c = 0.90$, CHCl_3).



(S)-ethyl-2-([1,1'-binaphthalen]-2-ylcarbamoyl)hydrazine-1-carboxylate (S2-5):

Following general procedure 2, crude **S2-4** (74 mg, 0.25 mmol) was reacted with ethyl carbazate (27 mg, 0.26 mmol) in toluene (2.5 mL) at RT for 4 hours. Crude material was purified by column chromatography to afford **S2-5** (64 mg) as a white solid containing 1 wt% ethyl acetate, 6 wt% diethyl ether, and 12 wt% ethyl carbazate (47% yield of **S2-5** over two steps).

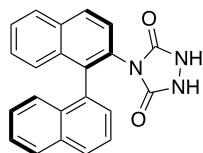
$R_f = 0.29$ (1:1 Hex:EtOAc) visualized by staining with cerium molybdate.

$^1\text{H NMR}$ (600 MHz, CDCl_3) δ 8.52 (d, $J = 9.1$ Hz, 1H), 7.96 (td, $J = 11.7, 8.2$ Hz, 3H), 7.89 (d, $J = 8.0$ Hz, 1H), 7.63 (dd, $J = 8.3, 6.9$ Hz, 1H), 7.50 (ddd, $J = 8.1, 6.6, 1.4$ Hz, 1H), 7.45 (dd, $J = 7.0, 1.2$ Hz, 1H), 7.38 (ddd, $J = 8.1, 6.7, 1.1$ Hz, 1H), 7.31 (ddd, $J = 7.9, 6.6, 1.3$ Hz, 1H), 7.29–7.27 (m, 1H), 7.23 (ddd, $J = 8.2, 6.7, 1.3$ Hz, 1H), 7.09 (d, $J = 8.5$ Hz, 1H), 6.94 (s, 1H), 3.98–3.77 (m, 2H), 1.16–1.10 (m, 3H).

$^{13}\text{C} \{^1\text{H}\}$ NMR (151 MHz, CDCl_3) δ 155.3 (2C), 134.1, 134.0, 133.3, 133.2, 132.4, 130.5, 129.1 (2C), 129.0, 128.5, 128.1, 127.0, 126.6, 126.5, 126.0, 125.82, 125.77, 124.7, 124.2, 119.8, 62.6, 14.4.

HRMS (ESI-TOF) m/z calcd for $\text{C}_{24}\text{H}_{21}\text{N}_3\text{O}_3\text{Na}$ ($\text{M} + \text{Na}$) $^+$: 422.1481, found 422.1482.

$[\alpha]_{\text{D}}^{23} = -0.5$ ($c = 0.56$. CHCl_3)



(S)-4-([1,1'-binaphthalen]-2-yl)-1,2,4-triazolidine-3,5-dione (2-24):

Following general procedure 3, **S2-5** (53 mg, 0.13 mmol) was treated with refluxing NaOEt (0.80 mmol, 0.1 M) in EtOH (2 mL). Crude material was purified by column chromatography (1:1 to

0:1 Hex:EtOAc) to afford the title compound as a white solid (27 mg) containing 9 wt% ethyl acetate (53% yield of **2-24**).

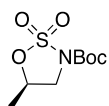
$R_f = 0.05$ (1:1 Hex:EtOAc) visualized by UV.

$^1\text{H NMR}$ (500 MHz, CDCl_3) δ 8.01 (d, $J = 8.7$ Hz, 1H), 7.93 (d, $J = 8.3$ Hz, 1H), 7.83 (d, $J = 7.5$ Hz, 1H), 7.79 (d, $J = 8.5$ Hz, 1H), 7.52 (t, $J = 7.6$ Hz, 1H), 7.48–7.42 (m, 2H), 7.39–7.32 (m, 2H), 7.32–7.24 (m, 2H), 7.21 (d, $J = 8.6$ Hz, 1H), 7.16 (t, $J = 7.6$ Hz, 1H).

$^{13}\text{C} \{^1\text{H}\}$ NMR (125 MHz, CDCl_3) δ 155.0, 154.4, 138.6, 133.8, 133.5, 133.4, 132.9, 132.4, 129.9, 128.8, 128.23, 128.19, 128.0, 127.3, 127.2, 127.1, 126.9, 126.7, 126.1, 126.0, 125.7, 125.3.

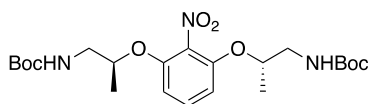
HRMS (ESI-TOF) m/z calcd for $\text{C}_{22}\text{H}_{15}\text{N}_3\text{O}_2\text{Na}$ ($\text{M} + \text{Na}$) $^+$: 376.1062, found 376.1064.

$[\alpha]_D^{22} = -0.2$ ($c = 0.69$, CHCl_3).



***tert*-butyl-(*R*)-5-methyl-1,2,3-oxathiazolidine-3-carboxylate 2,2-dioxide (**2-26**):**

Synthesized by known procedure, and all spectral data are consistent with those previously reported.³³



Di-*tert*-butyl-((2*S*,2'*S*)-((2-nitro-1,3-phenylene)bis(oxy))bis(propane-2,1-diyl))dicarbamate (S2-6**):**

To a solution of nitroresorcinol (0.200 g, 1.29 mmol) in DMF (8.6 mL) was added sodium hydride (0.108 g, 60 wt% in mineral oil, 2.71 mmol) and mixture was allowed to stir for 15 min at RT. After this time, **2-26** (0.612 g, 2.58 mmol) was added in one portion, and the solution was allowed to stir for 16 h. Subsequently, 6 M HCl (aq) (0.70 mL, 4.2 mmol) was added, and a vent needle was added to clear generated SO_3 gas from the headspace. The acidified solution was allowed to

stir for 2 h, followed by the addition of 1 M NaOH (aq). The mixture was extracted with diethyl ether (3 x 15 mL), and the organic extracts were washed with 1 M NaOH (aq) (3 x 15 mL) and water (3 x 15 mL). The organic phase was dried (MgSO₄) and concentrated *in vacuo*. The crude product was used in subsequent reactions but did not require further purification. The title compound was isolated as a white solid (0.560 g) containing 1 wt% DMF (92% yield of **S2-6**).

$R_f = 0.27$ (7:3 Hex:EtOAc) visualized by UV.

mp = 120–123 °C.

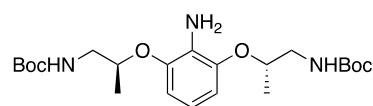
¹H NMR (500 MHz, CDCl₃) δ 7.30 (t, *J* = 8.5 Hz, 1H), 6.67 (d, *J* = 8.6 Hz, 2H), 5.04 (t, *J* = 6.1 Hz, 2H), 4.67–4.51 (m, 2H), 3.55–3.41 (m, 2H), 3.28–3.11 (m, 2H), 1.44 (s, 18H), 1.32 (d, *J* = 6.3 Hz, 6H).

¹³C {¹H} NMR (125 MHz, CDCl₃) δ 156.2, 150.7, 131.3, 107.3 (2C), 79.6, 76.0, 45.6, 28.5, 28.4, 17.3.

IR (neat) 2980, 2924, 2854, 1680, 1586, 1537, 1390, 1101, 859 cm⁻¹

HRMS (ESI-TOF) *m/z* calcd for C₂₂H₃₅N₃O₈H (M + H)⁺ : 470.2502, found 470.2509.

[α]_D²⁴ = +34.9 (c = 1.17, CHCl₃).



Di-tert-butyl-((2S,2'S)-((2-amino-1,3-phenylene)bis(oxy))bis(propane-2,1-diyl))dicarbamate (2-27):

A flame dried round bottom flask was charged with palladium on activated carbon (0.200 g, 10 wt%, 0.192 mmol) and ethyl acetate (2 mL). To this suspension was added **S2-6** (0.180 g, 0.384 mmol), and the mixture was sparged with a balloon of hydrogen gas for 15 min. The balloon was refilled, and the reaction was allowed to stir until there was no residual starting material (monitored by MS). The crude reaction mixture was filtered through Celite and washed with additional ethyl

acetate (15 mL). The combined washings were concentrated *in vacuo* to afford **2-27** as an orange oil (0.163 g) containing 1 wt% ethyl acetate (95% yield of **2-27**).

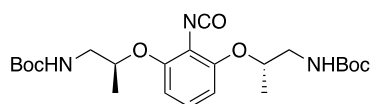
$R_f = 0.27$ (7:3 Hex:EtOAc) visualized by staining with KMnO_4 .

$^1\text{H NMR}$ (500 MHz, CDCl_3) δ 6.59 (t, $J = 8.2$ Hz, 1H), 6.50 (d, $J = 8.3$ Hz, 2H), 5.20–5.08 (m, 2H), 4.46–4.38 (m, 2H), 3.78 (s, 2H), 3.49–3.40 (m, 2H), 3.28–3.19 (m, 2H), 1.41 (s, 18H), 1.26 (d, $J = 6.6$ Hz, 6H).

$^{13}\text{C} \{^1\text{H}\}$ NMR (125 MHz, CDCl_3) δ 156.2, 145.8, 128.1, 117.1, 107.8, 79.3, 74.6, 45.8, 28.4, 17.6.

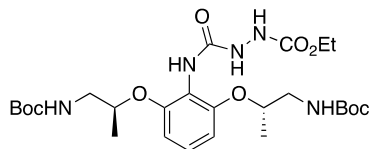
HRMS (ESI-TOF) m/z calcd for $\text{C}_{22}\text{H}_{37}\text{N}_3\text{O}_6\text{Na}$ ($\text{M} + \text{Na}$) $^+$: 462.2580, found 462.2586.

$[\alpha]_D^{23} = +48.0$ ($c = 1.00$, CH_2Cl_2).



Di-tert-butyl-((2S,2'S)-((2-isocyanato-1,3-phenylene)bis(oxy))bis(propane-2,1-diyl))dicarbamate (S2-7):

Following general procedure 1, the reaction of **2-27** (76 mg, 0.17 mmol) in CH_2Cl_2 (3.5 mL) with triphosgene (26 mg, 0.086 mmol) and diisopropylethylamine (90 μL , 0.52 mmol) afforded crude **2-7** as a yellow oil. The crude material was used in the next step without further purification.



Ethyl-2-((2,6-bis(((S)-1-((tert-butoxycarbonyl)amino)propan-2-yl)oxy)phenyl)carbamoyl)hydrazine-1-carboxylate (2-28):

Following general procedure 2, crude **S2-7** (97 mg, 0.17 mmol) in toluene (1.2 mL) was stirred with ethyl carbazate (18 mg, 0.17 mmol) to afford **2-28** as a white oil (80 mg) containing 9 wt% toluene (80% yield of **2-28** over two steps).

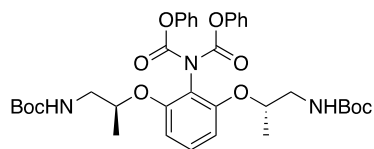
$R_f = 0.05$ (3:2 Hex:EtOAc) visualized by staining with cerium molybdate.

$^1\text{H NMR}$ (500 MHz, CDCl_3) δ 7.09 (t, $J = 8.3$ Hz, 1H), 6.98–6.85 (m, 1H), 6.57 (d, $J = 8.6$ Hz, 2H), 6.02–5.74 (m, 2H), 4.55–4.42 (m, 1H), 4.25–4.14 (m, 2H), 3.53–3.42 (m, 1H), 3.30–3.16 (m, 2H), 1.43 (s, 18H), 1.27 (d, $J = 6.4$ Hz, 6H).

^{13}C $\{^1\text{H}\}$ NMR (125 MHz, CDCl_3) δ 157.5, 156.6, 154.0, 138.0, 127.4, 116.6, 107.2, 79.3, 74.8, 62.3, 45.9, 28.5, 17.2, 14.5.

HRMS (ESI-TOF) m/z calcd for $\text{C}_{26}\text{H}_{43}\text{N}_5\text{O}_9\text{Na}$ ($\text{M} + \text{Na}$) $^+$: 592.2958, found 592.2949.

$[\alpha]_{\text{D}}^{23} = +94.9$ ($c = 1.08$, CHCl_3).



Phenyl-(2,6-bis(((S)-1-((tert-butoxycarbonyl)amino)propan-2-yl)oxy)phenyl)(phenoxy)carbonyl)carbamate (2-29a):

A two neck round bottom flask equipped with a reflux condenser was charged with **2-27** (0.150 g, 0.341 mmol) in CH_2Cl_2 (6.8 mL) and triethylamine (190 μL , 1.37 mmol). The solution was cooled to 0 $^\circ\text{C}$, and phenyl chloroformate (110 μL , 0.853 mmol) and 4-dimethylaminopyridine (0.0417 g, 0.341 mmol) were added. The reaction mixture was subsequently heated to reflux for 14 h. The mixture was cooled to RT and transferred to a separatory funnel. The solution was washed with water (3 x 5 mL) and 1 M HCl (aq) (3 x 5 mL), dried (Na_2SO_4), and concentrated *in vacuo*. The crude material was purified by silica gel chromatography (100:0 to 1:1 Hex:EtOAc) to afford **2-**

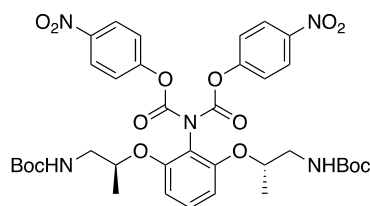
29a as a clear oil (0.214 g) containing 12 wt% CH₂Cl₂ and 3 wt% ethyl acetate (78% yield of **2-29a**).

¹H NMR (500 MHz, CDCl₃) δ 7.36 (dd, *J* = 8.5, 7.4 Hz, 4H), 7.27 (t, *J* = 8.5 Hz, 1H), 7.25–7.20 (m, 2H), 7.19–7.15 (m, 4H), 6.67 (d, *J* = 8.5 Hz, 2H), 5.05–4.95 (m, 2H), 4.70–4.60 (m, 2H), 3.55–3.44 (m, 2H), 3.34–3.21 (m, 2H), 1.38 (s, 18H), 1.33 (d, *J* = 6.2 Hz, 6H).

¹³C {¹H} NMR (125 MHz, CDCl₃) δ 156.2, 154.3, 151.5, 150.9, 130.0, 129.5, 126.2, 121.4, 106.9, 79.5, 74.6, 45.7, 28.5, 17.5, 14.3.

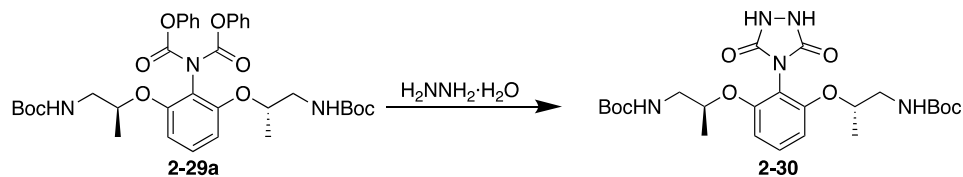
HRMS (ESI-TOF) *m/z* calcd for C₃₆H₄₅N₃O₁₀Na (M + Na)⁺ : 702.3003, found 702.2997.

[α]_D²³ = +61.6 (c = 1.02, CHCl₃).



4-nitrophenyl-(2,6-bis(((S)-1-((tert-butoxycarbonyl)amino)propan-2-yl)oxy)phenyl)((4-nitrophenoxy)carbonyl)carbamate (2-29b):

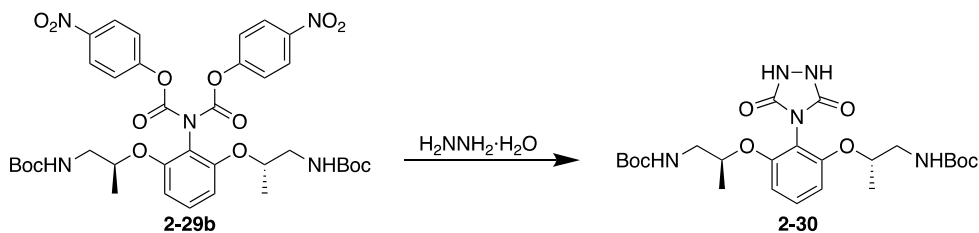
A two neck round bottom flask equipped with a reflux condenser was charged with **2-27** (0.153 g, 0.348 mmol) in CH₂Cl₂ (7.0 mL) and triethylamine (194 μL, 1.39 mmol). The solution was cooled to 0 °C, and *p*-nitrophenyl chloroformate (0.176 g, 0.870 mmol) and 4-dimethylaminopyridine (0.0430 g, 0.348 mmol) were added. The reaction mixture was subsequently heated to reflux for 14 h. The mixture was cooled to RT and transferred to a separatory funnel. The solution was washed with water (3 x 10 mL) and 1 M HCl (aq) (3 x 10 mL), dried (Na₂SO₄), and concentrated *in vacuo*. The crude material was purified by silica gel chromatography (100:0 to 1:1 Hex:EtOAc) to afford **2-29b** as a clear oil (0.0802 g) containing **S2-7** that was formed as an inseparable byproduct and confirmed by MS. This mixture of products was carried through the next step.



di-tert-butyl-((2S,2'S)-((2-(3,5-dioxo-1,2,4-triazolidin-4-yl)-1,3-phenylene)bis(oxy))bis(propane-2,1-diyl)dicarbamate (2-30):

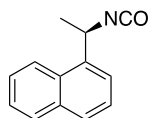
To a solution of **2-29a** (78 mg, 0.12 mmol) in CH₂Cl₂ (3.8 mL) was added hydrazine hydrate (7.0 μL, 0.14 mmol). The solution was allowed to stir for 12 h and was then concentrated *in vacuo*. The crude material was purified by column chromatography (3:2 to 0:1 Hex:EtOAc) to afford **2-30** as an oily solid (17 mg) as a mixture of products by NMR.

HRMS (ESI-TOF) *m/z* calcd for C₂₄H₃₇N₅O₈Na (M + Na)⁺: 546.2540, found 546.2533.



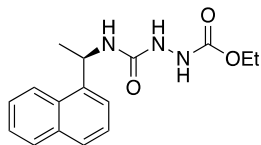
di-tert-butyl-((2S,2'S)-((2-(3,5-dinitro-1,2,4-triazolidin-4-yl)-1,3-phenylene)bis(oxy))bis(propane-2,1-diyl)dicarbamate (2-30):

To a solution of **2-29b** (37 mg, 0.048 mmol) in CH₂Cl₂ (2.3 mL) was added hydrazine hydrate (4.3 μL, 0.087 mmol). The solution was allowed to stir for 12 h and was then concentrated *in vacuo* to afford **2-30** as an oily solid (26 mg). This material was filtered through a plug of silica and was immediately used in the Diels–Alder reaction without further purification.



(R)-1-(1-isocyanatoethyl)naphthalene (S2-8):

Following general procedure 1, **2-31** (74 mg, 0.28 mmol) was reacted with triphosgene (43 mg, 0.15 mmol) and diisopropylethylamine (0.15 mL, 0.87 mmol) in CH₂Cl₂ (5.6 mL). Compound is known and all spectral data are consistent with those previously reported for this compound.³⁴



Ethyl-(R)-2-((1-(naphthalen-1-yl)ethyl)carbamoyl)hydrazine-1-carboxylate (S2-9):

Following general procedure 2, **S2-8** (0.410 g, 2.08 mmol) in toluene (6 mL) was reacted with ethyl carbazate (0.217 g, 2.08 mmol) to afford **S2-9** as a white solid (0.428 g, 68 %).

$R_f = 0.63$ (9:1 CH₂Cl₂:MeOH) visualized by UV.

mp = 131–134 °C.

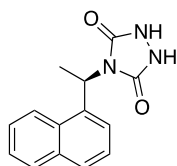
¹H NMR (500 MHz, CD₃OD) δ 8.17 (d, $J = 8.5$ Hz, 1H), 7.89 (d, $J = 8.1$ Hz, 1H), 7.79 (d, $J = 8.2$ Hz, 1H), 7.59 (d, $J = 7.2$ Hz, 1H), 7.55 (t, $J = 7.6$ Hz, 1H), 7.48 (dt, $J = 15.0, 7.7$ Hz, 2H), 5.75 (q, $J = 6.9$ Hz, 1H), 4.16 (q, $J = 7.1$ Hz, 2H), 1.62 (d, $J = 6.9$ Hz, 3H), 1.26 (t, $J = 7.1$ Hz, 3H).

¹³C {¹H} NMR (125 MHz, CD₃OD) δ 160.3, 141.1, 135.4, 132.1, 129.7, 128.7, 127.1, 126.5, 126.4, 126.3, 124.3, 123.3, 62.7, 46.9, 22.2, 14.8.

IR (neat) 3297, 2973, 1755, 1694, 1568, 1220, 772 cm⁻¹

HRMS (ESI-TOF) m/z calcd for C₁₆H₁₉N₃O₃Na (M + Na)⁺ : 324.1324, found 324.1321.

$[\alpha]_D^{23} = -2.7$ ($c = 1.02$, MeOH).



(R)-4-(1-(naphthalen-1-yl)ethyl)-1,2,4-triazolidine-3,5-dione (2-32):

Following general procedure 3, **S2-9** (0.238 g, 0.788 mmol) was treated with NaOEt (4.79 mmol, 0.16 M) in EtOH at reflux to afford **2-32** as a white solid (0.159 g, 79%).

R_f = 0.50 (9:1 CH₂Cl₂:MeOH) visualized by UV.

mp = 215–220 °C.

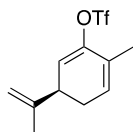
¹H NMR (500 MHz, CD₃OD) δ 8.19 (d, *J* = 8.5 Hz, 1H), 7.86–7.81 (m, 2H), 7.78 (d, *J* = 8.2 Hz, 1H), 7.49 (ddd, *J* = 8.4, 6.8, 1.5 Hz, 1H), 7.44 (dd, *J* = 8.3, 7.0 Hz, 2H), 6.02 (q, *J* = 7.1 Hz, 1H), 4.99 (s, 2H), 1.92 (d, *J* = 7.1 Hz, 3H).

¹³C {¹H} NMR (125 MHz, CD₃OD) δ 156.6, 135.6, 135.2, 132.3, 129.9, 129.6, 127.5, 126.7, 126.5, 126.0, 123.7, 47.7, 17.8.

IR (neat) 3099, 2979, 2923, 1682, 1449, 655 cm⁻¹

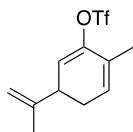
HRMS (ESI-TOF) *m/z* calcd for C₁₄H₁₃N₃O₂Na (M + Na)⁺ : 278.0905, found 278.0904.

[α]_D²³ = +47.8 (c = 1.02, MeOH).



(R)-6-methyl-3-(prop-1-en-2-yl)cyclohexa-1,5-dien-1-yl trifluoromethanesulfonate (2-33):

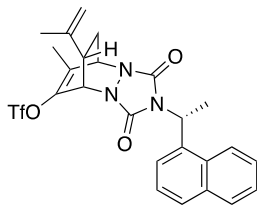
Compound was synthesized using known procedure, and all spectral data are consistent with those previously reported.²⁴



6-methyl-3-(prop-1-en-2-yl)cyclohexa-1,5-dien-1-yl trifluoromethanesulfonate (2-35):

Prepared in the same manner as **2-33**, but equal masses of (*R*)-carvone and (*S*)-carvone were mixed prior to the reaction to make a racemic sample. **[α]_D²³** = +0.1 (c = 1.02, CHCl₃).

2.6.8 *Diels–Alder Chemistry with TAD Reagents:*



(5*R*,8*S*,11*R*)-7-methyl-2-((*R*)-1-(naphthalen-1-yl)ethyl)-1,3-dioxo-11-(prop-1-en-2-yl)-2,3,5,8-tetrahydro-1*H*-5,8-ethano[1,2,4]triazolo[1,2-*a*]pyridazin-6-yl trifluoromethanesulfonate (2-34):

Following general procedure 4, intermediate **2-32** (17 mg, 0.067 mmol) was suspended in CH₂Cl₂ (0.5 mL) and was treated with (diacetoxyiodo)benzene (22 mg, 0.067 mmol). The resulting oxidized urazole was then added dropwise to a solution of **2-33** (25 mg, 0.067 mmol) in CH₂Cl₂ (0.5 mL) at –78 °C. The crude material was purified by silica gel chromatography (9:1 to 0:1 Hex:EtOAc) to afford **2-34** (19 mg, 54% yield) as a single diastereomer.

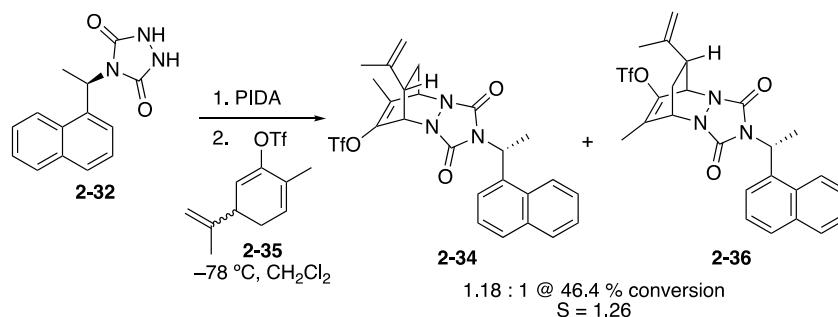
R_f = 0.05 (9:1 Hex:EtOAc) visualized by UV.

¹H NMR (600 MHz, CDCl₃) δ 8.05 (d, J = 8.7 Hz, 1H), 7.86 (t, J = 8.0 Hz, 2H), 7.81 (d, J = 8.3 Hz, 1H), 7.54 (t, J = 7.8 Hz, 1H), 7.50–7.44 (m, 2H), 5.99 (qd, J = 7.3, 2.0 Hz, 1H), 4.92 (s, 1H), 4.82 (s, 1H), 4.57 (s, 1H), 2.82 (t, J = 6.6 Hz, 1H), 2.26 (ddt, J = 11.3, 8.8, 2.6 Hz, 1H), 1.93 (d, J = 7.2 Hz, 2H), 1.89 (d, J = 2.1 Hz, 3H), 1.74 (s, 3H), 1.58–1.53 (m, 2H).

¹³C {¹H} NMR (151 MHz, CDCl₃) δ 157.1, 155.8, 142.8, 138.4, 133.9, 133.4, 131.2, 130.0, 129.1, 129.0, 126.9, 126.2, 125.6, 125.1, 122.8, 113.1, 56.2, 55.8, 47.3, 43.0, 28.2, 22.3, 17.4, 13.9.

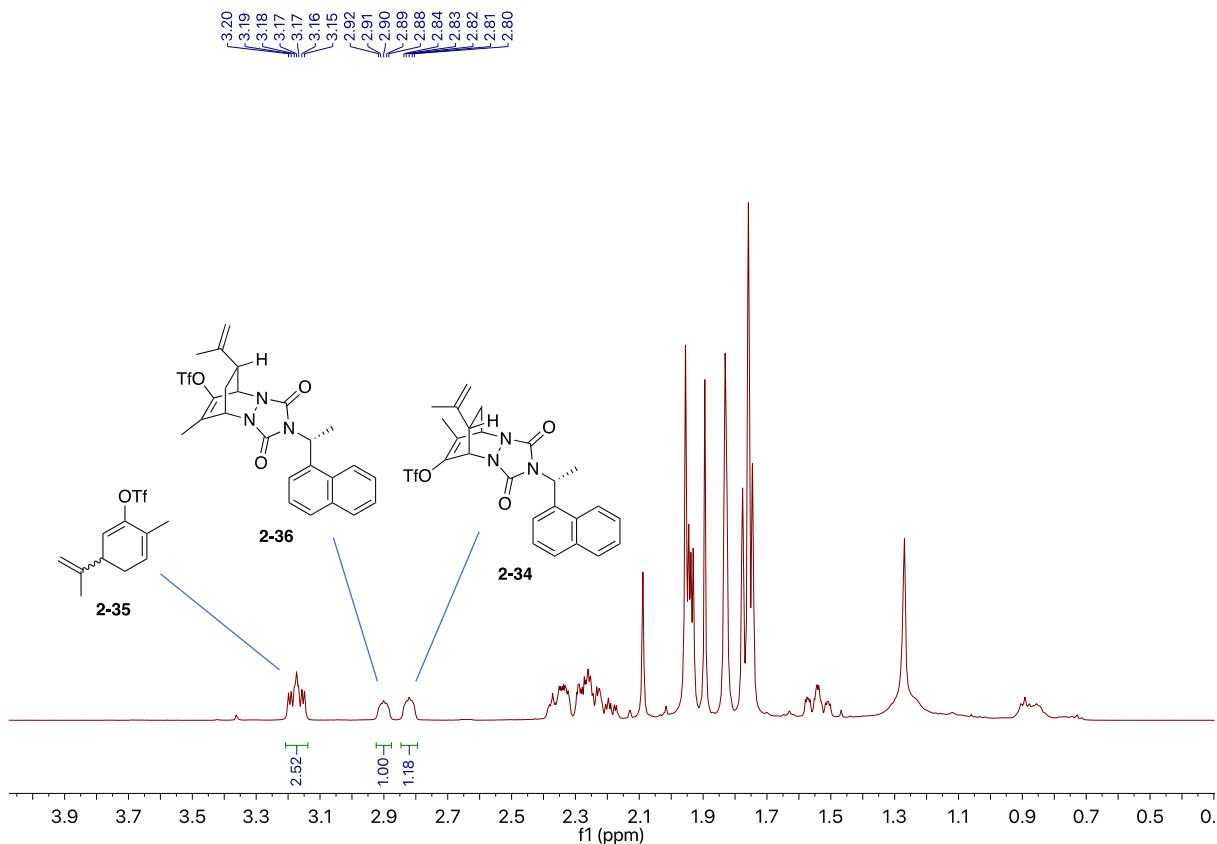
HRMS (ESI-TOF) m/z calcd for C₂₅H₂₄F₃N₃O₅SNa (M + Na)⁺ : 558.1287, found 558.1314.

Full 2D characterization for this compound can be found in Appendix A. All subsequent Diels–Alder reactions were assigned by analogy to this compound.



Kinetic resolution of **2-35**:

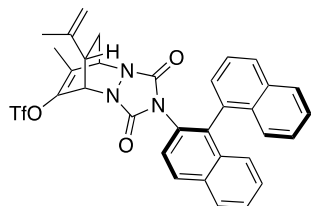
Following general procedure 5, intermediate **2-32** (18 mg, 0.071 mmol) was suspended in CH_2Cl_2 (0.5 mL), and was treated with (diacetoxyiodo)benzene (23 mg, 0.071 mmol). The resulting oxidized urazole was then added dropwise to a solution of **2-35** (40 mg, 0.14 mmol) in CH_2Cl_2 (0.5 mL) at $-78\text{ }^{\circ}\text{C}$. The solution was warmed to RT and concentrated *in vacuo*. The selectivity was determined by analysis of the crude NMR as follows:



$$(1) \text{ Conversion} = \frac{2.18}{2.52 + 2.18} = 0.464$$

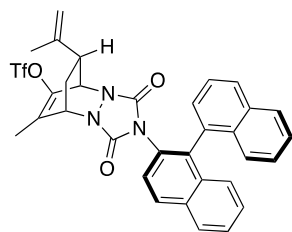
$$(2) \text{ Diastereomeric excess (de)} = \frac{1.18}{2.18} - \frac{1.00}{2.18} = 0.0826$$

$$(3) \text{ Selectivity} = \frac{\text{Log}[1 - 0.464(1 + 0.0826)]}{\text{Log}[1 - 0.464(1 - 0.0826)]} = 1.26$$



2-((S)-[1,1'-binaphthalen]-2-yl)-7-methyl-1,3-dioxo-11-(prop-1-en-2-yl)-2,3,5,8-tetrahydro-1H-5,8-ethano[1,2,4]triazolo[1,2-a]pyridazin-6-yl trifluoromethanesulfonate (2-37):

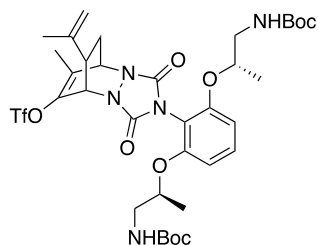
Following general procedure 4, intermediate **2-24** (26 mg, 0.074 mmol) was suspended in CH₂Cl₂ (2.0 mL), and was treated with (diacetoxyiodo)benzene (24 mg, 0.074 mmol). A portion of the resulting oxidized urazole solution (0.75 mL, 0.028 mmol) was then added dropwise to a solution of **2-33** (7.8 mg, 0.028 mmol) in CH₂Cl₂ (0.5 mL) at –78 °C. The solution was warmed to RT and concentrated *in vacuo*. Crude NMR revealed a 3.88:1 mixture of diastereomers of **2-37**. The material was used as a baseline data set for the kinetic resolution, and no further purification was performed.



2-((S)-[1,1'-binaphthalen]-2-yl)-7-methyl-1,3-dioxo-11-(prop-1-en-2-yl)-2,3,5,8-tetrahydro-1H-5,8-ethano[1,2,4]triazolo[1,2-a]pyridazin-6-yl trifluoromethanesulfonate (2-38):

Following general procedure 5, intermediate **2-24** (26 mg, 0.074 mmol) was suspended in CH₂Cl₂ (2.0 mL) and was treated with (diacetoxyiodo)benzene (24 mg, 0.074 mmol). A portion of the

resulting oxidized urazole solution (0.38 mL, 0.014 mmol) was then added dropwise to a solution of **2-35** (7.8 mg, 0.028 mmol) in CH₂Cl₂ (0.5 mL) at -78 °C. The solution was warmed to RT and concentrated *in vacuo*. Crude NMR revealed a 1:2.39 mixture of diastereomers of **2-38** at 34% conversion, but selectivity was not calculated due to the racemization of the TAD reagent.



2-(2,6-bis(((S)-1-((tert-butoxycarbonyl)amino)propan-2-yl)oxy)phenyl)-7-methyl-1,3-dioxo-11-(prop-1-en-2-yl)-2,3,5,8-tetrahydro-1H-5,8-ethano[1,2,4]triazolo[1,2-a]pyridazin-6-yl trifluoromethanesulfonate (2-39 + 2-40):

Following general procedure 5, intermediate **2-30** (16 mg, 0.031 mmol) was suspended in CH₂Cl₂ (0.75 mL) and was treated with (diacetoxyiodo)benzene (10 mg, 0.031 mmol). The resulting oxidized urazole was then added dropwise to a solution of **2-35** (17 mg, 0.061 mmol) in CH₂Cl₂ (0.5 mL) at -78 °C. The solution was warmed to RT and concentrated *in vacuo*. Due to overlapping signals in the crude NMR, the selectivity for this reagent was not calculated. Identity of the product was confirmed by HRMS.

HRMS (ESI-TOF) *m/z* calcd for C₃₅H₄₈F₃N₅O₁₁SNa (M + Na)⁺ : 826.2921, found 826.2922.

2.7 References

¹ Nicolaou, K. C.; Snyder, S. A. Chasing Molecules that Were Never There: Misassigned Natural Products and the Role of Chemical Synthesis in Modern Structure Elucidation. *Angew. Chem. Int. Ed.* **2005**, *44*, 1012–1044.

² (a) Wagner, A. J.; David, J. G.; Rychnovsky, S. D. Determination of Absolute Configuration Using Kinetic Resolution Catalysts. *Org. Lett.* **2011**, *13*, 4470–4473. (b) Wagner, A. J.; Rychnovsky, S. D. Determination of Absolute Configuration of Secondary Alcohols Using Thin-Layer Chromatography. *J. Org. Chem.* **2013**, *78*, 4594–

4598. (c) Wagner, A. J.; Miller, S. M.; King, R. P.; Rychnovsky, S. D. Nanomole-Scale Assignment and One-Use Kits for Determining the Absolute Configuration of Secondary Alcohols. *J. Org. Chem.* **2016**, *81*, 6253–6265. (d) Brito, G. A.; Della-Felice, F.; Luo, G.; Burns, A. S.; Pilli, R. A.; Rychnovsky, S. D.; Krische, M. J. Catalytic Enantioselective Allylations of Acetylenic Aldehydes via 2-Propanol-Mediated Reductive Coupling. *Org. Lett.* **2018**, *20*, 4144–4147. (e) Burns, A. S.; Ross, C. C.; Rychnovsky, S. D. Heteroatom-Directed Acylation of Secondary Alcohols To Assign Absolute Configuration. *J. Org. Chem.* **2018**, *83*, 2504–2515.
- ³ Burns, A. S.; Wagner, A. J.; Fulton, J. L.; Young, K.; Zakarian, A.; Rychnovsky, Scott. D. Determination of the Absolute Configuration of β -Chiral Primary Alcohols Using the Competing Enantioselective Conversion Method. *Org. Lett.* **2017**, *19*, 2953–2956.
- ⁴ Perry, M. A.; Trinidad, J. V.; Rychnovsky, S. D. Absolute Configuration of Lactams and Oxazolidinones Using Kinetic Resolution Catalysts. *Org. Lett.* **2013**, *15*, 472–475.
- ⁵ Miller, S. M.; Samame, R. A.; Rychnovsky, S. D. Nanomole-Scale Assignment of Configuration for Primary Amines Using a Kinetic Resolution Strategy. *J. Am. Chem. Soc.* **2012**, *134*, 20318–20321.
- ⁶ (a) Burtea, A.; Rychnovsky, S. D. Determination of the Absolute Configuration of Cyclic Amines with Bode's Chiral Hydroxamic Esters Using the Competing Enantioselective Conversion Method. *Org. Lett.* **2017**, *19*, 4195–4198. (b) Dooley, C. J., III.; Burtea, A.; Mitilian, C.; Dao, W. T.; Qu, B.; Salzameda, N. T.; Rychnovsky, S. D. Using the Competing Enantioselective Conversion Method to Assign the Absolute Configuration of Cyclic Amines with Bode's Acylation Reagents. *J. Org. Chem.* **2020**, *85*, 10750–10759.
- ⁷ Joyce, L. A.; Nawrat, C. C.; Sherer, E. C.; Biba, M.; Brunskill, A.; Martin, G. E.; Cohen, R. D.; Davies, I. W. Beyond optical rotation: what's left is not always right in total synthesis. *Chem. Sci.* **2018**, *9*, 415–424.
- ⁸ (a) Corey, E. J. Catalytic Enantioselective Diels–Alder Reactions: Methods, Mechanistic Fundamentals, Pathways, and Applications. *Angew. Chem. Int. Ed.* **2002**, *41*, 1650–1667. (b) Nicolaou, K. C.; Snyder, S. A.; Montagnon, T.; Vassilikogiannakis, G. The Diels–Alder Reaction in Total Synthesis. *Angew. Chem. Int. Ed.* **2002**, *41*, 1668–1698. (c) Funel, J.-A.; Abele, S. Industrial Applications of the Diels–Alder Reaction. *Angew. Chem. Int. Ed.* **2013**, *52*, 3822–3863.
- ⁹ Northrup, A. B.; MacMillan, D. W. C. The First General Enantioselective Catalytic Diels–Alder Reaction with Simple α,β -Unsaturated Ketones. *J. Am. Chem. Soc.* **2002**, *124*, 2458–2460.
- ¹⁰ Thiele, J.; Stange, O. *Justus Liebigs Ann. Chem.* **1894**, *283*, 1–46.

- ¹¹ (a) Cookson, R. C.; Gilani, S. S. H.; Stevens, I. D. R. 4-Phenyl-1,2,4-triazolin-3,5-dione: a powerful dienophile. *Tetrahedron Lett.* **1962**, *3*, 615–618. (b) Cookson, R. C.; Gilani, S. S. H.; Stevens, I. D. R. Diels–Alder reactions of 4-phenyl-1,2,4-triazoline-3,5-dione. *J. Chem. Soc. C*, **1967**, 1905–1909.
- ¹² (a) Pirkle, W. H.; Stickler, J. C. The reaction of 1,2,4-triazoline-3,5-diones with mono-olefins. *Chem. Commun. (London)* **1967**, 760–761. (b) Butler, G. B. Triazolinedione Modified Polydienes. *Ind. Eng. Chem. Prod. Res. Dev.* **1980**, *19*, 512–528. (c) Ohashi, S.; Leong, K.-W.; Matyjaszewski, K.; Butler, G. B. Ene reaction of triazolinediones with alkenes. 1. Structure and properties of products. *J. Org. Chem.* **1980**, *45*, 3467–3471. (d) Williams, A. G.; Butler, G. B. Mechanistic studies of the reaction of 4-substituted 1,2,4-triazoline-3,5-diones with .beta.-dicarbonyl compounds. *J. Org. Chem.* **1980**, *45*, 1232–1239. (e) Zolfigol, M. A.; Nasr-Isfahani, H.; Mallakpour, S.; Safaiee, M. Oxidation of Urazoles with 1,3-Dihalo-5,5-dimethylhydantoin, both in Solution and under Solvent-Free Conditions. *Synlett* **2005**, 761–764.
- ¹³ (a) Levandowski, B. J.; Houk, K. N. Theoretical Analysis of Reactivity Patterns in Diels–Alder Reactions of Cyclopentadiene, Cyclohexadiene, and Cycloheptadiene with Symmetrical and Unsymmetrical Dienophiles. *J. Org. Chem.* **2015**, *80*, 3530–3537. (b) Domingo, L. R.; Emamian, S. R. High reactivity of triazolinediones as superelectrophiles in polar reactions: A DFT study. *Ind. J. Chem. A* **2014**, *53*, 940–948. (c) Alajarín, M.; Cabrera, J.; Pastor, A.; Sánchez-Andrada, P. Polar Hetero-Diels–Alder Reactions of 4-Alkenylthiazoles with 1,2,4-Triazoline-3,5-diones: An Experimental and Computational Study. *J. Org. Chem.* **2008**, *73*, 963–973. (d) Alajarín, M.; Bonillo, B.; Marin-Luna, M.; Sánchez-Andrada, P.; Vidal, A. N-Phenyl-1,2,4-triazoline-3,5-dione (PTAD) as a Dienophilic Dinitrogen Equivalent: A Simple Synthesis of 3-Amino-1,2,4-benzotriazines from Arylcarbodiimides. *Eur. J. Org. Chem.* **2010**, 694–704. (e) Chen, J. S.; Houk, K. N.; Foote, C. S. Theoretical Study of the Concerted and Stepwise Mechanisms of Triazolinedione Diels–Alder Reactions. *J. Am. Chem. Soc.* **1998**, *120*, 12303–12309.
- ¹⁴ Morrison, C. F.; Vaters, J. P.; Miller, D. O.; Burnell, D. J. Facial Selectivity in the [4 + 2] Reactions of a Diene Derived From Carvone. *Org. Biomol. Chem.* **2006**, *4*, 1160–1166.
- ¹⁵ Giuliano, R. M.; Jordan, A. D., Jr; Gauthier, A. D. Diastereofacial Selectivity of Diels-Alder Reactions of Carbohydrate-Derived Dienes and Their Carbocyclic Analogs. *J. Org. Chem.* **1993**, *58*, 4979–4988.
- ¹⁶ (a) Carreño, M. C.; García Ruano, J. L.; Urbano, A. Synthesis and asymmetric diels-alder reactions of (*S*)-2-*p*-tolylsulfinyl-1,4-benzoquinone. *Tetrahedron Lett.* **1989**, *30*, 4003–4006. (b) Carreño, M. C.; García Ruano, J. L.; Urbano, A. Asymmetric Diels-Alder reactions of (*S*)-2-(*p*-tolylsulfinyl)-1,4-naphthoquinones. *J. Org. Chem.* **1992**,

- 57, 6870–6876. (c) Carreño, M. C.; García Ruano, J. L.; Toledo, M. A.; Urbano, A. Influence of the Sulfinyl Group on the Chemoselectivity and π -Facial Selectivity of Diels–Alder Reactions of (*S*)-2-(*p*-Tolylsulfinyl)-1,4-benzoquinone. *J. Org. Chem.* **1996**, *61*, 503–509. (d) Carreño, M. C.; García Ruano, J. L.; Urbano, A.; Hoyos, M. A. Studies of Diastereoselectivity in Diels–Alder Reactions of (*S,S*)-4a,5,8,8a-Tetrahydro-5,8-methano-2-(*p*-tolylsulfinyl)-1,4-naphtho-quinones with Cyclopentadiene. *J. Org. Chem.* **1996**, *61*, 2980–2985. (e) Carreño, M. C.; Urbano, A.; Di Vitta, C. Enantioselective Diels–Alder Cycloadditions with (*S,S*)-2-(*p*-Tolylsulfinyl)-1,4-naphthoquinone: Efficient Kinetic Resolution of Chiral Racemic Vinylcyclohexenes. *J. Org. Chem.* **1998**, *63*, 8320–8330. (f) Latorre, A.; Urbano, A.; Carreño, M. C. Synthesis and chiroptical properties of ferrocene-[4]-helicenequinones: kinetic resolution of a planar-chiral diene. *Chem. Commun.* **2011**, *47*, 8103–8105.
- ¹⁷ Paquette, L. A.; Doehner, R. F. Synthesis of optically active triazolinediones and examination of their utility for inducing asymmetry in Diels–Alder cycloaddition reactions. *J. Org. Chem.* **1980**, *45*, 5105–5113.
- ¹⁸ (a) Sakakura, A.; Suzuki, K.; Nakano, K.; Ishihara, K. Chiral 1,1'-Binaphthyl-2,2'-diammonium Salt Catalysts for the Enantioselective Diels–Alder Reaction with α -Acyloxyacroleins. *Org. Lett.* **2006**, *8*, 2229–2232. (b) Brunel, J. M. BINOL: A Versatile Chiral Reagent. *Chem. Rev.* **2005**, *105*, 857–897.
- ¹⁹ Uyanik, M.; Yasui, T.; Ishihara, K. Hydrogen Bonding and Alcohol Effects in Asymmetric Hypervalent Iodine Catalysis: Enantioselective Oxidative Dearomatization of Phenols. *Angew. Chem. Int. Ed.* **2013**, *52*, 9215–9218.
- ²⁰ Fujita, M. Mechanistic aspects of alkene oxidation using chiral hypervalent iodine reagents. *Tetrahedron Lett.* **2017**, *58*, 4409–4419.
- ²¹ De Bruycker, K.; Billiet, S.; Houck, H. A.; Chattopadhyay, S.; Winne, J. M.; Du Prez, F. E. Triazolinediones as Highly Enabling Synthetic Tools. *Chem. Rev.* **2016**, *116*, 3919–3974.
- ²² Yamada, H. A. S. Stereochemical studies—VIII: Unequivocal determination of the absolute configuration in biaryl systems. *Tetrahedron*, **1971**, *27*, 5999–6009.
- ²³ Handa, S.; Slaughter, L. M. Enantioselective Alkynylbenzaldehyde Cyclizations Catalyzed by Chiral Gold(I) Acyclic Diaminocarbene Complexes Containing Weak Au–Arene Interactions. *Angew. Chem. Int. Ed.* **2012**, *51*, 2912–2915.
- ²⁴ Chai, W.; Chang, Y.; Buynak, J. D. An efficient and general urazole synthesis. *Tetrahedron Lett.* **2012**, *53*, 3514–3517.

- ²⁵ Verboom, R. C.; Persson, B. A.; Bäckvall, J.-E. Palladium(II)-Catalyzed Intramolecular 1,4-Oxyacyloxylation of Conjugated Dienes. A Stereocontrolled Route to Fused Six-Membered Lactones and Pyrans. *J. Org. Chem.* **2004**, *69*, 3102–3111.
- ²⁶ Moriarty, R. M.; Prakash, I.; Penmasta, R. An Improved Synthesis of Ethyl Azodicarboxylate and 1,2,4-Triazoline-3,5-Diones Using Hypervalent Iodine Oxidation. *Synth. Commun.* **1987**, *17*, 409–413.
- ²⁷ (a) Heathcock, C. H.; White, C. T. Acyclic stereoselection. 5. Use of double stereodifferentiation to enhance 1,2 diastereoselection in aldol condensations of chiral aldehydes. *J. Am. Chem. Soc.* **1979**, *101*, 7076–7077; (b) Heathcock, C. H.; Pirrung, M. C.; Lampe, J.; Buse, C. T.; Young, S. D. Acyclic stereoselection. 12. Double stereodifferentiation with mutual kinetic resolution. A superior class of reagents for control of Cram's rule stereoselection in synthesis of erythro- α -alkyl- β -hydroxy carboxylic acids from chiral aldehydes. *J. Org. Chem.* **1981**, *46*, 2290–2300.
- ²⁸ Mamidala, R.; Kommuri, C.; Paulose, J.; Aswath, H.; Pawar, L.; Arunachalampillai, A.; Cherney, A. H.; Tedrow, J. S.; Röheli, A. R.; Ortiz, A. Convenient, Large-Scale Synthesis of (*S*)-TRIP Using Suzuki CrossCoupling Conditions. *Org. Process Res. Dev.* **2022**, *26*, 165–173.
- ²⁹ Pianowski, Z.; Gorska, K.; Oswald, L.; Merten, C. A.; Winssinger, N. Imaging of mRNA in Live Cells Using Nucleic Acid-Templated Reduction of Azidorhodamine Probes. *J. Am. Chem. Soc.* **2009**, *131*, 6492–6497.
- ³⁰ Mallakpour, S.; Rafiee, Z. Novel and Efficient Synthesis of 4-Substituted-1,2,4-triazolidine-3,5-diones from Anilines. *Synth. Commun.* **2007**, *37*, 1927–1934.
- ³¹ Vióquez, S. F.; Guillena, G.; Nájera, C.; Bradshaw, B.; Etxebarria-Jardi, G.; Bonjoch, J. (*Sa,S*)-N-[2'-(4-methylphenylsulfamido)-1,1'-binaphthyl-2-yl]pyrrolidine-2-carboxamide: An Organocatalyst For The Direct Aldol Reaction. *Org. Synth.* **2011**, *88*, 317–329.
- ³² Zhu, J.-B.; Chen, E. Y.-X. From *meso*-Lactide to Isotactic Polylactide: Epimerization by B/N Lewis Pairs and Kinetic Resolution by Organic Catalysts. *J. Am. Chem. Soc.* **2015**, *137*, 12506–12509.
- ³³ Hebeisen, P.; Weiss, U.; Alker, A.; Staempfli, A. Ring opening of cyclic sulfamidates with bromophenyl metal reagents: complementarity of sulfamidates and aziridines. *Tetrahedron Lett.* **2011**, *52*, 5229–5233.
- ³⁴ Huang, X.; Zhuang, T.; Kates, P. A.; Gao, H.; Chen, X.; Groves, J. T. Alkyl Isocyanates via Manganese-Catalyzed C–H Activation for the Preparation of Substituted Ureas. *J. Am. Chem. Soc.* **2017**, *139*, 15407–15413.

Chapter 3. Using the Competing Enantioselective Conversion Method to Assign the Absolute Configuration of Cyclic Amines with Bode's Acylation Reagents

Reprinted (adapted) with permission from Dooley, C. J., III.; Burtea, A.; Mitilian, C.; Dao, W. T.; Qu, B.; Salzameda, N. T.; Rychnovsky, S. D. Using the Competing Enantioselective Conversion Method to Assign the Absolute Configuration of Cyclic Amines with Bode's Acylation Reagents. *J. Org. Chem.* **2020**, *85*, 10750–10759. Copyright 2020 American Chemical Society.

3.1 Abstract

The competing enantioselective conversion (CEC) method is a quick and reliable means to determine absolute configuration. Previously, Bode's chiral acylated hydroxamic acids were used to determine the stereochemistry of primary amines, as well as cyclic and acyclic secondary amines. The enantioselective acylation has been evaluated for 4-, 5-, and 6-membered cyclic secondary amines, including medicinally relevant compounds. The limitations of the method were studied through computational analysis and experimental results. Piperidines with substituents at the 2-position did not behave well unless the axial conformer was energetically accessible, which is consistent with the transition state geometries proposed by Bode and Kozlowski. Control experiments were performed to investigate the cause of degrading selectivity under the CEC reaction conditions. The present study expands the scope of the CEC method for secondary amines and provides a better understanding of the reaction profile.

3.2 Introduction

Nitrogen-containing heterocycles are ubiquitous in active pharmaceutical ingredients and natural products. Alkaloids have long attracted the attention of medicinal and synthetic chemists due to their diverse biological activities and fascinating architectures. These structures have stimulated many new methods for the enantioselective installation of nitrogenous stereocenters.¹ Equally important in setting these stereocenters is the ability to accurately determine their absolute configuration. Frequently, this task is accomplished through new synthetic methodology to construct a compound of known absolute configuration and assigning other compounds by analogy. Also common is the use of computational predictions in conjunction with specific rotation or circular dichroism measurements.² However, there is rarely a straightforward method for assigning these newly formed stereocenters.

The gold standard in assigning absolute stereochemistry is generally considered X-ray crystallography. However, this requires the molecule of interest to be abundant, crystalline, and frequently necessitates derivatization to establish absolute stereochemistry. The process of crystallization can be also be arduous, as high-quality crystals of adequate size are required for reliable data to be obtained. Other approaches to assigning absolute configuration include chiral derivatization and subsequent NMR analysis,³ vibrational and electronic circular dichroism coupled with DFT calculation,⁴ and total synthesis.⁵ For more details on absolute structure assignment, see chapter 1.

In 2011, our lab reported a method to determine absolute configuration based on the enantioselective acylation of chiral secondary alcohols, for which we later coined the term Competing Enantioselective Conversion (CEC) method.⁶ The method was inspired by the work of Horeau, who performed pioneering studies on amplifying enantioenrichment through double

asymmetric induction.⁷ The CEC method is conducted with an enantioenriched substrate, which is reacted with both enantiomers of an acyl transfer catalyst/reagent, generally in two separate vessels. After sufficient time the reactions are quenched, and their conversions are assayed. The data were then compared to an empirically derived model, and the absolute configuration can be assigned by analogy. The method is predicated on a meaningful energy difference between the two diastereomeric transition states, with the faster reaction identified as the matched case between the enantioselective reagent and enantiopure substrate.

The CEC method has previously been applied to numerous substrate classes, including secondary alcohols,^{6,8} β -chiral primary alcohols,⁹ oxazolidinones, lactams,¹⁰ primary amines, and cyclic secondary amines.¹¹ In our work on alcohols, the reactions were run separately, and the conversion of each reaction was determined by NMR analysis. In some cases, we have been able to use pseudoenantiomeric reagents and run the competitive reactions in the same vessel.¹¹ Such an example is the CEC method for primary amines, which used deuterated derivatives of Mioskowski's reagents (chapter 1.4.4).¹² The use of pseudoenantiomeric reagents in this method allowed us to assign stereochemistry by mass spectrometry. However, this method was not very general due to low reactivity of the reagents with secondary amines. Additionally, it was surprisingly difficult to achieve high levels of deuterium enrichment with the Mioskowski's reagents, complicating data analysis.

3.2.1 *Inspiration from Bode's Work*

Seeking a more general solution that would allow for the assignment of secondary amines, our group looked to the literature and was inspired by work done in the Bode group.¹³ Bode had been examining the acylation of amines with N-heterocyclic carbenes (NHC) using α -hydroxy enones as the acylating agent. The reactions proceed through an initial retro-benzoin reaction to

generate an activated acyl-azolium, which can then undergo acyl transfer with amines. With good reactivity, Bode's group saw opportunity for asymmetric induction and began to evaluate chiral co-catalysts. While low enantioselectivity was observed for hydroxamic acids derived from glycine (**3-5**) and (*R,R*)-1,2-diaminocyclohexane (**3-6**), excellent results were obtained using aminoindanol derived hydroxamic acid **3-7**.^{13b} Notably, the synthesis of chiral piperidines was an unmet synthetic challenge, and this chemistry allowed facile generation of enantioenriched acylated-piperidines by resolution!

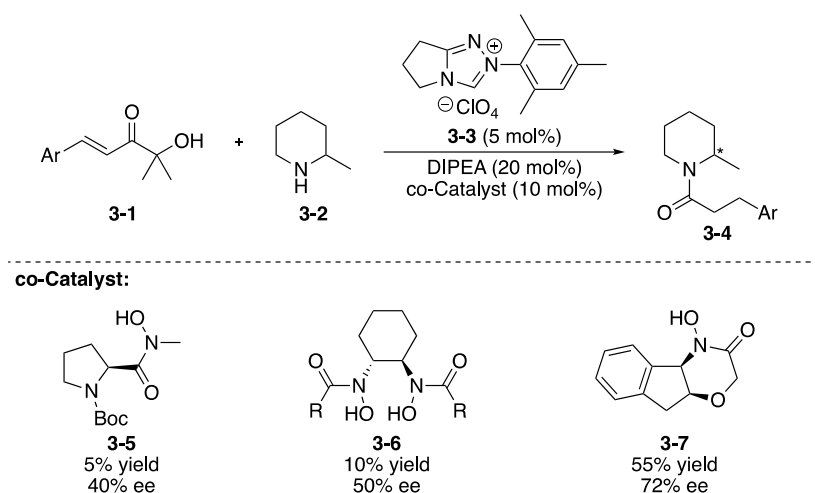


Figure 3-1 Enantioenrichment of N-heterocycles using α -hydroxy enones as acyl surrogates.

Bode's group then went on to apply this methodology to the kinetic resolution of various cyclic secondary amines (Figure 3-2).^{13b} Using modified reaction conditions, they were able to resolve an array of piperidines, protected azetidines, and morpholines with good to excellent selectivity. However, rings sizes other than 6-membered were typically challenging, as lower selectivity was often observed (**3-13**). Through collaboration with the Kozlowski group, they were able to computationally deduce the mechanism of the reaction.¹⁴ It was proposed that the acylation takes place in a concerted fashion, through a seven-membered transition state in which the α -substituent of the amine as well as the amine proton were placed in axial conformations (see

transition state, Figure 3-2). Other ring sizes likely distort the transition state and lead to less-selective reactions.

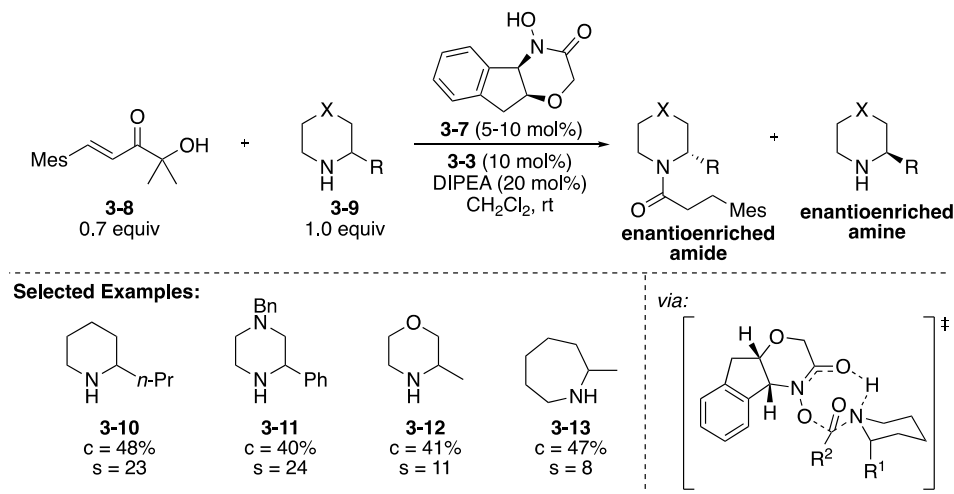


Figure 3-2 Kinetic resolution of secondary amines using hydroxamic acid **3-7**.

3.2.2 Prior work on CEC method for Secondary Amines

A former group member, Dr. Alex Burtea, was inspired by this work and thought that it could be applied to a CEC method to assign absolute configuration. Using the same enantiomeric hydroxamic acids, he found that acylation with butyryl and valeroyl chloride led to stable acyl transfer reagents **3-14** and **3-15**.^{11b} By using pseudoenantiomeric reagents which differ by a methylene, Dr. Burtea was able to assign the configuration of cyclic secondary amines through mass spectrometry. Additionally, it was a marked improvement over our previous method for assigning the configuration of primary amines, as the products were not plagued by loss of deuterium enrichment, leading to a simpler overall analysis.^{11a}

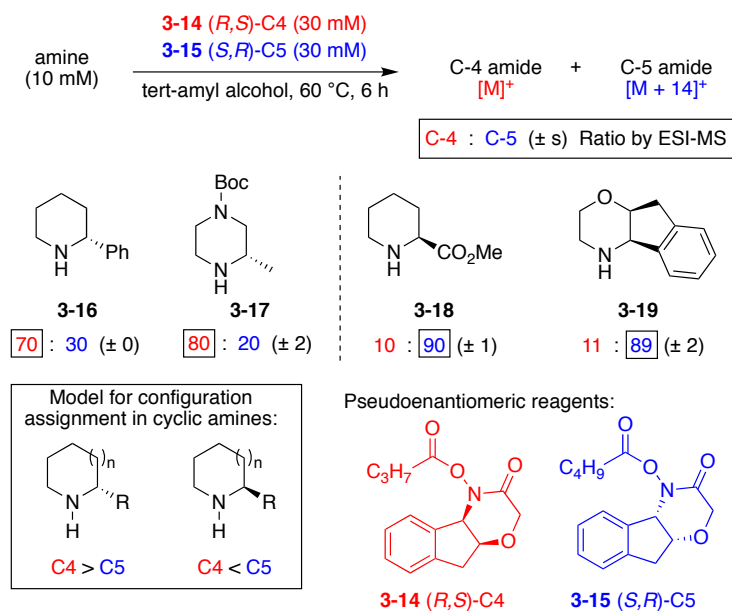


Figure 3-3 Basic CEC strategy for cyclic amines—published work with examples.

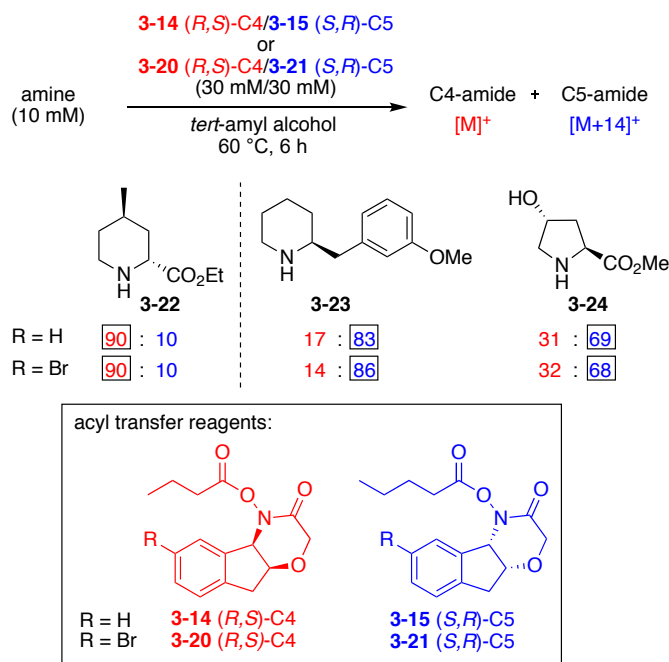
In our original report, we detailed the development of effective reaction conditions and briefly investigated the scope of the method.^{11b} However, we did not have a thorough understanding of the selectivity of the reaction or the limitations of the method. Given the mechanistic work performed by Bode and Kozłowski, the proposed mechanism for enantioselective acylation of 6-membered cyclic amines proceeds through a concerted 7-membered transition state, forcing the alpha substituent into an axial configuration.¹⁴ From this insight, one can imagine that the reaction would be either non-selective or unreactive in cases where the substituent cannot be placed in the axial position, and Bode's experimental work supports this conclusion. When I joined the project, we wanted to come to a better overall understanding of the scope and limitation of this CEC method. My work focused on expansion of substrate scope to various ring sizes, investigation of the origins of decaying selectivity through detailed kinetic modelling and control experiments, and examination of the effects of conformational preferences on the observed selectivity.

3.3 Results and Discussion

3.3.1 Brief Exploration of New Reagents and Mode of Analysis

We began our investigations by exploring a new set of reagents to optimize the selectivity for the CEC reaction. Bode has reported that brominated acyl transfer reagents **3-20** and **3-21** afford higher selectivity in the kinetic resolution of 6-membered cyclic amines.^{13c} Using previously optimized conditions for the CEC of cyclic amines,^{11b} the reaction of **3-22** and **3-23** exhibited equal selectivity with brominated and non-brominated acyl transfer reagents (Scheme 3-1). We also observed essentially identical selectivity for pyrrolidine **3-24** with both series of reagents. Our results indicate that the CEC method is equally effective with the brominated reagents. It is useful to note that the brominated hydroxamic acids are commercially available, which would make them a more suitable choice for any interested in using this methodology. However, since there was no increased selectivity with the **3-20** and **3-21**, we elected to continue using non-brominated reagents **3-14** and **3-15** for the purposes of our studies.

Scheme 3-1 Comparison of the Original and Brominated Acyl Transfer Reagents.



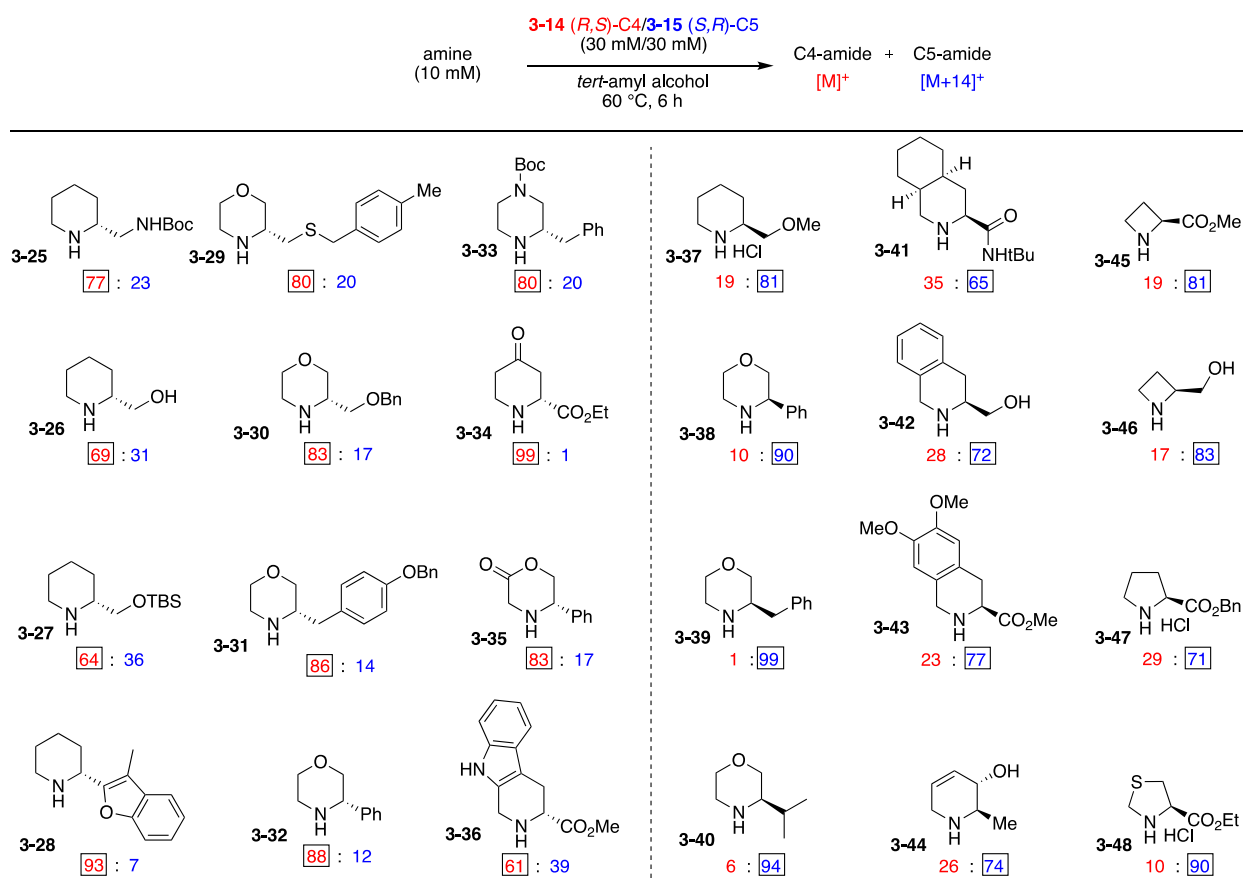
In our prior work, mass spectrometry for the CEC reactions was performed using a standard ESI-MS for simplicity and speed. However, one major drawback to this method of analysis is that at the end of the CEC reaction there are still superstoichiometric amounts of the acyl transfer reagents. These large concentrations of acyl transfer reagents can make it difficult to achieve sufficient signal of the desired compounds. More troubling is that substrates occasionally have the same molecular weight as the acyl transfer reagents, making data analysis impossible in this scenario. To circumvent this issue, we performed mass spectrometry for this work on a UPLC-QqQ-MS (see experimental section for more information). The combination of UPLC and the triple quadrupole mass analyzers allowed us to cleanly analyze the ions corresponding to the amide products without interference from the acyl transfer reagents. While this system is specialized and may not be widely available, we have also shown that standard LC-MS systems were able to achieve the same result for a series of compounds. The excess of acyl transfer reagents is quite apparent in the LC-MS trace; however, extracted ion chromatograms (EICs) can be used to easily quantify the ion count of the compound in question so long as it does not have the same molecular weight as the acyl transfer reagents.

3.3.2 *Expansion of Substrate Scope*

In our previous report, we demonstrated that the CEC method outlined above is effective for various 5-, 6-, and 7-membered cyclic amines bearing chirality alpha to the amine. Seeking to understand the scope and limitations of this method more fully, we evaluated an array of 6-membered cyclic amines (Scheme 3-2). Alkyl substituted piperidines **3-25** to **3-28** and **3-37** were evaluated and all reacted smoothly and could be assigned with confidence, even in the presence of an unprotected primary alcohol (**3-26**). Morpholines **3-29** to **3-32** and **3-38** to **3-40** also proved to be competent substrates and were assigned with good selectivity. The method was not sensitive to

other functional groups in the ring such as protected amines (**3-33**), ketones (**3-34**), esters (**3-35**) or alkenes (**3-44**). Substrate **3-36**, despite containing a potentially reactive indole, reacted with modest selectivity. The configuration of isoquinoline **3-41** and tetrahydroisoquinolones **3-42** and **3-43** were also successfully assigned using this method. Notably, piperidine **3-28**, bearing a benzofuran, reacted with excellent selectivity. Several piperidines with larger aryl groups were not selective in the CEC reaction. They are discussed later and presented in table 3-1.

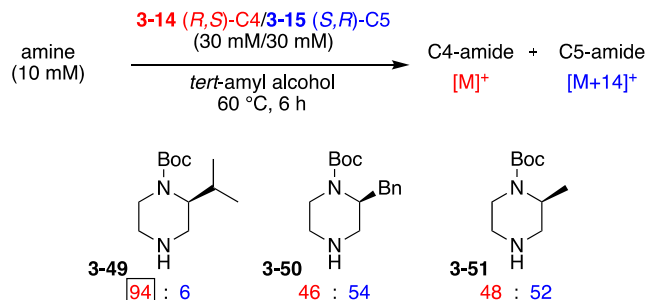
Scheme 3-2 CEC Results for Cyclic Secondary Amines.



It has been reported that acyl transfer reagents **3-14** and **3-15** are less selective in reactions with azetidines and pyrrolidines. As such, we sought to evaluate if our method would be effective for smaller ring sizes. Azetidines **3-45** and **3-46** were subjected to standard CEC conditions, and each reacted with good selectivity. Pyrrolidine **3-47** was also a competent substrate, albeit with

modest selectivity. Thiazolidine **3-48** displayed excellent selectivity, but the reaction took 48 hours and only achieved low conversion.

Scheme 3-3 CEC Results with 3-Alkyl Piperazines.

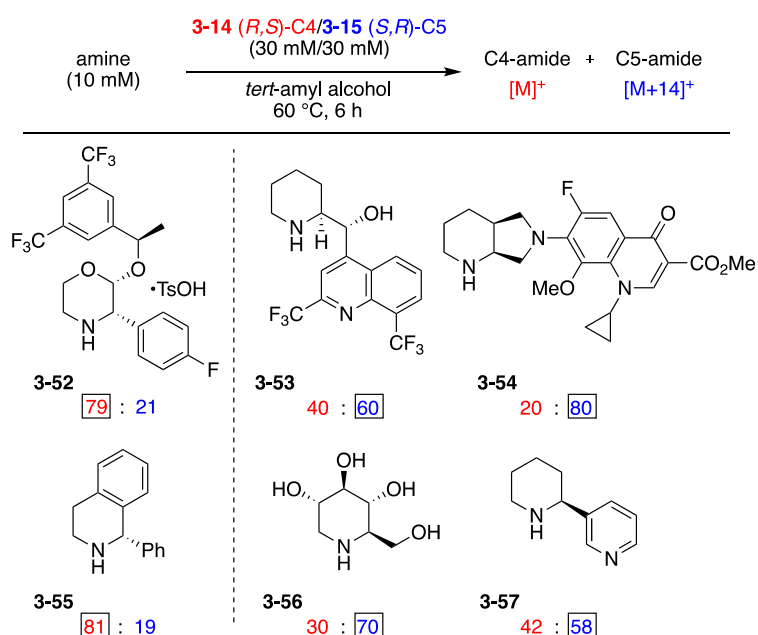


With an array of successful cases in hand, we wondered if the same selectivity would be observed with other substitution patterns. As such, *N*-Boc piperazines with 3-alkyl substituents were investigated (Scheme 3-3). Surprisingly, we found that isopropyl bearing piperazine **3-49** reacted with exquisite selectivity. This selectivity quickly proved to be unique, as **3-50** and **3-51** bearing benzyl and methyl substituents respectively displayed almost no selectivity. We speculate that in its reactive conformation, the isopropyl group in **3-49** could place a methyl group in an optimal position to influence the selectivity of the reaction, while benzyl and methyl substituents do not fill this space. Interestingly, the selectivity observed with **3-49** was at odds with the empirical model previously developed for cyclic amines.^{11b}

Following the success of the 6-membered ring substrates, we evaluated the utility of our method with biologically and medicinally relevant compounds (Scheme 3-4). Amines **3-52** and **3-55** are precursors to Aprepitant (Emend) and Solifenacin (Vesicare) respectively, and their configurations were successfully assigned with good selectivity. The configuration of Mefloquine (**3-53**) was also assigned successfully, but with diminished selectivity. This result is interesting, as Bode has previously reported a kinetic resolution of this compound with superior selectivity.^{13e} The methyl ester of Moxifloxacin (**3-54**), an antibiotic used to treat a number of bacterial

infections, also displayed good selectivity with our method. Finally, the stereocenter adjacent to the amine in the natural product 1-deoxynojirimycin (**3-56**) was successfully assigned by CEC. Anabasine (**3-57**) exhibits low levels of selectivity in the expected direction, despite having a similar A-value with substrate **3-32**; we consider the CEC method unreliable in this case. Ritalin hydrochloride, as well as the free amine were also tested, but lead to very low selectivity and could not be assigned using this method.

Scheme 3-4 CEC examples with clinically relevant cyclic amines.



3.3.3 Examination of Degrading Selectivity in the CEC Reaction

During the course of our studies, we noticed reactions that were allowed to reach high conversion (>70%) frequently resulted in lower levels of selectivity than those which proceeded to lower conversion (<70%). The CEC method was designed to be pseudo-first order with respect to the amine substrate, and the 1:3:3 ratio of amine to each acyl transfer reagent was previously shown to be effective.^{11b} However, the ratio is too low to be truly pseudo-first order. We

investigated the reduced selectivity because it seemed more significant than we would expect if it were simply a concentration effect.

To determine the underlying cause of this phenomenon, control experiments were performed in which the reaction of (*S*)-3-methylmorpholine (**3-58**) was quenched at different time points, and the selectivity and conversion were assayed. The results are summarized in Figure 3-2. At low conversion, the selectivity of the reaction was high, but the selectivity slowly faded as the reaction progressed. Hypothesizing that the change in concentration of acyl transfer reagents during the course of the reaction may play a key role, the CEC reaction was simulated using COPASI.¹⁵ Consistent with the mechanism proposed by Bode, we simulated the data on the assumption that the reaction of each pseudoenantiomer of acyl transfer reagent with the amine is a concerted, second order reaction. The rate constant (*k*) for the reaction of **3-14** was set to be nine times that of the reaction of **3-15**, in accord with the experimental result observed at 17% conversion (Figure 3-2). The initial concentrations were set to reflect the experimental CEC conditions, and the simulated data and ratio of C4 amide to C5 amide is shown below. The changing concentrations of acyl transfer reagents, based on these calculations, is likely to be a contributing factor, but the simulated data does not display a decrease large enough to be consistent with the experimental data.

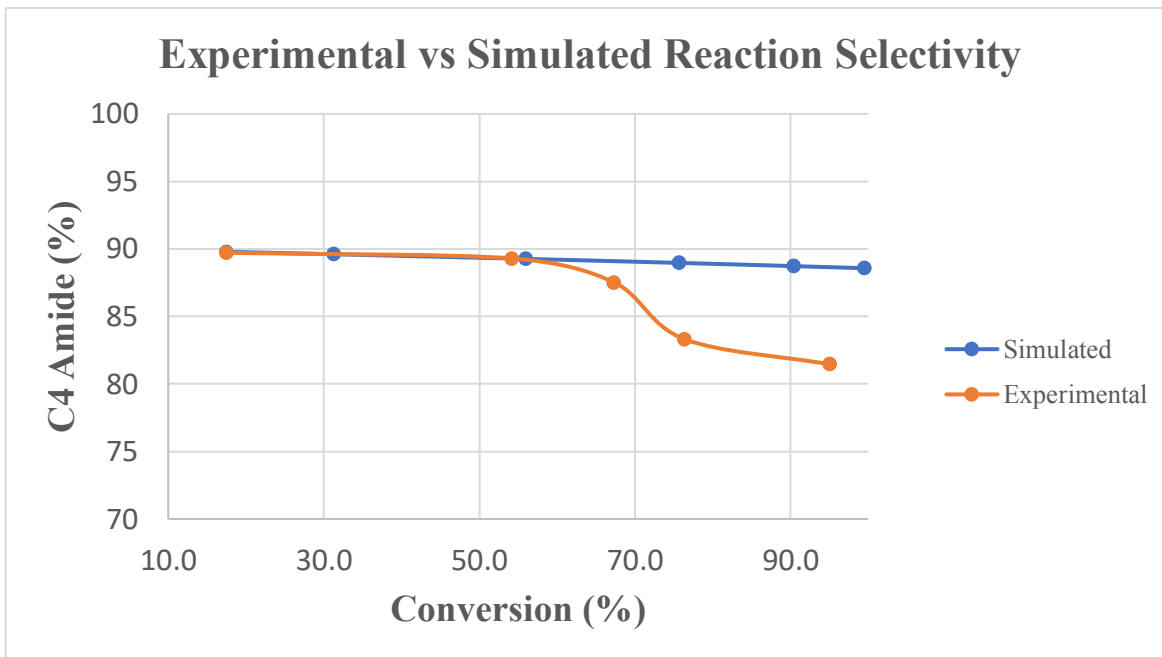
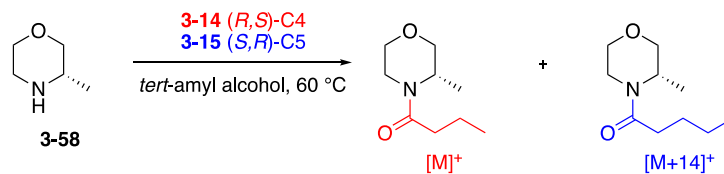
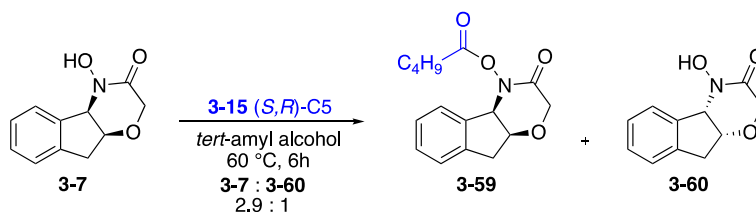


Figure 3-4 Acylation reaction and plot of experimental and simulated CEC kinetic data for **3-58**.

Mechanistically, the acyl transfer to the amine must generate the corresponding hydroxamic acid. At low conversion this concentration will be negligible, but at high conversion, there is close to one equivalent of combined enantiomeric hydroxamic acids in solution. A possible complication is acyl transfer between the hydroxamic acid and the acylated hydroxamic acid. For example, if (*R,S*)-hydroxamic acid **3-7** were acylated by **3-15** (*S,R*)-**C5**, it would generate **3-59** (*R,S*)-**C5**. In reaction with **3-58**, this enantiomeric acyl transfer reagent reacts faster than **3-15** (*S,R*)-**C5**. A buildup of **3-59** during the course of the reaction could artificially inflate the amount of C5 amide observed, leading to a lower ratio of C4/C5 amides. To test this hypothesis, we performed a crossover experiment to determine if acyl transfer is possible under the reaction conditions (Scheme 3-5).

Scheme 3-5 Hydroxamic Acid Crossover Experiment.



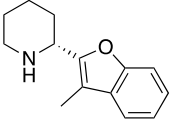
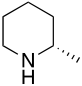
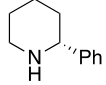
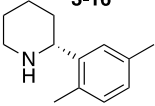
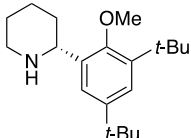
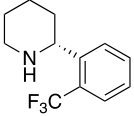
(*R,S*)-Hydroxamic acid **3-7** was mixed with an equimolar amount of **3-15** and was diluted to 30 mM in *tert*-amyl alcohol. This mixture was heated to 60 °C for 6 hours to simulate the CEC reaction conditions, and subsequently an aliquot was diluted and subjected to HPLC analysis. Consistent with acyl transfer, **3-7** and **3-60** were observed in a 2.9:1 ratio. Unfortunately, it is impossible to tell if this ratio reflects an equilibrium concentration, or simply a mid-point in the reaction. We attempted to use the results of this experiment to modify our COPASI simulations of the kinetic data for reaction of **3-58** by adding an additional acyl scrambling event in the series of reactions. However, the rate constant for this crossover had to be set equal to the rate of reaction of **3-58** with the matched pseudoenantiomer **3-14** for the simulated data to come close to the selectivity decay observed. While we could not directly quantify the effect of acyl crossover between enantiomeric hydroxamic acids **3-7** and **3-60**, we have shown that the change in concentration over the reaction course, in addition to a slow scrambling of the acyl groups accounts for some of the declining selectivity observed with long reaction times.

3.3.4 Effect of Conformation on the CEC Selectivity

With experimental results from an array of substrates, we became interested in systematically studying the effect of the size of substituents on the CEC reactivity. In Scheme 3-2, piperidine **3-28** was observed to react with excellent selectivity, giving a 93:7 ratio of C4 to C5 amides. However, we previously reported that a substrate with a similarly sized substituent (**3-16**) was assigned with a 70:30 ratio of C4 to C5 amides. In accord with the reactive conformation

proposed by Bode and Kozlowski,¹⁴ the 2-substituent and the proton on the nitrogen will adopt axial orientations during the acyl transfer. This conformation places an upper limit on the size of substituents which can be tolerated in the CEC reaction. To probe this, I performed CEC reactions with an array of arylated piperidines, which were graciously provided through collaboration with Dr. Bo Qu. After obtaining experimental results, Professor Rychnovsky then calculated the conformational energies for several of the substrates. Results are summarized in table 3-1.

Table 3-1 Selectivity and conversion data with calculated axial conformation energy.^a

cyclic amine	conversion (%)	amide ratio	C2 and N-H axial kcal/mol	Min C2 axial kcal/mol
 3-28	94	93 : 7	1.35	1.35
 3-61	—	78 : 22	2.32	2.14
 3-16	—	70 : 30	2.60	2.60
 3-62	24	45 : 55	3.96	3.96
 3-63	19	42 : 58	4.28	4.28
 3-64	0 ^b	0 : 0	6.51	5.56

^a Calculations were carried out using Spartan 18. Conformations were searched using MMFF force field, and low energy conformers were optimized using wB97xd/6-31G(d). The conformational energies in columns 4 and 5 are relative to the lowest energy conformation for each compound, which in all cases had the C2 substituent equatorial. Calculations were also carried out in Gaussian 16 and include solvation and free energy corrections; the conformational energies change some but the ordering and rationale for selectivity does not. ^b Determined by the insignificant ion counts of the C4 and C5 amides compared to the C3 amide.

Larger substituents lead to higher relative energies for the axial conformations. For piperidine **3-28**, the first conformation that places both the proton and substituent axial (column 4) occurred at a relative conformational energy of 1.35 kcal/mol. Additionally, this conformer also represents the lowest energy conformation that placed the aryl substituent axial (column 5).¹⁶ With respect to the previously reported piperidine **3-16**, the lowest energy axial conformation occurred at 2.60 kcal/mol. The difference in energy between **3-28** and **3-16** likely explains the variance in selectivity observed between these two substrates. Compound **3-61**, which was also reported in our prior work, had a lowest energy axial conformation at 2.14 kcal/mol, while the lowest energy conformation that places both the proton and methyl groups axial was 2.32 kcal/mol. The selectivity observed for this substrate fell nicely in the middle of **3-28** and **3-16**, corroborating the trend. We have observed that as the relative energy increases, both selectivity and reaction conversion will dramatically decrease (Table 3-1). As energies increase towards 4 kcal/mol (**3-62** and **3-63**) the reaction is no longer selective, and reaction conversion diminishes. As energies reach beyond 6 kcal/mol (**3-64**) the reaction does not proceed at all. Based upon the observed data from these substrates, we posit that if the substituent requires a relative energy around 3 kcal/mol or greater to adopt an axial conformation, then the CEC reaction is unlikely to be successful. This conformational energy requirement represents a limitation of the CEC method.

3.4 Conclusions

We have shown that the CEC method is a useful tool for the assigning absolute configuration of secondary cyclic amines and have extended the scope of the original method. Control experiments have helped to clarify the reaction profile and make sense of a slow erosion in selectivity at long reaction times. The Bode and Kozlowski model requires the C2 substituent and the proton on nitrogen to occupy axial positions in the reactive conformation for cyclic six-

membered amines. Our experimental and modeling results support this model and suggest an upper limit on the conformational energy for effective CEC reaction (and kinetic resolution) using these Bode acyl transfer reagents. The present study expands the scope of the CEC method for cyclic secondary amines and provides a better understanding for predicting and analyzing these enantioselective acyl transfer reactions.

3.5 Acknowledgements and Contributions

I would like to thank all my co-authors on this work. First, Dr. Burtea brought me onto the project when the project discussed in chapter 2 started failing. He showed me how to perform the reactions and put together the collaborations. I would also like to thank him and his undergraduate student Christina Mitilian for performing several of the CEC reactions in Schemes 3-1 and 3-2. Dr. Bo Qu provided enantiopure protected piperidines for analysis. Wendy Dao from the group of Professor Nick Salzameda synthesized the morpholine substrates. I have only included the synthesis of compounds which I made. The synthesis of the remainder of the compounds, as well as copies of all the spectroscopic data, can be found in our publication.¹⁷ I would also like to thank Dr. Felix Grun and Ben Katz for help with the mass spectrometry.

3.6 Supporting Information

3.6.1 General Experimental Details

Unless otherwise stated, synthetic reactions were carried out in flame- or oven-dried glassware under an atmosphere of argon. All CEC reactions were carried out under air, in 700 μ L amber mass spectrometry vials pre-loaded with 3 μ mol of each acyl transfer reagent. All commercially available reagents were used as received unless stated otherwise. Solvents were purchased as ACS grade or better and as HPLC-grade and passed through a solvent purification system equipped with activated alumina columns prior to use. Thin layer chromatography (TLC)

was carried out using glass plates coated with a 250 μm layer of 60 \AA silica gel. TLC plates were visualized with a UV lamp at 254 nm, or by staining with *p*-anisaldehyde, potassium permanganate, phosphomolybdic acid, or vanillin. Liquid chromatography was performed using forced flow (flash chromatography) with an automated purification system on prepacked silica gel (SiO_2) columns.

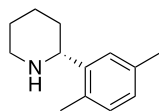
All volumetric glassware and NMR tubes were oven-dried prior to use. The ^1H NMR and $^{13}\text{C}\{^1\text{H}\}$ and spectra were recorded at 298.0 K unless stated otherwise. Chemical shifts (δ) were referenced to the residual solvent peak (7.26 ppm for CHCl_3) for ^1H NMR, and CDCl_3 (77.16 ppm) for $^{13}\text{C}\{^1\text{H}\}$ NMR. The ^1H NMR spectra data are presented as follows: chemical shift, multiplicity (s = singlet, d = doublet, t = triplet, q = quartet, p = pentet, sex = sextet, oct = octet, m = multiplet, app. = apparent, br. = broad), coupling constant(s) in hertz (Hz), and integration. Optical rotations were performed on a JACSO P-1010 spectrometer using a glass 50 mm cell with a D-line at 589 nm. High-resolution mass spectrometry was performed using ESI-TOF. Mass spectrometry for CEC reactions was performed on a UPLC-QqQ-MS system using an Acquity UPLC and a Quattro Premier XE QqQ-MS mass analyzer. LC-MS was performed using a Waters Acquity QDA UPLC-MS system.

3.6.2 *Chemicals*

All purchased chemicals were used without further purification unless otherwise noted. CDCl_3 was purchased from Cambridge Isotope Laboratories. UPLC grade water and MeCN were purchased from Fisher. Compounds **3-14**,^{13b} **3-15**,^{13b} **3-20**,^{13c} **3-21**,^{13c} **3-27**,¹⁸ **3-43**,¹⁹ and **3-54**²⁰ were synthesized according to known literature procedures. All piperidines were benzyl protected when acquired and were debenzylated for CEC analysis. All morpholines were synthesized according to a known preparation.²¹ All other compounds were purchased commercially.

General Procedure 1: Debenzylation of Piperidines

Benzylated piperidine and Pd/C (5 or 10 wt%, 0.5 equiv.) were suspended in either ethyl acetate, absolute ethanol, or a mixture of the two. Aqueous HCl (1 or 2 M, 1.2-1.5 equiv.) was added, and the mixture was sparged with hydrogen for 10 min. The mixture was then allowed to stir under an atmosphere of hydrogen until the reaction was complete as monitored by ESI-MS. Upon completion, the reaction mixture was filtered through a pad of Celite, and aqueous NaOH was added to free base the piperidine. The organic phase was separated, and the aqueous phase was extracted with ethyl acetate. The combined organic layers were dried over anhydrous sodium sulfate and concentrated *in vacuo*. Products were purified by flash chromatography on silica gel (0–10% MeOH in CH₂Cl₂).



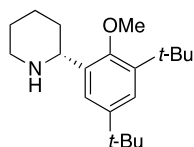
(R)-2-(2,4-dimethylphenyl)piperidine (3-62): Following general procedure 1, benzylated piperidine (58.7 mg, 0.210 mmol) and 10% Pd/C (111.8 mg, 0.105 mmol) were suspended in ethyl acetate (2.10 mL), and 2 M HCl (0.15 mL) was added. Subsequently, the mixture was sparged with hydrogen for 10 minutes, and was allowed to stir under hydrogen atmosphere for 36 hours. Upon completion of the reaction as monitored by ESI-MS, the mixture was filtered through a pad of Celite. Subsequently 1 M NaOH (3 mL) was added and the mixture was stirred for 20 minutes. The organic layer was separated, and the aqueous phase was extracted with ethyl acetate (3 x 5 mL). The product was isolated as stated to afford **3-62** as a yellow oil (21.3 mg, 54% yield).

¹H NMR (500 MHz, CDCl₃) δ 7.41 (d, *J* = 7.9 Hz, 1H), 7.01 (d, *J* = 7.9 Hz, 1H), 6.95 (s, 1H), 3.76 (d, *J* = 10.5 Hz, 1H), 3.21 (d, *J* = 11.6 Hz, 1H), 2.81 (dt, *J* = 11.7, 2.6 Hz, 1H), 2.29 (s, 3H), 1.89 (d, *J* = 11.9 Hz, 1H), 1.78–1.64 (m, 3H), 1.62–1.41 (m, 3H).

$^{13}\text{C}\{^1\text{H}\}$ NMR (126 MHz, CDCl_3) δ 140.7, 136.1, 134.7, 131.1, 127.0, 125.9, 58.1, 48.3, 34.0, 26.2, 25.8, 21.0, 19.2.

HRMS (ESI-TOF) m/z calcd for $\text{C}_{13}\text{H}_{19}\text{NH}$ ($\text{M} + \text{H}$) $^+$: 190.1591, found 190.1591.

$[\alpha]^{22}_{\text{D}} = +68.9$ (c 2.13, CDCl_3).



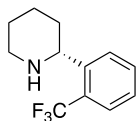
(R)-2-(3,5-di-tert-butyl-2-methoxyphenyl)piperidine (3-63): Following general procedure 1, benzylated piperidine (41.5 mg, 0.105 mmol) and 10% Pd/C (56.1 mg, 0.053 mmol) were suspended in ethanol (0.8 mL) and ethyl acetate (0.26 mL), and 2 M HCl (0.08 mL) was added. The product was isolated as stated to afford **3-63** as a white sticky solid (17.9 mg, 56%).

^1H NMR (500 MHz, CDCl_3) δ 7.36 (d, $J = 2.5$ Hz, 1H), 7.24 (d, $J = 2.6$ Hz, 1H), 3.95 (dd, $J = 10.6, 2.3$ Hz, 1H), 3.22 – 3.16 (m, 1H), 2.83 (td, $J = 11.6, 2.9$ Hz, 1H), 1.95 – 1.88 (m, 1H), 1.80 – 1.71 (m, 2H), 1.69 – 1.64 (m, 1H), 1.63 – 1.52 (m, 2H), 1.40 (s, 9H), 1.31 (s, 9H).

$^{13}\text{C}\{^1\text{H}\}$ NMR (126 MHz, CDCl_3) δ 154.8, 146.0, 141.5, 137.9, 123.1, 63.0, 56.0, 48.5, 35.5, 34.8, 34.5, 31.7, 31.4, 26.3, 26.0.

HRMS (ESI-TOF) m/z calcd for $\text{C}_{20}\text{H}_{33}\text{NOH}$ ($\text{M} + \text{H}$) $^+$: 304.2635, found 304.2628.

$[\alpha]^{22}_{\text{D}} = +34.8$ (c 1.79, CDCl_3).



(R)-2-(2-trifluoromethylphenyl)piperidine (3-64): Following general procedure 1, benzylated piperidine (67.2 mg, 0.210 mmol) and 10% Pd/C (112 mg, 0.105 mmol) were suspended in ethanol

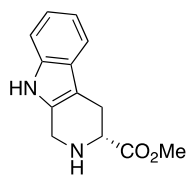
(1.6 mL) and ethyl acetate (0.53 mL), and 2 M HCl (0.15 mL) was added. The product was isolated as stated to afford **3-64** as a yellow oil (34.7 mg, 72%).

$^1\text{H NMR}$ (600 MHz, Chloroform-*d*) δ 7.85 (d, $J = 7.9$ Hz, 1H), 7.60 (d, $J = 7.9$ Hz, 1H), 7.52 (t, $J = 7.6$ Hz, 1H), 7.32 (t, $J = 7.6$ Hz, 1H), 3.98 (app. d, $J = 9.3$ Hz, 1H), 3.18 (app. d, $J = 11.4$ Hz, 1H), 2.83 (td, $J = 11.7, 2.6$ Hz, 1H), 2.01 (s, 1H), 1.92 – 1.83 (m, 1H), 1.81 – 1.74 (m, 1H), 1.71 – 1.65 (m, 1H), 1.59 (qt, $J = 12.3, 4.0$ Hz, 1H), 1.54 – 1.45 (m, 2H).

$^{13}\text{C}\{^1\text{H}\}$ NMR (151 MHz, CDCl_3) δ 144.4, 132.2, 128.9, 127.6 (q, $J = 29.5$ Hz), 127.0, 125.5 (q, $J = 5.9$ Hz), 124.7 (q, $J = 273.7$ Hz), 77.2, 57.8, 48.0, 34.9, 25.8, 25.5.

HRMS (ESI-TOF) m/z calcd for $\text{C}_{12}\text{H}_{14}\text{F}_3\text{NH}$ ($\text{M} + \text{H}$) $^+$: 230.1152, found 230.1149.

$[\alpha]^{22}_{\text{D}} = +50.9$ (c 3.47, CDCl_3).



Methyl (R)-2,3,4,9-tetrahydro-1H-pyrido[3,4-b]indole-3-carboxylate (3-36): (*R*)-2,3,4,9-tetrahydro-1H-pyrido[3,4-*b*]indole-3-carboxylic acid (30 mg, 0.14 mmol) was dissolved in methanol (1.4 mL), and thionyl chloride (15 μl , 0.21 mmol) was added. The mixture was heated to 80 $^{\circ}\text{C}$ for 2 h and was then evaporated *in vacuo*. The amine salt was suspended between a mixture of CH_2Cl_2 (1 mL) and saturated aq. NaHCO_3 (1 mL). The aqueous layer was extracted with CH_2Cl_2 (3 x 1 mL) and the combined organic layers were dried over MgSO_4 , and concentrated *in vacuo* to afford analytically pure **3-36** (26 mg, 80%).

$^1\text{H NMR}$ (500 MHz, CDCl_3) δ 8.03 (s, 1H), 7.47 (dd, $J = 7.6, 1.3$ Hz, 1H), 7.27 (dd, $J = 8.1, 1.0$ Hz, 1H), 7.15 (dd, $J = 8.1, 1.4$ Hz, 1H), 7.10 (td, $J = 7.4, 1.1$ Hz, 1H), 4.13–4.03 (m, 2H), 3.83–3.75 (m, 4H), 3.13 (dd, $J = 15.3, 1.2$ Hz, 1H), 2.90 (ddt, $J = 15.3, 9.6, 1.9$ Hz, 1H), 2.19 (s, 1H).

$^{13}\text{C}\{\text{1H}\}$ NMR (125 MHz, CDCl_3) δ 173.9, 136.1, 132.1, 127.3, 121.8, 119.6, 117.9, 110.9, 107.5, 56.0, 52.3, 42.2, 25.5.

HRMS (ESI-TOF) m/z calcd for $\text{C}_{13}\text{H}_{14}\text{N}_2\text{O}_2\text{H}$ ($\text{M} + \text{H}$) $^+$: 231.1129, found 231.1130.

$[\alpha]^{22}_{\text{D}} = +68.3$ (c 4.60, CHCl_3).

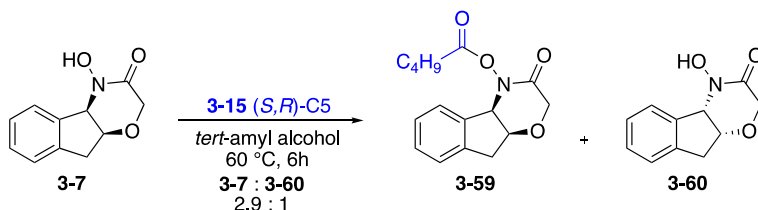
General Procedure 2: CEC Reactions

The amine was weighed into a volumetric flask and diluted to volume with methanol to make a 200 mM amine stock solution. This solution was subsequently diluted with *tert*-amyl alcohol to make a 10 mM stock solution for CEC reactions. 100 μl (1 μmol) of this solution was added to an amber mass spectrometry vial which had been pre-weighed with 3 μmol of each acyl transfer reagent, and the vial was sealed with an aluminum cap and shaken lightly to mix the contents. If the amine substrate was a salt, Et_3N (1 μL) was added to liberate the free amine *in situ*. The mixture was allowed to stand for the designated amount of time, at the designated temperature, after which time the cap was removed and 100 equivalents of propionic anhydride were added. The mixture was allowed to stand for 15 min, after which time the contents of the vial were pipetted into a dram vial.

For analysis, 3 μl of the CEC reaction mixture was diluted to 3 mL with 30% MeCN/ H_2O (UPLC grade solvents) to make a 10 μM stock solution. This solution was diluted to 1 μM and 3 μM in LC-MS vials, and the 1 μM , 3 μM , and 10 μM solutions were subjected to mass spectrometry analysis using an optimized method on a UPLC-QqQ-MS. Samples were subjected to UPLC using an Acquity UPLC system equipped with a C18 column eluting with a gradient of MeCN with 0.2% acetic acid (A1 buffer) in a mixture of 98:1.8:0.2 H_2O :MeCN:acetic acid (B1 buffer) from 10–90% of A1 buffer/B1 buffer. This system was coupled to a Quattro Premier XE QqQ MS using a learning method, allowing the user to input the expected ionic masses in each

sample. The instrument then optimizes itself to look for the desired mass transition through the QqQ.

As proof of concept, analysis was also performed for substrate **3-32**, **3-38**, and **3-43** using a Waters Acquity QDA UPLC-MS system. For analysis, 5 μL of the CEC reaction mixture was diluted to 1 mL with 10% $\text{H}_2\text{O}/\text{MeCN}$ (UPLC grade solvents) to make a 50 μM mass spectrometry sample. Samples were subjected to UPLC using a Waters Acquity UPLC system equipped with a C4 column eluting with a gradient from 0-100% $\text{MeCN}/\text{H}_2\text{O}$ + 0.1% formic acid. The TIC chromatogram was then used to prepare extracted ion chromatograms (EICs) for the $[\text{M} + \text{H}]^+$ peak of the C3, C4, and C5 amides in question. Data for these substrates is reported in the SI, and is in excellent agreement with the data from the UPLC-QqQ-MS.



Hydroxamic acid crossover experiment: (4*aS*,9*aR*)-3-oxo-2,3,9,9*a*-tetrahydroindeno[2,1-*b*][1,4]oxazin-4(4*aH*)-yl pentanoate (**3-15 (S,R)-C5**) (5.3 mg, 0.018 mmol) and (4*aR*,9*aS*)-4-hydroxy-4,4*a*,9,9*a*-tetrahydroindeno[2,1-*b*][1,4]oxazin-3(2*H*)-one (**3-7**) (3.8 mg, 0.018 mmol) were added to a dram vial equipped with a stir bar and *t*-amyl alcohol (0.6 mL, 0.03 M) was added. The mixture was heated to 60 $^\circ\text{C}$ for 6 h to replicate the CEC reaction conditions. The reaction mixture was cooled to room temperature, and a 240 μL aliquot was diluted to 2 mL with a solution of 10% *i*PrOH/Hexanes (both HPLC grade). This mixture was characterized by HPLC using a Chiralcel AD column (w/o guard) eluting with 15% *i*PrOH/Hexanes with a flow rate of 1.0

mL/min. The two hydroxamic acids were observed as a 2.9:1 ratio of **3-7** : **3-60**. HPLC traces can be found in our publication.¹⁶

3.7 References

¹ For reviews, see: (a) Crossley, S. W. M.; Shenvi, R. A. A Longitudinal Study of Alkaloid Synthesis Reveals Functional Group Interconversions as Bad Actors. *Chem. Rev.* **2015**, *115*, 9465–9531. (b) Wang, D.-S.; Chen, Q.-A.; Lu, S.-M.; Zhou, Y.-G. Asymmetric Hydrogenation of Heteroarenes and Arenes. *Chem. Rev.* **2012**, *112*, 2557–2590. (c) Chrzanowska, M.; Grajewska, A.; Rozwadowska, M. D. Asymmetric Synthesis of Isoquinoline Alkaloids: 2004–2015. *Chem. Rev.* **2016**, *116*, 12369–12465. (d) Mailyan, A. K.; Eickhoff, J. A.; Minakova, A. S.; Gu, Z.; Lu, P.; Zakarian, A. Cutting-Edge and Time-Honored Strategies for Stereoselective Construction of C–N Bonds in Total Synthesis. *Chem. Rev.* **2016**, *116*, 4441–4557. (e) Race, N. J.; Faulkner, A.; Fumagalli, G.; Yamauchi, T.; Scott, J. S.; Rydén-Landergren, M.; Sparkes, H. A.; Bower, J. F. Enantioselective Narasaka–Heck Cyclizations: Synthesis of Tetrasubstituted Nitrogen-Bearing Stereocenters. *Chem. Sci.* **2017**, *8* (3), 1981–1985. (f) Muthukrishnan, I.; Sridharan, V.; Menéndez, J. C. Progress in the Chemistry of Tetrahydroquinolines. *Chem. Rev.* **2019**, *119*, 5057–5191. (g) Xie, J.-H.; Zhu, S.-F.; Zhou, Q.-L. Transition Metal-Catalyzed Enantioselective Hydrogenation of Enamines and Imines. *Chem. Rev.* **2011**, *111*, 1713–1760.

² (a) Lattanzi, A.; Scettri, A.; Zanasi, R.; Devlin, F. J.; Stephens, P. J. Absolute Configuration Assignment of Norcamphor-Derived Furyl Hydroperoxide Using Density Functional Theory Calculations of Optical Rotation and Vibrational Circular Dichroism. *J. Org. Chem.* **2010**, *75*, 2179–2188. (b) Stephens, P. J.; Devlin, F. J.; Cheeseman, J. R.; Frisch, M. J.; Rosini, C. Determination of Absolute Configuration Using Optical Rotation Calculated Using Density Functional Theory. *Org. Lett.* **2002**, *4*, 4595–4598. (c) Stephens, P. J.; Pan, J. J.; Devlin, F. J.; Krohn, K.; Kurtán, T. Determination of the Absolute Configurations of Natural Products via Density Functional Theory Calculations of Vibrational Circular Dichroism, Electronic Circular Dichroism, and Optical Rotation: The Iridoids Plumericin and Isoplumericin. *J. Org. Chem.* **2007**, *72*, 3521–3536.

³ (a) Seco, J. M.; Quinoa, E.; Riguera, R. Assignment of the Absolute Configuration of Polyfunctional Compounds by NMR Using Chiral Derivatizing Agents. *Chem. Rev.* **2012**, *112*, 4603–4641. (b) Wenzel, T. J.; Chisholm, C. D. Assignment of Absolute Configuration Using Chiral Reagents and NMR Spectroscopy. *Chirality* **2011**, *23*, 190–214. (c) Seco, J. M.; Quinoa, E.; Riguera, R. The Assignment of Absolute Configuration by NMR. *Chem. Rev.* **2004**, *104*,

17–118. (d) Dale, J. A.; Mosher, H. S. Nuclear Magnetic Resonance Enantiomer Reagents. Configurational Correlations via Nuclear Magnetic Resonance Chemical Shifts of Diastereomeric Mandelate, *O*-Methylmandelate, and α -Methoxy- α -Trifluoromethylphenylacetate (MTPA) Esters. *J. Am. Chem. Soc.* **1973**, *95*, 512–519. (e) Ohtani, I.; Kusumi, T.; Kashman, Y.; Kakisawa, H. High-Field FT NMR Application of Mosher Method – the Absolute Configurations of Marine Terpenoids. *J. Am. Chem. Soc.* **1991**, *113*, 4092–4096. (f) Hoye, T. R.; Renner, M. K. Applications of MTPA (Mosher) Amides of Secondary Amines: Assignment of Absolute Configuration in Chiral Cyclic Amines. *J. Org. Chem.* **1996**, *61*, 8489–8495. (g) Hoye, T. R.; Jeffrey, C. S.; Shao, F. Mosher Ester Analysis for the Determination of Absolute Configuration of Stereogenic (Chiral) Carbinol Carbons. *Nat. Protoc.* **2007**, *2*, 2451–2458.

⁴ (a) Petrovic, A. G.; Berova, N.; Alonso-Gomez, J. L. Absolute Configuration and Conformational Analysis of Chiral Compounds via Experimental and Theoretical Prediction of Chiroptical Properties: ORD, ECD, and VCD. In *Structure Elucidation in Organic Chemistry*; Cid, M. Bravo, J., Eds.; Wiley-VCH: Weinheim, Germany, 2015; pp 65–104. (b) Merten, C.; Golub, T. P.; Kreienborg, N. M. Absolute Configurations of Synthetic Molecular Scaffolds From Vibrational CD Spectroscopy. *J. Org. Chem.* **2019**, *84*, 8797–8814. (c) Pescitelli, G.; Bruhn, T. Good Computational Practice in the Assignment of Absolute Configurations by TDDFT Calculations of ECD Spectra. *Chirality* **2016**, *28*, 466–474.

⁵ Maier, M. E. Structural Revisions of Natural Products by Total Synthesis. *Nat. Prod. Rep.* **2009**, *26*, 1105–1124.

⁶ Wagner, A. J.; David, J. G.; Rychnovsky, S. D. Determination of Absolute Configuration Using Kinetic Resolution Catalysts. *Org. Lett.* **2011**, *13*, 4470–4473.

⁷ (a) Horeau, A. Principe et applications d'une nouvelle methode de determination des configurations dite "par dedoublement partiel". *Tetrahedron Lett.* **1961**, *2*, 506–512. (b) Schoofs, A.; Horeau, A. Nouvelle methode generale de determination de la purete enantiomerique et de la configuration absolue des alcools secondaires chiraux. *Tetrahedron Lett.* **1977**, *18*, 3259–3262. (c) Horeau, A.; Nouaille, A. Micromethode de determination de la configuration des alcools secondaires par dedoublement cinetique. Emploi de la spectrographie de masse. *Tetrahedron Lett.* **1990**, *31*, 2707–2710. For an excellent review, see: (d) Harned, A. M. From determination of enantiopurity to the construction of complex molecules: The Horeau principle and its application in synthesis. *Tetrahedron* **2018**, *74*, 3797–3841.

- ⁸ (a) Wagner, A. J.; Miller, S. M.; King, R. P.; Rychnovsky, S. D. Nanomole-Scale Assignment and One-Use Kits for Determining the Absolute Configuration of Secondary Alcohols. *J. Org. Chem.* **2016**, *81*, 6253–6265. (b) Brito, G. A.; Della-Felice, F.; Luo, G.; Burns, A. S.; Pilli, R. A.; Rychnovsky, S. D.; Krische, M. J. Catalytic Enantioselective Allylations of Acetylenic Aldehydes via 2-Propanol-Mediated Reductive Coupling. *Org. Lett.* **2018**, *20*, 4144–4147. (c) Burns, A. S.; Ross, C. C.; Rychnovsky, S. D. Heteroatom-Directed Acylation of Secondary Alcohols To Assign Absolute Configuration. *J. Org. Chem.* **2018**, *83*, 2504–2515.
- ⁹ Burns, A. S.; Wagner, A. J.; Fulton, J. L.; Young, K.; Zakarian, A.; Rychnovsky, Scott. D. Determination of the Absolute Configuration of β -Chiral Primary Alcohols Using the Competing Enantioselective Conversion Method. *Org. Lett.* **2017**, *19*, 2953–2956.
- ¹⁰ Perry, M. A.; Trinidad, J. V.; Rychnovsky, S. D. Absolute Configuration of Lactams and Oxazolidinones Using Kinetic Resolution Catalysts. *Org. Lett.* **2013**, *15*, 472–475.
- ¹¹ (a) Miller, S. M.; Samame, R. A.; Rychnovsky, S. D. Nanomole-Scale Assignment of Configuration for Primary Amines Using a Kinetic Resolution Strategy. *J. Am. Chem. Soc.* **2012**, *134*, 20318–20321. (b) Burtea, A.; Rychnovsky, S. D. Determination of the Absolute Configuration of Cyclic Amines with Bode's Chiral Hydroxamic Esters Using the Competing Enantioselective Conversion Method. *Org. Lett.* **2017**, *19*, 4195–4198.
- ¹² (a) Arseniyadis, S.; Valleix, A.; Wagner, A.; Mioskowski, C. Kinetic Resolution of Amines: A Highly Enantioselective and Chemoselective Acetylating Agent with a Unique Solvent-Induced Reversal of Stereoselectivity. *Angew. Chem. Int. Ed.* **2004**, *43*, 3314–3317. (b) Arseniyadis, S.; Subhash, P. V.; Valleix, A.; Mathew, S. P.; Blackmond, D. G.; Wagner, A.; Mioskowski, C. Tuning the Enantioselective N-Acylation of Racemic Amines: A Spectacular Salt Effect. *J. Am. Chem. Soc.* **2005**, *127*, 6138–6139. (c) Arseniyadis, S.; Subhash, P. V.; Valleix, A.; Wagner, A.; Mioskowski, C. Unprecedented, Fully Recyclable, Solid-Supported Reagent for the Kinetic Resolution of Racemic Amines through Enantioselective N-Acylation. *Chem. Commun.* **2005**, 3310–3312. (d) Sabot, C.; Subhash, P. V.; Valleix, A.; Arseniyadis, S.; Mioskowski, C. Nonenzymatic Kinetic Resolution of Amines in Ionic Liquids. *Synlett* **2008**, 268–272.
- ¹³ (a) Kreituss, I.; Bode, J. W. Catalytic Kinetic Resolution of Saturated N-Heterocycles by Enantioselective Amidation with Chiral Hydroxamic Acids. *Acc. Chem. Res.* **2016**, *49*, 2807–2821. (b) Binanzer, M.; Hsieh, S.-Y.; Bode, J. W. Catalytic Kinetic Resolution of Cyclic Secondary Amines. *J. Am. Chem. Soc.* **2011**, *133*, 19698–19701. (c) Hsieh, S.-Y.; Binanzer, M.; Kreituss, I.; Bode, J. W. Expanded Substrate Scope and Catalyst Optimization for the

Catalytic Kinetic Resolution of *N*-Heterocycles. *Chem. Commun.* **2012**, *48*, 8892–8894. (d) Kreituss, I.; Murakami, Y.; Binanzer, M.; Bode, J. W. Kinetic Resolution of Nitrogen Heterocycles with a Reusable Polymer-Supported Reagent. *Angew. Chem. Int. Ed.* **2012**, *51*, 10660–10663. (e) Kreituss, I.; Chen, K.-Y.; Eitel, S. H.; Adam, J.-M.; Wuitschik, G.; Fettes, A.; Bode, J. W. A Robust, Recyclable Resin for Decagram Scale Resolution of (\pm)-Mefloquine and Other Chiral *N*-Heterocycles. *Angew. Chem. Int. Ed.* **2016**, *55*, 1553–1556. (f) Kreituss, I.; Bode, J. W. Flow Chemistry and Polymer-Supported Pseudoenantiomeric Acylating Agents Enable Parallel Kinetic Resolution of Chiral Saturated *N*-Heterocycles. *Nat. Chem.* **2017**, *9*, 446–452.

¹⁴ (a) Allen, S. E.; Hsieh, S.-Y.; Gutierrez, O.; Bode, J. W.; Kozlowski, M. C. Concerted Amidation of Activated Esters: Reaction Path and Origins of Selectivity in the Kinetic Resolution of Cyclic Amines via *N*-Heterocyclic Carbenes and Hydroxamic Acid Cocatalyzed Acyl Transfer. *J. Am. Chem. Soc.* **2014**, *136*, 11783–11791. (b) Wanner, B.; Kreituss, I.; Gutierrez, O.; Kozlowski, M. C.; Bode, J. W. Catalytic Kinetic Resolution of Disubstituted Piperidines by Enantioselective Acylation: Synthetic Utility and Mechanistic Insights. *J. Am. Chem. Soc.* **2015**, *137*, 11491–11497.

¹⁵ Hoops, S.; Sahle, S.; Gauges, R.; Lee, C.; Pahle, J.; Simus, N.; Singhal, M.; Xu, L.; Mendes, P.; Kummer, U. COPASI—a Complex Pathway Simulator. *Bioinformatics* **2006**, *22*, 3067–3074.

¹⁶ These two values are not mutually exclusive. The substituent can be in an axial configuration without the *N*-H proton being in an axial configuration.

¹⁷ Dooley, C. J., III.; Burtea, A.; Mitilian, C.; Dao, W. T.; Qu, B.; Salzameda, N. T.; Rychnovsky, S. D. Using the Competing Enantioselective Conversion Method to Assign the Absolute Configuration of Cyclic Amines with Bode's Acylation Reagents. *J. Org. Chem.* **2020**, *85*, 10750–10759.

¹⁸ (a) Grzyb, J. A.; Shen, M.; Yoshina-Ishii, C.; Chi, W.; Brown, R. S.; Batey, R. A. Carbamoylimidazolium and Thiocarbamoylimidazolium Salts: Novel Reagents for the Synthesis of Ureas, Thioureas, Carbamates, Thiocarbamates and Amides. *Tetrahedron* **2005**, *61*, 7153–7175. (b) So, S.; Yeom, C.-E.; Cho, S.; Choi, S.; Chung, Y.; Kim, B. A Short Synthesis of Conformationally Constrained Unnatural Bicyclic Amino Acids Containing a Nitrogen Atom at the Ring Junction: (9*aR*)- and (9*aS*)-Octahydropyrido[1,2-*a*]Pyrazine-(3*S*)-Carboxylic Acids (Opc). *Synlett* **2008**, *2008*, 702–706.

¹⁹ Bennett, M. R.; Thompson, M. L.; Shepherd, S. A.; Dunstan, M. S.; Herbert, A. J.; Smith, D. R. M.; Cronin, V. A.; Menon, B. R. K.; Levy, C.; Micklefield, J. Structure and Biocatalytic Scope of Coclaurine N-Methyltransferase. *Angew. Chem. Int. Ed.* **2018**, *57*, 10600–10604.

²⁰ Yang, X.; Ammeter, D.; Idowu, T.; Domalaon, R.; Brizuela, M.; Okunnu, O.; Bi, L.; Guerrero, Y. A.; Zhanel, G. G.; Kumar, A.; Schweizer, F. Amphiphilic Nebramine-Based Hybrids Rescue Legacy Antibiotics from Intrinsic Resistance in Multidrug-Resistant Gram-Negative Bacilli. *Eur. J. Med. Chem.* **2019**, *175*, 187–200.

²¹ Hu, P.; Hu, J.; Jiao, J.; Tong, X. Amine-Promoted Asymmetric (4+2) Annulations for the Enantioselective Synthesis of Tetrahydropyridines: A Traceless and Recoverable Auxiliary Strategy. *Angew. Chem. Int. Ed.* **2013**, *52*, 5319–5322.

Chapter 4. Crystallization of Liquid Alkenes and Diols as Osmate Ester Derivatives

Adapted with permission from Burns, A. S.; Dooley, C., III; Carlson, P. C.; Ziller, J. W.; Rychnovsky, S. D. Relative and Absolute Structure Assignments of Alkenes Using Crystalline Osmate Derivatives for X-ray Analysis. *Org. Lett.* **2019**, *21*, 10125–10129. Copyright 2022 American Chemical Society.

4.1 Abstract

Organic compounds containing alkenes are often challenging to crystallize. We have found that osmium tetroxide and TMEDA form stable crystalline adducts with alkenes, allowing the determination of absolute structure by X-ray crystallography. Osmium, a heavy atom, facilitates the crystallographic analysis and the determination of absolute configuration using common Mo X-ray sources. The utility of this method for determining absolute structure and configuration was demonstrated on several unsaturated substrates. We also investigated a redox-neutral crystallization strategy of 1,2- and 1,3- diols using potassium osmate, and results are reported.

4.2 Introduction

4.2.1 Motivation

As shown in chapters 1–3, our group has always had an interest in the determination of absolute structure. Our group has also had a long-standing interest in the synthesis of complex natural products. A former group member, Dr. Sunshine Burns, completed the first total synthesis of illisimonin A, an unprecedented *Illicium* sesquiterpene.¹ Sunshine had developed a synthesis of the racemic natural product, but wanted to render the synthesis asymmetric to either confirm or rebut the absolute configuration assigned by the isolation chemists. To do so, he used an intermediate with a free primary alcohol to perform some sort of derivatization with a chiral resolving agent. After several attempts, he was able to form a set of diastereomeric carbamates **4-1** and **4-2** using (*S*)- α -naphthylethyl isocyanate, an intermediate I had suggested after my experience with isocyanates (see chapter 2). These diastereomers were separable by chromatography, thus resolving the enantiomers of the complex intermediate.

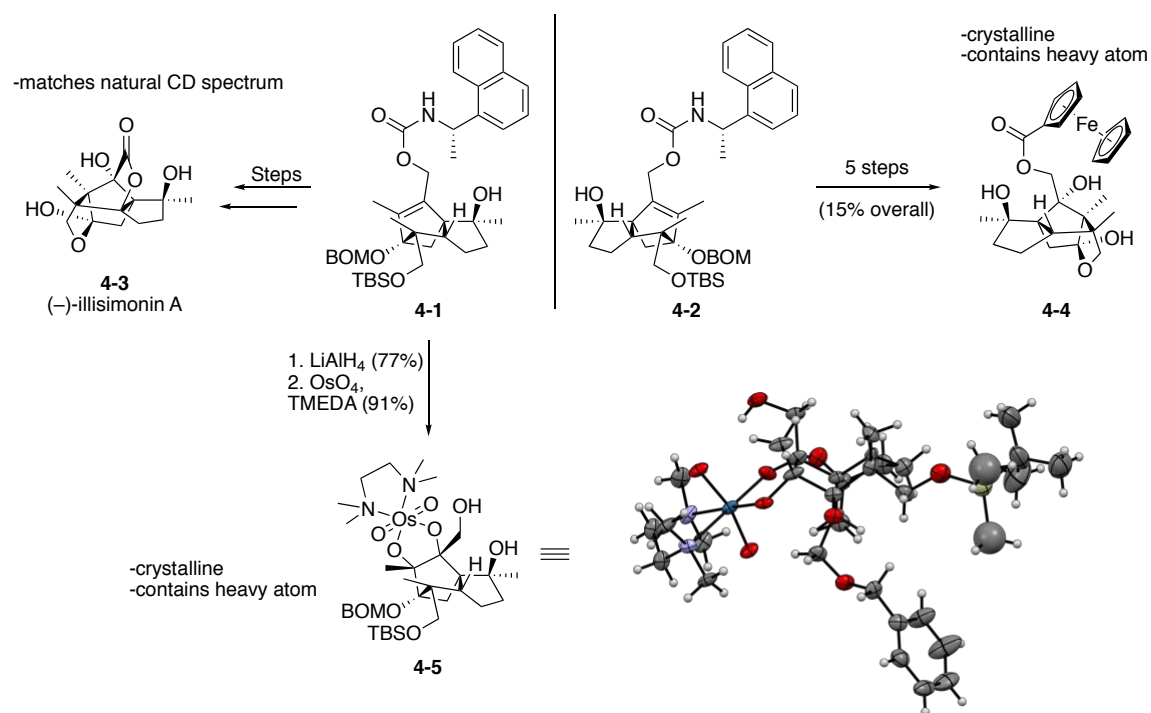


Figure 4-1 Determination and revision of the absolute configuration of (-)-illisimonin A. Our published assignment was based on ferrocene ester **4-4**, whose absolute configuration was determined through X-ray crystallography. Osmate ester **4-5** was prepared in fewer steps and retained greasy protecting groups.

Seeking to determine absolute configuration, Sunshine removed the carbamate from **4-1**, and carried it forward to the natural product (**4-3**). He found that the measured ECD spectrum for this enantiomer matched the ECD spectrum reported for the natural product. As the absolute configuration was still ambiguous, he also wanted to form a crystalline intermediate for X-ray analysis. With diastereomer **4-2**, Sunshine attempted to crystallize several of his intermediates by forming ferrocene esters with the primary alcohol. Ferrocene ester **4-4** was crystalline, allowing the establishment of its absolute structure through X-ray diffraction, thus reversing the absolute configuration of (-)-illisimonin A by inference. However, Sunshine had to push the material 5 steps before a suitably crystalline intermediate was found. At a suggestion from Professor Rychnovsky, Sunshine removed the carbamate from **4-1**, and attempted to form a TMEDA-osmate ester. Reaction of the allylic alcohol with osmium tetroxide in the presence of TMEDA at low

temperature afforded osmate **4-5** in excellent yield. This substance was readily crystalline, despite still retaining the TBS and BOM-ether protecting groups. This strategy was more concise and practical than the ferrocene ester **4-4**.

4.2.2 *Background*

As discussed in chapter 1, the determination of absolute configuration is a non-trivial and substrate dependent task. The gold standard for structure analysis is often considered to be X-ray crystallography. Absolute configuration can be determined from X-ray diffraction from the Flack parameter.² To have low uncertainty in the Flack parameter, and thus confidence in the assignment, a heavy atom has often been required. Heavy atoms increase anomalous dispersion in the diffraction data, allowing the position of that specific atom to be determined readily. One can think of a heavy atom on an organic molecule as essentially a target for the X-rays. Further improvements in the Flack method, as well as the use of higher energy Cu K α X-ray sources, have allowed the determination of absolute configuration for solely light-atom containing structures.³

To perform X-ray diffraction studies, it is necessary to obtain a suitable crystal from the substance in question. This can often be challenging with organic compounds, as organic compounds are not often crystalline. Several strategies have been developed to facilitate crystallization of organic compounds. Alcohols, amines, carboxylic acids, ketones, and aldehydes have all been derivatized to render them more crystalline. Alcohols and amines have been derivatized with 4-nitrobenzoyl chloride and 4-bromobenzoyl chloride. More recently, as showcased in Figure 4-1, acylation of alcohols and amines with ferrocene carboxylic acid has facilitated the crystallization of liquid compounds.⁴ These intermediates also contain a heavy atom (Fe), facilitating X-ray analysis. Carboxylic acids have been converted to amine salts, and ketones and aldehydes have been crystallized as 3,5-(NO₂)₂-phenylhydrazones. As we were preparing our

publication of this work, a new method was published by the Whitehead group which formed crystalline derivatives of alcohols as guanidinium sulfate salts.⁵

Several strategies have also been developed which do not rely on the derivatization of organic substrates. One strategy for dealing with liquid substances is to crystallize them at low temperatures.⁶ Another astounding strategy does not involve crystallization of organic substrates at all! Fujita *et. al.* have reported that tiny crystals of porous complexes can be soaked with solutions of liquid compounds, and the complex can absorb the target molecules.⁷ The host complexes can then be analyzed by X-ray diffraction, thus giving information about the organic substance trapped within it. This method completely circumvents crystallization but is rather specialized.

4.2.3 *Osmylation as a Crystallization Strategy*

Osmium tetroxide is known to be a highly reactive compound and has long been known to react with alkenes and form complexes with amines.⁸ Osmate esters have been used to generate crystalline intermediates. Crystalline osmates have been used to elucidate the stereoselectivity of the osmylation reaction,^{9,10} the regioselectivity of the reaction,¹¹ or to help explain the effect of chiral ligands in stoichiometric enantioselective osmylations.¹² Several studies investigating the interactions of OsO₄ with RNA and DNA have produced crystal structures of nucleoside and nucleotide-derived osmates.¹³

We were inspired by the work of Donohoe, who has shown that the OsO₄-TMEDA (tetramethylethylenediamine) complex displays excellent chemoselectivity in reactions with allylic alcohols.⁹ Additionally, it is estimated that the OsO₄-TMEDA is 100x more reactive than the OsO₄-pyridine complex, allowing reactions with alkenes at cryogenic temperatures. The dihydroxylation can be directed by hydrogen bonding, and often reacts with good

diastereoselectivity. These desirable characteristics spurred us to investigate the scope of alkenes which could be crystallized using this methodology.

4.3 Results and Discussion

4.3.1 *Crystallization of Liquid Alkenes*

To evaluate the utility of this method, we initially examined commercially available, liquid alkenes. The osmylation of prenol (**4-6a**), geraniol (**4-7a**), and (+)-2-carene (**4-8a**) was carried out by addition of a stock solution of OsO₄ in CH₂Cl₂ to a cooled (−78 °C) solution of alkene and TMEDA. These reactions all proceeded in good yield, and the osmate ester products were stable to silica gel chromatography. The substrates were readily crystallized by vapor diffusion, and their structures were determined using single crystal X-ray diffraction. Additionally, geraniol reacts proximal to the allylic alcohol, in accord with directing effect reported by Donohoe.⁹ The melting point of **4-7b** is 61 °C higher than the corresponding ferrocene ester, indicating enhanced crystallinity.^{4a} In the case of **4-8b**, the absolute configuration was confirmed by the Flack method.²

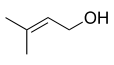
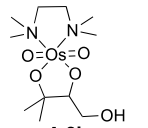
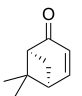
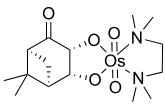
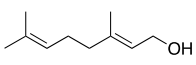
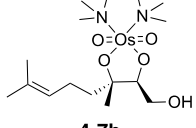
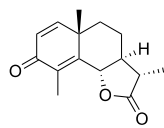
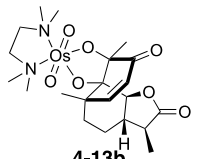
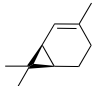
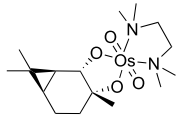
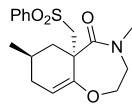
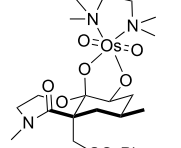
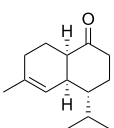
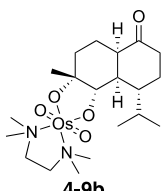
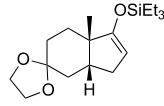
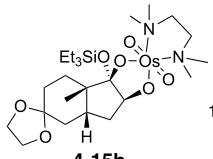
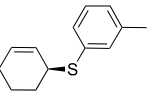
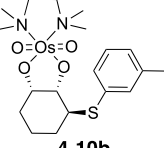
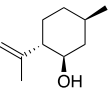
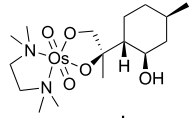
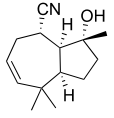
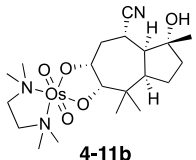
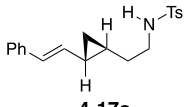
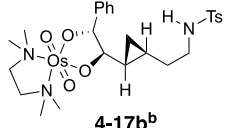
Decalin **4-9a**,¹⁴ and allylic sulfide **4-10a**¹⁵ are both oils. They both react under standard conditions (OsO₄ and TMEDA at −78 °C in CH₂Cl₂) to form osmate esters **4-9b** and **4-10b** in good yields. The structures and absolute configurations were determined by X-ray crystallography. Sulfide **4-10a** is a compelling example of the utility of this methodology. Its absolute configuration was originally inferred by analogy to a model substrate synthesized using the same enantioselective method. From 14 mg of **4-10a**, we prepared 36 mg of osmate **4-10b** that crystallized on the first attempt, providing experimental confirmation of its proposed absolute configuration.

Alkene **4-11a**¹⁶ reacted with the osmium complex selectively and the adduct **4-11b** crystallized readily. Initially, the crystals were twinned, making it challenging to determine

absolute configuration from the X-ray diffraction data. Fortuitously, changing solvents resulted in single crystals, allowing confirmation of the absolute configuration and structure.

Verbenone (**4-12a**), an oil, and the solid dienone α -santonin (**4-13a**) were both osmylated and the adducts readily crystallized, highlighting the method's applicability to electron-deficient alkenes. Notably, the osmylations are not sensitive to the reaction solvent, as **4-12a** reacted in CH₂Cl₂, MeOH, and THF without diminishment in yield. The chemoselectivity of the osmylation on **4-13a** was also notable, as a lack of selectivity could have led to lower yields and a more challenging crystallization.¹⁷

Table 4-1 Alkenes and the Derived Crystalline Osmate-TMEDDA Esters.^a

Alkene	Yield	Osmate	mp	Alkene	Yield	Osmate	mp
 4-6a achiral oil	59%		135 °C (dec)	 4-12a enantiopure oil	81%		192 °C (dec)
 4-7a achiral oil	60%		100-103 °C	 4-13a enantiopure solid mp = 172 °C	87%		202 °C (dec)
 4-8a enantiopure oil	85%		180 °C (dec)	 4-14a racemic oil	76%		182-185 °C
 4-9a racemic oil	93%		87-92 °C	 4-15a enantiopure oil	-		170 °C (dec)
 4-10a enantiopure oil	91%		170 °C (dec)	 4-16a enantiopure oil	87% 1.3:1		84-87 °C
 4-11a enantiopure solid mp = 59-63 °C	97%		231 °C (dec)	 4-17a racemic oil	68% 2.4:1		90-93 °C

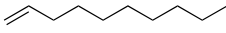
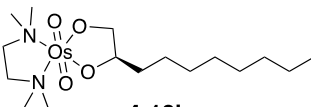
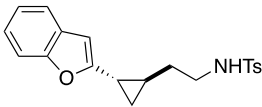
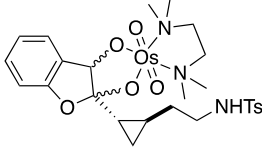
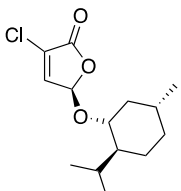
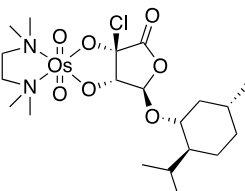
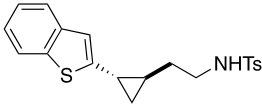
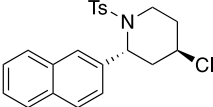
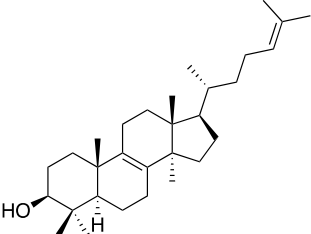
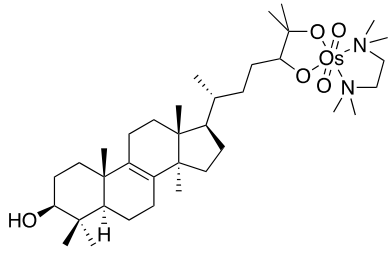
^aStandard Conditions: 1.0 equiv alkene, 1.0 equiv OsO₄, 1.1 equiv TMEDA, CH₂Cl₂, -78 °C, 1 h. ^bThe diastereomeric mixture of osmate esters was separated by chromatography prior to crystallization.

The dihydroxylation of enol ethers and silyl enol ethers typically leads to α -hydroxy ketone products.¹⁸ We hypothesized that the osmate esters of these motifs would be kinetically stable, and lead to crystalline products. Enol ether **4-14a**, an intermediate toward the total synthesis of batrachotoxin, formed a stable, crystalline osmate ester. Silyl enol ether **4-15a** formed a less stable

osmate ester. Osmate ester **4-15b** decomposed during chromatography on silica gel, but we found that the osmate ester could be crystallized directly from the reaction mixture, allowing structure determination of this challenging substrate.

One drawback of the functionalization of alkenes is the possible generation of diastereomers. All the substrates discussed thus far reacted with high diastereoselectivity. However, the osmylation of isopulegol **4-16a** generated a 1.3:1 mixture of diastereomers. In theory, a single diastereomer could be crystallized out of the mixture, but we did not have any success in our attempts. However, we found that the osmate diastereomers could be separated by chromatography after an extensive screen of eluents, and with a single diastereomer we were able to crystallize **4-16b**. Additionally, vinylcyclopropane **4-17a** generated a 2.4:1 mixture of diastereomers which were readily separated, allowing structure confirmation of this product. The generation of diastereomers is a drawback to the methodology, but we found it generally possible to separate the diastereomeric osmates when the osmate ester was formed proximal to other chiral centers in the molecule.

Table 4-2 Unsuccessful substrates.

Alkene	Osmate Product	Reason for Failure
 <p>4-18a</p>	 <p>4-18b</p>	Oil
 <p>4-19a</p>	 <p>4-19b</p>	Product was amorphous solid; it did not crystallize in our hands
 <p>4-20a</p>	 <p>4-20b</p>	Decomposed on isolation and purification
 <p>4-21a</p>	N/A	No reaction
 <p>4-22a</p>	N/A	No reaction
 <p>4-23a</p>	 <p>4-23b</p>	Osmate ester formed in a 1:1 dr. Mixture was not separable by chromatography and did not crystallize

Several alkenes could not be successfully analyzed with this methodology, and they are outlined in Table 4-2. Alkenes **4-18a** and **4-19a** underwent osmylation, but the osmate products could not be crystallized. Chloroalkene **4-20a** also underwent smooth osmylation, but the product decomposed during purification. Thiophene **4-21a** and naphthyl piperidine **4-22a** were unreactive.

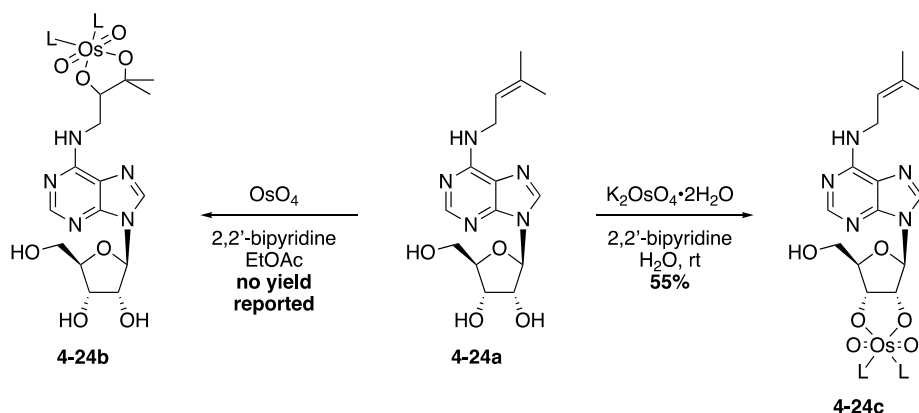
Lanosterol **4-23a** formed a 1:1 mixture of osmate diastereomers which were inseparable by chromatography and could not be crystallized away from one another.

4.4 Redox Neutral Crystallization of Diols as TMEDA-Osmate Esters

4.4.1 Introduction

Following the success of the osmate functionalization of alkenes, we were interested in applying a similar strategy to the crystallization of 1,2 and 1-3 diols, as well as amino alcohols. These motifs are ubiquitous in synthetic chemistry, particularly macrolide natural products, and the absolute configuration of these groups are often challenging to determine.¹⁹ We have previously shown that osmate esters enhance the crystallinity of organic compounds, making them suitable agents for crystallization.

Scheme 4-1 Regioselective osmylation of isopentenyl adenosine.

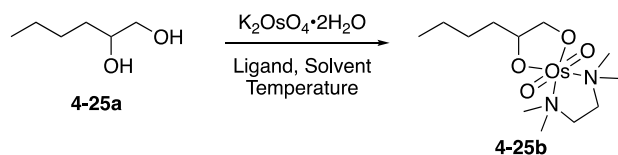


It has long been known that 1,2-diols can undergo redox neutral osmylation using potassium osmate in the presence of bidentate ligands.²⁰ In 1976, Behrman showed that it was possible to regioselectively osmylate isopentenyl adenosine **4-24a** through modification of reaction conditions. When reacted with osmium tetroxide in the presence of pyridine or 2,2'-bipyridine (bpy), osmate ester **4-24b** was formed by dihydroxylation of the alkene. However, the diol of the sugar residue could be selectively osmylated by reaction with potassium osmate in the presence of bpy to generate osmate ester **4-24c** in 55% isolated yield.^{20a} Behrman's group

performed several other studies on the kinetics and exchange equilibrium of these glycol-osmate complexes with other diols or bidentate amine ligands.^{20b,c} While these complexes were reported and utilized to study biological systems, we are not aware any examples using such a strategy to generate X-ray quality crystals.

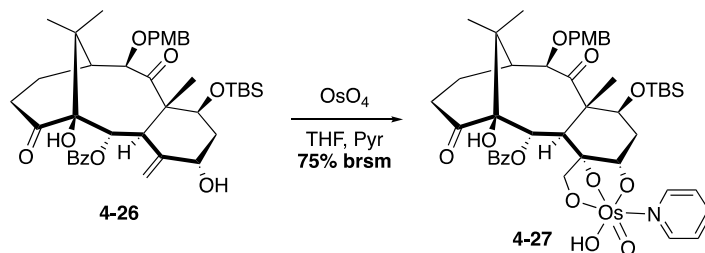
4.4.2 *Results and Discussion*

We began our studies by optimizing reaction conditions using 1,2-hexanediol **4-25a** as a model substrate. Results are reported in Table 4-3. Since potassium osmate is sparingly soluble in many organic solvents, we began our optimization by using methanol as solvent. Reaction of **4-25a** with potassium osmate in methanol using 1.1 equivalents of TMEDA as the ligand resulted in formation of osmate ester, but incomplete conversion. This was problematic, as the diol and osmate ester were inseparable by chromatography. By adding 3 equivalents of TMEDA (entry 2) we were able to drive the reaction to completion, but only achieved a 43% isolated yield of product. We rationalized that it would be possible to perform the reactions under heterogeneous conditions, as the osmate ester products are often highly soluble in organic solvent. Changing the solvent to CH₂Cl₂ and increasing the temperature to 40 °C (entry 3) led once again to a 43% isolated yield of product. Performing the reaction in THF (entry 4) and acetone/water (entry 5) resulted incomplete conversion once again. In the reaction shown in Scheme 4-1, the reaction mixture was brought to pH 7 by the addition of 1 M aq. HCl, presumably to attenuate any basicity. We thought that we could buffer the TMEDA as an acid salt, achieving essentially the same effect. As such, I synthesized TMEDA•2TsOH salt, and when it was used as the ligand in methanol (entry 6) osmate **4-25b** was isolated in 84% yield. This product crystallized on the first attempt, generating X-ray quality crystals.

Table 4-3 Optimization of redox neutral osmylation of 1,2-diols.

Entry	Ligand	Solvent	Temperature	Result
1	TMEDA (1.1 equiv)	MeOH	RT	Incomplete conversion
2	TMEDA (3 equiv)	MeOH	RT	43%
3	TMEDA (1.1 equiv)	CH ₂ Cl ₂	40 °C	43%
4	TMEDA (1.1 equiv)	THF	40 °C	Incomplete conversion
5	TMEDA (1.1 equiv)	Acetone:H ₂ O 19:1	40 °C	Incomplete conversion
6	TMEDA·2TsOH (1.1 equiv)	MeOH	RT	84%

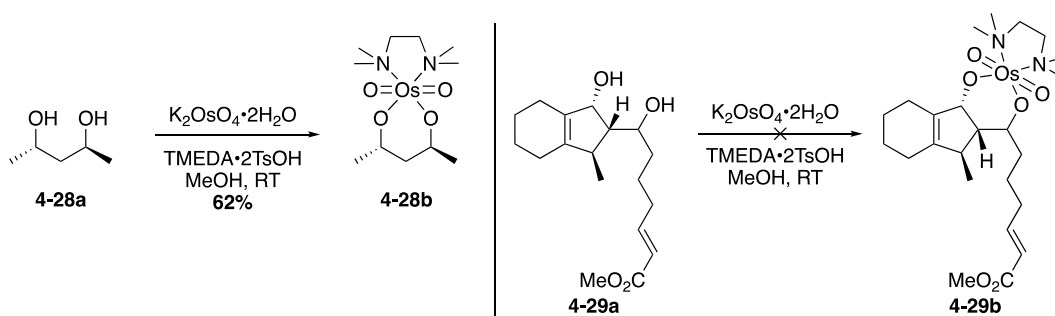
With optimal conditions for a 1,2-diol, we wanted to investigate the propensity of 1,3-diols to form osmate esters. There is exceedingly little precedent for a 1,3-diol osmate ester; in fact, it was noted by Behrman that 1,2-diols kinetically outcompete 1,3-diols in transesterification reactions with nucleosides.²⁰ The only example of a 1,3-diol osmate ester was from Paquette's approach to functionalized taxanes, wherein dihydroxylation of allylic alcohol **4-26** with OsO₄/pyridine led to the stable osmate ester **4-27**.²¹ This triol osmate ester is interesting but is clearly not directly applicable to simpler 1,3-diols.

Scheme 4-2 Isolation of a triol-osmate complex by Paquette.

To probe this unprecedented transformation, I subjected diol **4-28a** to the previously established optimal conditions (Table 4-3, entry 6) and observed a 62% yield of osmate **4-28b**. This osmate ester crystallized on the first attempt, allowing us to attain the first X-ray structure of

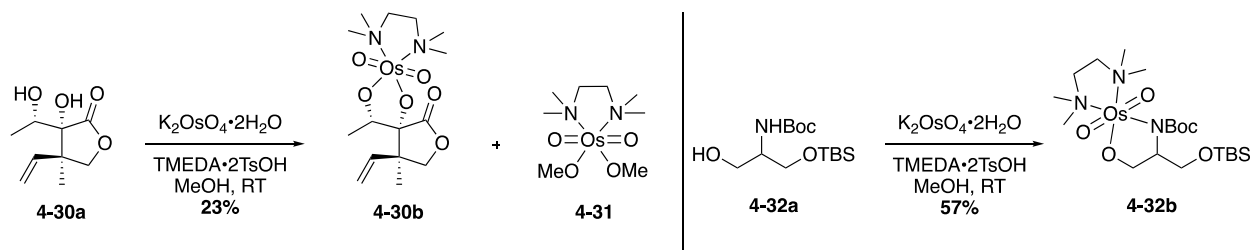
a 1,3-diol osmate ester. Optimistic that the osmylation would be general, we attempted to react diol **4-29a**, an intermediate from our group's silacycle-directed intramolecular Diels–Alder methodology.²² This compound would have been an excellent example of the utility of the method, as the compound was a single diastereomer, but the configuration of the secondary alcohol on the alkyl chain was unknown at the time. Unfortunately, reaction of **4-28a** under the previously established conditions did not lead to the isolation of any osmate ester, but rather seemed to eliminate one of the two alcohols (assignment was not made).

Scheme 4-3 Osmylation of 1,3-diols.



On the heels of this failed substrate, I attempted to look at other complex substrates. I attempted osmylation of diol **4-30a**, an intermediate in my work toward the synthesis of (2*R*)-hydroxynorneomajucin (for details, see Chapter 5), and isolated 23% of osmate ester **4-30b**, in addition to a significant amount of methanol osmate **4-31**. The low yield, coupled with the isolation of the methanol osmate adduct, led us to believe that complex or hindered substrates might pose a significant challenge for this methodology, greatly hindering the utility. Additionally, I tried to form an osmate ester from Boc-protected amino alcohol **4-32a**, and was pleased to observe a 57% yield of osmate **4-32b**. Unfortunately, the TBS and Boc protecting groups made the product very non-polar, and the compound was in fact soluble in our most common antisolvent (pentane). As such, I was unable to crystallize this substrate. However, the clean reactivity could be useful for further evaluation of amino-alcohol substrates in the future.

Scheme 4-4 Osmylation of complex 1,2-diol and amino alcohol substrates.



4.5 Conclusions and Future Directions

In this chapter, we have shown that osmate esters are excellent functional groups for the crystallization of organic compounds. The reaction of OsO_4 -TMEDA with alkenes is high yielding and insensitive to reaction conditions, and the osmate esters are often highly crystalline, enabling X-ray structure determination. The main limitation to this reactivity is the low diastereoselectivity observed with acyclic alkenes. We have shown that when the osmate ester is proximal to other chiral centers in the molecule, the diastereomers are often separable, allowing efficient crystallization.

We have also reported preliminary work toward a strategy to crystallize 1,2 and 1,3 diols as osmate esters. The use of $\text{TMEDA} \cdot 2\text{TsOH}$ was necessary for clean conversion diols. Simple 1,2 and 1,3 diols effectively undergo the redox neutral osmylation, but more complex substrates often fail, limiting the potential scope of the methodology. We also showed that protected amino alcohols cleanly form osmate complexes under the same conditions. The limited scope of the method, as well as low yields and challenging purifications are current problems for further development. Further reaction optimization is certainly necessary for more complicated substrates, beginning with avoiding alcoholic solvents due to the propensity to isolate the alcohol osmate esters (see **4-31**). There is significant potential for this methodology, but this project was re-prioritized and set aside during the course of my total synthesis of (2*R*)-hydroxynorneomajucin. I

hope that another graduate student will pick up the project and find a useful starting point in this chapter.

4.6 Acknowledgements and Contributions

The idea of using OsO₄-TMEDA complexes as a derivatization strategy for alkenes was initially proposed by Professor Scott Rychnovsky, and much of the initial literature searching was done by him. Sunshine Burns led the project, and we owe the speed of development to him. Sunshine, Paul Carlson, and I collaborated on the design of experiments and synthesis of substrates. I have only included the synthesis of compounds which I made during the alkene derivatization project. Additional experimental details, including spectral data for osmates in Section 4.3, are described in our communication.²³ Dr. Joseph Ziller, Sunny Chen, and Daniel Huh are responsible for obtaining and solving the crystal structures of the osmate esters. I performed all the work on diol osmylation strategy reported here, but Jordan Thompson worked on some additional optimization on the methodology. I thank Ryan Davison, Kirsten A. Hewitt, Dr. Nicholas Weires, Dr. Jonathon Chung, Dr. Matthias Göhl, Nicholas Foy, Ryan Kozlowski, Leah Salituro, and Paul Carlson for providing compounds for osmylation.

4.7 Supporting Information

4.7.1 *General Information*

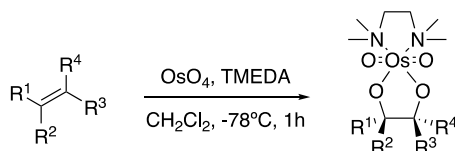
Chemical shifts (δ) were referenced to either TMS or the residual solvent peak. The ¹H NMR spectra data are presented as follows: chemical shift, multiplicity (s = singlet, d = doublet, t = triplet, q = quartet, m = multiplet, dd = doublet of doublets, ddd = doublet of doublet of doublets, dddd = doublet of doublet of doublet of doublets, dt = doublet of triplets, dq = doublet of quartets, ddq = doublet of doublet of quartets, app. = apparent), coupling constant(s) in hertz (Hz), and integration. High-resolution mass spectrometry was performed using ESI-TOF. An internal

standard was used to calibrate the exact mass of each compound. For accuracy, the osmium isotope selected for comparison was that which most closely matched the ion intensity of the internal standard. The isotope of osmium which corresponds to the nominal mass of this peak is reported.

Unless otherwise stated, synthetic reactions were carried out in flame- or oven-dried glassware under an atmosphere of argon. All commercially available reagents were used as received unless stated otherwise. Solvents were purchased as ACS grade or better and as HPLC-grade and passed through a solvent purification system equipped with activated alumina columns prior to use. Thin layer chromatography (TLC) was carried out using glass plates coated with a 250 μm layer of 60 Å silica gel. TLC plates were visualized with a UV lamp at 254 nm, or by staining with Hanessian's stain.²⁴ Liquid chromatography was performed using forced flow (flash chromatography) with an automated purification system on prepacked silica gel (SiO_2) columns unless otherwise stated. Electrospray ionization mass spectrometry (ESI-MS) was analyzed in positive mode with flow injection. Optical rotations were performed on a JACSO P-1010 spectrometer using a glass 50 mm cell with the sodium D-line at 589 nm.

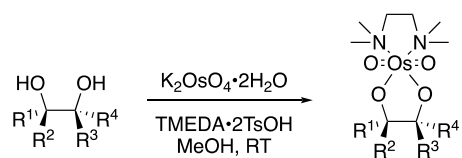
All purchased chemicals were used without further purification unless otherwise noted. CDCl_3 was purchased from Cambridge Isotope Laboratories. Tetramethylethylene diamine (TMEDA) was distilled over calcium hydride into a storage Schlenk and was stored under an atmosphere of argon. Osmium tetroxide was purchased as a pure solid from Fisher Scientific and used without further purification.

4.7.2 General Procedure 1: Formation of Osmate Esters from Alkenes^{9b}



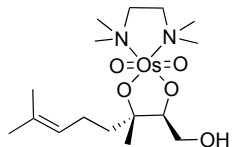
To a solution of alkene in dichloromethane was added TMEDA (1.1 equiv). The solution was cooled to $-78\text{ }^{\circ}\text{C}$, and OsO_4 (1 equiv) was added as a solution in dichloromethane. Reactions were run at concentrations anywhere from 0.01–0.3 M. The clear solution turned red upon addition of OsO_4 , then brown/black as the osmium complex reacted with the alkene. When the starting material was consumed as indicated by TLC (generally less than 15 min), the reaction was allowed to warm to room temperature, and the solvent was removed *in vacuo*. The crude material was purified by flash column chromatography (0 – 20% MeOH in CH_2Cl_2) to yield the brown osmate ester. The osmate esters were most often crystallized by vapor diffusion for X-ray crystallographic analysis.

4.7.3 General Procedure 2: Redox Neutral Formation of Osmate Esters from Diols



To a stirred solution of diol (or amino alcohol) in methanol (0.1 M) was added $\text{TMEDA}\cdot 2\text{TsOH}$ (1.05 equiv). Potassium osmate (1.0 equiv) was then added, and the reaction was stirred at ambient temperature. The reaction was monitored by TLC, as well as observing the solubilization of potassium osmate. When the reaction was complete, the mixture was filtered through a pad of celite, and the filtrate was evaporated. The crude material was purified by flash chromatography (0 – 20% MeOH in CH_2Cl_2) to yield the brown osmate ester.

4.7.4 Compound Synthesis and Characterization



Geraniol osmate ester (4-7b): Geraniol (10 μ L, 0.060 mmol) was converted to geraniol osmate **4-7b** (19.0 mg, 60%) following general procedure 1. Osmate **4-7b** was a brown foam when initially concentrated from $\text{CH}_2\text{Cl}_2/\text{MeOH}$ fractions.

Crystallization attempts				
	Method	Solvent	Antisolvent	Result
1	Vapor Diffusion	CHCl_3	Pentanes	X-ray quality crystals

R_f: 0.38 (10% MeOH in CH_2Cl_2 , visualized by UV)

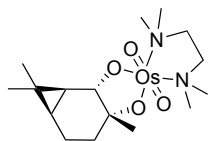
¹H NMR (500 MHz, CDCl_3) δ 5.20 – 5.09 (app. t, $J = 7.0$ Hz, 1H), 3.95–3.87 (m, 2H), 3.74 (q, $J = 7.8$ Hz, 1H), 3.18–3.07 (m, 2H), 3.07–2.97 (m, 2H), 2.87 (s, 3H), 2.85 (s, 3H), 2.81 (s, 6H), 2.11–2.04 (m, 2H), 1.91–1.83 (m, 1H), 1.70–1.67 (m, 1H), 1.65 (s, 3H), 1.59 (s, 3H), 1.31 (s, 3H)

¹³C NMR (126 MHz, CDCl_3) δ 130.7, 125.7, 92.6, 88.6, 64.7, 64.0, 63.2, 52.5, 51.7, 51.5, 50.7, 39.2, 25.9, 22.4, 19.9, 17.8.

Melting Point: 100–103 $^\circ\text{C}$

HRMS m/z calcd for $\text{C}_{16}\text{H}_{34}\text{N}_2\text{O}_5^{192}\text{OsNa}$ ($\text{M} + \text{Na}$)⁺ : 549.1976, found 549.1954.

Crystal Structure: CCDC 1966638



(+)-2-Carene osmate ester (4-8b): (+)-2-Carene (9.5 μ L, 0.060 mmol) was converted to osmate **4-8b** (26 mg, 85% yield) following the general procedure outlined above. Osmate **4-8b** was a brown oily solid when initially concentrated from $\text{CH}_2\text{Cl}_2/\text{MeOH}$ fractions.

Crystallization attempts				
	Method	Solvent	Antisolvent	Result
1	Vapor Diffusion	CHCl ₃	Pentanes	oil
2*	Vapor Diffusion	CHCl ₃	Pentanes	oil
3	Vapor Diffusion	THF	Pentanes	X-ray quality crystals

*This trial used half the volume of solvent as trial 1.

R_f: 0.47 (10% MeOH in CH₂Cl₂, visualized by UV)

¹H NMR (500 MHz, CDCl₃) δ 3.66 (s, 1H), 3.13–3.05 (m, 2H), 3.05–2.97 (m, 2H), 2.83 (s, 6H), 2.81 (s, 6H), 2.04–1.84 (m, 3H), 1.57–1.46 (m, 1H), 1.24 (s, 3H), 1.04 (s, 3H), 1.01 (s, 3H), 0.65 (m, 1H), 0.56 (d, *J* = 9.6 Hz, 1H).

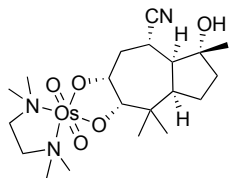
¹³C NMR (126 MHz, CDCl₃) δ 86.9, 85.9, 64.4, 63.9, 51.7, 51.4, 51.2, 50.9, 32.9, 29.8, 26.5, 26.0, 21.5, 16.4, 15.8, 15.3.

Melting Point: decomposed at 180 °C

HRMS *m/z* calcd for C₁₆H₃₂N₂O₄¹⁹²OsNa (M + Na)⁺ : 531.1870, found 531.1890.

[α]_D²² +146.8 (*c* 1.26, CHCl₃)

Crystal Structure: CCDC 1966635



(3*R*,3*aS*,4*S*,8*aR*)-3-Hydroxy-3,8,8-trimethyl-1,2,3,3*a*,4,5,8,8*a*-octahydroazulene-4-

carbonitrile Osmate Ester (4-11b): Nitrile **4-11a**⁶ (20 mg, 0.091 mmol) was converted to osmate **4-11b** (52 mg, 97% yield) following the general procedure outlined above. Osmate **4-11b** was a brown solid when initially concentrated from CH₂Cl₂/MeOH fractions.

Crystallization attempts				
	Method	Solvent	Antisolvent	Result
1	Vapor diffusion	7:4 THF:CHCl ₃	Cyclopentane	X-ray crystals, twinned
2	Vapor diffusion	CHCl ₃	<i>n</i> -Pentane	X-ray crystals, twinned
3	Vapor diffusion	3:1 PhH:CH ₂ Cl ₂	Et ₂ O	X-ray crystals

R_f: 0.43 (10% MeOH in CH₂Cl₂, visualized by UV)

¹H NMR (500 MHz, CDCl₃) δ 4.14 (d, *J* = 3.7 Hz, 1H), 3.89 (app. dt, *J* = 11.7, 4.2 Hz, 1H), 3.14–3.04 (m, 4H), 2.99–2.90 (m, 2H), 2.86 (s, 3H), 2.85 (s, 3H), 2.84 (s, 3H), 2.81 (s, 3H), 2.47 (q, *J* = 11.3 Hz, 1H), 2.26 (t, *J* = 12.6 Hz, 1H), 2.09 (dd, *J* = 13.8, 4.5 Hz, 1H), 1.81–1.68 (m, 4H), 1.45–1.37 (m, 1H), 1.32 (s, 3H), 1.11 (s, 3H), 1.03 (s, 3H).

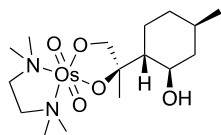
¹³C{¹H} NMR (126 MHz, CDCl₃) δ 123.6, 101.5, 83.6, 79.9, 77.4, 64.53, 64.49, 55.8, 52.1, 51.9, 51.3, 40.4, 40.3, 38.2, 34.5, 29.9, 24.9, 24.2, 23.8, 22.8.

Melting Point: decomposed at 231 °C

HRMS *m/z* calcd for C₂₀H₃₇N₃O₅¹⁹⁰OsNa (M + Na)⁺ : 612.2215, found 612.2223.

[α]_D²² –953.2 (*c* 1.18, CHCl₃)

Crystal Structure: CCDC 1966640



(–)-Isopulegol Osmate (4-16b): (–)-Isopulegol **4-16a** (24 μL, 0.14 mmol) was dissolved in CH₂Cl₂ (4.8 mL, 0.03 M), and TMEDA (24 μL, 0.16 mmol) was added. The solution was cooled to –78 °C, and OsO₄ prepared as a 0.25 M solution in CH₂Cl₂ (0.57 mL, 0.14 mmol) was added. The reaction was allowed to warm to room temperature after 30 min, and the solvent was evaporated *in vacuo*. The crude residue was purified by preparative TLC eluting with 3%

MeCN/Me₂CO to provide **4-16b** as a brown foam (36 mg, 47%) and *epi*-**4-16b** as a brown foam (30 mg, 40%). Crystals for X-ray analysis were grown as described in the tables below.

Diastereomer 1 (4-16b, Higher R_f):

Crystallization attempts				
	Method	Solvent	Antisolvent	Result
1	Vapor Diffusion	Et ₂ O	<i>n</i> -Pentane	Amorphous Solids
2	Vapor Diffusion	3:1 THF:CH ₂ Cl ₂	<i>n</i> -Pentane	Amorphous Solids
3	Liquid Diffusion	CHCl ₃	Cyclopentane	No solids formed
4	Vapor Diffusion	CHCl ₃	<i>n</i> -Pentane	Amorphous Solids
5	Vapor Diffusion	THF	Cyclopentane	X-ray Quality Crystals

R_f: 0.42 (10% MeOH in CH₂Cl₂, visualized by UV)

¹H NMR (600 MHz, CDCl₃) δ 6.30 (s, 1H), 4.19 (d, *J* = 9.9 Hz, 1H), 4.06 (d, *J* = 9.9 Hz, 1H), 3.84 (td, *J* = 10.4, 4.3 Hz, 1H), 3.11–3.05 (m, 4H), 2.87 (s, 3H), 2.86 (s, 3H), 2.81 (s, 3H), 2.79 (s, 3H), 1.98–1.93 (m, 2H), 1.76 (ddd, *J* = 12.8, 9.9, 3.4 Hz, 1H), 1.64–1.57 (m, 2H), 1.42 (s, 3H), 1.15 (qd, *J* = 13.3, 12.7, 3.9 Hz, 1H), 1.03 (app q, *J* = 11.7 Hz, 1H), 0.97–0.91 (m, 1H), 0.90 (d, *J* = 6.6 Hz, 3H).

¹³C{¹H} NMR (151 MHz, CDCl₃) δ 92.3, 89.9, 72.3, 64.6, 64.3, 52.1 (2C), 51.74, 51.73, 49.4, 44.1, 35.0, 31.1, 28.6, 22.3, 17.9.

Melting Point: 84–87 °C

HRMS : *m/z* calcd for C₁₆H₃₄N₂O₅¹⁸⁶OsNa (M + Na)⁺ : 543.1899, found 543.1904.

[α]²²_D +217.5 (*c* 1.25, CDCl₃)

Crystal Structure: CCDC 1966646

Diastereomer 2 (*epi*-4-16b, Lower R_f):

Crystallization attempts				
	Method	Solvent	Antisolvent	Result
1	Vapor Diffusion	PhH	Cyclopentane	Amorphous Solids
2	Vapor Diffusion	Et ₂ O	<i>n</i> -Pentane	No solids formed
3	Vapor Diffusion	3:1 PhH:CHCl ₃	<i>n</i> -Pentane	Amorphous Solids
4	Vapor Diffusion	THF	Cyclopentane	Amorphous Solids
5	Vapor Diffusion	THF	<i>n</i> -Pentane	Amorphous Solids
6	Vapor Diffusion	THF	Cyclopentane	Amorphous Solids

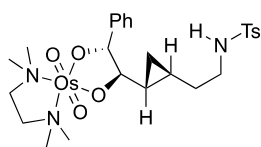
R_f: 0.41 (10% MeOH in CH₂Cl₂, visualized by UV)

¹H NMR (600 MHz, CDCl₃) δ 6.18 (s, 1H), 4.46 (d, *J* = 10.0 Hz, 1H), 3.99 (d, *J* = 10.0 Hz, 1H), 3.82 (td, *J* = 10.2, 4.4 Hz, 1H), 3.15–3.09 (m, 2H), 3.09–3.02 (m, 2H), 2.88 (s, 3H), 2.87 (s, 3H), 2.83 (s, 3H), 2.80 (s, 3H), 1.99 (s, 1H), 1.95 (dt, *J* = 12.4, 4.3 Hz, 1H), 1.91–1.83 (m, 2H), 1.66–1.60 (m, 1H), 1.40 (s, 3H), 1.04–0.95 (m, 2H), 0.90 (d, *J* = 6.5 Hz, 3H), 0.93–0.85 (m, 1H).

¹³C{¹H} NMR (151 MHz, CDCl₃) δ 92.5, 85.6, 77.2, 71.9, 64.7, 64.4, 52.1, 51.9, 51.8 (2C), 51.7, 44.0, 35.6, 31.2, 29.1, 24.4, 22.3.

HRMS : *m/z* calcd for C₁₆H₃₄N₂O₅¹⁸⁶OsNa (M + Na)⁺ : 543.1899, found 543.1918.

[α]_D²² –592.8 (*c* 1.24, CDCl₃)



Vinylcyclopropane osmate ester (4-17b): (±)-Vinylcyclopropane **4-17a** (7.5 mg, 0.022 mmol) was converted to osmate **4-17b** (7.4 mg) and its diastereomer (3.2 mg, 68% combined yield) following the general procedure outlined above. Osmate **4-17b** readily separable from its diastereomer, and was a brown solid when initially concentrated from CH₂Cl₂/MeOH fractions.

Crystallization attempts				
	Method	Solvent	Antisolvent	Result
1	Vapor diffusion	PhH	<i>n</i> -pentane	amorphous solids
2	Vapor diffusion	CH ₂ Cl ₂	<i>n</i> -pentane	oil
3	Vapor diffusion	THF	<i>n</i> -pentane	amorphous solids
4	Vapor diffusion	Me ₂ CO	cyclopentane	amorphous solids
5	Vapor diffusion	THF	cyclopentane	amorphous solids
6	Vapor diffusion	THF	Et ₂ O	No solids
7	Liquid Diffusion	CH ₂ Cl ₂	<i>n</i> -pentane	X-ray quality crystals

R_f: 0.55 (10% MeOH/CH₂Cl₂, UV). Diastereomer: 0.50 (10% MeOH/CH₂Cl₂, UV).

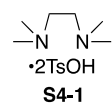
¹H NMR (500 MHz, CDCl₃) δ 7.84 (s, 1H), 7.35–7.28 (m, 4H), 7.29–7.27 (m, 2H), 7.23–7.19 (m, 1H), 4.98 (d, *J* = 9.3 Hz, 1H), 3.46 (ddd, *J* = 13.4, 8.8, 4.7 Hz, 1H), 3.26–3.15 (m, 4H), 3.13–3.05 (m, 2H), 3.04 (s, 3H), 3.02 (s, 3H), 2.97 (s, 3H), 2.89 (s, 3H), 2.44 (s, 3H), 1.82–1.75 (m, 1H), 0.51 (dtd, *J* = 14.0, 10.2, 4.3 Hz, 1H), 0.45–0.36 (m, 1H), 0.24 (tt, *J* = 9.3, 4.9 Hz, 1H), –0.12 (dt, *J* = 8.6, 5.3 Hz, 1H), –0.38 (dt, *J* = 10.0, 5.1 Hz, 1H).

¹³C{¹H} NMR (151 MHz, CDCl₃) δ 142.7, 142.5, 139.5, 129.7 (2C), 127.84 (2C), 127.77 (2C), 127.4, 127.3 (2C), 101.3, 95.2, 64.9, 64.7, 52.9, 52.3, 51.8, 51.2, 44.5, 31.2, 21.7, 20.0, 14.1, 9.5.

Melting Point: 90–93 °C

HRMS *m/z* calcd for C₂₆H₃₉N₃O₆¹⁸⁶OsSNa (M + Na)⁺ : 730.1991, found 730.2000.

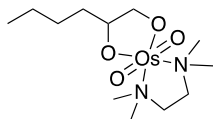
Crystal Structure: CCDC 1966645



TMEDA•2TsOH (S4-1): To a solution of TMEDA (0.218 g, 1.88 mmol) in acetone (9.4 mL) was added TsOH•H₂O (0.713 g, 3.75 mmol), and the mixture was stirred at ambient temperature. After an hour, a white precipitate had formed. The mixture was cooled to 0 °C, and the mixture was filtered through a sintered glass funnel. The solid was collected and dried *in vacuo*, affording **S4-1** (0.795 g, 92%) as a white solid.

¹H NMR (600 MHz, CD₃OD) δ 7.72 (d, *J* = 8.3 Hz, 2H), 7.26 (d, *J* = 7.9 Hz, 2H), 3.63 (s, 2H), 2.97 (s, 7H), 2.38 (s, 3H).

¹³C{¹H} NMR (151 MHz, CD₃OD) δ 143.2, 142.0, 130.0, 126.9, 52.5, 44.3, 21.3.



Hexane-1,2-Diol Osmate (4-25b): hexane-1,2-diol **4-25a** (12.6 mg, 0.107 mmol) was converted to its osmate ester (40.7 mg, 84%) following general procedure 2.

Crystallization Attempts				
	Method	Solvent	Antisolvent	Result
1	Vapor Diffusion	CHCl ₃	Pentane	Oil
2	Vapor Diffusion	3:1 Et ₂ O:CH ₂ Cl ₂	Pentane	Oil
3	Vapor Diffusion	THF	Pentane	X-ray Quality Crystals

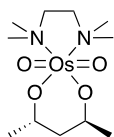
R_f: 0.44 (10% MeOH in CH₂Cl₂, visualized by UV)

¹H NMR (500 MHz, CDCl₃): δ 4.28–4.16 (m, 2H), 3.98 (dd, *J* = 9.3, 7.6 Hz, 1H), 3.12–3.02 (m, 4H), 2.86 (s, 6H), 2.84 (s, 6H), 1.92–1.84 (m, 1H), 1.81–1.71 (m, 1H), 1.53–1.42 (m, 1H), 1.42–1.31 (m, 3H), 0.89 (t, *J* = 7.1 Hz, 3H).

¹³C{¹H} NMR (126 MHz, CDCl₃): δ 90.0, 85.0, 64.6, 64.3, 52.1, 51.9, 51.5, 51.4, 32.5, 29.2, 23.2, 14.3.

Melting Point: 74–76°C

HRMS: *m/z* calcd for C₁₂H₂₈N₂O₄¹⁹²OsNa (M + Na)⁺ : 479.1557, found 479.1547.



(2*S*,4*S*)-pentanediol Osmate (4-28b): (2*S*,4*S*)-pentanediol **4-28a** (10.2 mg, 86.3 μmol) was converted to osmate ester **4-28b** (23.5 mg, 62%) following general procedure 2.

Crystallization Attempts				
	Method	Solvent	Antisolvent	Result
1	Vapor Diffusion	CHCl ₃	Pentane	X-ray Quality Crystals

R_f: 0.40 (10% MeOH in CH₂Cl₂, visualized by UV)

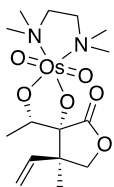
¹H NMR (600 MHz, CDCl₃): δ 4.77 (dq, *J* = 6.2, 5.0 Hz, 2H), 3.14 – 3.02 (m, 4H), 2.72 (s, 10H), 2.41 (t, *J* = 5.1 Hz, 2H), 1.23 (d, *J* = 6.1 Hz, 6H).

¹³C{¹H} NMR (151 MHz, CDCl₃) δ 74.1, 64.8, 50.3, 50.0, 49.2, 23.0.

Melting Point: decomposed at 150 °C

HRMS: *m/z* calcd for C₁₁H₂₆N₂O₄¹⁹²OsNa (M + Na)⁺ : 465.1400, found 465.1398.

[α]_D²² –364.9 (*c* 1.01, CHCl₃)



(3*R*,4*R*)-3-hydroxy-3-((*S*)-1-hydroxyethyl)-4-methyl-4-vinyldihydrofuran-2(3*H*)-one

Osmate Ester (4-30b): Diol **4-30a** (25.0 mg, 0.134 mmol) was converted to osmate ester **4-30b** (16.1 mg, 23%) according to general procedure 2 with the addition of extra TMEDA (100. μL, 0.670 mmol) after 2 h. Compound **4-31** was also isolated during chromatography, and spectral data are reported below.

Osmate 4-30b:

Crystallization Attempts				
	Method	Solvent	Antisolvent	Result
1	Vapor Diffusion	CHCl ₃	Pentane	X-ray Quality Crystals

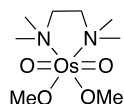
R_f: 0.51 (10% MeOH in CH₂Cl₂, visualized by UV)

¹H NMR (600 MHz, CDCl₃) δ 6.61 (dd, *J* = 17.9, 11.0 Hz, 1H), 5.09 (d, *J* = 11.1 Hz, 1H), 4.94 (d, *J* = 17.9 Hz, 1H), 4.50 (q, *J* = 6.9 Hz, 1H), 4.36 (d, *J* = 8.5 Hz, 1H), 4.19 (s, 1H), 3.20 – 3.13 (m, 2H), 3.08 – 3.01 (m, 2H), 2.95 (s, 3H), 2.91 (s, 3H), 2.86 (s, 3H), 2.85 (s, 3H), 1.58 (d, *J* = 6.9 Hz, 3H), 1.20 (s, 3H).

¹³C{¹H} NMR (151 MHz, CDCl₃) δ 176.8, 142.2, 113.2, 92.8, 91.5, 75.3, 64.9, 64.3, 52.6, 52.5, 51.5, 48.7, 22.2, 16.2.

HRMS: *m/z* calcd for C₁₅H₂₈N₂O₆¹⁹²OsH (M + H)⁺ : 525.1641, found 525.1655.

[α]_D²² –630.1 (*c* 1.07, CHCl₃)

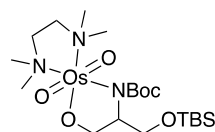


Osmate 4-31:

¹H NMR (600 MHz, CDCl₃) δ 4.59 (s, 3H), 3.04 (s, 2H), 2.77 (s, 6H).

¹³C{¹H} NMR (151 MHz, CDCl₃) δ 66.7, 65.4, 50.9.

HRMS: *m/z* calcd for C₈H₂₂N₂O₄¹⁹²OsNa (M + Na)⁺ : 425.1092, found 425.1096.



Amino alcohol Osmate (4-32b): Amino alcohol **4-32a** (17.0 mg, 0.0556 mmol) was converted to osmate **4-32b** (20.2 mg, 57%) following general procedure 2. The product was soluble in pentane, and we were unable to crystallize this compound.

R_f: 0.67 (10% MeOH in CH₂Cl₂, visualized by UV)

¹H NMR (500 MHz, CDCl₃) δ 4.62 (d, *J* = 9.7 Hz, 1H), 4.20 (ddd, *J* = 9.8, 4.4, 1.2 Hz, 1H), 3.79 – 3.72 (m, 2H), 3.71 – 3.63 (m, 2H), 3.58 (ddd, *J* = 8.9, 4.4, 1.2 Hz, 1H), 3.14 (qd, *J* = 12.8, 11.7,

9.4 Hz, 2H), 3.02 (s, 3H), 2.94 (s, 3H), 2.85 (s, 3H), 2.70 (s, 3H), 1.48 (s, 9H), 0.90 (s, 9H), 0.07 (s, 3H), 0.06 (s, 3H).

$^{13}\text{C}\{^1\text{H}\}$ NMR (126 MHz, CDCl_3) δ 162.1, 80.9, 78.6, 68.6, 65.0, 62.4, 61.1, 51.7, 51.1, 49.8, 48.2, 28.8 (3C), 26.2 (3C), 18.5, -4.9, -5.0.

HRMS: m/z calcd for $\text{C}_{20}\text{H}_{45}\text{N}_3\text{O}_6^{192}\text{OsSiNa}$ ($\text{M} + \text{Na}$) $^+$: 666.2590, found 666.2576.

4.8 References

- ¹ Burns, A. S.; Rychnovsky, S. D. Total Synthesis and Structure Revision of (–)-Illisimonin A, a Neuroprotective Sesquiterpene from the Fruits of *Illicium simonsii*. *J. Am. Chem. Soc.* **2019**, *141*, 13295–13300.
- ² Flack, H. D. On Enantiomorph-Polarity Estimation. *Acta Crystallogr., Sect. A* **1983**, *39*, 876–881.
- ³ (a) Hooft, R. W. W.; Straver, L. H.; Spek, A. L. Determination of Absolute Structure Using Bayesian Statistics on Bijvoet Differences. *J. Appl. Cryst.* **2008**, *41*, 96–103. (b) Parsons, S.; Wagner, T.; Presly, O.; Wood, P. A.; Cooper, R. I. Applications of Leverage Analysis in Structure Refinement. *J. Appl. Cryst.* **2012**, *45*, 417–429.
- ⁴ (a) Holstein, P. M.; Holstein, J. J.; Escudero-Adán, E. C.; Baudoin, O.; Echavarren, A. M. Ferrocene Derivatives of Liquid Chiral Molecules Allow Assignment of Absolute Configuration by X-Ray Crystallography. *Tetrahedron Asymm.* **2017**, *28*, 1321–1329. (b) Shibata, T.; Arai, Y.; Takami, K.; Tsuchikama, K.; Fujimoto, T.; Takebayashi, S.; Takagi, K. Iridium-Catalyzed Enantioselective [2+2+2] Cycloaddition of Dienes and Monoalkynes for the Generation of Axial Chiralities. *Adv. Synth. Catal.* **2006**, *348*, 2475–2483.
- ⁵ Brummel, B. R.; Lee, K. G. McMillen, C. D.; Kolis, J. W.; Whitehead, D. C. Simple One-Pot Absolute Stereochemical Identification of Alcohols via Guanidinium Sulfate Crystallization. *Org Lett.* **2019**, *21*, 9622–9627.
- ⁶ Boese, R. Z. Special issue on *In Situ* Crystallization. *Kristallog.* **2014**, *229*, 595–601.
- ⁷ Inokuma, Y.; Yoshioka, S.; Ariyoshi, J.; Arai, T.; Hitora, Y.; Takada, K.; Matsunaga, S.; Rissanen, K.; Fujita, M. X-ray analysis on the nanogram to microgram scale using porous complexes. *Nature* **2013**, *495*, 461–466.
- ⁸ (a) Kobs, S. F.; Behrman, E. J. Complexation of Osmium Tetroxide with Tertiary Amines. *Inorganica Chim. Acta* **1987**, *128*, 21–26. (b) Nielson, A. J.; Griffith, W. P. Tissue Fixation by Osmium Tetroxide. *J. Histochem. Cytochem.* **1979**, *27*, 997–999.

⁹ (a) Donohoe, T. J.; Blades, K.; Moore, P. R.; Waring, M. J.; Winter, J. J. G.; Helliwell, M.; Newcombe, N. J.; Stemp, G. Directed Dihydroxylation of Cyclic Allylic Alcohols and Trichloroacetamides Using OsO₄/TMEDA. *J. Org. Chem.* **2002**, *67*, 7946–7956. (b) Donohoe, T. J.; Blades, K.; Helliwell, M.; Waring, M. J.; Newcombe, N. J. The Synthesis of (+)-Pericosine B. *Tetrahedron Lett.* **1998**, *39*, 8755–8758. (c) Donohoe, T. J.; Mitchell, L.; Waring, M. J.; Helliwell, M.; Bell, A.; Newcombe, N. J. Scope of the Directed Dihydroxylation: Application to Cyclic Homoallylic Alcohols and Trihaloacetamides. *Org. Biomol. Chem.* **2003**, *1*, 2173–2186.

¹⁰ (a) Sivik, M. R.; Gallucci, J. C.; Paquette, L. A. Crystal Structure Analysis of an Osmium(VI) Bisglycolate Produced by Reaction of a Sterically Hindered Chiral Nonracemic Alkene with Osmium Tetroxide. *J. Org. Chem.* **1990**, *55*, 391–393. (b) Landais, Y.; Mahieux, C.; Schenk, K.; Surange, S. S. A New Synthesis and Stereocontrolled Functionalization of Substituted Silacyclopent-3-Enes. *J. Org. Chem.* **2003**, *68*, 2779–2789. (c) Lang, Y.; Souza, F. E. S.; Xu, X.; Taylor, N. J.; Assoud, A.; Rodrigo, R. Pentacyclic Furanosteroids: the Synthesis of Potential Kinase Inhibitors Related to Viridin and Wortmannolone. *J. Org. Chem.* **2009**, *74*, 5429–5439. (d) VanVeller, B.; Miki, K.; Swager, T. M. Rigid Hydrophilic Structures for Improved Properties of Conjugated Polymers and Nitrotyrosine Sensing in Water. *Org. Lett.* **2010**, *12*, 1292–1295.

¹¹ (a) Prangé, T.; Pascard, C. Osmium Tetroxide–9-Methylbenzanthracene–Bis(Pyridine) Adduct (Toluene Solvate). *Acta Crystallogr. Sect. B* **1977**, *33*, 621–623. (b) Wallis, J. M.; Kochi, J. K. Electron-Transfer Activation in the Thermal and Photochemical Osmylations of Aromatic Electron Donor-Acceptor Complexes with Osmium(VIII) Tetroxide. *J. Am. Chem. Soc.* **1988**, *110*, 8207–8223. (c) Groy, T. L.; Hartman, R. F.; Rose, S. D. Structure of a Bis(Osmate Ester) Produced by Addition of Osmium Tetroxide to Diethyl 3,4-Furandicarboxylate. *Acta Crystallogr. Sect. C* **1991**, *47*, 273–275. (d) Herrmann, W. A.; Eder, S. J.; Scherer, W. Catalytic Oxidation of Partially and Fully Fluorinated Olefins with Osmium Tetroxide. *Angew. Chem. Int. Ed.* **1992**, *31*, 1345–1347. (e) Herrmann, W. A.; Roesky, P. W.; Elison, M.; Artus, G.; Oefele, K. Oxy Functionalization of Metal-Coordinated Heterocyclic Carbenes. *Organometallics* **1995**, *14*, 1085–1086.

¹² (a) Tomioka, K.; Nakajima, M.; Iitaka, Y.; Koga, K. Mechanistic Aspects of Asymmetric Cis-Dihydroxylation of Olefins with Osmium-Tetroxide Employing a C₂-Symmetric Chiral Diamine. *Tetrahedron Lett.* **1988**, *29*, 573–576. (b) Oishi, T.; Hiramata, M. Highly Enantioselective Dihydroxylation of Trans-Disubstituted and Monosubstituted Olefins. *J. Org. Chem.* **1989**, *54*, 5834–5835. (c) Pearlstein, R. M.; Blackburn, B. K.; Davis, W. M.; Sharpless, K. B. Structural Characterization of the Pseudoenantiomeric Cis-Dioxo Osmium(VI) Esters of Chiral Diols with Cinchona

Alkaloid Ligands. *Angew. Chem. Int. Ed.* **1990**, *29*, 639–641. (d) Hanessian, S.; Meffre, P.; Girard, M.; Beaudoin, S.; Sanceau, J. Y.; Bennani, Y. Asymmetric Dihydroxylation of Olefins with a Simple Chiral Ligand. *J. Org. Chem.* **1993**, *58*, 1991–1993. (e) Donohoe, T. J.; Harris, R. M.; Butterworth, S.; Burrows, J. N.; Cowley, A.; Parker, J. S. New Osmium-Based Reagent for the Dihydroxylation of Alkenes. *J. Org. Chem.* **2006**, *71*, 4481–4489.

¹³ (a) Conn, J. F.; Kim, J. J.; Suddath, F. L.; Blattmann, P.; Rich, A. Crystal and Molecular Structure of an Osmium Bispyridine Ester of Adenosine. *J. Am. Chem. Soc.* **1974**, *96*, 7152–7153. (b) Umemoto, T.; Okamoto, A. Synthesis and Characterization of the 5-Methyl-2'-Deoxycytidine Glycol–Dioxoosmium–Bipyridine Ternary Complex in DNA. *Org. Biomol. Chem.* **2008**, *6*, 269–271. (c) Sugizaki, K.; Ikeda, S.; Yanagisawa, H.; Okamoto, A. Facile Synthesis of Hydroxymethylcytosine-Containing Oligonucleotides and Their Reactivity Upon Osmium Oxidation. *Org. Biomol. Chem.* **2011**, *9*, 4176–4176.

¹⁴ Taber, D. F.; Gunn, B. P. Control Elements in the Intramolecular Diels-Alder Reaction. Synthesis of (±)-Torreyol. *J. Am. Chem. Soc.* **1979**, *101*, 3992–3993.

¹⁵ Yang, X.-H.; Davison, R.; Dong, V. M. Catalytic Hydrothiolation: Regio- and Enantioselective Coupling of Thiols and Dienes. *J. Am. Chem. Soc.* **2018**, *140*, 10443.

¹⁶ Slutskyy, Y.; Jamison, C. R.; Zhao, P.; Lee, J.; Rhee, Y. H.; Overman, L. E. Versatile Construction of 6-Substituted cis-2,8-Dioxabicyclo[3.3.0]octan-3-ones: Short Enantioselective Total Synthesis of Cheloviolenes A and B and Dendrillolide C. *J. Am. Chem. Soc.* **2017**, *139*, 7192–7195.

¹⁷ The reactivity of the tetrasubstituted alkene in α -santonin has previously been noted for the dihydroxylation with potassium permanganate: Paknikar, S. K.; Malik, B. L.; Bates, R. B.; Caldera, S.; Wijayaratne, T. V. Stereochemistry of 4,5-Dihydroxy- α -Santonin and Structure of a New Santonin Oxidation-Product. *Tetrahedron Lett.* **1994**, *35*, 8117–8118.

¹⁸ McCormick, J. P.; Tomasik, W.; Johnson, M. W. α -Hydroxylation of Ketones - Osmium Tetroxide-*N*-Methylmorpholine-*N*-Oxide Oxidation of Silyl Enol Ethers. *Tetrahedron Lett.* **1981**, *22*, 607–610.

¹⁹ (a) Schreiber, S. L.; Goulet, M. T. Application of a Two-Directional Chain Synthesis Strategy to the First Stereochemical Assignment of Structure to Members of the Skipped-Polyol Polyene Macrolide Class: Mycoticin A and B. *J. Am. Chem. Soc.* **1987**, *109*, 8120–8122. (b) Rychnovsky, S. D.; Rogers, B.; Yang, G. Analysis of Two ¹³C NMR Correlations for Determining the Stereochemistry of 1,3-Diol Acetonides. *J. Org. Chem.* **1993**, *58*, 3511–3515.

- ²⁰ (a) Ragazzo, J. A.; Behrman, E. J. The reactions of oxo-osmium ligand complexes with isopentenyl adenine and its nucleoside. *Bioinorg. Chem.* **1976**, *5*, 343–352. (b) Midden, W. R.; Chang, C.-H.; Clark, R. L.; Behrman, E. J. Transesterification of Oxo-Osmium(VI) Ligand Complexes of Thymine Derivatives. *J. Inorg. Biochem.* **1980**, *12*, 93–105. (c) Mohapatra, S. K.; Behrman, E. J. Effects of Glycol Structure on the Transesterification Equilibria of Oxo-Osmium(VI) Esters. *J. Inorg. Biochem.* **1982**, *16*, 85–89. (d) Seddon, E. A. Osmium. *Coor. Chem. Rev.* **1985**, *67*, 243–295.
- ²¹ Paquette, L. A.; Lo, H. Y. Chemical Modifications of a Highly Functionalized Taxane. The Consequences of an Absent Bridgehead Double Bond on Oxetane D-Ring Construction. *J. Org. Chem.* **2003**, *68*, 2282–2289.
- ²² Carlson, P. R.; Burns, A. S.; Shimizu, E. A.; Wang, S.; Rychnovsky, S. D. Silacycle-Templated Intramolecular Diels–Alder Cyclizations for the Diastereoselective Construction of Complex Carbon Skeletons. *Org. Lett.* **2021**, *23*, 2183–2188.
- ²³ Burns, A. S.; Dooley, C., III; Carlson, P. C.; Ziller, J. W.; Rychnovsky, S. D. Relative and Absolute Structure Assignments of Alkenes Using Crystalline Osmate Derivatives for X-ray Analysis. *Org. Lett.* **2019**, *21*, 10125–10129.
- ²⁴ Khadem, El, H.; Hanessian, S. Ammonium Molybdate as Spraying Agent for Paper Chromatograms of Reducing Sugars. *Anal. Chem.* **1958**, *30*, 1965–1965.

Chapter 5. Development of Strategies Toward the Total Synthesis of (2*R*)-Hydroxynorneomajucin and Related *Illicium* Sesquiterpenes

5.1 Abstract

Efforts toward the first total synthesis of (2*R*)-hydroxynorneomajucin are described herein. Our synthetic strategy initially hinged on utilizing a Pauson–Khand reaction of an advanced bis-lactone intermediate to construct the core of the natural product which, unfortunately, was not successful. The key features of our revised synthetic strategy include an asymmetric Tsuji–Trost allylic alkylation to set a key quaternary center, a Pauson–Khand to close the core of the molecule, and a late-stage conjugate addition to install the final quaternary center. This strategy has allowed us to complete the first total synthesis of (2*R*)-hydroxynorneomajucin to date in 18 steps.

5.2 Introduction

5.2.1 Introduction to the *Illicium* Sesquiterpenes

The *Illicium* genus comprises a group of flowering trees and shrubs native to areas of eastern Asia, Australia, New Zealand, and the Southeastern United States.¹ From this genus of plant, hundreds of interesting sesquiterpene natural products have been isolated, displaying varying carbon skeletons, as can be seen in Figure 5-1.² There have been around 100 *seco*-prezizaane type sesquiterpenes isolated from the *Illicium* genus, and this sub-class will be the focus of this chapter.

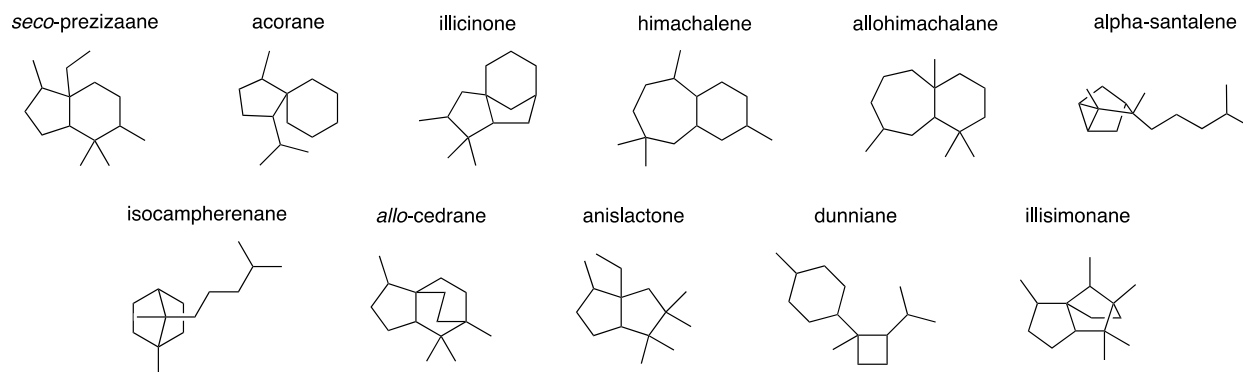


Figure 5-1 Different carbon skeletons of the *Illicium* sesquiterpenes.

The history of *seco*-prezizaane natural products dates back to the isolation of anisatin (**5-1**), the toxin derived from the Japanese star anise in 1952.³ However, it was not until 1968 when the x-ray structure of anisatin was solved by Yamada and coworkers that the chemical community would see the complexity of this family of natural products.⁴ Over the next several decades, the field of *seco*-prezizaane natural products would flourish. In the early nineties, the group of Fukuyama initiated a campaign searching for exogenous, small molecule neurotrophic factors derived from the *Illicium* species of plants.¹ From this work, several new natural products were isolated, some of which are shown in Figure 5-2. The *seco*-prezizaanes have become very popular synthetic targets, owing to their challenging structure and potent neurotrophic activity.

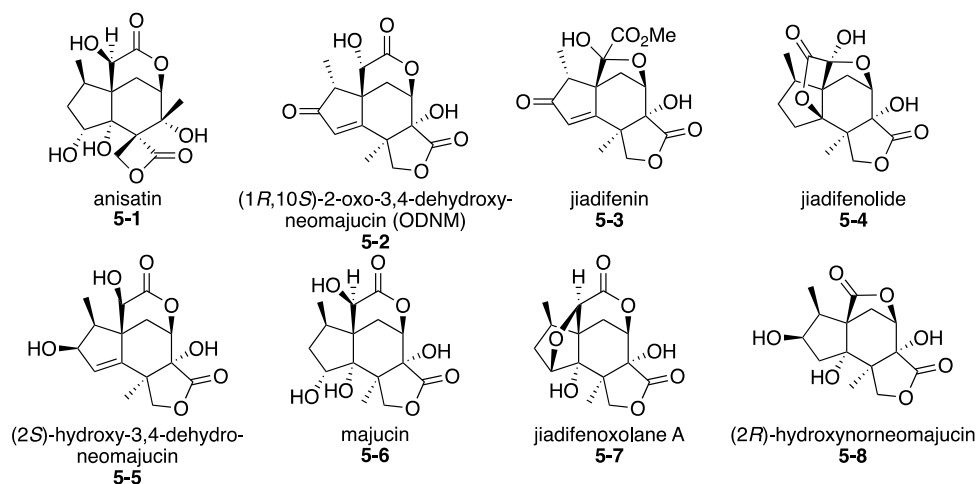


Figure 5-2 Representative seco-prezizaane sesquiterpenes.

From a biological perspective, the mechanism of action that lends the *seco*-prezizaanes their neurotrophic benefits is not very well understood. Anisatin is known to be one of the most potent neurotoxins of plant origin (LD50=1mg/kg in mice). Studies have shown that anisatin is a potent, non-competitive γ -aminobutyric acid (GABA) antagonist.⁵ GABA is a major inhibitory neurotransmitter in vertebrates and is important for regulation within the central nervous system.⁶ Specifically, GABA acts as an inhibitor on neuronal chloride channels, causing hyperpolarization and inhibiting the propagation of action potentials. Several of the *Illicium* sesquiterpenes are thought to act as GABA receptor antagonists. Antagonism of an inhibitory neurotransmitter is net excitatory and can lead to increased action potential firing through depolarization of the neuron. For example, anisatin, acting as a non-competitive GABA antagonist, inhibits the action of GABA on chloride channels, and leads to convulsions of the organism.

Unlike **5-1**, the other *seco*-prezizaanes listed in Figure 5-2 have been shown to elicit neurotrophic effects, such as promoting the survival or growth of neural cells. The neurotrophic effect of these natural products is not very well understood, as they also act as GABA antagonists. Among the best studied of these natural products is jiadifenolide (**5-4**), owing to an elegant gram-

scale synthesis of this natural product by the Shenvi group.⁷ In pharmacological assays, **5-4** was shown not to induce convulsions, and reportedly mice dosed at 15 μM intracerebroventricularly (ICV) were more alert and active than the rest of the host mice.⁸ Interestingly, while **5-4** was shown to antagonize GABA receptors, it exhibited significantly weaker potency. Compared to known convulsants, which blocked the GABA_A currents in the single digit μM range, **5-4** blocked the same currents only at 100 μM concentration. This weaker potency has been implicated in the safety of **5-4**, as dosing at high concentrations did not elicit any convulsant side effects. However, it does not adequately explain exactly how **5-4** elicits its neuroprotective effects. Shenvi has also pointed out that, at very low concentration, analogous GABA antagonists elicit similar neurotrophic effects.⁹ This is especially interesting, as these compounds have other known binding sites in the Cys-loop family of neurotransmitter-gated ion channels. Lastly, Shenvi points out that the PC12 cell line frequently used as an *in vitro* model for these natural products lacks functional GABA receptors, meaning that the antagonistic effect of **5-4** on GABA receptors does not necessarily underly its neurotrophic activity.

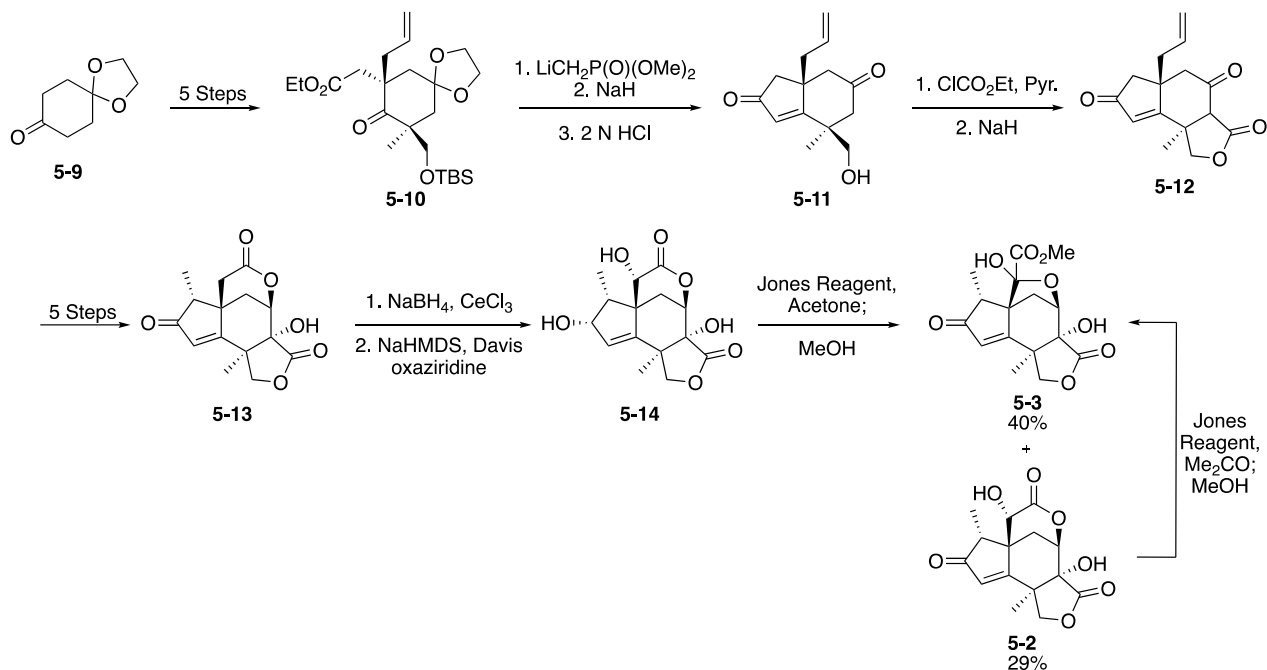
Though the mechanism of action is poorly understood, the interesting structures and potent neurotrophic activity of these compounds has made them popular synthetic targets. Given their homology to our target compound **5-8**, it is instructive to examine the prior syntheses of these compounds, which will be covered mostly chronologically. Excellent reviews on the topic of *Illicium* and *seco-prezizaane* syntheses are available for further reading.¹⁰

5.2.2 Danishefsky's Total Synthesis of (\pm)-*Jiadifenin*

In 2004, Danishefsky's group published the first total synthesis of (\pm)-**5-3**.¹¹ Their synthesis commenced by conversion of readily available **5-9** to **5-10** in a 5-step sequence of alkylations. The ester of **5-10** was converted to a β -ketophosphonate, followed by an

intramolecular Horner–Wadsworth–Emmons reaction and deprotection to produce **5-11**. The primary alcohol of **5-11** was converted to an ethyl carbonate, and the intermediate was subjected to sodium hydride to effect a Dieckmann condensation generating β -ketolactone **5-12**. A series of functional group and redox manipulations led to compound **5-13**.

Scheme 5-1 Danishefsky's synthesis of **5-2** and **5-3**.



With **5-13** in hand, a simple set of reactions led to **5-3**. First, **5-13** was subjected to a Luche reduction, followed by oxidation of the δ -lactone with Davis oxaziridine to generate **5-14**. Following precedent from Fukuyama¹², treatment of **5-14** with Jones Reagent, followed by the addition of methanol led to a mixture of **5-2** and **5-3** in 69% overall yield. **5-2** could be converted to **5-3** by resubjection of the material to the oxidative rearrangement conditions. A brief validation of the biological activity interestingly revealed that **5-2** was a more potent promoter of neurite outgrowth than **5-3**. In 2006, Danishefsky's group published another paper investigating some of the structure-activity relationship (SAR) around these natural products.¹³ Through discreet

changes in their synthetic strategy, they additionally synthesized compounds **5-15** to **5-17** and investigated their potential to promote neurite outgrowth (Figure 5-3).

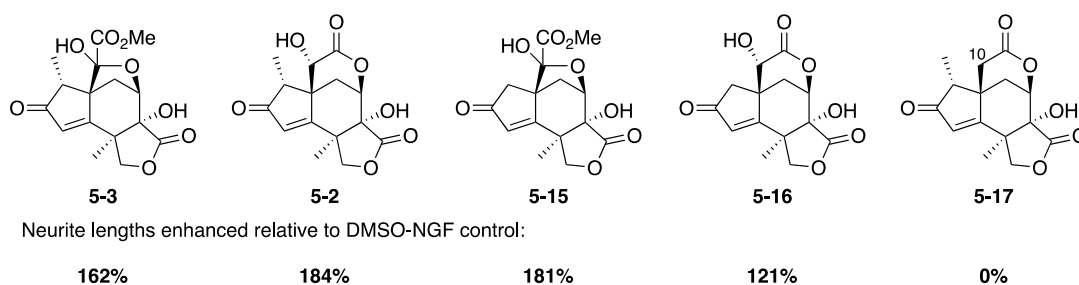


Figure 5-3 Initial SAR mapping of jiadifenin-like compounds.

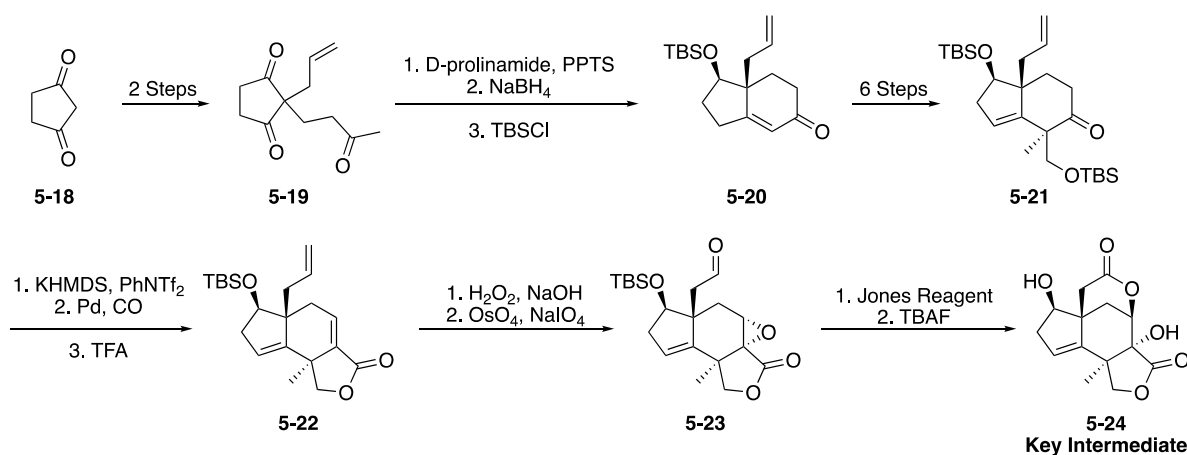
Comparing the activity of **5-3** to **5-15**, it appears that methylation of the cyclopentenone A-ring in fact diminishes the neurotrophic activity. Oddly, **5-16** has far diminished activity relative to **5-2**, making any assessment of the function of this methyl group unclear. It is, however, clear that oxidation of C10 (labelled in compound **5-17**) is necessary for activity, as compound **5-17** elicited no effect in these assays. One other important finding was that these compounds only promoted neurite outgrowth in the presence of neurite growth factor (NGF), suggesting a synergistic mechanism of action with this growth factor. This work sparked significant interest in the field, and several elegant syntheses followed.

5.2.3 Theodorakis's Enantioselective Syntheses of (-)-Jiadifenolide and (-)-Jiadifenin

Following Danishefsky's pioneering racemic synthesis of **5-3**, in 2011 the group of Theodorakis disclosed the first total synthesis of enantiopure **5-4**.¹⁴ Their synthesis commenced from compound **5-18**, which was readily converted to **5-19** in two steps. To render the synthesis asymmetric, compound **5-19** was subjected to an enantioselective aldol condensation catalyzed by D-prolinamide. Subsequent reduction of the remaining ketone with NaBH₄, followed by protection led to **5-20**. A sequence of 6 steps converted enone **5-20** to **5-21** bearing a new quaternary center. Treatment of this intermediate with KHMDS and *N*-phenyl triflimide led to a vinyl triflate, which

could then undergo a palladium-catalyzed carbomethoxylation and lactonization to access **5-22**. Nucleophilic epoxidation of the α,β -unsaturated lactone, followed by Johnson–Lemieux oxidative cleavage of the alkene afforded aldehyde **5-23**. Oxidation of the aldehyde with Jones reagent led to a carboxylic acid, which concomitantly underwent a nucleophilic opening of the epoxide leading to a δ -lactone intermediate. Desilylation with TBAF gave compound **5-24**, which is a key intermediate for the syntheses of both jiadifenolide (**5-4**) and jiadifenin (**5-3**).

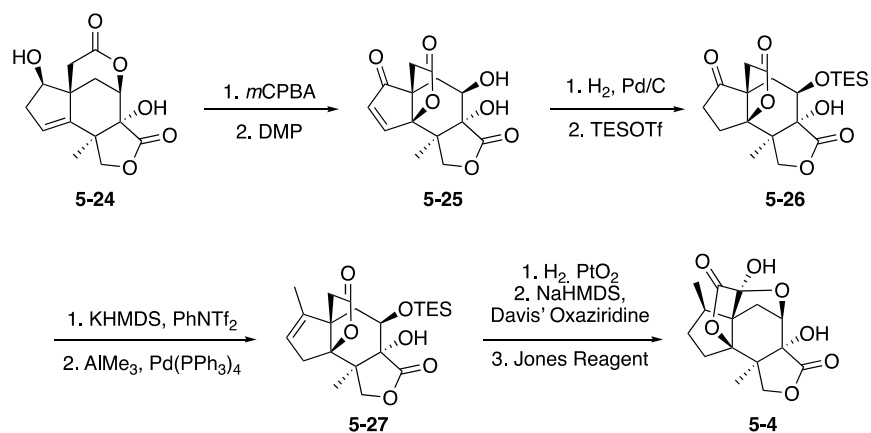
Scheme 5-2 Theodorakis's Synthesis of key intermediate **5-24**.



With intermediate **5-24** in hand, there remained some work to access jiadifenolide. First, the oxidation pattern of the A-ring cyclopentene needed to be adjusted. As such, diastereoselective epoxidation of compound **5-24** directed by the free alcohol occurred upon treatment with *m*CPBA. Subsequently, the alcohol was oxidized with Dess–Martin periodinane. Under the reaction conditions, the newly formed ketone eliminated the β -epoxide, and the tertiary alcohol thus formed underwent translactonization, cleanly affording compound **5-25**. Reduction of the enone via hydrogenation, followed by silyl protection of the secondary alcohol led to **5-26**. In order to convert the ketone functionality to a β -disposed methyl group, the ketone was first converted to a vinyl triflate, which then underwent palladium-catalyzed methylation upon treatment with AlMe₃ to generate **5-27**. Hydrogenation of this alkene with PtO₂ (Adam's catalyst) occurred selectively

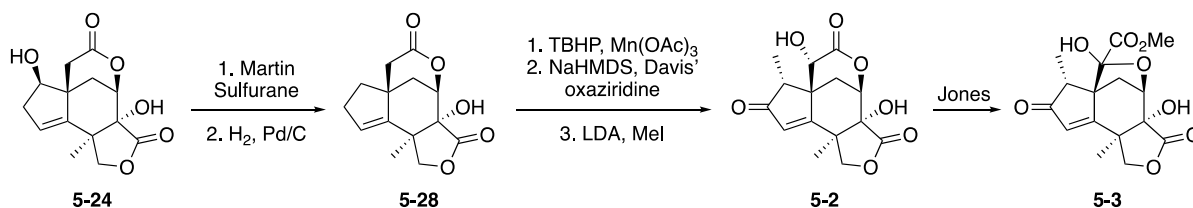
from the bottom face, giving the desired methyl configuration. To complete the synthesis, the γ -lactone was oxidized by treatment with NaHMDS and Davis' oxaziridine, followed by further oxidation with Jones reagent. When treated under the acidic conditions of Jones reagent, cleavage of the TES-group occurs with concomitant lactol formation to complete the first total synthesis of jiadifenolide in 27 steps from **5-18**.

Scheme 5-3 Completion of the total synthesis of **5-4**.



Later in 2011, the Theodorakis group published a total synthesis of enantiopure jiadifenin utilizing **5-24** as a common intermediate.¹⁵ As such, the secondary alcohol of **5-24** was eliminated by treatment with Martin's sulfurane. Hydrogenation of the less hindered alkene smoothly generated **5-28**. Allylic oxidation mediated by Mn(OAc)₃ and TBHP generated an enone intermediate. Oxidation of the lactone ring with Davis' oxaziridine, followed by diastereoselective methylation of the enone afforded **5-2**. Following the precedent of Danishefsky¹¹ and Fukuyama¹², treatment of **5-2** with Jones reagent completed the synthesis of (–)-**5-3** in 24 steps from **5-18**.

Scheme 5-4 Theodorakis's synthesis of **5-3** from common intermediate **5-24**.



Following these publications, the Theodorakis group also set about further investigating the SAR of these natural products to complement the work done previously by Danishefsky.¹⁶ Following the routes outlined in Schemes 5-2 to 5-4, a small library of analogues were synthesized and subjected to biological assays. Each compound was added to cultured PC12 cells in the presence NGF, and neurite outgrowth was monitored. The results are summarized in Table 5-1. Note that inactive compounds showed neurite outgrowth less than 110% relative to NGF alone, and active compounds elicited outgrowth greater than 110% relative to control. From the results, the substitution around the cyclopentane A-ring does not seem to control the activity, but substitution on the lactone does seem to be crucial. Specifically, having an α -disposed substituent is necessary for activity. Compounds containing either no substituent or a β -substituent on the lactone were shown to be inactive. Lastly, the Theodorakis group showed that oxidation of the lactone does not underly the activity of these compounds, as having an α -methyl group (Table 4-1, bottom row) also promoted neurite outgrowth. This work provides a much more thorough understanding of the SAR of these molecules, but the specific mechanism of action remains unclear.

Table 5-1 Pharmacophore mapping of ODNM analogues.

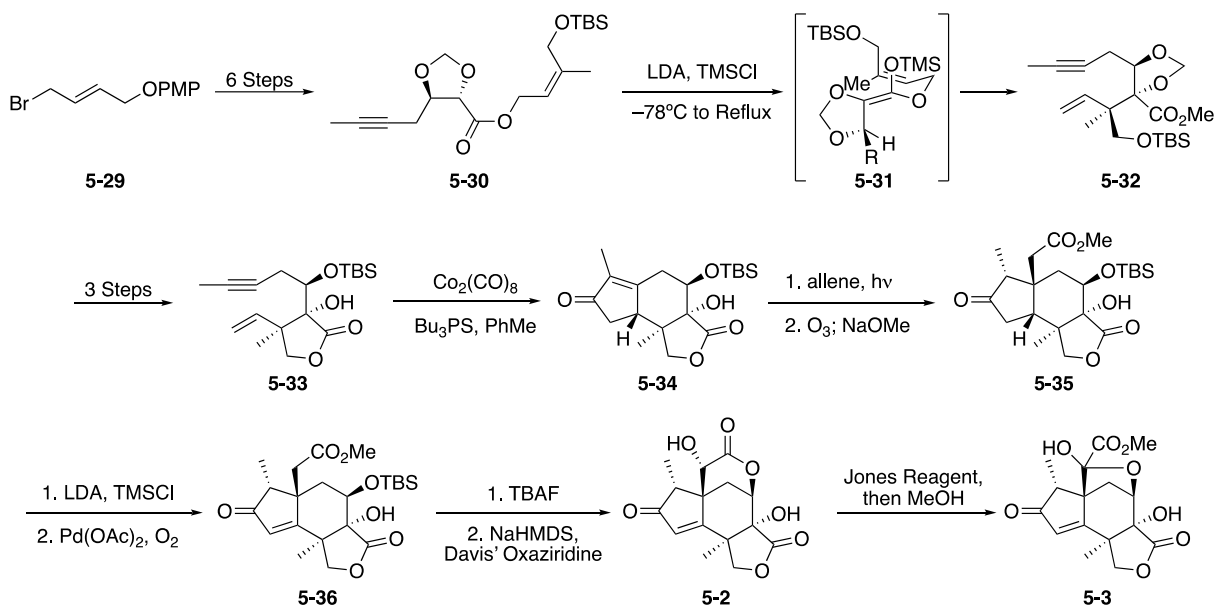
	inactive	–	inactive	–	inactive	inactive	inactive
	–	inactive	inactive	–	–	–	inactive
	active	–	active	active	active	–	active
	active	–	active	–	–	–	–

5.2.4 Zhai's Total Synthesis of Jiadifenin

In 2012, the group of Hongbin Zhai published an elegant route to jiadifenin (**5-3**) utilizing a distinct set of bond disconnections.¹⁷ The synthesis started from **5-29**, available in 3 steps from commercial material. A sequence of 6 steps converted this compound to enantiopure **5-30**. The absolute stereochemistry of this intermediate was set via a Sharpless asymmetric dihydroxylation. Treatment of **5-30** with LDA and TMSCl at low temperature generated silyl-ketene acetal **5-31**, which, upon heating, underwent a diastereoselective Ireland–Claisen rearrangement to set the quaternary center in **5-32**. A further sequence of protecting group manipulations led to compound **5-33**, which, upon treatment with stoichiometric dicobaltoctacarbonyl and tributylphosphane sulfide, underwent a smooth Pauson–Khand reaction to give tricycle **5-34**. To set the other necessary quaternary center, the Zhai group used a clever sequence consisting of a [2+2] photocycloaddition with allene, followed by ozonolysis of the resulting alkene to generate a

cyclobutanone. Treatment of the *in situ* generated cyclobutanone with NaOMe led directly to **5-35**.

Scheme 5-5 Zhai's synthesis of **5-3**.



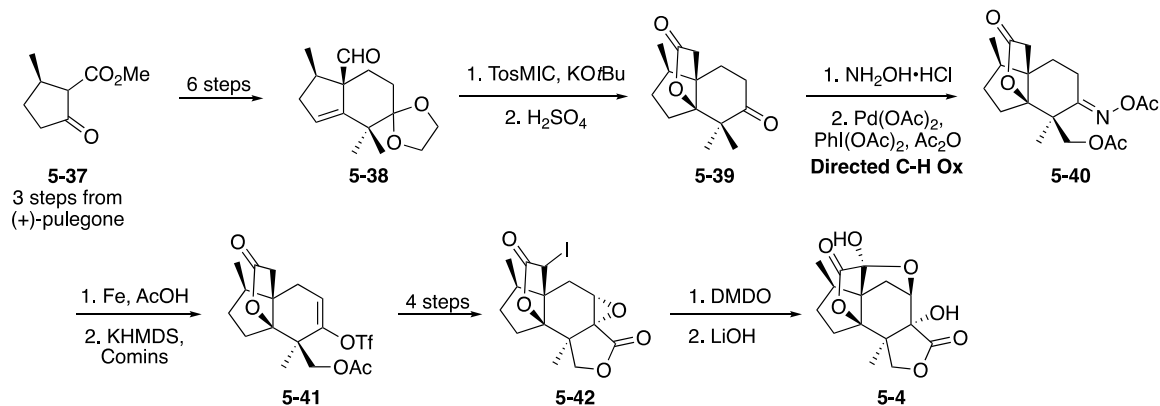
With all of the requisite carbons installed, all that remained was a sequence of functional group and redox manipulations to complete the synthesis. Transformation of **5-35** to the enone via a two-step Saegusa–Ito oxidation generated **5-36**. Treatment of this compound with TBAF elicited desilylation and subsequent lactonization. From here, oxidation of the lactone with Davis' oxaziridine afforded **5-2**, which could once again be converted to **5-3** by treatment with Jones reagent. Overall, this elegant synthesis was completed in 18 steps from **5-29**, and is one of few approaches to this family of natural products that does not start with the A-ring cyclopentane intact.

5.2.5 Sorensen's Total Synthesis of (–)-Jiadifenolide

In 2014, the Sorensen group published an approach to **5-4** taking advantage of a clever directed C-H oxidation as a key step.¹⁸ Their synthesis begins with **5-37**, derived in 3 steps from (+)-pulegone. It is worth mentioning that **5-37** will appear as a starting material in several other

approaches to **5-4**. Compound **5-37** was converted to **5-38** in a series of 6 standard manipulations. One carbon homologation of the aldehyde in **5-38** was achieved using the Van Leusen reaction, generating a homologated nitrile intermediate. Hydrolysis of the nitrile with sulfuric acid occurred with concomitant lactonization to generate **5-39**. Subsequently, the ketone was converted to an oxime, which they used as a functional handle to direct a palladium catalyzed C–H oxidation of the neighboring gem-dimethyl group generating **5-40**. Unfortunately, while the oxidation was regioselective for the methyl groups, it generated a 1:1 mixture of diastereomers from equal oxidation of each methyl group. Further experimentation did not improve this ratio, but fortunately the diastereomers were separable by silica gel chromatography.

Scheme 5-6 Sorensen's synthesis of **5-4**.



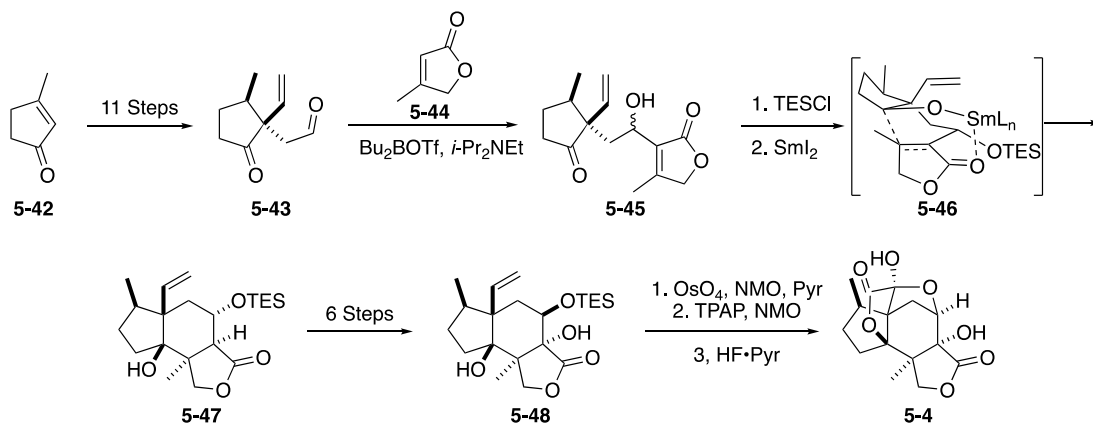
With access to suitable quantities of **5-40**, the synthesis could be completed in short order. Cleavage of the oxime with iron powder in acetic acid, followed by treatment with KHMDS and Comins reagent generated alkenyl triflate **5-41**. A sequence of 4 steps reminiscent of Theodorakis's approach led to intermediate **5-42**. Treatment of this material with DMDO effected an oxidation of the iodide to an iodoso intermediate, which underwent an iodoso Pummerer

rearrangement to generate an α -keto lactone.¹⁹ Final treatment of this ketone with LiOH formed the final ring and completed the synthesis of **5-4** in 18 steps LLS from pulegone-derived **5-37**.

5.2.6 Paterson's Total Synthesis of (\pm)-Jiadifenolide

Exactly one month after the Sorensen group published their synthesis of jiadifenolide, the Paterson group published their work on the synthesis of racemic jiadifenolide utilizing an elegant intramolecular Giese addition to close the central 6-membered ring and set a key quaternary center.²⁰ Their synthesis commenced by performing an 11-step sequence on enone **5-42** to access compound **5-43**. Boron-mediated aldol of butenolide **5-44** with aldehyde **5-43** generated **5-45** as a 2:1 mixture of separable diastereomers. The newly formed alcohol was silyl protected, leading to the key step of the synthesis. Treatment of this intermediate with SmI₂ generated an intermediate ketyl radical, which underwent intramolecular Giese addition with the pendant butenolide to generate **5-47** as a single diastereomer. The authors propose that the exquisite diastereoselectivity is due to chelated, boat-like transition state **5-46**. Notably, the poor diastereoselectivity in the aldol reaction was relatively inconsequential, as only the α -alcohol underwent productive cyclization. This is likely due to the pseudoaxial position of the β -configured alcohol, which impedes the samarium chelate.

Scheme 5-7 Paterson's synthesis of **5-4**.

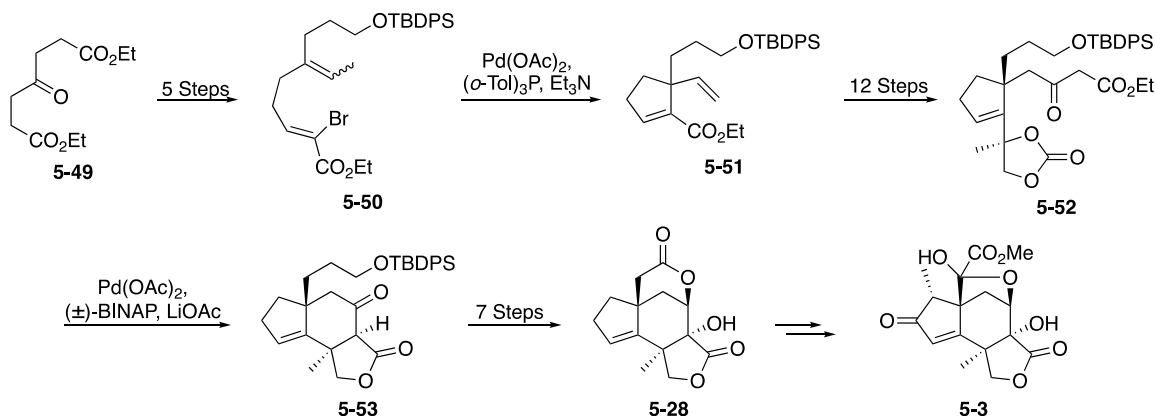


With a successful route to tricycle **5-47**, a series of manipulations was performed to access **5-48**. Pyridine accelerated dihydroxylation of the monosubstituted alkene, followed by oxidative lactonization under Ley conditions led to an intermediate α -keto lactone, similar to Sorensen's approach. Final desilylation with Olah's reagent (HF•Pyr) occurred with concurrent hemiacetalization to complete the synthesis of **5-4** in 23 steps LLS from **5-42**. While not the shortest approach, the creative strategy employed to close the core of the molecule would inspire other approaches in this family of natural products.

5.2.7 *Fukuyama's Formal Synthesis of (\pm)-Jiadifenin*

In 2015, Fukuyama's group disclosed a formal synthesis of jiadifenin utilizing clever palladium catalyzed reactions to form all of the rings and quaternary centers. Their approach began with **5-49**, which was converted to **5-50** in a sequence of 5 steps. The alkenyl bromide of **5-50** was utilized to template a palladium-catalyzed Heck cyclization to form **5-51**. A series of 12 steps led to cyclic carbonate **5-52**, which Fukuyama's group used to template an intramolecular Tsuji–Trost reaction. Treatment with Pd(OAc)₂ and racemic BINAP generated a π -allyl palladium species, which underwent cyclization from the keto-ester and further lactonization to afford **5-53**. A final sequence of manipulations led to Theodorakis's intermediate **5-28**, completing the formal synthesis of **5-3**. The creative use of palladium catalysis, specifically the Tsuji–Trost reaction, partially inspired our own approach to **5-8**.

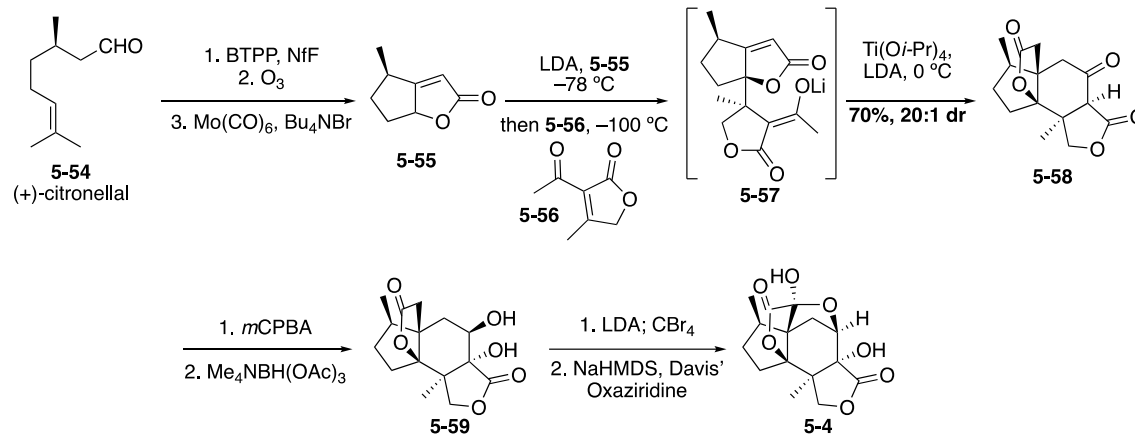
Scheme 5-8 Fukuyama's formal synthesis of **5-3**.



5.2.8 Shenvi's Gram-Scale Synthesis of (-)-Jiadifenolide

In 2015, Ryan Shenvi's group published an 8-step, gram-scale synthesis of **5-4**; a major advance in the field of *seco*-prezizaane synthesis.⁷ Their synthesis began with **5-54**, conveniently bearing the methyl stereocenter necessary in the A-ring. The aldehyde was initially converted to a terminal alkyne through elimination of an intermediate alkenyl nonafluorobutanesulfonate with *tert*-butyl-imino-tri(pyrrrolidino)phosphorane (BTTP). This transformation could also be performed in two steps by conversion of the aldehyde to the geminal dibromide, followed by elimination with potassium *tert*-butoxide, which was a more convenient solution on large scale. Ozonolysis of the trisubstituted alkene led to another aldehyde, which underwent a molybdenum catalyzed hetero Pauson–Khand reaction to generate **5-55**. Treatment of **5-55** with LDA at low temperature, followed by addition of acetylbutenolide **5-56**, formed Michael adduct **5-57**. Addition of titanium(IV) isopropoxide and additional LDA at 0 °C equilibrated the enolate and allowed a second Michael addition to occur, forming **5-58** as a single diastereomer. Notably, in one operation, the entire core of **5-4** was formed from two relatively simple fragments.

Scheme 5-9 Shenvi's total synthesis of (–)-jiadifenolide.



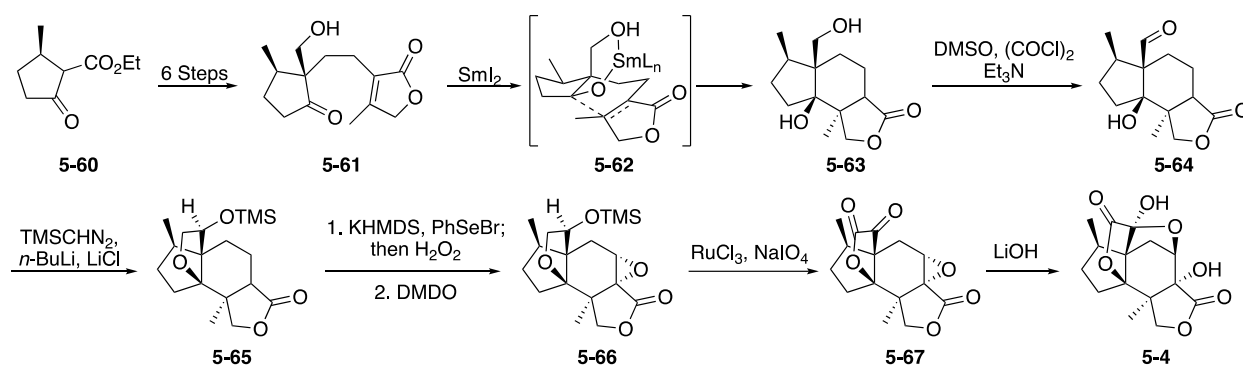
To complete the synthesis of **5-4**, a few manipulations remained. First, Rubottom oxidation of keto-ester **5-58** occurred diastereoselectively upon treatment with *m*CPBA. Subsequent directed reduction of the ketone using tetramethylammonium triacetoxyborohydride delivered **5-59**. Enolization of the lactone with LDA, followed by addition of CBr₄ led to an intermediate bromolactone. Oxidation of this bromolactone with Davis' oxaziridine yielded **5-4**. In a single pass of this sequence, the Shenvi group prepared 1 gram of synthetic jiadifenolide, showcasing the power of synthetic chemistry. To isolate 1 gram of jiadifenolide from natural sources, it would require approximately 117 kilograms of *Illicium jiadifengpi* pericarps. While syntheses of other classes of *Illicium* sesquiterpenes is beyond the scope of discussion, it is noteworthy that Shenvi's group has applied this highly stereocontrolled Michael addition to the syntheses of (–)-11-*O*-debenzoyltashironin and merrilactone A.^{21,22}

5.2.9 Zhang's Protecting Group Free Synthesis of (–)-Jiadifenolide

In 2015, Zhang and coworkers published a protecting group free total synthesis of **5-4**, utilizing an unprecedented formal [4+1] annulation that was discovered in the course of their work.²³ Their synthesis commenced with **5-60**, the ethyl ester derivative of Sorensen's starting material. In a similar sequence of reactions covered in Paterson's synthesis, **5-60** was converted to

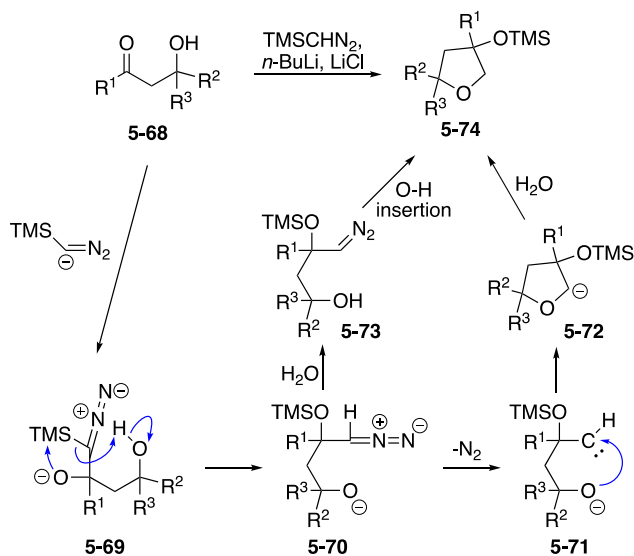
5-61. Drawing inspiration from Paterson's work, Zhang utilized a ketyl radical cyclization to construct the core tricycle of the natural product. As such, treatment of **5-61** with SmI_2 led to **5-63** with good stereocontrol, which was postulated to be controlled by samarium chelate **5-62**. This altered execution of Paterson's key transformation led to tricycle **5-63** in 7 steps, as opposed to the 14 steps required to synthesize **5-47**. A Swern oxidation of the primary alcohol led to aldehyde **5-64**, the substrate for the key formal [4+1] cyclization.

Scheme 5-10 Zhang's total synthesis of **5-4**.



At this stage, Zhang's group had hoped to close the final lactone ring by functionalizing an alkyne derivative. As such, they attempted to transform **5-64** to a terminal alkyne through use of the Colvin rearrangement.²⁴ Serendipitously, treatment of **5-64** with lithiated TMS-diazomethane smoothly led to tetrahydrofuran **5-65**. The proposed mechanism of this transformation can be seen in Scheme **5-11** and will be discussed below. With **5-65** in hand, a one-step selenoxide elimination delivered an intermediate enone, which was epoxidized by the action of DMDO to afford **5-66**. Oxidation with *in situ* generated RuO_4 delivered α -keto lactone **5-67**, which, upon treatment with LiOH , formed **5-4**. To showcase the scalability and utility of their route, Zhang's group synthesized >300 mg of jiadifenolide. This 13-step route, while not as short as Shenvi's route, was still a significant achievement in the context of *Illicium* syntheses.

Scheme 5-11 Proposed mechanism of the formal [4+1] annulation.



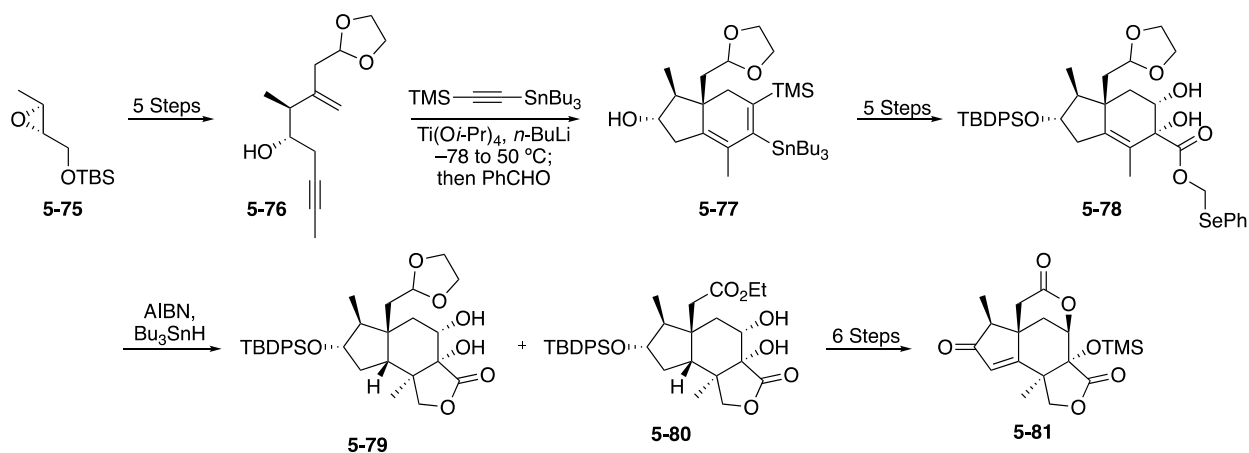
Mechanistically, the key formal [4+1] cyclization takes a simple turn from the originally proposed mechanism of the Colvin rearrangement.²⁴ After initial addition of lithiated TMS-diazomethane to generalized β -hydroxy ketone **5-68** to give **5-69**, a Brook rearrangement occurs, followed by intramolecular proton transfer to give intermediate **5-70**. From here, two pathways are possible. In the first pathway, extrusion of N_2 occurs to give carbene intermediate **5-71**, followed by addition of the alkoxide to the carbene to give **5-72**, which is a simple proton transfer from the product. It is also possible that the alkoxide intermediate **5-70** is protonated, giving intermediate **5-73**. Subsequent carbene formation and O-H insertion would also plausibly lead to the generalized product **5-74**. The authors show that this reactivity is general for a variety of β -hydroxy ketones and aldehyde derivatives. While unplanned, this reaction was a very convenient means of constructing a necessary ring in **5-4**.

5.2.10 Micalizio's Synthesis of (-)-Jiadifenin and (2S)-Hydroxy-3,4-dehydroneomajucin

In 2016, the group of Micalizio at Dartmouth published a divergent approach to **5-3** and **5-5**, making use of a metallacycle-mediated [2+2+2] cyclization to construct the A,B-ring system.²⁵

Their route began with enyne **5-76**, available in 5 steps from chiral epoxide **5-75**. Treatment of stannyl-substituted TMS-acetylene to the combination of $\text{Ti}(\text{O}i\text{-Pr})_4$ and $n\text{-BuLi}$ generated a titanium metallacycle, which reacted with the lithium alkoxide of **5-76** to generate hydrindane **5-77** with exquisite regio- and diastereoselectivity with respect to the quaternary center formed. A detailed discussion of the mechanism for this transformation is beyond the scope of this discussion, but details of similar studies can be found in Micalizio's prior work.²⁶ A series of 5 steps transformed **5-77** into selenide **5-78**. Treatment of selenide **5-78** with AIBN and tributyltin hydride in refluxing benzene elicited a 5-exo radical cyclization, forming the final quaternary center and generating a 1:1 mixture of **5-79** and **5-80**. The formation of **5-80** is thought to occur via a 1,5-hydrogen atom transfer to the dioxolane, followed by fragmentation of the protecting group to give the ethyl ester after final hydrogen atom transfer. While the ratio is low, both **5-79** and **5-80** can be converted to **5-81** in a sequence of 6 or 7 steps.

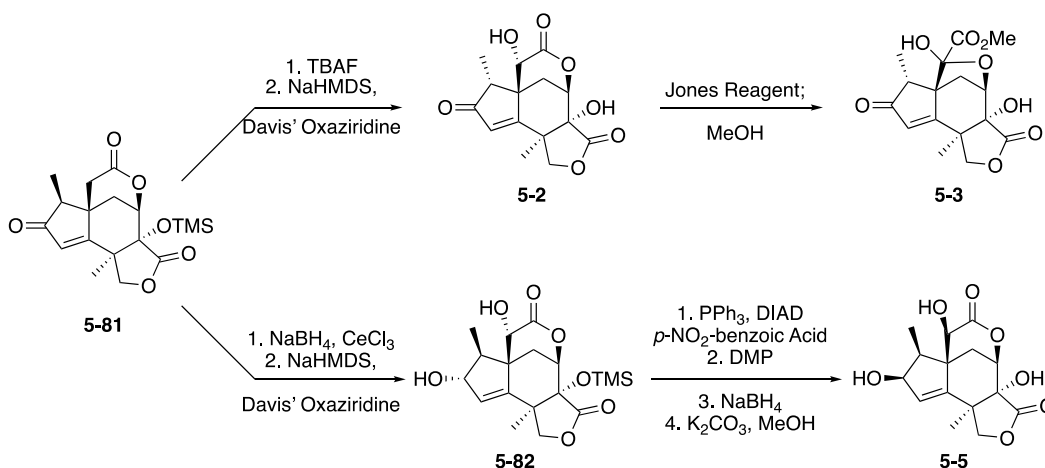
Scheme 5-12 Micalizio's approach to **5-81**.



Compound **5-81** serves as a divergency point in the synthesis, as shown in Scheme 5-13. To complete the synthesis of jiadifenin, **5-81** was treated with TBAF to epimerize the acidic methyl center. Treatment of the epimerized intermediate with NaHMDS and Davis' oxaziridine led to **5-2**, which could be easily converted to **5-3** upon treatment with Jones reagent. To access **5-5**,

intermediate **5-81** was first subjected to a diastereoselective Luche reduction, followed once again by oxidation with Davis' oxaziridine to afford hydroxylactone **5-82**. Unfortunately, both the Luche reduction and α -oxidation gave the incorrect stereochemistry of the alcohols necessary for the completion of **5-5**. To rectify the stereochemistry, first the A-ring alcohol was inverted through Mitsunobu reaction with *p*-nitrobenzoic acid, affording a *p*-nitrobenzoate intermediate. Subsequently, the hydroxylactone was oxidized to an α -keto lactone upon treatment with Dess–Martin periodinane. Reduction of the ketone with sodium borohydride led once again to an α -hydroxylactone, but with the desired configuration. Final deprotection of the benzoate completed the first total synthesis of **5-5**. Overall, this divergent approach afforded jiadifenin in 21 steps and (2*S*)-hydroxy-3,4-dehydroneomajucin in 24 steps from **5-75**.

Scheme 5-13 Divergence of **5-81** to **5-3** and **5-5**.

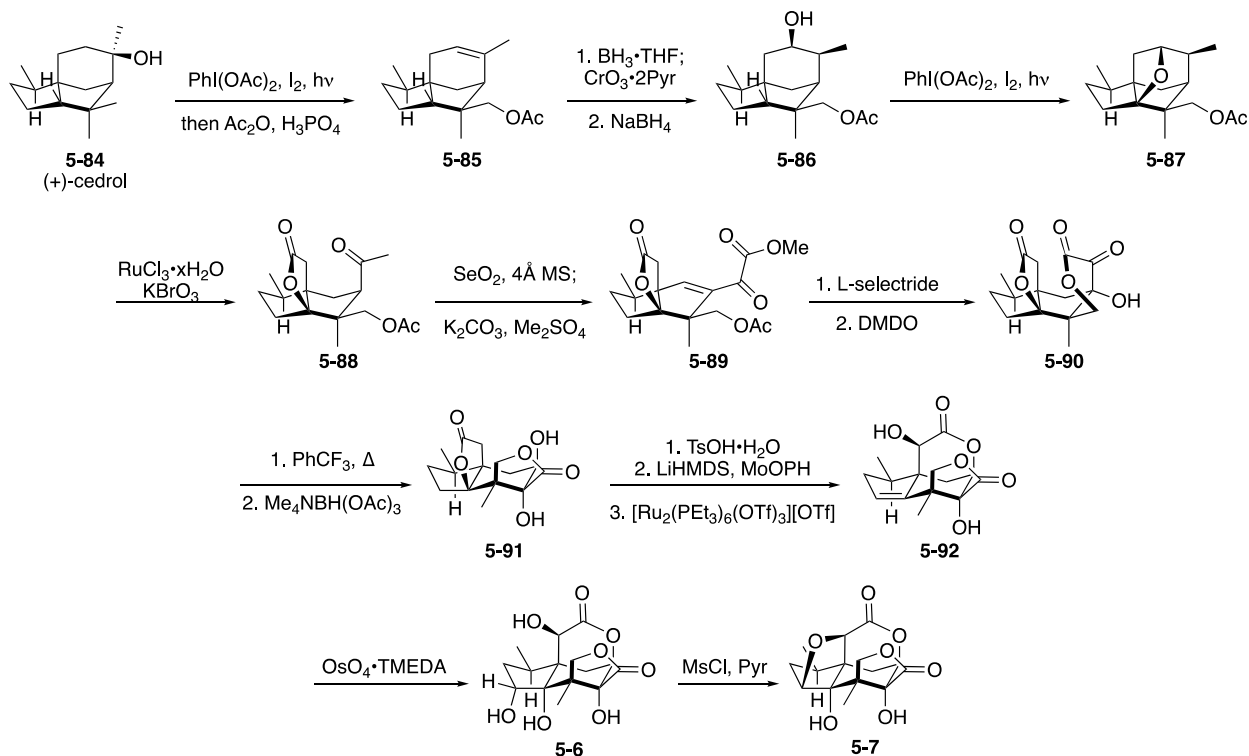


5.2.11 Maimone's Oxidative Approach to (–)-Majucin and (–)-Jiadifenoxolane A

In 2017, Maimone's group disclosed a very clever approach to the syntheses of majucin (**5-6**) and jiadifenoxolane A (**5-7**) which relied on the heavy use of C-H oxidation reactions.²⁷ The authors quite brilliantly recognized that by beginning from commercially available cedrol, they could start their synthetic efforts in the middle of the proposed biosynthesis, affording them maximum

divergency.^{1,28} Initial Suárez oxidation of **5-84** was used to selectively oxidize the neighboring methyl group and generate an intermediate tetrahydrofuran ring. Direct addition of acetic anhydride and phosphoric acid afforded acetate **5-85**. Hydroboration of the alkene, followed by double oxidation with Collins reagent led to a ketone, which, upon treatment with sodium borohydride, gave alcohol **5-86**. With this alcohol, another Suárez oxidation was performed to oxidize the bridging methine position, generating **5-87**. The tetrahydrofuran was then oxidized by the action of *in situ* generated RuO_4 , leading cleanly to triple oxidation product **5-88**. Subjection to anhydrous Riley oxidation conditions further oxidized **5-88**, followed by addition of dimethylsulfate and base formed unsaturated keto ester **5-89**. This two-step sequence of events affected 7 total oxidations. Reduction of the ketone with L-selectride, followed by quenching with basic methanol led to an intermediate keto-lactone, which was oxidized with DMDO to afford **5-90**.

Scheme 5-14 Maimone's Synthesis of **5-6** and **5-7**.



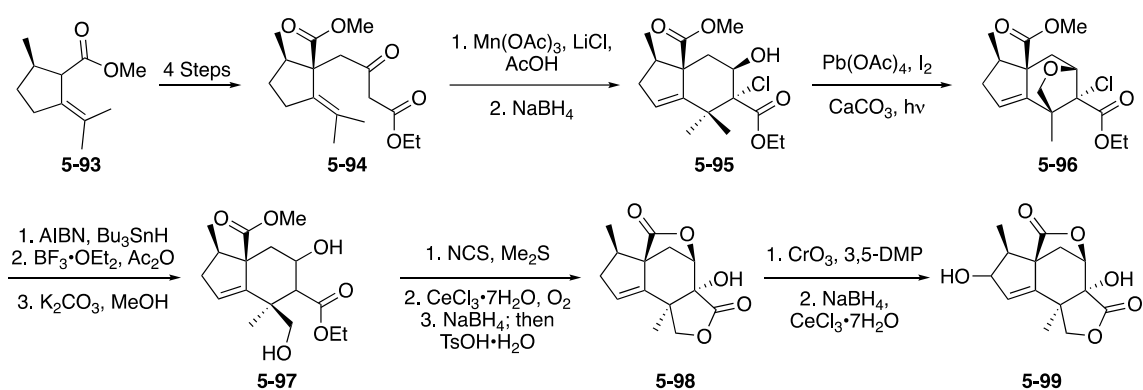
Having established much of the oxidation for the natural products, the authors needed to rearrange the carbon skeleton to access the necessary hydrindane of the *seco*-prezizaanes. To do so, **5-90** was simply heated in trifluorotoluene to effect an α -ketol rearrangement to access the hydrindane core. Subsequent directed reduction gave trans-diol intermediate **5-91**, which resembles the core of jiadifenolide. It was then necessary to transactonize **5-91** to achieve the necessary δ -lactone. This could be achieved by treatment of **5-91** with TsOH, giving the δ -lactone with elimination to generate the A-ring alkene. Treatment with base and MoOPH oxidized the lactone to a hydroxylactone, which occurred from the less hindered face. To place the alcohol on the concave face of the lactone, the authors made use of a Ru-catalyzed transfer hydrogenation that had been recently reported by Hartwig.²⁹ As such, subjection of the intermediate to $[\text{Ru}_2(\text{PEt}_3)_6(\text{OTf})_3][\text{OTf}]$ in isopropanol cleanly epimerized this center and afforded **5-92**. Dihydroxylation with stoichiometric $\text{OsO}_4 \cdot \text{TMEDA}$ complex gave **5-6**. Mesylation of the secondary alcohol, followed by heating elicited an intramolecular etherification, completing the synthesis of **5-7**. This powerful oxidative strategy allowed Maimone and coworkers to complete the first total synthesis of **5-6** and **5-7** in 14 and 15 steps respectively. The group has applied this general strategy to the synthesis of a total of 12 *Illicium* sesquiterpenes.²⁸

5.2.12 Gademann's Approach to (2R)-Hydroxynorneomajucin

In 2016, in a report on their formal synthesis of jiadifenolide, the Gademann group published the first, and to my knowledge only, approach targeting the nor-*seco*-prezizaane **5-8**.³⁰ Their efforts began from compound **5-93**, which was derived from (+)-pulegone in 2 steps. 4-step elaboration of **5-93** led to keto ester **5-94**. This intermediate underwent a low-yielding oxidative radical cyclization when treated with $\text{Mn}(\text{OAc})_3$ in the presence of LiCl. Subsequent reduction of the ketone afforded **5-95**. To oxidize the gem-dimethyl position, alcohol **5-95** was treated with

$\text{Pd}(\text{OAc})_4$ and iodine to form tetrahydrofuran **5-96** through a Suárez oxidation. Radical dechlorination ensued upon treatment of **5-96** with AIBN and Bu_3SnH . The bridging ether was then opened by treatment with acetic anhydride in the presence of $\text{BF}_3 \cdot \text{OEt}_2$ to give an intermediate diacetate, which was cleaved with basic methanol to generate diol **5-97**. Corey–Kim oxidation led to an intermediate keto-ester with a neighboring aldehyde, which was α -hydroxylated by the action of $\text{CeCl}_3 \cdot 7\text{H}_2\text{O}$ and atmospheric oxygen. Reduction of the aldehyde and ketone occurred upon treatment with sodium borohydride, and the intermediate underwent double lactonization upon heating with TsOH to afford **5-98**.

Scheme 5-15 Gademann's Approach to **5-8**.



Compound **5-98** was the last compound reported in the 2016 paper, but in 2017, Christophe Daepfen disclosed some further studies in his dissertation.³¹ On small scale, **5-98** could undergo allylic oxidation upon treatment with chromium trioxide, generating an intermediate enone. Luche reduction of this enone gave allylic alcohol **5-99**. The stereochemistry of the alcohol was unspecified since the reaction was performed on a scale small enough that NOE experiments could not be performed. This work has achieved the most advanced intermediate toward **5-8** published to date, and it is noteworthy that this approach was only one alcohol shy of the natural product.

5.2.13 Introduction to (2*R*)-hydroxynorneomajucin

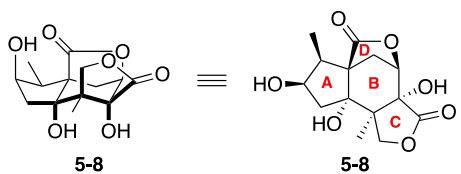
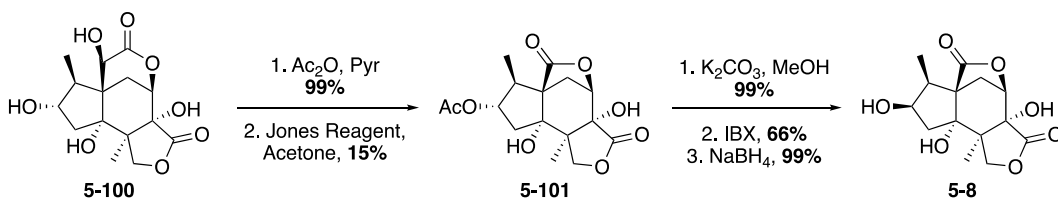


Figure 5-4 (2*R*)-hydroxynorneomajucin.

In 2012, Fukuyama's group published the isolation and neurotrophic activity of (2*R*)-hydroxynorneomajucin (**5-8**). This natural product was the first example of a *seco*-prezizaane norsesquiterpene from the dried pericarps of *Illicium jiadifengpi*.³² The connectivity and relative configuration of the natural product were assigned by extensive 2D-NMR studies. Additionally, IR data was used to deduce the presence of a γ -lactone ring, as opposed to the δ -lactone ring of other majucin-like compounds. To assign absolute configuration, **5-8** was synthesized from (2*S*)-hydroxynorneomajucin (**5-100**), the absolute configuration of which was determined by Kusumi's modification of Mosher's method.³³ Acylation of the A-ring secondary alcohol of **5-100**, followed by oxidative rearrangement mediated by Jones reagent formed compound **5-101**. Cleavage of the acetate with basic methanol, followed by oxidation and reduction then formed **5-8**, whose spectral data matched the isolated natural product, thus confirming the assigned absolute configuration.

Scheme 5-16 Derivatization of **5-8** from **5-100**.



With the isolated material, Fukuyama was able to perform some initial biological assays of **5-8**. They found that **5-8**, like many of the other *seco*-prezizaanes (Figure 5-2) was able to promote neurite outgrowth in primary cultures of fetal rat cortical neurons at concentrations ranging from 1 to 10 μ M. However, additional biological studies were likely challenging due to the poor isolated yield. From 3.5 kg of dried plant material, only 1.2 mg of **5-8** was isolated, an overall yield of

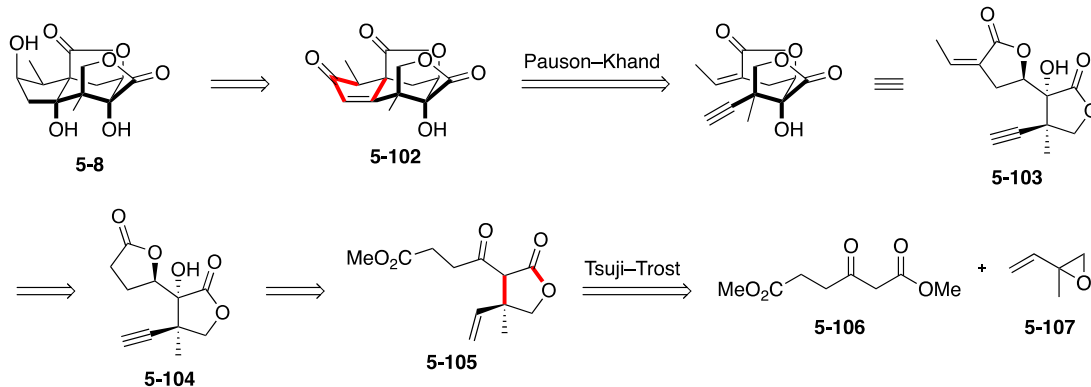
0.000034%. Because of its unprecedented structure, coupled with its biological implications in neurodegenerative disease, our group was particularly interested in developing a laboratory synthesis of **5-8**.

5.3 Initial Efforts Toward the Synthesis of (2*R*)-hydroxynorneomajucin

5.3.1 Retrosynthesis

Structurally, **5-8** is a highly oxidized tetracycle, with an embedded *trans*-hydrindane core and two quaternary centers. Our synthetic strategy is outlined in Scheme 5-17. We envisioned that the *trans*-fusion would be set at a late stage utilizing a strategic Mukaiyama hydration, which is preceded from Maimone's work.²⁸ Based on retrosynthetic analysis, late-stage redox manipulations would lead back to tetracyclic enone **5-102**. To access the core of the molecule and set one of the quaternary centers, we imagined forming the A and B rings in one step using a Pauson–Khand reaction from enyne **5-103**. By having the alkene of the enyne appended to a lactone ring, we believed that the conformational restriction would allow us to control the stereochemical outcome at the quaternary center. Functional group manipulations could trace **5-103** back to bis-lactone **5-104**. To access **5-104**, we envisioned accessing the neopentyl alkyne from an alkene, via the intermediacy of an aldehyde. We also envisioned setting the *trans*-diol motif via a diastereoselective Rubottom oxidation, and subsequent directed reduction, leading back to compound **5-105**. Given the lack of steric differentiation between the methyl and vinyl groups attached to the quaternary center, it was not clear at the outset how these groups might influence the diastereoselectivity of the ensuing Rubottom oxidation. Finally, we imagined setting the β -quaternary center of lactone **5-105** by using a tandem Tsuji–Trost asymmetric allylic alkylation/lactonization, tracing back to the known β -keto ester **5-106** and commercially available isoprene monoxide (**5-107**).

Scheme 5-17 Initial synthetic plan.



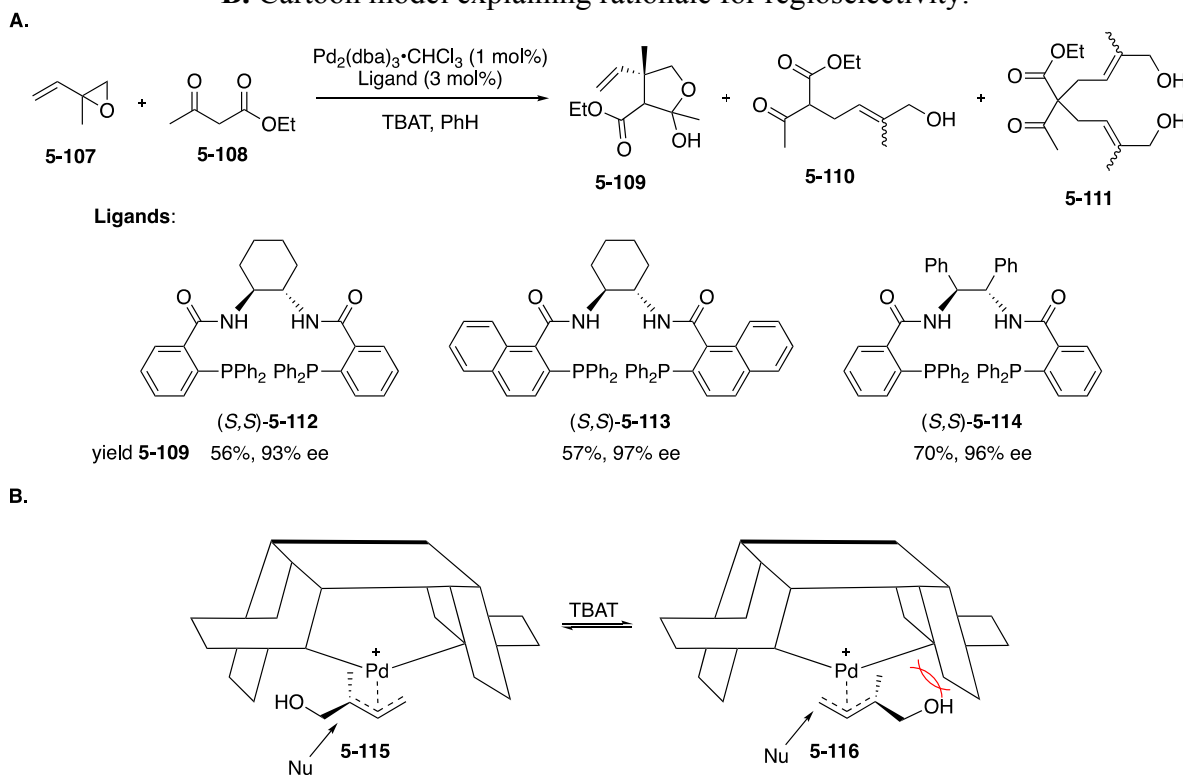
5.3.2 Investigation of Tsuji–Trost Reactivity

The Tsuji–Trost asymmetric allylic alkylation has a rich history in the field of organic synthesis, particularly in the realm of total synthesis.³⁴ This methodology has found vast use, due to the ordinarily high fidelity of the reaction. We hoped to utilize this methodology to set a quaternary center early on in our route toward **5-8**. Before discussing our results, it is imperative to discuss some key pieces of literature for this transformation.

In 2001, Trost reported that quaternary centers can be formed via an asymmetric allylic alkylation with high regio- and stereoselectivity.³⁵ Their optimization efforts looked at the reaction of ethyl acetoacetate (**5-108**) and isoprene monoxide (**5-107**) catalyzed by 1 mol% of Pd₂(dba)₃•CHCl₃, 1 mol % of tetra-*n*-butylammonium triphenyldifluorosilicate (TBAT) additive, and 3 mol% of various ligands. The results are summarized in Scheme **5-18A**. Using ligand (*S,S*)-**5-112**, they were able to achieve a 56% yield of **5-109** with 93% ee with respect to the newly formed quaternary center. Changing the ligand to naphthyl ligand **5-113** gave no substantial increase in yield but boosted the enantioselectivity to 97% ee. Switching to ligand **5-114**, with a more flexible backbone, **5-109** could be formed in 70% yield and 96% ee. Regiosomeric products **5-110** and **5-111** were observed in all reactions performed. This is due to the diastereomeric π -allyl palladium complexes **5-115** and **5-116** which were formed upon ionization of the racemic

epoxide. As seen in Scheme 5-18B, the nucleophile approaches from the less sterically encumbered side of the complex to set the stereochemistry of the resulting quaternary center. However, when π -allyl complex 5-116 was formed, the nucleophilic addition lead to the undesired linear addition products. These diastereomeric complexes can interconvert through a π - σ - π mechanism, which Trost found to be accelerated in the presence of certain additives. Specifically, TBAT was found to accelerate this interconversion, which increases the regioselectivity of the overall process by favoring complex 5-115 (Scheme 5-18B).

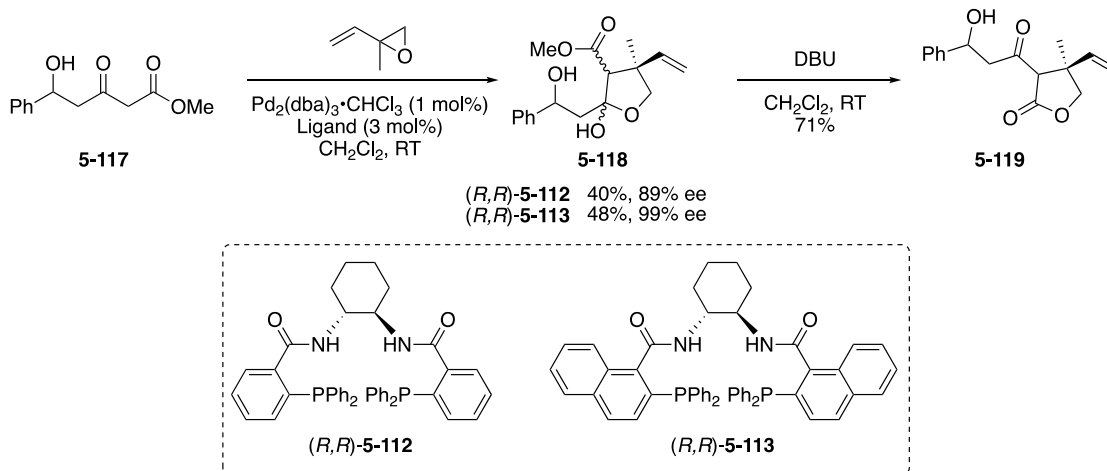
Scheme 5-18A. Formation of quaternary centers by Pd-catalyzed asymmetric allylic alkylation.
B. Cartoon model explaining rationale for regioselectivity.



Further precedent can be found in Xie's total synthesis of the hyperolactones.³⁶ In their 2011 biomimetic work toward the hyperolactones, the authors used a similar Tsuji–Trost reaction. Treatment of 5-117 with isoprene monoxide in the presence of $\text{Pd}_2(\text{dba})_3 \cdot \text{CHCl}_3$ and either (*R,R*)-5-112 or (*R,R*)-5-113 led to the formation of hemiacetal 5-118. When ligand (*R,R*)-5-112 was used,

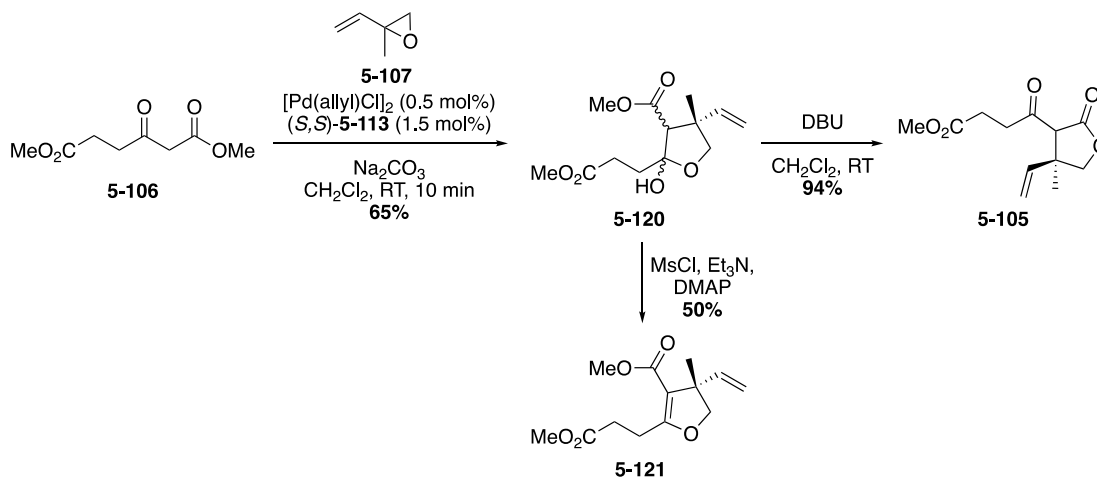
the product was formed in 40% yield and 89% ee. Changing the ligand to *(R,R)*-**5-113** led to formation of **5-118** in 48% yield and an astounding 99% ee. The authors also showed that the hemiacetal could be cleaved with the addition of DBU which was followed by lactonization onto the methyl ester, generating **5-119** in 71% yield.

Scheme 5-19 Xie's use of a Tsuji–Trost toward the hyperolactones.

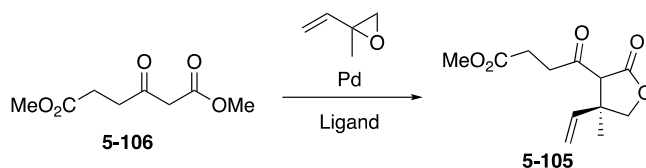


With this precedent in mind, I began investigating the Tsuji–Trost reaction between **5-106** and **5-107**. I began by using the reaction conditions that Xie had used in their system, but changing to the enantiomeric ligand *(S,S)*-**5-113** to access the desired product. In the first several reactions to access lactone **5-105**, the reactions were performed in two operations. This was due to the need to independently access the dihydrofuran **5-121** to confirm the enantiomeric purity about the quaternary center by chiral HPLC. Since the lactone was formed as a 1:1 mixture of diastereomers, it was challenging to determine enantiomeric purity from this intermediate. It was also found that these steps could be combined, and simply adding DBU to the reaction mixture once the reaction had reached completion directly formed **5-105** in one pot.

Scheme 5-20 Initial attempts to access **5-105** from keto-ester **5-106**.



The conditions were then optimized for further scalability. Typically, these reactions have been reported at 0.1 M concentration, which was troublesome for two reasons. First, these reactions are very sensitive to the presence of oxygen, so the solvent needs to be rigorously degassed, which becomes quite time consuming on large scale. Second, on large scale the reaction required significant quantities of solvent. As such, we were interested in seeing if we could increase the reaction concentration without effecting the yield or enantiopurity of the product. Additionally, (*S,S*)-**5-113** was an expensive ligand. To run the reaction on a 15 g scale, it required the use of approximately \$220 worth of ligand alone. To make the process more economically friendly, we also sought to decrease the palladium and ligand loadings while maintaining suitable reactivity. Lastly, the report from Trost suggested that using (*S,S*)-**5-114** might increase the overall yield. A convenient consequence of using this ligand was that it is readily prepared from inexpensive starting materials, making it a more economical choice if the yields and enantiopurity were comparable.

Table 5-2 Optimization of the Tsuji–Trost.

Entry	Condition	Pd (mol %)	Ligand (mol %)	Concentration	Result
1	A	0.5	1.5	0.1 M	64%, 96% ee
2	A	0.5	1.5	0.3 M	48%, 92% ee
3	A	0.5	1.5	0.2 M	61%, 95% ee
4	A	0.25	0.75	0.2 M	63%, 95% ee
5	B	0.25	0.75	0.2 M	61%, 90% ee

Condition A: **5-107** (1.2 equiv), [Pd(allyl)Cl]₂, (*S,S*)-**5-113**, Na₂CO₃, CH₂Cl₂, RT; then DBU

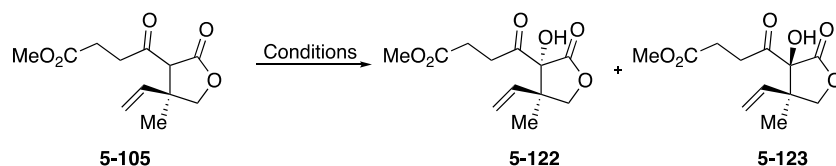
Condition B: **5-107** (1.2 equiv), Pd₂(dba)₃·CHCl₃, (*S,S*)-**5-114**, TBAT, PhH, 40°C; then DBU

With these goals in mind, I first examined the effect of concentration on the reaction (Table 5-2). Under standard conditions (entry 1), the reaction generated **5-105** in 64% yield and 96% ee at the quaternary center. When the overall concentration was tripled (entry 2), the yield decreased to 48% and the enantiomeric excess dropped to 92%. However, when the reaction was run at 0.2 M, the yield and enantiopurity were almost identical to entry 1, forming **5-105** in 61% yield and 95% ee. Having cut the total solvent use in half, I looked into decreasing the loading of palladium and ligand. By dropping the loadings of palladium and ligand to 0.25 and 0.75 mol% respectively (entry 4) the yield increased to 63% while maintaining the enantioselectivity. Interestingly, while the overall concentration with respect to the limiting amount of **5-106** was doubled, the concentration of palladium and ligand in entry 4 were identical to their respective concentrations in entry 1. Decreasing the loadings beyond entry 4 proved fruitless and impractical, as the reaction was significantly retarded using 0.1 and 0.3 mol% of palladium and ligand respectively. Subsequently, to observe the effect of ligand **5-114**, the loadings and concentration from entry 4 were replicated while mirroring Trost's original reaction conditions (entry 5). This led to formation

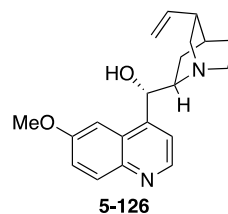
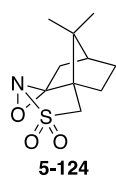
of product in similar yield, but the enantioselectivity of the process diminished, forming the quaternary center with only 90% ee. While the conditions were in fact more economical, we elected to use the conditions in entry 4 to scale the process for material throughput due to the higher enantiopurity of the product. By performing the reaction according to entry 4 on about 10 g scale, we were able to replicate the optimization result and showcase the scalability. The desired lactone **5-105** was isolated in a 63% yield with 95% ee.

5.3.3 Optimization of α -Hydroxylation

Having established scalable access to lactone **5-105**, the next challenge was to diastereoselectively install an α -hydroxyl group. Having set the quaternary center with high enantiomeric excess, we hoped that the slight steric difference between the methyl and ethylene groups might confer some inherent diastereoselectivity. With these hopes in mind, I first tried α -hydroxylation under standard Rubottom-type conditions employing *m*-CPBA and observed a 1:2 ratio of **5-122** to **5-123**. Unfortunately, the substrate displayed a slight bias for the undesired diastereomer. There was precedent from Xie's synthesis of the hyperolactones suggesting that this selectivity could be inverted under radical generating conditions.³⁵ As such, treatment of **5-105** with cerium trichloride heptahydrate in *i*PrOH under an atmosphere of oxygen as described by Christoffers,³⁷ generated a 2:1 ratio favoring the desired **5-122**. This result seemed promising at first, but inconsistent results and low overall yields made material throughput an impediment on scale. Other oxidizing metals were used to try and boost overall yield, such as Mn(OAc)₂, Mn(OAc)₃, and CAN, but to no avail.³⁸

Table 5-3 Optimization of the α -hydroxylation.

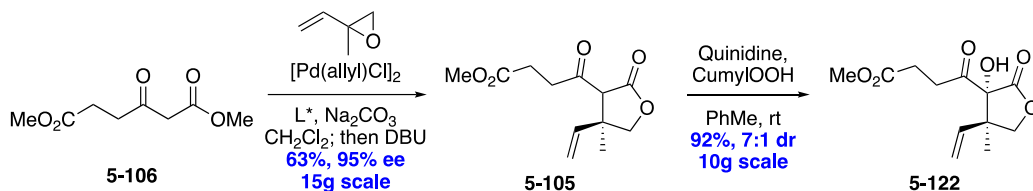
Entry	Conditions	5-122 : 5-123
1	<i>m</i> CPBA, CH ₂ Cl ₂	1 : 2
2	CeCl ₃ ·7H ₂ O, O ₂ (1 atm), <i>i</i> PrOH	2 : 1
3	K ₂ CO ₃ , 5-124 , THF	1 : 4
4	K ₂ CO ₃ , 5-125 , THF	1 : 1
5	5-126 (20 mol%), Cumyl-OOH, PhMe	7 : 1



Rationalizing that the substrate only has a small stereochemical bias, we hoped that we could use an external source of chirality to overcome the inherent bias. As such, I thought that Davis' chiral camphor-derived oxaziridines might elicit the desired transformation.³⁹ However, oxidation with **5-124** led to a 1:4 ratio favoring undesired **5-123**, and oxidation with **5-125** gave a 1:1 ratio of diastereomers. Having failed with chiral oxidants, we hoped the chirality could be derived from a different external source, such as an organocatalyst. Along these lines, we found a protocol developed by Jørgensen in which they performed an enantioselective α -hydroxylations of β -keto esters using cinchona alkaloid catalysis in the presence of cumyl hydroperoxide.⁴⁰ We gratifyingly found that treatment of **5-105** with catalytic quantities of quinidine (**5-126**) in the presence of cumyl hydroperoxide led to a 7:1 diastereomeric ratio favoring the desired **5-122**! It is also worth noting that this reaction was incredibly simple to perform, as the reaction was run in untreated toluene under an ambient atmosphere. On decagram scale, I was able to consistently

perform this reaction in 92% overall yield to generate a 7:1 mixture of separable diastereomers (Scheme 5-21).

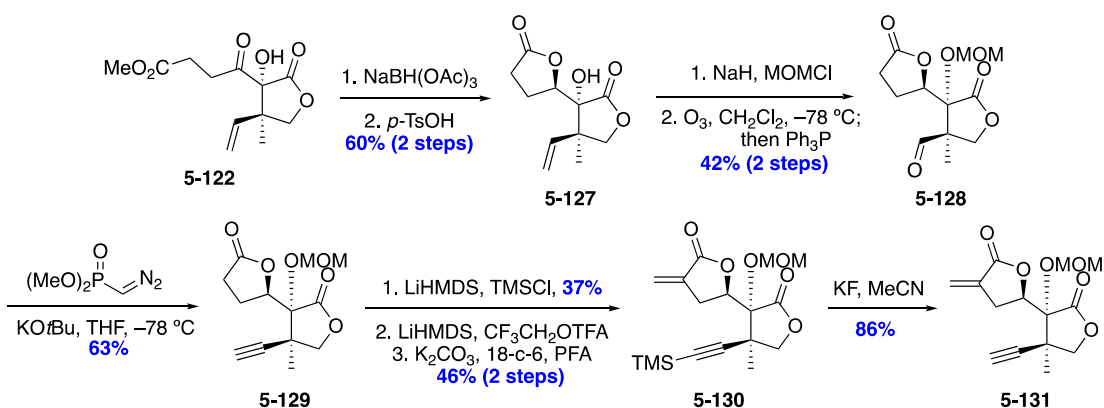
Scheme 5-21 Decagram scale synthesis of **5-122**.



5.3.4 *Forward Synthesis*

With access to suitable quantities of **5-122**, we could continue forward to synthesize the enyne precursor necessary to investigate the Pauson–Khand reaction. We elected to initially target simplified enyne **5-131** (Scheme 5-22), which lacks a methyl group on the exo-methylene functionality. We envisioned this would incur less of a steric clash in the transition state of the Pauson–Khand, and it also simplified synthesis. Furthermore, we imagined it would be possible to methylate subsequent to the Pauson–Khand reaction.

Scheme 5-22 Synthesis of enyne **5-131**.



Reduction of the ketone in **5-122** under modified Saksena reduction conditions led to an intermediate diol, which could be fully lactonized upon treatment with tosic acid to generate **5-127** in 51% yield over two steps.⁴¹ We initially investigated the ozonolysis of the free tertiary alcohol but found that the compound readily underwent a retro-aldol/aldol pathway, scrambling the configuration of the quaternary center. Therefore, the tertiary alcohol was first protected as a MOM-ether, which was subsequently ozonolyzed to yield aldehyde **5-128**. Conversion to the alkyne was achieved by utilizing the Seyferth–Gilbert homologation, generating alkyne **5-129**.⁴² It is worth noting that the Ohira–Bestmann reaction,⁴³ Corey–Fuchs reaction,⁴⁴ and the Colvin rearrangement⁴⁵ were all ineffective for this substrate. We found it necessary to protect the alkyne to install the requisite alkene. Unfortunately, silylation of the alkyne proceeded in low yield, owing to a competitive C-silylation of the lactone. Methylenation of the protected intermediate led to enyne **5-130**. The silyl group was removed upon heating the alkyne in the presence of KF to yield enyne **5-131**. With a suitable enyne substrate, we began investigating the feasibility of our key Pauson–Khand reaction.

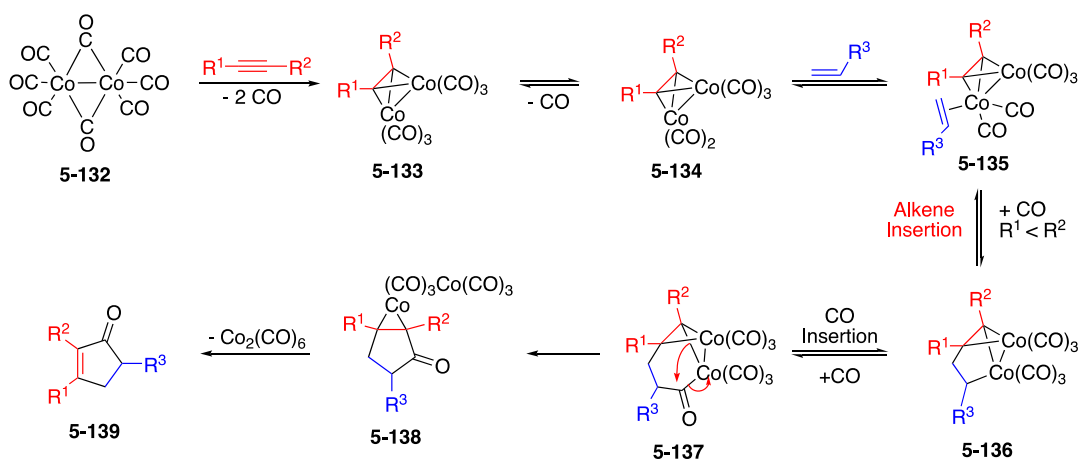
5.3.5 *Investigation of Pauson–Khand Reactivity*

Having successfully synthesized **5-131**, we began probing the Pauson–Khand cyclization. Before discussing our efforts in this area, it is imperative to briefly discuss the utility of the Pauson–Khand reaction (PKR) in the context of total synthesis. This discussion will not be all-encompassing but will highlight some recent examples of Pauson–Khand reactions in total synthesis. Several excellent reviews on the subject have been published, in which there are more thorough detail on mechanism and early examples.⁴⁶

The Pauson–Khand reaction was first reported in 1971. This seminal report was investigating the reaction between cobalt-alkyne complexes with norbornadiene to generate

cobalt-cyclopentadiene and cobalt-arene complexes.⁴⁷ The reaction between norbornadiene and the cobalt-alkyne complex to generate an enone was viewed as a side product in the transformation. Since its discovery, the reaction has become particularly useful to construct complex cyclopentenones. The mechanism for the cobalt-mediated reaction was first proposed by Magnus in 1985 and can be seen in Scheme 5-23.⁴⁸

Scheme 5-23 Mechanism of the Pauson–Khand reaction.



The mechanism proposed by Magnus began with coordination of $\text{Co}_2(\text{CO})_8$ to an alkyne, to generate intermediate **5-133**. Loss of a carbon monoxide ligand generated complex **5-134**, which has an open site to coordinate an alkene, thus forming **5-135**. Subsequently, a migratory insertion occurred to generate **5-136** after the addition of a CO ligand. This intermediate can undergo a ring expanding CO insertion, followed again by addition of a CO ligand to generate complex **5-137**. After CO insertion, **5-137** could undergo a reductive elimination pathway to generate **5-138**, with the other cobalt atom still bound to the alkyne carbons. After loss of $\text{Co}_2(\text{CO})_6$, enone **5-139** was formed. While this mechanism was specific for dicobalt octacarbonyl, the most prevalent mediator of the Pauson–Khand reaction, similar mechanisms can be invoked for several other transition metal carbonyl complexes.

Since its discovery, the Pauson–Khand reaction has found significant utility in total synthesis. Figure 5-5 shows natural products that have been recently synthesized using a Pauson–Khand reaction; the resulting ring from the reaction is highlighted. As seen earlier in Scheme 5-5, the Zhai group made use of a cobalt-mediated Pauson–Khand reaction to construct the core of jiadifenin in 2012.¹⁷ The synthesis of crinipellin A by Zhen Yang and coworkers was a testament to the power of this transformation.⁴⁹ As seen in **5-140**, the entire tetracyclic natural product was made by two Pauson–Khand reactions (PKR). The rings highlighted in red were formed through a cobalt mediated PKR, while the blue rings were formed through a palladium catalyzed Pauson–Khand. In addition to this synthesis, the Pauson–Khand reaction was also featured in the synthesis of astellatol (**5-141**),⁵⁰ waihoensene (**5-142**),⁵¹ 5-*epi*-cyanthiwigin I (**5-143**),⁵² ryanodol (**5-144**),⁵³ phorbol (**5-145**),⁵⁴ ingenol (**5-146**),⁵⁵ and indoxamycin A (**5-147**).⁵⁶ While not a complete list, these complex natural products showcase the utility of the Pauson–Khand reaction and were inspiration for us as we pursued this transformation.

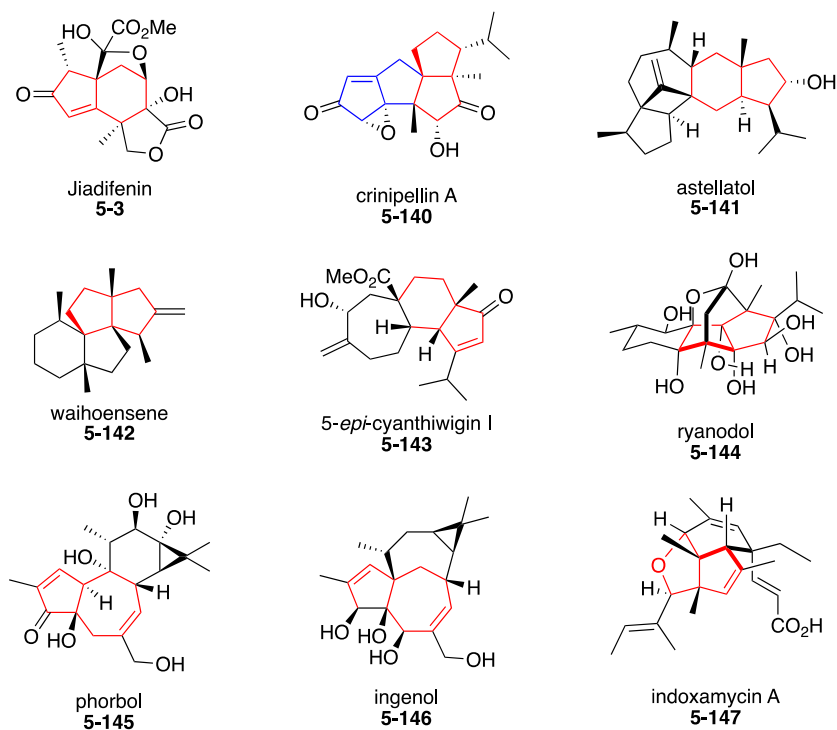


Figure 5-5 Natural products recently synthesized using Pauson–Khand reactions.

With inspiration from the literature, as well as access to compound **5-131**, we were ready to probe the feasibility of our key disconnection. Unfortunately, subjecting **5-131** to stoichiometric $\text{Co}_2(\text{CO})_8$ and tetramethylthiourea (TMTU) in refluxing toluene failed to elicit the desired Pauson–Khand reaction. Additionally, switching to a rhodium catalyzed PKR, similar to that reported in Reisman’s ryanodol synthesis, did not change the outcome of the reaction.⁵² With these results, we wanted to understand what was impeding the reaction. We rationalized that the preferred conformation of **5-131** likely has the alkene and alkyne far apart. Conformations in which these functionalities are close in space might be sparsely populated.

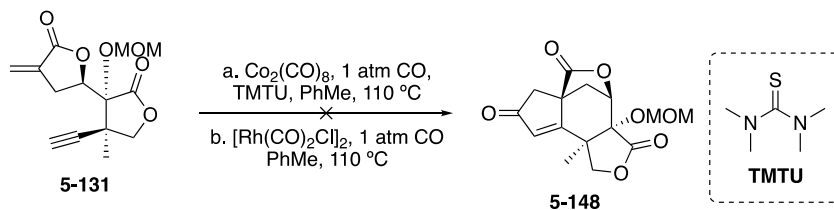


Figure 5-6 Initial attempts at the key Pauson–Khand reaction.

To investigate the conformational preferences of the molecule, I performed calculations on compound **5-131**. Initial conformer searching was performed on **5-131** in Spartan⁵⁷ using molecular mechanics. Subsequently, the conformers were minimized using Hartree–Fock with the 6-31G* basis set. I then selected only the conformers which put the reactive atoms close in space and performed a final DFT minimization of these conformers using ω B97X-D and the 6-31G* basis set. I found that there were several conformers which placed the atoms close in space; the lowest in energy of the conformers was found at 1.78 kcal/mol relative to the ground state (Figure 5-6). In this conformation, the highlighted atoms, which would need to form a bond, are 3.434 Å apart. While this did not paint the whole picture, since the conformations can significantly change once a metal is bound to the alkyne, it gave us hope that the system could undergo a Pauson–Khand reaction.

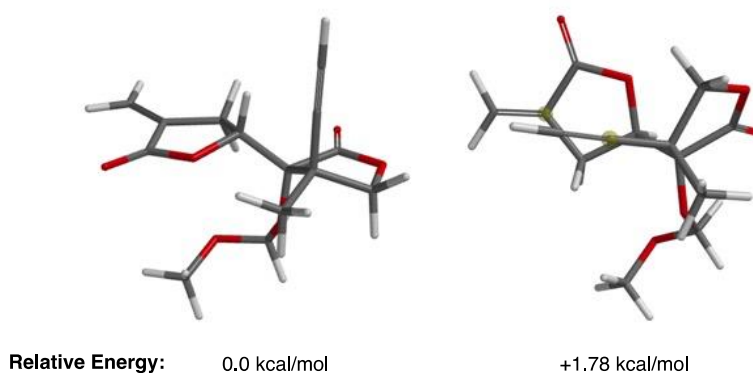
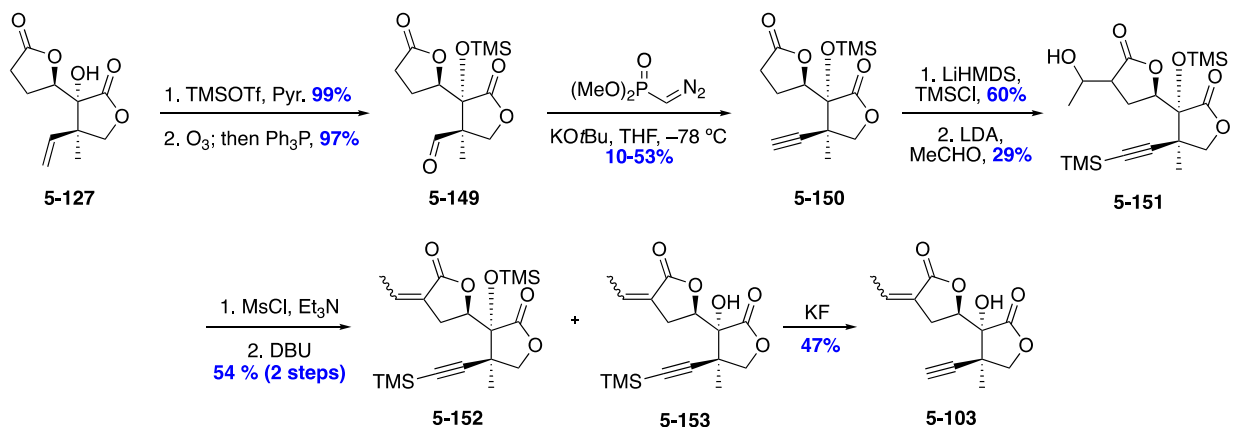


Figure 5-7 Calculated conformers for **5-131**.

Unwilling to give up on this transformation, we synthesized several other enyne substrates hypothesizing that other functionalities around the enyne may play a key role in changing the conformation enough to allow the PKR to proceed. We elected to change the substitution on the alkyne, on the alkene, and on the tertiary alcohol to investigate their effect on the outcome of the PKR. Synthesis of these substrates began with compound **5-127**. Silylation of the tertiary alcohol proceeded in excellent yield, followed by a high yielding ozonolysis afforded **5-149**. Seyferth–

Gilbert homologation on this compound was particularly irreproducible, resulting in yields of **5-150** between 10 and 53%. This was likely due to an undesired silyl transfer that can occur during the course of the reaction, halting the formation of the oxaphosphetane intermediate. Subsequent silylation of the alkyne, followed by a low-yielding aldol reaction with acetaldehyde led to **5-151** as a mixture of diastereomers. Elimination of the alcohol to the *exo*-enone was realized upon mesylation of the secondary alcohol and treatment of the mesylate with DBU to generate **5-152**. Alcohol **5-153** was also observed from the elimination, a consequence of desilylation under the reaction conditions. Both **5-152** and **5-153** were desired PKR synthons. A portion of the free alcohol was desilylated by treatment with KF to afford PKR precursor **5-103** in 47% yield.

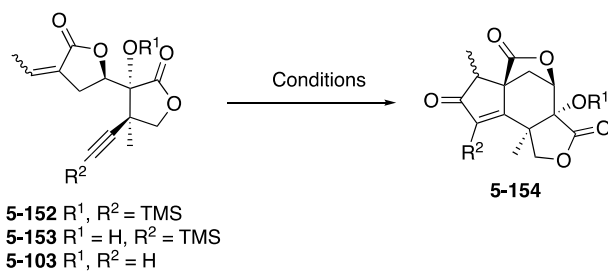
Scheme 5-24 Synthesis of alternate enyne substrates.



With these enynes prepared, we embarked on a more thorough investigation of the Pauson–Khand reactivity. Results can be seen in Table 5-3 below. Using doubly silylated **5-152**, rhodium catalyzed conditions (entries 1 and 2) resulted in decomposition of the starting material and no formation of product. Changing to a cobalt mediated process at room temperature utilizing NMO to promote ligand exchange (entry 3) simply returned starting material.⁵⁸ Using **5-153** (entry 4), a similar cobalt mediated process also failed to elicit any reaction. As the silyl groups did not seem to be helping the reactivity, further studies were performed on **5-103**. However, even with the

unprotected material, rhodium mediated reactions (entries 5-7), cobalt mediated reactions (entries 8-10), molybdenum mediated reactions (entries 11-13), and *in situ* generated Ni(CO)₄ (entry 14) all failed to yield even traces of **5-154**. Rationalizing that if this system were likely to undergo a productive Pauson–Khand reaction, at least a trace amount of product would have been detected during the studies outlined in Table 5-3. It seems that having the alkene appended to the second lactone ring placed too much of a conformational constraint on the system, making it unlikely that the alkene and alkyne would come close enough to form a bond. After these failures, we went back and revised our overall synthetic strategy.

Table 5-4 Attempted Pauson–Khand reactions using a variety of enynes.



Entry	Compound	CO	Solvent	Temp.	Metal	Result
1	5-152	1 atm	PhMe	100 °C	[Rh(CO) ₂ Cl] ₂ , AgOTf	Decomp
2	5-152	1 atm	Bu ₂ O	140 °C	[Rh(CO) ₂ Cl] ₂	Decomp
3	5-152	-	PhMe	RT	Co ₂ (CO) ₈ , NMO	N.R.
4	5-153	-	CH ₂ Cl ₂	RT	Co ₂ (CO) ₈ , TMANO	N.R.
5	5-103	1 atm	PhMe	110 °C	[Rh(CO) ₂ Cl] ₂	N.R.
6	5-103	1 atm	Bu ₂ O	130 °C	[Rh(CO) ₂ Cl] ₂	N.R.
7	5-103	1 atm	Bu ₂ O	150 °C	[Rh(CO) ₂ Cl] ₂	Decomp
8	5-103	-	CH ₂ Cl ₂	RT	Co ₂ (CO) ₈ , TMANO	N.R.
9	5-103	-	PhMe	110 °C	Co ₂ (CO) ₈	Decomp
10	5-103	1 atm	DCE	76 °C	Co ₂ (CO) ₈ , NMO	N.R.
11	5-103	-	CH ₂ Cl ₂	RT	Mo(CO) ₃ (DMF) ₃	N.R.
12	5-103	-	PhMe	60 °C	Mo(CO) ₃ (DMF) ₃	N.R.
13	5-103	-	PhMe	110 °C	Mo(CO) ₃ (DMF) ₃	N.R.
14	5-103	1 atm	PhMe	RT	Ni(COD) ₂ , bpy	N.R.

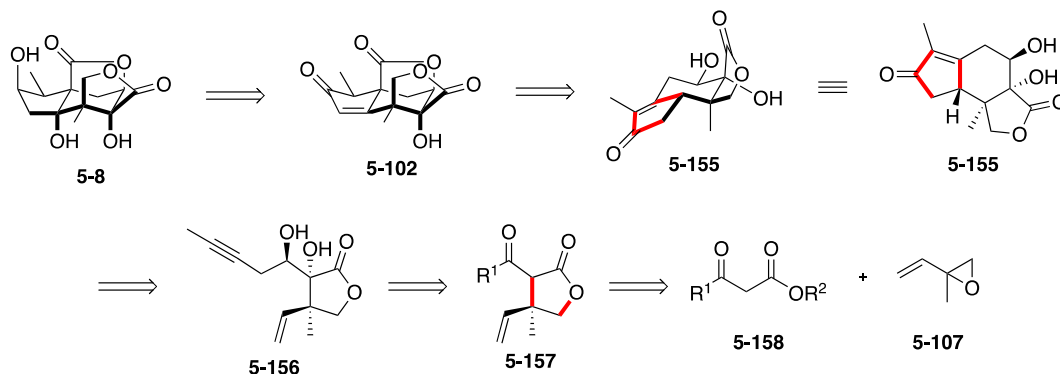
5.4 Second Generation Route Toward (2*R*)-hydroxynorneomajucin

5.4.1 Revised Retrosynthesis

After the failure of the key Pauson–Khand, I needed to step back and reevaluate the synthetic strategy. It was clear from Table 5-3 that having the alkene bound to the lactone did not allow for the reaction to proceed. The most likely explanation was that the alkene and alkyne were unable to come close enough in space to form a bond once a metal was bound to one of these functionalities. However, the Pauson–Khand reaction still seemed like the most efficient means of

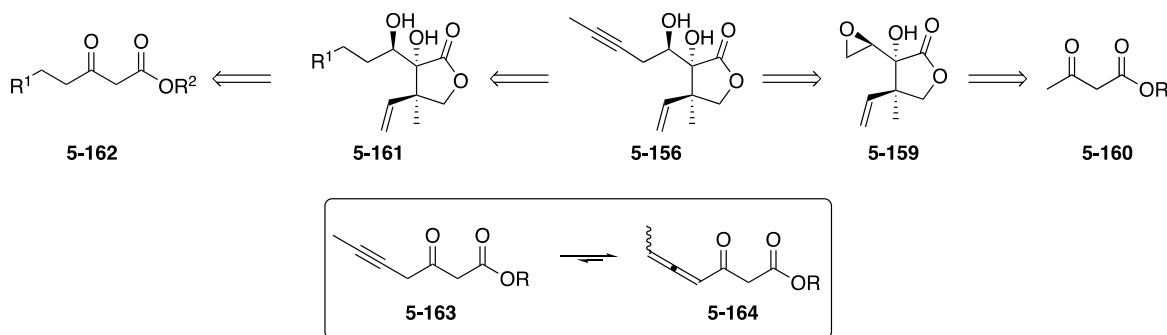
forming the core ring system of **5-8**. I thought that the strategy could be salvaged by redesigning the enyne substrate to allow for more conformational flexibility. The simplest means of doing this would be to close the lactone ring after the Pauson–Khand reaction. As such, I devised the following retrosynthesis (Scheme 5-25).

Scheme 5-25 Revised retrosynthesis of **5-8**.



Strategically, I wanted to retain the two major reactions from the previous approach, namely the Pauson–Khand reaction to close the core, and the Tsuji–Trost asymmetric allylic alkylation to set the quaternary center. As such, I envisioned taking **5-8** back to **5-102** through late-stage redox manipulations. The lactone was envisioned to be closed at a later stage in the synthesis, from a conjugate addition into enone **5-155**. The tricyclic core of **5-155** could once again be formed through a Pauson–Khand reaction with enyne **5-156**. Functional group manipulations could lead back to **5-157**, which would once again arise from a Tsuji–Trost reaction between **5-158** and **5-107**. However, it was unclear at the outset what specific functionalities would be necessary in **5-157** to synthesize **5-156**, and our efforts commenced by investigating this.

Scheme 5-26 Potential approach to **5-156**.



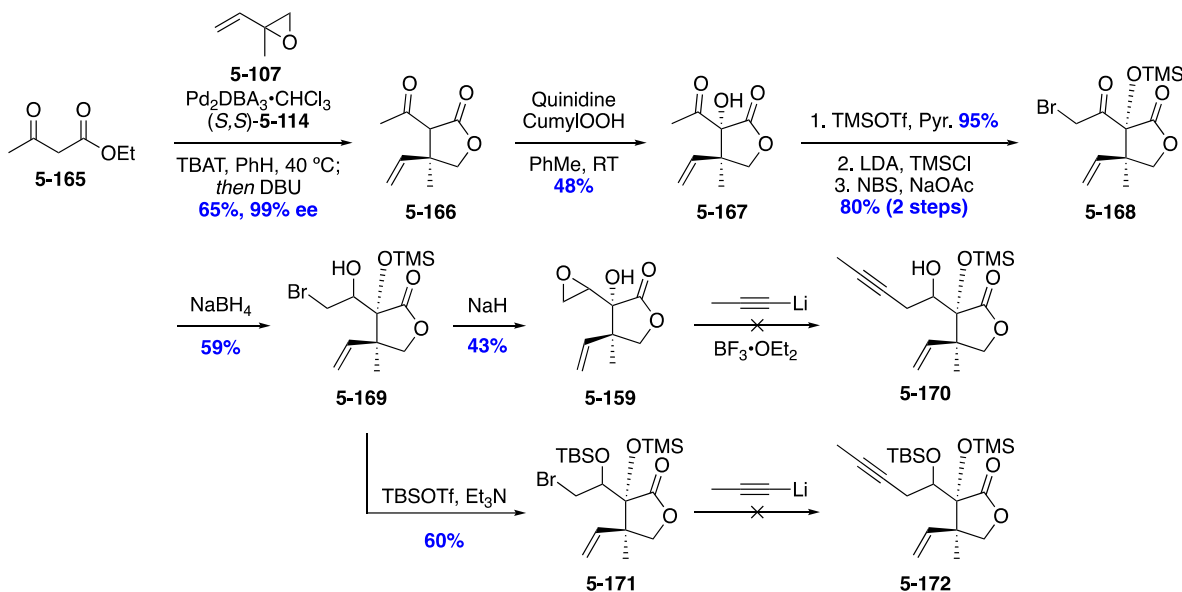
As shown in Scheme 5-26, two potential sequences could lead to **5-156**. We could potentially trace this material back to epoxide **5-159**, which would be opened with lithiated propyne to directly give **5-156**. This epoxide could come back to a Tsuji–Trost reaction of methyl or ethyl acetoacetate with **5-107**. This pathway would have the benefit of coming back to commodity chemicals. Alternatively, the alkyne of **5-156** could be installed by functionalizing an aldehyde intermediate, which would trace back to **5-161** bearing some sort of β -heteroatom functionality. This would also arise from a Tsuji–Trost reaction from ketoester **5-162**. While it was conceptually possible to perform the Tsuji–Trost with **5-163**, we found this approach to not be feasible due to challenges in the synthesis of the substrate. Attempts to form **5-163** all resulted in isomerization to the conjugated allene **5-164**, and as such will not be discussed further.

5.4.2 *Synthesis of the Enyne Precursor*

With several ideas of where to start this new route, I began by investigating the formation of **5-156** through the intermediacy of epoxide **5-159**. The Tsuji–Trost reaction between ethyl acetoacetate (**5-165**) and **5-107** has been reported previously, so the conditions reported were utilized.³⁴ As such, **5-165** was treated **5-107** in the presence of Pd₂DBA₃•CHCl₃ and **5-114**, followed by the addition of DBU to elicit lactonization to afford **5-166** in 65% yield, and excellent enantiomeric purity. Subsequent α -hydroxylation using the previously optimized conditions

resulted in a 48% isolated yield of **5-167**. However, analysis of the crude NMR revealed only a 2.7:1 dr in contrast to the good selectivity observed previously on **5-105**. Silylation of the tertiary alcohol, followed by two-step bromination of the methyl ketone led to **5-168** in good yield. The ketone was reduced non-diastereoselectively with sodium borohydride to yield **5-169**. Treatment of this compound with sodium hydride resulted in the desired epoxide **5-159**. Unfortunately, after several attempts to open the epoxide with propyne derivatives, no productive reaction was observed. Alternatively, we could potentially perform an S_N2 reaction with bromide **5-169** after protection of the secondary alcohol. As such, TBS protection gave **5-171**, but unfortunately attempts at performing an S_N2 of this substrate proved challenging and inconsistent. Due to these challenges, we ultimately abandoned this approach to pursue the other strategy laid out in Scheme 5-26.

Scheme 5-27 Synthesis of enyne **5-156** through epoxide **5-159**.



The alternative approach to **5-156** required keto ester starting materials bearing β -functionalization to manipulate at a later stage to form the alkyne. Several potential starting materials were synthesized bearing protected β -alcohols, but none of them were particularly

reactive in the Tsuji–Trost reaction (Figure 5-8). These compounds either resulted in partial conversion to product, or no conversion. Concerned that the β -functionality could potentially eliminate or poison the palladium catalyst, we sought literature precedent for performing this type of reaction with potential β -leaving groups. We found that Trost had utilized **5-173** in an approach to viridenomycin,⁵⁹ and thought that this could be useful to us, as the sulfide could be converted to an aldehyde via a Pummerer rearrangement. I synthesized **5-173** and under modified conditions from Trost's report **5-174** was isolated in 49% yield and 96% ee. The reaction was found to be robust and scalable, but the lactonization required cooling of the solution to $-10\text{ }^{\circ}\text{C}$ and dropwise addition of DBU to limit the side product that resulted from elimination of thiophenol.

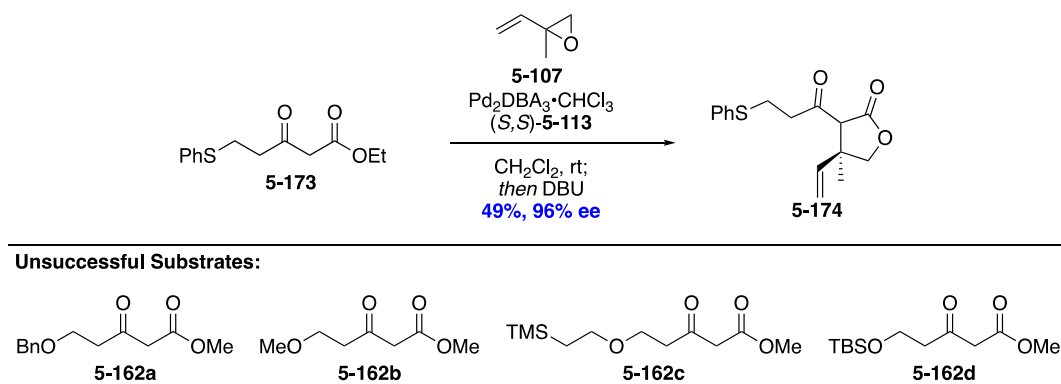
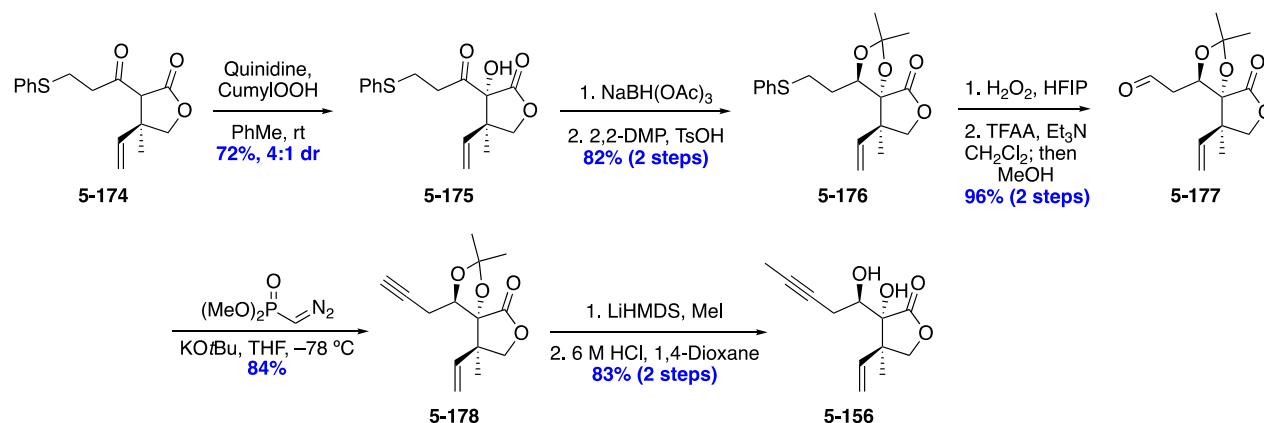


Figure 5-8 Investigation of potential Tsuji–Trost starting materials.

Having established scalable access to **5-174**, the material was pushed forward toward enyne **5-156** using a similar sequence to the one previously established. Oxidation of **5-174** with quinidine and cumyl hydroperoxide yielded **5-175** in 72% overall yield, as a 4:1 mixture of separable diastereomers. Importantly, it was necessary to cool the reaction mixture prior to the addition of cumyl hydroperoxide to circumvent competitive oxidation of the sulfide under the reaction conditions. Additionally, the cumyl alcohol byproduct formed in the reaction has a very similar R_f value to the desired compound. It was necessary to remove the byproduct by distillation either before or after chromatography. Saksena reduction of the ketone, followed by treatment with

2,2-dimethoxypropane and TsOH led to acetonide **5-176**. Oxidation of the sulfide to the sulfoxide, followed by Pummerer rearrangement promoted by TFAA led to aldehyde **5-177** in 96% yield over two steps. Seyferth–Gilbert homologation proceeded smoothly, giving terminal alkyne **5-178** in 84% yield. Methylation of the alkyne, followed by deprotection afforded **5-156**, in a total of 9 steps LLS.

Scheme 5-28 Synthesis of **5-156**.

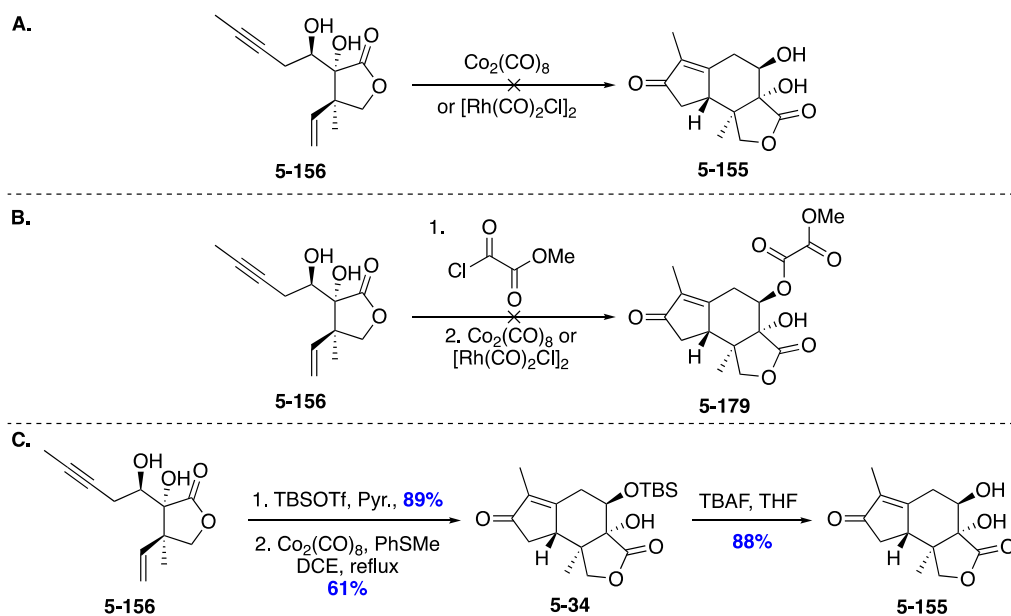


5.4.3 Constructing the Core

With access to **5-156**, we were once again able to investigate the Pauson–Khand reaction on this substrate. Given the precedent from Zhai’s synthesis of jiadifenin (Scheme 5-5),¹⁷ we were very confident about the outlook for this transformation. In terms of minimizing protecting group manipulations, we were interested in the possibility of performing this reaction with **5-156** directly. However, under cobalt mediated and rhodium catalyzed conditions, only starting material was recovered (Scheme 5-29A). PKR reactions have been reported with unprotected tertiary alcohols, so we postulated that the secondary alcohol was inhibiting the reactivity. Once again, to minimize protecting group manipulation, we attempted to protect the secondary alcohol as a dialkyl oxalate. This would serve both as a protecting group and as a functional handle to form a cesium oxalate, which can be leveraged to perform an intramolecular alkoxy carbonyl radical cyclization.⁶⁰

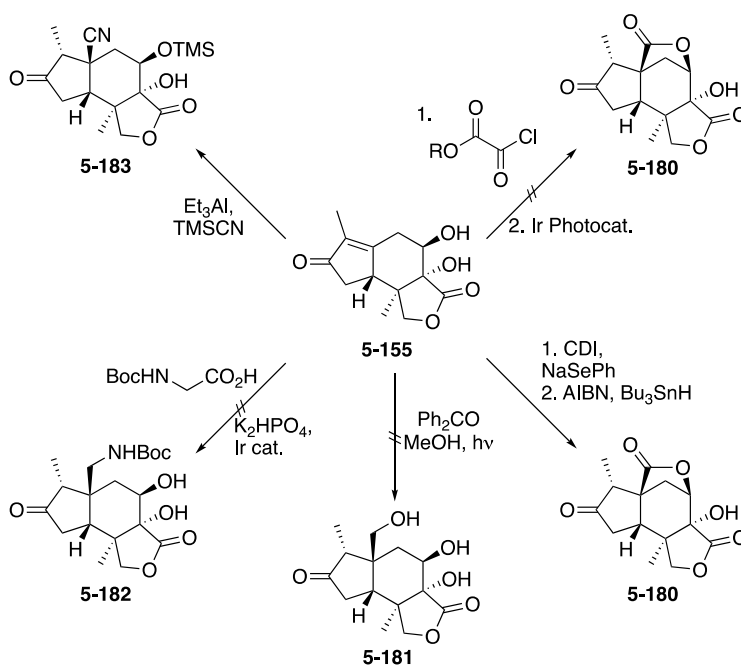
Treatment of **5-156** with methyl chlorooxoacetate produced an intermediate dialkyl oxalate, however this intermediate unfortunately did not undergo the desired Pauson-Khand (Scheme 5-29B). Ultimately, we elected to silylate the secondary alcohol in a similar manner to Zhai and use this known intermediate to perform the Pauson–Khand. However, we elected not to use the same reaction conditions as Zhai. Specifically, the Zhai group used tributylphosphane sulfide as an additive in the PKR, but this material can only be made from tributyl phosphine in poor yield.^{17,61} Additionally, it is known that simpler sulfide additives will also serve the same role in the Pauson–Khand reaction.⁶² As such, we chose to use readily available thioanisole to mediate our reaction. Treatment of the silylated alcohol with $\text{Co}_2(\text{CO})_8$, followed by refluxing the solution in the presence of thioanisole gratifyingly led to **5-180** in 61% yield. This material was subsequently desilylated by treatment with TBAF to give **5-155** in 88% yield. The structure and absolute configuration of **5-155** were unambiguously confirmed through X-ray crystallography.

Scheme 5-29A. Pauson–Khand of the free diol **5-156**. **B.** Protection of the secondary alcohol as an oxalate. **C.** Silylation of the secondary alcohol.



Having secured scalable access to **5-155**, we needed to install the final carbon atom and quaternary center necessary for **5-8**. At the outset of this sequence, we were hoping to leverage the secondary alcohol of **5-155** to perform an intramolecular alkoxy carbonyl radical cyclization to set the quaternary center and close the final ring in one step.^{59,63} We intended to do this by converting the secondary alcohol into a cesium oxalate, and using conditions developed in the Overman laboratory to perform the intramolecular Giese addition to yield **5-180**.⁵⁹ Unfortunately, these efforts were not fruitful (Scheme 5-30). The secondary alcohol could be selectively acylated with methyl chlorooxoacetate, but we found that saponification with CsOH resulted in non-regioselective saponification. Under these conditions we also observed elimination of the secondary alcohol to generate a conjugated dienone product. It is also possible to access cesium oxalates by treatment of TMS-ethyl oxalates with CsF to generate the cesium hemioxalate.⁶⁴ However, attempts to form the cesium oxalate on our system resulted primarily in elimination to the dienone side product.

Scheme 5-30 Attempts to install the final quaternary center.



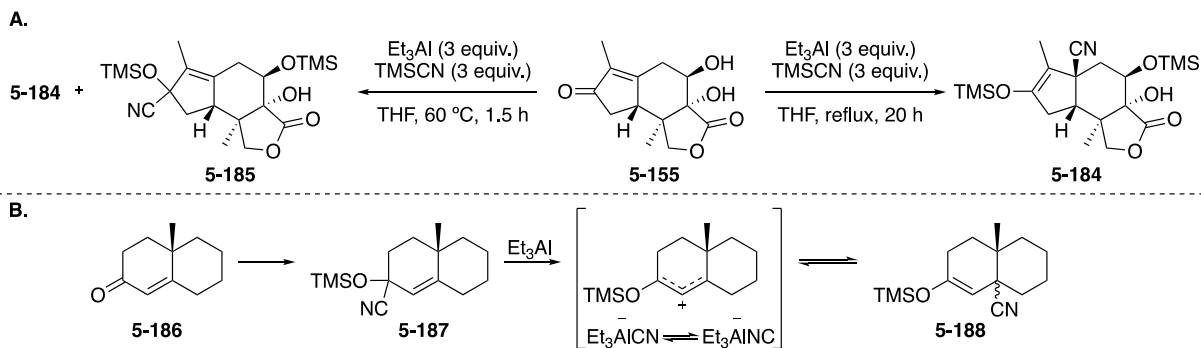
Having failed to form the cesium oxalates, we attempted to access the desired alkoxycarbonyl radicals through selenocarbonates. Treatment of **5-155** with CDI followed by sodium phenylselenide led to the desired selenocarbonate. Subsequent radical cyclization mediated by AIBN and Bu₃SnH successfully afforded the desired lactone **5-180**; however the selenocarbonate intermediate was plagued by the same elimination issues as the oxalates, making it challenging to access meaningful quantities of this lactone. We then turned our attention to intermolecular conjugate additions into enone **5-155**. I reasoned that radical chemistry might still be productive, as the early transition states that radicals often go through make them less sensitive to steric effects, which was particularly important when adding into a tetrasubstituted enone. It is possible to perform Giese additions with hydroxymethyl radicals generated in methanol by photolysis of enones in the presence of photosensitizers.⁶⁵ Initially, the reaction seemed to be productive on small scale when irradiating with a 450W mercury arc lamp. However, the reaction was sensitive to scale and overall irreproducible, as no two reactions gave the same results, even if the scale, stoichiometry, and vessel were identical.

Recently, Dr. Alex Burtea of our group used photoredox catalysis to generate the α -amino radical of Boc-glycine to perform a Giese addition as one of the key steps in the total synthesis of himeradine A.⁶⁶ I attempted to use these conditions to perform a Giese addition into **5-155**, and the reaction seemed robust when using several equivalents of Boc-glycine on <5 mg scale. However, the reaction did not scale well, as increasing the scale to 15 mg resulted in complete deterioration of the reaction conversion. Additionally, it was not readily apparent how to best convert the protected primary amine into an aldehyde/ester. Due to the polarity of the product after removal of the amine protecting group, none of the desired primary amine product was isolated.

After significant failure in eliciting either an intra- or intermolecular Giese addition into **5-155**, I began to pursue polar approaches for the conjugate addition. Ideally, the nucleophile would be in the acid oxidation state to minimize late-stage redox manipulations. With this idea, we became interested in the hydrocyanation chemistry developed by Nagata.⁶⁷ We initially attempted additions of Nagata's reagent (Et_2AlCN) to both **5-155** and **5-34** but found no success. Nagata also frequently used triethyl aluminum and HCN to enact this transformation, but I was hesitant to synthesize and use neat HCN due to its inherent toxicity. However, after some evaluation of the literature, I found that TMS-CN is often used as a surrogate for HCN in these reactions.⁶⁸ Treatment of enone **5-155** with TMS-CN and AlEt_3 successfully afforded ketone **5-183**.

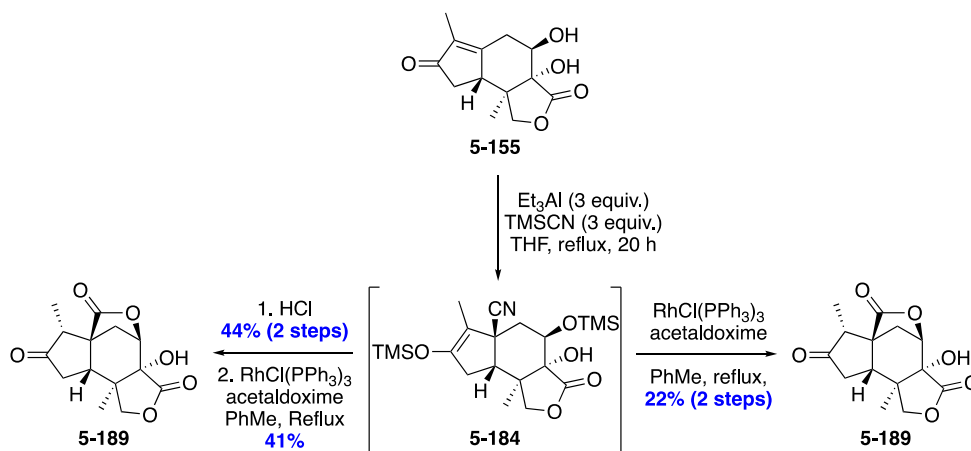
The initial reaction conditions for the hydrocyanation were modeled after the conditions that Snyder reported in their synthesis of the annotinolides.^{66c} Compound **5-155** was added to a mixture of Et_3Al and TMS-CN, and the reaction was heated to 60 °C for 1.5 hours (Figure 5-9a). Under these conditions, TMS-cyanohydrin **5-185** was isolated in large quantities along with the desired 1,4-addition product **5-184**. Utimoto and coworkers proposed that in the early stages of the reaction, TMS-cyanohydrin **5-187** predominates (Scheme 5-31B), but in the presence of excess Et_3Al this intermediate can reionize and equilibrate to the thermodynamic 1,4-addition product **5-188**.^{67b} By allowing the reaction to proceed for 20 hours at reflux, **5-155** was cleanly converted to **5-184**.

Scheme 5-31A. Divergent results for hydrocyanation of **5-155**. **B.** Mechanistic pathway proposed by Utimoto.



Now that the final carbon was installed, we next needed to evaluate the most prudent way of forming the lactone. Attempts to directly form the lactone by treatment of **5-184** with concentrated acid led to decomposition of the material. Dilute hydrochloric acid achieved hydrolysis of the TMS-enol ether. Subsequent treatment of this the ketone with Wilkinson's catalyst and acetaldoxime enacted an anhydrous hydration of the nitrile,⁶⁹ which spontaneously lactonized under these conditions, generating **5-189** in 41% yield. It was also possible to form **5-189** directly by treatment of the crude TMS-enol ether **5-184** with Wilkinson's catalyst and acetaldoxime, albeit in low yield. Regardless of yield, these steps led to the installation of the final carbon atom, quaternary center, and ring of the natural product.

Scheme 5-32 Conversion of **5-155** into desired lactone **5-189**.



5.4.4 End Game Strategy

Having developed a route to **5-189**, we could evaluate the endgame of the synthesis. To convert **5-189** to **5-8**, we needed to epimerize the methyl stereocenter at carbon 1 in the A ring, as well as manipulate the oxidation states at carbon 2 and 4 (Figure 5-9). Unfortunately, **5-189** exists in a twist-boat which makes direct epimerization challenging due to the concave nature of the α -face of the molecule. However, conversion to enone **5-190** through a Saegusa–Ito dehydrogenation would generate a more planar A-ring, thus increasing the probability that a successful epimerization could be achieved. Epimerization of **5-190** would generate an intermediate from Gademann’s approach to **5-8**.³⁰ Gademann’s group synthesized the same enone through allylic oxidation of **5-98** (Scheme 5-15) and performed a Luche reduction to generate **5-99** with unassigned stereochemistry. While a full discussion will follow below, we believed that the allylic alcohol stereochemistry set by this Luche reduction contradicts that of the natural product at C2. After the 1,2-reduction, a Mukaiyama hydration would install the final oxygenation and complete the synthesis of **5-8**.

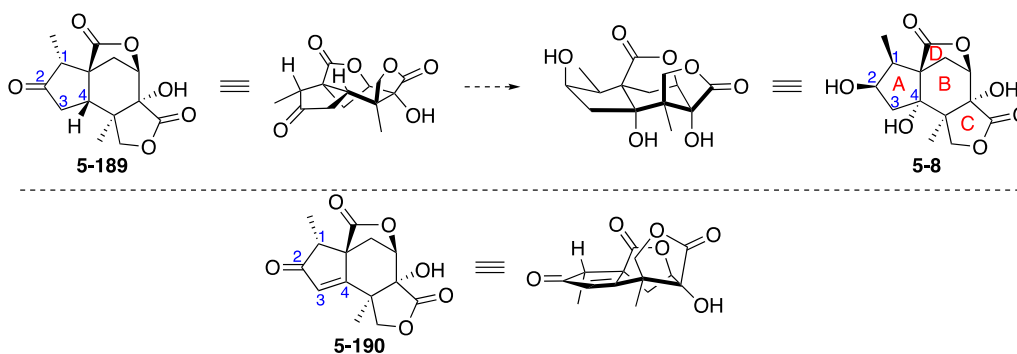
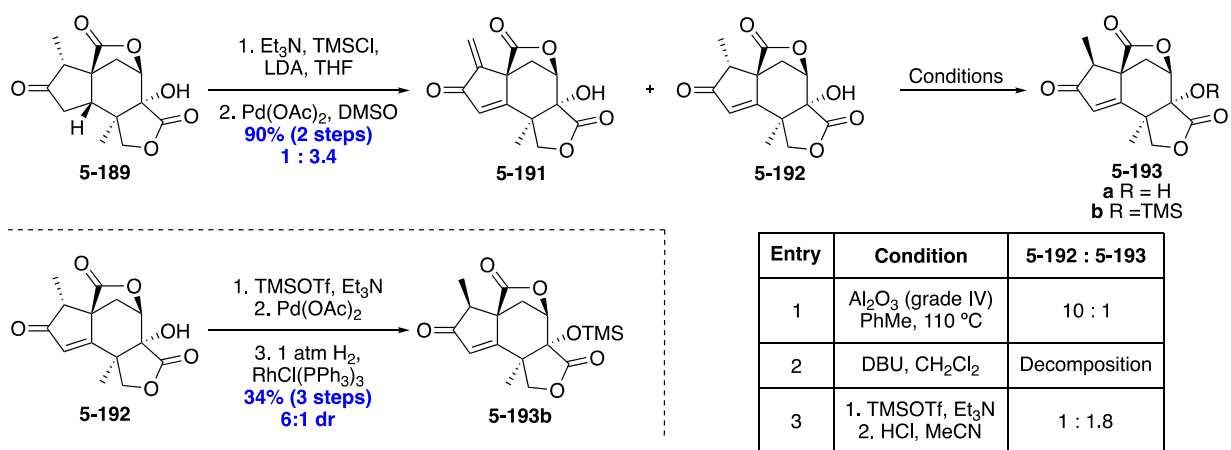


Figure 5-9 Highlighting the final manipulations necessary for the conversion of **5-189** to **5-8**.

To begin investigating the stereochemical complexity of the A ring, a Saegusa–Ito oxidation was performed on **5-189** (Scheme 5-33). Interestingly, when using the protocol established in Zhai’s synthesis of jiadifenin, we observed a 1:3.4 ratio of dienone **5-191** and desired

enone **5-192**. Precedent for this double dehydrogenation is scarce, making it an intriguing side product. Unfortunately, **5-191** and **5-192** were not separable by silica gel chromatography, so the mixture was taken forward to attempt epimerization of the methyl center. We first attempted epimerization using grade IV basic alumina in refluxing toluene,⁷⁰ but we only observed **5-193a** in a 1:10 ratio with **5-192**. Decomposition of the starting material occurred upon treatment of **5-192** with DBU at room temperature. We also attempted a kinetic protonation of the corresponding silyl enol ether using a procedure developed by Zimmerman.⁷¹ As such, **5-192** was converted to its silyl enol ether upon treatment with TMSOTf and triethylamine and was subsequently protonated with 6 M HCl in acetonitrile generating a mixture of **5-193a** and **5-193b**. The diastereomeric ratio of this transformation (for both **5-193a** and **5-193b**) was 1.8:1. Unfortunately, the silylated diastereomers were inseparable, but the free alcohol diastereomers were conveniently separable by chromatography and the stereochemistry was confirmed by NOESY.

Scheme 5-33 Efforts toward epimerizing the A-ring methyl stereocenter.



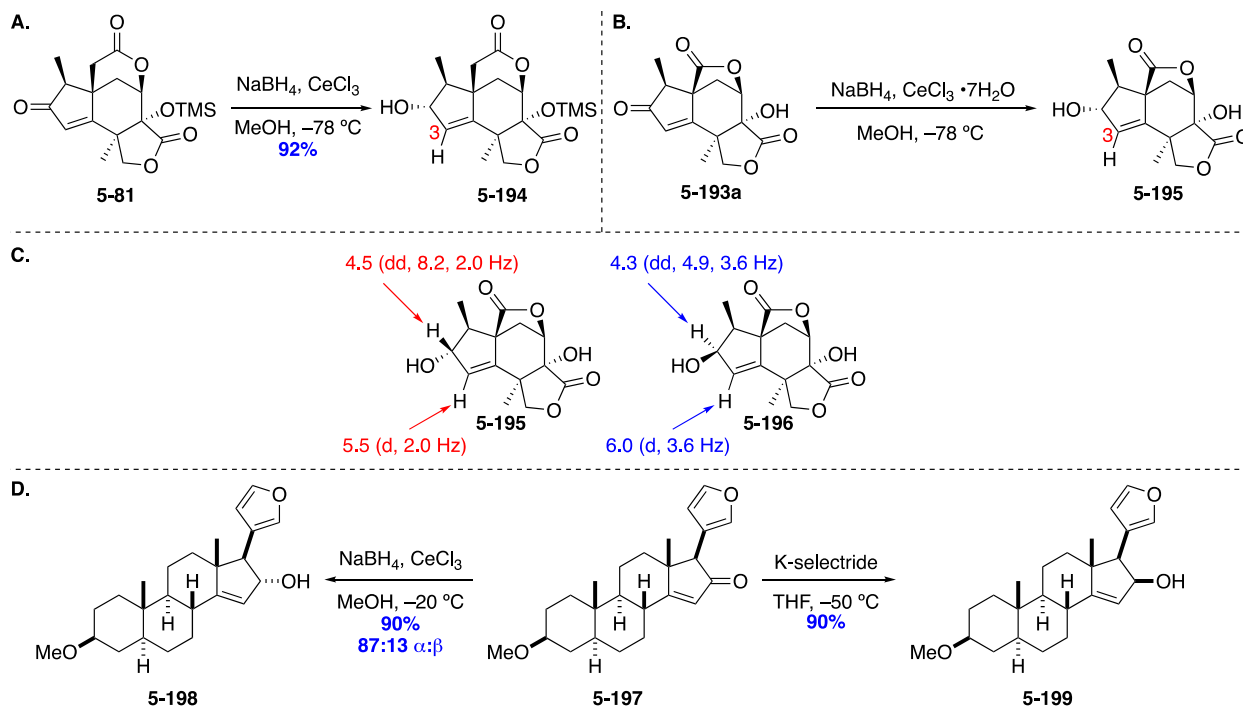
Having achieved partial epimerization, we were still interested in improving the ratio, and thought that **5-191** could serve as a useful intermediate. Professor Rychnovsky suggested that hydrogenation with Wilkinson's catalyst to reduce the *exo*-alkene might give greater diastereoselectivity, as the catalyst is known to be sensitive to sterics.⁷² Since **5-191** was

inseparable form **5-192**, the mixture of material was subject to a Saegusa–Ito oxidation to funnel it to the desired dienone. Subsequent hydrogenation of the crude material with Wilkinson’s catalyst then provided **5-193b** as a 6:1 mixture of diastereomers at C2. While an excellent result, the process was not reproducible, as pure samples of dienone **5-191** failed to hydrogenate by the action of Wilkinson’s catalyst under otherwise identical conditions. This seemed to be a lesson in tracking metal impurities, as the crude mixture that successfully hydrogenated likely contained Pd(OAc)₂ from the previous transformation. Verification of this hypothesis by hydrogenating a sample of pure **5-191** with 40 mol % Pd(OAc)₂ led to **5-193** as a 2.5:1 mixture of diastereomers.

With **5-193** in hand, we were ready to perform the final manipulations of the synthesis. Our rationale for stereoselectivity was informed by an evaluation of the literature. In Micalizio’s synthesis of **5-3** and **5-5**, they reported a Luche reduction on an enone very similar to **5-193**. Luche reduction of **5-81** gave **5-194** in 92% yield as a single diastereomer (Scheme 5-34A) and the stereochemistry was confirmed by NOESY.²⁵ In this report, the vinylic proton at position 3 is reported as a doublet with a coupling constant of 0.9 Hz. The only difference between **5-194** and our desired product is the size of the bridging lactone ring, which is unlikely to drastically change the conformation of the A ring. Based upon this coupling constant and completed synthesis by Micalizio, I propose that the unassigned allylic alcohol of **5-99** in Gademann’s approach to **5-8** was in an α -orientation (Scheme 5-34B). This is based on the tabulated NMR data reported in Christophe Daeppen’s dissertation,³⁰ in which he stated that the vinylic proton at carbon 3 appears as a doublet with a coupling constant of 1.0 Hz. The NMR spectra for diastereomers **5-195** and **5-196** were calculated using Spartan,^{56,73} and the coupling constant for the vinyl proton was calculated to be 2.0 Hz in **5-195** and 3.6 Hz in **5-196**. In addition to these calculated values, the vinyl proton of **5-5** is known to appear as a doublet with 3.1 Hz coupling, which gives credibility

to the calculated values.²⁵ While the coupling constants are not exact, the evidence from Micalizio's synthesis in addition to the calculated coupling lend credence to the assertion that a Luche reduction will set the alcohol stereochemistry incorrectly.

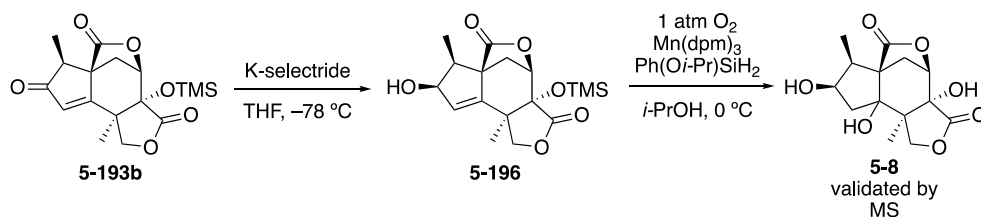
Scheme 5-34A. Luche reduction reported by Micalizio.²⁵ **B.** Proposed stereochemistry for the Luche reduction reported by Gademann and Daepen.³⁰ **C.** Calculated NMR data for the alcohol diastereomers. **D.** Precedent from Wicha describing stereochemical divergent results.



Confident that a Luche reduction would give the incorrect diastereoselectivity, I searched the literature for relevant examples of 1,2-reductions of enones resulting in a syn relationship between the alcohol and an α -substituent. In 2016, Wicha reported a very relevant result in which they were performing 1,2-reductions on steroidal enone **5-197** (Scheme 5-34D).⁷⁴ They observed that 1,2-reduction of **5-197** under Luche conditions gave predominantly **5-198**, but reduction with K-selectride at low temperature gave exclusively **5-199** in 90% yield. Eager to see if this result would be fruitful, **5-193b** was treated with K-selectride at -78 °C on small scale. In our case **5-196** was formed, and the proton at carbon 3 appeared as a doublet at 6.36 ppm with a 3.2 Hz coupling

constant, consistent with the calculated value for this compound and the value from **5-5**. Excited that the stereochemistry seemed to match, we attempted Mukaiyama hydration with the very minimal material recovered from the reduction. Treatment of this crude material with $\text{Mn}(\text{dpm})_3$ and $\text{Ph}(\text{O}i\text{Pr})\text{SiH}_2$ in isopropanol under an oxygen atmosphere resulted in complete conversion as observed by TLC. After workup with aqueous HCl, **5-8** was formed. Unfortunately, the NMR of the crude material in a low-volume NMR tube resulted in peaks barely discernable from the baseline noise. The sample was sufficient to observe a **5-8** by LRMS, but the stereochemistry at the tertiary alcohol could not be confirmed at the time.

Scheme 5-35 Completion of the synthesis of **5-8** on small scale.



Having validated that the final steps work, additional material was necessary to confirm the stereochemistry of the Mukaiyama hydration. The sequence in Scheme 5-33 was overall low yielding, and almost every step generated a mixture of products. However, in one of the hydrocyanation reactions of **5-155**, the crude material was treated with $\text{Pd}(\text{OAc})_2$ to effect a Saegusa–Ito oxidation. In addition to the expected *exo*-enone, we observed a significant quantity of the double dehydrogenation product. This outcome was unexpected, as precedent for double dehydrogenations on systems similar to ours is scarce in the literature. We found that we could perform the hydrocyanation as before to generate **5-184**, and subsequent treatment with superstoichiometric $\text{Pd}(\text{OAc})_2$ in DMSO at 55–70 °C led cleanly to β -cyano dienone **5-200** in 34% yield over two steps. While the yield is relatively low, this sequence cuts out several of the manipulations shown in Scheme 5-33. We also found that when the mixture was heated further,

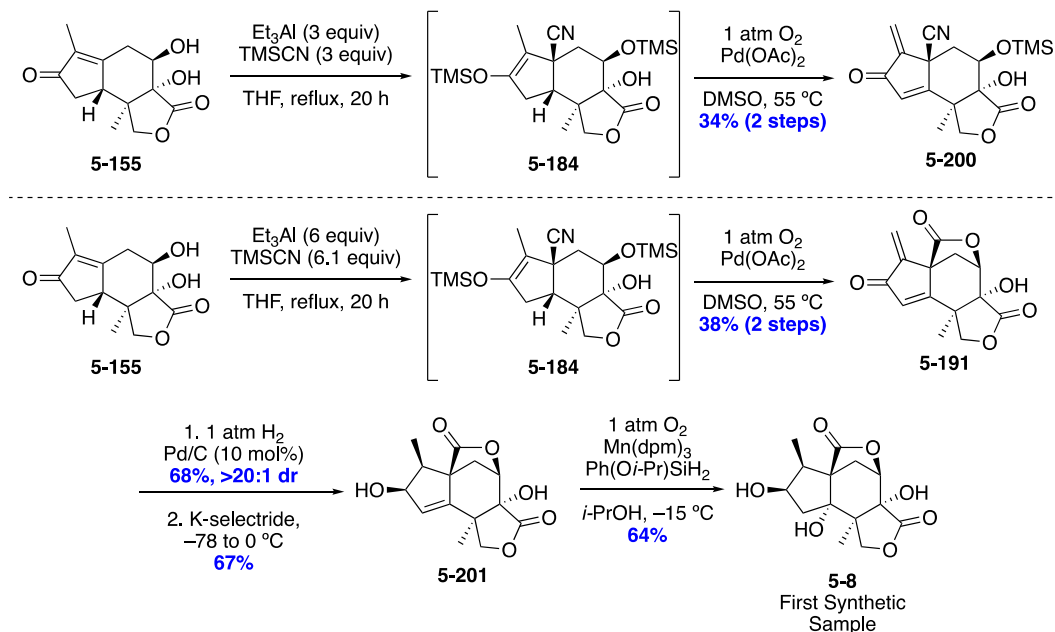
we began to observe hydrolysis of the nitrile, presumably by trace moisture. Gratifyingly, treatment of crude **5-184** with 2.5 equivalents of Pd(OAc)₂ at 110 °C in an oxygen atmosphere directly led to dienone lactone **5-191** in 38% yield over 2 steps, eliminating the rhodium-catalyzed hydration we had previously been using.

With improved access to clean samples of dienone **5-191**, we attempted to improve the diastereoselectivity of the final steps. We had previously shown that hydrogenation of enone **5-191** with Pd(OAc)₂ led to **5-193a** as an intermediate as a 2.5:1 dr at the methyl stereocenter (see Scheme **5-33** and accompanying discussion). In this reaction, the mixture would often turn black, potentially indicating the presence of highly active palladium nanoparticles.⁷⁵ We thought that using a less active palladium species might increase the diastereoselectivity of the process. As such, we attempted hydrogenation over 10 mol% Pd/C and were delighted to find that the diastereoselectivity was essentially perfect! However, the material needed to be sufficiently pure and free of excess palladium from the preceding Saegusa–Ito reaction. Subsequent 1,2-reduction of the enone with K-selectride generated **5-201** as a single diastereomer in 67% yield, and the stereochemistry of this material was confirmed by NOESY. Mukaiyama hydration of **5-201** under the previously described conditions yielded the first synthetic sample of **5-8** as a 7:1 mixture of diastereomers presumably about the tertiary alcohol. However, when the temperature was decreased, and the reaction was performed at –15 °C, we only observed a single diastereomer. After chromatography, we isolated the first synthetic sample of **5-8** in 64% yield. The ¹H and ¹³C NMR spectra of our synthetic material matched well with those reported by Fukuyama.³²

The NMR data of isolated **5-8** are worth briefly discussing. In the isolation paper, Fukuyama reported isolation of 1.2 mg of **5-8** from 3.5 kg of dried plant material. While the ¹H NMR spectrum reported was clean, there is some discrepancy in the purity of the sample (Figure

5-10 and 5-11). In the COSY data reported for isolated **5-8**, there are several impurities between 3.8 and 3.3 ppm that do not appear in the normal ^1H NMR spectrum. Additionally, in the reported proton spectrum there is no water peak at 4.87 ppm as seen in the COSY, and the ^{13}C satellites for the methanol signal are seemingly missing. These discrepancies lead us to question the overall purity of the isolated material. While we are not attempting to disparage the work of Fukuyama's group, these inconsistencies simply lead to some question about the purity and reliability of the data reported, particularly the specific rotation value. However, as the absolute configuration of intermediate **5-155** was determined through X-ray crystallography, we are confident that the absolute configuration of **5-8** is indeed correct.

Scheme 5-36 Alternate end-game strategy leading to the **5-8**.

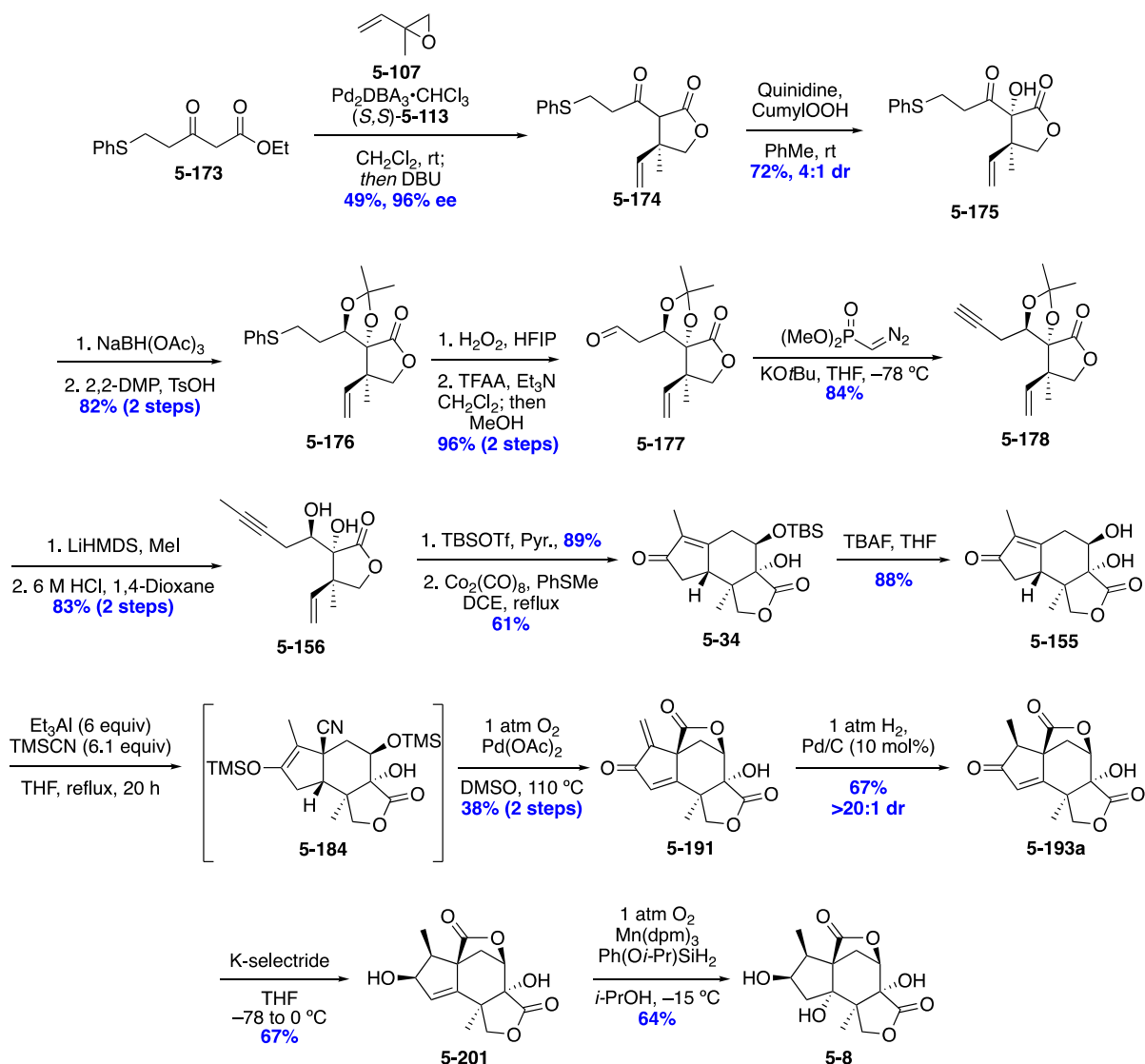


5.5 Summary

In this chapter, we have reported the first completed total synthesis of (2R)-hydroxynorneomajucin (**5-8**). Efforts toward an initial route which disconnected the molecule to a complex bis-lactone enyne substrate for a key Pauson–Khand cyclization are described in detail.

A revised strategy beginning from 5-173 led to the first completed total synthesis of 5-8 in 18 steps LLS. Our strategy relied on the use of 5-34, a known intermediate from the Zhai group's route to jiadifenin. Our sequence to 5-34 is 11 steps LLS in an overall 8.4% yield, while the route published by Zhai is also 11 steps but proceeds in 5.7% overall yield. Additionally, we observed excellent control of the quaternary center in 5-34, while the Ireland–Claisen that was used in the reported sequence sets the quaternary center as an inseparable 7:1 mixture of diastereomers. Our strategy allowed us to complete the first total synthesis of 5-8 in 17 steps LLS. At the time of writing, we are working on a manuscript of this work, and results will be published in due course.

Scheme 5-37 The first total synthesis of **5-8**, completed in 17 steps from **5-173**.



5.6 Supporting Information

5.6.1 General Experimental Details

Unless otherwise stated, all reactions were carried out under an atmosphere of argon in flame- or oven-dried glassware. Solvents were purchased as ACS grade or better and as HPLC-grade and passed through a solvent purification system equipped with activated alumina columns prior to use. Thin layer chromatography (TLC) was carried out using glass plates coated with a 250 μm layer of 60 \AA silica gel. TLC plates were visualized with a UV lamp at 254 nm, or by

staining with potassium permanganate or Hanessian's stain.⁷⁶ Liquid chromatography was performed using forced flow (flash chromatography) with an automated purification system on prepacked silica gel (SiO₂) columns unless otherwise stated.

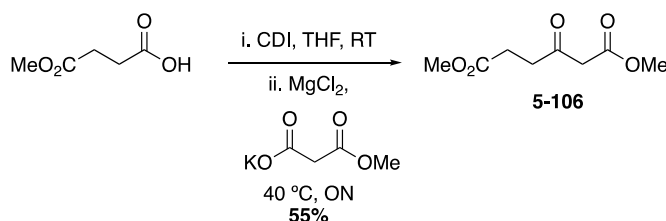
The ¹H and ¹³C{¹H} NMR spectra were recorded at 298.0 K unless otherwise stated. Chemical shifts (δ) were referenced to the residual solvent peak (7.26 ppm for CHCl₃, 3.31 ppm for CH₃OH) for ¹H NMR and CDCl₃ (77.16 ppm) or CD₃OD (49.00 ppm) for ¹³C{¹H} NMR. The ¹H NMR spectra data are presented as follows: chemical shift, multiplicity (s = singlet, d = doublet, t = triplet, q = quartet, m = multiplet, dd = doublet of doublets, ddd = doublet of doublet of doublets, dddd = doublet of doublet of doublet of doublets, dt = doublet of triplets, dq = doublet of quartets, ddq = doublet of doublet of quartets, app. = apparent), coupling constant(s) in hertz (Hz), and integration. High-resolution mass spectrometry was performed using ESI-TOF. An internal standard was used to calibrate the exact mass of each compound. Optical rotations were performed on a JACSO P-1010 spectrometer using either a 10 or 50 mm glass cell with the sodium D-line at 589 nm.

5.6.2 Chemicals

All commercially available reagents were used as received unless stated otherwise. (*S,S*)-DACH-Naphthyl (**5-113**) and Pd₂DBA₃•CHCl₃ were purchased from Strem and stored in a desiccator. We later found that **5-113** could be purchased from AmBeed at a lower price while retaining the quality of ligand. (*S,S*)-**5-114** was prepared as described by Trost.⁷⁷ Compound **5-107** was purchased from Sigma, but it could also be prepared on large scale following the procedure of Stoltz.⁷⁸ Compounds **5-162a**,⁷⁹ **5-162b**,⁸⁰ and **5-162c**⁸¹ were prepared from the Weiler dianion of methylacetoacetate according to literature procedures. Compound **5-162d**⁸² was prepared according to literature procedure. [Rh(CO)₂Cl]₂, and Co₂(CO)₈ were purchased from Strem and

were stored in a $-20\text{ }^{\circ}\text{C}$ freezer in a nitrogen-filled glovebox. $\text{Mo}(\text{CO})_3\text{DMF}_3$ was made according to a literature procedure, and the material was stored in a $-20\text{ }^{\circ}\text{C}$ freezer in a nitrogen-filled glovebox.⁸³

5.6.3 Compound Synthesis and Characterization



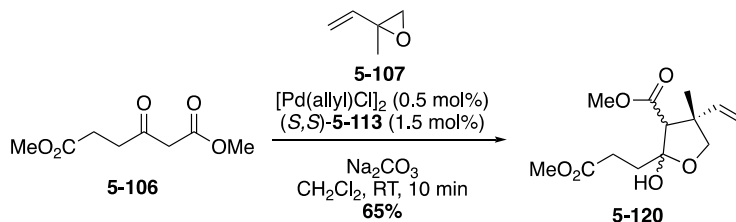
dimethyl 3-oxohexanedioate (5-106): A flame-dried 2L three-neck round bottom flask equipped with a mechanical stirrer (using an adapter to maintain argon atmosphere) and a reflux condenser was charged with mono-methyl succinate (38.5 g, 0.291 mol) and THF (500 mL, 0.58 M). The solution was stirred, and 1,1'-carbonyldiimidazole (56.8 g, 0.350 mol) was added portion wise under an argon counterflow. The solution was then stirred for 1 h at room temperature. After this time, potassium 3-methyl-3-oxopropanoate (45.5 g, 0.291 mol) and MgCl_2 (dried at $150\text{ }^{\circ}\text{C}$ under vacuum for 24 h, 27.8 g, 0.291 mol) were added successively, and the solution was heated to $40\text{ }^{\circ}\text{C}$ overnight. During this time, CO_2 evolution was observed, and the suspension became thicker as the reaction progressed. Once CO_2 evolution had ceased, the slurry was cooled to room temperature and filtered through a pad of celite washing with additional portions of THF. The filtrate was concentrated *in vacuo*, and the crude material was suspended between EtOAc (300 mL) and aq. 1 M HCl (300 mL). The organic layer was collected, and the aqueous layer was extracted with EtOAc (3 x 150 mL). The combined organic extracts were washed with saturated aq. NaHCO_3 (2 x 200 mL), brine (1 x 200 mL), dried over Na_2SO_4 and concentrated *in vacuo*. The crude oil was vacuum distilled in an oil bath ($\sim 300\text{ mTorr}$, $83\text{ }^{\circ}\text{C}$ vapor temperature, $130\text{ }^{\circ}\text{C}$ bath temperature) to afford **5-106** as a clear oil which turned yellow upon storage (30.0 g, 55%). All

spectral data were consistent with those reported previously.

R_f = 0.51 (50% EtOAc in hexanes) visualized by UV.

$^1\text{H NMR}$ (500 MHz, CDCl_3) δ 3.73 (s, 3H), 3.67 (s, 3H), 3.50 (s, 2H), 2.86 (t, J = 6.6 Hz, 2H), 2.61 (t, J = 6.6 Hz, 2H).

$^{13}\text{C}\{^1\text{H}\}$ NMR (126 MHz, CDCl_3) δ 201.0, 172.9, 167.5, 52.5, 52.0, 49.1, 37.5, 27.8.



methyl (4*S*)-2-hydroxy-2-(3-methoxy-3-oxopropyl)-4-methyl-4-vinyltetrahydrofuran-3-carboxylate (5-120): A flame-dried 100 mL round bottom flask was charged with **5-106** (0.397 g, 2.11 mmol), [Pd(allyl)Cl]₂ (7.7 mg, 0.021 mmol), (*S,S*)-DACH-naphthyl (50.0 mg, 0.0633 mmol), and Na₂CO₃ (0.268 g, 2.53 mmol). The flask was evacuated and backfilled with argon three times. Dichloromethane (degassed by sparging, 21 mL) was added and the solution was stirred for 5 minutes, during which time a bright orange color was observed. 2-methyl-2-vinyloxirane (0.25 mL, 2.5 mmol) was added, and the solution turned pale yellow immediately. Once the orange color of the palladium complex had returned, the solvent was evaporated and the crude material was purified by flash chromatography on silica gel eluting with 30% EtOAc/hexanes to afford **5-120** as a colorless oil (0.376 g, 65%) as an inseparable mixture of 3 diastereomers. The diastereomers were integrated together when signals were overlapping to simplify analysis, however it should be noted that once the hemiacetal is eliminated, the diastereomers converge to one isomer.

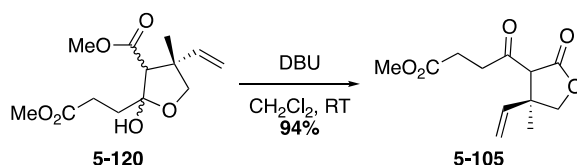
R_f = 0.67 (50% EtOAc in hexanes) visualized by staining with KMnO_4 .

$^1\text{H NMR}$ (500 MHz, CDCl_3) δ 6.14–5.83 (m, 1H), 5.22–4.95 (m, 2H), 4.22 (d, J = 9.0 Hz, 0.13H),

4.02 (dd, $J = 8.9, 7.9$ Hz, 0.49H), 3.86–3.78 (m, 1H), 3.73 (s, 2H), 3.69–3.61 (m, 5H), 2.83 (s, 0.48H), 2.70 (s, 0.37H), 2.62–2.44 (m, 2H), 2.13–2.04 (m, 0.82H), 2.04–1.94 (m, 0.82H), 1.36 (s, 1.43H), 1.22 (s, 1.47H).

$^{13}\text{C}\{^1\text{H}\}$ NMR (126 MHz, CDCl_3) δ 174.3, 174.2, 173.2, 173.0, 172.8, 170.3, 165.8, 144.2, 143.1, 141.3, 114.4, 112.8, 112.7, 105.2, 105.1, 82.4, 77.95, 77.87, 61.9, 59.4, 52.32, 52.31, 51.81, 51.76, 51.75, 50.7, 49.0, 47.83, 47.80, 35.7, 35.4, 30.9, 28.64, 28.57, 28.5, 24.8, 24.1, 23.6, 20.5.

HRMS (ESI/TOF) m/z : $[\text{M}+\text{Na}]^+$ Calcd for $\text{C}_{13}\text{H}_{20}\text{O}_6\text{Na}$ 295.1158; Found 295.1159.



methyl 4-((4*S*)-4-methyl-2-oxo-4-vinyltetrahydrofuran-3-yl)-4-oxobutanoate (5-105):

Compound **5-120** (0.249 g, 0.914 mmol) was dissolved in CH_2Cl_2 (9 mL) and DBU (0.15 mL, 1.0 mmol) was added dropwise. The mixture was allowed to stir until complete consumption of **5-120** was observed. The reaction was quenched by the addition of 2 M aq. HCl (9 mL). The mixture was transferred to a separatory funnel, the organic phase was separated, and the aqueous phase was extracted with CH_2Cl_2 (3 x 10 mL). The combined organic extracts were dried over Na_2SO_4 , the drying agent was filtered off, and the solution was concentrated. The crude material was purified by flash chromatography on silica gel eluting with 50% EtOAc/hexanes. Pure **5-105** was isolated as a clear oil (0.205 g, 94%) as a 1:1 mixture of diastereomers with 7% of the enol tautomer. The diastereomers were integrated together when possible to simplify analysis.

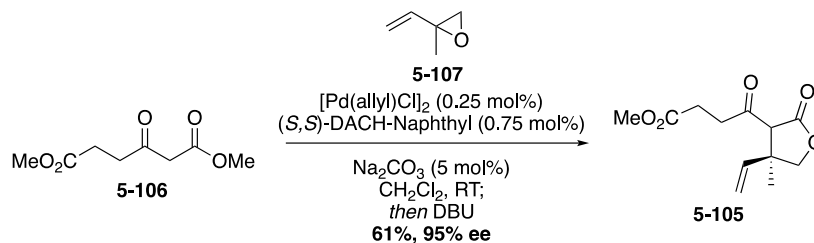
$R_f = 0.51$ (50% EtOAc in hexanes) visualized by UV.

^1H NMR (500 MHz, CDCl_3) δ 11.62 (s, 0.08H), 5.98–5.86 (m, 1H), 5.29–5.16 (m, 2H), 4.42 (d, $J = 8.8$ Hz, 0.36 H), 4.11 (q, $J = 8.8$ Hz, 1H), 4.02–3.96 (m, 0.47H), 3.73 (s, 0.63H), 3.67 (s, 3H), 3.59 (s, 0.48H), 3.50 (s, 0.40H), 3.43 (s, 0.35H), 3.03–2.83 (m, 2H), 2.71–2.49 (m, 2H), 1.39 (s,

1.5H), 1.27 (s, 1.5H).

$^{13}\text{C}\{^1\text{H}\}$ NMR (126 MHz, CDCl_3) δ 202.2, 201.6, 201.0, 172.8, 172.7, 172.5, 172.1, 167.5, 141.8, 140.3, 136.9, 117.1, 115.9, 114.8, 79.1, 76.6, 76.6, 63.9, 60.9, 52.5, 52.0, 52.0, 49.1, 46.7, 46.6, 39.6, 39.6, 37.5, 29.8, 27.8, 27.4, 27.4, 26.9, 23.8, 23.7, 18.5.

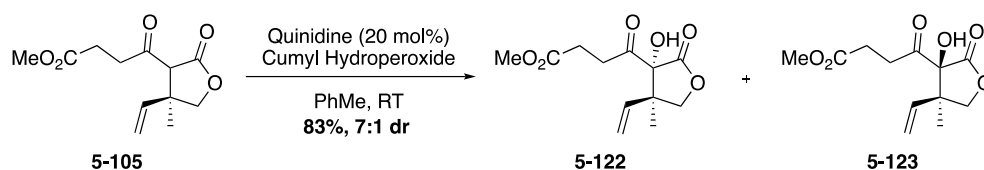
HRMS (ESI/TOF) m/z : $[\text{M}+\text{Na}]^+$ Calcd for $\text{C}_{12}\text{H}_{16}\text{O}_5\text{Na}$ 263.0890; Found 263.0889.



methyl 4-((4*S*)-4-methyl-2-oxo-4-vinyltetrahydrofuran-3-yl)-4-oxobutanoate (5-105): A dry 1L 3-neck round bottom flask was charged with beta-keto ester (9.82 g, 52.2 mmol), [Pd(allyl)Cl]₂ (47.6 mg, 0.130 mmol), (*S,S*)-DACH-naphthyl (0.310 g, 0.391 mmol), and Na₂CO₃ (0.277 g, 2.61 mmol). The flask was evacuated and backfilled with argon three times. Dichloromethane* (260 mL) was added via cannula under a positive pressure of argon and the solution was stirred for 5 minutes, during which time a bright orange color was observed. 2-methyl-2-vinylloxirane (5.9 mL, 60. mmol) was added, and the solution turned pale yellow immediately. The mixture was stirred at room temperature until the orange color of the palladium complex returned. If TLC reveals starting material, 0.2 equivalents of epoxide can be added and the reaction can be stirred until the orange color returns to ensure full conversion. At this time, a 0.5 mL aliquot of the reaction mixture was removed and was dehydrated to the dihydrofuran to assay the enantioselectivity of the reaction. DBU (8.6 mL, 57 mmol) was then added, and the solution was stirred for 1 h. Subsequently, the reaction was quenched with aq. 2 M HCl (200 mL) and the mixture was transferred to a separatory funnel. The organic layer was separated, and the aqueous layer was extracted with CH₂Cl₂ (2 x 150 ml). The combined organic extracts were dried over Na₂SO₄ and

concentrated *in vacuo*. The crude material was purified by flash chromatography on silica gel (500 g) eluting with 30% EtOAc/hexanes to afford the title compound as a peach-colored oil (7.92 g, 63%). The material was spectroscopically identical to characterization for **5-105** described above.

*The reaction was found to be very sensitive to oxygen. Prior to reaction, the solvent was degassed (sparging) with argon for 45 minutes to ensure the solvent was oxygen free. Rigorous Schlenk technique should be used, as traces of ambient atmosphere will retard formation of the active catalyst.



methyl 4-((3*R*,4*R*)-3-hydroxy-4-methyl-2-oxo-4-vinyltetrahydrofuran-3-yl)-4-

oxobutanoate (5-122): Lactone **5-105** (7.92 g, 33.0 mmol) was dissolved in toluene (330 mL) in a non-dried round bottomed flask open to air. Quinidine (2.15 g, 6.59 mmol) was added, and the solution was stirred for 10 minutes at ambient temperature. Cumene hydroperoxide (80% assay) (7.3 mL, 39.6 mmol) was then added, and the mixture was stirred overnight (~15 h) at room temperature. After the reaction was complete (TLC) the solvent was evaporated *in vacuo*. NMR analysis of the crude material revealed a 7:1 dr favoring the desired diastereomer. The crude material was purified by flash chromatography on silica gel eluting with a gradient from 15-25% EtOAc/hexanes to afford **5-122** as a clear oil (6.24 g, 74%) as a single diastereomer.

Desired Diastereomer (5-122):

R_f = 0.27 (25% EtOAc in hexanes) visualized by $KMnO_4$.

1H NMR (600 MHz, $CDCl_3$) δ 5.77 (dd, J = 17.5, 10.8 Hz, 1H), 5.28 (d, J = 10.8 Hz, 1H), 5.19 (d, J = 17.5 Hz, 1H), 4.48 (d, J = 8.8 Hz, 1H), 4.19 (br. s, 1H), 4.04 (d, J = 8.8 Hz, 1H), 3.67 (s, 3H), 3.15 (ddd, J = 18.7, 7.6, 6.0 Hz, 1H), 2.71 (dt, J = 18.7, 6.2 Hz, 1H), 2.61 (ddd, J = 17.4, 7.6,

6.0 Hz, 1H), 2.53 (dt, $J = 17.4, 6.2$ Hz, 1H), 1.29 (s, 3H).

$^{13}\text{C}\{^1\text{H}\}$ NMR (151 MHz, CDCl_3) δ 208.1, 174.9, 173.2, 135.5, 118.4, 87.2, 74.5, 52.2, 49.7, 34.2, 27.9, 19.6.

HRMS (ESI/TOF) m/z : $[\text{M}+\text{Na}]^+$ Calcd for $\text{C}_{12}\text{H}_{16}\text{O}_6\text{Na}$ 279.0840; Found 279.0846.

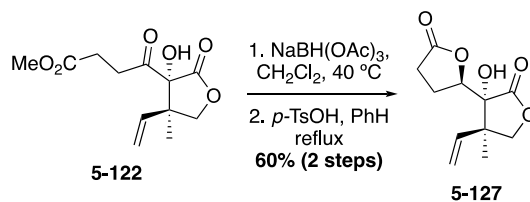
$[\alpha]_D^{21} +106.3$ (c 1.58, CHCl_3)

Undesired Diastereomer (5-123):

$R_f = 0.23$ (25% EtOAc in hexanes) visualized by KMnO_4 .

^1H NMR (600 MHz, CDCl_3) δ 5.93 (dd, $J = 17.6, 10.9$ Hz, 1H), 5.35 (d, $J = 10.9$ Hz, 1H), 5.28 (d, $J = 17.5$ Hz, 1H), 4.26 (dd, $J = 20.2, 8.9$ Hz, 2H), 3.78 (s, 1H), 3.67 (s, 3H), 3.18 (ddd, $J = 19.3, 7.1, 5.1$ Hz, 1H), 2.91 – 2.82 (m, 1H), 2.61 (ddd, $J = 10.8, 7.3, 5.3$ Hz, 2H), 1.20 (s, 3H).

$^{13}\text{C}\{^1\text{H}\}$ NMR (151 MHz, CDCl_3) δ 207.8, 174.6, 173.2, 136.7, 117.3, 85.8, 74.1, 52.1, 34.6, 27.5, 16.2.



(2*R*,3'*R*,4'*R*)-3'-hydroxy-4'-methyl-4'-vinyltetrahydro-[2,3'-bifuran]-2',5(2*H*,3'*H*)-dione (5-127): To a stirred solution of α -ketol **5-122** (4.52 g, 17.6 mmol) in CH_2Cl_2 (176 mL) was added $\text{NaBH}(\text{OAc})_3$ (11.3 g, 52.9 mmol) at room temperature. The solution was then heated to reflux overnight (~18 h). The mixture was then cooled to room temperature and aq. 2 M HCl (150 mL) was added and the solution was stirred vigorously for 1.5 h. Subsequently, the mixture was transferred to a separatory funnel, and the organic layer was separated. The aqueous layer was extracted with CH_2Cl_2 (3 x 100 mL), and the combined organic extracts were dried over Na_2SO_4 and concentrated *in vacuo*. The crude diol was used directly without further purification.

The crude diol was dissolved in benzene (200 mL) in a 500 mL round bottom flask equipped with a Dean–Stark apparatus under argon. TsOH•H₂O (0.837 g, 4.40 mmol) was added, and the solution was heated to reflux for 18 h. The solution was cooled, and the solvent was evaporated. The crude material was chromatographed by flash chromatography on silica gel eluting with a gradient from 20-50% EtOAc/hexanes to afford bislactone **5-127** as a yellow oil (2.39 g, 60% over two steps).

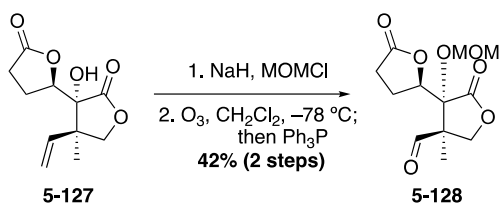
R_f = 0.23 (25% EtOAc in hexanes) visualized by KMnO₄.

¹H NMR (500 MHz, CDCl₃) δ 5.95 (dd, *J* = 17.6, 10.9 Hz, 1H), 5.27 (d, *J* = 10.9 Hz, 1H), 5.23 (d, *J* = 17.6 Hz, 1H), 4.73 – 4.69 (m, 1H), 4.28 (d, *J* = 8.9 Hz, 1H), 4.19 (d, *J* = 9.0 Hz, 1H), 3.57 (app. s, 1H), 2.64 – 2.43 (m, 3H), 2.43 – 2.33 (m, 1H), 1.30 (s, 3H).

¹³C{¹H} NMR (126 MHz, CDCl₃) δ 177.3, 174.3, 137.5, 116.3, 79.6, 78.9, 74.7, 49.8, 28.2, 22.6, 17.3.

HRMS (ESI/TOF) *m/z*: [M+Na]⁺ Calcd for C₁₁H₁₄O₅Na 249.0739; Found 249.0742.

[**a**]²²_D –30.1 (*c* 1.35, CHCl₃)



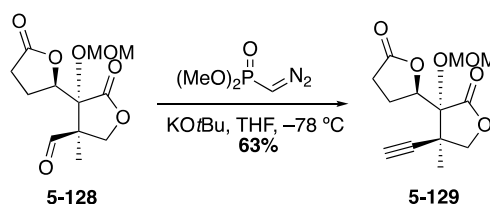
(2*R*,3'*R*,4'*R*)-3'-(methoxymethoxy)-4'-methyl-2',5-dioxooctahydro-[2,3'-bifuran]-4'-

carbaldehyde (5-128): To a cooled (0 °C) solution of bislactone **5-127** (1.57 g, 6.94 mmol) and MOMCl (1.05 mL, 13.9 mmol) in THF (69 mL) was added NaH (60% dispersion, 1.39 g, 34.7 mmol) in 5 portions. The solution was warmed to room temperature and stirred until the reaction as complete by TLC. The mixture was cooled to 0 °C and quenched by the addition of saturated aq. NH₄Cl (150 mL). The mixture was transferred to a separatory funnel, and the aqueous layer

was extracted with ethyl acetate (3 x 50 mL). The combined organic extracts were dried over Na₂SO₄ and concentrated *in vacuo*. This material was used immediately in the subsequent step without purification.

A solution of crude methoxymethyl ether in CH₂Cl₂ (69 mL) was cooled to -78 °C, and O₃/O₂ (generated by a ClearWater Tech corona discharge M-1500 ozone generator) was bubbled through the solution until the solution was saturated with ozone (visualized by the persistence of a blue color in the solution). Once saturated, the excess ozone was purged from the solution by bubbling O₂ through the solution until it became colorless, and Ph₃P (2.18 g, 8.33 mmol) was added. The reaction mixture was warmed to room temperature and allowed to stir for 12 h. The solution was concentrated, and the crude residue was purified by flash chromatography on silica gel (40-90% EtOAc/Hex) to afford aldehyde **5-128** as a colorless oil (787 mg, 42% over two steps). ¹H NMR (500 MHz, CDCl₃) δ 9.75 (s, 1H), 4.93 (d, *J* = 7.0 Hz, 1H), 4.88 (d, *J* = 7.0 Hz, 1H), 4.60 (d, *J* = 9.4 Hz, 1H), 4.06 (dd, *J* = 9.4, 0.8 Hz, 1H), 3.45 (s, 3H), 2.63–2.54 (m, 2H), 2.54–2.46 (m, 1H), 2.45–2.37 (m, 1H), 1.47 (s, 3H).

HRMS (ESI/TOF) *m/z*: [M+Na]⁺ Calcd for C₁₂H₁₆O₇Na 295.0794; Found 295.0781.



(2*R*,3'*R*,4'*R*)-4'-ethynyl-3'-(methoxymethoxy)-4'-methyltetrahydro-[2,3'-bifuran]-

2',5(2*H*,3'*H*)-dione (5-129): Potassium *tert*-butoxide (0.341 g, 3.03 mmol) was weighed into a flame dried 200 mL Schlenk flask in a nitrogen filled glovebox. The flask containing the KO^tBu was brought out of the glovebox and was placed under inert atmosphere. THF (15 mL) was added to the solid, and the solution was cooled to -78 °C. Seyferth–Gilbert reagent (0.477 g, 3.18 mmol)

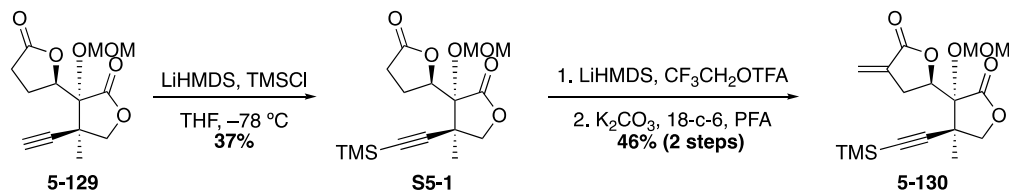
was added dropwise, during which time the contents of the flask turned bright orange. The mixture was allowed to stir for 20 minutes, after which time a solution of **5-128** (azeotroped 3x with PhMe, 0.787 g, 2.89 mmol) in THF (8 mL) was added dropwise, rinsing with another 8 mL portion of THF. The mixture was allowed to stir at $-78\text{ }^{\circ}\text{C}$ for 2 h, and was subsequently quenched by the addition of saturated aq. NH_4Cl (30 mL) at $-78\text{ }^{\circ}\text{C}$. The mixture was warmed to ambient temperature, diluted with 50 mL of H_2O , and was transferred to a separatory funnel. The aqueous phase was extracted with ethyl acetate (3 x 30 mL), and the combined organic extracts were dried over Na_2SO_4 , filtered, and concentrated. The crude material was purified by MPLC (ISCO) on silica gel eluting with a gradient from 40–80% EtOAc in hexanes to afford alkyne **5-129** as a colorless oil (0.490 g, 63%).

$R_f = 0.71$ (75% EtOAc in hexanes) visualized by KMnO_4 .

$^1\text{H NMR}$ (500 MHz, CDCl_3) δ 5.23–5.15 (m, 1H), 4.92 (d, $J = 7.1$ Hz, 1H), 4.82 (d, $J = 7.1$ Hz, 1H), 4.33 (d, $J = 8.4$ Hz, 1H), 4.18 (d, $J = 8.4$ Hz, 1H), 3.44–3.35 (m, 3H), 2.60–2.44 (m, 4H), 2.39 (s, 1H), 1.50 (s, 3H).

$^{13}\text{C}\{^1\text{H}\}$ NMR (126 MHz, CDCl_3) δ 176.6, 171.8, 95.0, 84.0, 81.4, 80.8, 76.5, 74.0, 57.0, 45.3, 27.9, 22.7, 18.1.

HRMS (ESI/TOF) m/z : $[\text{M}+\text{Na}]^+$ Calcd for $\text{C}_{13}\text{H}_{16}\text{O}_6\text{Na}$ 291.0845; Found 291.0847.



(2*R*,3'*R*,4'*R*)-3'-(methoxymethoxy)-4'-methyl-4'-((trimethylsilyl)ethynyl)tetrahydro-[2,3'-bifuran]-2',5(2*H*,3'*H*)-dione (S5-1): LiHMDS (0.643 g, 3.84 mmol) was weighed into a flame dried 100 mL Schlenk flask in a nitrogen filled glovebox, and the flask was removed from the

glovebox and placed under argon. THF (10 mL) was added to the solid LiHMDS, and the solution was cooled to $-78\text{ }^{\circ}\text{C}$. A solution of alkyne **5-129** (0.490 g, 1.83 mmol) in THF (5 ml) was added, and the mixture was allowed to stir for 30 minutes. Freshly distilled TMSCl (0.49 mL, 3.9 mmol) was added, and the mixture was allowed to stir for 20 minutes. The reaction was quenched by the addition of saturated aq. NH_4Cl (6 mL) at $-78\text{ }^{\circ}\text{C}$, and the mixture was warmed to ambient temperature. The mixture was diluted with H_2O (20 mL), transferred to a separatory funnel, and extracted with ethyl acetate (3 x 15 mL). The combined organic extracts were dried over Na_2SO_4 , filtered, and concentrated *in vacuo*. The crude material was purified by MPLC (ISCO) on silica gel eluting with a gradient from 0–50% EtOAc in hexanes to yield **S5-1** as a colorless oil (0.232 g, 37%).

^1H NMR (500 MHz, CDCl_3) δ 5.20–5.14 (m, 1H), 4.95 (d, $J = 7.1$ Hz, 1H), 4.84 (d, $J = 7.1$ Hz, 1H), 4.33 (d, $J = 8.3$ Hz, 1H), 4.17 (d, $J = 8.3$ Hz, 1H), 3.43 (s, 3H), 2.62–2.47 (m, 4H), 1.49 (s, 3H), 0.15 (s, 9H).

$^{13}\text{C}\{^1\text{H}\}$ NMR (151 MHz, CDCl_3) δ 176.8, 172.1, 105.5, 95.1, 90.9, 81.6, 80.9, 76.8, 57.1, 46.0, 28.0, 22.9, 18.5, -0.1.

HRMS (ESI/TOF) m/z : $[\text{M}+\text{H}]^+$ Calcd for $\text{C}_{16}\text{H}_{24}\text{O}_6\text{SiH}$ 341.1420; Found 341.1408.

(2*R*,3'*R*,4'*R*)-3'-(methoxymethoxy)-4'-methyl-4-methylene-4'-

((trimethylsilyl)ethynyl)tetrahydro-[2,3'-bifuran]-2',5(2*H*,3'*H*)-dione (5-130):

LiHMDS (0.164 g, 0.981 mmol) was weighed into a flame dried 25 mL Schlenk flask in a nitrogen filled glovebox, and the flask was removed from the glovebox and placed under argon. THF (2.5 mL) was added to the solid LiHMDS, and the solution was cooled to $-78\text{ }^{\circ}\text{C}$. A solution of alkyne **S5-1** (0.163 g, 0.479 mmol) in THF (2.5 ml) was added, and the mixture was allowed to stir for 30 minutes. Freshly distilled 2,2,2-Trifluoroethyl trifluoroacetate (0.14 mL, 1.0 mmol) was added,

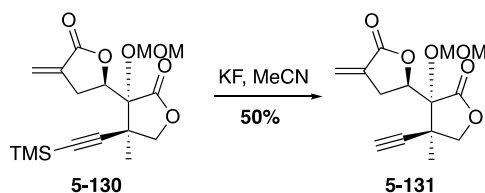
and the solution was stirred at $-78\text{ }^{\circ}\text{C}$ for 30 minutes. The reaction mixture was subsequently warmed to $0\text{ }^{\circ}\text{C}$ for 10 minutes, and then quenched by the addition of saturated aq. NH_4Cl (5 mL). The mixture was extracted with ethyl acetate (3 x 5 mL), and the combined organic extracts were dried over Na_2SO_4 , filtered, and concentrated by rotary evaporation. The crude trifluoroacetate was used directly in the next step without further purification.

A flame dried 2-neck round bottom flask equipped with a reflux condenser was charged with 18-crown-6 (33 mg, 0.13 mmol), paraformaldehyde (0.494 g, 16.3 mmol) and K_2CO_3 (0.205 g, 1.48 mmol). Crude trifluoroacetate was added as a solution in benzene (24 mL total volume), and the mixture was heated to reflux for 2 hours. Subsequently the mixture was cooled to room temperature and was quenched with saturated aq. NH_4Cl . The mixture was extracted with ethyl acetate (3 x 10 mL), and the combined organic extracts were dried over Na_2SO_4 , filtered, and concentrated by rotary evaporation. The crude material was purified by MPLC (ISCO) on silica gel eluting with 0-50% EtOAc in hexanes to yield **5-130** as a colorless oil (77 mg, 46% over 2 steps).

^1H NMR (500 MHz, CDCl_3) δ 6.18 (t, $J = 3.0$ Hz, 1H), 5.61 (t, $J = 2.6$ Hz, 1H), 5.20 (dd, $J = 8.8$, 4.5 Hz, 1H), 4.86 (d, $J = 7.3$ Hz, 1H), 4.71 (d, $J = 7.3$ Hz, 1H), 4.31 (d, $J = 8.4$ Hz, 1H), 4.12 (d, $J = 8.5$ Hz, 1H), 3.40 – 3.32 (m, 4H), 3.11 (ddt, $J = 18.2$, 8.7, 3.0 Hz, 1H), 1.47 (s, 3H), 0.11 (s, 9H).

^{13}C $\{^1\text{H}\}$ NMR (126 MHz, CDCl_3) δ 172.0, 169.8, 134.1, 121.1, 105.4, 95.0, 91.0, 77.7, 76.6, 60.4, 57.0, 45.9, 29.0, 18.4, -0.2.

HRMS (ESI/TOF) m/z : $[\text{M}+\text{Na}]^+$ Calcd for $\text{C}_{17}\text{H}_{24}\text{O}_6\text{SiNa}$ 375.1240; Found 375.1242.



(2*R*,3'*R*,4'*R*)-4'-ethynyl-3'-(methoxymethoxy)-4'-methyl-4-methylenetetrahydro-[2,3'-

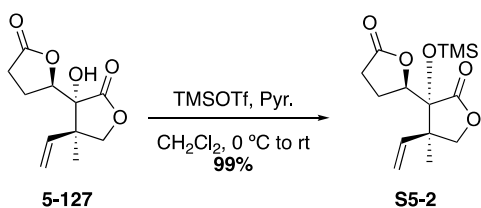
bifuran]-2',5(2*H*,3'*H*)-dione (5-131): To a solution of **5-130** (49.5 mg, 0.140 mmol) in MeCN (2.8 mL) was added KF (0.163 g, 2.80 mmol) and the mixture was stirred for 18 h. The solvent was evaporated, and the crude residue was purified by flash chromatography on silica gel eluting with EtOAc to afford **5-131** (34.0 mg, 86%) as a colorless oil.

R_f = 0.45 (40% EtOAc in hexanes) visualized by $KMnO_4$.

1H NMR (500 MHz, $CDCl_3$) δ 6.20 (s, 1H), 5.63 (s, 1H), 5.27 (dd, J = 8.7, 4.5 Hz, 1H), 4.87 (d, J = 7.2 Hz, 2H), 4.72 (d, J = 7.2 Hz, 2H), 4.35 (d, J = 8.4 Hz, 1H), 4.17 (d, J = 8.4 Hz, 1H), 3.42 – 3.29 (m, 4H), 3.14 (ddt, J = 18.2, 8.7, 2.9 Hz, 1H), 2.40 (s, 1H), 1.52 (s, 3H).

^{13}C { 1H } NMR (151 MHz, $CDCl_3$) δ 171.8, 169.8, 134.0, 121.3, 95.1, 84.0, 81.2, 77.7, 76.4, 74.2, 57.1, 45.4, 28.9, 18.1.

HRMS (ESI/TOF) m/z : $[M+Na]^+$ Calcd for $C_{14}H_{16}O_6Na$ 303.0845; Found 303.0852.



(2*R*,3'*R*,4'*R*)-4'-methyl-3'-((trimethylsilyl)oxy)-4'-vinyltetrahydro-[2,3'-bifuran]-

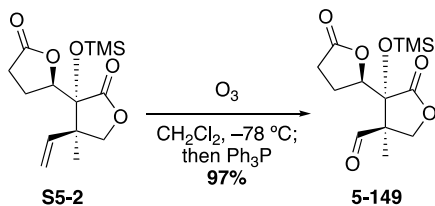
2',5(2*H*,3'*H*)-dione (S5-2): To a solution of **5-127** (1.38 g, 6.10 mmol) in CH_2Cl_2 (60 mL) was added pyridine (1.2 mL, 15 mmol). The solution was cooled to 0 °C, and TMSOTf (1.6 mL, 8.6 mmol) was added dropwise. The solution was stirred for 20 minutes at 0 °C, then it was warmed to room temperature and allowed to stir an additional 30 minutes. The reaction was quenched with

saturated aq. NH₄Cl, and the mixture was extracted with CH₂Cl₂ (3 x 50 mL). The combined organic extracts were dried over Na₂SO₄, filtered, and concentrated *in vacuo*. The crude material was purified by flash chromatography on silica gel eluting with 30% EtOAc in hexanes to afford **S5-2** (1.80 g, 99%) as a colorless oil.

¹H NMR (600 MHz, CDCl₃) δ 5.97 (dd, *J* = 17.7, 10.9 Hz, 2H), 5.25 (d, *J* = 11.0 Hz, 1H), 5.22 (d, *J* = 17.6 Hz, 1H), 4.70 – 4.67 (m, 1H), 4.31 (d, *J* = 9.1 Hz, 1H), 4.04 (d, *J* = 9.1 Hz, 1H), 2.56 – 2.42 (m, 3H), 2.40 – 2.30 (m, 1H), 1.25 (s, 3H), 0.23 (s, 9H).

¹³C {¹H} NMR (151 MHz, CDCl₃) δ 176.8, 174.4, 138.2, 115.9, 81.2, 80.7, 74.6, 50.6, 28.0, 22.3, 17.9, 1.6.

[α]_D²² –8.7 (*c* 1.77, CDCl₃)



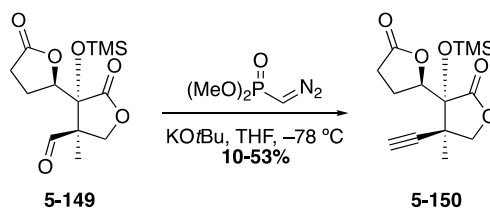
(2*R*,3'*R*,4'*R*)-4'-methyl-2',5-dioxo-3'-((trimethylsilyl)oxy)octahydro-[2,3'-bifuran]-4'-

carbaldehyde (5-149): A solution of **S5-2** (2.00g, 6.70 mmol) in CH₂Cl₂ (67 mL) was cooled to –78 °C, and O₃/O₂ (generated by a ClearWater Tech corona discharge M-1500 ozone generator) was bubbled through the solution until the solution was saturated with ozone (visualized by the persistence of a blue color in the solution). Once saturated, the excess ozone was purged from the solution by bubbling O₂ through the solution until it became colorless, and Ph₃P (2.11 g, 8.04 mmol) was added. The reaction mixture was warmed to room temperature and allowed to stir for 16 h. The solution was concentrated, and the crude residue was purified by flash chromatography on silica gel (0-35% EtOAc in hexanes) to afford aldehyde **5-149** (1.95 g, 97%) as a white solid.

¹H NMR (500 MHz, CDCl₃) δ 9.70 (s, 1H), 4.71 (d, *J* = 9.9 Hz, 1H), 4.62 (dd, *J* = 8.1, 4.3 Hz, 1H), 3.94 (d, *J* = 9.8 Hz, 1H), 2.61 – 2.44 (m, 3H), 2.35 – 2.24 (m, 1H), 1.38 (s, 3H), 0.27 (s, 9H).
¹³C {¹H} NMR (126 MHz, CDCl₃) δ 199.5, 175.8, 172.7, 81.9, 78.8, 70.6, 57.9, 27.8, 21.7, 15.4, 1.7.

Melting Point: 57–61 °C

[α]²²_D +18.5 (*c* 1.38, CDCl₃)



(2*R*,3'*R*,4'*R*)-4'-ethynyl-4'-methyl-3'-((trimethylsilyl)oxy)tetrahydro-[2,3'-bifuran]-

2',5(2*H*,3'*H*)-dione (5-150): Potassium *tert*-butoxide (0.620 g, 5.52 mmol) was weighed into a flame dried 200 mL Schlenk flask in a nitrogen filled glovebox. The flask containing the KO*t*Bu was brought out of the glovebox and was placed under inert atmosphere. THF (30 mL) was added to the solid, and the solution was cooled to –78 °C. Seyferth–Gilbert reagent (0.947 g, 6.31 mmol) was added dropwise, during which time the contents of the flask turned bright orange. The mixture was allowed to stir for 20 minutes, after which time a solution of **5-149** (azeotroped 3x with PhMe, 0.790 g, 2.63 mmol) in THF (15 mL) was added dropwise, rinsing with another 10 mL portion of THF. The mixture was allowed to stir at –78 °C for 3 h, and was subsequently warmed to –20 °C. After 20 minutes at –20 °C, the reaction was quenched by the addition of saturated aq. NH₄Cl (30 mL). The mixture was warmed to ambient temperature, diluted with 50 mL of H₂O, and was transferred to a separatory funnel. The aqueous phase was extracted with ethyl acetate (3 x 30 mL), and the combined organic extracts were dried over Na₂SO₄, filtered, and concentrated. The crude

material was purified by MPLC (ISCO) on silica gel eluting with a gradient from 0–50% EtOAc in hexanes to afford alkyne **5-150** as a white semisolid (0.264 g, 34%).

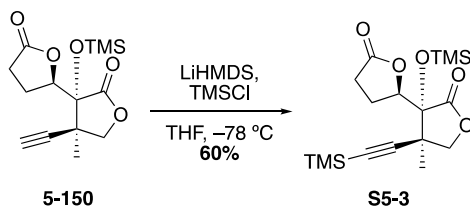
R_f = 0.56 (40% EtOAc in hexanes) visualized by $KMnO_4$.

1H NMR (500 MHz, $CDCl_3$) δ 5.03 (dd, J = 8.3, 6.9 Hz, 1H), 4.42 (d, J = 8.6 Hz, 1H), 4.05 (d, J = 8.6 Hz, 1H), 2.73 – 2.64 (m, 1H), 2.54 (dd, J = 9.8, 7.2 Hz, 2H), 2.43 (s, 1H), 2.42 – 2.35 (m, 1H), 1.43 (s, 3H), 0.22 (s, 9H).

^{13}C $\{^1H\}$ NMR (151 MHz, $CDCl_3$) δ 176.6, 174.4, 83.2, 81.3, 80.0, 76.2, 74.7, 43.2, 28.0, 22.3, 20.6, 1.6.

HRMS (ESI/TOF) m/z : $[M+Na]^+$ Calcd for $C_{14}H_{20}O_5SiNa$ 319.0978; Found 319.0978.

$[a]_D^{22}$ –37.7 (c 1.84, $CDCl_3$)



(2*R*,3'*R*,4'*R*)-4'-methyl-4'-((trimethylsilyl)ethynyl)-3'-((trimethylsilyl)oxy)tetrahydro-[2,3'-bifuran]-2',5(2*H*,3'*H*)-dione (S5-3): A solution of **5-150** (0.180 g, 0.607 mmol) in THF (5.0 mL) was cooled to -78°C , and LiHMDS (1.0 M, 1.34 mL, 1.34 mmol) was added dropwise. The solution was stirred 1 h at -78°C , then TMSCl (0.23 mL, 1.8 mmol) was added and the mixture was stirred for another 30 minutes. Subsequently, the reaction was quenched with saturated aq. NH_4Cl (5 mL) at -78°C , and the mixture was warmed to rt. The mixture was extracted with ethyl acetate (3 x 5 mL), and the combined organic extracts were dried over Na_2SO_4 , filtered, and concentrated. The crude material was purified by flash chromatography on silica gel eluting with 10-20% EtOAc in hexanes to afford **S5-3** (0.135 g, 60%) as a colorless oil.

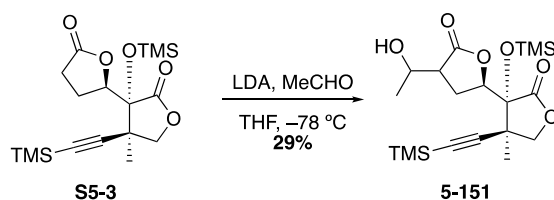
R_f = 0.24 (10% EtOAc in hexanes) visualized by $KMnO_4$.

¹H NMR (600 MHz, CDCl₃) δ 4.92 (dd, *J* = 8.3, 7.3 Hz, 1H), 4.38 (d, *J* = 8.5 Hz, 1H), 4.00 (d, *J* = 8.5 Hz, 1H), 2.71 (dddd, *J* = 13.5, 10.6, 8.8, 7.3 Hz, 1H), 2.54 – 2.48 (m, 2H), 2.33 (dtd, *J* = 13.4, 8.4, 6.0 Hz, 1H), 1.36 (s, 3H), 0.19 (s, 9H), 0.13 (s, 9H).

¹³C {¹H} NMR (151 MHz, CDCl₃) δ 176.4, 174.8, 104.4, 91.6, 81.4, 80.1, 76.3, 43.5, 28.0, 22.3, 21.4, 1.6, -0.1.

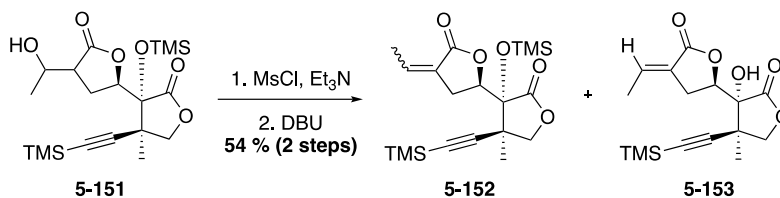
HRMS (ESI/TOF) *m/z*: [M+Na]⁺ Calcd for C₁₇H₂₈O₅Si₂Na 391.1373; Found 391.1375.

[*a*]_D²¹ –41.7 (*c* 0.83, CDCl₃)



(2*R*,3'*R*,4'*R*)-4-(1-hydroxyethyl)-4'-methyl-4'-((trimethylsilyl)ethynyl)-3'-

((trimethylsilyl)oxy)tetrahydro-[2,3'-bifuran]-2',5(2*H*,3'*H*)-dione (5-151): A solution of **S5-3** (0.130 g, 0.353 mmol) in THF (3.6 mL) was cooled to –78 °C, and LiHMDS (1.0 M, 0.39 mL, 0.39 mmol) was added dropwise. The solution was allowed to stir at this temperature for 1 hour, and subsequently acetaldehyde (60. mL, 1.06 mmol) was added and the mixture was stirred for an additional 20 minutes. The reaction was quenched by the addition of saturated aq. NH₄Cl, the mixture was extracted with ethyl acetate (3 x 5 mL). The combined organic extracts were dried over Na₂SO₄, filtered, and concentrated. The crude material was purified by MPLC (ISCO) on silica gel eluting with a gradient from 10–100% EtOAc in hexanes to give **5-151** (41.9 mg, 29%) as a mixture of 4 diastereomers. For simplicity, the data will not be tabulated, but an expansion of the relevant peaks can be found in Appendix C.



(2*R*,3'*R*,4'*R*)-4-ethylidene-4'-methyl-4'-((trimethylsilyl)ethynyl)-3'-

((trimethylsilyl)oxy)tetrahydro-[2,3'-bifuran]-2',5(2*H*,3'*H*)-dione (5-152): To a solution of **5-151** (85 mg, 0.206 mmol) in CH₂Cl₂ (4.1 mL) was added triethylamine (90. mL, 0.62 mmol). The mixture was cooled to 0 °C, and MsCl (20. mL, 0.27 mmol) was added. The solution was allowed to stir at 0 °C for 30 minutes, and was subsequently quenched by the addition of saturated aq. NH₄Cl. The mixture was extracted with CH₂Cl₂ (3 x 5 mL), and the combined extracts were dried (Na₂SO₄), filtered and concentrated. The crude material was taken into the next step without further purification.

The crude mesylate was dissolved in CH₂Cl₂ (4.1 mL), and DBU (34 mL, 0.23 mmol) was added at room temperature. The solution was stirred for 2 hours and was subsequently diluted with water (5 mL) and extracted with CH₂Cl₂ (3 x 5 mL). The combined extracts were dried over Na₂SO₄, filtered, and concentrated. The crude material was purified by MPLC (ISCO) on silica gel, eluting with a gradient from 0-20% EtOAc in hexanes to give **5-152** (28.8 mg, 35%, 1.7:1 E:Z) as a colorless oil, as well as **5-153** (13.0 mg, 19%, >20:1 E:Z) as a white solid. These compounds were subsequently combined for desilylation.

Data for 5-152: The proton NMR was a 1.7:1 mixture of isomers. Integrations shown are exactly as they appear. The mixture was inconsequential going forward.

¹H NMR (500 MHz, CDCl₃) δ 6.83 – 6.71 (m, 1.7H, major), 6.28 (q, *J* = 7.6 Hz, 1H, minor), 5.01 (dd, *J* = 8.8, 5.6 Hz, 1.7H, major), 4.92 (t, *J* = 7.6 Hz, 1H, minor), 4.41 (dd, *J* = 8.5, 4.6 Hz, 3.3H), 4.00 (d, *J* = 8.6 Hz, 3.4H), 3.91 (d, *J* = 8.7 Hz, 1H), 3.63 (d, *J* = 8.7 Hz, 1H), 3.48 – 3.38 (m, 1.7H),

3.29 (d, $J = 18.6$ Hz, 2.5H), 3.06 (s, 1H), 2.92 (dd, $J = 18.5, 8.5$ Hz, 3.5H), 2.50 (dq, $J = 14.2, 7.9, 7.0$ Hz, 1H), 2.18 (d, $J = 7.0$ Hz, 3.5H), 1.87 (d, $J = 7.1$ Hz, 5.5H), 1.64 (d, $J = 6.2$ Hz, 1H), 1.39 (s, 10H), 0.17 (s, 29H), 0.14 (s, 10.7H), 0.11 (s, 23.9H).

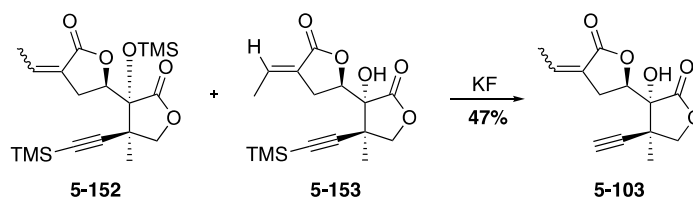
HRMS (ESI/TOF) m/z : $[M+Na]^+$ Calcd for $C_{19}H_{30}O_5Si_2Na$ 417.1530; Found 417.1531.

Data for 5-153:

1H NMR (500 MHz, $CDCl_3$) δ 6.80 (dq, $J = 10.2, 4.1, 3.6$ Hz, 1H), 5.02 (dd, $J = 8.4, 6.8$ Hz, 1H), 4.37 (d, $J = 8.3$ Hz, 1H), 4.17 (d, $J = 8.3$ Hz, 1H), 3.46 (s, 1H), 3.26 (ddt, $J = 17.8, 6.4, 2.9$ Hz, 1H), 3.07 (ddt, $J = 18.0, 8.5, 2.3$ Hz, 1H), 1.88 (dt, $J = 7.3, 2.1$ Hz, 3H), 1.47 (s, 3H), 0.14 (s, 9H).

^{13}C NMR { **1H** } **NMR** (126 MHz, $CDCl_3$) δ 174.2, 170.2, 136.8, 126.5, 104.3, 91.7, 77.9, 77.7, 76.6, 43.8, 27.1, 19.3, 16.0, -0.1.

HRMS (ESI/TOF) m/z : $[M+Na]^+$ Calcd for $C_{16}H_{22}O_5SiNa$ 345.1134; Found 345.1135.



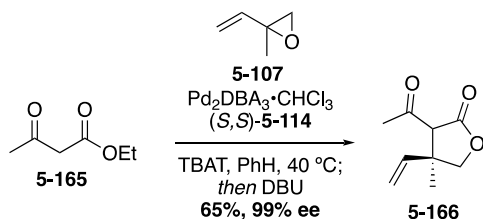
(2*R*,3'*R*,4'*R*)-4-ethylidene-4'-ethynyl-3'-hydroxy-4'-methyltetrahydro-[2,3'-bifuran]-

2',5(2*H*,3'*H*)-dione (5-103): To a solution of **5-152** (28.8 mg, 0.0730 mmol) and **5-153** (13.0 mg, 0.0403 mmol, 0.113 mmol combined) in MeCN (2.3 mL) was added KF (65 mg, 1.1 mmol). The mixture was heated to 40 °C and was stirred for 20 hours. Subsequently, the mixture was cooled and the solvent was evaporated by rotary evaporation. The mixture was re-suspended in 50% EtOAc in hexanes, and was filtered through a plug of silica gel, eluting also with 50% EtOAc in hexanes to yield **5-103** (13.1 mg, 47%) as a 3:1 mixture of E:Z alkene isomers.

1H NMR (500 MHz, $CDCl_3$) δ 6.82 – 6.75 (m, 3H), 6.36 (qt, $J = 7.4, 2.4$ Hz, 1H), 5.16 (dd, $J = 8.5, 6.6$ Hz, 3H), 5.08 (t, $J = 7.7$ Hz, 1H), 4.36 (d, $J = 8.5$ Hz, 3H), 4.33 (d, $J = 8.8$ Hz, 1H), 4.20

(d, $J = 8.4$ Hz, 5H), 3.64 (dd, $J = 18.2, 8.7$ Hz, 1H), 3.47 – 3.43 (m, 1H), 3.38 – 3.22 (m, 4H), 3.14 – 3.05 (m, 5H), 2.39 (s, 4H), 2.25 (d, $J = 4.8$ Hz, 1H), 2.14 (dt, $J = 7.4, 2.4$ Hz, 3H), 1.88 (dt, $J = 7.2, 2.1$ Hz, 9H), 1.52 (s, 9H), 1.50 (s, 3H).

HRMS (ESI/TOF) m/z : $[M+Na]^+$ Calcd for $C_{13}H_{14}O_5Na$ 273.0739; Found 273.0743.



(4S)-3-acetyl-4-methyl-4-vinyldihydrofuran-2(3H)-one (5-166): Based off of the protocol of Trost.³⁴ A dry 1L 3-neck round bottom flask was charged with $\text{Pd}_2\text{DBA}_3 \cdot \text{CHCl}_3$ (0.155 g, 0.150 mmol), (*S,S*)-**5-114** (0.355 g, 0.450 mmol), and TBAT (0.162 g, 0.300 mmol). The flask was evacuated and backfilled with argon five times. Benzene* (300 mL) was added via cannula under a positive pressure of argon and the solution was submerged in an oil bath preheated to 40 °C for 10 minutes, during which time a bright orange color was observed. Ethyl acetoacetate **5-165** (7.6 mL, 60. mmol) was added, followed by 2-methyl-2-vinyloxirane (6.5 mL, 66 mmol), and the solution turned pale yellow immediately. The mixture was stirred at 40 °C until the orange color of the palladium complex returned (3 h). At this time the solution was cooled to room temperature, and a 0.5 mL aliquot of the reaction mixture was removed and was subsequently dehydrated to the dihydrofuran to assay the enantioselectivity of the reaction. DBU (9.9 mL, 66 mmol) was then added, and the solution was stirred for 1 h. Subsequently, the reaction was quenched with aq. 2 M HCl (200 mL) and the mixture was transferred to a separatory funnel. The organic layer was separated, and the aqueous layer was extracted with CH_2Cl_2 (2 x 150 mL). The combined organic extracts were dried over Na_2SO_4 and concentrated *in vacuo*. The crude material was purified by MPLC (ISCO) on silica gel eluting with a gradient from 10-30% EtOAc in hexanes to afford **5-**

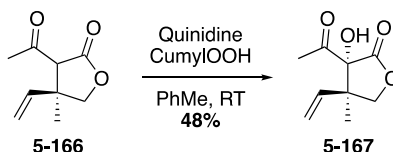
166 as a yellow oil (6.60 g, 65%). The material is a 1.2:1 mixture of diastereomers and exists approximately 34% as the enol tautomer. Several of the peaks in the proton did not resolve, and are integrated together.

*The reaction was found to be very sensitive to oxygen. Prior to reaction, the solvent was degassed (sparging) with argon for 45 minutes to ensure the solvent was oxygen free.

¹H NMR (500 MHz, CDCl₃) δ 11.52 (s, 1H), 6.06 – 5.75 (m, 3H), 5.28 – 5.13 (m, 6H), 4.40 (d, *J* = 8.7 Hz, 1H), 4.12 (d, *J* = 8.9 Hz, 1H), 4.10 – 4.06 (m, 2H), 3.99 (dd, *J* = 10.3, 8.8 Hz, 2H), 3.55 (s, 1H), 3.40 (s, 1H), 2.32 (s, 3H), 2.28 – 2.25 (m, 4H), 1.94 (s, 3H), 1.39 (s, 6H), 1.26 (s, 3H).

¹³C {¹H} NMR (126 MHz, CDCl₃) δ 202.0, 201.4, 176.4, 172.7, 172.3, 171.0, 141.8, 140.4, 136.9, 117.1, 115.8, 114.5, 102.9, 79.0, 76.5, 76.5, 64.5, 61.6, 61.5, 50.3, 46.5, 46.4, 43.5, 32.3, 32.3, 30.3, 23.8, 23.4, 18.6, 18.4, 14.2.

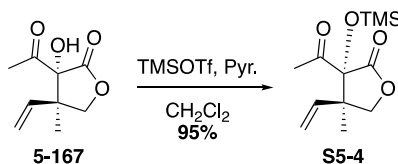
HRMS (ESI/TOF) *m/z*: [M+Na]⁺ Calcd for C₉H₁₂O₃Na 191.0684; Found 191.0687.



(3*R*,4*R*)-3-acetyl-3-hydroxy-4-methyl-4-vinyldihydrofuran-2(3*H*)-one (5-167): Lactone **5-166** (3.48 g, 20.7 mmol) was dissolved in toluene (200 mL) in a non-dried round bottomed flask open to air. Quinidine (1.35 g, 4.14 mmol) was added, and the solution was stirred for 10 minutes at ambient temperature. Cumene hydroperoxide (80% assay) (4.6 mL, 25 mmol) was then added, and the mixture was stirred overnight (~15 h) at room temperature. After the reaction was complete (TLC) the solvent was evaporated *in vacuo*. The crude material was purified by MPLC (ISCO) on silica gel eluting with a gradient from 10-30% EtOAc/hexanes to afford **5-167** (1.84 g, 48%) as a colorless oil.

$^1\text{H NMR}$ (500 MHz, CDCl_3) δ 5.76 (dd, $J = 17.6, 10.9$ Hz, 1H), 5.29 (d, $J = 10.9$ Hz, 1H), 5.20 (d, $J = 17.6$ Hz, 1H), 4.54 (d, $J = 8.9$ Hz, 1H), 4.11 (d, $J = 8.9$ Hz, 1H), 3.54 (s, 1H), 2.27 (s, 3H), 1.29 (d, $J = 0.9$ Hz, 3H).

$^{13}\text{C } \{^1\text{H}\}$ NMR (151 MHz, CDCl_3) δ 207.5, 175.5, 135.4, 118.1, 87.4, 74.5, 49.4, 27.4, 19.6.



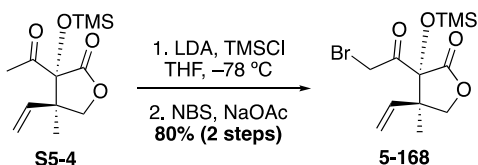
(3*R*,4*R*)-3-acetyl-4-methyl-3-((trimethylsilyloxy)-4-vinyldihydrofuran-2(3*H*)-one (**S5-4**):

Compound **5-167** (1.83 g, 9.94 mmol) was dissolved in CH_2Cl_2 (50 mL) and the solution was cooled to 0 °C. Pyridine (2.01 mL, 24.9 mmol) was added followed by TMSOTf (2.16 mL, 11.9 mmol), and the mixture was stirred at 0 °C for 15 minutes. The mixture was then warmed to room temperature, and stirred overnight (16 h). The reaction was quenched by the addition of saturated aq. NH_4Cl (30 mL), and the layers were separated. The aqueous layer was extracted with CH_2Cl_2 (3 x 30 mL), and the combined organic extracts were dried over Na_2SO_4 , filtered, and concentrated. The crude material was purified by flash chromatography on silica gel eluting with 15% EtOAc in hexanes to afford **S5-4** (2.43 g, 95%) as a colorless oil.

$^1\text{H NMR}$ (500 MHz, CDCl_3) δ 5.70 (dd, $J = 17.6, 10.9$ Hz, 1H), 5.25 (d, $J = 10.9$ Hz, 1H), 5.13 (d, $J = 17.6$ Hz, 1H), 4.36 (d, $J = 9.1$ Hz, 1H), 3.99 (d, $J = 8.8$ Hz, 1H), 2.19 (s, 3H), 1.23 (s, 3H), 0.24 (s, 9H).

$^{13}\text{C } \{^1\text{H}\}$ NMR (126 MHz, CDCl_3) δ 208.5, 173.8, 135.9, 117.8, 90.0, 73.4, 50.1, 27.4, 20.0, 1.7.

$[\alpha]^{22}_{\text{D}} +106.9$ (c 1.15, CHCl_3)



(3*R*,4*R*)-3-(2-bromoacetyl)-4-methyl-3-((trimethylsilyl)oxy)-4-vinyldihydrofuran-2(3*H*)-one

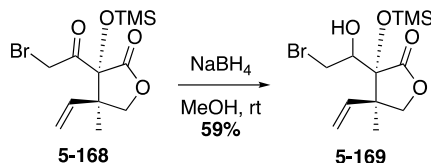
(5-168): A solution of diisopropylamine (0.62 mL, 4.4 mmol) in THF (25 mL) was cooled to -78 °C, and *n*-BuLi (2.5 M, 1.7 mL, 4.2 mmol) was added dropwise. The solution was stirred for 30 minutes at this temperature. A solution of **S5-4** (0.987 g, 3.85 mmol) in THF (10 mL) was then added dropwise, and the solution was stirred at -78 °C for another 30 minutes. TMSCl (0.59 mL, 4.6 mmol) was added, and the solution was stirred at -78 °C for 20 minutes. The solution was then warmed to room temperature and stirred for another hour. The reaction was quenched by the addition of saturated aq. NaHCO₃ (30 mL) and the mixture was extracted with EtOAc (3 x 30 mL). The combined organic extracts were washed with saturated aq. NaHCO₃ (2 x 30 mL), brine (1 x 30 mL), and were dried over Na₂SO₄. The drying agent was filtered off, and the solvent was evaporated by rotary evaporation. The crude TMS-enol ether was used immediately in the next step.

N-Bromosuccinimide (1.03 g, 5.78 mmol) and sodium acetate (0.537 g, 6.55 mmol) were dissolved in a mixture of 5:1 Acetone:H₂O (39 mL), and the solution was cooled to 0 °C. The crude TMS-enol ether was added dropwise as a solution in acetone (8 mL), and the reaction was allowed to warm to room temperature overnight (16 h). The reaction was subsequently quenched by the addition of 20% aqueous NaHSO₃ (15 mL) and brine (30 mL), and the mixture was extracted with CH₂Cl₂ (3 x 40 mL). The combined organic extracts were dried over Na₂SO₄, filtered, and concentrated *in vacuo*. The crude material was purified by MPLC (ISCO) on silica gel eluting with a gradient from 0-20% EtOAc in hexanes to give **5-168** (1.024 g, 80%) as a slightly yellow oil.

¹H NMR (500 MHz, CDCl₃) δ 5.66 (dd, *J* = 17.5, 10.9 Hz, 1H), 5.34 (d, *J* = 10.9 Hz, 1H), 5.20 (d, *J* = 17.5 Hz, 1H), 4.39 (d, *J* = 9.0 Hz, 1H), 4.27 (d, *J* = 16.0 Hz, 1H), 4.22 (d, *J* = 16.0 Hz, 1H), 4.02 (d, *J* = 9.0 Hz, 1H), 1.25 (s, 3H), 0.26 (s, 9H).

¹³C {¹H} NMR (126 MHz, CDCl₃) δ 200.4, 172.4, 135.1, 119.2, 90.0, 73.5, 50.5, 34.7, 19.7, 1.8.

HRMS (ESI/TOF) *m/z*: [M+Na]⁺ Calcd for C₁₂H₁₉⁷⁹BrO₄SiNa 357.0134; Found 357.0132.

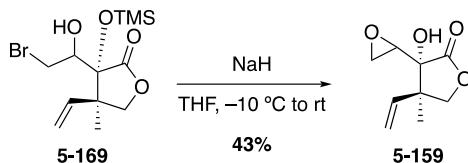


(3*R*,4*R*)-3-(2-bromo-1-hydroxyethyl)-4-methyl-3-((trimethylsilyloxy)-4-vinyldihydrofuran-2(3*H*)-one (5-169): Sodium borohydride (21.0 mg, 0.543 mmol) was added to a solution of **5-168** (0.121 g, 0.362 mmol) in MeOH (3 mL), and the mixture was stirred until the starting material had been consumed (TLC). The reaction was quenched by the addition of saturated aq. NH₄Cl (10 mL), and the mixture was extracted with CH₂Cl₂ (3 x 5 mL). The combined organic extracts were dried over Na₂SO₄, filtered, and concentrated. The crude material was purified by flash chromatography on silica gel eluting with a gradient of 10-15-20-25% EtOAc in hexanes to afford **5-169** (73.0 mg, 59%) as a 1.6:1 mixture of unassigned diastereomers.

¹H NMR (500 MHz, CDCl₃) δ 6.16 (dd, *J* = 17.7, 10.9 Hz, 1H, minor), 6.01 (dd, *J* = 17.6, 11.0 Hz, 2H, major), 5.41 (d, *J* = 11.0 Hz, 2H, major), 5.34 (d, *J* = 10.9 Hz, 1H, minor), 5.28 (d, *J* = 17.6 Hz, 2H, major), 4.46 (d, *J* = 8.3 Hz, 1H, minor), 4.40 (d, *J* = 8.4 Hz, 2H, major), 4.28 (dd, *J* = 7.9, 2.0 Hz, 1H, minor), 4.22 (dd, *J* = 7.9, 2.1 Hz, 2H, major), 4.07 (d, *J* = 8.3 Hz, 2H, major), 3.98 (d, *J* = 8.3 Hz, 1H, minor), 3.95 (dd, *J* = 11.2, 2.2 Hz, 2H, major), 3.92 (dd, *J* = 10.9, 1.9 Hz, 1H, minor), 3.58 (dd, *J* = 10.9, 7.9 Hz, 1H, minor), 3.34 (s, 1H), 3.33 (dd, *J* = 11.1, 7.9 Hz, 2H, major), 1.30 (s, 5H, major), 1.29 (s, 3H, minor), 0.29 (s, 12H, major), 0.26 (s, 9H, minor).

^{13}C $\{^1\text{H}\}$ NMR (126 MHz, CDCl_3) δ 178.7 (minor), 176.8 (major), 137.6 (minor), 136.4 (major), 117.6 (major), 117.2 (minor), 81.3 (minor), 80.9 (major), 80.0 (minor), 76.6 (major), 76.1 (minor), 75.7 (major), 48.2 (major), 48.1 (minor), 35.0 (minor), 34.7 (major), 20.0 (major), 19.9 (minor), 1.0 (major), 0.5 (minor).

HRMS (ESI/TOF) m/z : $[\text{M}+\text{Na}]^+$ Calcd for $\text{C}_{12}\text{H}_{21}^{79}\text{BrO}_4\text{SiNa}$ 359.0290; Found 359.0275.

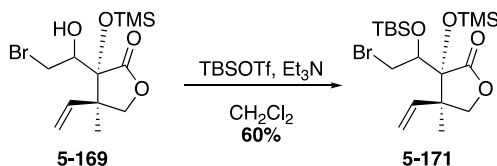


(3*R*,4*R*)-3-hydroxy-4-methyl-3-(oxiran-2-yl)-4-vinyldihydrofuran-2(3*H*)-one (5-159):

Sodium hydride (95% assay, 21.1 mg, 0.838 mmol) was weighed into a flame dried Schlenk flask and was suspended in THF (7.5 mL). The mixture was cooled to $-10\text{ }^\circ\text{C}$, and a solution of **5-169** (0.257 g, 0.762 mmol) in THF (7.5 mL) was added. The reaction mixture was stirred at $-10\text{ }^\circ\text{C}$ for 30 minutes, and was then warmed to room temperature and stirred for an additional 3 hours. The reaction was quenched by the addition of saturated aq. NH_4Cl , and the mixture was extracted with EtOAc (3 x 15 mL). The combined organic extracts were dried over Na_2SO_4 , filtered, and concentrated. The crude material was purified by MPLC (ISCO) on silica gel eluting with a gradient from 0-25% EtOAc in hexanes to afford **5-159** (84.2 mg, 43%) as a colorless oil.

^1H NMR (500 MHz, CDCl_3) δ 5.96 (dd, $J = 17.9, 10.9$ Hz, 2H, major), 5.93 (dd, $J = 18.0, 10.9$ Hz, 1H, minor), 5.37 (d, $J = 11.0$ Hz, 2H, major), 5.25 (d, $J = 11.0$ Hz, 1H, minor), 5.13 (d, $J = 17.6$ Hz, 2H, major), 5.13 (d, $J = 17.6$ Hz, 1H, minor), 4.80 (t, $J = 6.7$ Hz, 2H, major), 4.68 (t, $J = 6.2$ Hz, 2H, major), 4.43 (t, $J = 6.3$ Hz, 2H, major), 4.20 (d, $J = 9.0$ Hz, 1H, minor), 4.13 (d, $J = 9.0$ Hz, 2H, major), 4.01 (d, $J = 9.1$ Hz, 1H, minor), 3.98 (d, $J = 8.9$ Hz, 2H, major), 3.07 (dd, $J = 4.0, 2.7$ Hz, 1H, minor), 2.79 (t, $J = 4.4$ Hz, 1H, minor), 2.71 (dd, $J = 4.7, 2.6$ Hz, 1H, minor), 1.18 (s, 3H, minor), 1.15 (s, 6H, major), 0.20 (s, 9H, minor), 0.05 (s, 18H, major).

^{13}C $\{^1\text{H}\}$ NMR (126 MHz, CDCl_3) δ 173.4 (major), 173.3 (minor), 137.1 (major), 137.0 (minor), 117.3 (major), 116.4 (minor), 95.8 (major), 80.5 (minor), 76.7 (major), 73.8 (minor), 72.1 (major), 67.2 (minor), 52.6 (major), 50.1 (minor), 46.4 (minor), 44.9 (major), 19.1 (minor), 18.3 (major), 1.7 (minor), -0.2 (major).

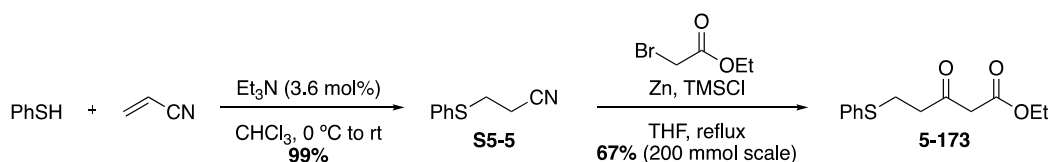


(3*R*,4*R*)-3-(2-bromo-1-((*tert*-butyldimethylsilyl)oxy)ethyl)-4-methyl-3-((trimethylsilyl)oxy)-4-vinyldihydrofuran-2(3*H*)-one (5-171): A solution of **5-169** (70.1 mg, 0.208 mmol) in CH_2Cl_2 (2.0 mL) was cooled to 0 °C, and triethylamine (70. μL , 0.52 mmol) was added. TBSOTf (60. mL, 0.27 mmol) was added dropwise, and the solution was warmed to room temperature and stirred for 3 hours. The reaction was quenched by the addition of saturated aq. NH_4Cl , the layers were separated, and the aqueous phase was extracted with CH_2Cl_2 (3 x 15 mL). The combined organic extracts were dried over Na_2SO_4 , filtered, and concentrated. The crude material was purified by MPLC (ISCO) on silica gel eluting with a gradient from 0-20% EtOAc in hexanes to afford **5-171** (54 mg, 60%) as a colorless oil.

^1H NMR (500 MHz, CDCl_3) δ 6.09 (dd, $J = 17.6, 10.9$ Hz, 1H, minor), 5.89 (dd, $J = 17.7, 11.0$ Hz, 2H, major), 5.34 (d, $J = 10.9$ Hz, 2H, major), 5.21 (d, $J = 10.9$ Hz, 1H, minor), 5.16 (overlapping d, $J = 17.7$ Hz, 3H), 4.35 (d, $J = 8.8$ Hz, 2H, major), 4.32 (d, $J = 7.7$ Hz, 1H, minor), 4.16 (dd, $J = 7.6, 1.1$ Hz, 2H, major), 3.93 (d, $J = 8.8$ Hz, 2H, major), 3.87 – 3.85 (m, 1H, minor), 3.85 – 3.81 (m, 3H, major), 1.20 (s, 7H, major), 1.18 (s, 3H, minor), 0.91 (s, 9H, minor), 0.90 (s, 19H, major), 0.37 (s, 7H, major), 0.34 (s, 3H, minor), 0.20 (s, 19H, major), 0.19 (s, 9H, minor), 0.11 (s, 6H, major), 0.11 (s, 3H, minor).

^{13}C $\{^1\text{H}\}$ NMR (126 MHz, CDCl_3) δ 177.1 (minor), 174.4 (major), 138.4 (minor), 136.9 (major), 117.4 (major), 116.3 (minor), 85.7 (major), 84.5 (minor), 81.8 (minor), 77.7 (major), 75.9 (minor), 74.6 (major), 49.1 (major), 49.0 (minor), 36.6 (major), 35.9 (minor), 26.4 (major), 26.3 (minor), 21.8 (major), 20.8 (minor), 19.4 (major), 19.0 (minor), 0.9 (major), 0.4 (minor), -2.2 (major), -3.1 (minor).

HRMS (ESI/TOF) m/z : $[\text{M}+\text{Na}]^+$ Calcd for $\text{C}_{18}\text{H}_{35}^{79}\text{BrO}_4\text{Si}_2\text{Na}$ 473.1155; Found 473.1149.



Compound **5-173** can be prepared through alkylation of the dianion of ethyl acetoacetate according to the procedure of Trost,⁸⁴ but we found it more convenient and scalable to synthesize **5-173** from **S5-5** via a Blaise reaction.

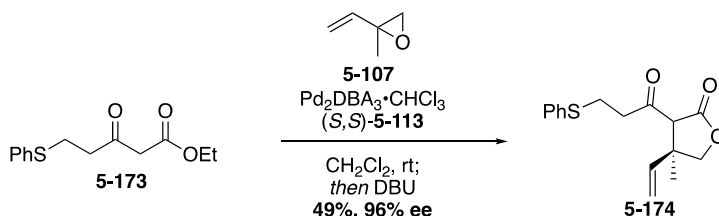
3-(phenylthio)propanenitrile (S5-5): Prepared according to a literature procedure.⁸⁵ To a cooled (0 °C) solution of thiophenol (25.8 mL, 251 mmol) and acrylonitrile (16.4 mL, 250 mmol) in CHCl_3 (50 mL) was added Et_3N (1.25 mL, 9.00 mmol). The cooling bath was removed, and the solution was stirred at room temperature for 2 hours. The reaction was diluted with Et_2O (500 mL), and the organics were washed with aq. 1 M NaOH (2 x 150 mL), water (1 x 150 mL) and brine (1 x 150 mL). The organic layer was dried over MgSO_4 , filtered, and concentrated, yielding **S5-5** (40.77 g, 99%) as a clear oil. All spectral data are in accord with the literature.

^1H NMR (500 MHz, CDCl_3) δ 7.44 – 7.40 (m, 2H), 7.37 – 7.32 (m, 2H), 7.31 – 7.27 (m, 1H), 3.13 (t, $J = 7.3$ Hz, 2H), 2.59 (t, $J = 7.3$ Hz, 2H).

ethyl 3-oxo-5-(phenylthio)pentanoate (5-173): Prepared according to a literature protocol.⁸⁶ A flame dried 3-neck 1L round bottom flask equipped with a reflux condenser and two pressure-equalizing addition funnels was charged with Zn dust (26.16 g, 400 mmol) and THF (166 mL).

TMSCl (0.76 mL, 6.0 mmol) was added, and the mixture was refluxed for 20 minutes to activate the zinc. One of the addition funnels was charged with ethyl bromoacetate (45.0 mL, 400 mmol), and the other was charged with **S5-5** (32.64 g, 200 mmol). **S5-5** and ethyl bromoacetate were added simultaneously and dropwise over the course of an hour to the refluxing mixture of zinc (caution: highly exothermic. Controlling addition rate, as well as choosing an adequately sized flask and reflux condenser is extremely important). After the addition was complete, the mixture was refluxed for another 3 hours. Subsequently, the mixture was cooled to 0 °C, and aq. 3 M HCl (125 mL) was added dropwise over 45 minutes with vigorous stirring. The mixture warmed to room temperature over an hour and was stirred for 2 hours at this temperature to ensure adequate hydrolysis. The mixture was then transferred to a separatory funnel, and the mixture was extracted with Et₂O (3 x 180 mL). The combined organic extracts were washed with water (1 x 350 mL) and brine (1 x 100 mL), dried over Na₂SO₄, filtered and concentrated. The crude material was loaded onto a silica gel column (270 g silica), and was eluted with a gradient from 0-1-2-3-4-5% EtOAc in hexanes to afford **5-173** as a yellow oil (33.90 g, 67%). Spectral data are in accord with those reported in the literature. Compound exhibits 7% of the enol tautomer.

¹H NMR (500 MHz, CDCl₃) δ 7.36 – 7.32 (m, 2H), 7.32 – 7.27 (m, 2H), 7.22 – 7.19 (m, 1H), 4.18 (q, *J* = 7.2 Hz, 2H), 3.42 (s, 2H), 3.16 (t, *J* = 7.3 Hz, 2H), 2.87 (t, *J* = 7.3 Hz, 2H), 1.26 (t, *J* = 7.2 Hz, 3H).



(4S)-4-methyl-3-(3-(phenylthio)propanoyl)-4-vinyldihydrofuran-2(3H)-one (5-174): A dry 1L 3-neck round bottom flask was charged with Pd₂DBA₃•CHCl₃ (0.180 g, 0.174 mmol) and (S,S)-

5-113 (0.413 g, 0.522 mmol). The flask was evacuated and backfilled with argon five times. CH₂Cl₂* (350 mL) was added via cannula under a positive pressure of argon and the solution was stirred at room temperature, during which time the color went from deep purple to orange/burnt orange. **5-173** (17.56 g, 69.59 mmol) was added, followed by 2-methyl-2-vinylloxirane (8.9 mL, 91 mmol), and the solution turned pale yellow/green immediately. The mixture was stirred at room temperature until the orange color of the palladium complex returned (20 h). At this time a 0.5 mL aliquot of the reaction mixture was removed and was subsequently dehydrated to the dihydrofuran to assay the enantioselectivity of the reaction. The reaction mixture was cooled to 0 °C, and DBU (11.4 mL, 76.6 mmol) was added dropwise over the course of an hour, and the reaction was stirred for another hour while warming to room temperature after the addition was complete. Subsequently, the solution was transferred to a separatory funnel, and the organics were washed with aq. 1 M HCl (2 x 100 mL). The combined aqueous phase was back-extracted with CH₂Cl₂ (2 x 50 mL), and the combined organic extracts were dried over Na₂SO₄, filtered, and concentrated. The crude material was purified by flash chromatography on silica gel eluting with 20% EtOAc in hexanes to afford **5-174** as a red oil (9.86 g, 49%). The material is a 1.3:1 mixture of diastereomers and exists 24% as the enol tautomer. Signals were deconvoluted as appropriate, but several of the peaks in the proton did not resolve, and are integrated together.

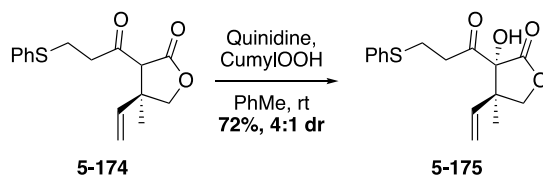
*The reaction was found to be very sensitive to oxygen. Prior to reaction, the solvent was degassed (sparging) with argon for 45 minutes to ensure the solvent was oxygen free.

Note: If the rate of addition of the DBU is fast, or if the reaction is directly quenched with dilute HCl and then extracted, a portion of the product will eliminate thiophenol to give an enone byproduct. Working up the reaction in this way has been the most effective at reducing this elimination.

¹H NMR (500 MHz, CDCl₃) δ 11.57 (s, 0.48H), 7.37 – 7.27 (m, 8H), 7.23 – 7.19 (m, 2H), 5.88 (dd, *J* = 17.3, 10.7 Hz, 1H), 5.83 (dd, *J* = 17.1, 10.5, 1H), 5.81 (dd, *J* = 17.5, 10.5 Hz, 1H), 5.21 (d, *J* = 10.8 Hz, 1H), 5.17 (d, *J* = 9.7 Hz, 1H), 5.16 (d, *J* = 9.9 Hz, 1H), 5.06 – 4.98 (m, 1H), 4.41 (d, *J* = 8.8 Hz, 1H), 4.10 (d, *J* = 8.9 Hz, 1H), 4.08 (d, *J* = 8.9 Hz, 1H), 4.05 (d, *J* = 8.9 Hz, 1H), 3.98 (d, *J* = 8.9 Hz, 1H), 3.97 (d, *J* = 8.7 Hz, 1H), 3.51 (s, 1H), 3.35 (s, 1H), 3.19 – 3.09 (m, 4H), 2.99 – 2.86 (m, 3H), 2.66 – 2.49 (m, 1H), 1.37 (s, 2H), 1.29 (s, 1H), 1.22 (s, 3H).

¹³C {¹H} NMR (126 MHz, CDCl₃) δ 202.2, 201.5, 176.4, 172.5, 172.0, 170.9, 141.7, 140.2, 136.7, 135.52, 135.48, 129.9, 129.8, 129.7, 129.23, 129.21, 129.17, 126.64, 126.62, 126.60, 117.4, 116.0, 114.8, 104.1, 79.0, 77.4, 76.61, 76.58, 64.1, 61.1, 46.7, 46.6, 44.7, 43.5, 32.0, 29.9, 27.0, 26.8, 23.9, 23.8, 18.6.

HRMS (ESI/TOF) *m/z*: [M+Na]⁺ Calcd for C₁₆H₁₈O₃SNa 313.0874; Found 313.0870.



(3*R*,4*R*)-3-hydroxy-4-methyl-3-(3-(phenylthio)propanoyl)-4-vinyldihydrofuran-2(3*H*)-one

(5-175): Lactone **5-174** (9.26 g, 31.9 mmol) was dissolved in toluene (320 mL) in a non-dried round bottomed flask open to air. Quinidine (2.61 g, 7.97 mmol) was added, and the solution was stirred for 10 minutes at ambient temperature. After this time, the solution was cooled to –30 °C, and cumene hydroperoxide (80% assay) (7.1 mL, 38 mmol) was added. The mixture was allowed to warm to room temperature overnight (~14 h). After the reaction was complete (TLC) the solvent was evaporated *in vacuo*. To remove the cumyl alcohol side product which co-elutes with the product, the side product can be distilled away under vacuum (0.5 Torr) at 100 °C on a Kugelrohr distillation apparatus. Crude NMR of this material revealed a 4:1 dr. The material after distillation was purified by flash chromatography on silica gel eluting with 20% EtOAc in hexanes to afford

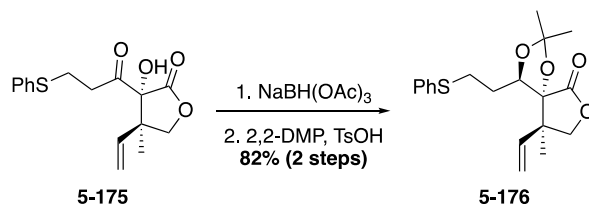
a single diastereomer of **5-175** (2.81 g, 29%) as a colorless oil, as well as a fraction containing an 11:1 mixture of alcohol diastereomers (1.28 g, 13%), and another fraction containing a further mixture of diastereomers (2.91 g, 30%) totaling a 72% yield. The mixed fractions could be re-purified to isolate additional **5-175**. Note: The distillation can be done before or after chromatography. The side product does not seem to affect the separation.

¹H NMR (600 MHz, CDCl₃) δ 7.35 – 7.29 (m, 4H), 7.24 – 7.20 (m, 1H), 5.70 (dd, *J* = 17.5, 10.9 Hz, 1H), 5.20 (d, *J* = 10.9 Hz, 1H), 5.16 (d, *J* = 17.5 Hz, 1H), 4.53 (d, *J* = 8.8 Hz, 1H), 4.07 (d, *J* = 8.8 Hz, 1H), 3.35 (s, 1H), 3.15 – 3.01 (m, 3H), 2.93 – 2.86 (m, 1H), 1.26 (s, 3H).

¹³C {¹H} NMR (151 MHz, CDCl₃) δ 207.1, 174.7, 135.5, 135.2, 129.7, 129.2, 126.6, 118.6, 86.9, 74.7, 49.8, 39.7, 27.0, 19.7.

HRMS (ESI/TOF) *m/z*: [M+Na]⁺ Calcd for C₁₆H₁₈O₄SNa 329.0823; Found 329.0823.

[α]_D²² +79.5 (*c* 1.67, CHCl₃)



(4*R*,5*R*,9*R*)-2,2,9-trimethyl-4-(2-(phenylthio)ethyl)-9-vinyl-1,3,7-trioxaspiro[4.4]nonan-6-

one (5-176): To a stirred solution of **5-175** (2.99 g, 9.76 mmol) in CH₂Cl₂ (93 mL) and glacial AcOH (4.6 mL) was added NaBH(OAc)₃ (6.21 g, 29.3 mmol) at room temperature. The solution was stirred at room temperature overnight (~18 h) and was quenched by the addition of aq. 2 M HCl (100 mL). The mixture was stirred vigorously for 1 hour at room temperature, and was subsequently transferred to a separatory funnel. The organic layer was separated, and the aqueous layer was extracted with CH₂Cl₂ (3 x 50 mL). The combined organic extracts were washed with water (2 x 50 mL) and brine (1 x 50 mL), dried over Na₂SO₄, filtered, and concentrated *in vacuo*.

The crude diol was used directly without further purification.

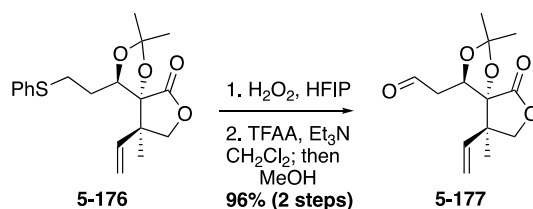
The crude diol was dissolved in 2,2-dimethoxypropane (98 mL) in a 250 mL round bottom flask equipped with a reflux condenser. TsOH•H₂O (58.1 mg, 0.305 mmol) was added, and the solution was heated to reflux for 20 h. The solution was cooled, and the solvent was evaporated. The crude material was chromatographed by MPLC (ISCO) on silica gel eluting with a gradient from 0-40% EtOAc in hexanes to afford **5-176** as a yellow oil (2.78 g, 82% over 2 steps).

¹H NMR (500 MHz, CDCl₃) δ 7.33 – 7.26 (m, 4H), 7.21 – 7.15 (m, 1H), 5.67 (dd, *J* = 17.5, 10.9 Hz, 1H), 5.16 (d, *J* = 11.0 Hz, 1H), 5.06 (d, *J* = 17.6 Hz, 1H), 4.35 (d, *J* = 13.7 Hz, 2H), 4.03 – 3.94 (m, 2H), 3.26 – 3.19 (m, 1H), 3.03 – 2.94 (m, 1H), 2.19 – 2.10 (m, 1H), 1.72 – 1.64 (m, 1H), 1.56 (s, 3H), 1.34 (s, 3H), 1.23 (d, *J* = 1.5 Hz, 3H).

¹³C {¹H} NMR (126 MHz, CDCl₃) δ 174.2, 136.6, 135.9, 129.3, 129.1, 126.2, 117.1, 110.6, 86.7, 76.0, 73.9, 45.8, 30.7, 29.9, 27.5, 26.9, 19.5.

HRMS (ESI/TOF) *m/z*: [M+Na]⁺ Calcd for C₁₉H₂₄O₄SNa 371.1293; Found 371.1287.

[α]²¹_D +70.6 (*c* 1.22, CDCl₃)



2-((4*R*,5*R*,9*R*)-2,2,9-trimethyl-6-oxo-9-vinyl-1,3,7-trioxaspiro[4.4]nonan-4-yl)acetaldehyde

(5-177): A solution of **5-176** (2.50 g, 7.17 mmol) in HFIP (48 mL) was cooled to 0 °C, and H₂O₂ (30%, 0.88 mL, 8.6 mmol) was added dropwise. The solution was stirred at 0 °C for 20 minutes, and was then warmed to room temperature and stirred for another 25 minutes. The reaction was quenched by the addition of saturated aq. Na₂S₂O₃ (25 mL) and saturated aq. NaHCO₃ (25 mL), and the mixture was extracted with EtOAc (3 x 50 mL). The combined organic extracts were dried

over Na₂SO₄, filtered, and concentrated. The crude sulfoxide was used in the next step without purification.

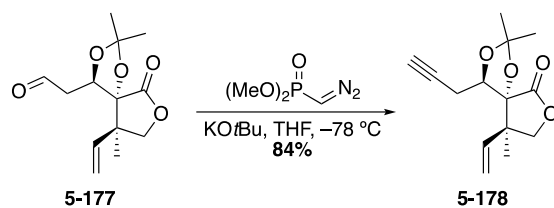
The crude sulfoxide was azeotroped with PhMe (5x), and was then dissolved in anhydrous CH₂Cl₂ (48 mL). The solution was sparged with Ar for 15 minutes, during which time Et₃N (5.0 mL, 36 mmol) was added. The solution was cooled to 0 °C, and freshly distilled TFAA (2.0 mL, 14 mmol) was added dropwise. The solution was stirred at 0 °C for 5 minutes, and was then warmed to room temperature and stirred for an hour. Anhydrous methanol (3 mL) was added, and the solution was stirred for 5 minutes before being transferred to a separatory funnel. The material was washed with aq. 1 M HCl (40 mL), and the aqueous phase was back-extracted with CH₂Cl₂ (3 x 30 mL). The combined organic layer was dried over Na₂SO₄, filtered, and concentrated. The crude material was purified by MPLC (ISCO) eluting with a gradient from 20-70% EtOAc in hexanes to afford **5-177** as an orange oil (1.74 g, 96% over 2 steps).

¹H NMR (600 MHz, CDCl₃) δ 9.76 (s, 1H), 5.77 (dd, *J* = 17.6, 10.9 Hz, 1H), 5.32 (d, *J* = 10.9 Hz, 1H), 5.23 (d, *J* = 17.6 Hz, 1H), 4.65 (dd, *J* = 9.0, 3.1 Hz, 1H), 4.20 (d, *J* = 8.9 Hz, 1H), 4.12 (d, *J* = 8.9 Hz, 1H), 3.16 (dd, *J* = 17.6, 9.1 Hz, 1H), 2.62 (dd, *J* = 17.7, 3.0 Hz, 1H), 1.54 (s, 3H), 1.42 (s, 3H), 1.28 (s, 3H).

¹³C {¹H} NMR (151 MHz, CDCl₃) δ 198.9, 173.8, 136.5, 117.6, 111.5, 86.0, 74.4, 71.8, 46.3, 45.1, 27.5, 27.1, 18.0.

HRMS (ESI/TOF) *m/z*: [M+Na]⁺ Calcd for C₁₃H₁₈O₅Na 277.1052; Found 277.1055.

[α]_D²¹ +25.1 (*c* 1.23, CDCl₃)



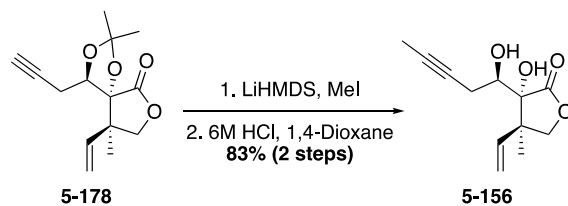
(4*R*,5*R*,9*R*)-2,2,9-trimethyl-4-(prop-2-yn-1-yl)-9-vinyl-1,3,7-trioxaspiro[4.4]nonan-6-one (5-178): Performed according to the procedure of Gilbert. Potassium *tert*-butoxide (0.410 g, 3.65 mmol) was dissolved in THF (20 mL) in a flame-dried 200 mL Schlenk flask. The solution was cooled to $-78\text{ }^{\circ}\text{C}$ (maintained by a Cryocool) and dimethyl (diazomethyl)phosphonate (0.548 g, 3.65 mmol) was added dropwise, and the solution was stirred for 30 minutes. Subsequently a solution of **5-177** (0.830 g, 3.26 mmol) in THF (10 mL) was added, and the solution was stirred at $-78\text{ }^{\circ}\text{C}$ overnight (20 h). The reaction was then warmed to room temperature and stirred for 1 hour. The reaction was quenched by addition of saturated aq. NH_4Cl (50 mL), and the mixture was transferred to a separatory funnel and was extracted with EtOAc (3 x 50 mL). The combined organic extracts were dried over Na_2SO_4 , filtered, and concentrated. The crude material was purified by flash chromatography on silica gel eluting with 20% EtOAc in hexanes to afford **5-178** as a yellow oil (0.682 g, 84%).

^1H NMR (600 MHz, CDCl_3) δ 5.87 (dd, $J = 17.6, 10.9$ Hz, 1H), 5.36 (d, $J = 10.9$ Hz, 1H), 5.23 (d, $J = 17.6$ Hz, 1H), 4.37 – 4.30 (m, 2H), 4.07 (d, $J = 9.0$ Hz, 1H), 2.82 (ddd, $J = 17.1, 7.7, 2.7$ Hz, 1H), 2.47 (ddd, $J = 17.2, 5.3, 2.7$ Hz, 1H), 2.09 (t, $J = 2.7$ Hz, 1H), 1.58 (s, 3H), 1.41 (s, 3H), 1.28 (s, 3H).

^{13}C $\{^1\text{H}\}$ NMR (151 MHz, CDCl_3) δ 173.8, 136.6, 117.7, 111.3, 87.0, 80.1, 77.1, 74.1, 70.8, 46.3, 27.7, 27.2, 21.8, 19.1.

HRMS (ESI/TOF) m/z : $[\text{M}+\text{Na}]^+$ Calcd for $\text{C}_{14}\text{H}_{18}\text{O}_4\text{Na}$ 273.1103; Found 273.1097.

$[\alpha]_D^{25} +51.1$ (c 1.28, CDCl_3)



(3*R*,4*R*)-3-hydroxy-3-((*R*)-1-hydroxypent-3-yn-1-yl)-4-methyl-4-vinyldihydrofuran-2(3*H*)-

one (5-156): A solution of **5-178** (0.925 g, 3.70 mmol) in THF (12.5 mL) was cooled to $-78\text{ }^{\circ}\text{C}$, and a solution of LiHMDS (0.53 M, 12.5 mL, 6.63 mmol) was added dropwise. The mixture was stirred for 1 hour at $-78\text{ }^{\circ}\text{C}$, then MeI (2.30 mL, 37.0 mmol) was added, and the solution was allowed to warm to room temperature overnight (16 h). The reaction was quenched by the addition of saturated aq. NH_4Cl , and the mixture was extracted with EtOAc (3 x 25 mL). The combined organic extracts were dried over Na_2SO_4 , filtered, and concentrated. The crude material was used in the next step without further purification.

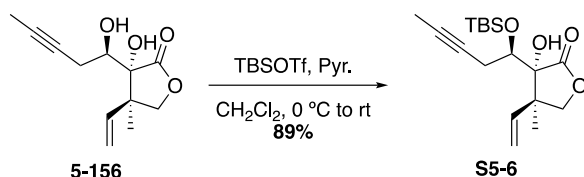
The crude material was dissolved in 1,4-dioxane (12.5 mL) and aq. 6 M HCl (12.5 mL) was added. The solution was heated to $60\text{ }^{\circ}\text{C}$ and was stirred vigorously for 5 hours. The solution was cooled to room temperature, diluted with water (50 mL) and was transferred to a separatory funnel. The mixture was extracted with EtOAc (3 x 25 mL), and the organic extracts were washed with water (2 x 20 mL). The combined organic layer was dried over Na_2SO_4 , filtered, and concentrated. The crude material was purified by MPLC (ISCO) eluting with a gradient from 20-60% EtOAc in hexanes to afford **5-156** as an orange oil (0.692 g, 83% over 2 steps).

^1H NMR (600 MHz, CDCl_3) δ 6.05 (dd, $J = 17.5, 11.0$ Hz, 1H), 5.26 (d, $J = 10.9$ Hz, 1H), 5.16 (d, $J = 17.6$ Hz, 1H), 4.29 (d, $J = 9.0$ Hz, 1H), 4.07 (d, $J = 9.0$ Hz, 1H), 3.91 (dd, $J = 11.9, 6.0$ Hz, 1H), 3.36 (s, 1H), 2.66 – 2.62 (m, 2H), 1.81 (t, $J = 2.6$ Hz, 3H), 1.28 (s, 3H).

^{13}C { ^1H } NMR (151 MHz, CDCl_3) δ 175.9, 137.7, 115.9, 80.5, 80.0, 74.3, 74.3, 69.1, 49.1, 23.1, 19.1, 3.7.

HRMS (ESI/TOF) m/z : $[M+Na]^+$ Calcd for $C_{12}H_{16}O_4Na$ 247.0946; Found 249.0953.

$[\alpha]^{23}_D +30.6$ (c 1.20, $CDCl_3$)

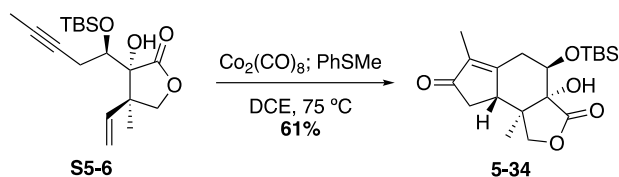


(3*R*,4*R*)-3-((*R*)-1-((*tert*-butyldimethylsilyloxy)pent-3-yn-1-yl)-3-hydroxy-4-methyl-4-

vinyl-dihydrofuran-2(3*H*)-one (S5-6): A solution of **5-156** (0.692 g, 3.09 mmol) in CH_2Cl_2 (21 mL) was cooled to 0 °C, and pyridine (1.25 mL, 15.5 mmol) was added. The solution was stirred for 5 minutes, then TBSOTf (1.80 mL, 7.73 mmol) was added dropwise. The solution was stirred at 0 °C for 15 minutes, and was then warmed to room temperature and stirred for 6 hours. The reaction was quenched by the addition of saturated aq. NH_4Cl (20 mL), and the mixture was transferred to a separatory funnel. The layers were partitioned, and the aqueous phase was extracted with CH_2Cl_2 (3 x 20 mL). The combined organic extracts were dried over Na_2SO_4 , filtered, and concentrated. The crude material was purified by flash chromatography on silica gel, eluting with 15% EtOAc in hexanes to afford **S5-6** as a colorless oil (0.932 g, 89%). The spectral data match those reported by Zhai.

1H NMR (600 MHz, $CDCl_3$) δ 6.10 (dd, $J = 17.7, 10.9$ Hz, 1H), 5.25 (d, $J = 10.9$ Hz, 1H), 5.18 (d, $J = 17.7$ Hz, 1H), 4.38 (d, $J = 8.4$ Hz, 1H), 4.07 (t, $J = 5.6$ Hz, 1H), 3.92 (d, $J = 8.3$ Hz, 1H), 3.13 (s, 1H), 2.77 (ddq, $J = 17.2, 5.3, 2.6$ Hz, 1H), 2.44 (ddq, $J = 17.2, 5.4, 2.6$ Hz, 1H), 1.77 (t, $J = 2.6$ Hz, 3H), 1.25 (s, 3H), 0.91 (s, 9H), 0.17 (s, 3H), 0.11 (s, 3H).

^{13}C { 1H } NMR (151 MHz, $CDCl_3$) δ 178.4, 137.9, 116.4, 80.9, 79.2, 76.6, 76.1, 75.4, 48.4, 26.0 (3C), 24.1, 20.2, 18.2, 3.7, -4.3, -4.7.



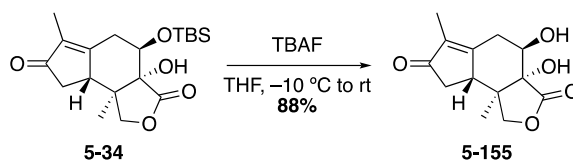
(3a*R*,4*R*,8a*R*,8b*R*)-4-((*tert*-butyldimethylsilyl)oxy)-3a-hydroxy-6,8b-dimethyl-

3a,4,5,8a,8b-hexahydro-1*H*-indeno[4,5-*c*]furan-3,7-dione (5-34): A solution of $\text{Co}_2(\text{CO})_8$ (1.184 g, 3.29 mmol) in DCE (10 mL) was added to a solution of **S5-6** (0.928 g, 2.74 mmol) in DCE (10 mL) and the mixture was stirred at room temperature for 3 hours. If incomplete complexation occurs during this period, the mixture can be gently heated to 30 °C to facilitate complex formation. Thioanisole (1.16 mL, 9.86 mmol) was added, and the solution was stirred at room temperature for 15 minutes, and then at 75 °C overnight (18 h). The reaction mixture was cooled to room temperature, and the solvent was evaporated. The crude residue was purified by MPLC (ISCO) on silica gel eluting with a gradient from 20-85% EtOAc in hexanes to afford **5-34** as a white solid (0.617 g, 61%). The spectral data are in accord with those reported by Zhai, however in the ^{13}C in CDCl_3 there was some unexpected line-broadening which largely eliminated 3 carbon signals. Expansions of the relevant areas show the presence of the broadened peaks in the expected locations. Both sets of data are reported for clarity.

$^1\text{H NMR}$ (500 MHz, CD_3OD) δ 4.34 (dd, $J = 3.9, 2.6$ Hz, 1H), 4.27 (d, $J = 8.5$ Hz, 1H), 4.18 (d, $J = 8.6$ Hz, 1H), 3.54 (app. s, 1H), 3.03 (dd, $J = 19.2, 3.2$ Hz, 1H), 2.64 (d, $J = 19.2$ Hz, 1H), 2.42 – 2.39 (m, 2H), 1.68 (s, 3H), 0.89 (overlapping s, 12H), 0.13 (s, 3H), 0.12 (s, 3H).

$^1\text{H NMR}$ (600 MHz, Chloroform-*d*) δ 4.20 (d, $J = 8.4$ Hz, 1H), 4.16 (d, $J = 8.4$ Hz, 1H), 4.09 (app. t, $J = 5.0$ Hz, 1H), 3.24 (s, 1H), 3.06 (dd, $J = 17.2, 4.4$ Hz, 1H), 2.70 (s, 1H), 2.54 (dd, $J = 17.3, 5.3$ Hz, 1H), 2.41 (dd, $J = 18.7, 6.4$ Hz, 1H), 2.35 (dd, $J = 18.8, 2.6$ Hz, 1H), 1.72 (t, $J = 1.7$ Hz, 3H), 0.92 (s, 3H), 0.90 (s, 9H), 0.14 (s, 3H), 0.12 (s, 3H).

^{13}C $\{^1\text{H}\}$ NMR (151 MHz, CDCl_3) δ 207.6, 167.2, 137.0, 77.6, 72.0, 45.1, 42.5, 35.5, 32.0, 25.8, 18.0, 8.2, -4.3, -5.0.



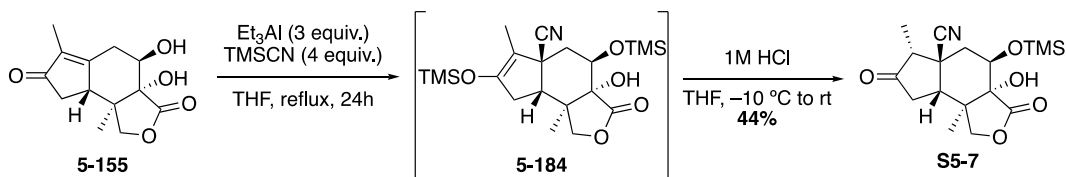
(3a*R*,4*R*,8a*R*,8b*R*)-3a,4-dihydroxy-6,8b-dimethyl-3a,4,5,8,8a,8b-hexahydro-1*H*-indeno[4,5-*c*]furan-3,7-dione (5-155): A solution of **5-34** (0.606 g, 1.65 mmol) in THF (18 mL) was cooled to $-10\text{ }^\circ\text{C}$, and TBAF (1.0 M, 5.4 mL, 5.4 mmol) was added dropwise. The solution was stirred at $-10\text{ }^\circ\text{C}$ for 15 minutes, and was then warmed to room temperature and stirred for another 2 hours. The reaction was quenched by the addition of saturated aq. NH_4Cl (20 mL), and the mixture was extracted with EtOAc (3 x 15 mL). The combined organic extracts were dried over Na_2SO_4 , filtered, and concentrated. The crude material was purified by MPLC (ISCO) on silica gel eluting with a gradient from 20-85% EtOAc in hexanes to afford **5-155** as a white solid (0.417 g, 88%). A portion of the material was crystallized using vapor diffusion with EtOAc as the solvent and hexanes as the anti-solvent to generate x-ray quality crystals. See section 5.6.4 for details.

^1H NMR (600 MHz, CDCl_3) δ 4.38 (d, $J = 8.5$ Hz, 1H), 4.04 (d, $J = 8.5$ Hz, 1H), 3.83 (s, 1H), 3.79 (dt, $J = 11.4, 6.3$ Hz, 1H), 3.62 (d, $J = 11.4$ Hz, 1H), 3.38 (dd, $J = 13.8, 5.8$ Hz, 1H), 2.82 (dq, $J = 7.1, 1.9$ Hz, 1H), 2.50 (dd, $J = 18.8, 6.9$ Hz, 1H), 2.41 – 2.33 (m, 2H), 1.82 (t, $J = 1.7$ Hz, 3H), 0.94 (s, 3H).

^{13}C $\{^1\text{H}\}$ NMR (151 MHz, CDCl_3) δ 207.4, 177.4, 164.1, 137.8, 76.1, 75.3, 71.1, 47.3, 43.0, 35.4, 34.4, 8.1, 8.0.

HRMS (ESI/TOF) m/z : $[\text{M}+\text{H}]^+$ Calcd for $\text{C}_{14}\text{H}_{18}\text{O}_4\text{DH}$ 269.1374; Found 269.1368. Observed partial deuterium exchange of presumably one of the alcohols in the MS sample.

$[\alpha]_D^{23} +66.8$ (c 0.49, CDCl_3)



(3*aR*,4*R*,5*aS*,6*R*,8*aR*,8*bR*)-3*a*-hydroxy-6,8*b*-dimethyl-3,7-dioxo-4-

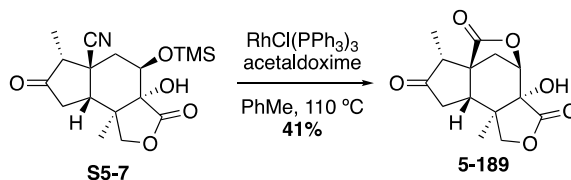
((trimethylsilyl)oxy)decahydro-5*aH*-indeno[4,5-*c*]furan-5*a*-carbonitrile (5-189): A flame dried 2-dram vial was charged with Et₃Al (1.0 M, 0.59 mL, 0.59 mmol) and TMSCN (0.10 mL, 0.79 mmol) at room temperature, and the mixture was stirred for 5 minutes. **5-155** (50.1 mg, 0.198 mmol) was added as a solution in THF (2.0 mL), and the mixture was heated to 66 °C in an oil bath for 24 hours. The solution was subsequently cooled to 0 °C, and water was added dropwise until ethane evolution ceased. The solution was then filtered through a short plug of MgSO₄ and the solution was concentrated. The material was used directly in the next step.

Crude **5-184** was re-dissolved in THF (2.0 mL), and the solution was cooled to –10 °C. Aqueous 1 M HCl (1.0 mL) was added, and the mixture was warmed to room temperature and was stirred vigorously for 30 minutes. The solution was diluted with water (3 mL), and the mixture was extracted with EtOAc (3 x 3 mL). The combined extracts were dried over Na₂SO₄, filtered, and concentrated. The crude material was purified by MPLC (ISCO) eluting with a gradient from 60-85% EtOAc in hexanes to afford **S5-7** as a colorless oil (30.3 mg, 44% over 2 steps). The material contains unknown peaks at 3.17 and 1.37 ppm respectively, and the carbon has two additional carbons because of it.

¹H NMR (600 MHz, CDCl₃) δ 5.13 (d, *J* = 8.3 Hz, 1H), 4.05 (t, *J* = 2.7 Hz, 1H), 3.92 (d, *J* = 8.2 Hz, 1H), 3.12 (s, 1H), 2.79 (q, *J* = 7.0 Hz, 1H), 2.66 (dd, *J* = 11.7, 8.7 Hz, 1H), 2.52 (dd, *J* = 19.5, 8.7 Hz, 1H), 2.43 (dd, *J* = 19.5, 11.8 Hz, 1H), 1.90 (dd, *J* = 14.6, 3.3 Hz, 1H), 1.53 (dd, *J* = 14.5, 2.3 Hz, 1H), 1.19 (d, *J* = 7.1 Hz, 3H), 1.18 (s, 3H), 0.17 (s, 9H).

^{13}C $\{^1\text{H}\}$ NMR (126 MHz, CDCl_3) δ 211.1, 178.3, 123.9, 77.6, 74.1, 71.8, 57.1, 43.0, 41.0, 37.6, 36.9, 27.6, 22.0, 7.5, -0.2.

HRMS (ESI/TOF) m/z : $[\text{M}+\text{Na}]^+$ Calcd for $\text{C}_{17}\text{H}_{25}\text{NO}_5\text{SiNa}$ 374.1400; Found 374.1395.



(3aR,4R,6aS,7R,9aS,9bR)-3a-hydroxy-7,9b-dimethylhexahydro-3H,6H-4,6a-

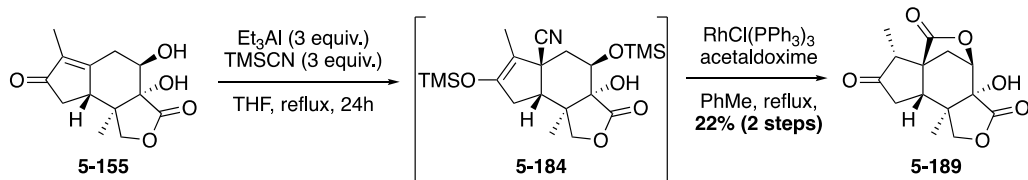
methanocyclopenta[c]furo[3,4-e]oxepine-3,6,8(7H)-trione (5-189): To a solution of **S5-7** (25 mg, 0.071 mmol) in PhMe (0.7 mL) was added $\text{RhCl(PPh}_3)_3$ (13 mg, 0.014 mmol). The solution was sparged with argon for 10 minutes, during which time acetaldoxime (86 μL , 1.4 mmol) was added. The solution was then heated to 110 $^\circ\text{C}$ in a preheated oil bath overnight (18 h). The mixture was cooled to room temperature, and MeOH (0.7 mL) was added. The solution was stirred for 5 minutes, and was subsequently concentrated *in vacuo*. The crude material was purified by flash chromatography on silica gel eluting with a gradient from 40-50-60% EtOAc in hexanes to afford **5-189** as a colorless oil (8.1 mg, 41%).

^1H NMR (600 MHz, CDCl_3) δ 4.71 (d, $J = 5.9$ Hz, 1H), 4.10 (d, $J = 9.4$ Hz, 1H), 4.05 (d, $J = 9.4$ Hz, 1H), 2.99 (s, 1H), 2.79 (q, $J = 7.1$ Hz, 1H), 2.56 (ddd, $J = 17.1, 6.5, 1.1$ Hz, 1H), 2.37 – 2.27 (m, 3H), 2.20 (d, $J = 12.8$ Hz, 1H), 1.21 (s, 3H), 1.07 (d, $J = 7.0$ Hz, 3H).

^{13}C $\{^1\text{H}\}$ NMR (151 MHz, CDCl_3) δ 212.3, 177.3, 176.7, 78.4, 77.9, 73.8, 50.5, 49.0, 42.1, 41.2, 38.8, 26.0, 21.1, 8.8.

HRMS (ESI/TOF) m/z : $[\text{M}-\text{H}]^-$ Calcd for $\text{C}_{14}\text{H}_{15}\text{O}_6$ 279.0869; Found 279.0860.

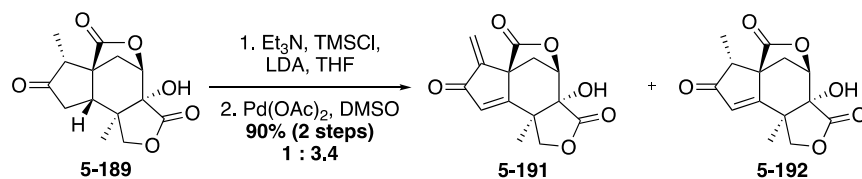
$[\alpha]_D^{21} -79.5$ (c 0.80, CDCl_3)



(3a*R*,4*R*,6a*S*,7*R*,9a*S*,9b*R*)-3a-hydroxy-7,9b-dimethylhexahydro-3*H*,6*H*-4,6a-

methanocyclopenta[*c*]furo[3,4-*e*]oxepine-3,6,8(7*H*)-trione (5-189): A flame dried 2-dram vial was charged with Et₃Al (1.0 M, 0.28 mL, 0.28 mmol) and TMSCN (30. μL, 0.28 mmol) at room temperature, and the mixture was stirred for 5 minutes. **5-155** (23.4 mg, 0.093 mmol) was added as a solution in THF (0.93 mL), and the mixture was heated to 66 °C in an oil bath for 24 hours. The solution was subsequently cooled to 0 °C, and water was added dropwise until ethane evolution ceased. The solution was then filtered through a short plug of MgSO₄ and the solution was concentrated. The material was used directly in the next step.

To a solution of crude **5-184** in PhMe (0.93 mL) was added RhCl(PPh₃)₃ (17.2 mg, 0.0186 mmol). The solution was sparged with argon for 10 minutes, during which time acetaldoxime (0.14 mL, 2.33 mmol) was added. The solution was then heated to 110 °C in a preheated oil bath overnight (18 h). The mixture was cooled to room temperature, and MeOH (0.7 mL) was added. The solution was stirred for 5 minutes and was subsequently concentrated *in vacuo*. The crude material was purified by MPLC (ISCO) on silica gel eluting with a gradient from 20-90% EtOAc in hexanes to afford **5-189** as a colorless oil (5.7 mg, 22% over 2 steps). Spectral data are consistent with those reported above.

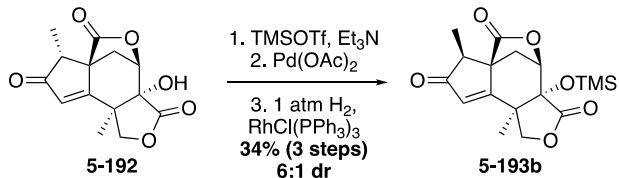


Compounds 5-191 and 5-192: Triethylamine (30. μ L, 0.21 mmol) was added to a solution of **5-189** (azeotroped 3x with PhMe, 12 mg, 0.043 mmol) in THF (0.86 mL). Freshly distilled TMSCl (30. mL, 0.21 mmol) was added at room temperature, and the solution was stirred for 5 minutes before being cooled to -78 $^{\circ}$ C. A 1.0 M stock solution of LDA (0.17 mL, 0.17 mmol) was added dropwise, and the solution was stirred at -78 $^{\circ}$ C for 1.5 hours. The mixture was then warmed to 0 $^{\circ}$ C for 5 minutes, and was then quenched with saturated aq. NaHCO₃ (1.5 mL). The mixture was extracted with EtOAc (3 x 1 mL), and the combined extracts were dried over MgSO₄, filtered, and concentrated. The crude silyl enol ether was used directly in the next step.

The silyl enol ether was dissolved in dry DMSO (0.43 mL), and Pd(OAc)₂ (19 mg, 0.086 mmol) was added. The solution was evacuated and backfilled with O₂ 5 times, and the mixture was then heated to 75 $^{\circ}$ C in a preheated oil bath for 18 h. The solution was then cooled to room temperature and was diluted with H₂O (0.5 mL). The mixture was extracted with EtOAc (5 x 1 mL), and the combined organic extracts were washed with brine (4 x 1 mL). The organic phase was dried over MgSO₄, filtered, and concentrated. The crude material was purified by flash chromatography on silica gel eluting with 50% EtOAc in hexanes to afford **5-191** and **5-192** as an inseparable mixture of products in a 1:3.4 ratio respectively (10.7 mg, 90% combined over 2 steps). **¹H NMR** (500 MHz, CDCl₃) δ 6.44 (s, 1H), 6.43 (s, 1H), 6.19 (s, 3H), 5.64 (s, 1H), 4.87 (d, J = 5.9 Hz, 1H), 4.85 (d, J = 5.9 Hz, 4H), 4.15 – 4.07 (m, 9H), 3.33 (s, 1H), 3.30 (s, 3H), 3.03 (q, J = 7.7 Hz, 3H), 2.87 (dd, J = 12.5, 5.6 Hz, 1H), 2.67 – 2.61 (m, 5H), 2.45 (d, J = 12.5 Hz, 3H), 1.54 (s, 3H), 1.50 (s, 11H), 1.17 (d, J = 7.7 Hz, 12H).

HRMS 5-191 (ESI/TOF) m/z : [M-H]⁻ Calcd for C₁₄H₁₁O₆ 275.0556; Found 275.0557.

HRMS 5-192 (ESI/TOF) m/z: [M-H]⁻ Calcd for C₁₄H₁₃O₆ 277.0712; Found 277.0723.



(3aR,4R,6aR,7S,9bR)-7,9b-dimethyl-3a-((trimethylsilyl)oxy)-1,3a,4,9b-tetrahydro-3H,6H-4,6a-methanocyclopenta[*c*]furo[3,4-*e*]oxepine-3,6,8(7H)-trione (5-193b): Compound **5-192** (3.4:1 mix with **5-191**, 4.3 mg, 0.015 mmol) was dissolved in CH₂Cl₂ (0.3 mL) and Et₃N (0.01 mL, 0.09 mmol) was added. The solution was cooled to 0 °C, and TMSOTf (0.01 mL, 0.06 mmol) was added dropwise. The solution was warmed to room temperature and was stirred for 1 hour. The reaction was quenched by the addition of saturated aq. NaHCO₃, and the mixture was extracted with CH₂Cl₂ (3 x 1 mL). The combined extracts were dried over MgSO₄, filtered, and concentrated. The crude material was used directly in the next step.

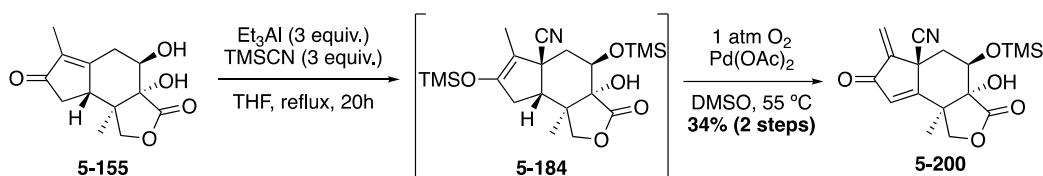
Crude TMS-enol ether was dissolved in MeCN (0.3 mL) under argon, and Pd(OAc)₂ (4.4 mg, 0.020 mmol) was added. The solution was stirred under argon for 22 h at room temperature, and was subsequently concentrated *in vacuo*. The crude material was filtered through a plug of silica gel eluting with 60% EtOAc in hexanes to afford crude dienone. This material was used crude in the next step without intensive purification.

The crude material was re-dissolved in THF (0.3 mL) under argon, and RhCl(PPh₃)₃ (0.7 mg, 0.0008 mmol) was added. The solution was sparged with hydrogen gas for 5 minutes, and the mixture was then allowed to stir under hydrogen atmosphere for 18 h. The reaction mixture was filtered over silica gel with EtOAc, and the filtrate was concentrated. The crude material was purified by silica gel chromatography eluting with a gradient from 20-30-40-50% EtOAc in pentanes to afford **5-193b** as a 5.6:1 mixture of diastereomers (1.8 mg, 34% over 3 steps). ***It is

now clear that this final reaction was not truly catalyzed by Wilkinson's catalyst, but the protocol is reported for completeness. NMR data is tabulated for the major diastereomer.

¹H NMR (600 MHz, CDCl₃) δ 6.25 (s, 1H), 4.80 (d, *J* = 5.7 Hz, 1H), 4.09 (d, *J* = 9.8 Hz, 1H), 3.98 (d, *J* = 9.8 Hz, 1H), 2.68 (dd, *J* = 12.3, 5.8 Hz, 1H), 2.53 (q, *J* = 7.5 Hz, 1H), 2.50 (d, *J* = 12.3 Hz, 1H), 1.44 (d, *J* = 0.9 Hz, 3H), 1.40 (d, *J* = 7.4 Hz, 3H), 0.25 (s, 9H).

¹³C {¹H} NMR (151 MHz, CDCl₃) δ 205.4, 174.3, 172.5, 171.2, 130.6, 78.5, 76.0, 53.9, 46.0, 45.4, 34.7, 29.9, 22.0, 9.0, 1.9.



(3*aR*,4*R*,5*aS*,8*bR*)-3*a*-hydroxy-8*b*-methyl-6-methylene-3,7-dioxo-4-((trimethylsilyl)oxy)-

1,3,3*a*,4,5,6,7,8*b*-octahydro-5*aH*-indeno[4,5-*c*]furan-5*a*-carbonitrile (5-200): A flame dried 2-

dram vial was charged with Et₃Al (1.0 M, 0.16 mL, 0.16 mmol) and TMSCN (30. μL, 0.28 mmol) at room temperature, and the mixture was stirred for 5 minutes. **5-155** (20. mg, 0.079 mmol) was added as a solution in THF (0.80 mL), and the mixture was heated to 66 °C in an oil bath for 22 hours. The solution was subsequently cooled to 0 °C, and saturated aq. NH₄Cl (2.0 mL) was added. The mixture was extracted with EtOAc (3 x 1.5 mL), and the combined organic extracts were dried over MgSO₄, filtered, and concentrated. The material was used directly in the next step.

Crude **5-184** was re-dissolved in dry DMSO (0.8 mL) under an argon atmosphere, and Pd(OAc)₂ (24.8 mg, 0.110 mmol) was added. The solution was evacuated and backfilled with oxygen (5x), and the solution was heated to 55 °C in a preheated oil bath for 27 hours. The solution was cooled to room temperature and diluted with H₂O (0.8 mL). The mixture was extracted with EtOAc (3 x 1.5 mL) and the combined organic layers were washed with brine (3 x 1 mL).

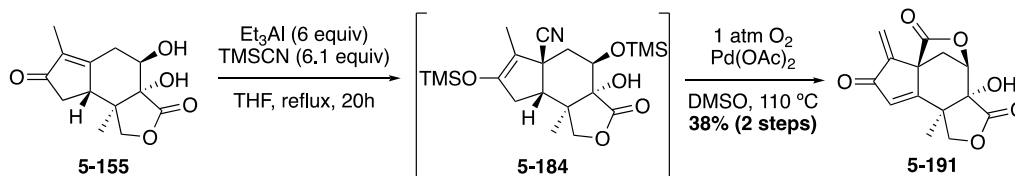
The organic phase was dried over MgSO₄, filtered, and concentrated. The crude material was purified by MPLC (ISCO) eluting with a gradient from 0-40% EtOAc in hexanes to afford **5-200** as a white solid (9.4 mg, 34 % over 2 steps).

¹H NMR (600 MHz, CDCl₃) δ 6.57 (s, 1H), 6.38 (d, *J* = 1.0 Hz, 1H), 5.83 (d, *J* = 0.9 Hz, 1H), 5.30 (d, *J* = 8.6 Hz, 1H), 4.12 (dd, *J* = 3.2, 2.1 Hz, 1H), 4.09 (d, *J* = 8.7 Hz, 1H), 2.95 (s, 1H), 2.54 (dd, *J* = 14.1, 3.1 Hz, 1H), 2.00 (dd, *J* = 14.1, 2.1 Hz, 1H), 1.47 (s, 3H), 0.23 (s, 9H).

¹³C {¹H} NMR (151 MHz, CDCl₃) δ 190.2, 176.9, 166.7, 145.2, 136.1, 120.9, 120.1, 81.6, 73.0, 72.1, 47.2, 39.5, 38.7, 20.8, -0.2.

HRMS (ESI/TOF) *m/z*: [M-H]⁻ Calcd for C₁₇H₂₀NO₅Si 346.1111; Found 346.1120.

[α]_D²¹ -54.1 (*c* 1.00, CDCl₃)



(3a*R*,4*R*,6a*S*,9*bR*)-3a-hydroxy-9*b*-methyl-7-methylene-1,3*a*,4,9*b*-tetrahydro-3*H*,6*H*-4,6*a*-methanocyclopenta[*c*]furo[3,4-*e*]oxepine-3,6,8(7*H*)-trione (5-191): A flame dried Schlenk flask was charged with Et₃Al (1.0 M, 0.12 mL, 0.12 mmol), TMSCN (15.0 μL, 0.122 mmol), and THF (0.5 mL) at room temperature, and the mixture was stirred for 10 minutes. **5-155** (5.0 mg, 0.020 mmol) was added neat under heavy argon counterflow. The flask was sealed, and the mixture was heated to reflux in an oil bath (75 °C oil temp.) for 22 hours. The solution was subsequently cooled to 0 °C and quenched with half saturated aq. Rochelle's salt (1.0 mL). The mixture was warmed to room temperature and was vigorously stirred for 1.5 h. The mixture was extracted with EtOAc (3 x 1.0 mL), and the combined organic extracts were dried over MgSO₄, filtered, and concentrated. The material was used directly in the next step without purification.

Crude **5-184** was re-dissolved in dry DMSO (0.5 mL) under an argon atmosphere, and Pd(OAc)₂ (11.2 mg, 0.0499 mmol) was added. The solution was evacuated and backfilled with oxygen (5x), and the solution was heated to 110 °C in a preheated oil bath for 24 hours. The solution was cooled to room temperature and diluted with H₂O (0.8 mL). The mixture was extracted with EtOAc (3 x 1.0 mL) and the combined organic layers were washed with brine (3 x 1 mL). The organic phase was dried over MgSO₄, filtered, and concentrated. The crude material was purified by flash chromatography on silica gel eluting with a gradient from 40-50% EtOAc in hexanes to afford **5-191** as a pale yellow oil (2.2 mg, 38 % over 2 steps).

¹H NMR (600 MHz, CDCl₃) δ 6.44 (s, 2H), 5.64 (s, 1H), 4.85 (d, *J* = 5.6 Hz, 1H), 4.13 – 4.12 (m, 2H), 3.02 (s, 1H), 2.86 (ddd, *J* = 12.5, 5.6, 0.7 Hz, 1H), 2.65 (d, *J* = 12.5 Hz, 1H), 1.53 (s, 3H).

¹³C {¹H} NMR (151 MHz, CDCl₃) δ 192.2, 175.9, 172.7, 166.6, 139.9, 131.8, 121.8, 78.2, 75.8, 75.7, 53.7, 44.7, 36.8, 20.7.

HRMS (ESI/TOF) *m/z*: [M-H]⁻ Calcd for C₁₄H₁₁O₆ 275.0556; Found 275.0557.

[α]_D²² +10.1 (*c* 0.30, CDCl₃)



(3a*R*,4*R*,6a*R*,7*S*,9b*R*)-3a-hydroxy-7,9b-dimethyl-1,3a,4,9b-tetrahydro-3*H*,6*H*-4,6a-

methanocyclopenta[*c*]furo[3,4-*e*]oxepine-3,6,8(7*H*)-trione (5-193a): To a solution of **5-191** (1.9 mg, 0.0069 mmol) in EtOAc (0.5 mL) was added Pd/C (10% w/w, 0.7 mg, 0.00069 mmol). The solution was sparged with hydrogen for 5 minutes and was allowed to stir under hydrogen atmosphere overnight. The reaction mixture was subsequently filtered over celite, and the solvent was evaporated giving **5-193a** (1.3 mg, 68%) as a white solid. The crude material was

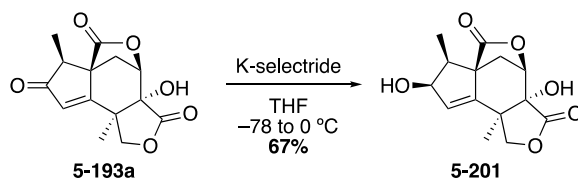
spectroscopically pure and was not purified further.

¹H NMR (600 MHz, CDCl₃) δ 6.29 (s, 1H), 4.79 (d, *J* = 5.7 Hz, 1H), 4.13 (d, *J* = 9.7 Hz, 1H), 4.06 (dd, *J* = 9.7, 0.9 Hz, 1H), 2.92 (s, 1H), 2.74 (ddd, *J* = 12.5, 5.8, 0.9 Hz, 1H), 2.57 (d, *J* = 12.4 Hz, 1H), 2.57 (q, *J* = 7.4 Hz, 1H), 1.51 (d, *J* = 0.9 Hz, 3H), 1.41 (d, *J* = 7.4 Hz, 3H). The signals at 2.57 are overlapping but can be deconvoluted.

¹³C {¹H} NMR (151 MHz, CDCl₃) δ 205.2, 176.1, 172.4, 170.2, 130.7, 78.2, 76.8, 75.3, 53.9, 46.1, 44.5, 34.8, 21.2, 8.9.

HRMS (ESI/TOF) *m/z*: [M-H]⁻ Calcd for C₁₄H₁₃O₆ 277.0712; Found 277.0699.

[α]²²_D +34.4 (*c* 0.44, CDCl₃)



(3aR,4R,6aR,7S,8R,9bR)-3a,8-dihydroxy-7,9b-dimethyl-1,3a,4,7,8,9b-hexahydro-3H,6H-4,6a-methanocyclopenta[c]furo[3,4-e]oxepine-3,6-dione (5-201): Enone **5-193a** (1.5 mg, 0.0054 mmol) was azeotroped 5x with dry PhMe, and was subsequently dissolved in THF (0.3 mL). The solution was cooled to -78 °C, and K-selectride (1.0 M, 22 μL, 0.022 mmol) was added in one portion. The solution was stirred at -78 °C for 3 hours, and was subsequently warmed to 0 °C and stirred for an additional hour. The reaction was quenched by the addition of 2 M HCl (1.0 mL) and the mixture was stirred at room temperature for 15 min. The mixture was then extracted with EtOAc (3 x 1.0 mL), dried over MgSO₄, and concentrated. The crude material was purified by flash chromatography on silica gel eluting with 60% EtOAc in hexanes to afford **5-201** (1.0 mg, 67%) as a white solid.

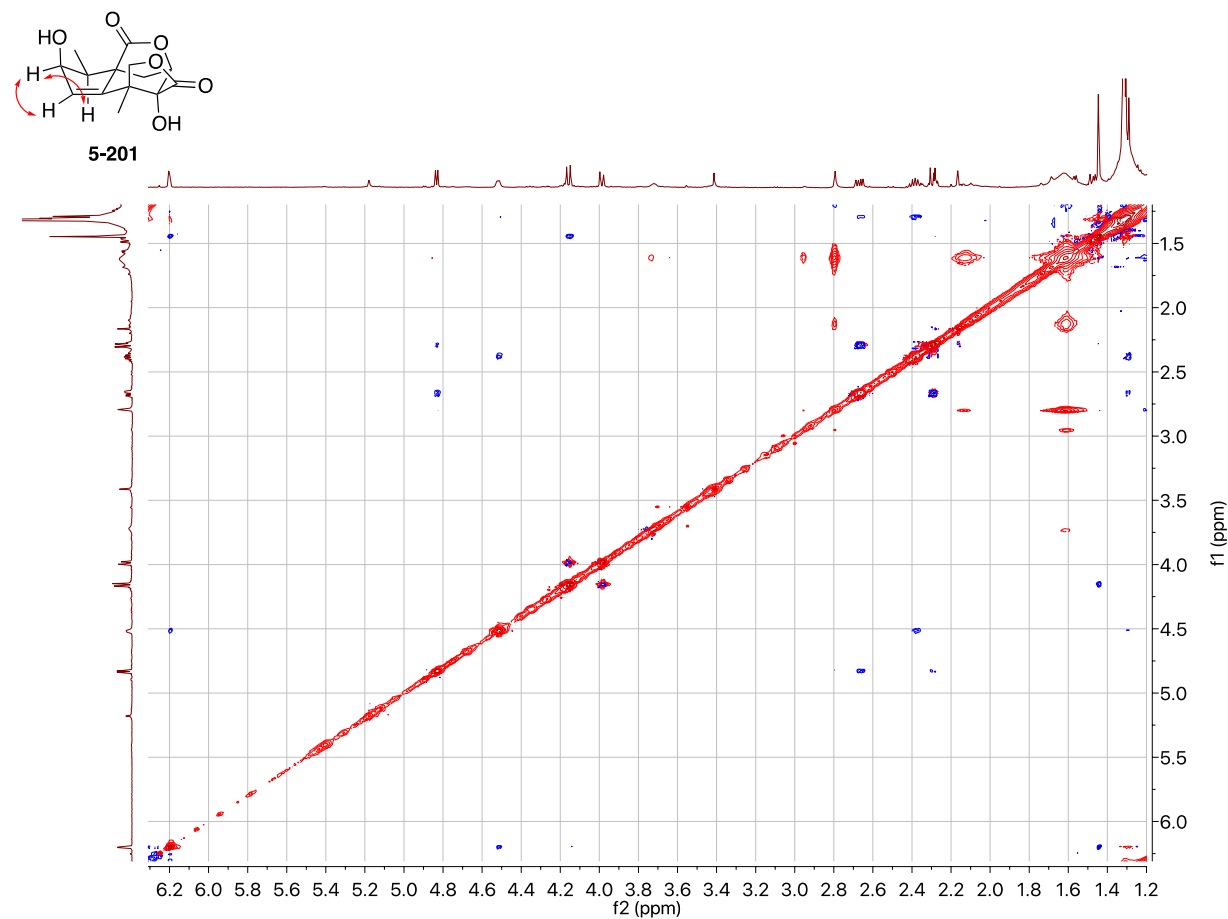
^1H NMR (600 MHz, CDCl_3) δ 6.14 (d, $J = 2.8$ Hz, 1H), 4.77 (d, $J = 5.9$ Hz, 1H), 4.46 (ddd, $J = 11.8, 5.9, 2.9$ Hz, 1H), 4.10 (d, $J = 9.6$ Hz, 1H), 3.93 (dd, $J = 9.5, 0.9$ Hz, 1H), 2.77 (s, 1H), 2.61 (ddd, $J = 12.2, 5.9, 1.0$ Hz, 1H), 2.32 (dq, $J = 7.4, 6.1$ Hz, 1H), 2.23 (d, $J = 12.2$ Hz, 1H), 2.07 (d, $J = 12.0$ Hz, 1H), 1.38 (d, $J = 0.9$ Hz, 3H), 1.24 (d, $J = 7.4$ Hz, 3H).

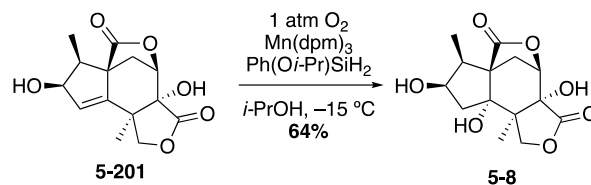
^{13}C $\{^1\text{H}\}$ NMR (151 MHz, CDCl_3) δ 177.6, 177.1, 145.9, 132.6, 80.0, 78.2, 76.1, 74.0, 57.2, 43.1, 41.0, 32.3, 21.3, 7.8.

HRMS (ESI/TOF) m/z : $[\text{M}-\text{H}]^-$ Calcd for $\text{C}_{14}\text{H}_{15}\text{O}_6$ 279.0869; Found 279.0864.

$[\alpha]_D^{22} +12.0$ (c 0.10, CDCl_3)

Key NOE correlations: NOESY was performed on a less-pure sample of **5-201**, but key correlations are still apparent.





(2R)-hydroxynorneomajucin (5-8): To a solution of **5-201** (1.0 mg, 0.0036 mmol) in HPLC grade *i*-PrOH (0.1 mL) was added a stock solution of Mn(dpm)₃ (2.0 mg/mL, 0.1 mL, 0.00036 mmol). The solution was then sparged with O₂ for 5 minutes, and was then cooled to −15 °C while still sparging. Ph(O*i*-Pr)SiH₂ (1.3 μL, 0.0071 mmol) was then added while still actively sparging, and then the solution was allowed to stir at −15 °C under an oxygen atmosphere for 1 h. The solution was warmed to room temperature, and the solvent was removed *in vacuo*. The crude residue was purified by column chromatography on silica gel eluting with CH₂Cl₂ (2 column volumes) followed by 5% MeOH in CH₂Cl₂ to afford **5-8** (0.7 mg, 64%) as a white solid.

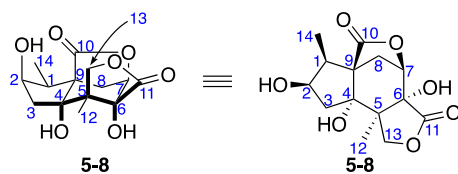
¹H NMR (600 MHz, CD₃OD) δ 4.67 (d, *J* = 5.7 Hz, 1H), 4.32 (td, *J* = 7.9, 4.9 Hz, 1H), 4.10 (dd, *J* = 10.0, 1.2 Hz, 1H), 3.93 (d, *J* = 9.9 Hz, 1H), 2.76 (d, *J* = 12.3 Hz, 1H), 2.61 (p, *J* = 7.6 Hz, 1H), 2.46 (ddd, *J* = 14.7, 7.6, 1.0 Hz, 1H), 2.30 (ddd, *J* = 12.3, 5.7, 1.0 Hz, 1H), 1.89 (s, 1H), 1.46 (dd, *J* = 14.7, 4.9 Hz, 1H), 1.23 (d, *J* = 1.1 Hz, 3H), 1.05 (d, *J* = 7.5 Hz, 3H).

¹³C {¹H} NMR (151 MHz, CD₃OD) δ 181.0, 178.8, 82.0, 80.2, 76.2, 75.4, 73.0, 60.6, 49.6, 43.7, 38.8, 30.2, 19.9, 7.7.

HRMS (ESI/TOF) *m/z*: [M-H][−] Calcd for C₁₄H₁₇O₇ 297.0974; Found 297.0971.

[α]²³_D −27.1 (*c* 0.30, CH₃OH); Isolated [α]²³_D −24.0 (*c* 0.003, CH₃OH).³²

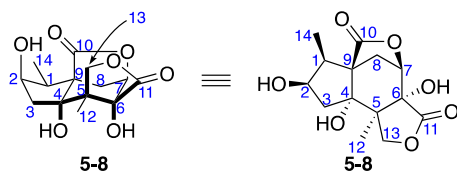
Table 5-5 Comparison of ^1H NMR spectra of isolated and synthetic **5-8**.³²



^1H Shifts (CD_3OD , ppm; J (Hz) in parenthesis)

Position	Natural 5-8	Synthetic 5-8
1	2.60 (dq, 7.8, 7.6)	2.61 (p, 7.6)
2	4.31 (dt, 7.8, 4.9)	4.32 (td, 7.9, 4.9)
3 α	2.44 (dd, 14.7, 7.8)	2.46 (ddd, 14.7, 7.6, 1.0)
3 β	1.45 (dd, 14.7, 4.9)	1.46 (dd, 14.7, 4.9)
7	4.66 (d, 5.6)	4.67 (d, 5.7)
8 α	2.75 (d, 12.2)	2.76 (d, 12.3)
8 β	2.28 (dd, 12.2, 5.6)	2.30 (ddd, 12.3, 5.7, 1.0)
12	1.22 (s)	1.23 (d, 1.1)
13 α	3.92 (d, 10.0)	3.93 (d, 9.9)
13 β	4.09 (d, 10.0)	4.10 (dd, 10.0, 1.1)
14	1.04 (d, 7.6)	1.05 (d, 7.5)

Table 5-6 Comparison of ^{13}C NMR spectra of isolated and synthetic **5-8**.³²



^{13}C Shifts (CD_3OD , ppm)

Position	Natural 5-8	Synthetic 5-8
1	38.8	38.8
2	73.0	73.0
3	43.7	43.7
4	80.2	80.2
5	49.6*	49.6
6	76.2	76.2
7	82.0	82.0
8	30.2	30.2
9	60.7	60.6
10	181.1	181.0
11	178.8	178.8
12	19.9	19.9
13	75.4	75.4
14	7.7	7.7

*Listed as 47.5 in publication, but appears at 49.6 in ^{13}C spectrum in supporting information

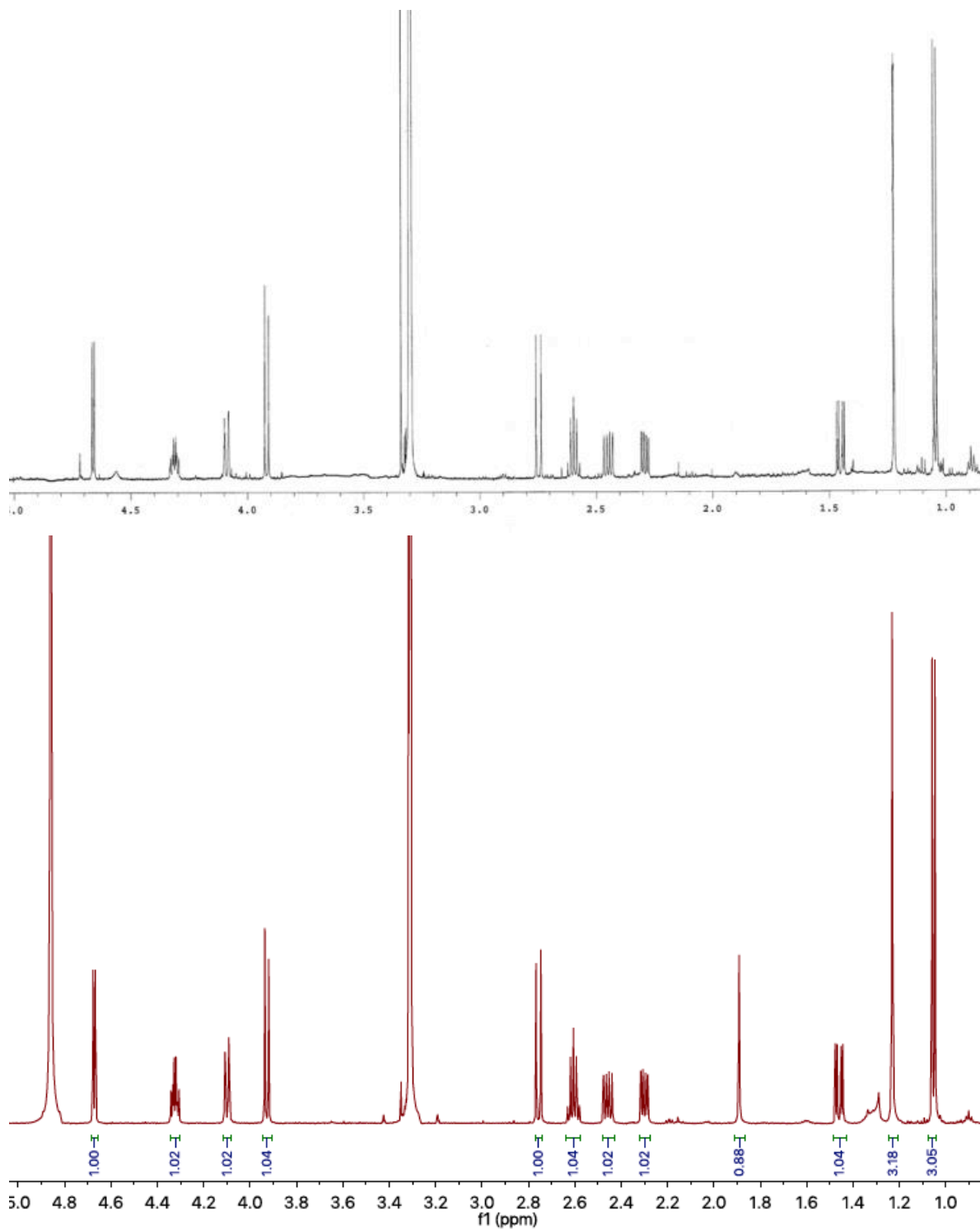


Figure 5-10 Overlaid ^1H NMR Spectra of **5-8**. Top: Isolated.³² Bottom: Synthetic.

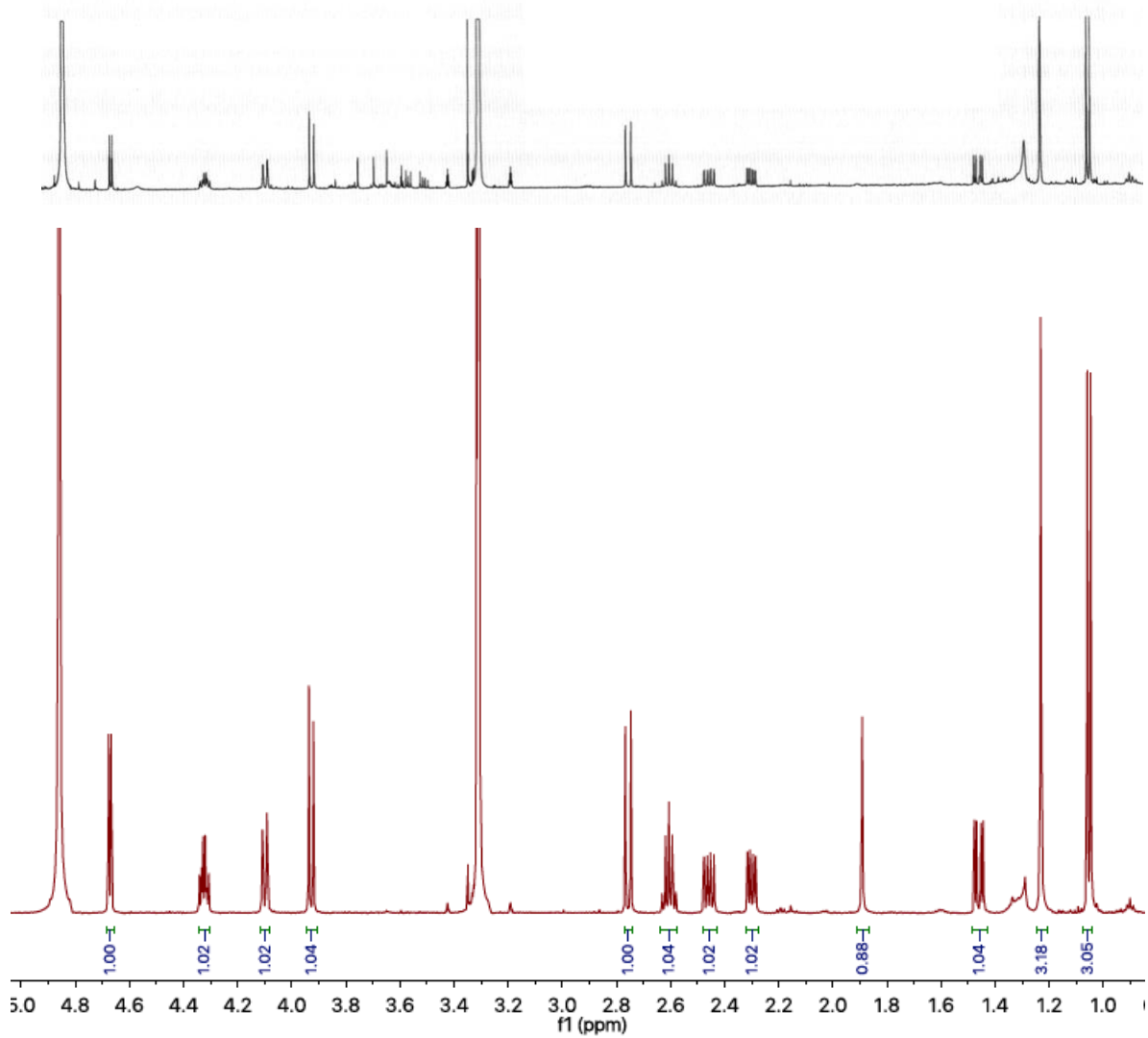
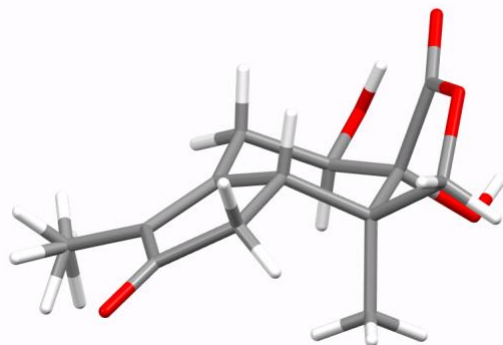


Figure 5-11 Overlaid ¹H NMR of the F1 domain from the COSY reported in the isolation paper and synthetic **5-8**.

5.6.4 X-ray Crystallography Data

X-ray data for 5-155:



A colorless crystal of approximate dimensions 0.091 x 0.117 x 0.175 mm was mounted on a glass fiber and transferred to a Bruker SMART APEX II diffractometer system. The APEX3⁸⁷ program package was used to determine the unit-cell parameters and for data collection (10 sec/frame scan time). The raw frame data was processed using SAINT⁸⁸ and SADABS⁸⁹ to yield the reflection data file. Subsequent calculations were carried out using the SHELXTL⁹⁰ program package. The diffraction symmetry was *mmm* and the systematic absences were consistent with the orthorhombic space group *P2₁2₁2₁* that was later determined to be correct.

The structure was solved by direct methods and refined on F^2 by full-matrix least-squares techniques. The analytical scattering factors⁹¹ for neutral atoms were used throughout the analysis. Hydrogen atoms H3, H4, and disordered hydrogen atoms H13A-H13F were located from a difference-Fourier map and refined (x, y, z and U_{iso}). All other hydrogen atoms were included using a riding model.

Least squares analysis yielded $wR2 = 0.0648$ and $Goof = 1.083$ for 191 variables refined against 2208 data (0.83\AA), $R1 = 0.0254$ for those 2171 data with $I > 2.0\sigma(I)$. The absolute structure was assigned by refinement of the Flack parameter.⁹²

Definitions:

$$wR2 = [\Sigma[w(F_o^2 - F_c^2)^2] / \Sigma[w(F_o^2)^2]]^{1/2}$$

$$R1 = \Sigma||F_o| - |F_c|| / \Sigma|F_o|$$

$Goof = S = [\Sigma[w(F_o^2 - F_c^2)^2] / (n-p)]^{1/2}$ where n is the number of reflections and p is the total number of parameters refined.

Table 5-7 Crystal data and structure refinement for **5-155** (sdr60).

Identification code	sdr60 [Charles Dooley]	
Empirical formula	C ₁₃ H ₁₆ O ₅	
Formula weight	252.26	
Temperature	93(2) K	
Wavelength	1.54178 Å	
Crystal system	Orthorhombic	
Space group	P2 ₁ 2 ₁ 2 ₁	
Unit cell dimensions	$a = 6.3157(4)$ Å	$\alpha = 90^\circ$.
	$b = 12.3291(8)$ Å	$\beta = 90^\circ$.
	$c = 15.3236(10)$ Å	$\gamma = 90^\circ$.
Volume	1193.20(13) Å ³	
Z	4	
Density (calculated)	1.404 Mg/m ³	
Absorption coefficient	0.905 mm ⁻¹	
F(000)	536	

Crystal color	colorless
Crystal size	0.175 x 0.117 x 0.091 mm ³
Theta range for data collection	4.603 to 69.060°
Index ranges	-7 ≤ h ≤ 7, -13 ≤ k ≤ 14, -18 ≤ l ≤ 18
Reflections collected	46956
Independent reflections	2208 [R(int) = 0.0473]
Completeness to theta = 67.679°	100.0 %
Absorption correction	Semi-empirical from equivalents
Max. and min. transmission	0.7532 and 0.7032
Refinement method	Full-matrix least-squares on F ²
Data / restraints / parameters	2208 / 0 / 191
Goodness-of-fit on F ²	1.083
Final R indices [I > 2σ(I) = 2171 data]	R1 = 0.0254, wR2 = 0.0645
R indices (all data, 0.83 Å)	R1 = 0.0259, wR2 = 0.0648
Absolute structure parameter	0.02(5)
Largest diff. peak and hole	0.150 and -0.185 e.Å ⁻³

5.7 References

- ¹ Fukuyama, Y.; Huang, J.-M. Chemistry and neurotrophic activity of seco-prezizaane- and anisactone-type sesquiterpenes from *Illicium* species. *Studies in Nat. Prod. Chem.* **2005**, *32*, 395–427.
- ² (a) Song, T.-F.; Zhang, W.-F.; Xia, X.-H.; Shen, Y.-H.; Liu, C.-M.; Lin, S.; Jin, L.-H.; Li, H.-L. Two new acorane sesquiterpenes from *Illicium henryi*. *Arch. Pharm. Res.* **2009**, *32*, 1233–1236. (b) Y.; Shida, N.; Kodama, M.; Chaki, H.; Yumagi, T. Tricycloillicinone, a Novel Prenylated C₆-C₃ Compound Increasing Choline Acetyltransferase (ChAT) Activity, Isolated from *Illicium tashiroi*. *Chem. Pharm. Bull.* **1995**, *43*, 2270–2272. (c) Ngo, K.-S.; Brown, G. D. *Tetrahedron* **1999**, *55*, 759–770. (e) Huang, J.-m.; Yokoyama, R.; Yang, C.-s.; Fukuyama, Y. Merrillactone A, a novel neurotrophic sesquiterpene dilactone from *Illicium merrillianum*. *Tetrahedron Lett.* **2000**, *41*, 6111–6114. (f) Sy, L.-K.; Brown, G. D. A sesquiterpene class from *Illicium dunnianum*. *Phytochemistry* **1998**, *47*, 301–302.
- ³ Lane, J. F.; Koch, W. T.; Leeds, N. S.; Gorin, G. On the Toxin of *Illicium Anisatum*. I. The Isolation and Characterization of a Convulsant Principle: Anisatin. *J. Am. Chem. Soc.* **1952**, *74*, 3211–3215.
- ⁴ (a) Yamada, K.; Takada, S.; Nakamura, S.; Hirata, Y. The structure of anisatin. *Tetrahedron Lett.* **1965**, *6*, 4797–4801. (b) Yamada, K.; Takada, S.; Nakamura, S.; Hirata, Y. The structures of anisatin and neoanisatin: Toxic sesquiterpenes from *Illicium Anisatum* L. *Tetrahedron* **1968**, *24*, 199–229.
- ⁵ Schmidt, T. J.; Gurrath, M.; Ozoe, Y. Structure–activity relationships of *seco*-prezizaane and picrotoxane/picrodendrane terpenoids by *Quasar* receptor-surface modeling. *Bioorg. Med. Chem.* **2004**, *12*, 4159–4165.
- ⁶ Bormann, J. The ‘ABC’ of GABA receptors. *Trends Pharmacol. Sci.* **2000**, *21*, 16–19.
- ⁷ Lu, H.-H.; Martinez, M. D.; Shenvi, R. A. An eight-step gram-scale synthesis of (–)-jiadifenolide. *Nature Chem.* **2015**, *7*, 604–607.
- ⁸ Witkin, J. M.; Shenvi, R. A.; Li, X.; Gleason, S. D.; Weiss, J.; Morrow, D.; Catow, J. T.; Wakulchik, M.; Ohtawa, M.; Lu, H.-H.; Martinez, M. D.; Schkeryantz, J. M.; Carpenter, T. S.; Lightstone, F. C.; Cerne, R. Pharmacological characterization of the neurotrophic sesquiterpene jiadifenolide reveals a non-convulsant signature and potential for progression in neurodegenerative disease studies. *Biochem. Pharm.* **2018**, *155*, 61–70.
- ⁹ Shenvi, R. A. Neurite outgrowth enhancement by jiadifenolide: possible targets. *Nat. Prod. Rep.* **2016**, *33*, 535–539.

- ¹⁰ (a) Urabe, D.; Inoue, M. Total syntheses of sesquiterpenes from *Illicium* species. *Tetrahedron* **2009**, *65*, 6271–6289.
- (b) Condakes, M. L.; Novaes, L. F. T.; Maimone, T. J. Contemporary Synthetic Strategies toward *seco*-Prezizaane Sesquiterpenes from *Illicium* Species. *J. Org. Chem.* **2018**, *83*, 14843–14852.
- ¹¹ Cho, Y. S.; Carcache, D. A.; Tian, Y.; Li, Y.-M.; Danishefsky, S. J. Total Synthesis of (±)-Jiadifenin, a Non-peptidyl Neurotrophic Modulator. *J. Am. Chem. Soc.* **2004**, *126*, 14358–14359.
- ¹² Yokoyama, R.; Huang, J.-M.; Yang, C.-S.; Fukuyama, Y. New *seco*-Prezizaane-Type Sesquiterpenes, Jiadifenin with Neurotrophic Activity and 1,2-Dehydroneomajucin from *Illicium jiadifengpi*. *J. Nat. Prod.* **2002**, *65*, 527–531.
- ¹³ Carcache, D. A.; Cho, Y. S.; Hua, Z.; Tian, Y.; Li, Y.-M.; Danishefsky, S. J. Total Synthesis of (±)-Jiadifenin and Studies Directed to Understanding Its SAR: Probing Mechanistic and Stereochemical Issues in Palladium-Mediated Allylation of Enolate-Like Structures. *J. Am. Chem. Soc.* **2006**, *128*, 1016–1022.
- ¹⁴ Xu, J.; Trzoss, L.; Chang, W. K.; Theodorakis, E. A. Enantioselective Total Synthesis of (–)-Jiadifenolide. *Angew. Chem. Int. Ed.* **2011**, *50*, 3672–3676.
- ¹⁵ Trzoss, L.; Xu, J.; Lacoske, M. H.; Mobley, W. C.; Theodorakis, E. A. Enantioselective Synthesis of (–)-Jiadifenin, a Potent Neurotrophic Modulator. *Org. Lett.* **2011**, *13*, 4554–4557.
- ¹⁶ Trzoss, L.; Xu, J.; Lacoske, M. H.; Mobley, W. C.; Theodorakis, E. A. *Illicium* Sesquiterpenes: Divergent Synthetic Strategy and Neurotrophic Activity Studies. *Chem. Eur. J.* **2013**, *19*, 6398–6408.
- ¹⁷ Yang, Y.; Fu, X.; Chen, J.; Zhai, H. Total Synthesis of (–)-Jiadifenin. *Angew. Chem. Int. Ed.* **2012**, *51*, 9825–9828.
- ¹⁸ Siler, D. A.; Mighion, J. D.; Sorensen, E. J. An Enantiospecific Synthesis of Jiadifenolide. *Angew. Chem. Int. Ed.* **2014**, *53*, 5332–5335.
- ¹⁹ Reich, H. J.; Peake, S. L. Hypervalent organoiodine chemistry. Syn elimination of alkyl iodoso compounds. *J. Am. Chem. Soc.* **1978**, *100*, 4888–4889.
- ²⁰ Paterson, I.; Xuan, M.; Dalby, S. M. Total Synthesis of Jiadifenolide. *Angew. Chem. Int. Ed.* **2014**, *53*, 7286–7289.
- ²¹ Ohtawa, M.; Krambis, M. J.; Cerne, R.; Schkeryantz, J. M.; Witkin, J. M.; Shenvi, R. A. Synthesis of (–)-11-O-Debenzoyltashironin: Neurotrophic Sesquiterpenes Cause Hyperexcitation. *J. Am. Chem. Soc.* **2017**, *139*, 9637–9644.
- ²² Huffman, B. J.; Chu, T.; Hanaki, Y.; Wong, J. J.; Chen, S.; Houk, K. N.; Shenvi, R. A. Stereodivergent Attached-Ring Synthesis via Non-Covalent Interactions: A Short Formal Synthesis of Merrilactone A. *Angew. Chem. Int. Ed.* **2022**, e202114514.

- ²³ Shen, Y.; Li, L.; Pan, Z.; Wang, Y.; Li, J.; Wang, K.; Wang, X.; Zhang, Y.; Hu, T.; Zhang, Y. Protecting-Group-Free Total Synthesis of (–)-Jiadifenolide: Development of a [4 + 1] Annulation toward Multisubstituted Tetrahydrofurans. *Org. Lett.* **2015**, *17*, 5480–5483.
- ²⁴ Colvin, E. W.; Hamill, B. J. One-step conversion of carbonyl compounds into acetylenes. *J. Chem. Soc., Chem. Commun.* **1973**, 151–152.
- ²⁵ Cheng, X.; Micalizio, G. C. Synthesis of Neurotrophic *Seco*-prezizaane Sesquiterpenes (1R,10S)-2-Oxo-3,4-dehydroneomajucin, (2S)-Hydroxy-3,4-dehydroneomajucin, and (–)-Jiadifenin. *J. Am. Chem. Soc.* **2016**, *138*, 1150–1153.
- ²⁶ (a) Greszler, S. N.; Reichard, H. A.; Micalizio, G. C. Asymmetric Synthesis of Dihydroindanes by Convergent Alkoxide-Directed Metallacycle-Mediated Bond Formation. *J. Am. Chem. Soc.* **2012**, *134*, 2766–2774. (b) Jeso, V.; Aquino, C.; Cheng, X.; Mizoguchi, H.; Nakashige, M.; Micalizio, G. C. Synthesis of Angularly Substituted Trans-Fused Hydroindanes by Convergent Coupling of Acyclic Precursors. *J. Am. Chem. Soc.* **2014**, *136*, 8209–8212. (c) Cheng, X.; Micalizio, G. C. An Annulation Reaction for the Synthesis of Cross-Conjugated Triene-Containing Hydroindanes from Acyclic Precursors. *Org. Lett.* **2014**, *16*, 5144–5147. (d) Mizoguchi, H.; Micalizio, G. C. Synthesis of Highly Functionalized Decalins via Metallacycle-Mediated Cross-Coupling. *J. Am. Chem. Soc.* **2015**, *137*, 6624–6628.
- ²⁷ Condakes, M. L.; Hung, K.; Harwood, S. J.; Maimone, T. J. Total Syntheses of (–)-Majucin and (–)-Jiadifenoxolane A, Complex Majucin-Type *Illicium* Sesquiterpenes. *J. Am. Chem. Soc.* **2017**, *139*, 17783–17786.
- ²⁸ Hung, K.; Condakes, M. L.; Novaes, L. F. T.; Harwood, S. J.; Morikawa, T.; Yang, Z.; Maimone, T. J. Development of a Terpene Feedstock-Based Oxidative Synthetic Approach to the *Illicium* Sesquiterpenes. *J. Am. Chem. Soc.* **2019**, *141*, 3083–3099.
- ²⁹ Hill, C. K.; Hartwig, J. F. Site-selective oxidation, amination and epimerization reactions of complex polyols enabled by transfer hydrogenation. *Nat. Chem.* **2017**, *9*, 1213–1221.
- ³⁰ Gomes, J.; Daeppen, C.; Liffert, R.; Roesslein, J.; Kaufmann, E.; Heikinheimo, A.; Neuburger, M.; Gademann, K. Formal Total Synthesis of (–)-Jiadifenolide and Synthetic Studies toward *seco*-Prezizaane-Type Sesquiterpenes. *J. Org. Chem.* **2016**, *81*, 11017–11034.
- ³¹ Daeppen, C. A. Total Syntheses of (–)-Fragin and Valdiazen, and Synthetic Studies Toward Complex Neuritogenic Terpenoids, PhD Thesis, University of Basel, 2017; DOI: 10.5451/unibas-006781426

- ³² Kubo, M.; Kobayashi, K.; Huang, J.-M.; Harada, K.; Fukuyama, Y. The first examples of *seco*-prezizaane-type norsesquiterpenoids with neurotrophic activity from *Illicium jiadifengpi*. *Tetrahedron Lett.* **2012**, *53*, 1231–1235.
- ³³ Ohtani, I.; Kusumi, T.; Kashman, Y.; Kakisawa, H. High-field FT NMR application of Mosher's method. The absolute configurations of marine terpenoids. *J. Am. Chem. Soc.* **1991**, *113*, 4092–4096.
- ³⁴ (a) Trost, B. M.; Crawley, M. L. Asymmetric Transition-Metal-Catalyzed Allylic Alkylations: Applications in Total Synthesis. *Chem. Rev.* **2003**, *103*, 2921. (b) Trost, B. M. Metal catalyzed allylic alkylation: its development in the Trost laboratories. *Tetrahedron* **2015**, *71*, 5708–5733.
- ³⁵ Trost, B. M.; Jiang, C. Atom Economic Asymmetric Creation of Quaternary Carbon: Regio- and Enantioselective Reactions of a Vinylepoxyde with a Carbon Nucleophile. *J. Am. Chem. Soc.* **2001**, *123*, 12907–12908.
- ³⁶ Wu, Y.; Du, C.; Hu, C.; Li, Y.; Xie, Z. Biomimetic Synthesis of Hyperolactones. *J. Org. Chem.* **2011**, *76*, 4075–4081.
- ³⁷ (a) Christoffers, J.; Werner, T. Cerium-catalyzed α -Oxidation of β -Dicarbonyl Compounds with Molecular Oxygen. *Synlett* **2002**, *1*, 119–121. (b) Christoffers, J.; Kauf, T.; Werner, T.; Rössle, M. Cerium-Catalyzed α -Hydroxylation Reactions of α -Cyclopropyl β -Dicarbonyl Compounds with Molecular Oxygen. *Eur. J. Org. Chem.* **2006**, *2006*, 2601–2608.
- ³⁸ For a review on α -hydroxylation methods, see: Christoffers, J.; Baro, A.; Werner, T. α -Hydroxylation of β -Dicarbonyl Compounds. *Adv. Synth. Catal.* **2004**, *346*, 143–151.
- ³⁹ (a) Davis, F. A.; Sheppard, A. C. Applications of oxaziridines in organic synthesis. *Tetrahedron* **1989**, *45*, 5703–5742. (b) Davis, F. A.; Chen, B.-C. Asymmetric hydroxylation of enolates with N-sulfonyloxaziridines. *Chem. Rev.* **1992**, *92*, 919–934. (c) Chen, B.-C.; Zhou, P.; Davis, F. A.; Ciganek, E. α -Hydroxylation of Enolates and Silyl Enol Ethers. *Org. React.* **2003**, *62*, 1–356.
- ⁴⁰ Acocella, M. R.; Mancheño, O. G.; Bella, M.; Jørgensen, K. A. Organocatalytic Asymmetric Hydroxylation of β -Keto Esters: Metal-Free Synthesis of Optically Active *anti*-Diols. *J. Org. Chem.* **2004**, *69*, 8165–8167.
- ⁴¹ Saksena, A. K.; Mangiaracina, P. Recent studies on veratrum alkaloids: a new reaction of sodium triacetoxyborohydride [NaBH(OAc)₃]. *Tetrahedron Lett.* **1983**, *24*, 273–276.
- ⁴² (a) Seyferth, D.; Marmor, R. S.; Hilbert, P. Reactions of dimethylphosphono-substituted diazoalkanes. (MeO)₂P(O)CR transfer to olefins and 1,3-dipolar additions of (MeO)₂P(O)C(N₂)R. *J. Org. Chem.* **1971**, *36*, 1379–1386. (b) Gilbert, J. C.; Weerasooriya, U. Diazoethenes: their attempted synthesis from aldehydes and aromatic

ketones by way of the Horner-Emmons modification of the Wittig reaction. A facile synthesis of alkynes. *J. Org. Chem.* **1982**, *47*, 1837–1845.

⁴³ (a) Ohira, S. Methanolysis of Dimethyl (1-Diazo-2-oxopropyl) Phosphonate: Generation of Dimethyl (Diazomethyl) Phosphonate and Reaction with Carbonyl Compounds. *Synth. Commun.* **1986**, *19*, 561–564. (b) Müller, S. G.; Liepold, B.; Roth, G. J.; Bestmann, H. J. An Improved One-pot Procedure for the Synthesis of Alkynes from Aldehydes. *Synlett* **1996**, *1996*, 521–522. (c) Roth, G. J.; Liepold, B.; Müller, S. G.; Bestmann, H. J. Further Improvements of the Synthesis of Alkynes from Aldehydes. *Synthesis* **2004**, *1*, 59–62.

⁴⁴ Corey, E. J.; Fuchs, P. L. A synthetic method for formyl→ethynyl conversion ($\text{RCHO} \rightarrow \text{RC} \equiv \text{CH}$ or $\text{RC} \equiv \text{CR}'$). *Tetrahedron Lett.* **1972**, *13*, 3769–3772.

⁴⁵ Colvin, E. W.; Hamill, B. J. A simple procedure for the elaboration of carbonyl compounds into homologous alkyne. *J. Chem. Soc., Perkin Trans I*, **1977**, 869–874.

⁴⁶ (a) Pauson, P. L. The khand reaction : A convenient and general route to a wide range of cyclopentenone derivatives. *Tetrahedron* **1985**, *41*, 5855–5860. (b) Chung, Y. K. Transition metal alkyne complexes: the Pauson–Khand reaction. *Coor. Chem. Rev.* **1999**, *188*, 297–341. (c) Blanco-Urgoiti, J.; Añorbe, L.; Pérez-Serrano, L.; Domínguez, G.; Pérez-Castells, J.; The Pauson–Khand reaction, a powerful synthetic tool for the synthesis of complex molecules. *Chem. Soc. Rev.* **2004**, *33*, 32–42. (d) Strübing, D.; Beller, M. The Pauson–Khand Reaction. *Top. Organomet. Chem.* **2006**, *18*, 165–178. (e) Chen, S.; Jiang, C.; Zheng, N.; Yang, Z.; Shi, L. Evolution of Pauson-Khand Reaction: Strategic Applications in Total Syntheses of Architecturally Complex Natural Products (2016–2020). *Catalysts* **2020**, *10*, 1199.

⁴⁷ (a) Khand, I. U.; Knox, G. R.; Pauson, P. L.; Watts, W. E. A cobalt induced cleavage reaction and a new series of arenecobalt carbonyl complexes. *J. Chem. Soc. D; Chem. Commun.* **1971**, 36. (b) Khand, I. U.; Knox, G. R.; Pauson, P. L.; Watts, W. E. Organocobalt complexes. Part I. Arene complexes derived from dodecacarbonyltetracobalt. *J. Chem. Soc., Perkin Trans. I*, **1973**, 975–977.

⁴⁸ Magnus, P.; Exon, C.; Albaugh-Robertson, P. Dicobaltoctacarbonyl-alkyne complexes as intermediates in the synthesis of bicyclo[3.3.0]octenones for the synthesis of coriolin and hirsutic acid. *Tetrahedron* **1985**, *41*, 5861–5869.

⁴⁹ Huang, Z.; Huang, J.; Qu, Y.; Zhang, W.; Gong, J.; Yang, Z. Total Syntheses of Crinipellins Enabled by Cobalt-Mediated and Palladium-Catalyzed Intramolecular Pauson–Khand Reactions. *Angew. Chem. Int. Ed.* **2018**, *57*, 8744–8748.

- ⁵⁰ Zhao, N.; Xie, S.; Tian, P.; Tong, R.; Ning, C.; Xu, J. Asymmetric total synthesis of (+)-astellatol and (–)-astellatene. *Org. Chem. Front.* **2019**, *6*, 2014–2022.
- ⁵¹ (a) Qu, Z.; Wang, Z.; Zhang, Z.; Zhang, W.; Huang, J.; Yang, Z. Asymmetric Total Synthesis of (+)-Waihoensene. *J. Am. Chem. Soc.* **2020**, *142*, 6511–6515. (b) Peng, C.; Arya, P.; Zhou, Z.; Snyder, S. A. A Concise Total Synthesis of (+)-Waihoensene Guided by Quaternary Center Analysis. *Angew. Chem. Int. Ed.* **2020**, *59*, 13521–13525
- ⁵² Chang, Y.; Shi, L.; Huang, J.; Shi, L.; Zhang, Z.; Hao, H.-D.; Gong, J.; Yang, Z. Stereoselective Total Synthesis of (±)-5-epi-Cyanthiwigin I via an Intramolecular Pauson–Khand Reaction as the Key Step. *Org. Lett.* **2018**, *20*, 2876–2879.
- ⁵³ Chuang, K. V.; Xu, C.; Reisman, S. E. A 15-step synthesis of (+)-ryanodol. *Science* **2016**, *353*, 912–915.
- ⁵⁴ Kawamura, S.; Chu, H.; Felding, J.; Baran, P. S. Nineteen-step total synthesis of (+)-phorbol. *Nature* **2016**, *532*, 90–93.
- ⁵⁵ Jørgensen, L.; McKerrall, S. J.; Kuttruff, C. A.; Ungeheuer, F.; Felding, J.; Baran, P. S. 14-Step Synthesis of (+)-Ingenol from (+)-3-Carene. *Science* **2013**, *341*, 878–882.
- ⁵⁶ Jørgensen, L.; McKerrall, S. J.; Kuttruff, C. A.; Ungeheuer, F.; Felding, J.; Baran, P. S. 14-Step Synthesis of (+)-Ingenol from (+)-3-Carene. *Science* **2013**, *341*, 878–882.
- ⁵⁷ (a) Spartan, Wavefunction Inc., Irvine CA. (b) Shao, Y.; Gan, Z.; Epifanovsky, E.; Gilbert, A. T. B.; Wormit, M.; Kussmann, J.; Lange, A. W.; Behn, A.; Deng, J.; Feng, X.; Ghosh, D.; Goldey, M.; Horn, P. R.; Jacobson, L. D.; Kaliman, I.; Khaliullin, R. Z.; Kuś, T.; Landau, A.; Liu, J.; Proynov, E. I.; Rhee, Y. M.; Richard, R. M.; Rohrdanz, M. A.; Steele, R. P.; Sundstrom, E. J.; Woodcock, H. L., III; Zimmerman, P. M.; Zuev, D.; Albrecht, B.; Alguire, E.; Austin, B.; Beran, G. J. O.; Bernard, Y. A.; Berquist, E.; Brandhorst, K.; Bravaya, K. B.; Brown, S. T.; Casanova, D.; Chang, C.-M.; Chen, Y.; Chien, S. H.; Closser, K. D.; Crittenden, D. L.; Diedenhofen, M.; DiStasio, R. A., Jr.; Do, H.; Dutoi, A. D.; Edgar, R. G.; Fatehi, S.; FustiMolnar, L.; Ghysels, A.; Golubeva-Zadorozhnaya, A.; Gomes, J.; Hanson-Heine, M. W. D.; Harbach, P. H. P.; Hauser, A. W.; Hohenstein, E. G.; Holden, Z. C.; Jagau, T.-C.; Ji, H.; Kaduk, B.; Khistyayev, K.; Kim, J.; Kim, J.; King, R. A.; Klunzinger, P.; Kosenkov, D.; Kowalczyk, T.; Krauter, C. M.; Lao, K. U.; Laurent, A. D.; Lawler, K. V.; Levchenko, S. V.; Lin, C. Y.; Liu, F.; Livshits, E.; Lochan, R. C.; Luenser, A.; Manohar, P.; Manzer, S. F.; Mao, S.-P.; Mardirossian, N.; Marenich, A. V.; Maurer, S. A.; Mayhall, N. J.; Neuscamman, E.; Oana, C. M.; Olivares-Amaya, R.; O’Neill, D. P.; Parkhill, J. A.; Perrine, T. M.; Peverati, R.; Prociuk, A.; Rehn, D. R.; Rosta, E.; Russ, N. J.; Sharada, S. M.; Sharma, S.; Small, D. W.; Sodt, A.; Stein, T.; Stück,

D.; Su, Y.-C.; Thom, A. J. W.; Tsuchimochi, T.; Vanovschi, V.; Vogt, L.; Vydrov, O.; Wang, T.; Watson, M. A.; Wenzel, J.; White, A.; Williams, C. F.; Yang, J.; Yeganeh, S.; Yost, S. R.; You, Z.-Q.; Zhang, I. Y.; Zhang, X.; Zhao, Y.; Brooks, B. R.; Chan, G. K. L.; Chipman, D. M.; Cramer, C. J.; Goddard III, W. A.; Gordon, M. S.; Hehre, W. J.; Klamt, A.; Schaefer, H. F., III; Schmidt, M. W.; Sherrill, C. D.; Truhlar, D. G.; Warshel, A.; Xu, X.; Aspuru-Guzik, A.; Baer, R.; Bell, A. T.; Besley, N. A.; Chai, J.-D.; Dreuw, A.; Dunietz, B. D.; Furlani, T. R.; Gwaltney, S. R.; Hsu, C.-P.; Jung, Y.; Kong, J.; Lambrecht, D. S.; Liang, W.; Ochsenfeld, C.; Rassolov, V. A.; Slipchenko, L. V.; Subotnik, J. E.; Van Voorhis, T.; Herbert, J. M.; Krylov, A. I.; Gill, P. M. W.; Head-Gordon, M. *Advances in Molecular Quantum Chemistry Contained in the Q-Chem 4 Program Package. Molecular Physics* **2014**, *113*, 184–215.

⁵⁸ Shambayani, S.; Crowe, W. E.; Schreiber, S. L. N-oxide promoted pauson-khand cyclizations at room temperature. *Tetrahedron Lett.* **1990**, *31*, 5289–5292.

⁵⁹ Trost, B. M.; Jiang, C. Pd-Catalyzed Asymmetric Allylic Alkylation. A Short Route to the Cyclopentyl Core of Viridenomycin. *Org. Lett.* **2003**, *5*, 1563–1565.

^{60(a)} Weires, N. A.; Slutskyy, Y.; Overman, L. E. Facile Preparation of Spirolactones by an Alkoxy-carbonyl Radical Cyclization–Cross-Coupling Cascade. *Angew. Chem. Int. Ed.* **2019**, *58*, 8561–8565. (b) Allred, T. K.; Dieskau, A. P.; Zhao, P.; Lackner, G. L.; Overman, L. E. General Access to Concave-Substituted *cis*-Dioxabicyclo[3.3.0]octanones: Enantioselective Total Syntheses of Macfarlandin C and Dendrillolide A. *J. Org. Chem.* **2020**, *85*, 15532–15551.

⁶¹ Hayashi, M.; Hashimoto, Y.; Yamamoto, Y.; Usuki, J.; Saigo, K. Phosphane Sulfide/Octacarbonyldicobalt-Catalyzed Pauson–Khand Reaction Under an Atmospheric Pressure of Carbon Monoxide. *Angew. Chem. Int. Ed.* **2000**, *39*, 631–633.

⁶² Sugihara, T.; Yamada, M.; Yamaguchi, M.; Nishizawa, M. The Intra- and Intermolecular Pauson-Khand Reaction Promoted by Alkyl Methyl Sulfides. *Synlett* **1999**, *6*, 771–773.

⁶³ (a) Togo, H.; Fujii, M.; Yokoyama, M. Conversion of Hydroxyl Groups in Alcohols to Other Functional Groups with N-Hydroxy-2-thiopyridone, and Its Application to Dialkylamines and Thiols. *Bull. Chem. Soc. Jpn.* **1991**, *64*, 57–67. (b) Bachi, M. D.; Bosch, E. Synthesis of γ - and δ -lactones by free-radical annelation of Se-phenyl selenocarbonates. *J. Org. Chem.* **1992**, *57*, 4696–4705.

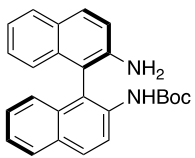
⁶⁴ McQueney, M. S.; Lee, S.-I.; Swartz, W. H.; Ammon, H. L.; Mariano, P. S.; Dunaway-Mariano, D. Evidence for an intramolecular, stepwise reaction pathway for PEP phosphomutase catalyzed phosphorus-carbon bond formation. *J. Org. Chem.* **1991**, *56*, 7121–7130.

- ⁶⁵ Fraser-Reid, B.; Holder, N. L.; Hicks, D. R.; Walker, D. L. Synthetic applications of the photochemically induced addition of oxycarbonyl species to α -enones. Part I. The addition of simple alcohols. *Can. J. Chem.* **1977**, *55*, 3978–3985.
- ⁶⁶ (a) Burtea, A.; DeForest, J.; Li, X.; Rychnovsky, S. D. Total Synthesis of (–)-Himeradine A. *Angew. Chem. Int. Ed.* **2019**, *58*, 16193–16197. (b) Chu, L.; Ohta, C.; Zuo, Z.; MacMillan, D. W. C. Carboxylic Acids as A Traceless Activation Group for Conjugate Additions: A Three-Step Synthesis of (\pm)-Pregabalin. *J. Am. Chem. Soc.* **2014**, *136*, 10886–10889.
- ⁶⁷ For a review, see: Nagata, W.; Yoshioka, M. Hydrocyanation of Conjugated Carbonyl Compounds. *Org. React.* **1977**, *25*, 255–476. For recent applications, see: (a) Murphy, S. K.; Zeng, M.; Herzon, S. B. A modular and enantioselective synthesis of the pleuromutilin antibiotics. *Science* **2017**, *356*, 956–959. (b) Johnson, R. E.; Ree, H.; Hartmann, M.; Lang, L.; Sawano, S.; Sarpong, R. Total Synthesis of Pentacyclic (–)-Ambiguine P Using Sequential Indole Functionalizations. *J. Am. Chem. Soc.* **2019**, *141*, 2233–2237. (c) Qu, P.; Snyder, S. A. Concise and Stereoselective Total Syntheses of Annotinolides C, D, and E. *J. Am. Chem. Soc.* **2021**, *143*, 11951–11956.
- ⁶⁸ (a) Utimoto, K.; Obayashi, M.; Shishiyama, Y.; Inoue, M.; Nozaki, H. Conjugated addition of cyanotrimethylsilane to α,β -unsaturated ketones. *Tetrahedron Lett.* **1980**, *21*, 3389–3392. (b) Utimoto, K.; Wakabayashi, Y.; Horie, T.; Inoue, M.; Shishiyama, Y.; Obayashi, M.; Nozaki, H. Cyanotrimethylsilane as a versatile reagent for introducing cyanide functionality. *Tetrahedron* **1983**, *39*, 967–973.
- ⁶⁹ Lee, J.; Kim, M.; Chang, S.; Lee, H.-Y. Anhydrous Hydration of Nitriles to Amides using Aldoximes as the Water Source. *Org. Lett.* **2009**, *11*, 5598–5601.
- ⁷⁰ (a) Kienzle, F.; Stadlwieserb, J.; Rank, W.; Schönholder, P. Die Synthese des Labdanditerpenes Erigerol und analoger Verbindungen. *Helv. Chim. Acta*, **1990**, *73*, 1108–1138. (b) Hylse, P.; Maier, L.; Kucera, R.; Perecko, T.; Svobodava, A.; Kubala, L.; Paruch, K.; Švenda, J. A Concise Synthesis of Forskolin. *Angew. Chem. Int. Ed.* **2017**, *56*, 12586–12589. (c) Thomas, W. P.; Schatz, D. J.; George, D. T.; Pronin, S. V. A Radical-Polar Crossover Annulation To Access Terpenoid Motifs. *J. Am. Chem. Soc.* **2019**, *141*, 12246–12250.
- ⁷¹ Zimmerman, H. E.; Wang, P. Inter- and Intramolecular Stereoselective Protonation of Enols. *J. Org. Chem.* **2002**, *67*, 9216–9226.
- ⁷² Birch, A.; Williamson, D. H. Homogeneous Hydrogenation Catalysts in Organic Synthesis. *Org. React.* **1976**, *24*, 1–186 and references cited therein.

- ⁷³ (a) Rychnovsky, S. D. Predicting NMR Spectra by Computational Methods: Structure Revision of Hexacyclinol. *Org. Lett.* **2006**, *8*, 2895–2898. (b) Cimino, P.; Gomez-Paloma, L.; Duca, D.; Riccio, R.; Bifulco, G. *Magn. Reson. Chem.* **2004**, *42*, S26–S33. (c) Lodewyk, M. W.; Siebert, M. W.; Tantillo, D. J. Computational Prediction of ¹H and ¹³C Chemical Shifts: A Useful Tool for Natural Product, Mechanistic, and Synthetic Organic Chemistry. *Chem. Rev.* **2012**, *112*, 1839–1862.
- ⁷⁴ Michalak, K.; Morawiak, M.; Wicha, J. Synthetic Approach to the Core Structure of Oleandrin and Related Cardiac Glycosides with Highly Functionalized Ring D. *Org. Lett.* **2016**, *18*, 6148–6151.
- ⁷⁵ For discussion of palladium nanoparticles, see: Wang, D.; Weinstein, A. B.; White, P. B.; Stahl, S. S. Ligand-Promoted Palladium-Catalyzed Aerobic Oxidation Reactions. *Chem. Rev.* **2018**, *118*, 2636–2679 and references therein.
- ⁷⁶ Khadem, El, H.; Hanessian, S. Ammonium Molybdate as Spraying Agent for Paper Chromatograms of Reducing Sugars. *Anal. Chem.* **1958**, *30*, 1965–1965.
- ⁷⁷ Trost, B. M.; Van Vranken, D. L.; Bingel, C. A modular approach for ligand design for asymmetric allylic alkylations via enantioselective palladium-catalyzed ionizations. *J. Am. Chem. Soc.* **1992**, *114*, 8327–9343.
- ⁷⁸ Hong, A. Y.; Stoltz, B. M. Enantioselective Total Synthesis of the Reported Structures of (–)-9-*epi*-Presilphiperfolan-1-ol and (–)-Presilphiperfolan-1-ol: Structural Confirmation and Reassignment and Biosynthetic Insights. *Angew. Chem. Int. Ed.* **2012**, *51*, 9674–9678.
- ⁷⁹ Murphy, G. K.; West, F. G. [1,2]- or [2,3]-Rearrangement of Onium Ylides of Allyl and Benzyl Ethers and Sulfides via in Situ-Generated Iodonium Ylides. *Org. Lett.* **2006**, *8*, 4359–4361.
- ⁸⁰ Sum, P.-E.; Weiler, L. Alkylation of β -keto-ester dianions with α -chloroethers. *J. Chem Soc., Chem. Commun.* **1977**, *3*, 91–92.
- ⁸¹ Masahiro, H.; Takeshi, N.; Shô, I. Trifunctional Chiral Synthons via Stereocontrolled Yeast Reduction. Preparation of Chiral Pentane-1,3,5-triol Derivatives. *Chem. Lett.* **1986**, *15*, 1381–1384.
- ⁸² (a) Mohapatra, D. K.; Umamaheshwar, G.; Rao, M. M.; Umadevi, D.; Yadav, J. S. Concise total synthesis of botryolide B. *RSC Adv.* **2014**, *4*, 8335–8340. (b) Lin, L.; Romano, C.; Mazet, C. Palladium-Catalyzed Long-Range Deconjugative Isomerization of Highly Substituted α,β -Unsaturated Carbonyl Compounds. *J. Am. Chem. Soc.* **2016**, *138*, 10344–10350.

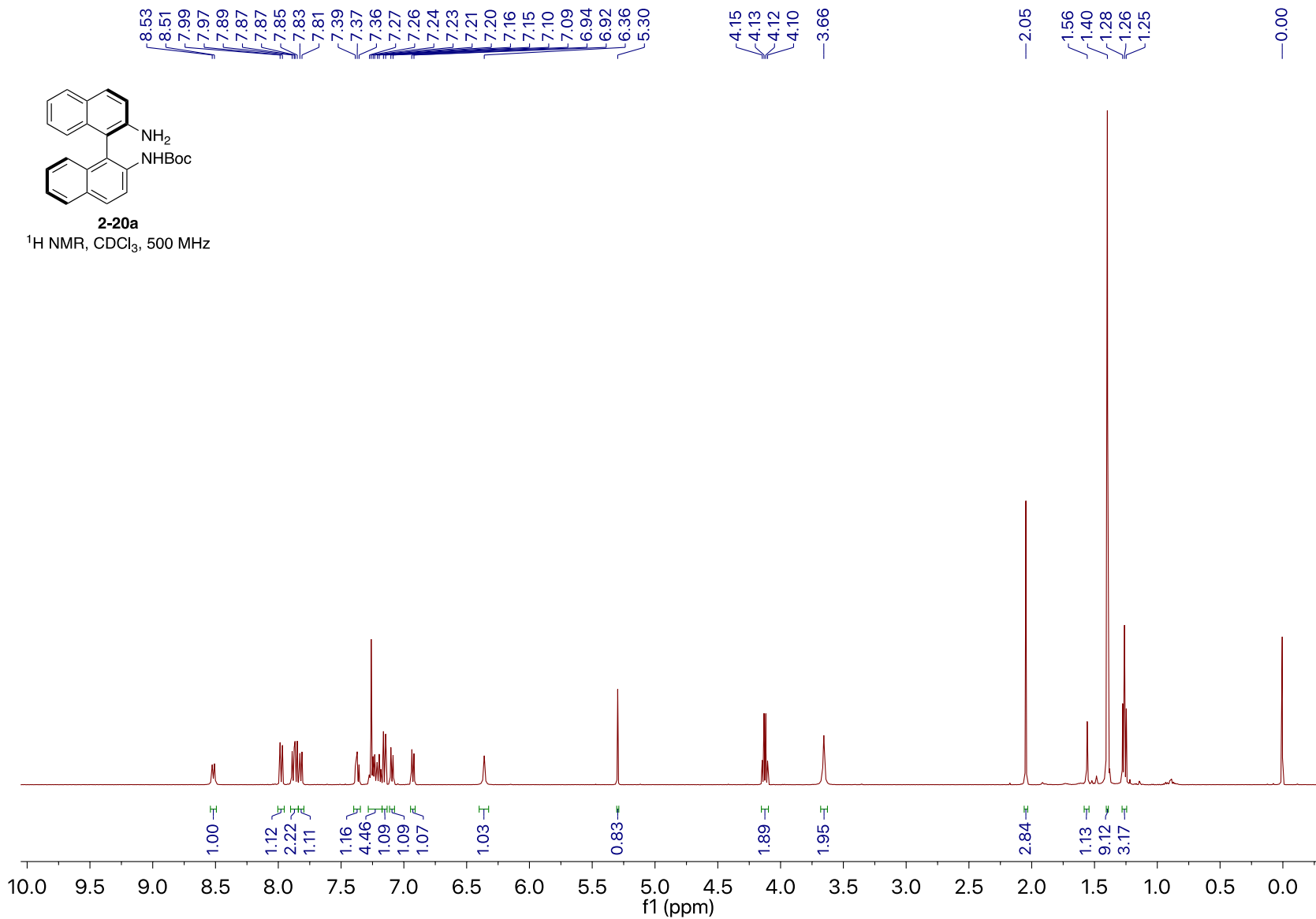
- ⁸³ Pasquali, M.; Leoni, P.; Sabatino, P.; Braga, D. Synthesis, Structure, and Reactivity of *fac*-Mo(CO)₃(DMF)₃ – Effect of Lewis Acids on the Substitution of DMF Ligands. *Gazz. Chim. Ital.* **1992**, *122*, 275–277.
- ⁸⁴ Trost, B. M.; Kunz, R. A. New synthetic reactions. Convenient approach to methyl 3-oxo-4-pentenoate. *J. Org. Chem.* **1974**, *39*, 2648–2650.
- ⁸⁵ Bakuzis, P.; Bakuzis, M. L. Oxidative functionalization of the β -carbon in α,β -unsaturated systems. Preparation of 3-phenylthio enones, acrylates, and other vinyl derivatives. *J. Org. Chem.* **1981**, *46*, 235–239.
- ⁸⁶ Rao, H. S. P.; Rafi, S.; Padmavathy, K. Facile and Efficient Synthesis of Ethyl 3-Oxo-5-arylthiopentanoates, the Precursors for Nazarov Reagent. *Lett. Org. Chem.* **2008**, *5*, 527–529.
- ⁸⁷ APEX3 Version 2017.3-0, Bruker AXS, Inc.; Madison, WI 2014.
- ⁸⁸ SAINT Version 8.38a, Bruker AXS, Inc.; Madison, WI 2013.
- ⁸⁹ Sheldrick, G. M. SADABS, Version 2014/5, Bruker AXS, Inc.; Madison, WI 2014.
- ⁹⁰ Sheldrick, G. M. SHELXTL, Version 2014/7, Bruker AXS, Inc.; Madison, WI 2014.
- ⁹¹ International Tables for Crystallography 1992, Vol. C., Dordrecht: Kluwer Academic Publishers.
- ⁹² Parsons, S., Flack, H. D., Wagner, T. Use of intensity quotients and differences in absolute structure refinement. *Acta Cryst.* **2013**, *B69*, 249–259.

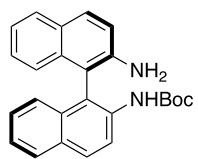
Appendix A: Spectral Data for Compounds in Chapter 2



2-20a

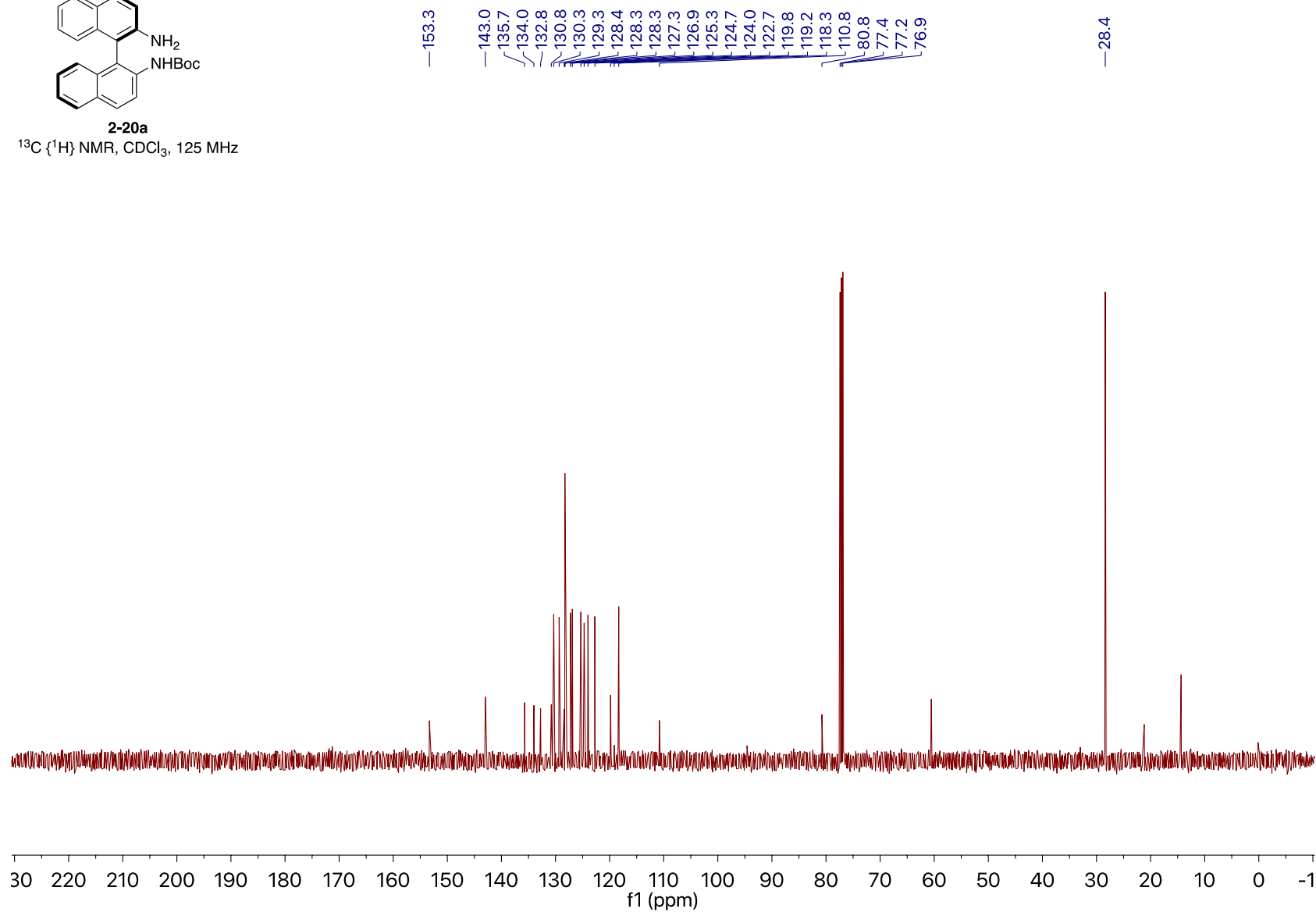
¹H NMR, CDCl₃, 500 MHz

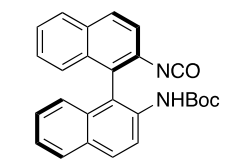




2-20a

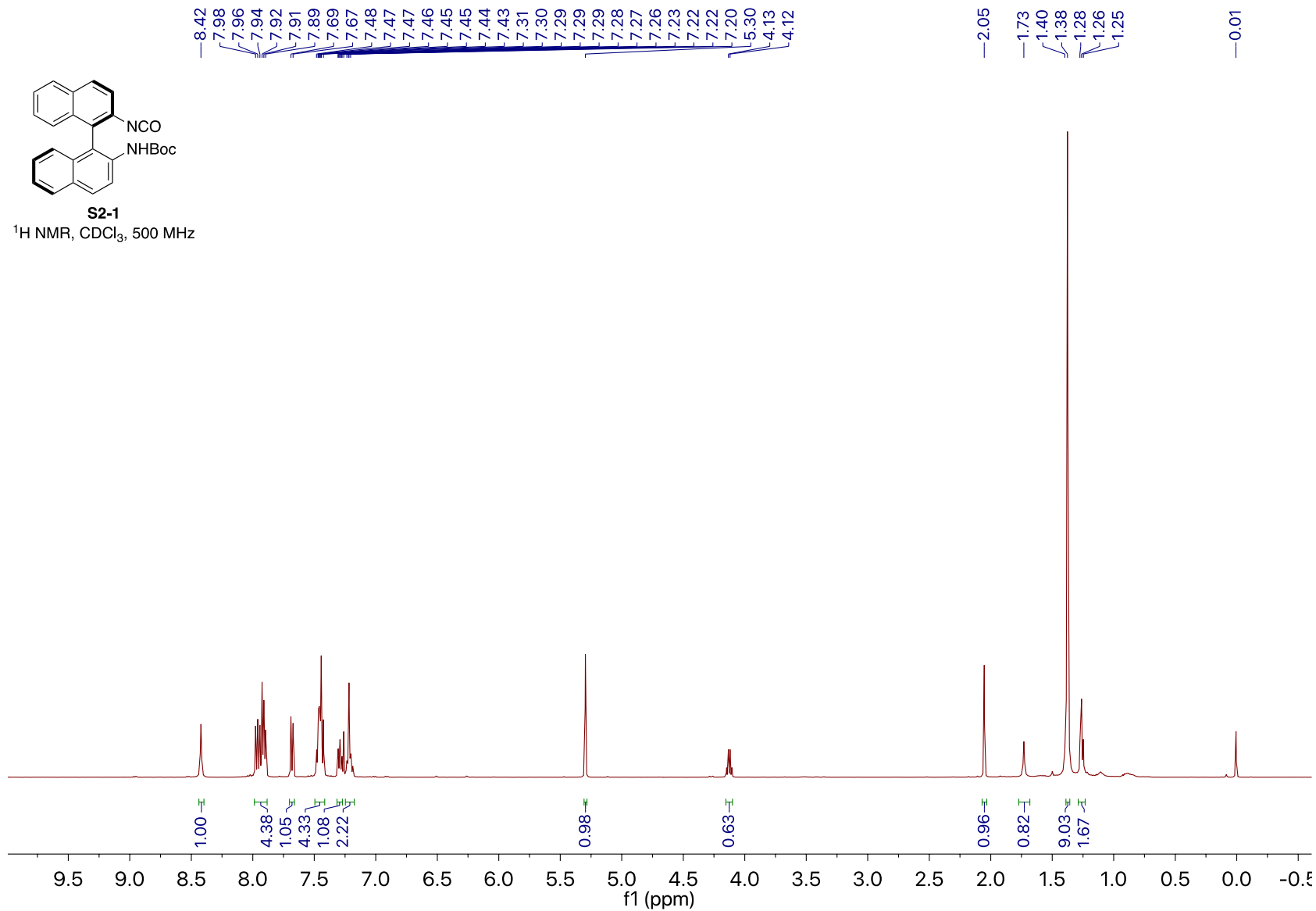
^{13}C $\{^1\text{H}\}$ NMR, CDCl_3 , 125 MHz

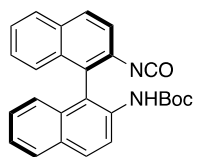




S2-1

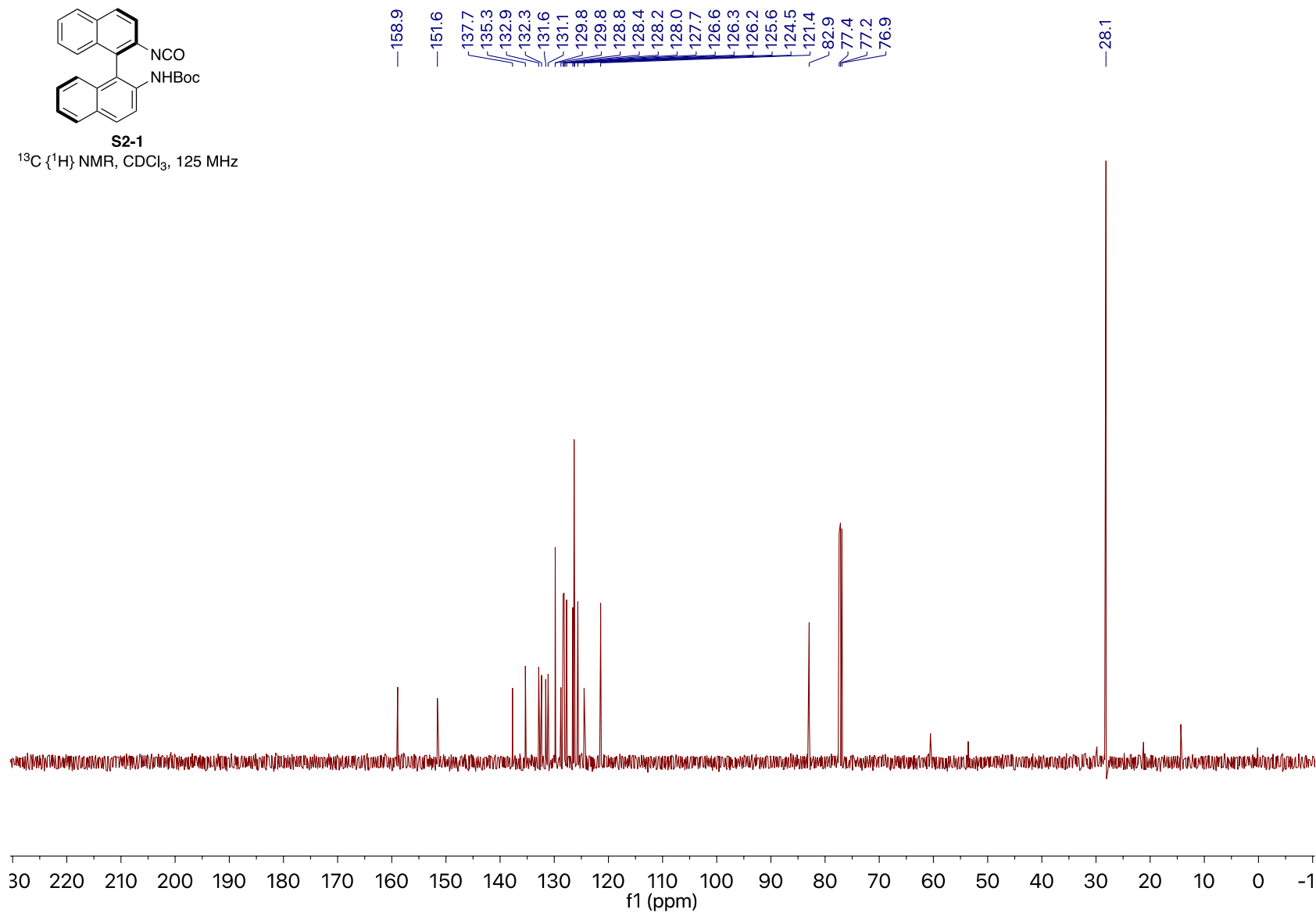
¹H NMR, CDCl₃, 500 MHz

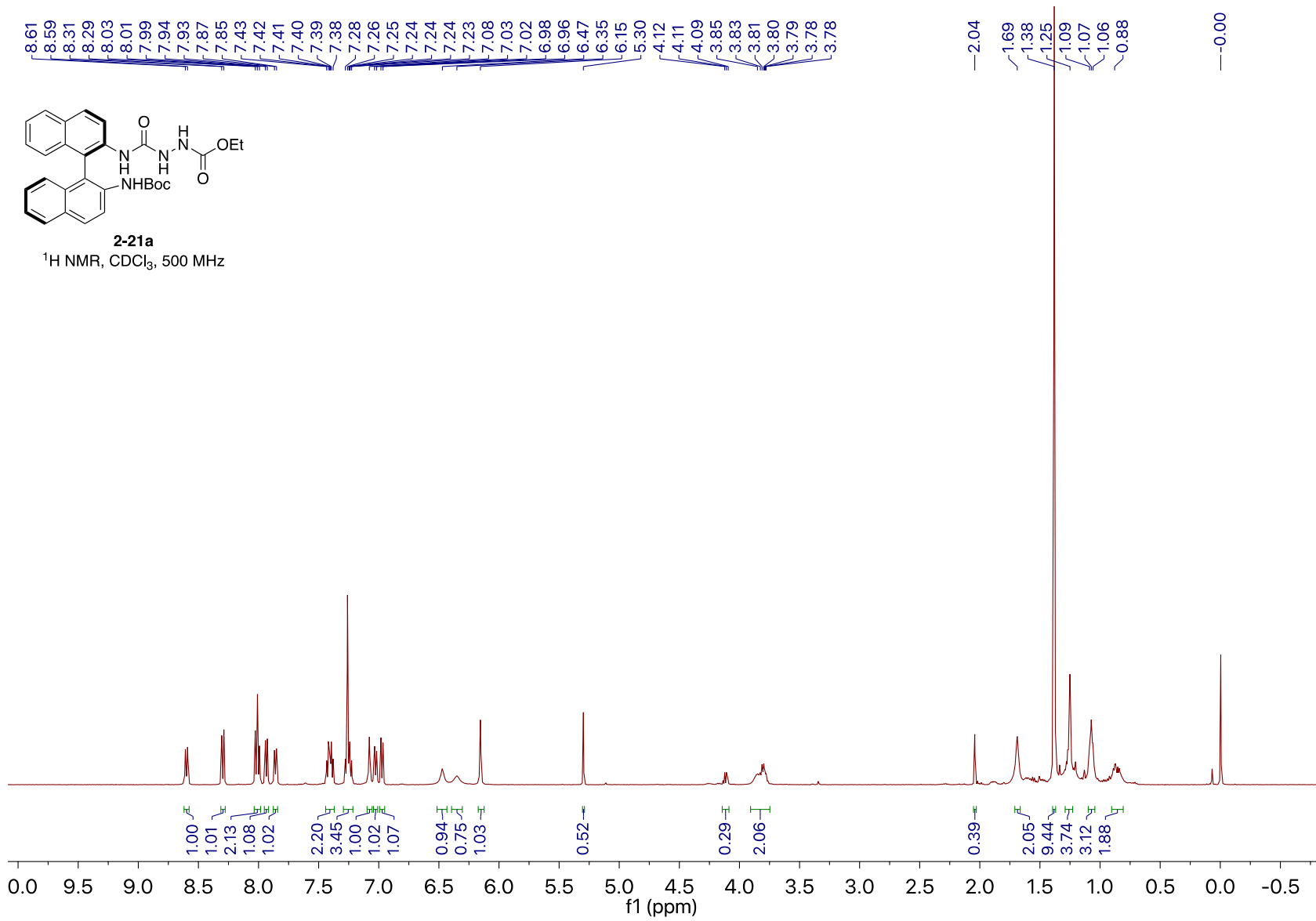


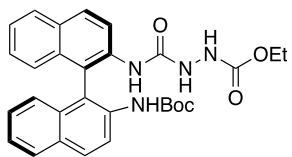


S2-1

^{13}C (^1H) NMR, CDCl_3 , 125 MHz

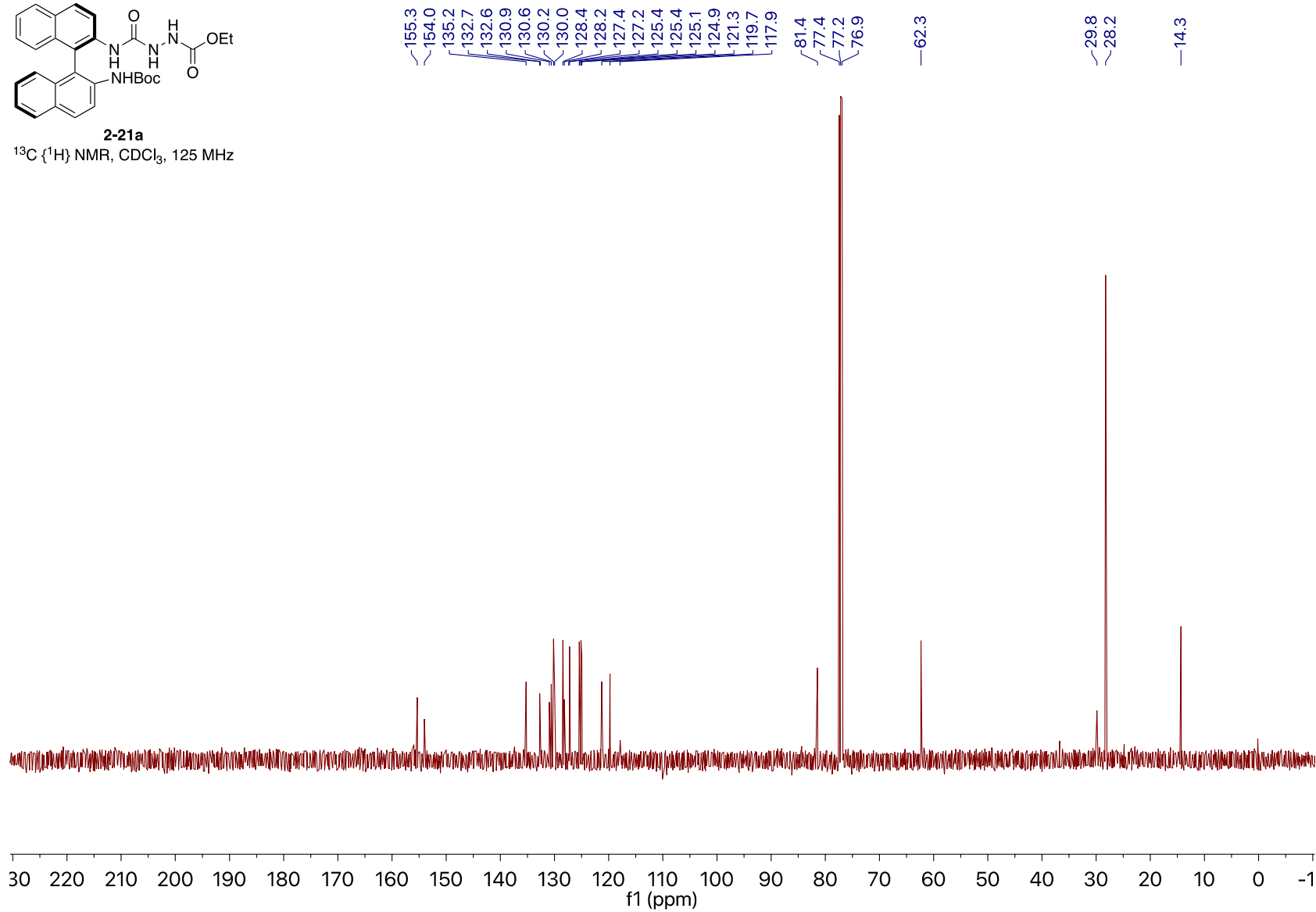


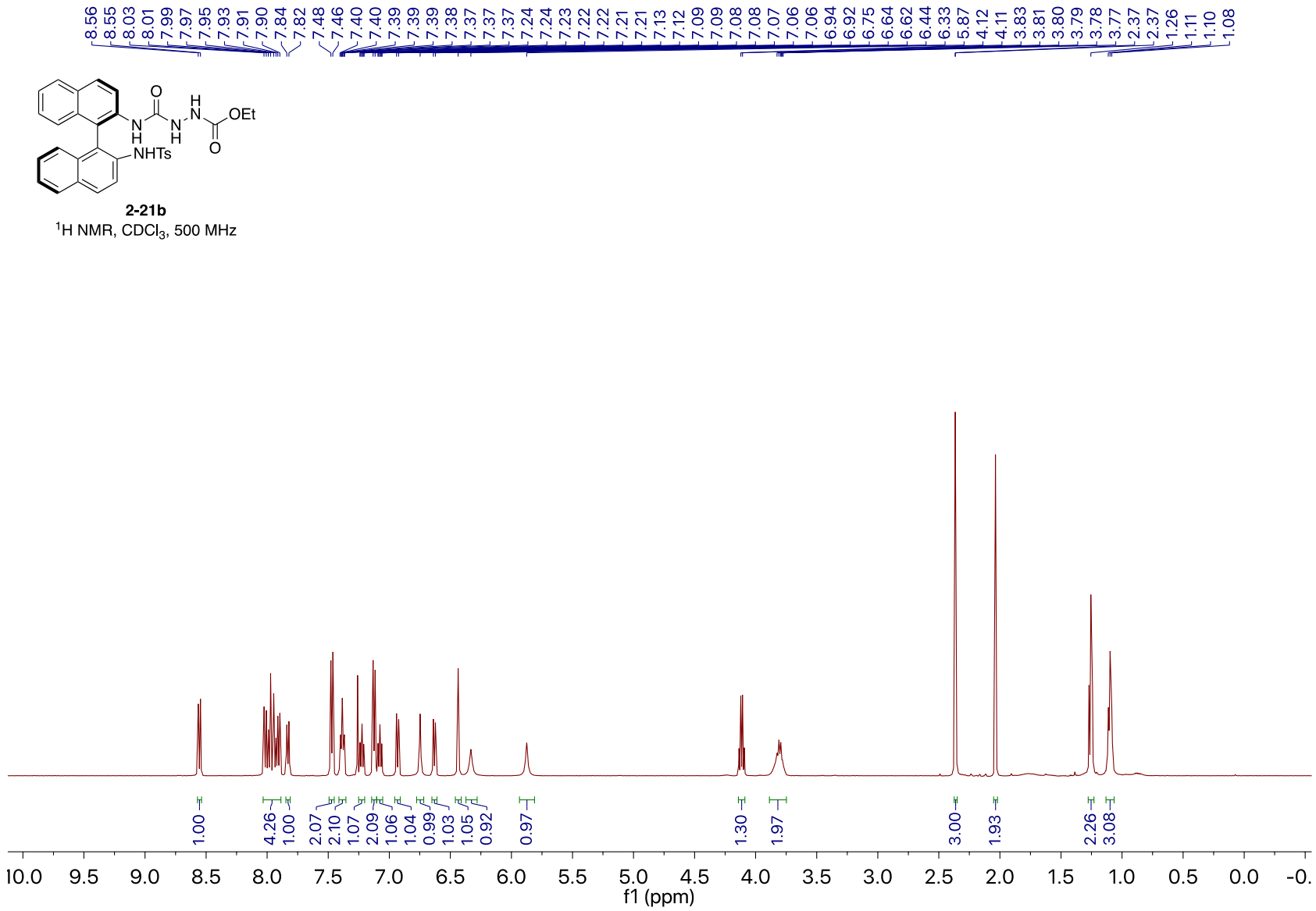


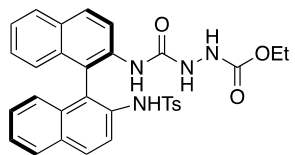


2-21a

^{13}C { ^1H } NMR, CDCl_3 , 125 MHz





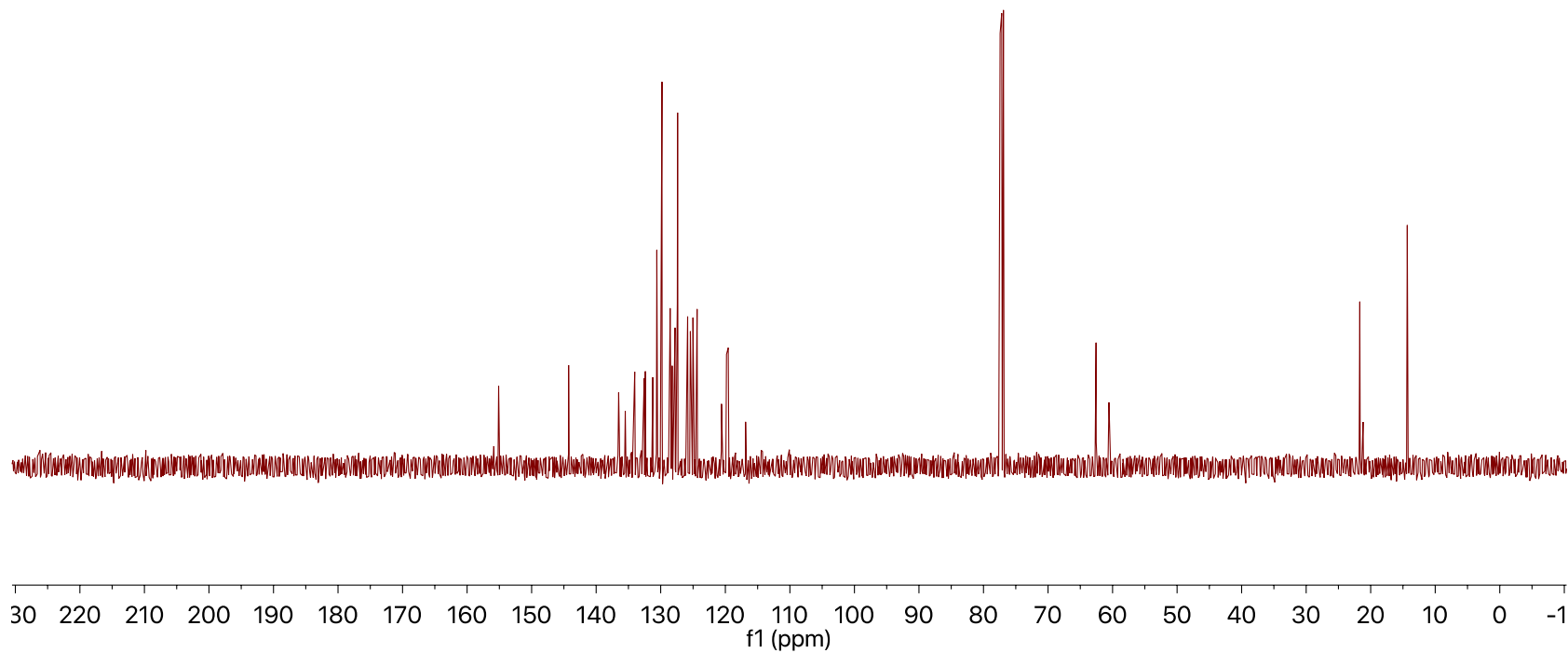


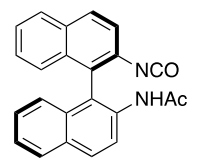
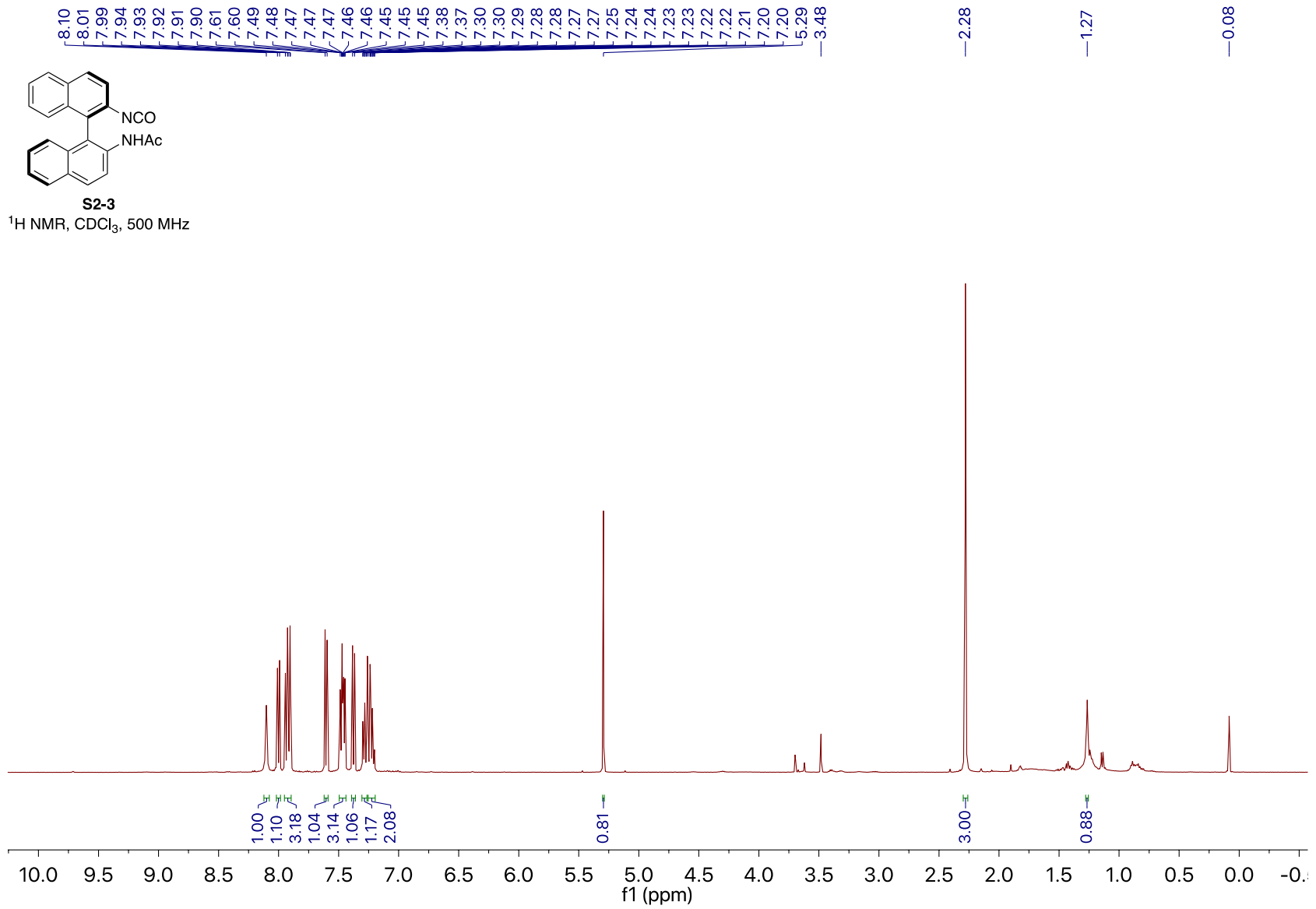
2-21b

^{13}C $\{^1\text{H}\}$ NMR, CDCl_3 , 125 MHz

— 155.12
— 144.28
— 136.53
— 135.50
— 134.04
— 132.56
— 132.39
— 131.24
— 130.62
— 130.51
— 129.80
— 128.54
— 128.23
— 127.79
— 127.44
— 127.38
— 125.84
— 125.42
— 125.01
— 124.37
— 120.59
— 119.81
— 119.55
— 116.86
— 77.41
— 77.16
— 76.91
— 62.56
— 60.54

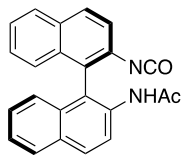
— 21.69
— 21.18
— 14.33





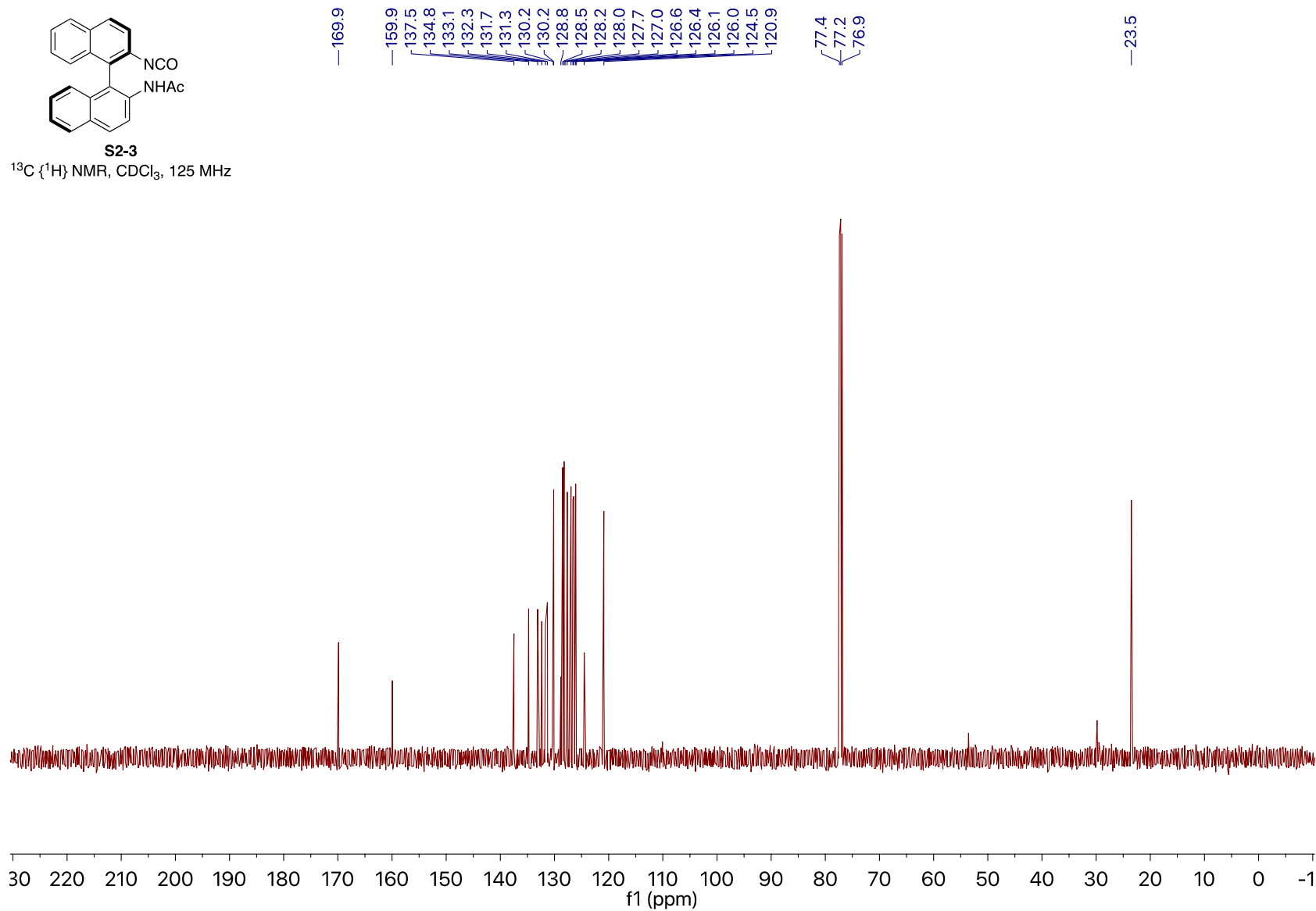
S2-3

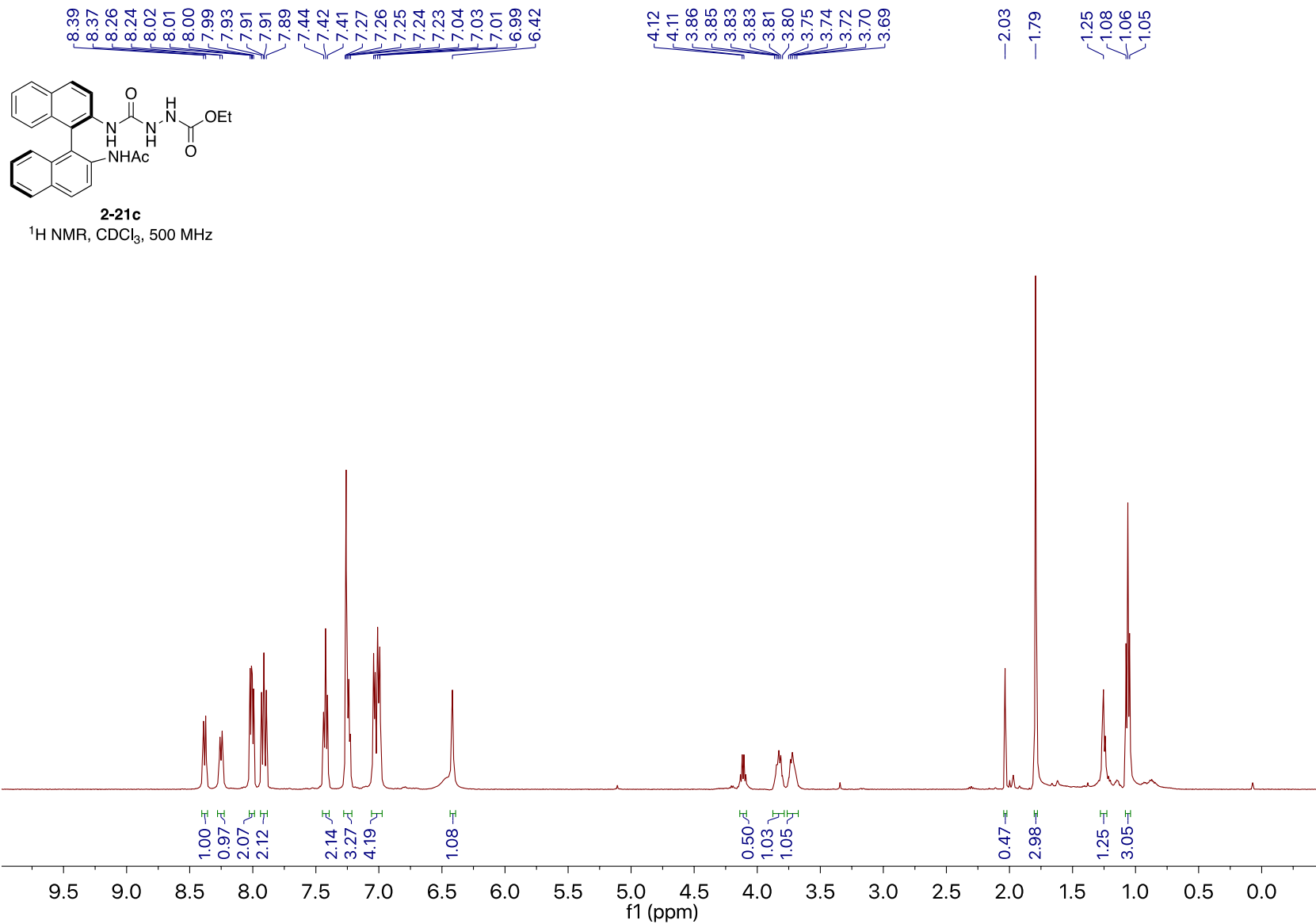
¹H NMR, CDCl₃, 500 MHz

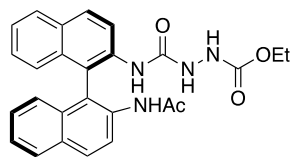


S2-3

^{13}C { ^1H } NMR, CDCl_3 , 125 MHz

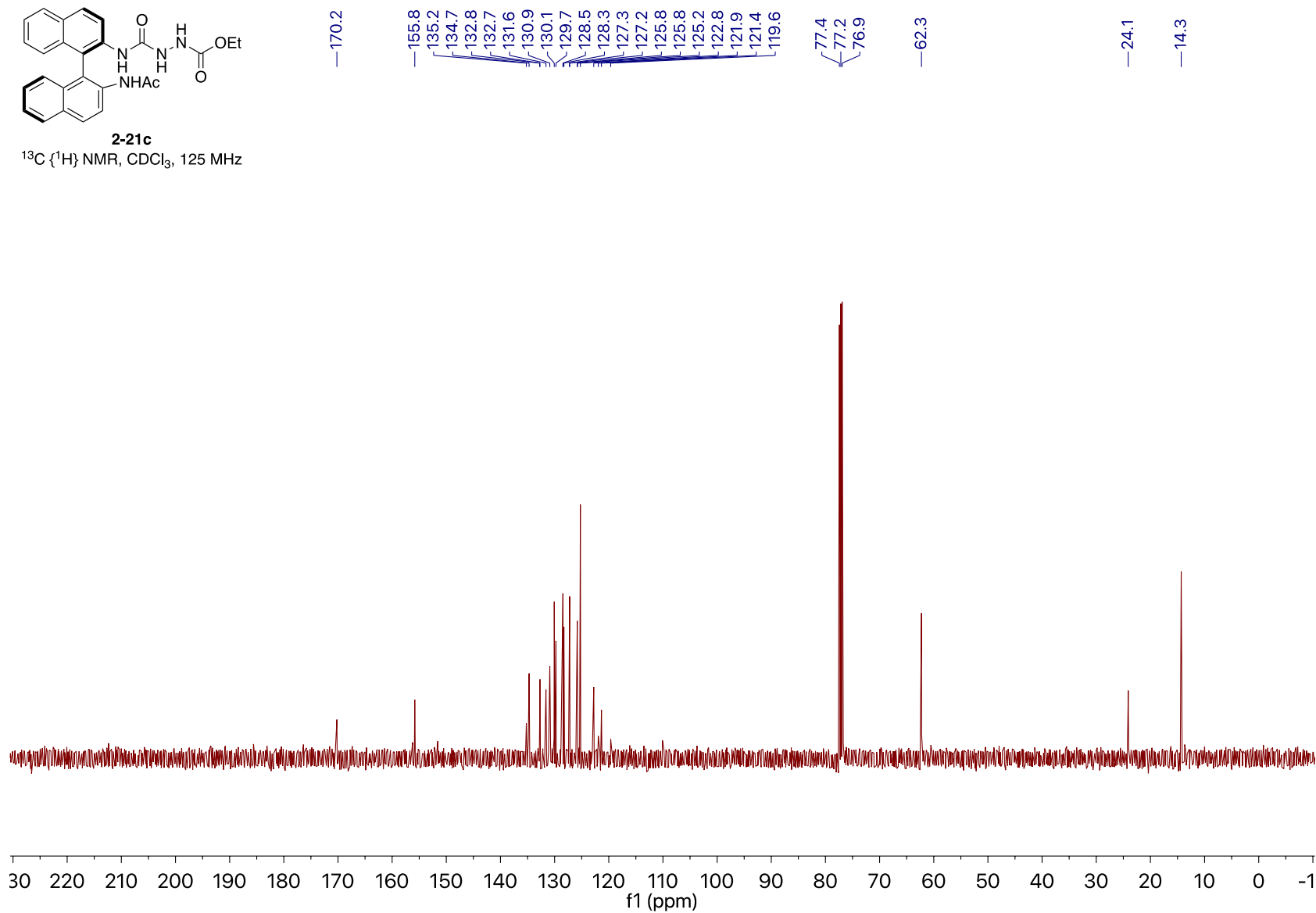




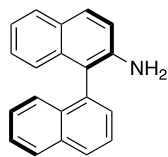


2-21c

^{13}C $\{^1\text{H}\}$ NMR, CDCl_3 , 125 MHz

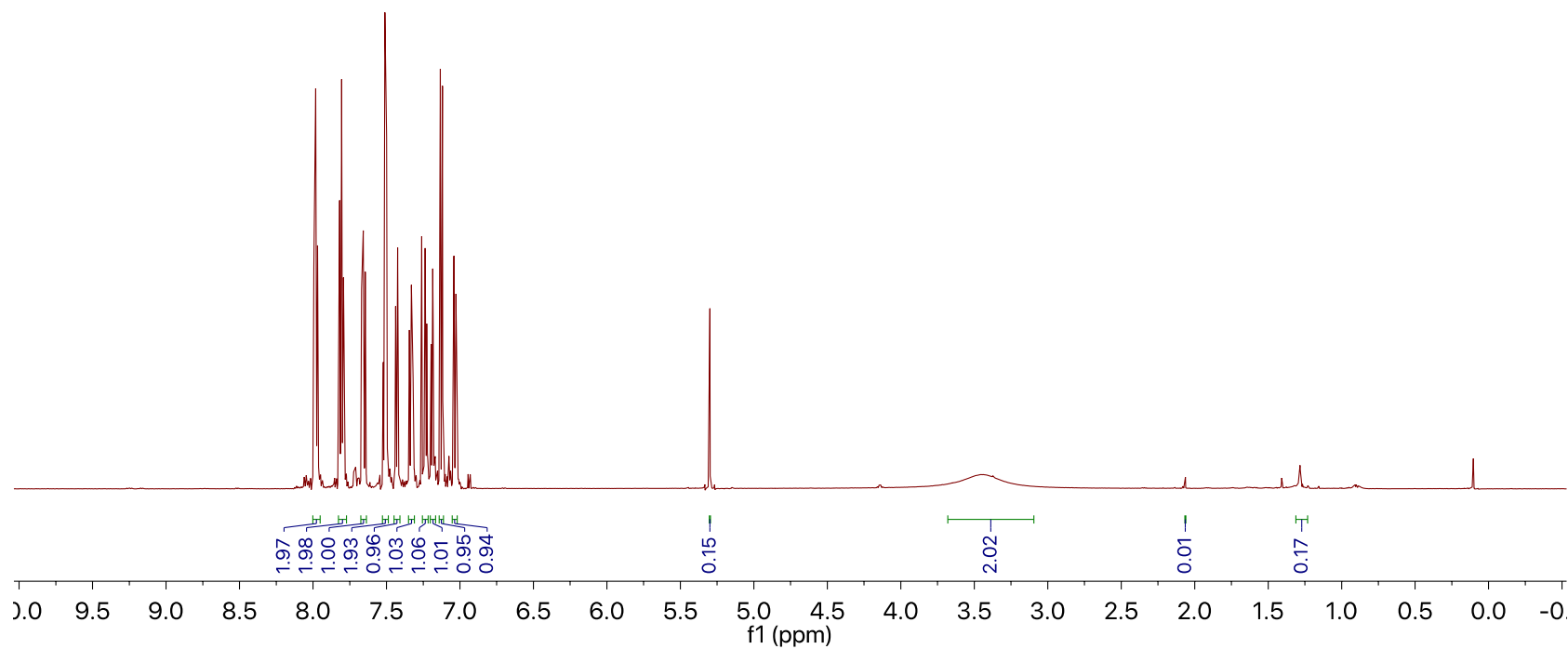


7.99
7.98
7.98
7.98
7.97
7.97
7.97
7.82
7.81
7.81
7.80
7.79
7.67
7.66
7.66
7.64
7.52
7.52
7.51
7.51
7.50
7.50
7.44
7.44
7.42
7.42
7.34
7.34
7.33
7.33
7.33
7.32
7.25
7.25
7.24
7.24
7.23
7.23
7.22
7.20
7.20
7.19
7.18
7.18
7.17
7.17
7.12
7.12
7.04
7.04
7.03
7.03
5.30
1.28

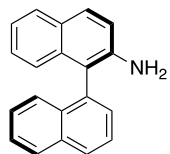


2-23

¹H NMR, CDCl₃, 500 MHz

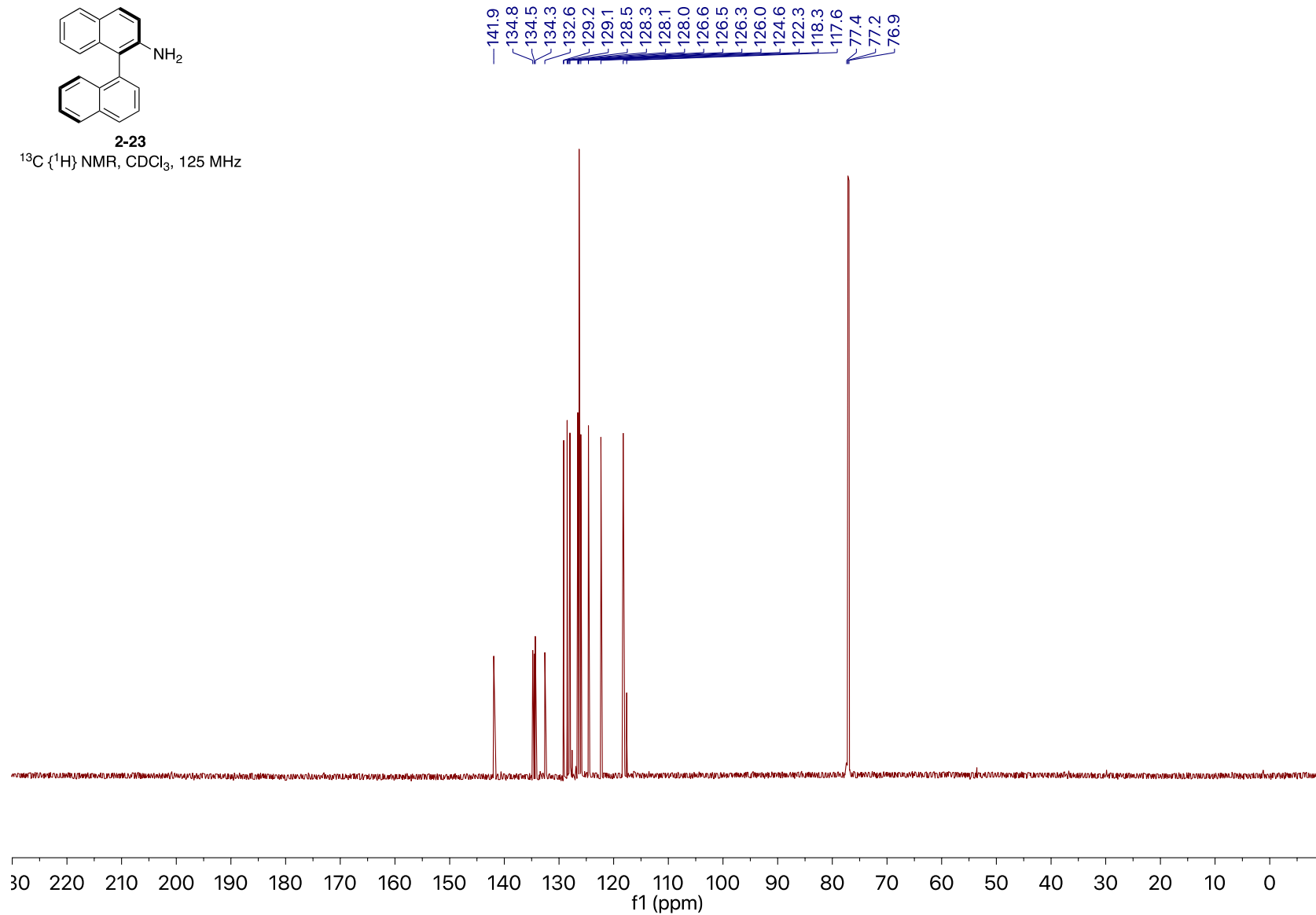


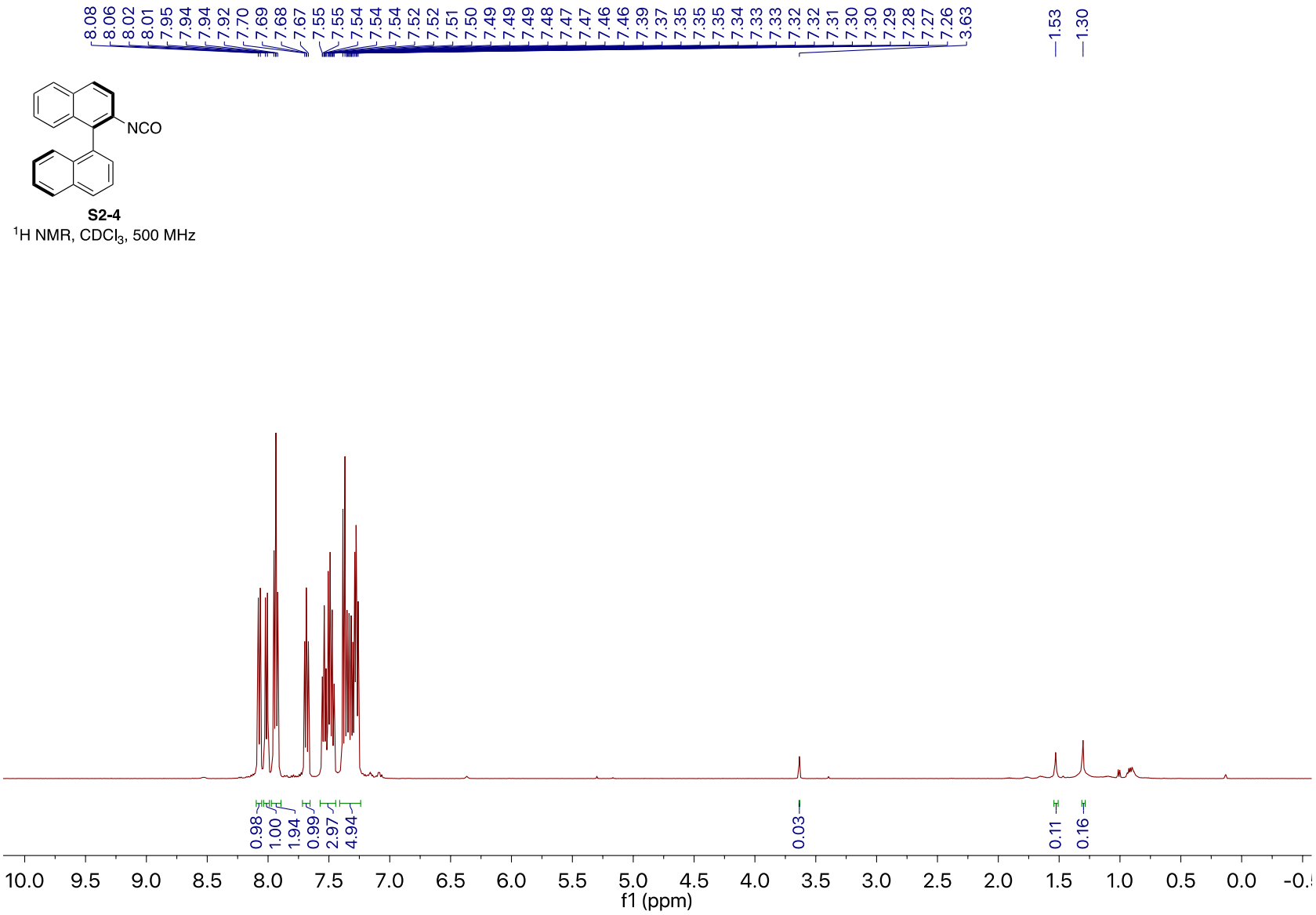
—0.10

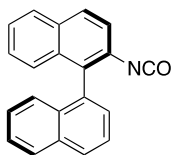


2-23

^{13}C (^1H) NMR, CDCl_3 , 125 MHz





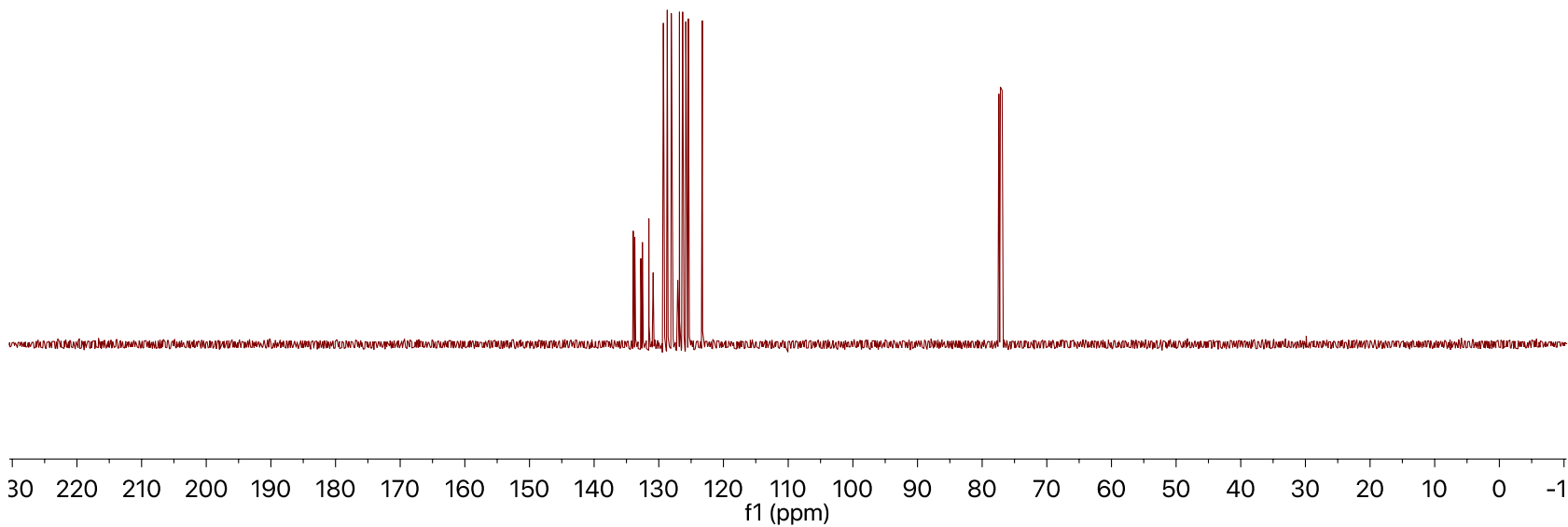


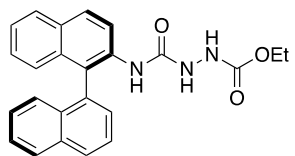
S2-4

^{13}C (^1H) NMR, CDCl_3 , 125 MHz

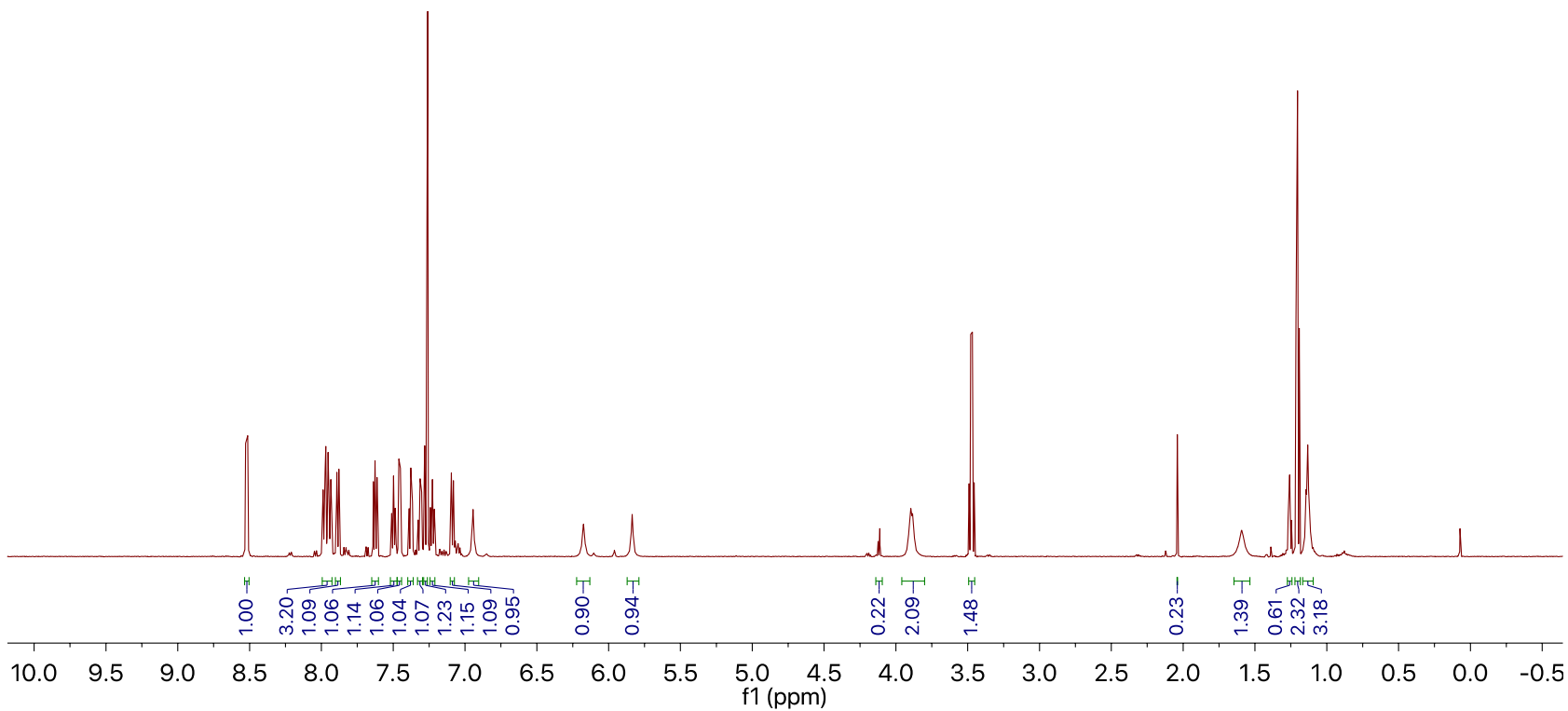
134.0
133.9
133.7
132.8
132.5
131.5
130.9
129.4
129.3
128.7
128.7
128.1
127.1
126.8
126.4
126.3
125.8
125.7
125.4
125.4
125.4
123.3

77.4
77.2
76.9

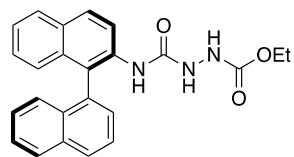




S2-5
 $^1\text{H NMR}$, CDCl_3 , 600 MHz



8.53
 8.51
 7.99
 7.97
 7.95
 7.93
 7.89
 7.88
 7.64
 7.63
 7.62
 7.61
 7.51
 7.50
 7.50
 7.48
 7.46
 7.45
 7.38
 7.38
 7.36
 7.33
 7.31
 7.30
 7.28
 7.26
 7.24
 7.23
 7.22
 7.09
 7.08
 6.94
 5.84
 4.12
 3.89
 3.88
 3.47
 — 2.04
 1.20
 1.14
 1.14
 1.13
 1.13
 1.12
 1.12
 — 0.07



S2-5

^{13}C $\{^1\text{H}\}$ NMR, CDCl_3 , 151 MHz

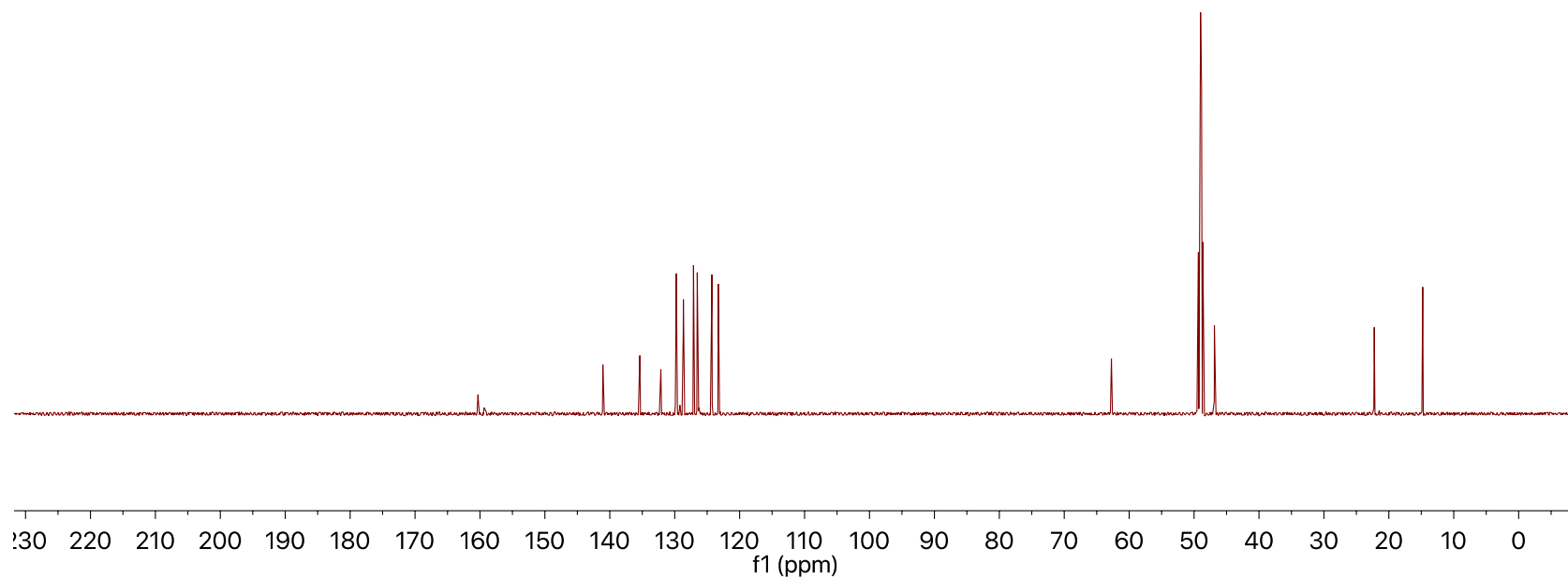
—160.3

141.1
135.4
132.1
129.7
128.7
127.1
126.5
126.4
126.3
124.3
123.3

—62.7
49.5
49.3
49.2
49.0
48.8
48.7
48.5
46.9

—22.2

—14.8



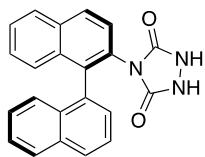
8.01
8.00
7.94
7.92
7.84
7.84
7.83
7.80
7.78
7.53
7.52
7.50
7.47
7.46
7.44
7.43
7.38
7.36
7.35
7.33
7.30
7.29
7.27
7.26
7.25
7.22
7.21
7.17
7.16
7.14

4.14
4.13
4.11
4.10

2.04
1.98

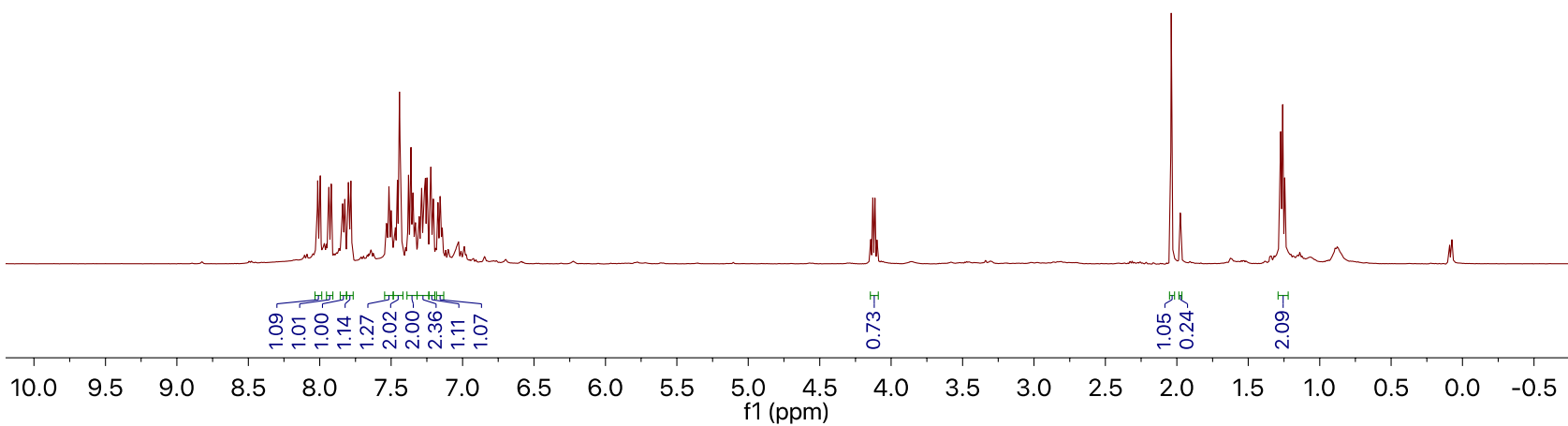
1.27
1.26
1.24
-0.89

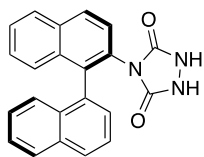
-0.07



2-24

¹H NMR, CDCl₃, 500 MHz

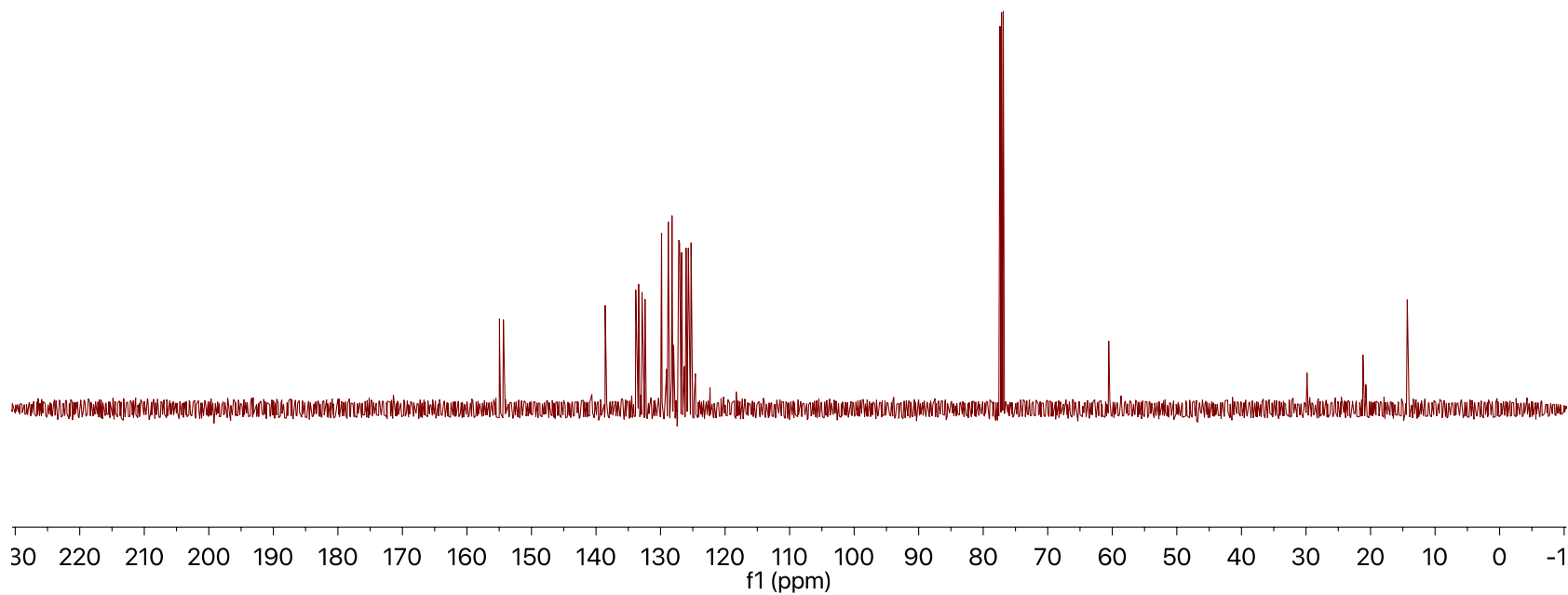


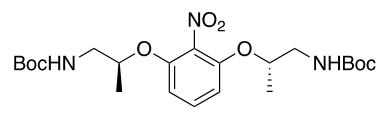


2-24

^{13}C $\{^1\text{H}\}$ NMR, CDCl_3 , 125 MHz

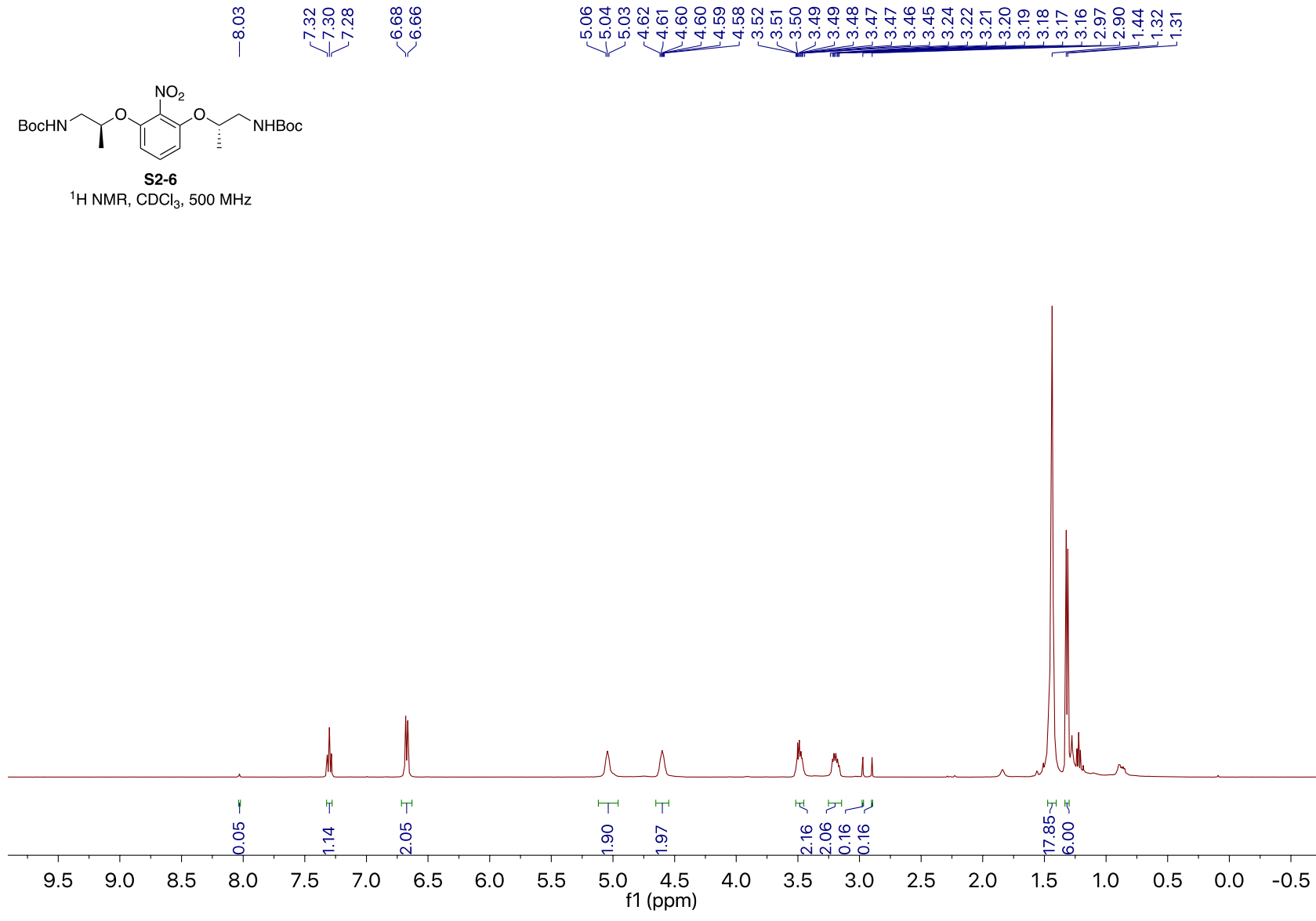
155.0
154.4
138.6
133.8
133.5
133.4
132.9
132.4
129.9
128.8
128.2
128.0
127.3
127.2
127.1
126.9
126.7
126.1
126.0
125.7
125.3
77.4
77.2
76.9

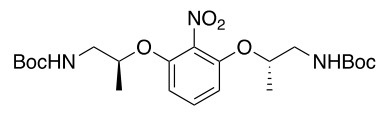




S2-6

¹H NMR, CDCl₃, 500 MHz





S2-6

¹³C {¹H} NMR, CDCl₃, 125 MHz

—156.2
—150.7

—131.3

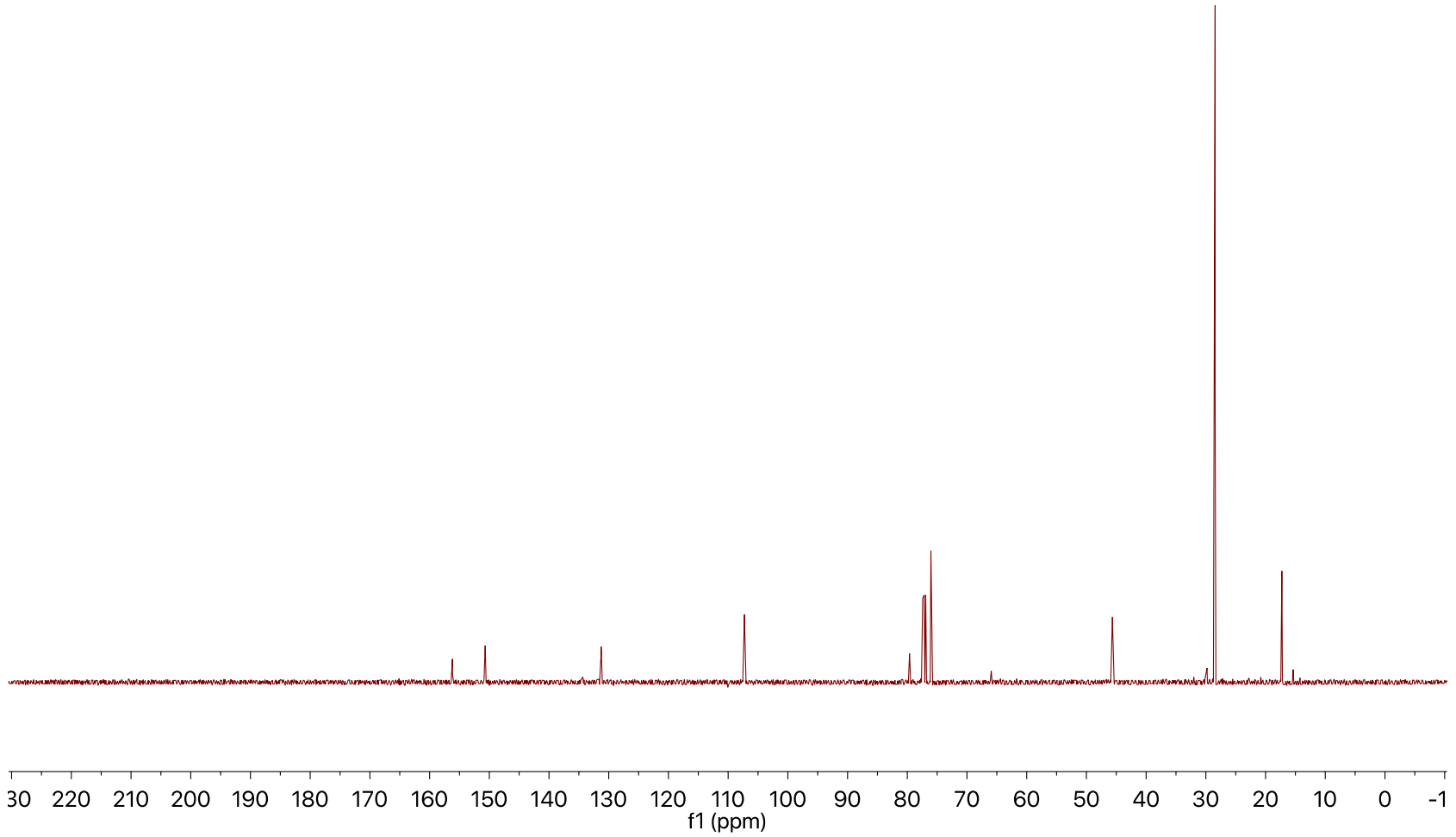
—107.3

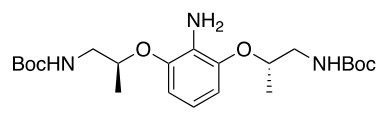
79.6
77.4
77.2
76.9
76.0

—45.6

28.5
28.4

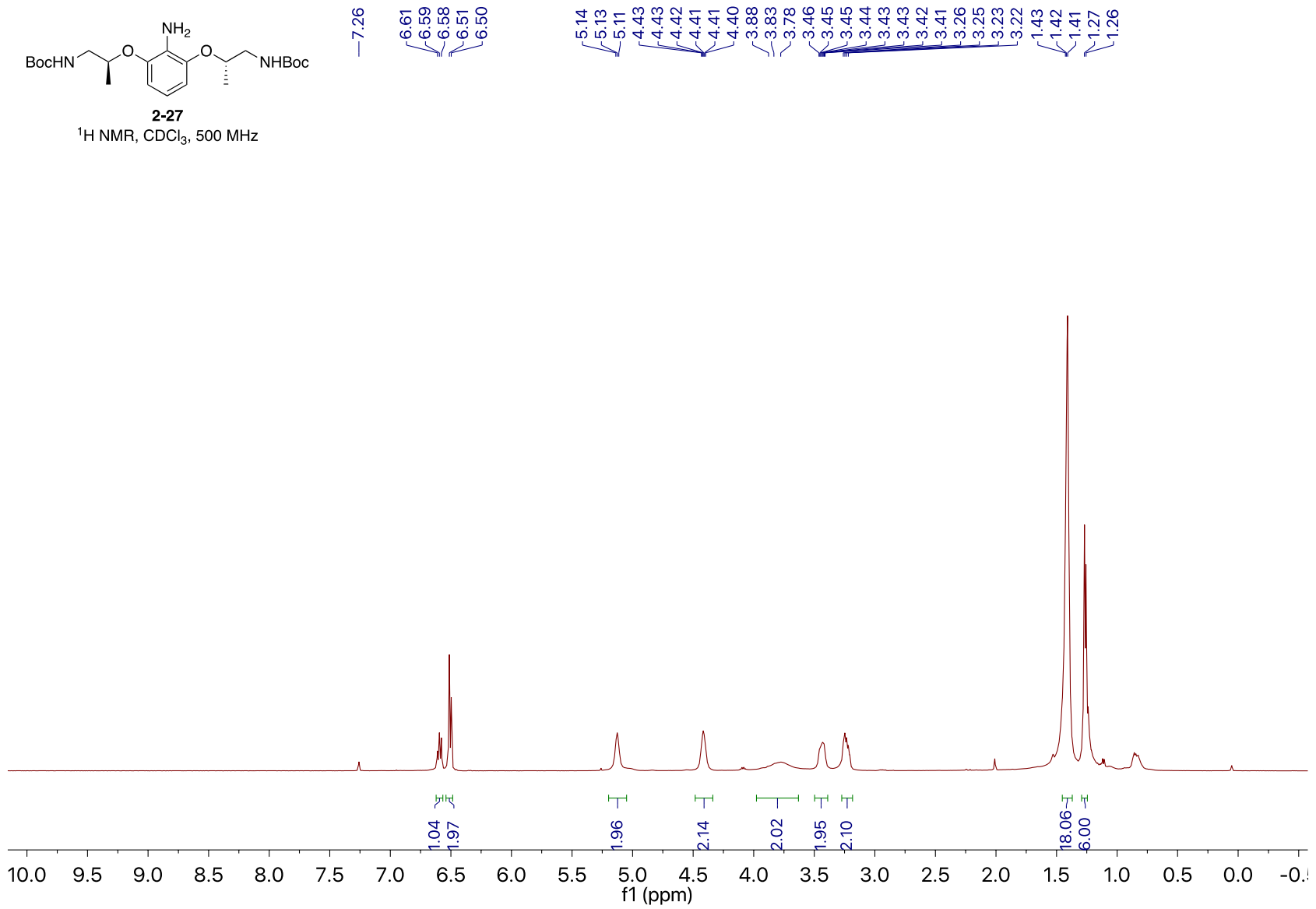
—17.3

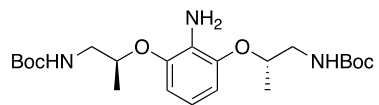




2-27

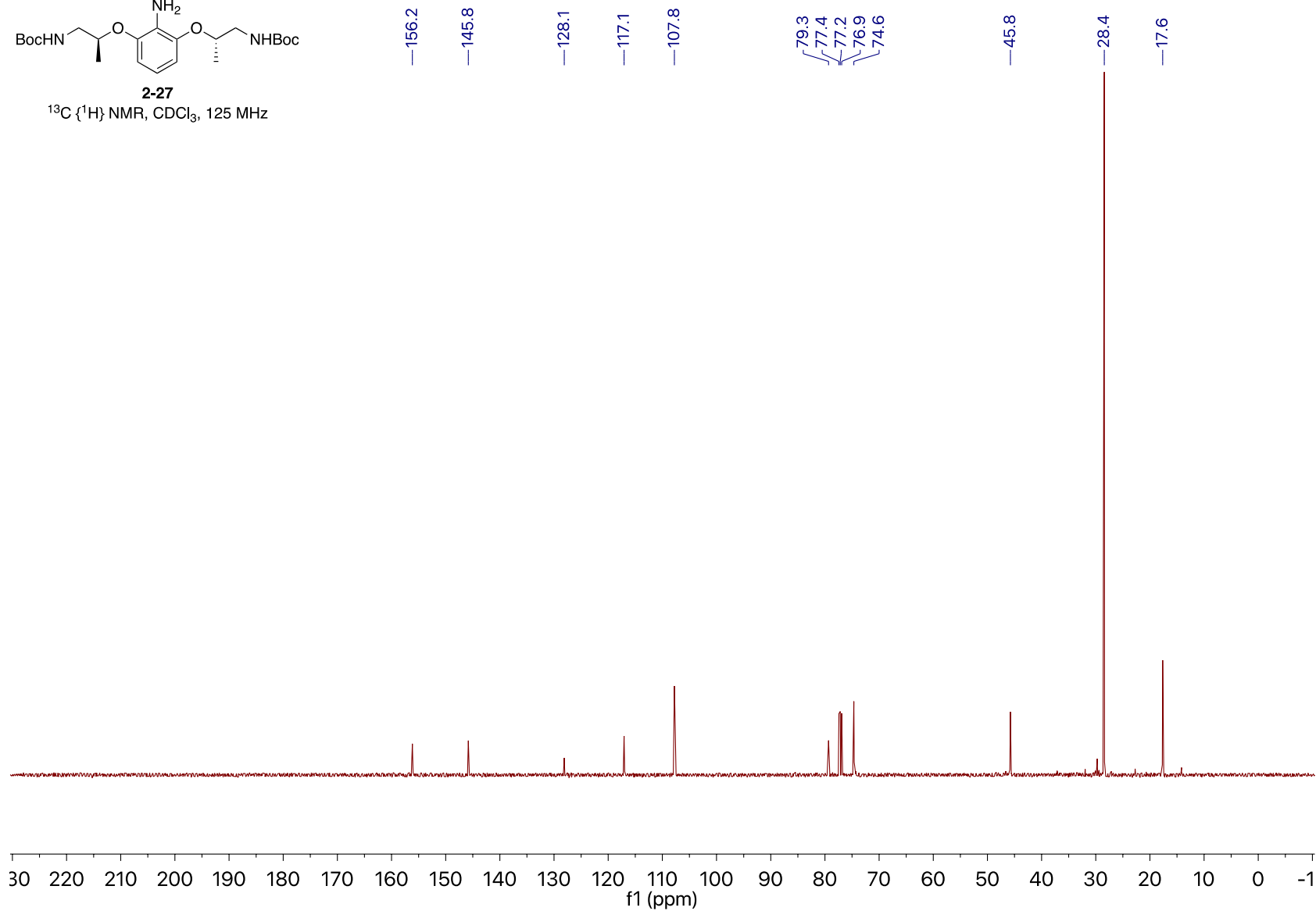
¹H NMR, CDCl₃, 500 MHz

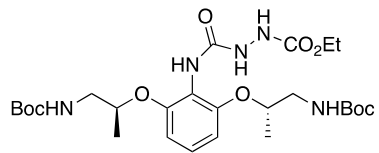




2-27

^{13}C { ^1H } NMR, CDCl_3 , 125 MHz

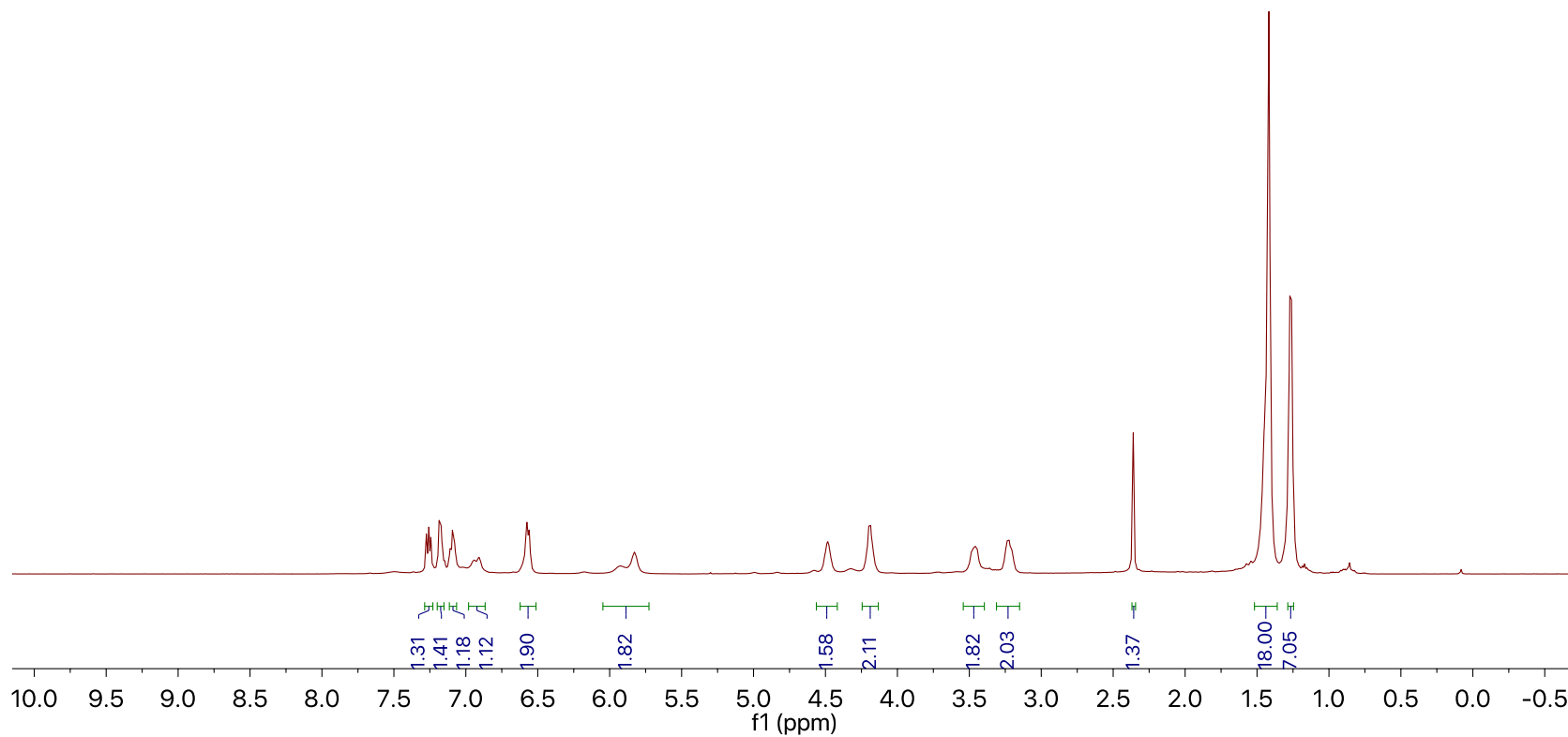


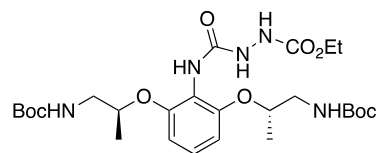


2-28

¹H NMR, CDCl₃, 500 MHz

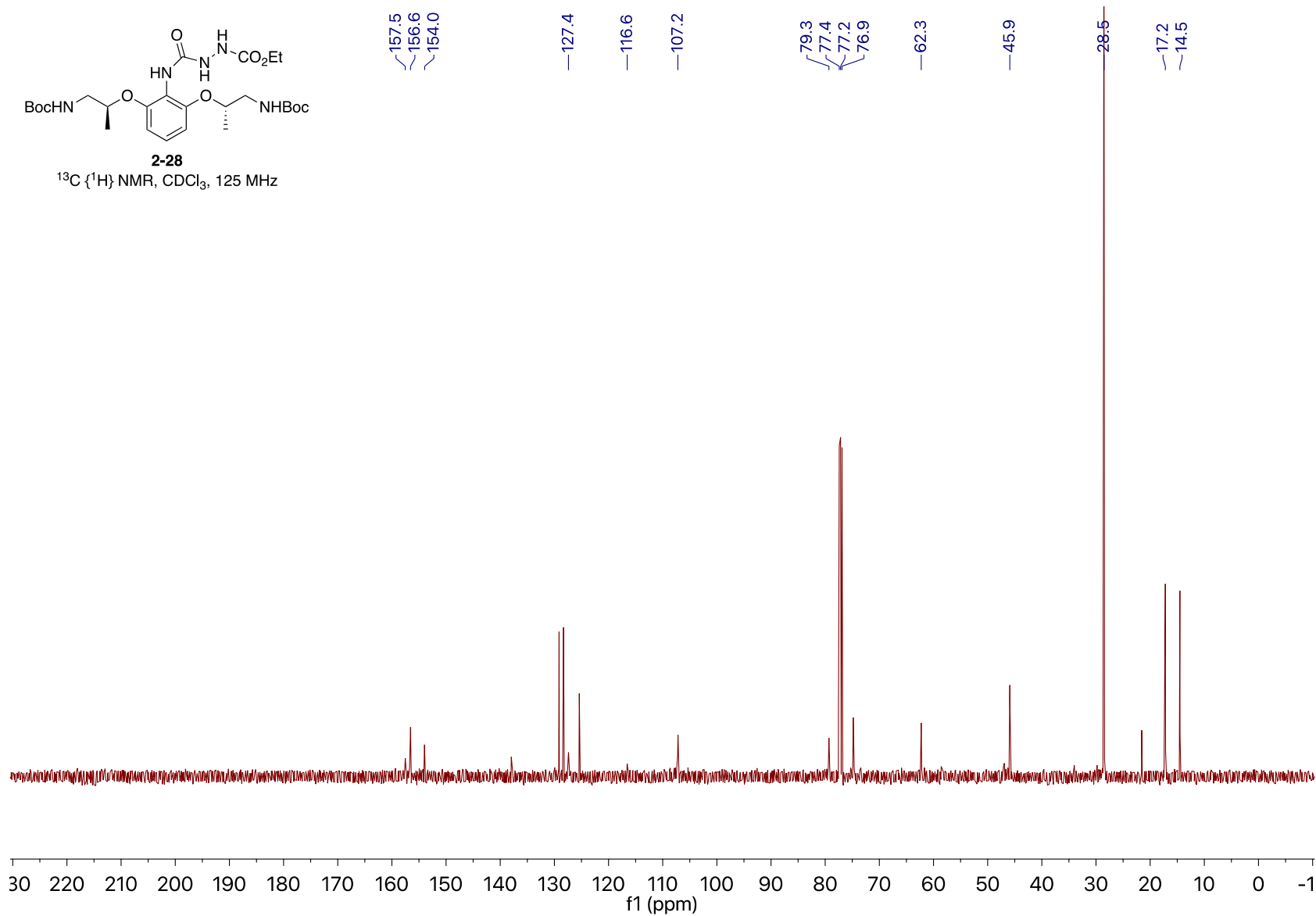
7.11
7.09
7.08
6.95
6.91
6.58
6.56
5.93
5.83
4.50
4.48
4.47
4.21
4.20
4.19
4.17
3.49
3.47
3.46
3.44
3.25
3.24
3.22
3.21
2.36
1.45
1.42
1.27
1.26
1.25

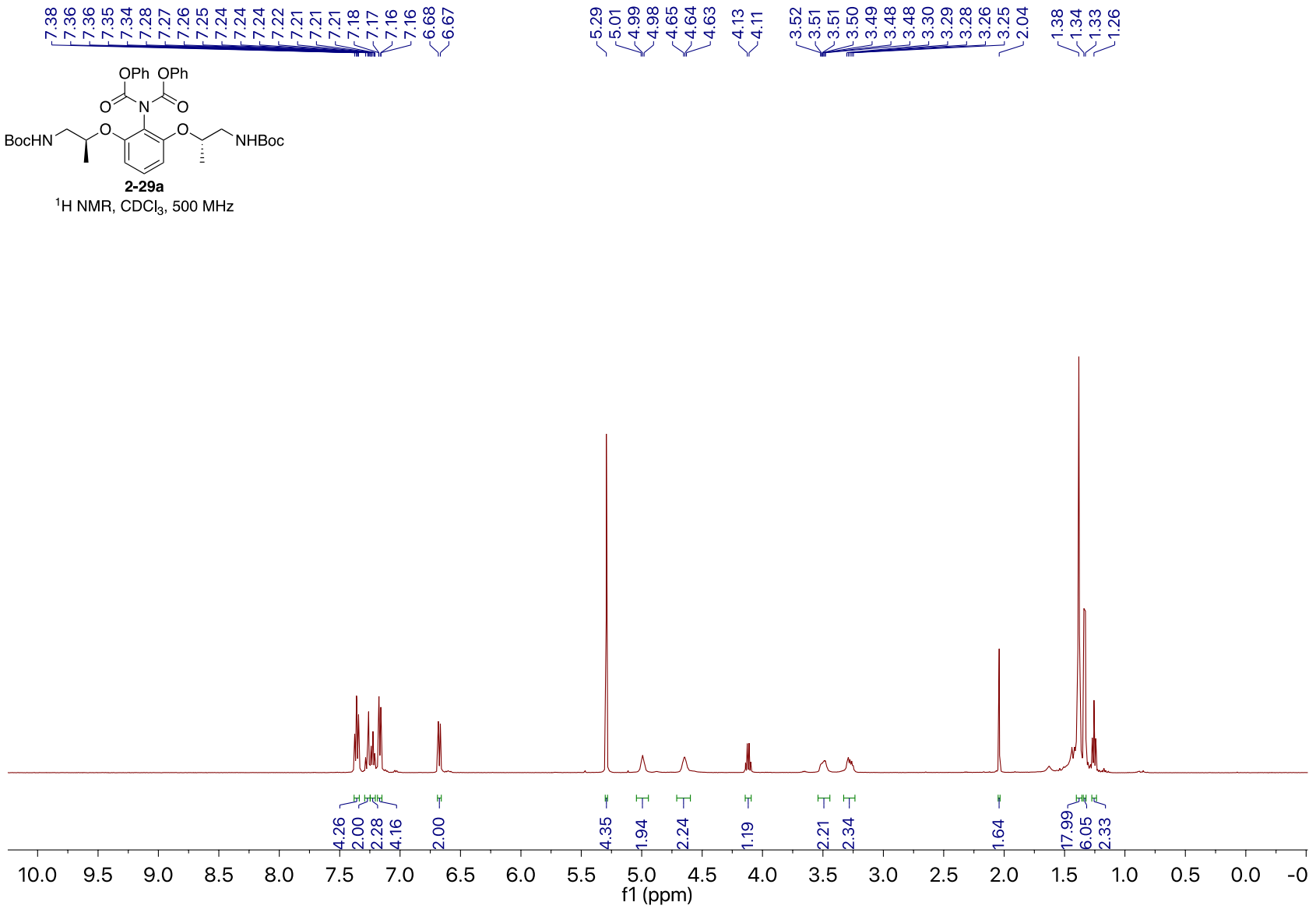
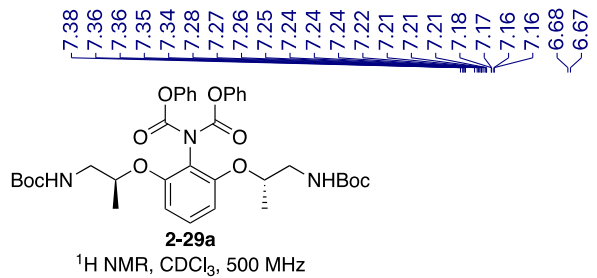


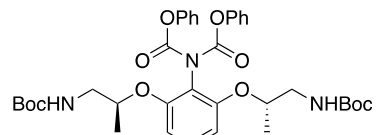


2-28

^{13}C { ^1H } NMR, CDCl_3 , 125 MHz







2-29a

^{13}C $\{^1\text{H}\}$ NMR, CDCl_3 , 125 MHz

156.2
154.3
151.5
150.9

130.0
129.5
126.2
121.4

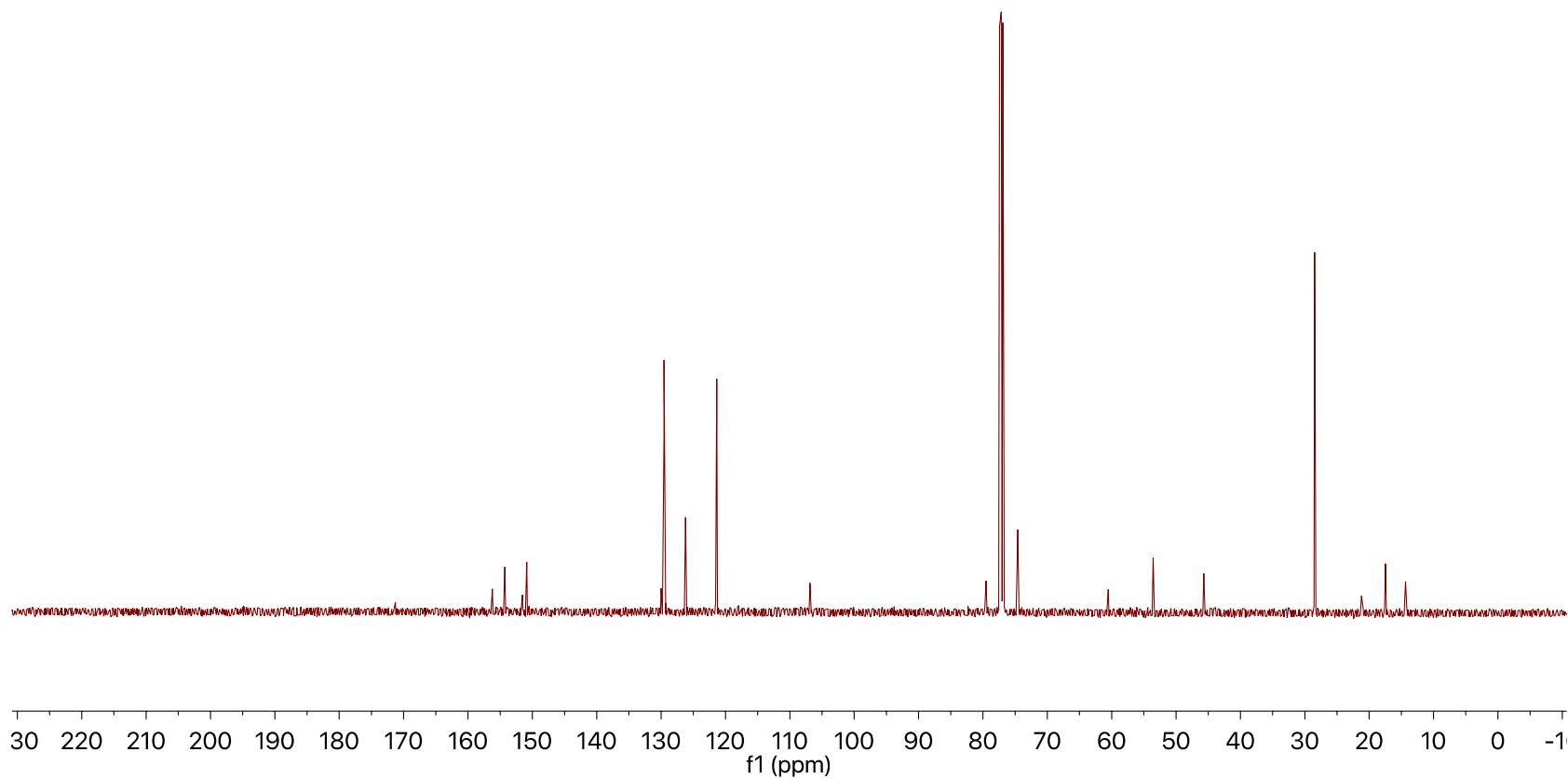
106.9

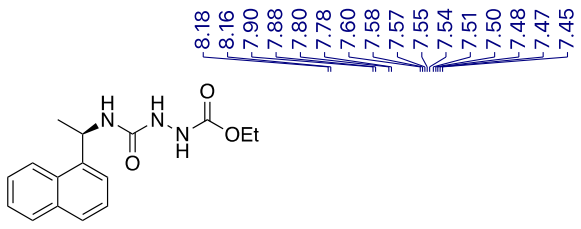
79.5
77.4
77.2
76.9
74.6

45.7

28.5

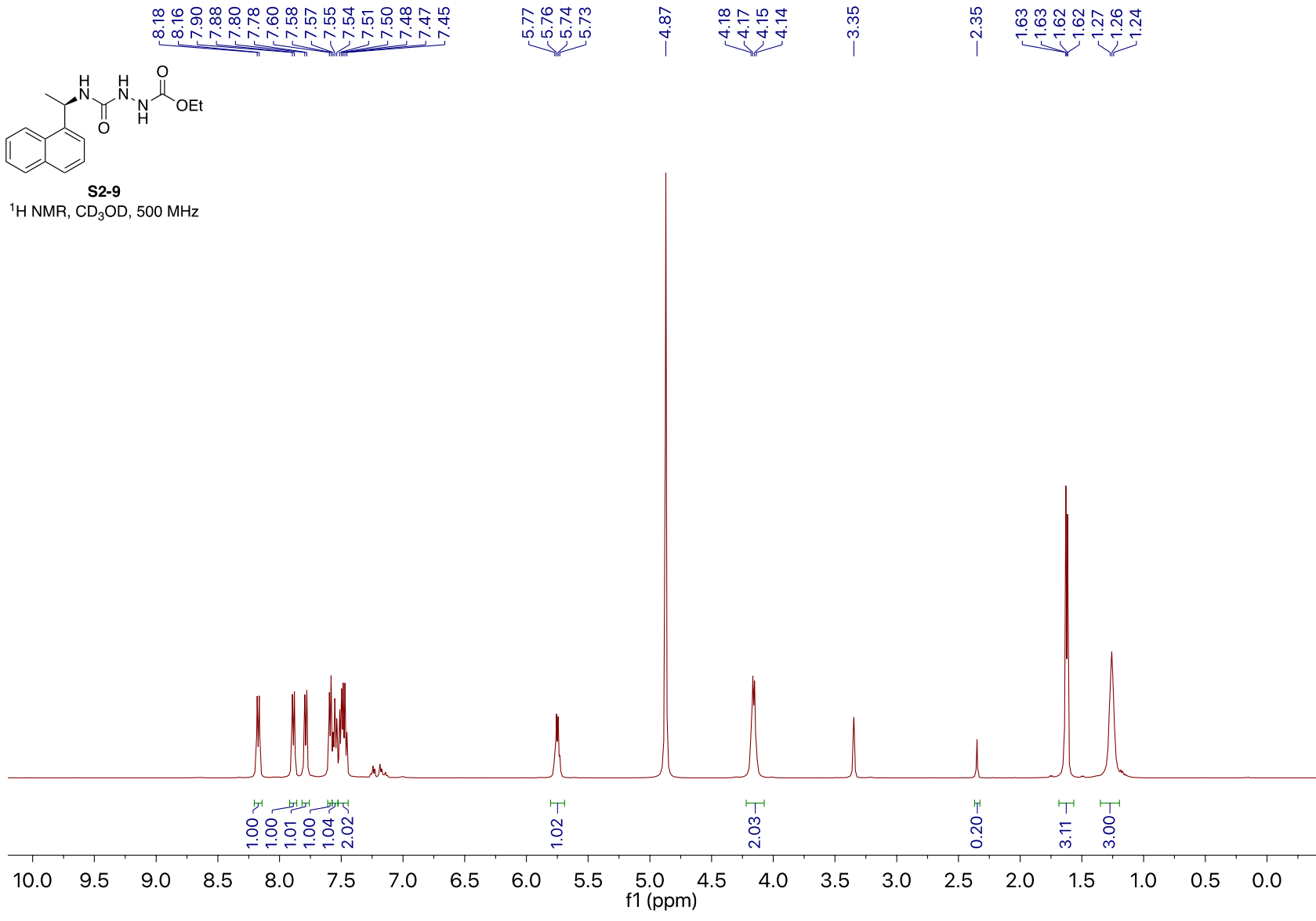
17.5
14.3

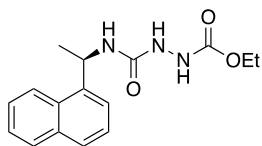




S2-9

¹H NMR, CD₃OD, 500 MHz





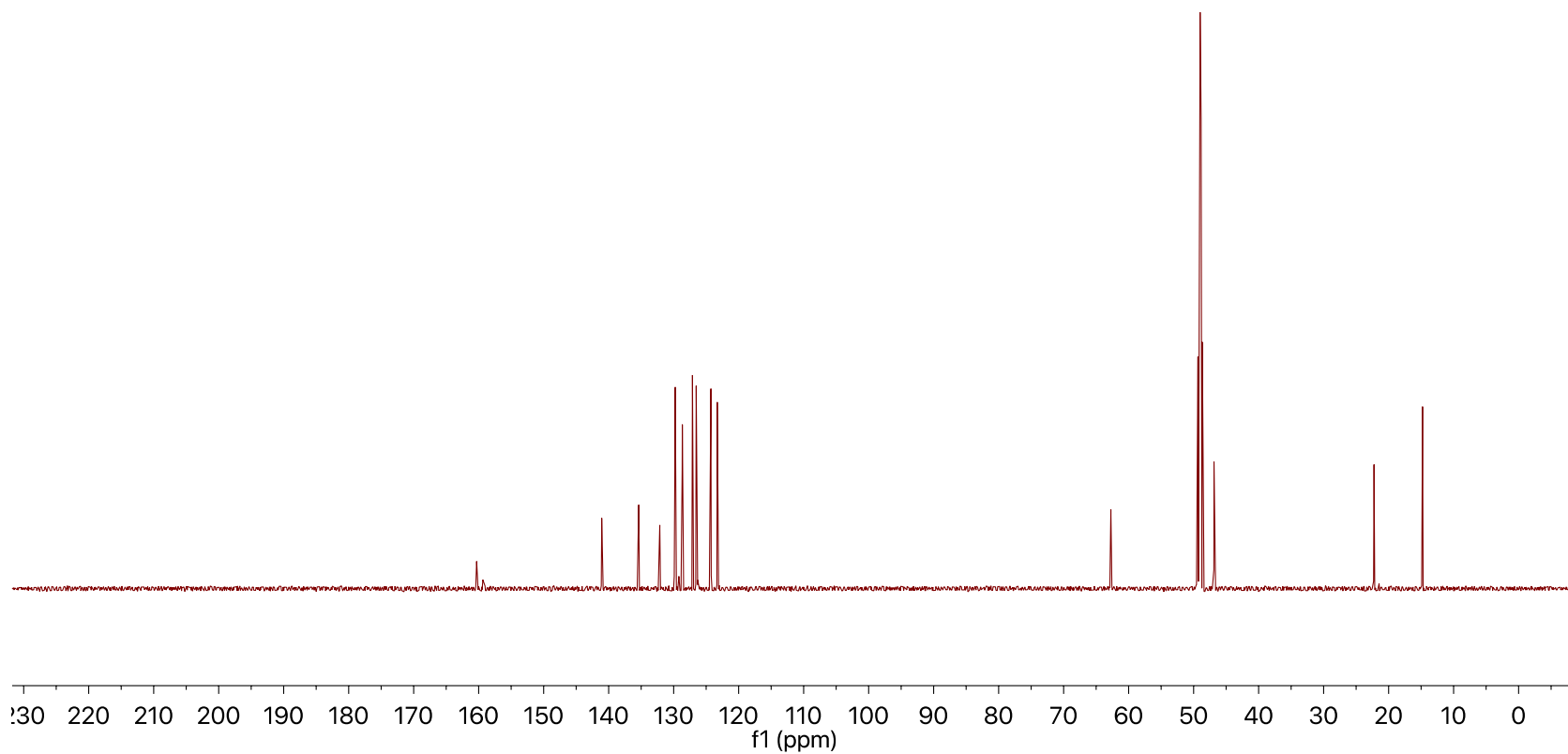
S2-9

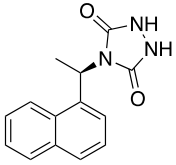
$^{13}\text{C}\{^1\text{H}\}$ NMR, CD_3OD , 125 MHz

160.3
159.3
141.1
135.4
132.1
129.9
129.7
129.2
128.7
127.1
126.5
126.4
126.3
124.3
123.3

62.7
49.5
49.3
49.2
49.0
48.8
48.7
48.5
46.9

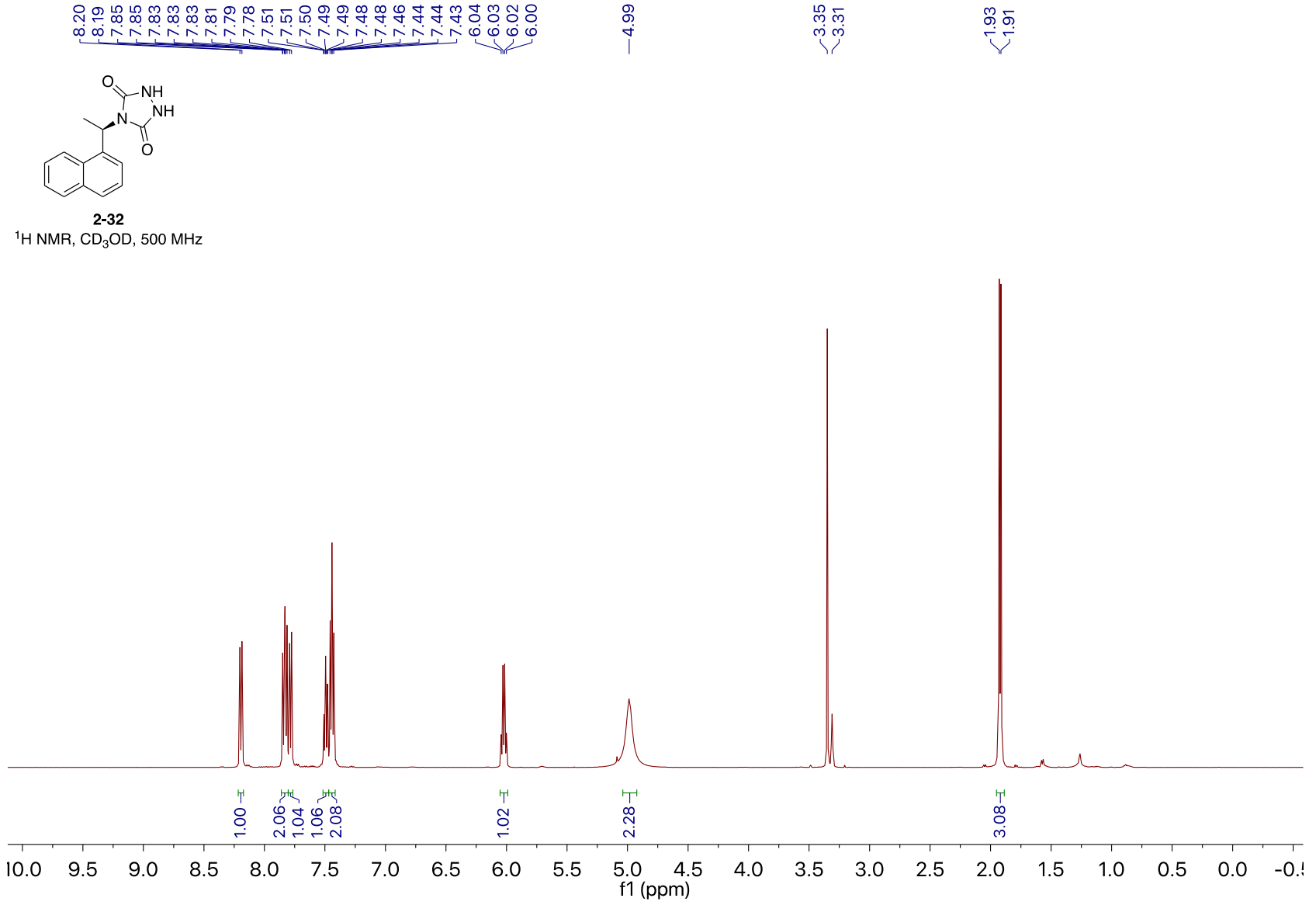
22.2
14.8

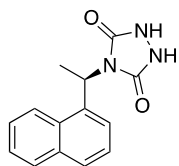




2-32

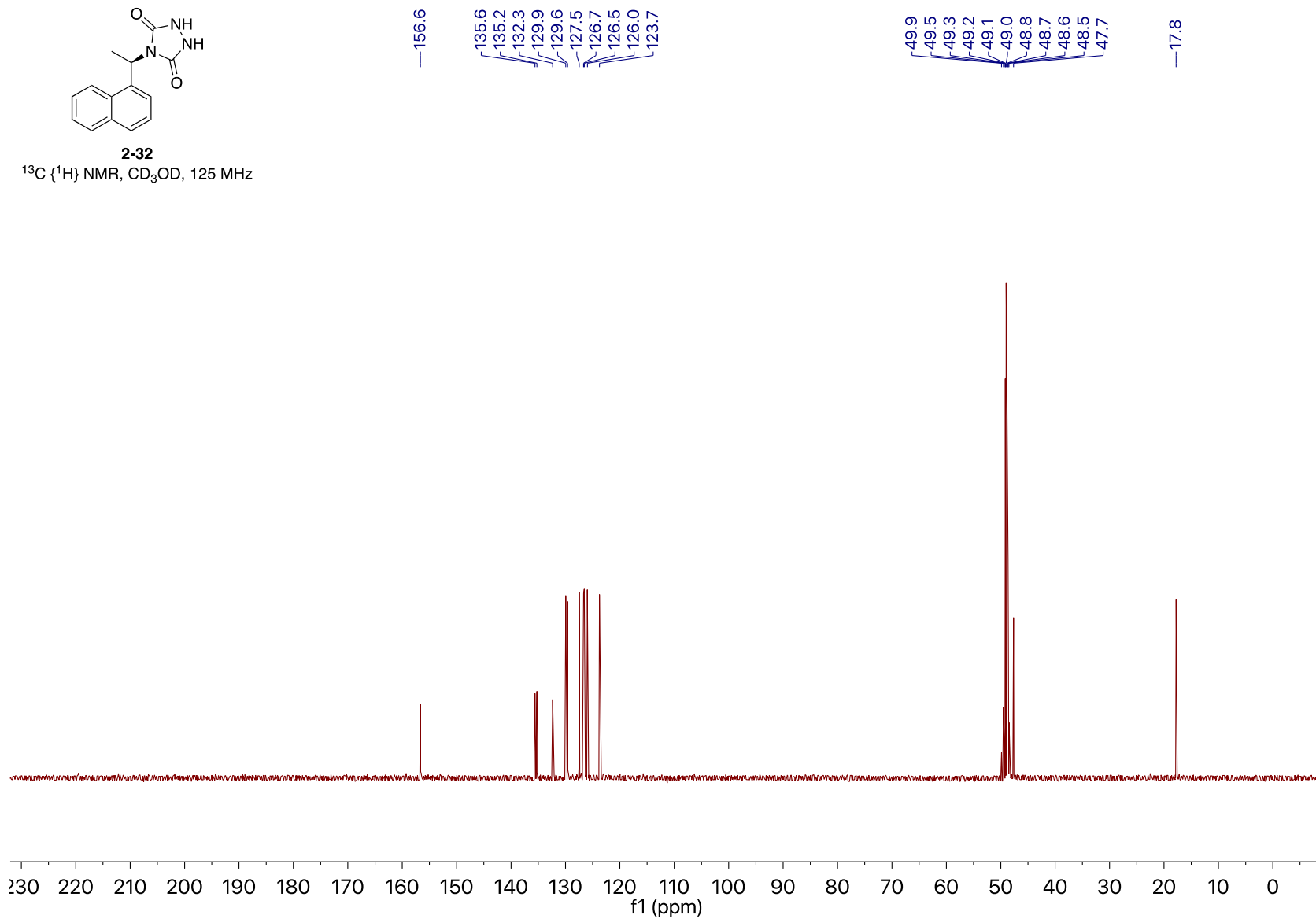
¹H NMR, CD₃OD, 500 MHz

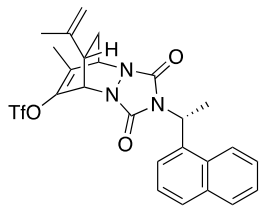




2-32

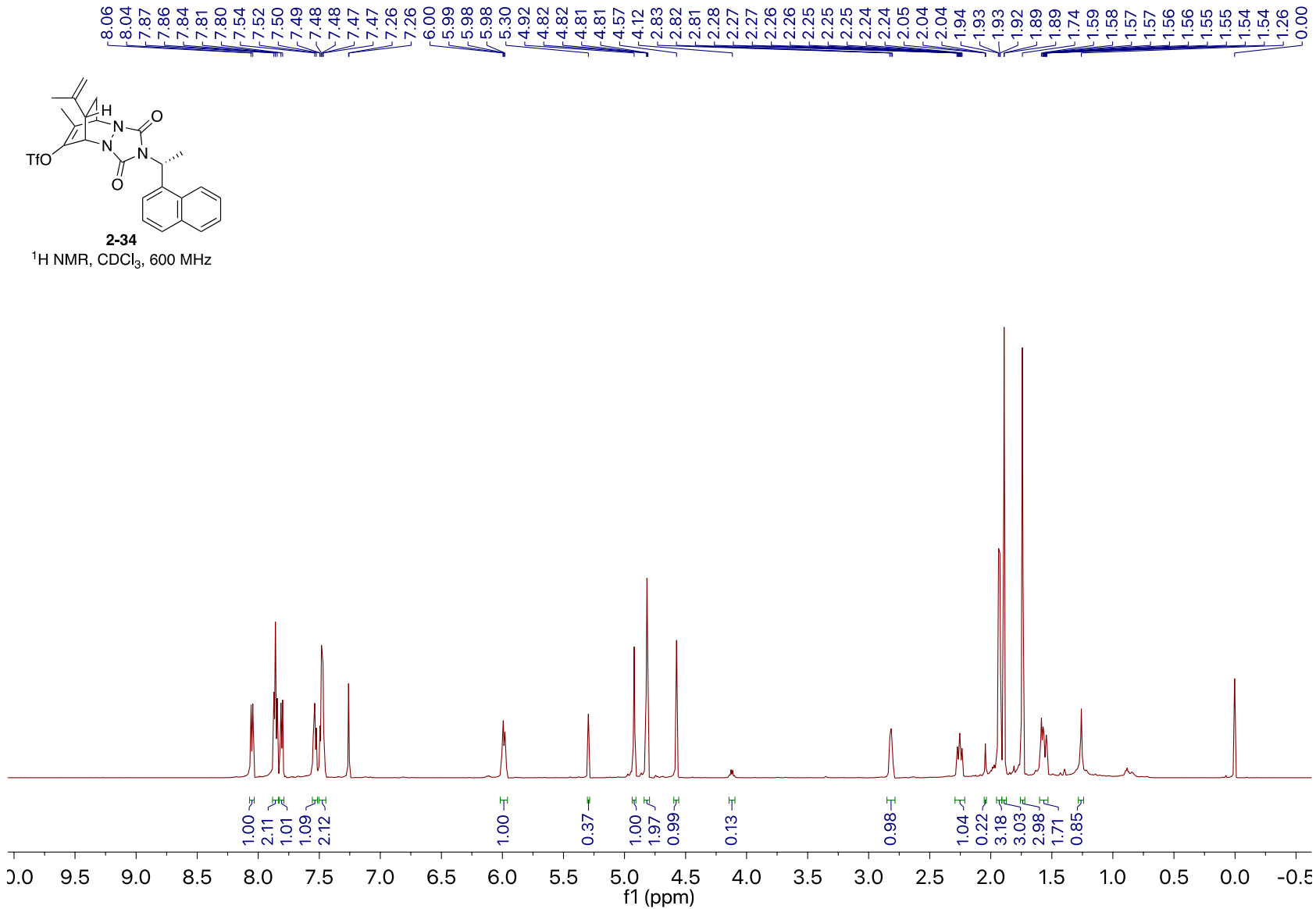
^{13}C $\{^1\text{H}\}$ NMR, CD_3OD , 125 MHz

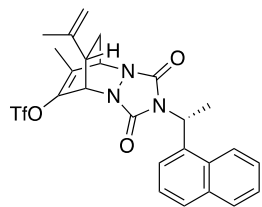




2-34

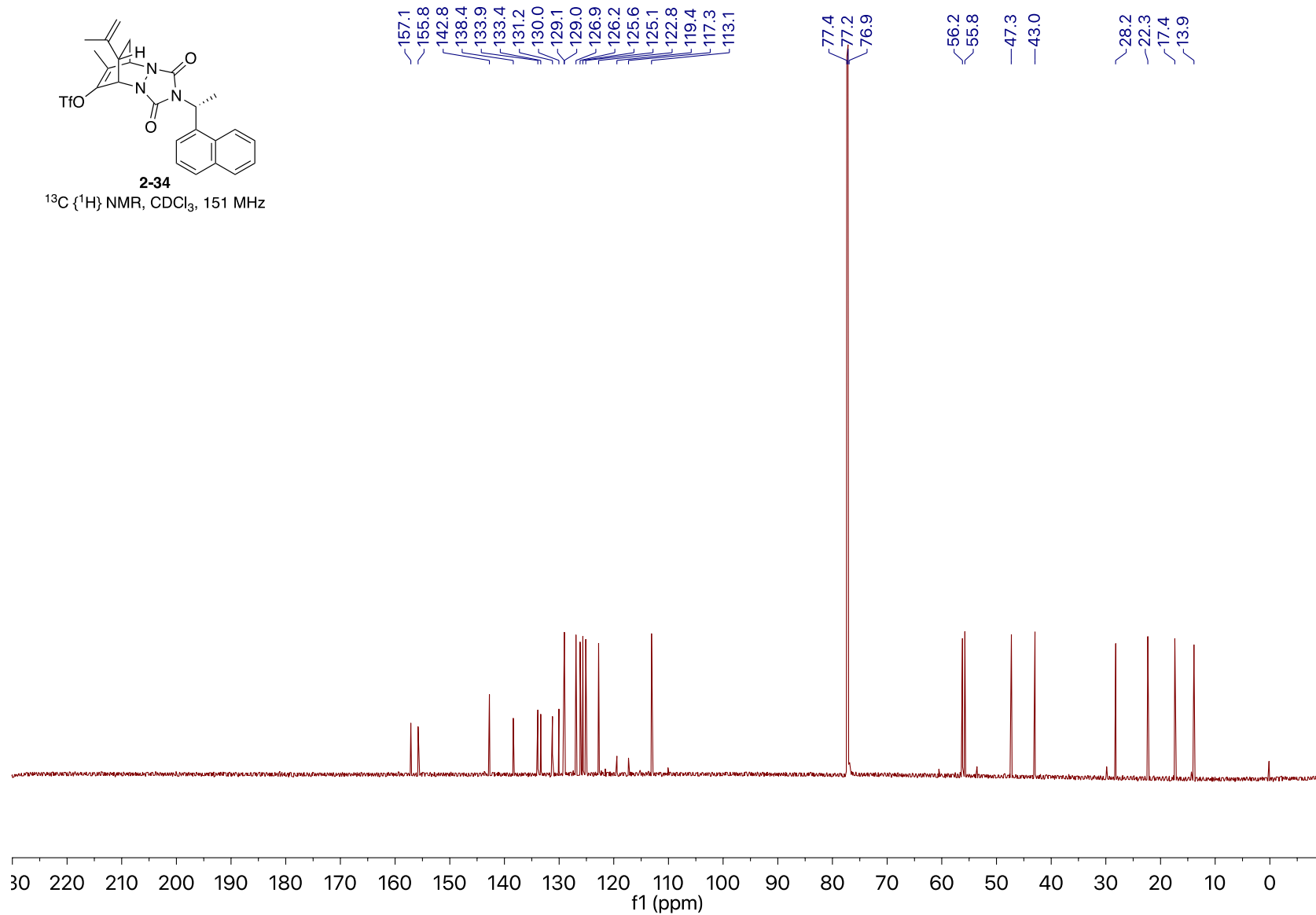
¹H NMR, CDCl₃, 600 MHz

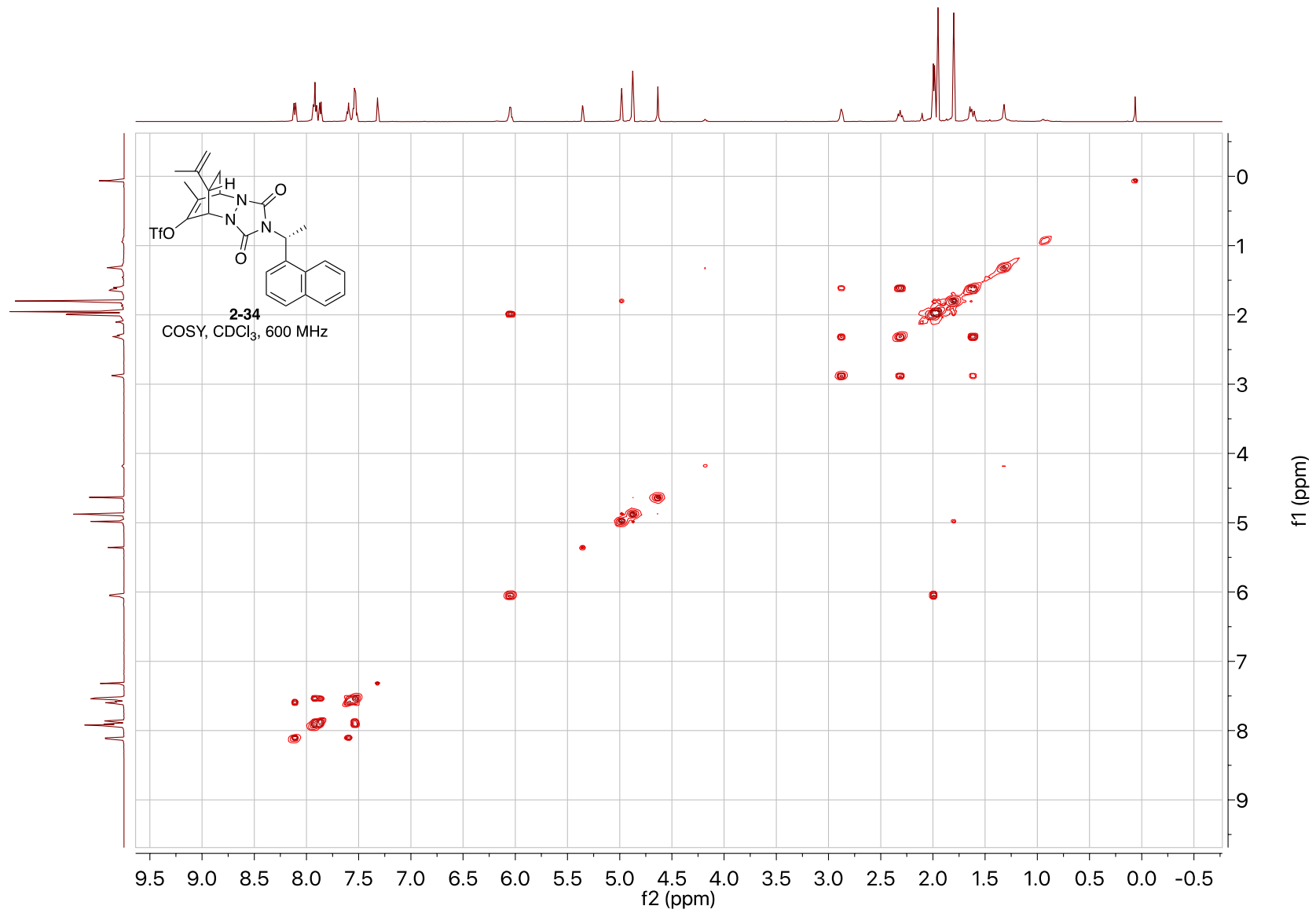


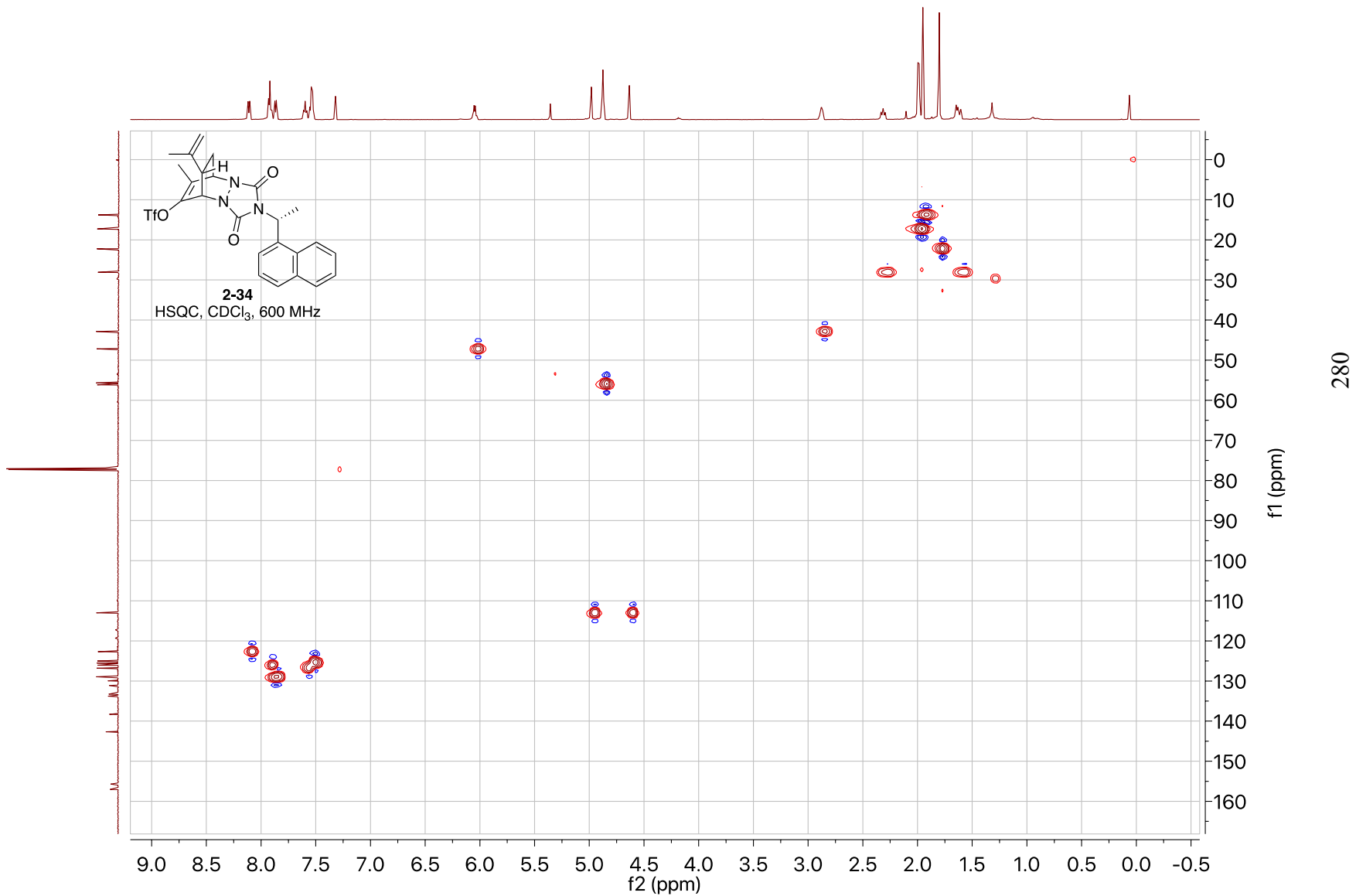


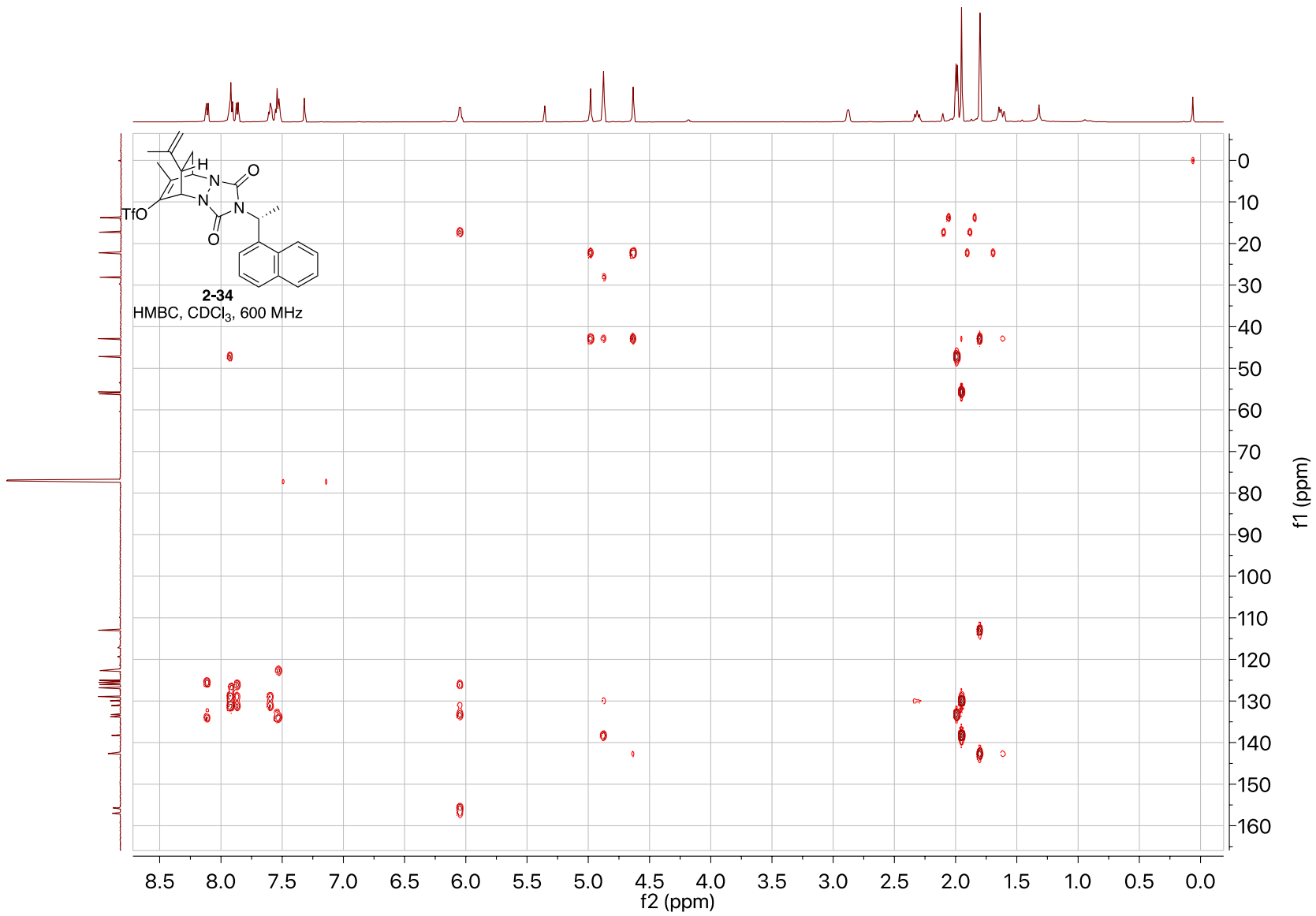
2-34

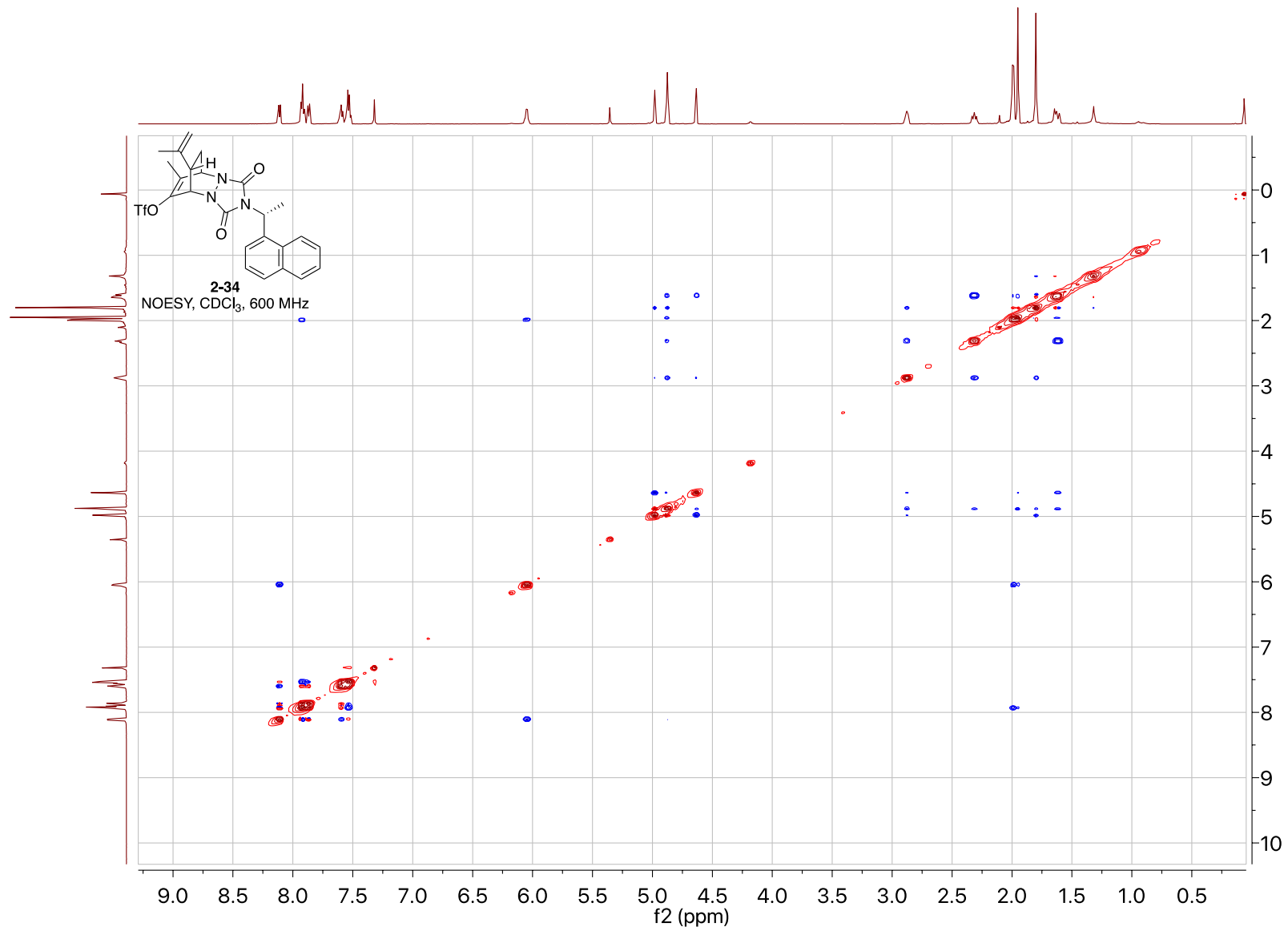
^{13}C $\{^1\text{H}\}$ NMR, CDCl_3 , 151 MHz

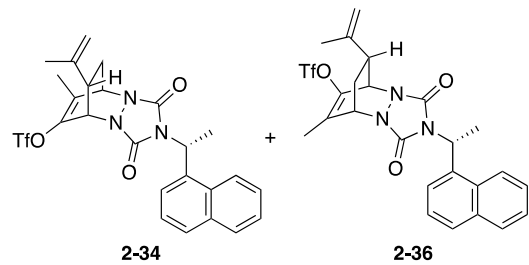






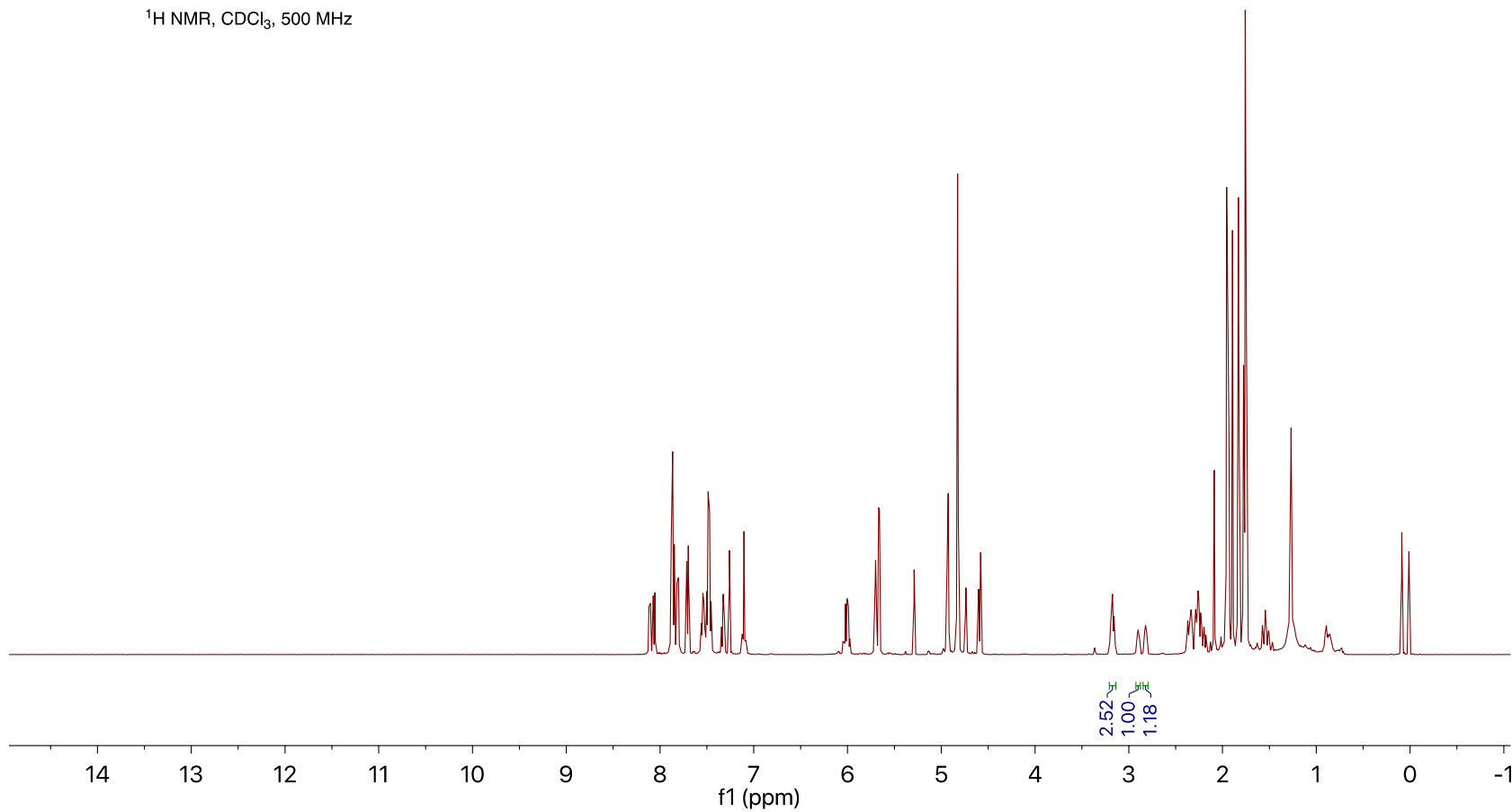


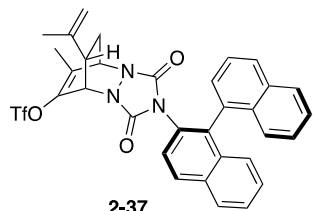




¹H NMR, CDCl₃, 500 MHz

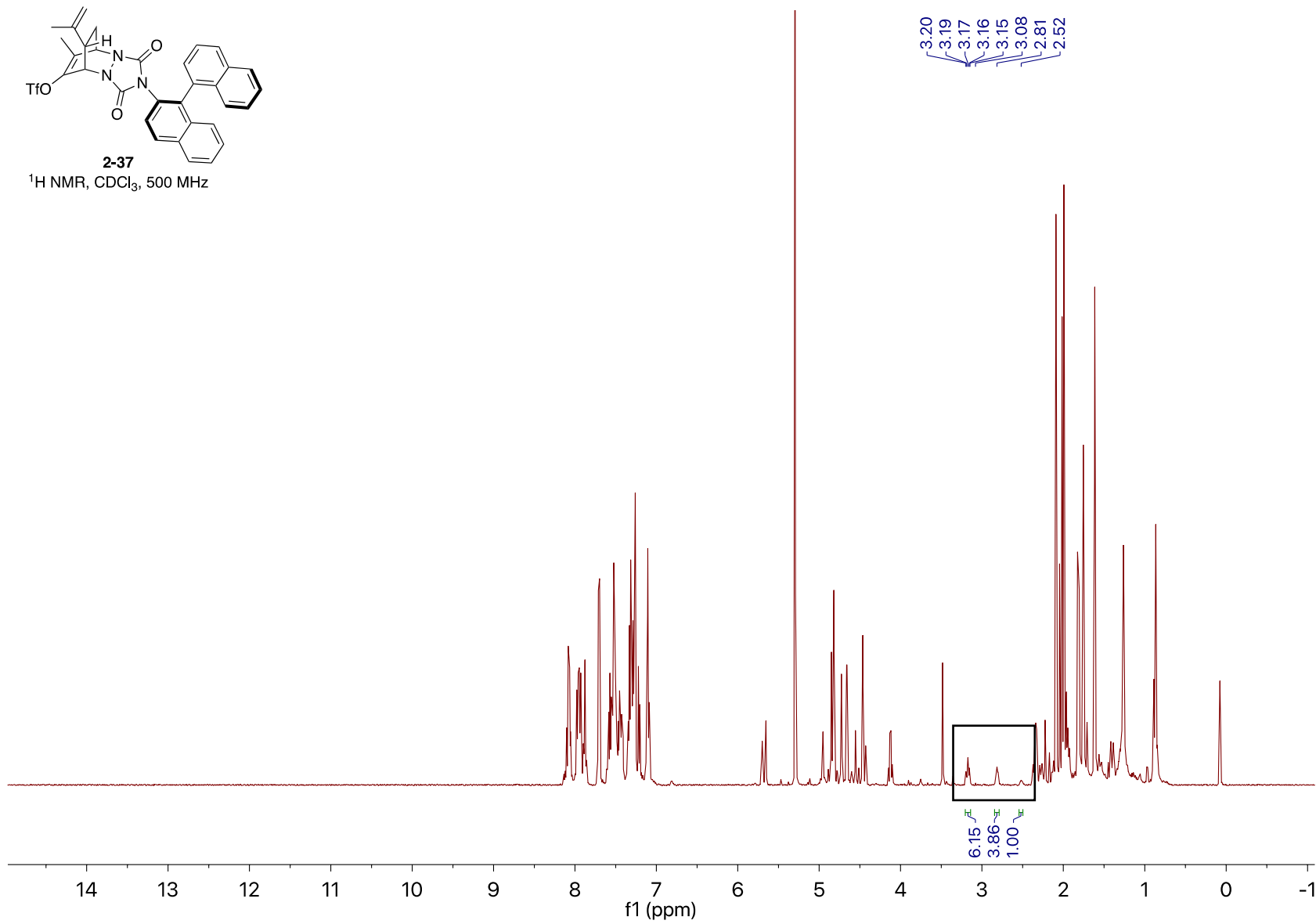
3.20
 3.19
 3.18
 3.17
 3.16
 3.15
 2.92
 2.91
 2.90
 2.89
 2.88
 2.84
 2.83
 2.82
 2.81
 2.80

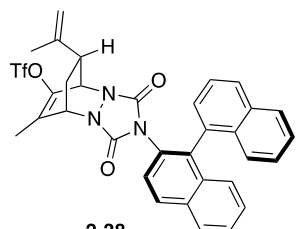




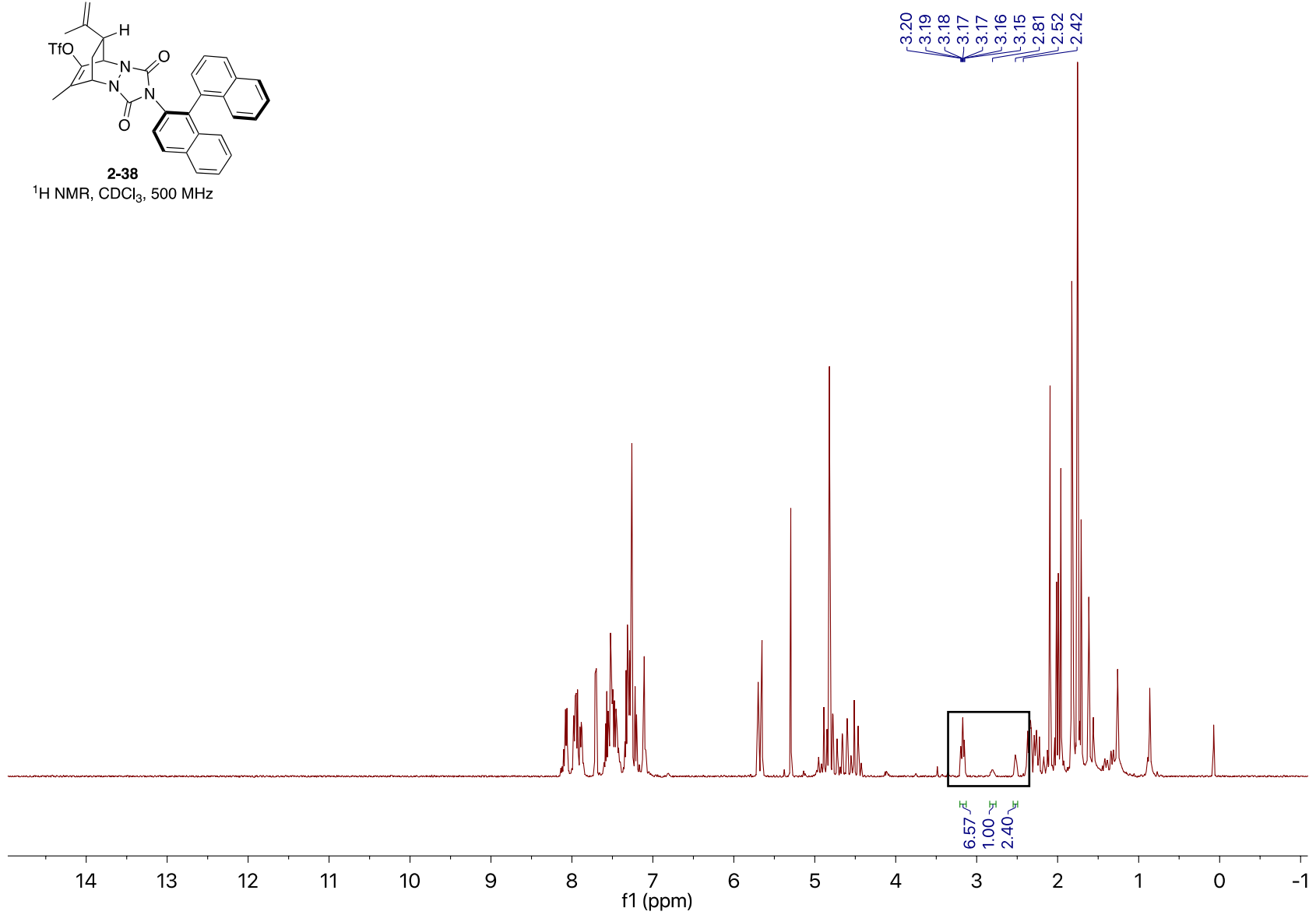
2-37

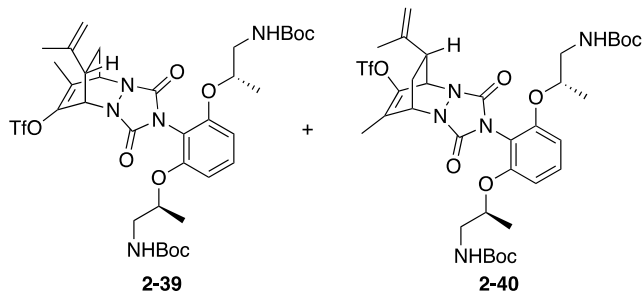
¹H NMR, CDCl₃, 500 MHz



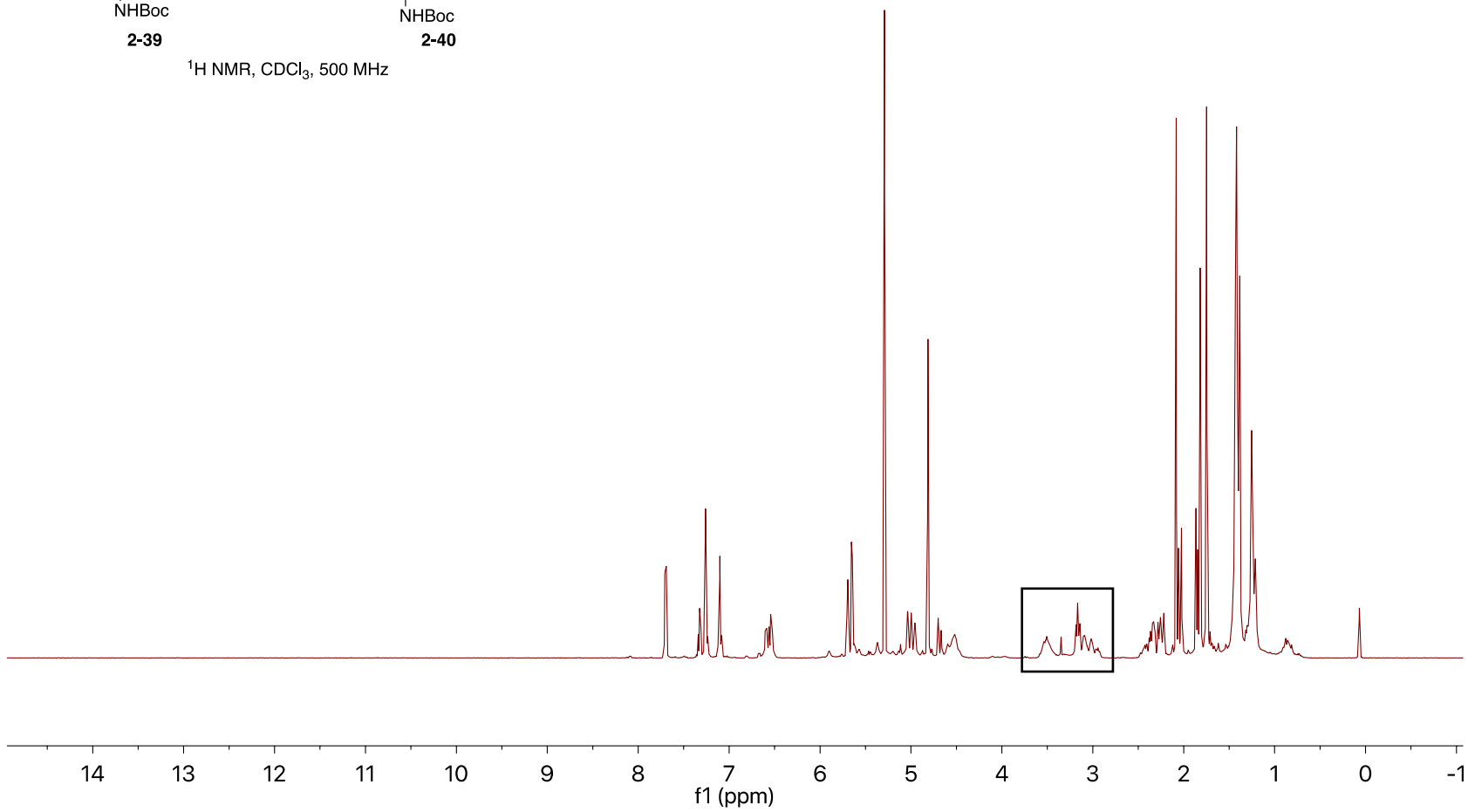


2-38
¹H NMR, CDCl₃, 500 MHz

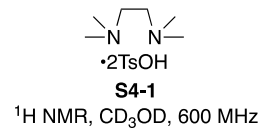




$^1\text{H NMR}$, CDCl_3 , 500 MHz

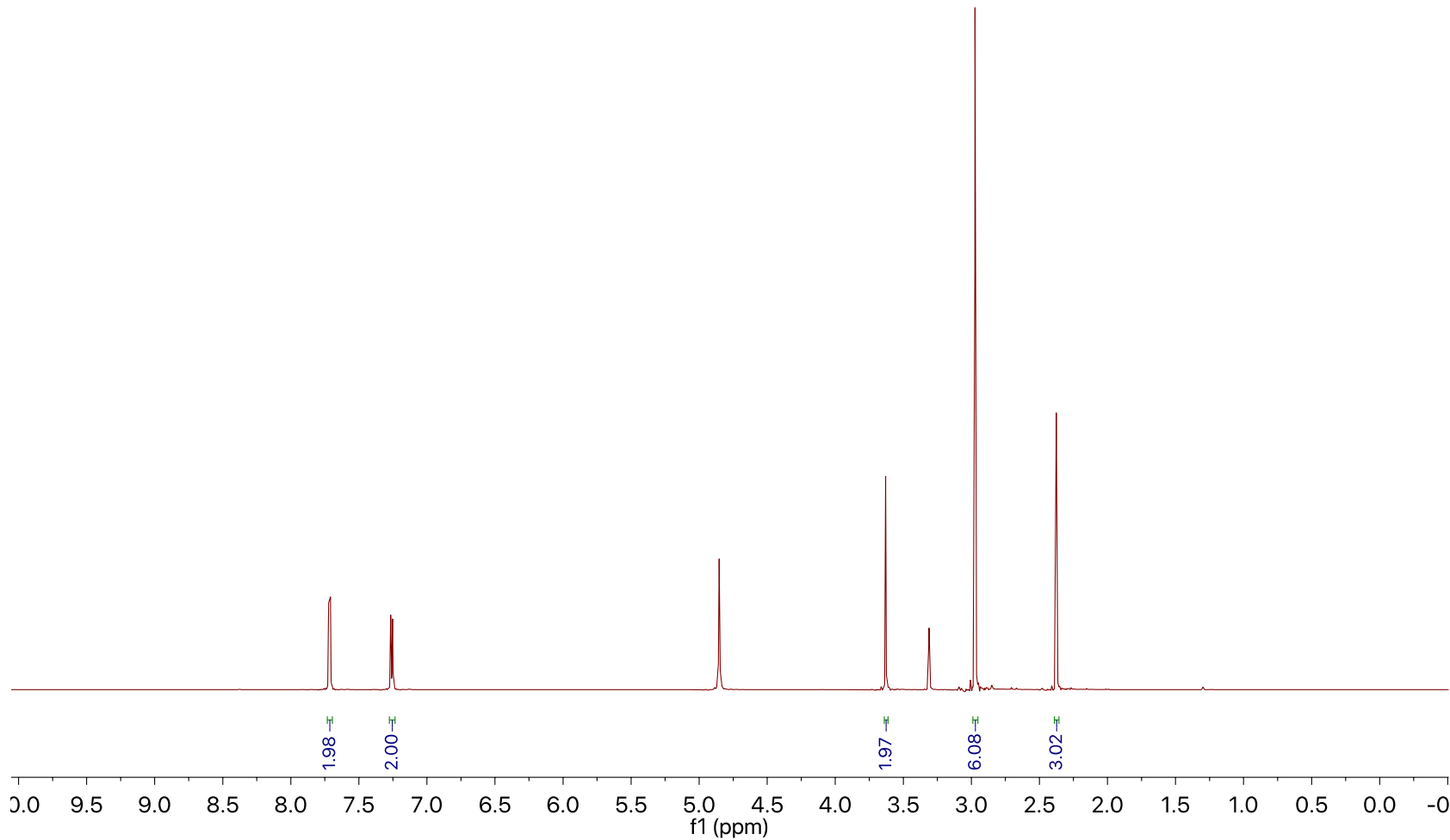


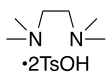
Appendix B: Spectral Data for Compounds in Chapter 4



7.72
7.72
7.71
7.27
7.25

3.64
3.63
3.62
3.61
3.60
2.97
2.96
2.96
2.95
2.38
2.36

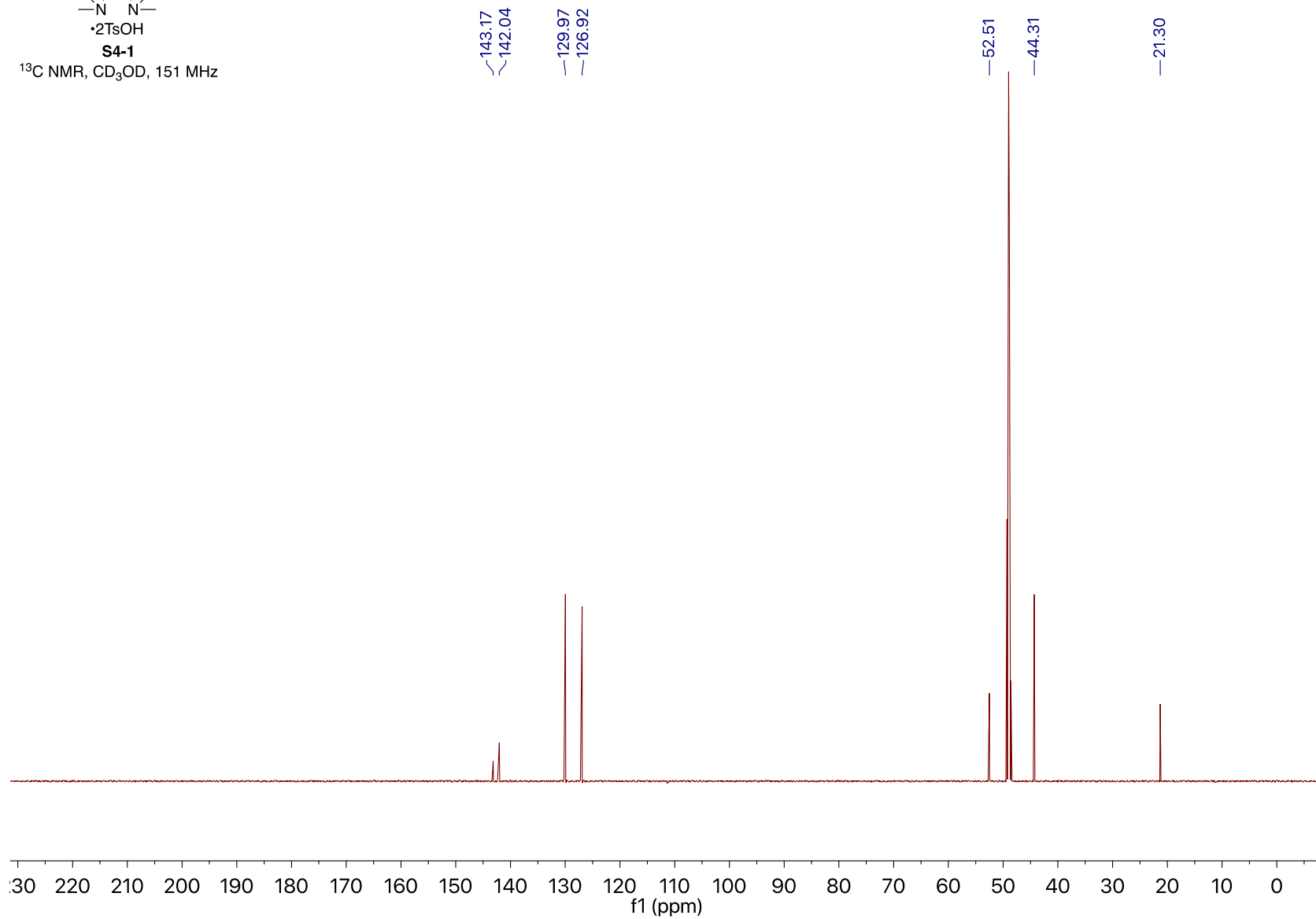


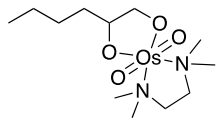


•2TsOH

S4-1

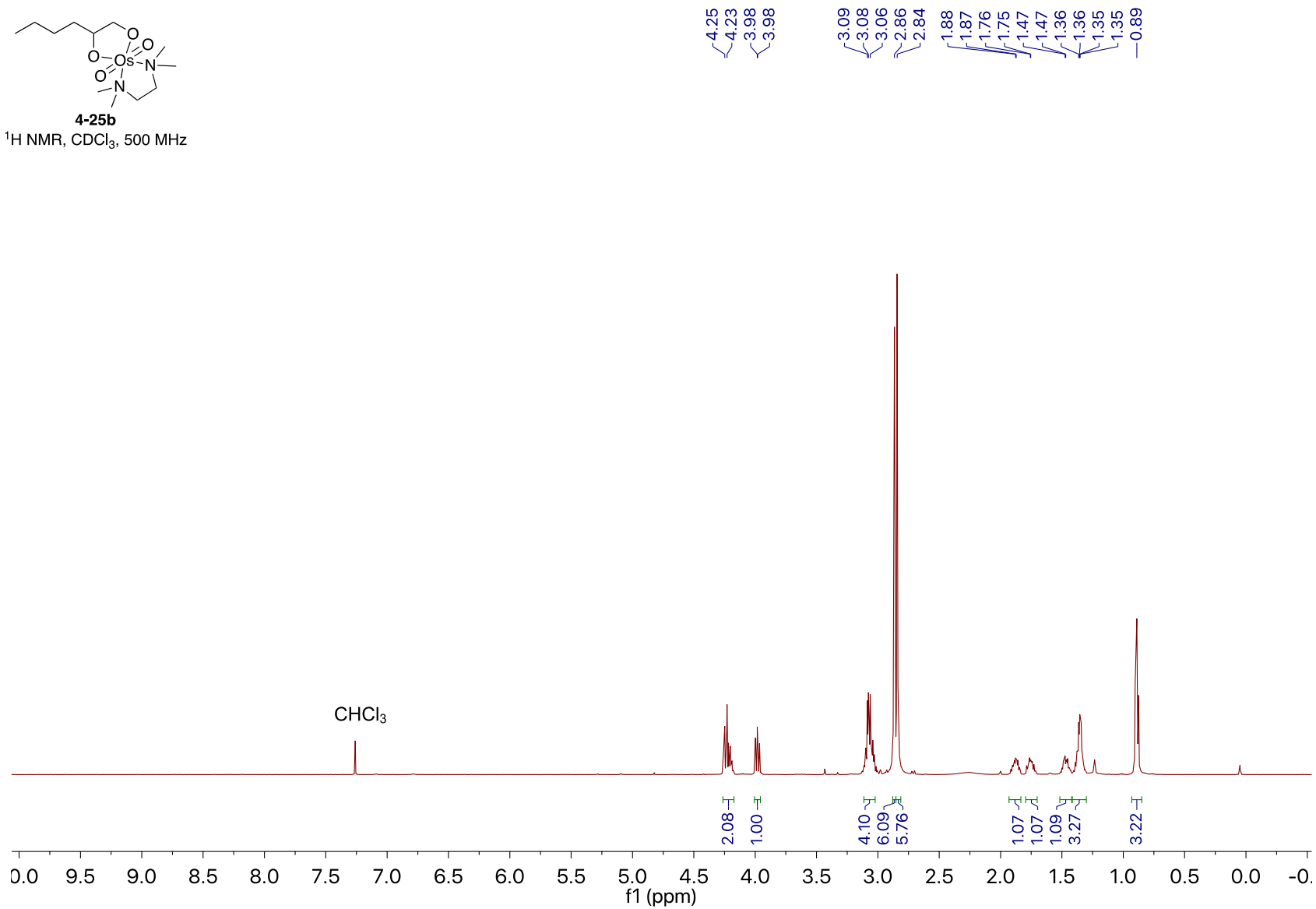
¹³C NMR, CD₃OD, 151 MHz

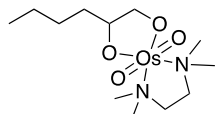




4-25b

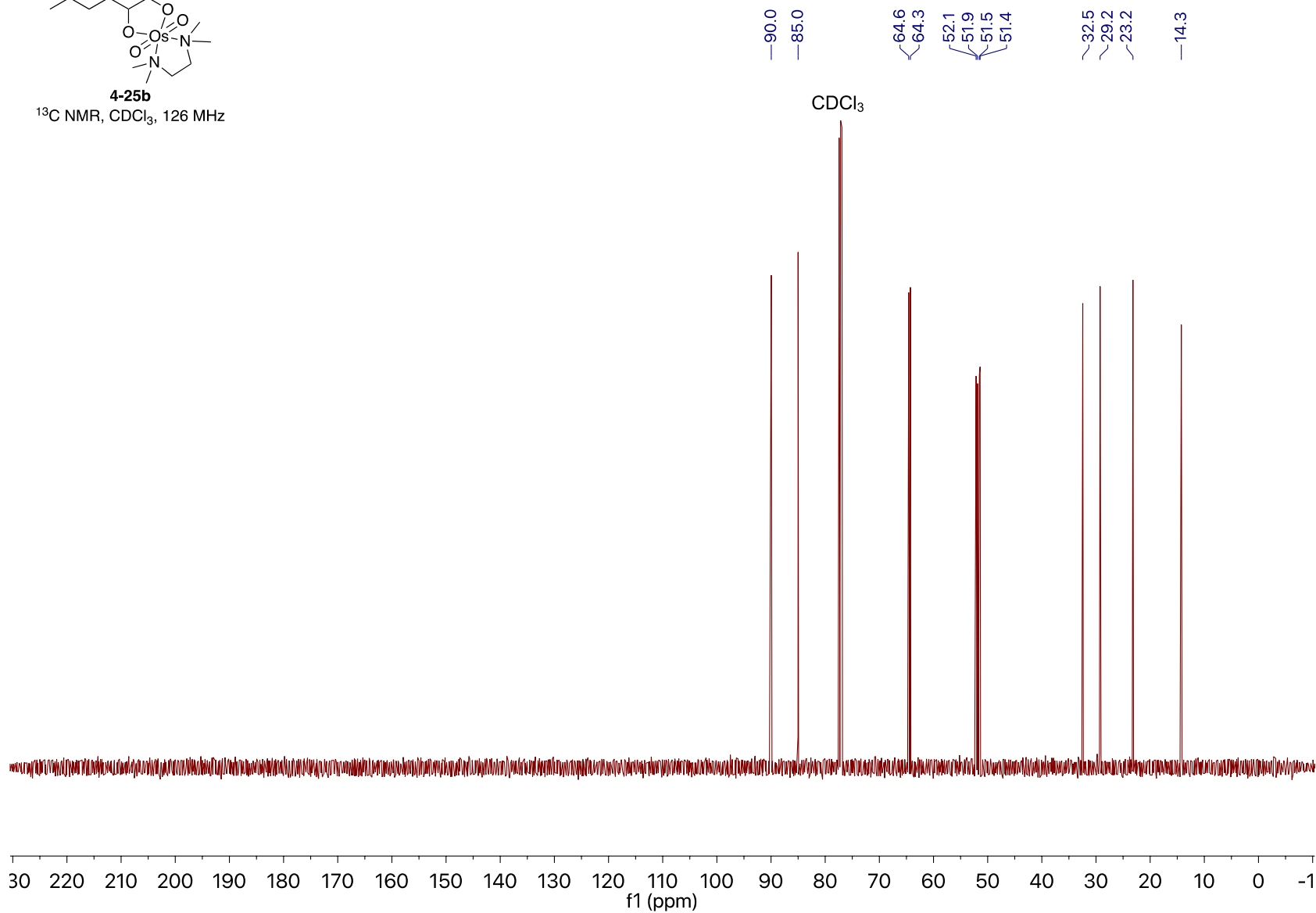
¹H NMR, CDCl₃, 500 MHz

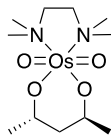




4-25b

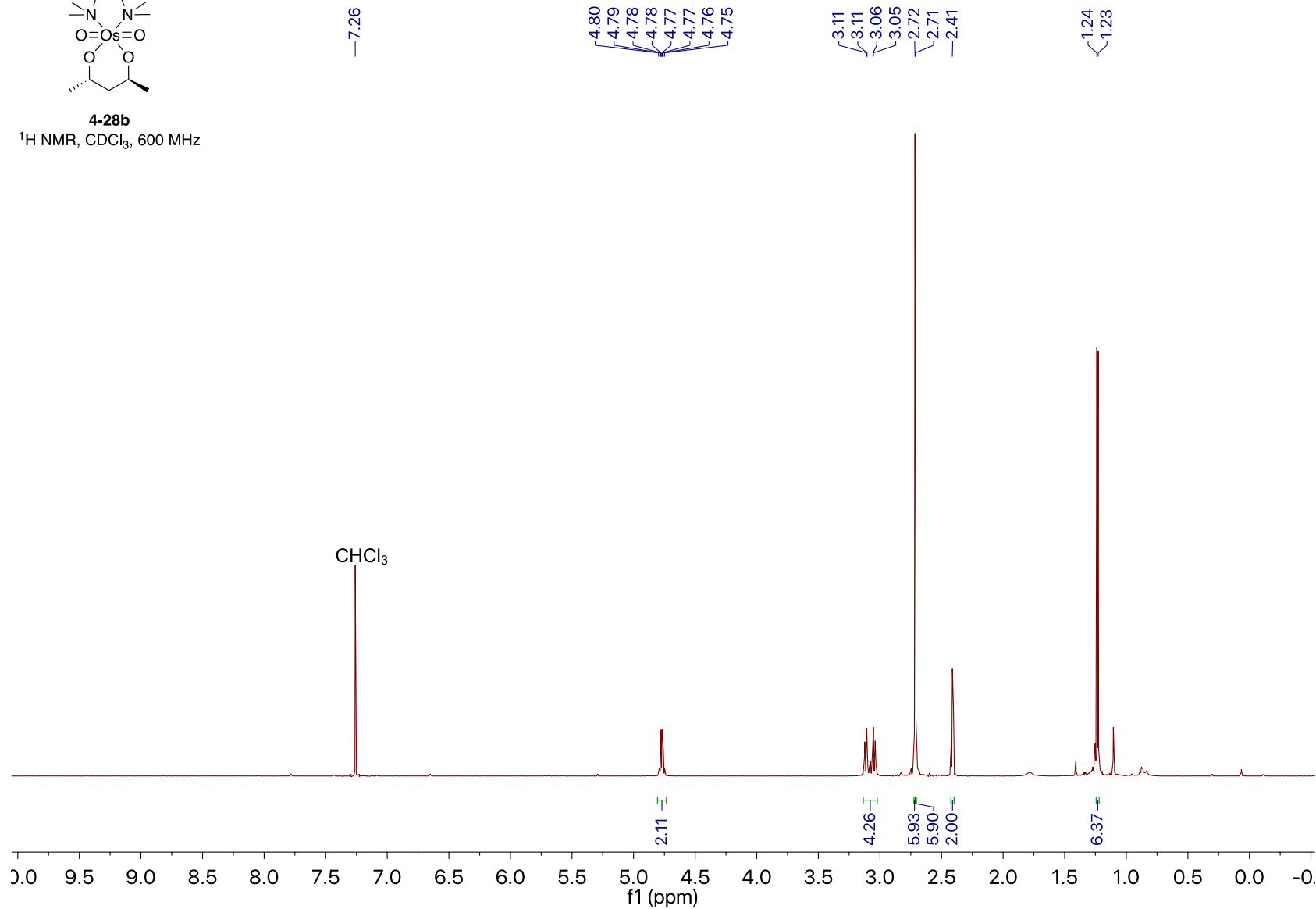
^{13}C NMR, CDCl_3 , 126 MHz

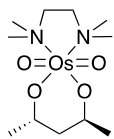




4-28b

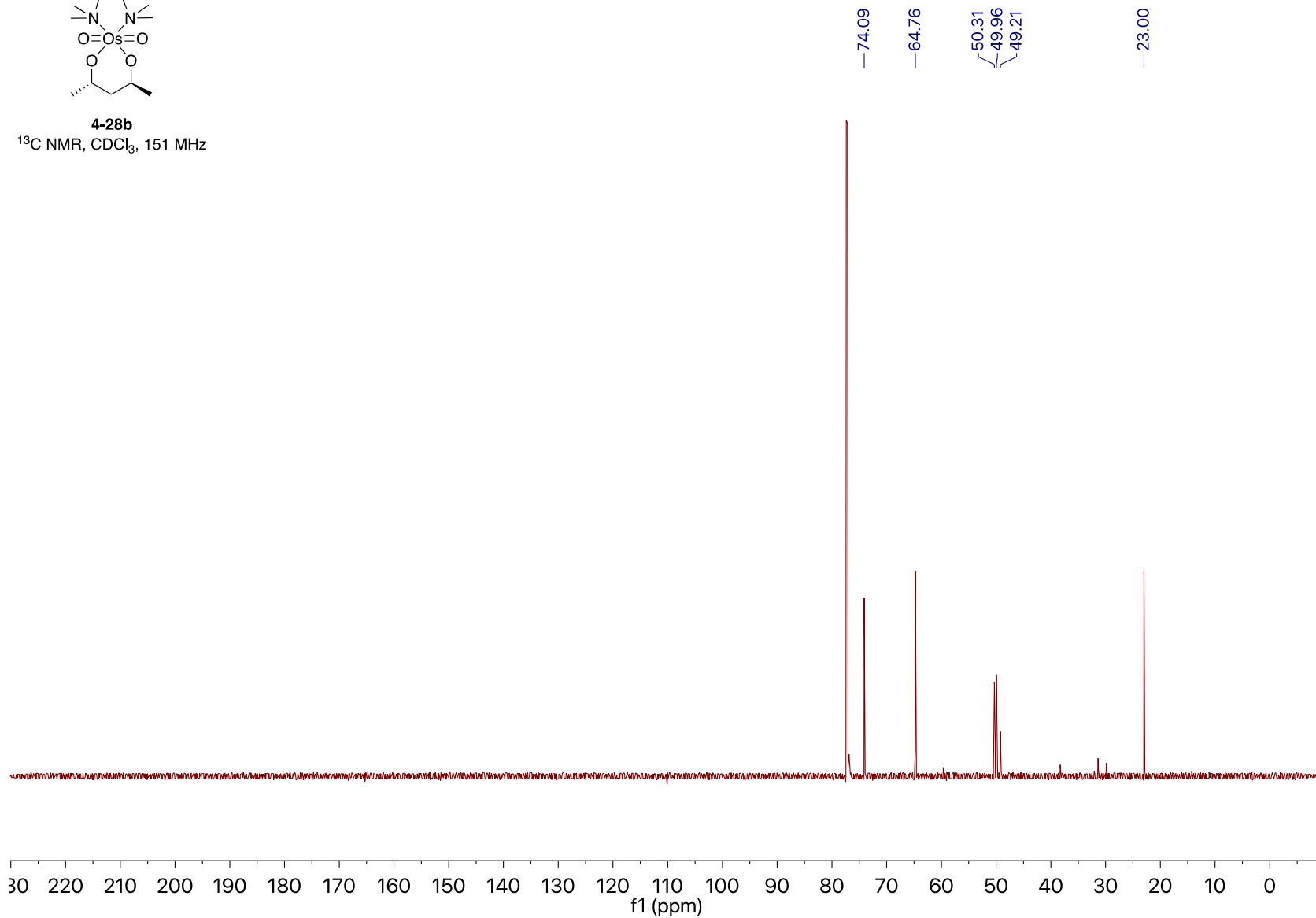
¹H NMR, CDCl₃, 600 MHz

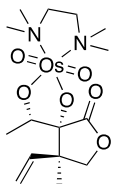




4-28b

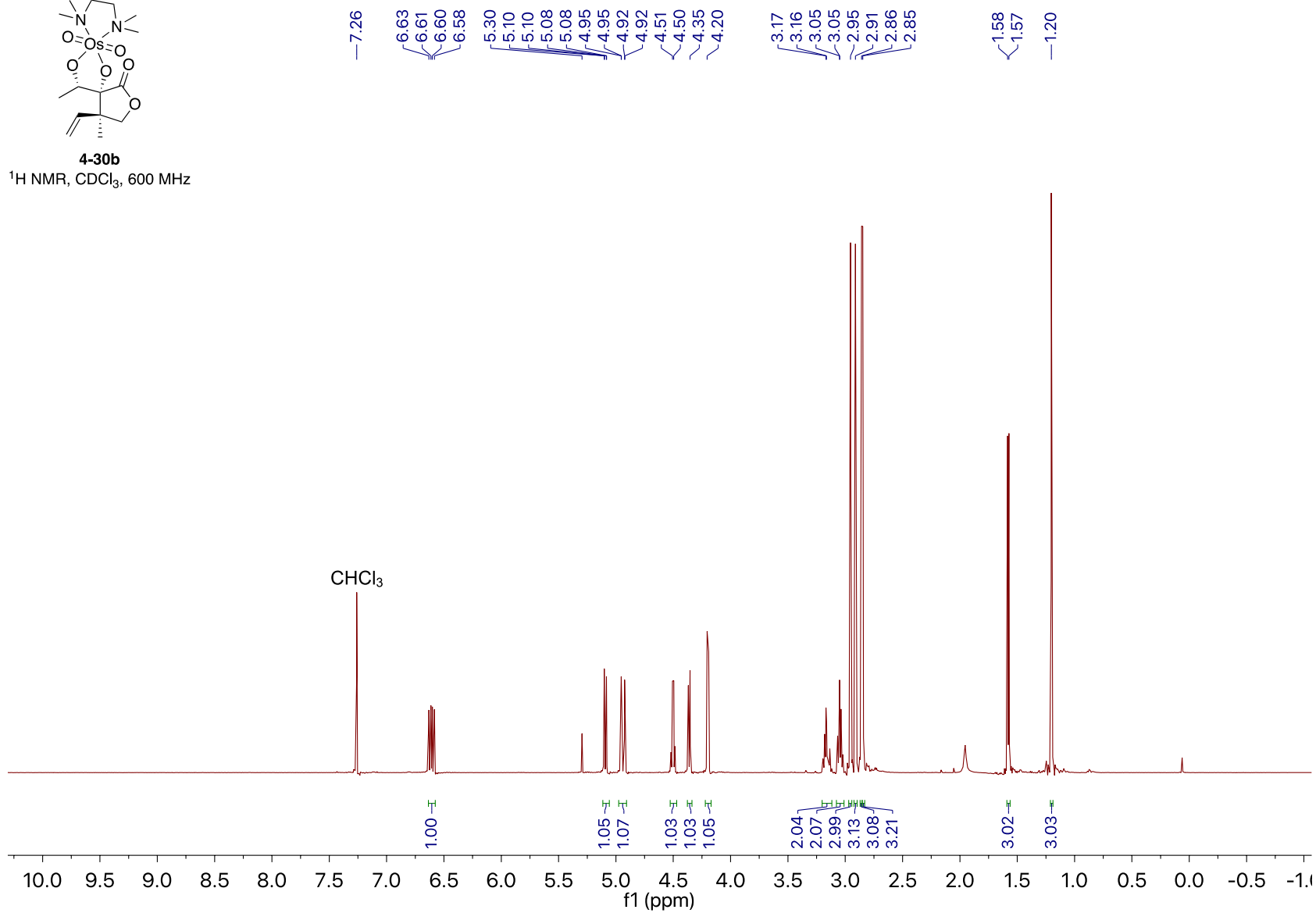
^{13}C NMR, CDCl_3 , 151 MHz

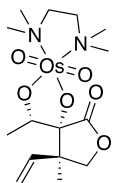




4-30b

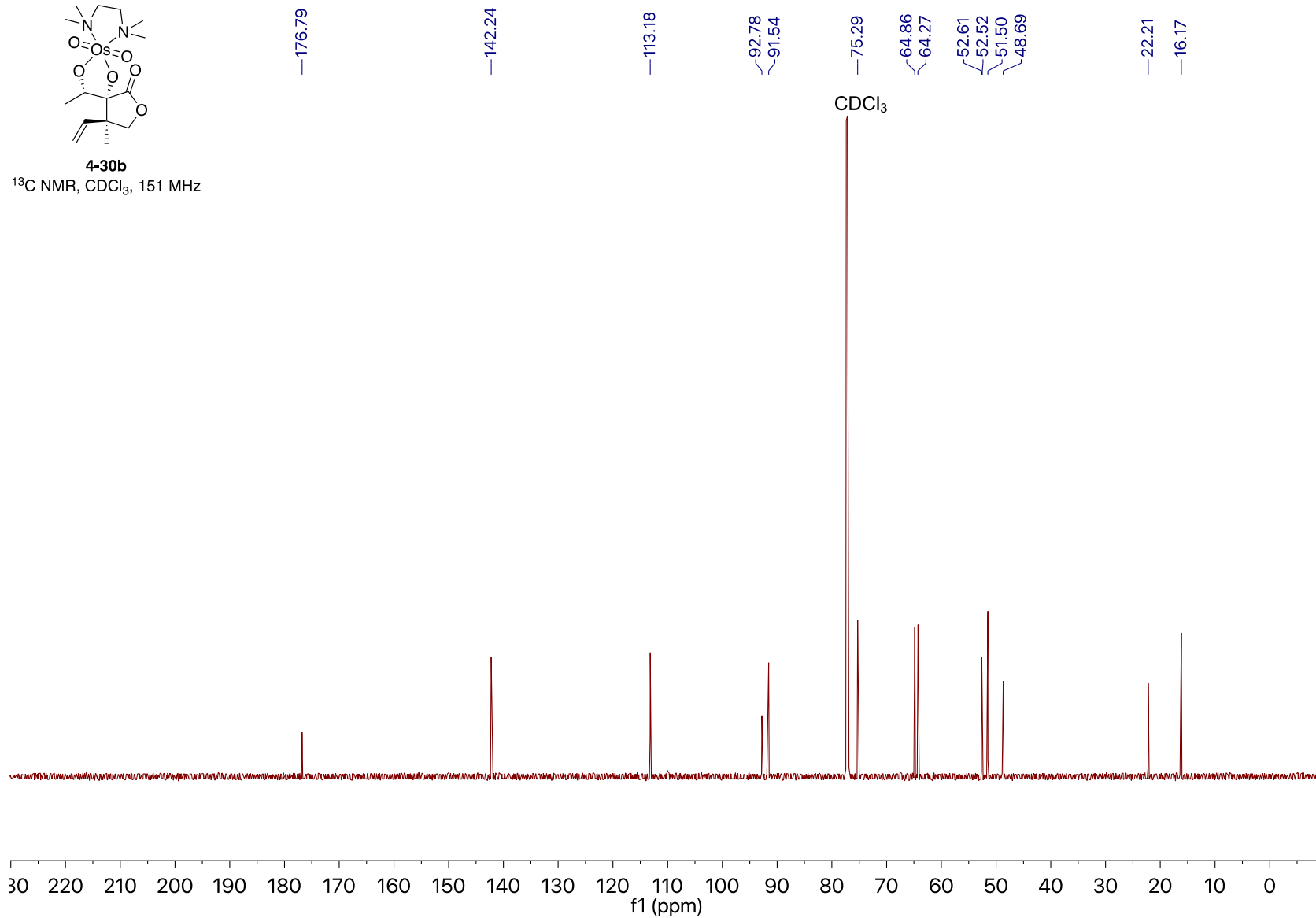
¹H NMR, CDCl₃, 600 MHz

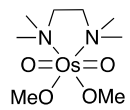




4-30b

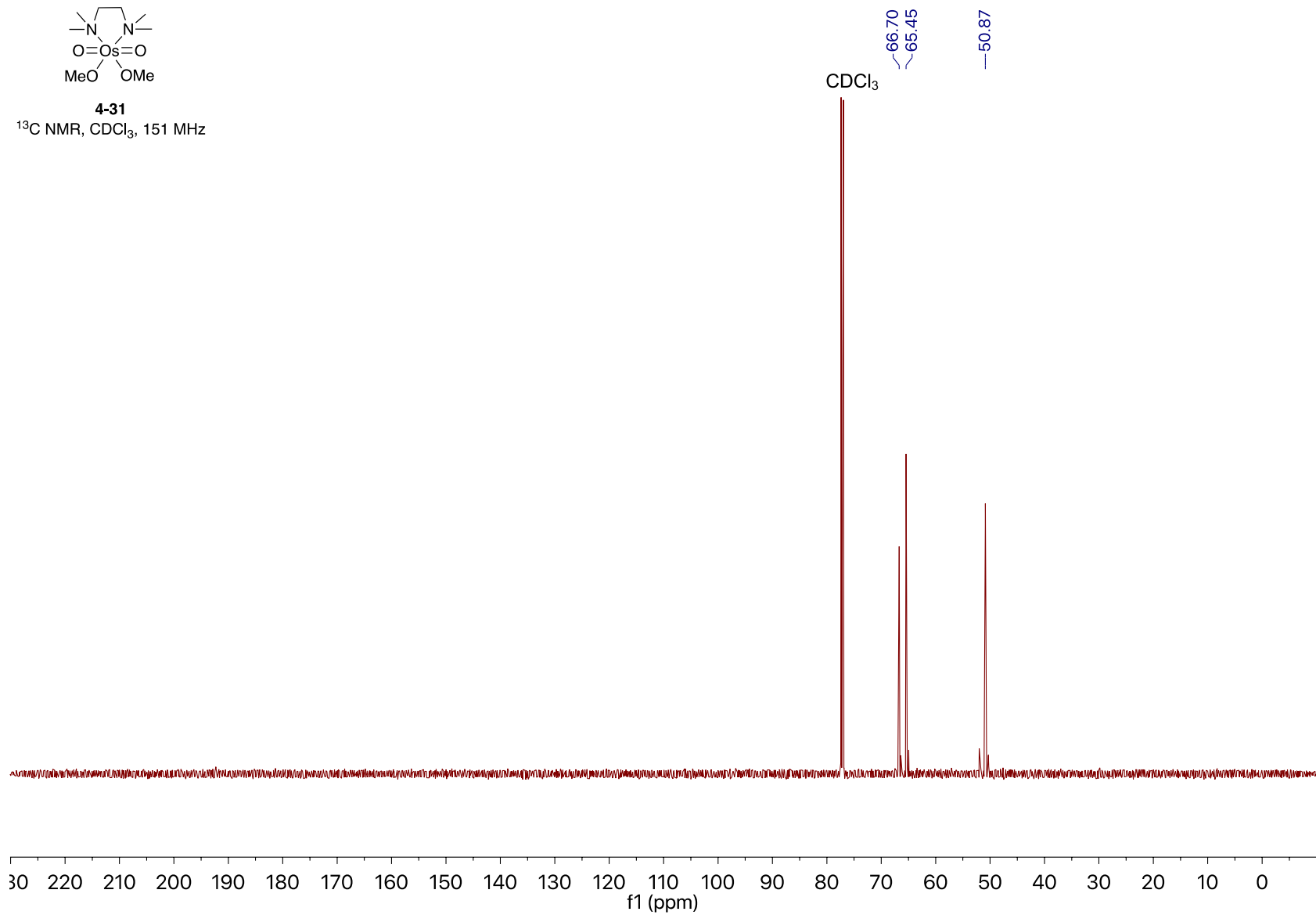
^{13}C NMR, CDCl_3 , 151 MHz

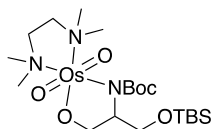




4-31

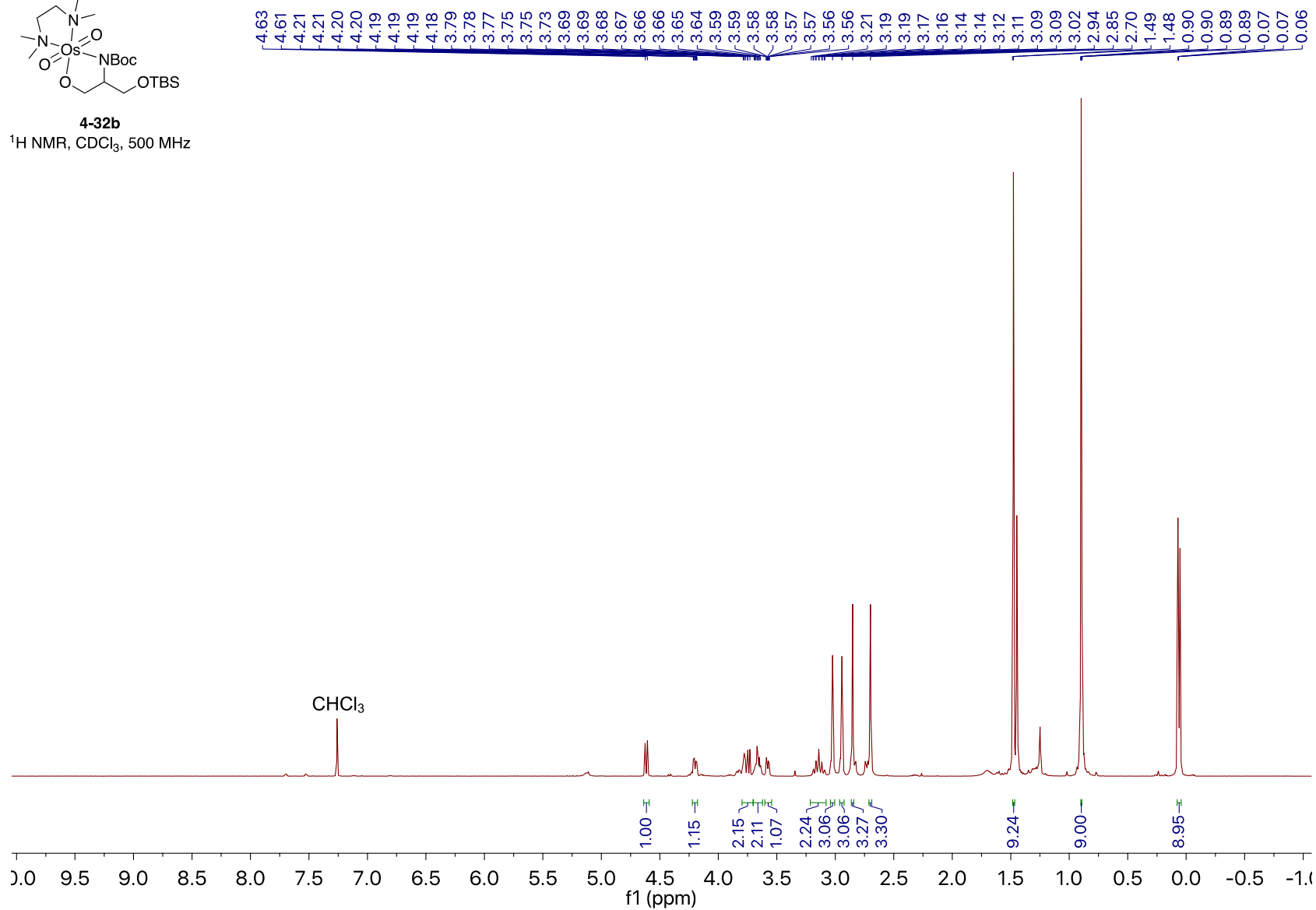
^{13}C NMR, CDCl_3 , 151 MHz

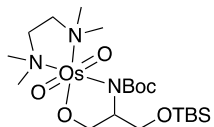




4-32b

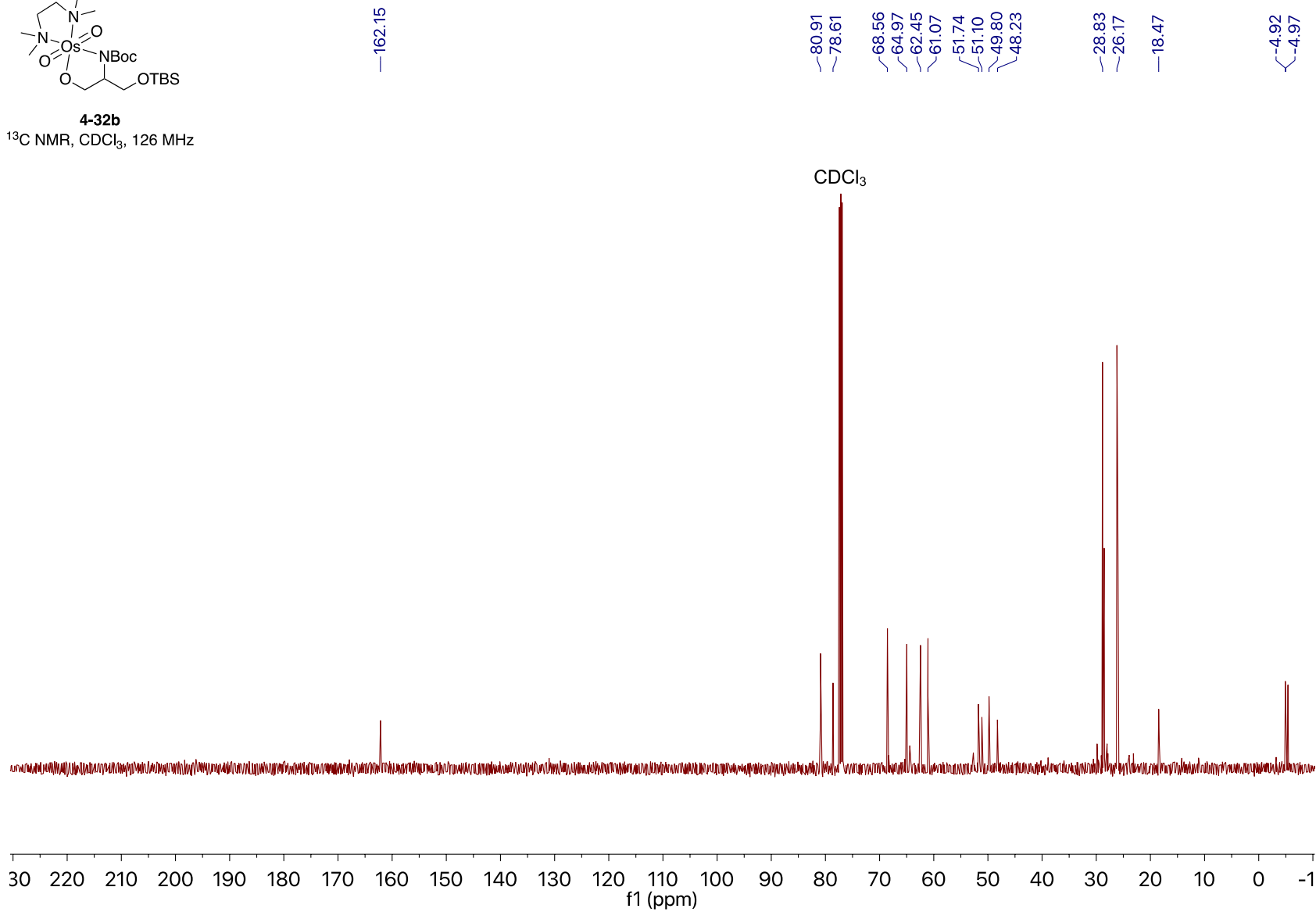
¹H NMR, CDCl₃, 500 MHz



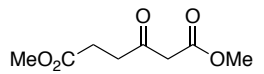


4-32b

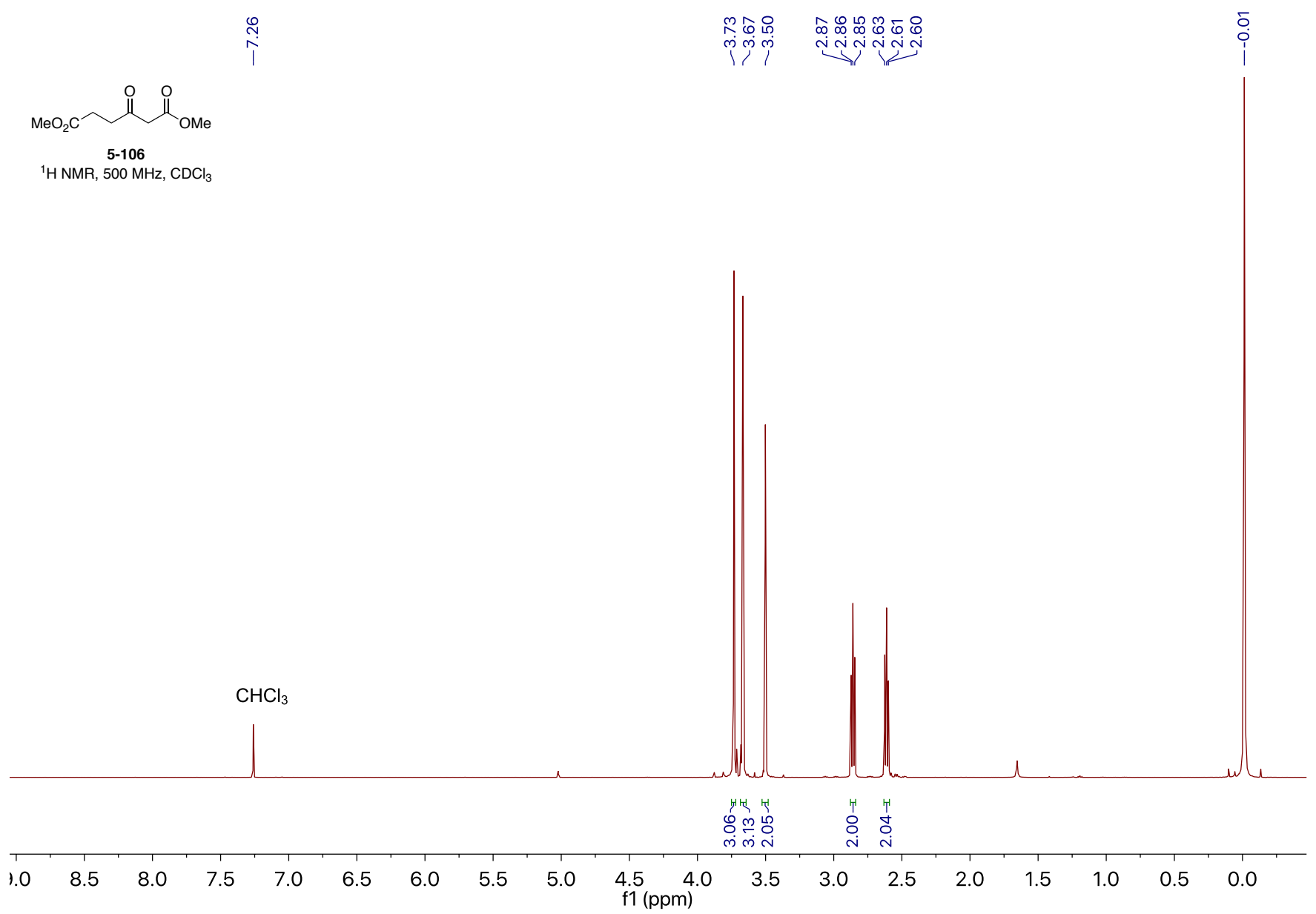
^{13}C NMR, CDCl_3 , 126 MHz

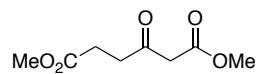


Appendix C: Spectral Data for Compounds in Chapter 5



5-106
¹H NMR, 500 MHz, CDCl₃





5-106

$^{13}\text{C}\{^1\text{H}\}$ NMR, 126 MHz, CDCl_3

— 200.98

— 172.93

— 167.51

— 52.52

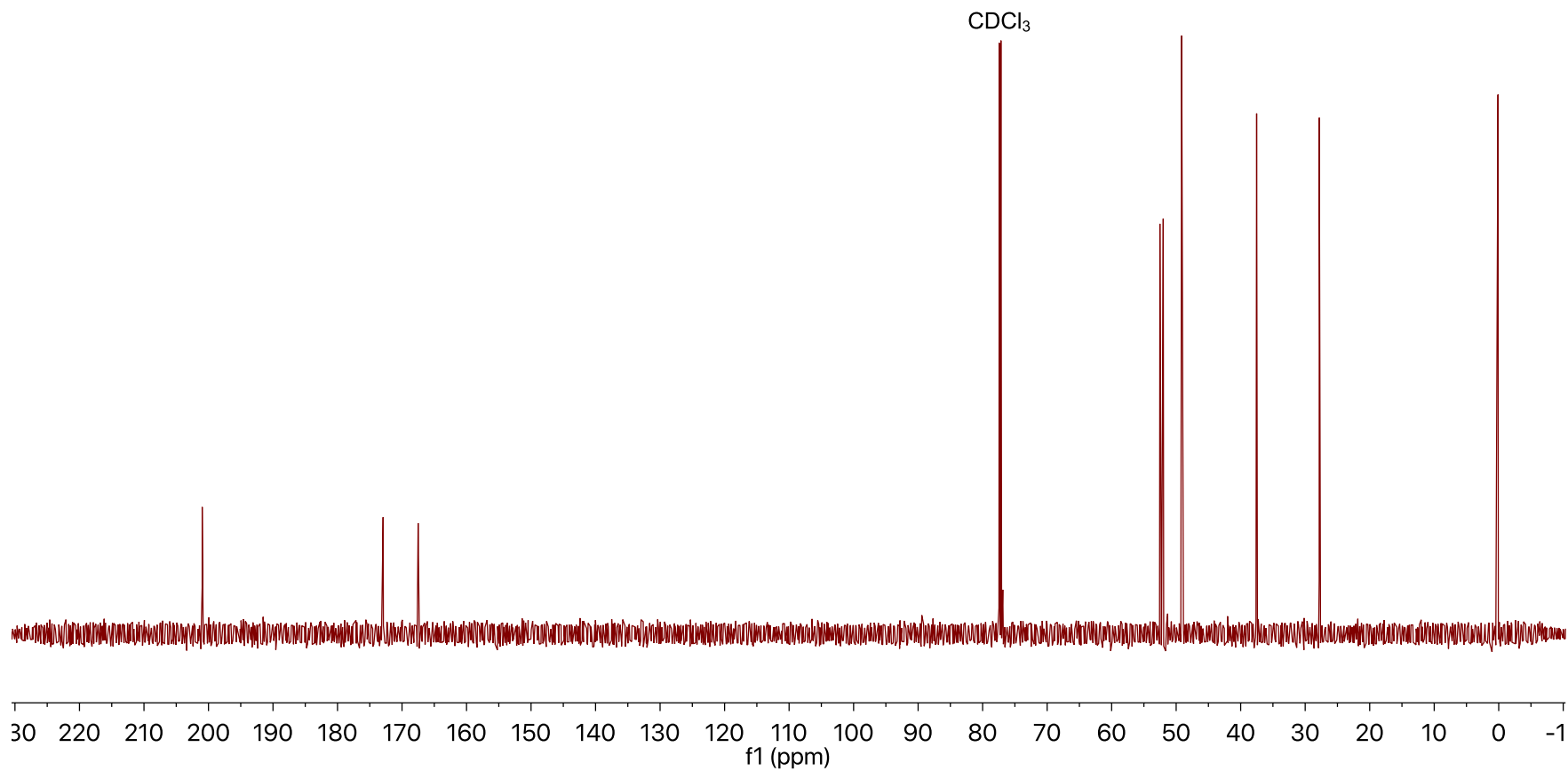
— 52.00

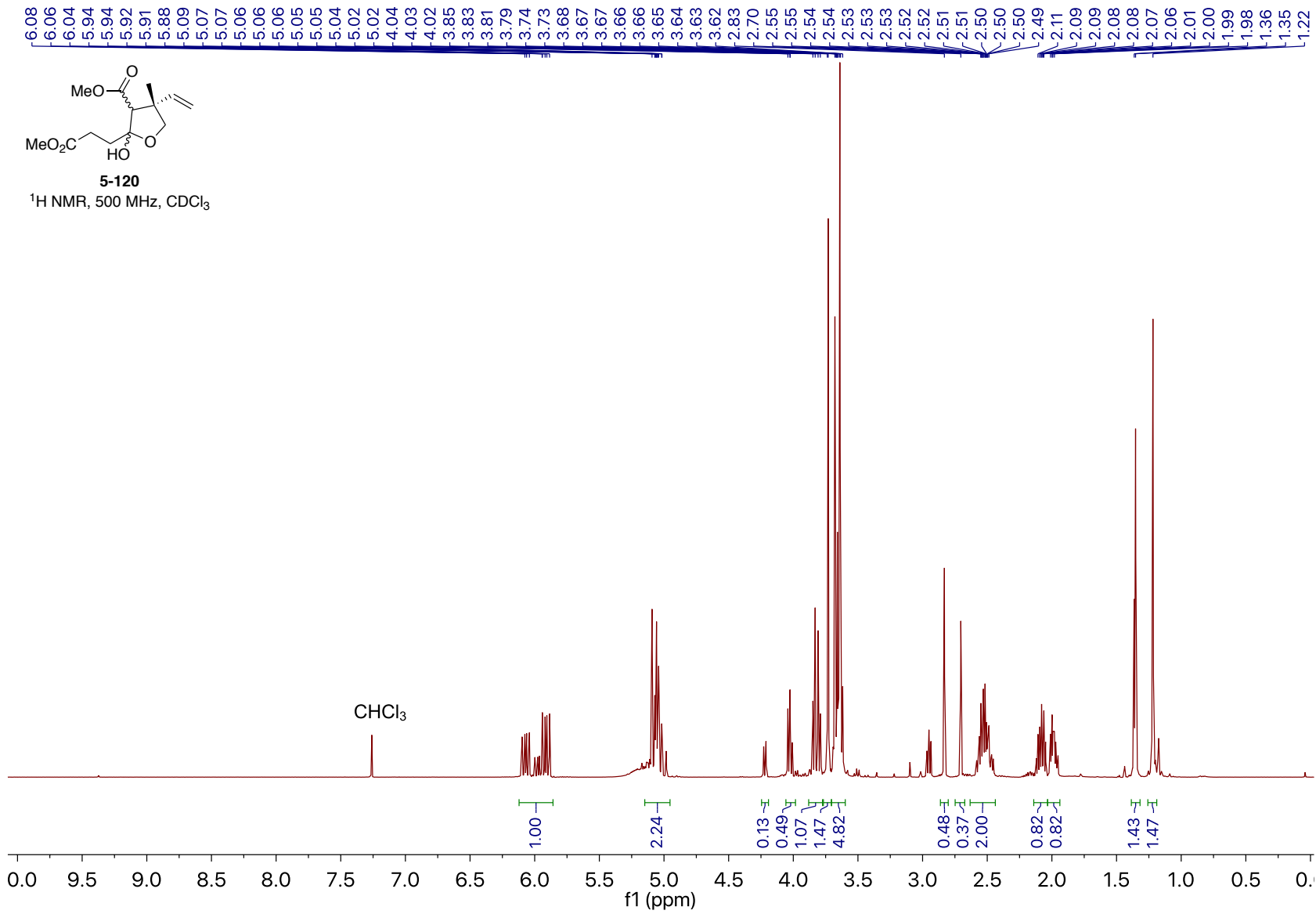
— 49.15

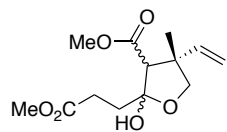
— 37.53

— 27.82

— 0.11







5-120

$^{13}\text{C}\{^1\text{H}\}$ NMR, 126 MHz, CDCl_3

174.28
174.21
173.22
172.96
172.84
170.31
165.78

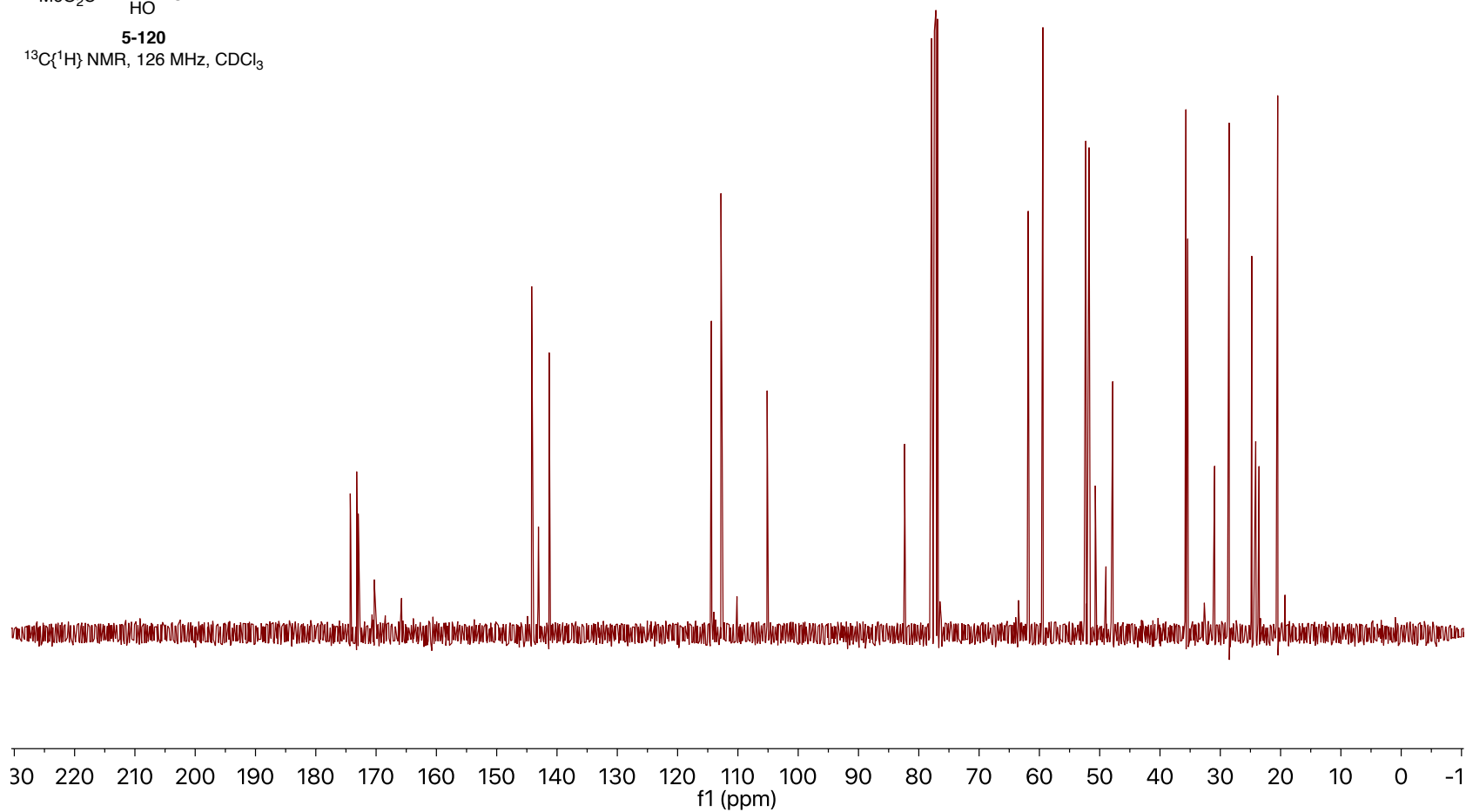
144.20
143.07
141.30

114.40
112.81
112.74
105.15
105.11

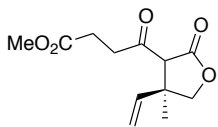
82.36
77.95
77.87

61.86
59.42
52.32
52.31
51.81
51.76
51.75
50.73
48.96
47.83
47.80
35.70
35.40
30.94
28.64
28.57
28.54
24.78
24.12
23.57
20.48

CDCl_3

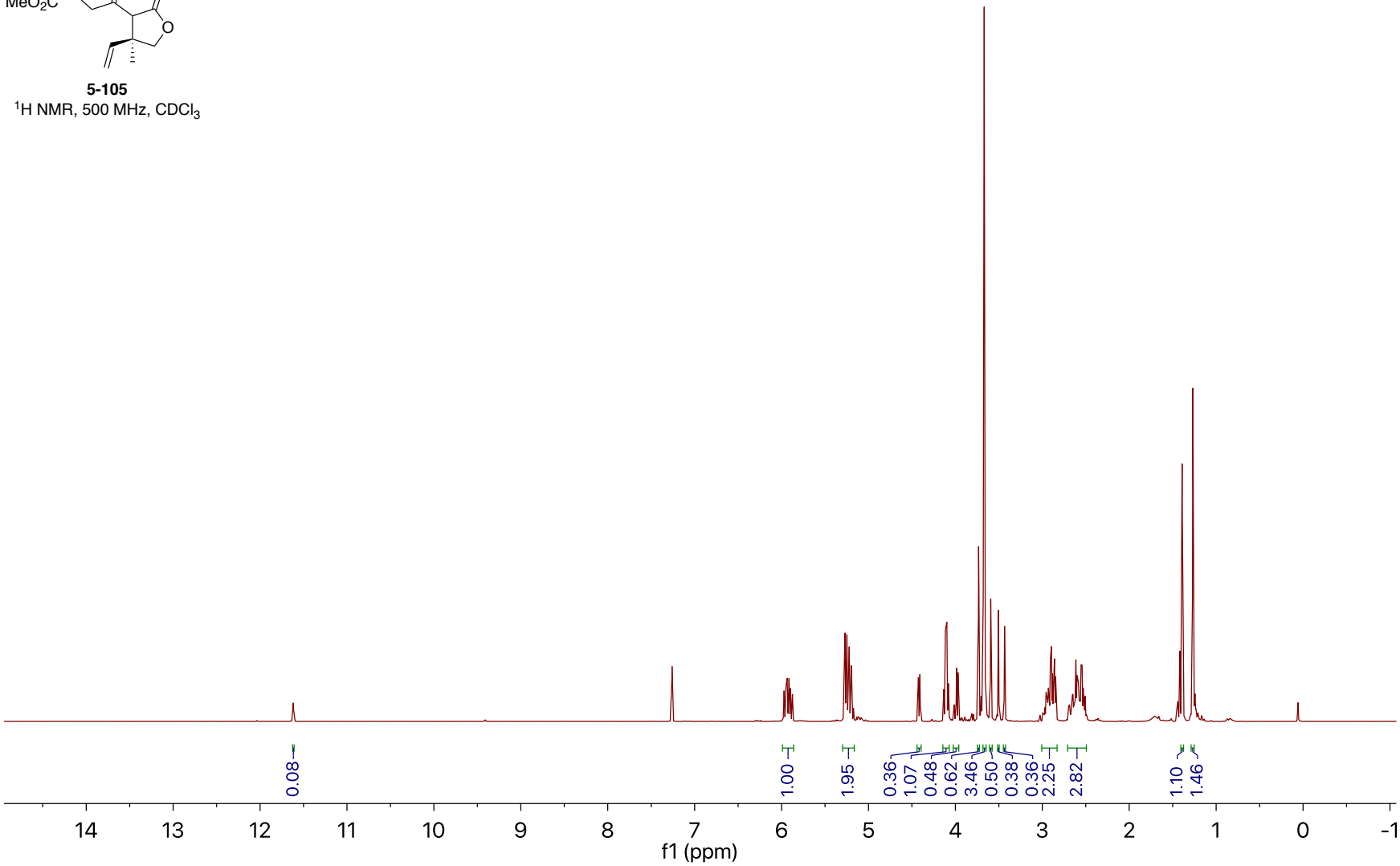


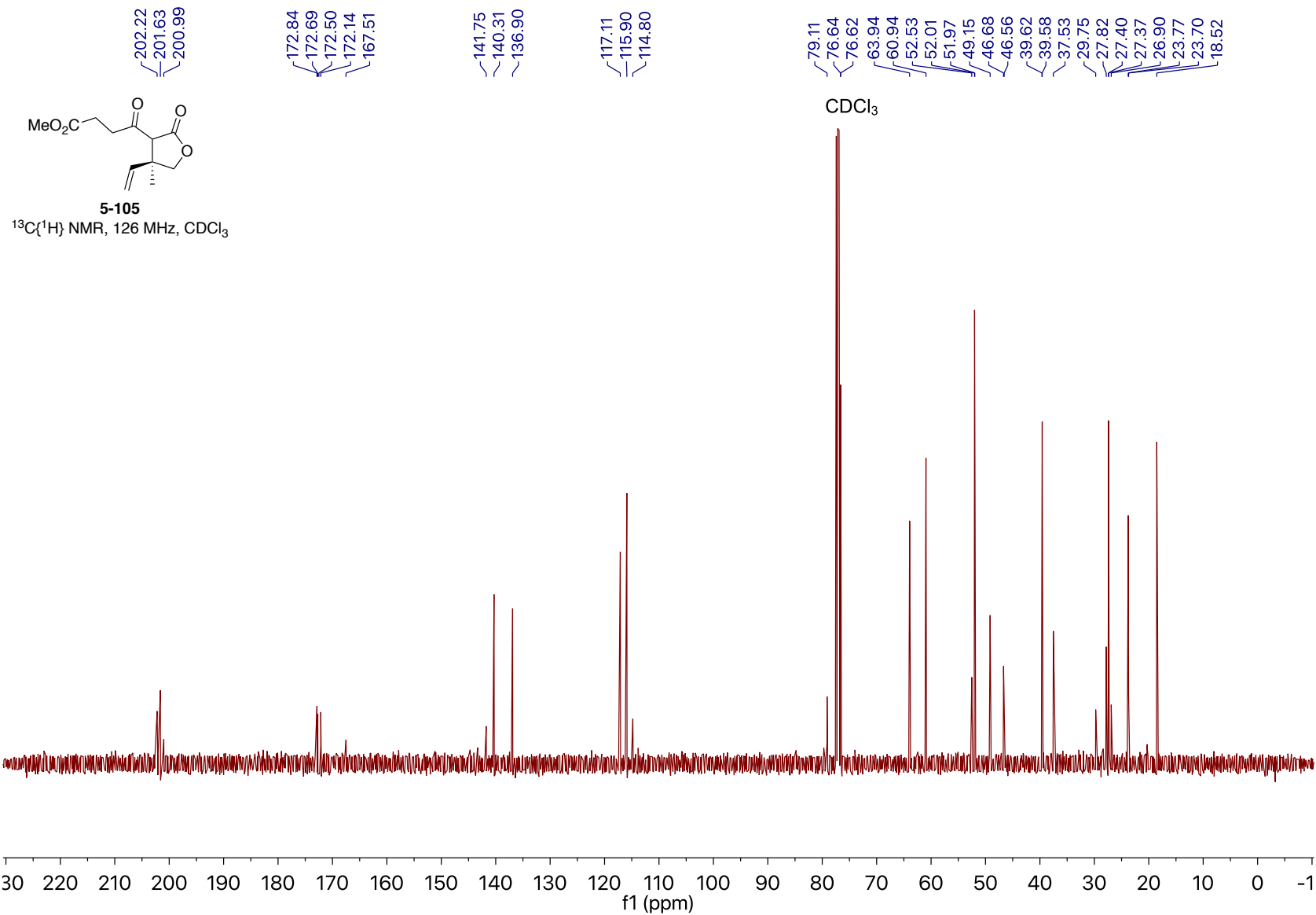
5.97
5.95
5.94
5.93
5.91
5.90
5.88
5.27
5.26
5.25
5.25
5.23
5.22
5.20
4.43
4.41
4.13
4.12
4.10
4.08
3.99
3.97
3.73
3.67
3.59
3.50
3.43
2.96
2.95
2.94
2.93
2.92
2.92
2.91
2.90
2.88
2.87
2.87
2.86
2.86
2.85
2.85
2.66
2.65
2.65
2.64
2.63
2.63
2.61
2.60
2.60
2.59
2.58
2.58
2.57
2.57
2.55
2.54
2.53
2.52
2.52
2.51
1.39
1.27

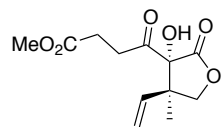


5-105

¹H NMR, 500 MHz, CDCl₃

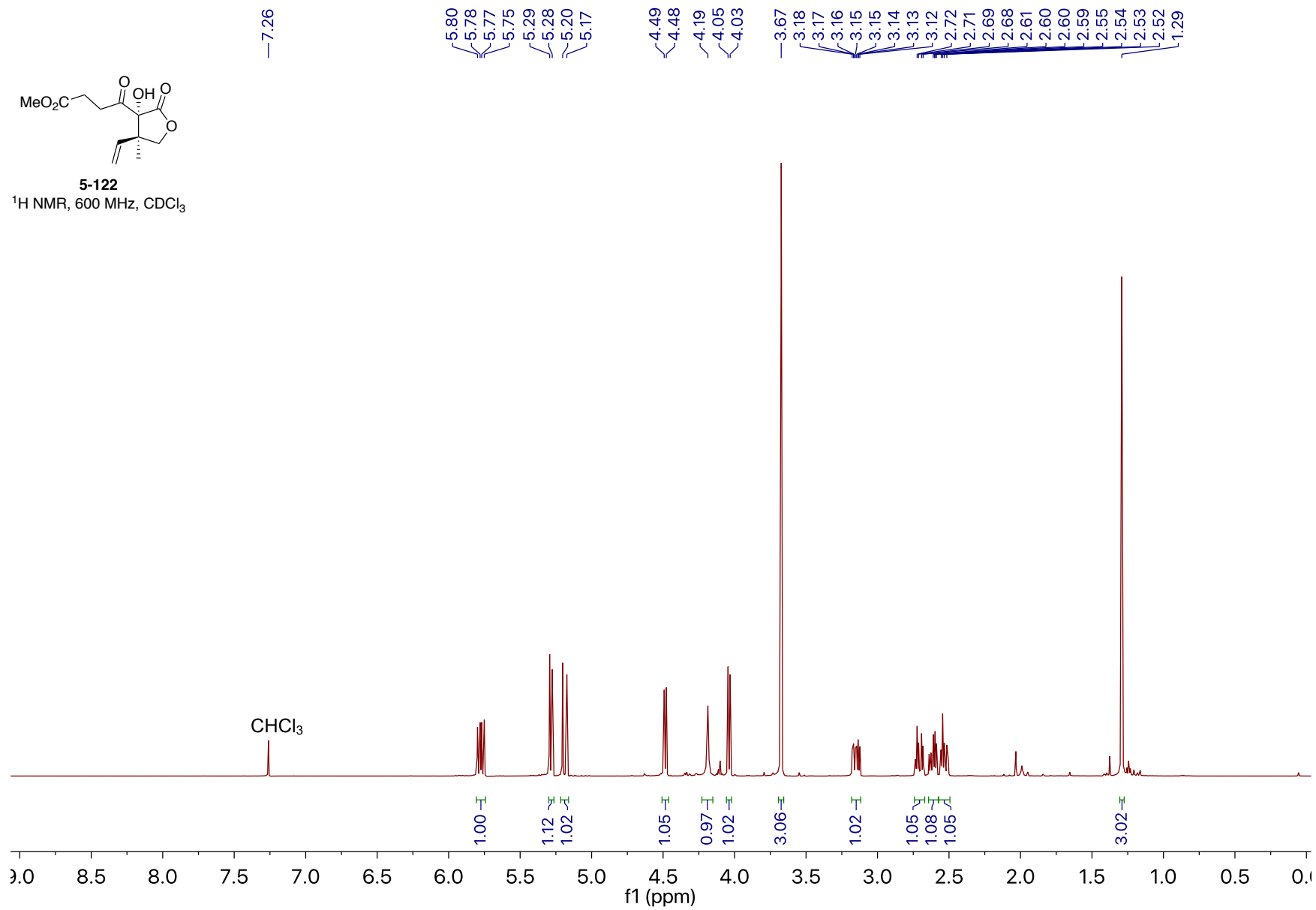


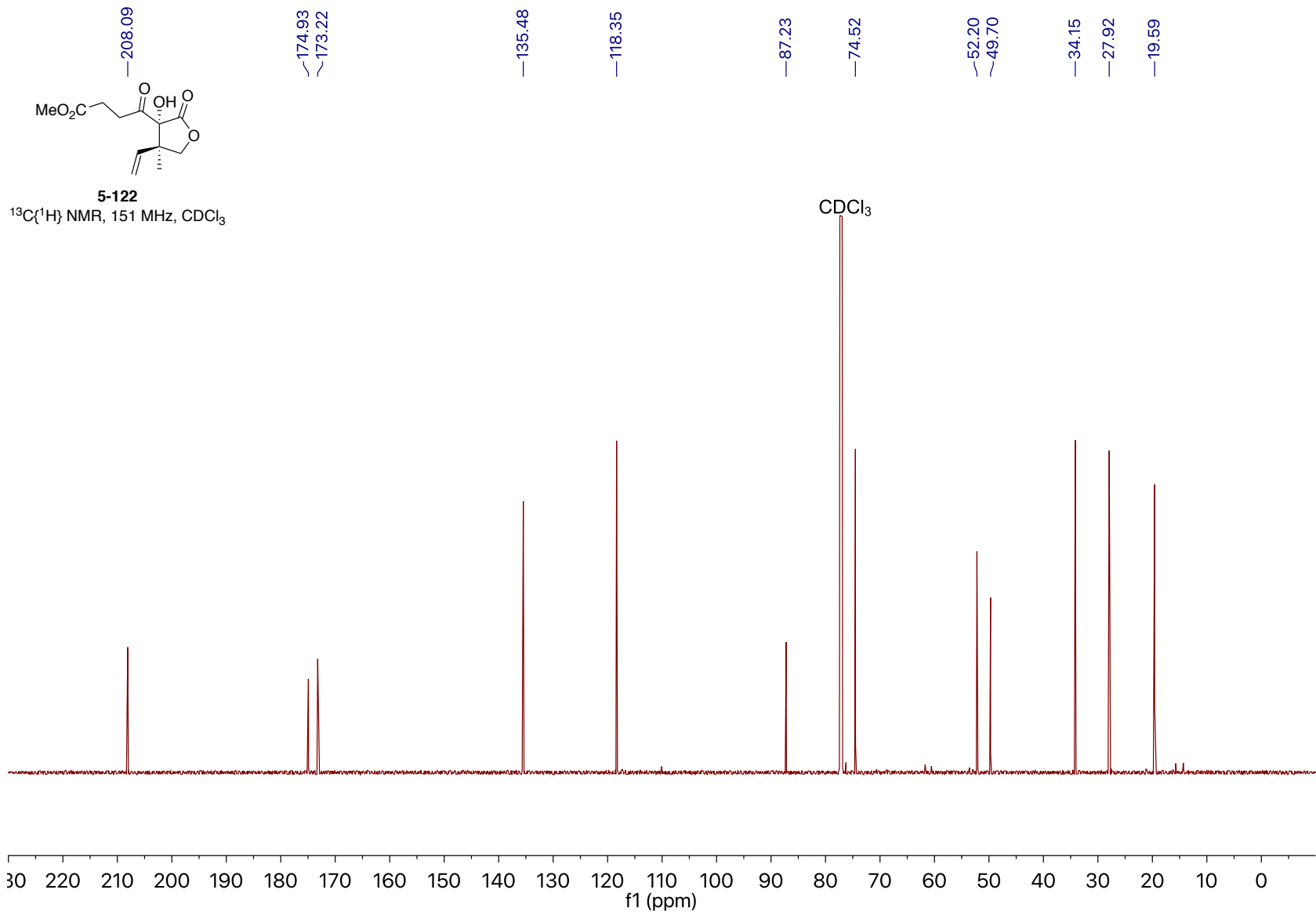


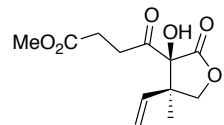


5-122

¹H NMR, 600 MHz, CDCl₃

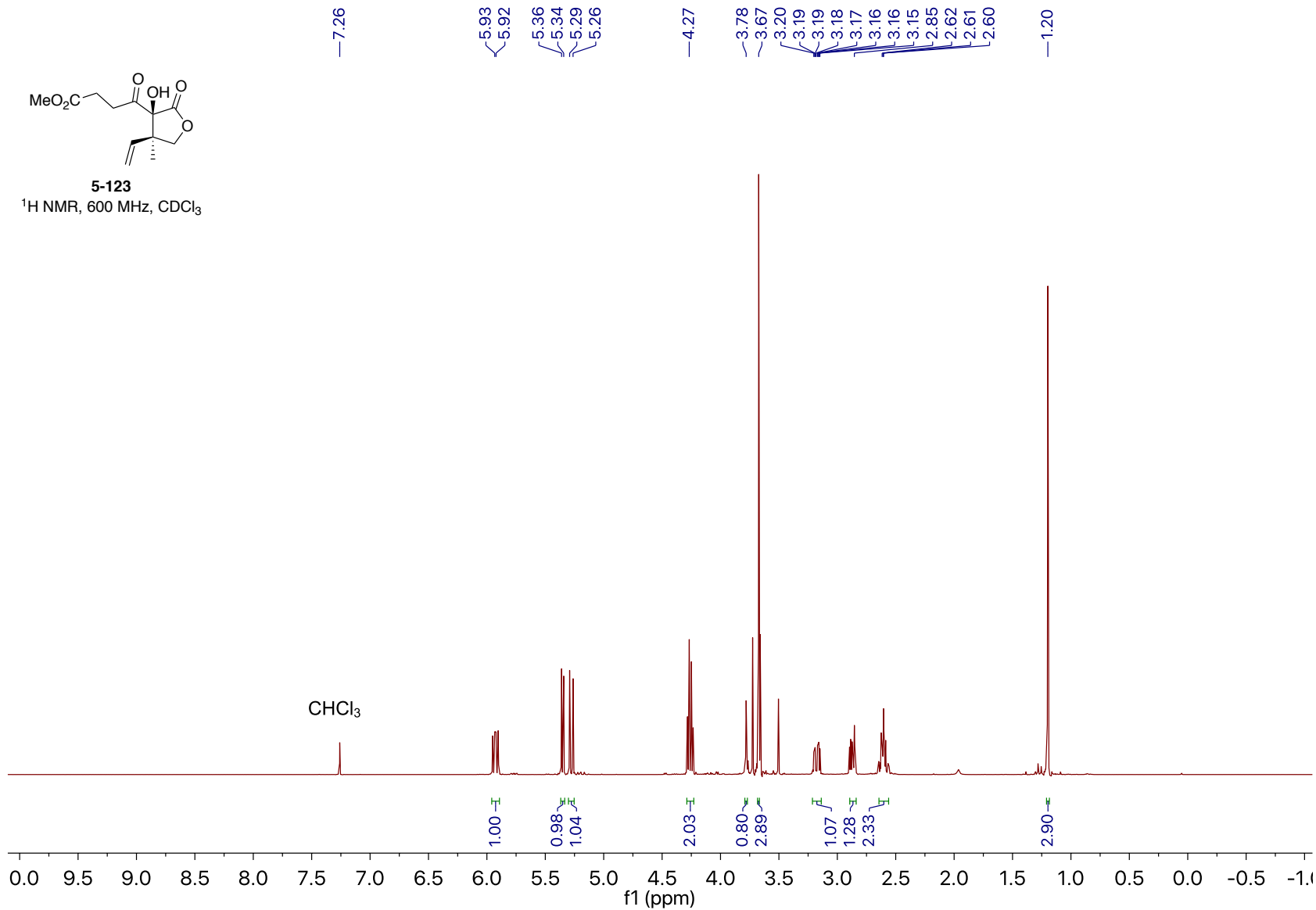


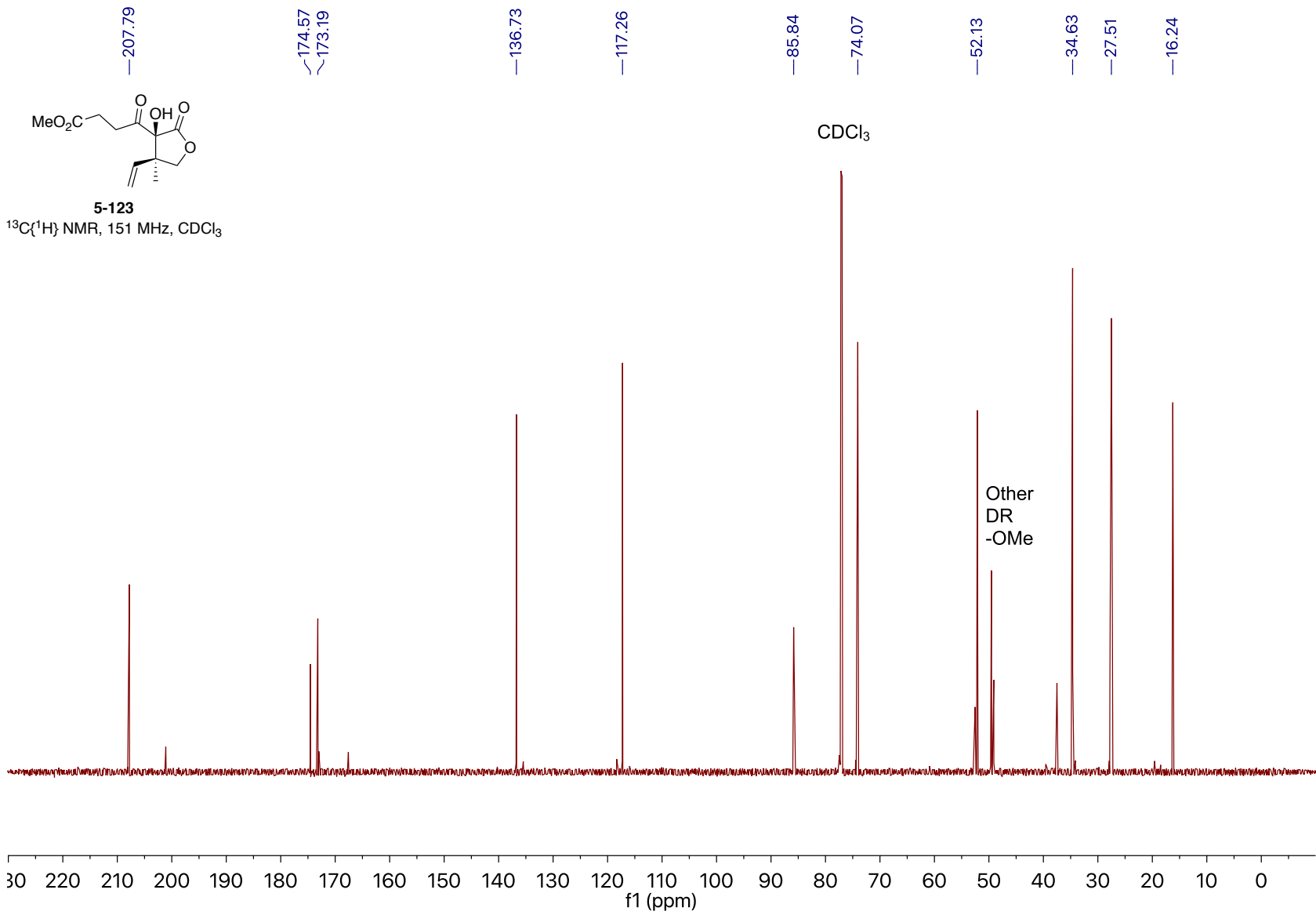


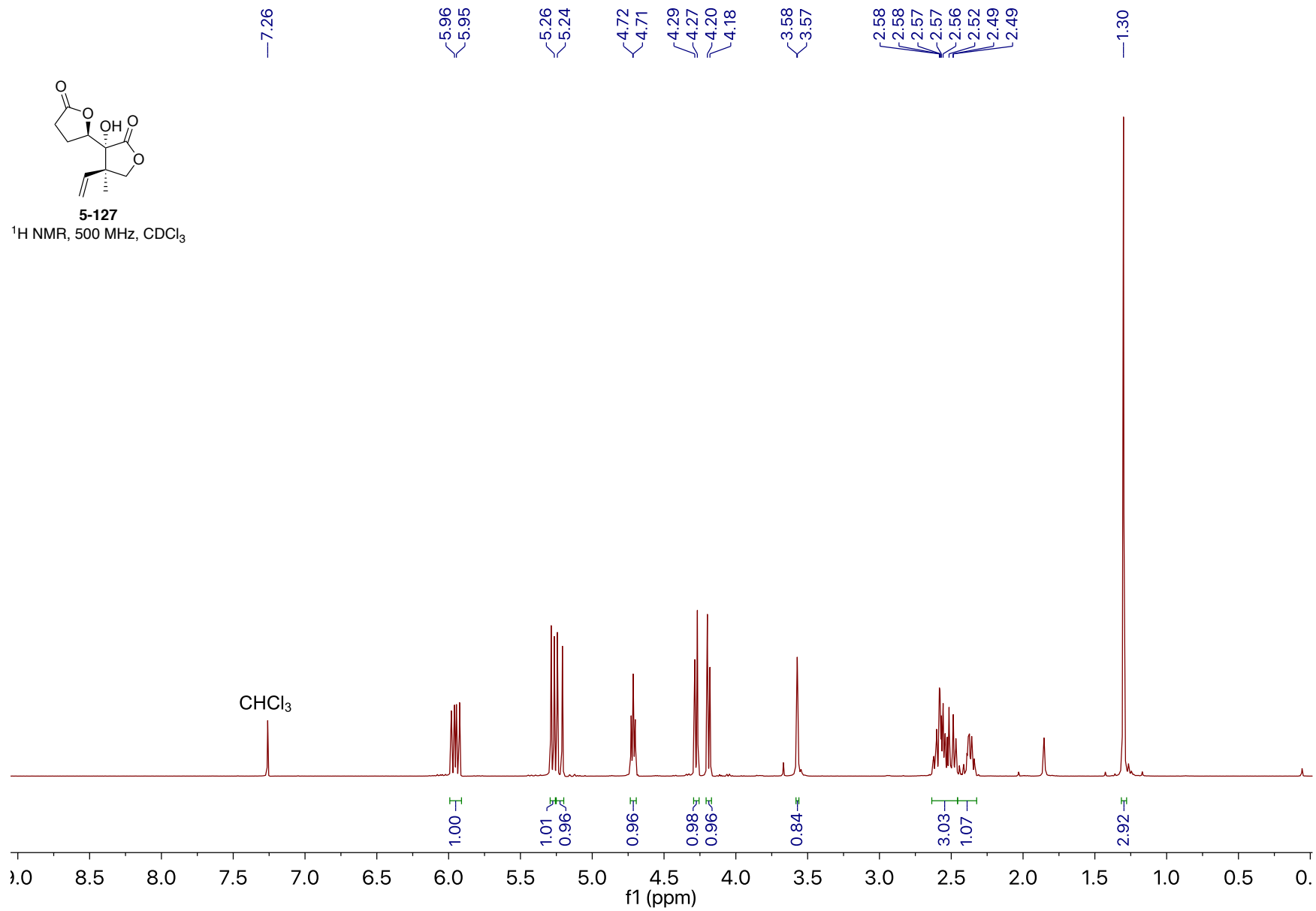
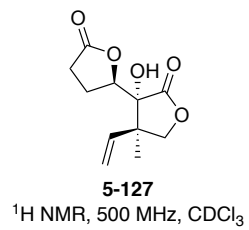


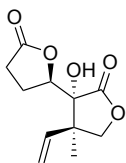
5-123

¹H NMR, 600 MHz, CDCl₃



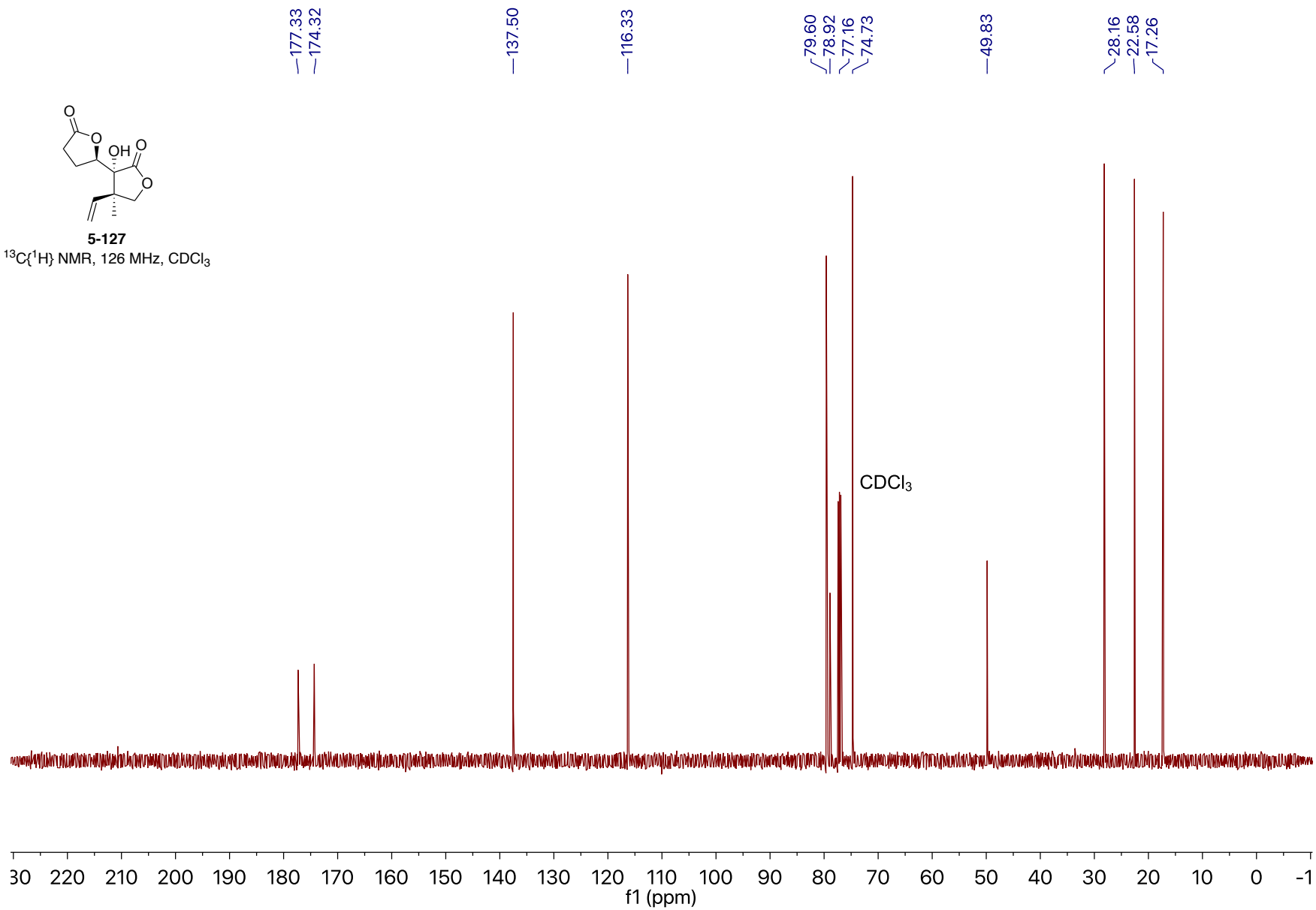


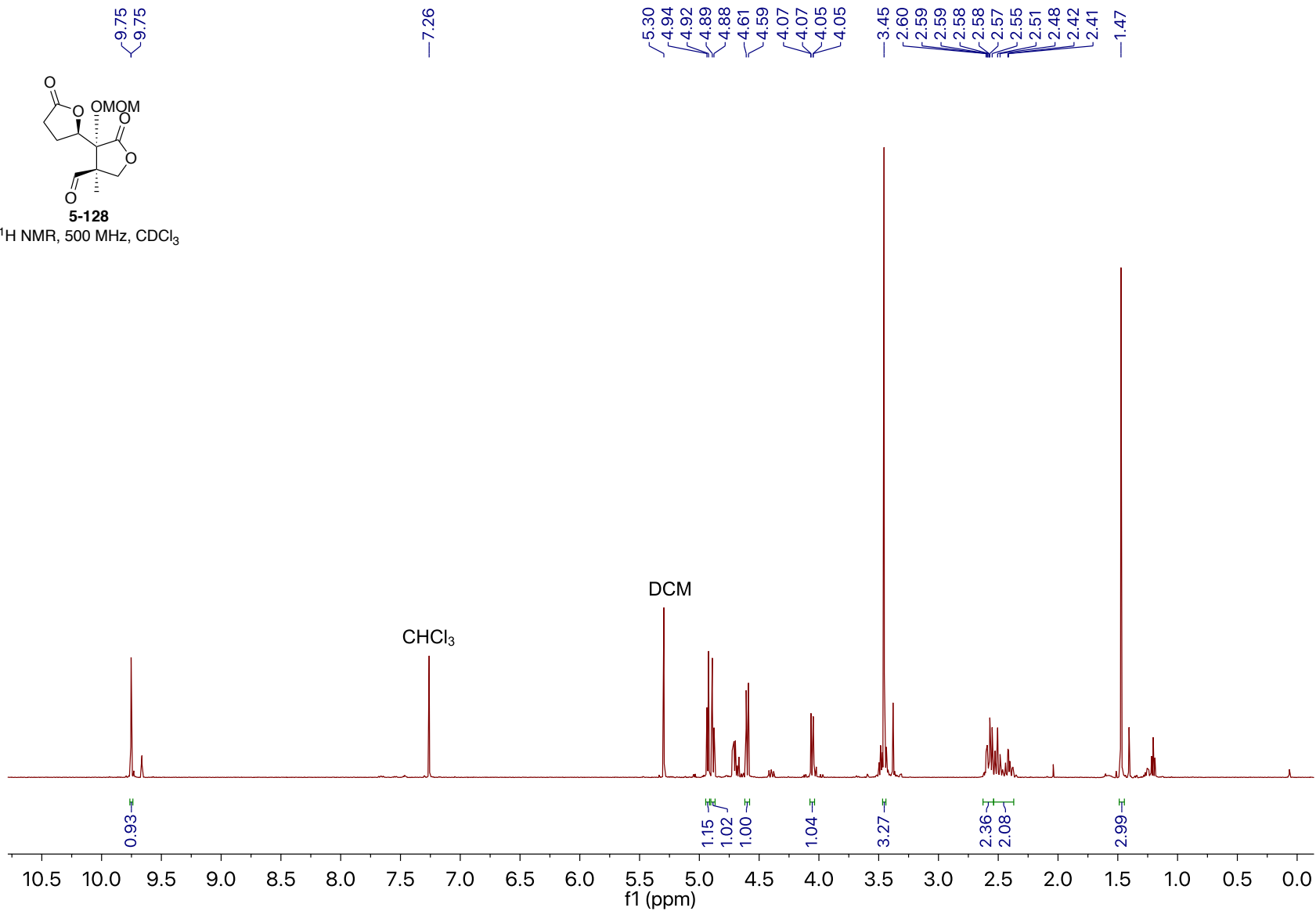
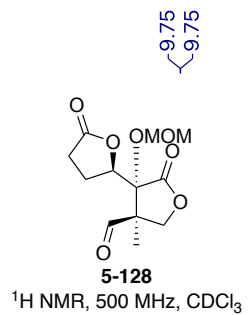


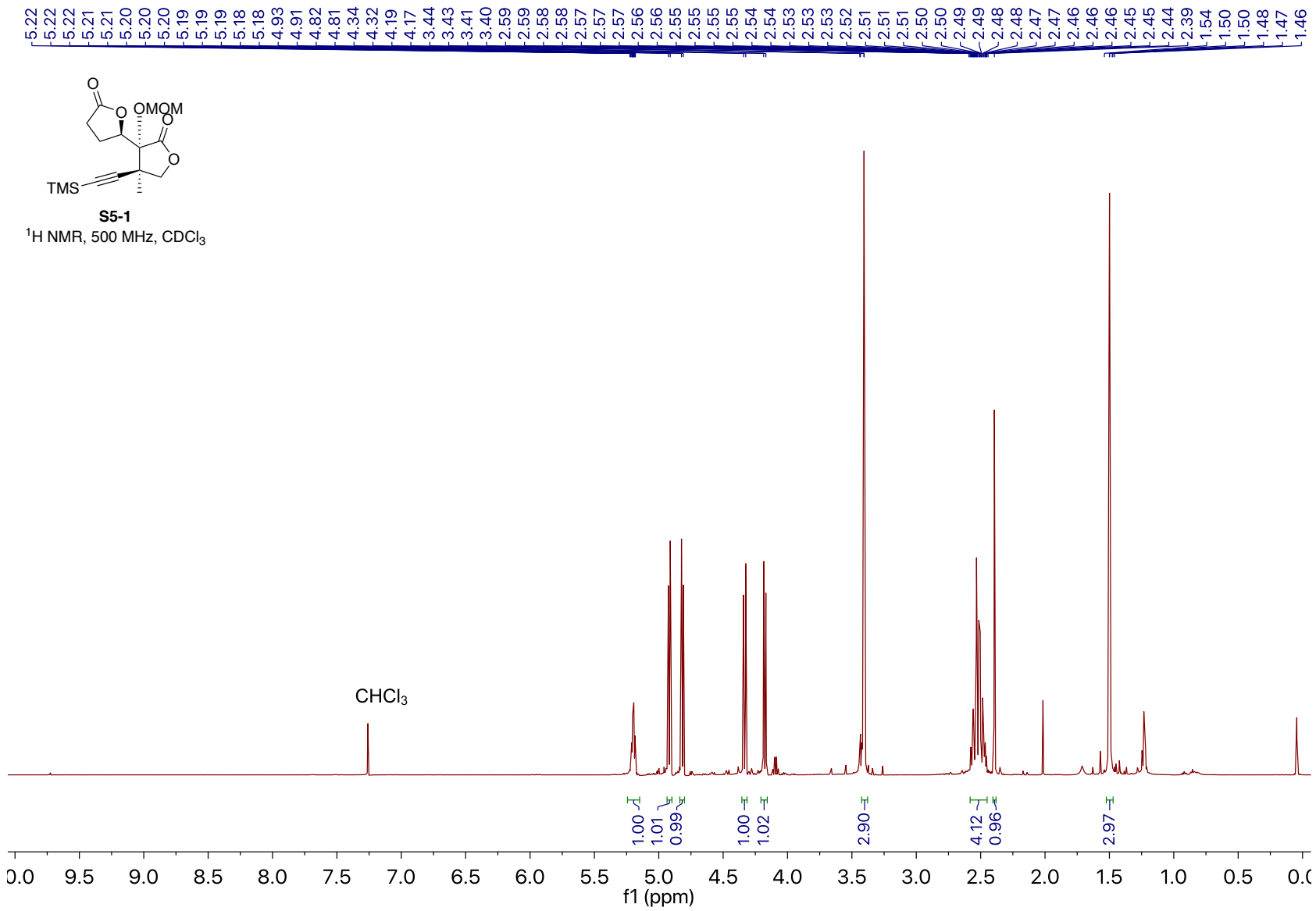


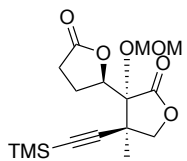
5-127

$^{13}\text{C}\{^1\text{H}\}$ NMR, 126 MHz, CDCl_3









S5-1

$^{13}\text{C}\{^1\text{H}\}$ NMR, 126 MHz, CDCl_3

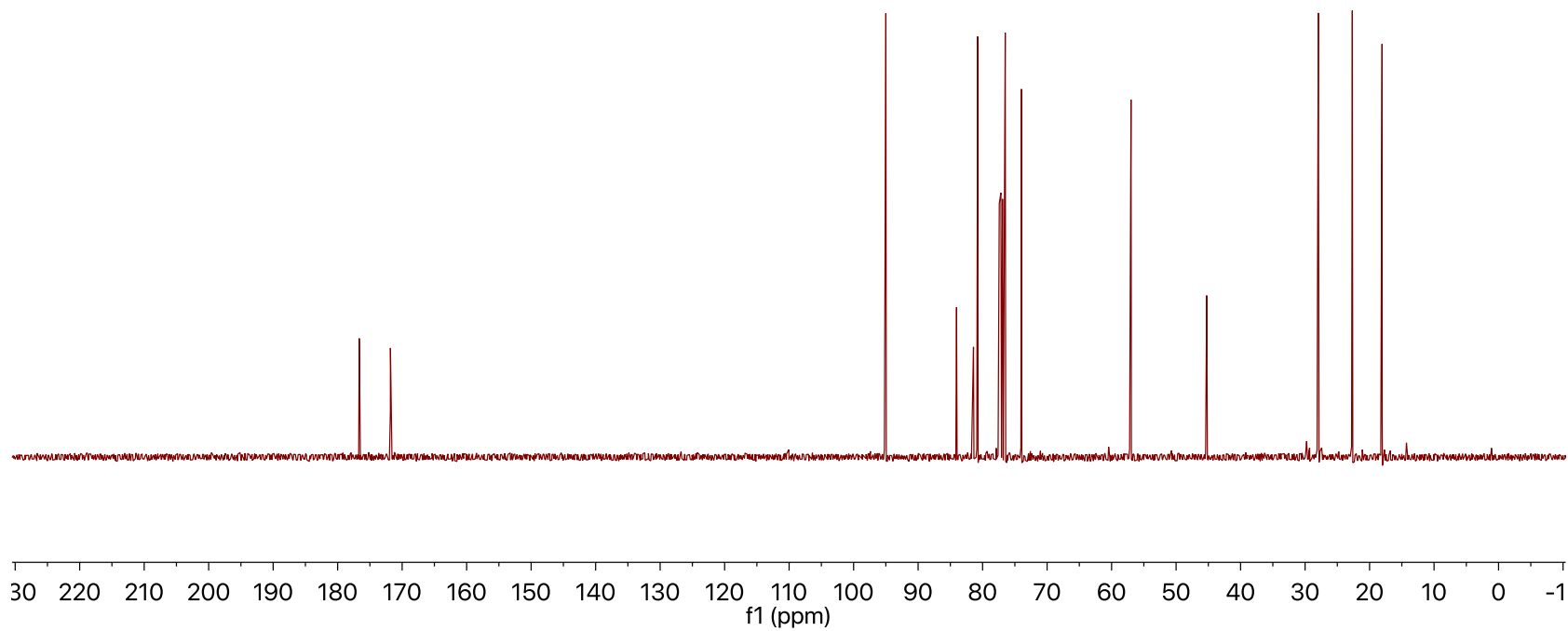
—176.65
—171.82

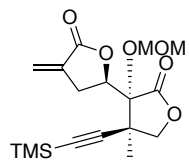
—95.00
/84.04
/81.41
/80.77
/76.49
/73.99

—56.99

—45.26

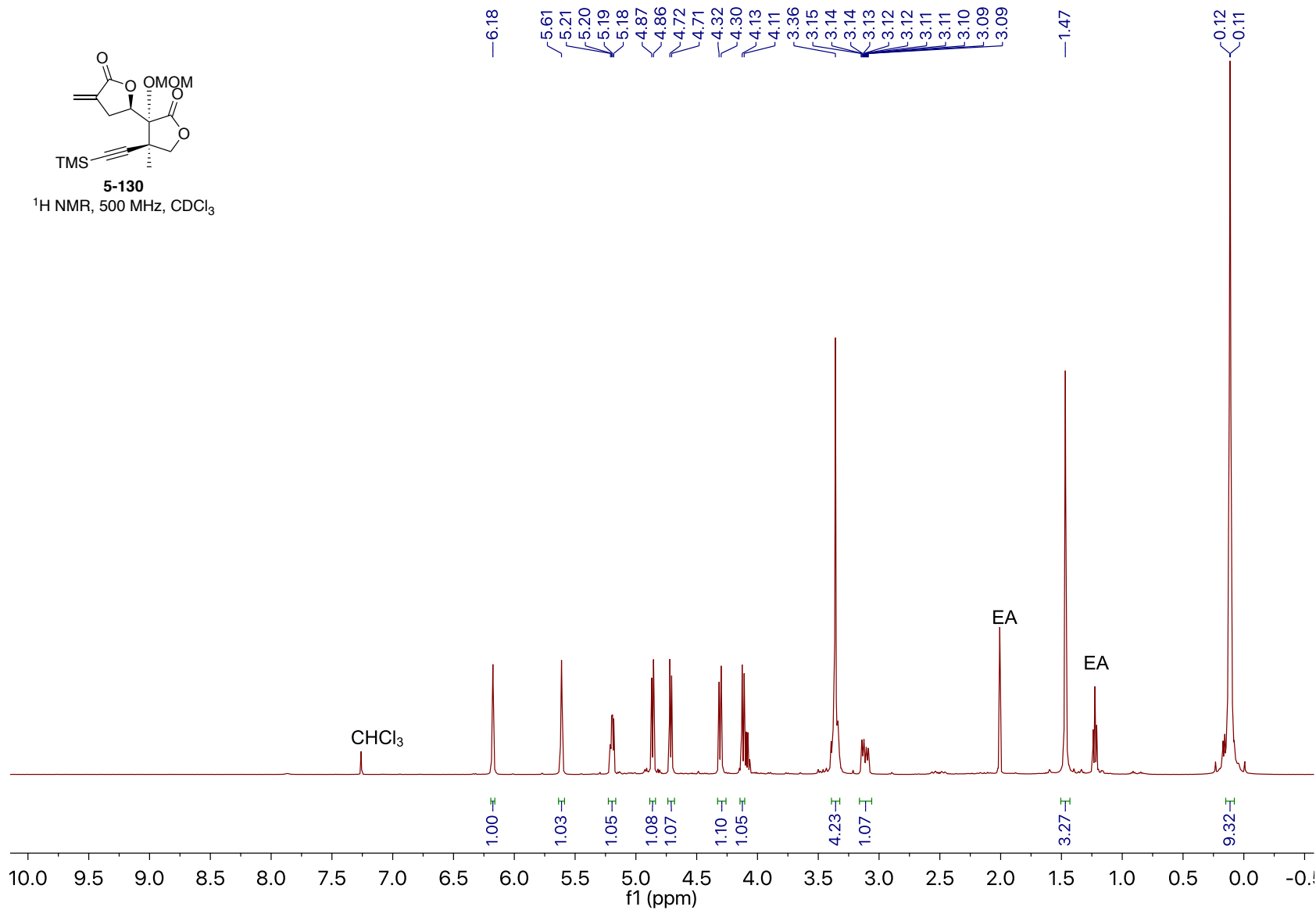
/27.95
/22.67
/18.06

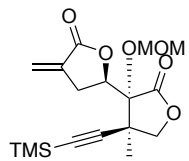




5-130

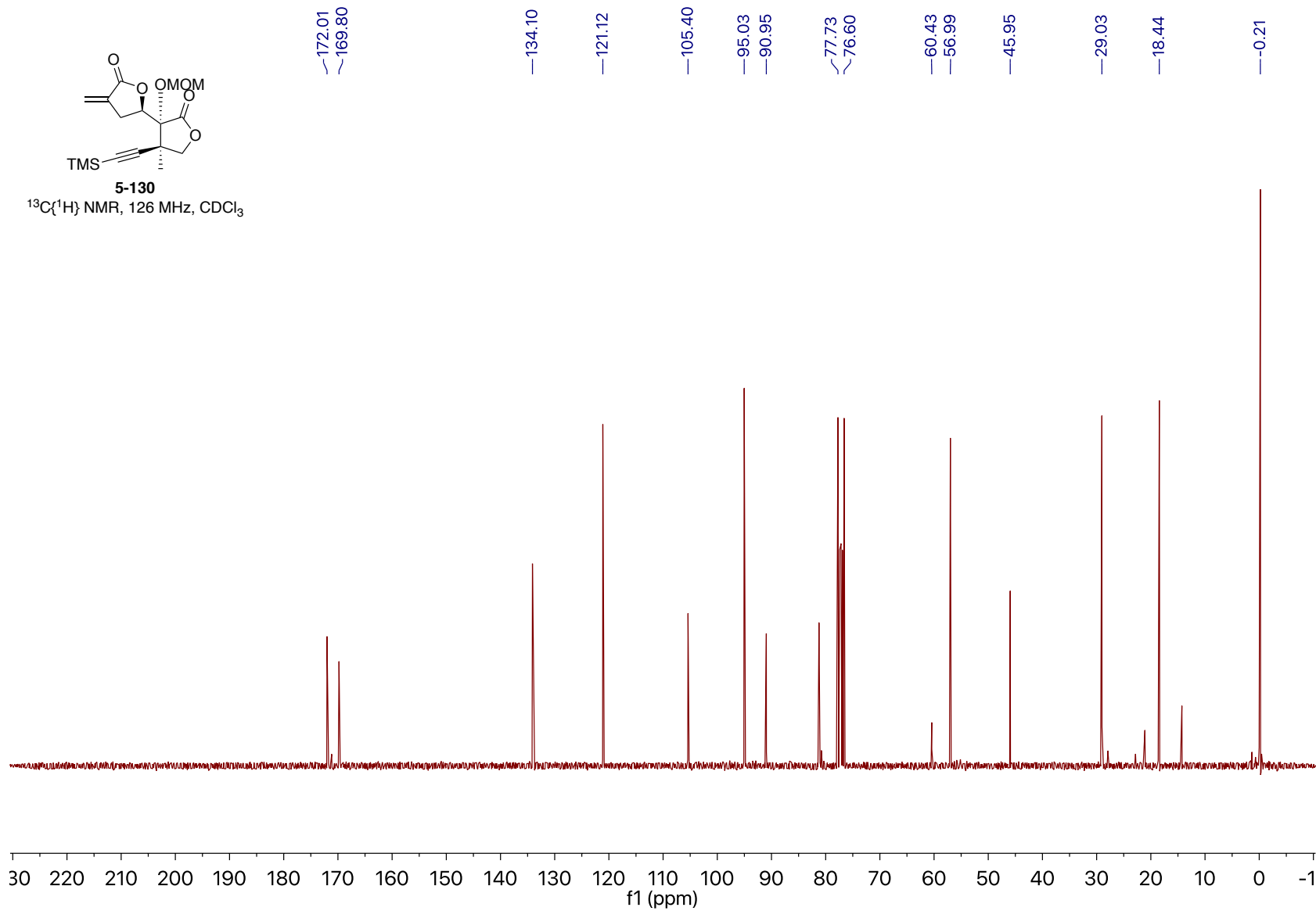
¹H NMR, 500 MHz, CDCl₃

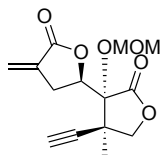




5-130

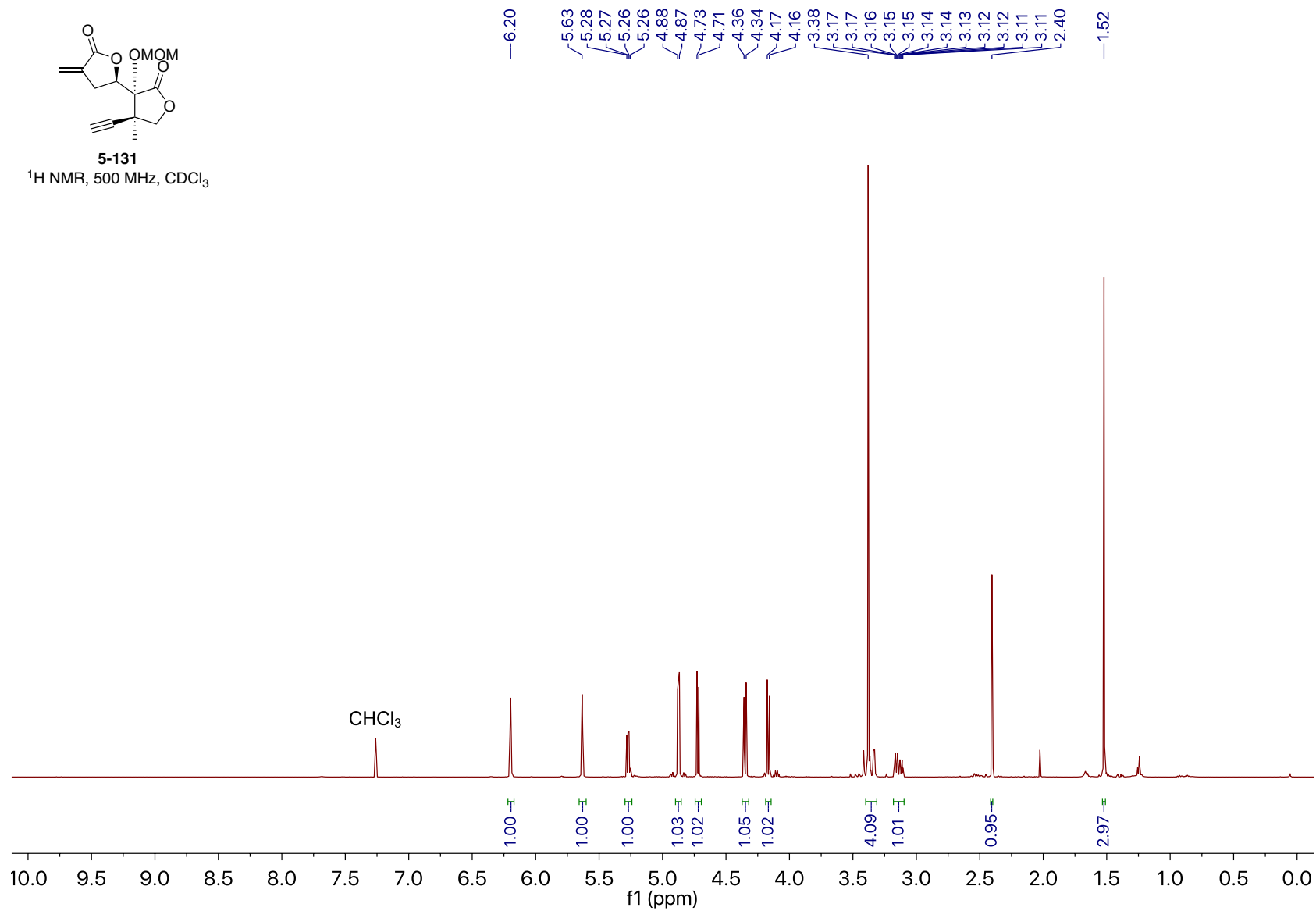
$^{13}\text{C}\{^1\text{H}\}$ NMR, 126 MHz, CDCl_3

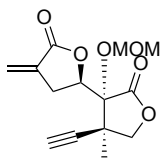




5-131

$^1\text{H NMR}$, 500 MHz, CDCl_3





5-131

$^{13}\text{C}\{^1\text{H}\}$ NMR, 151 MHz, CDCl_3

~171.81
~169.79

—133.99

—121.30

—95.13

~84.00

~81.23

~77.70

~76.44

~74.19

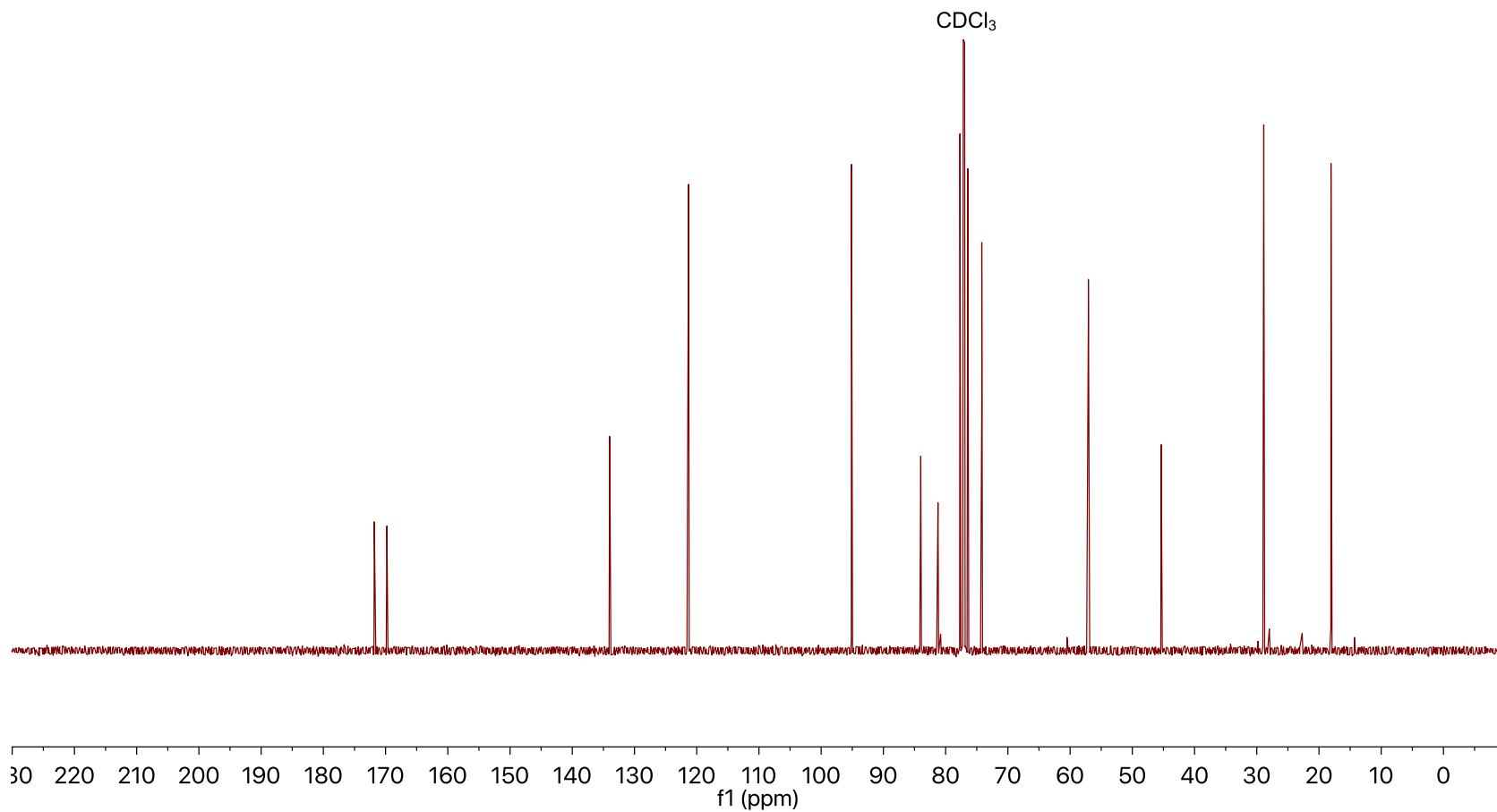
—57.07

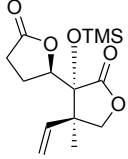
—45.35

—28.88

—18.07

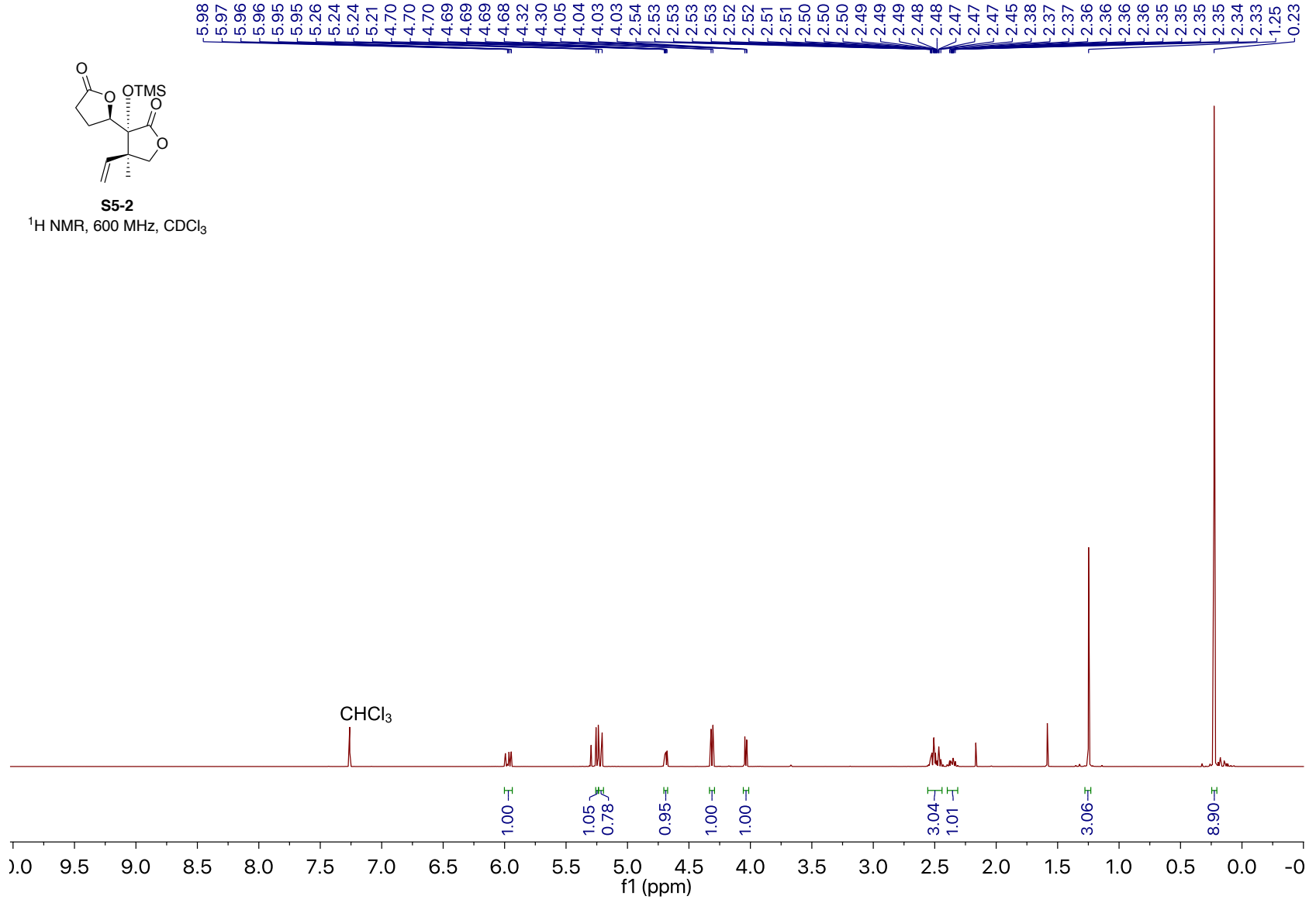
CDCl_3

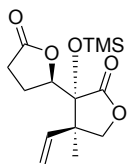




S5-2

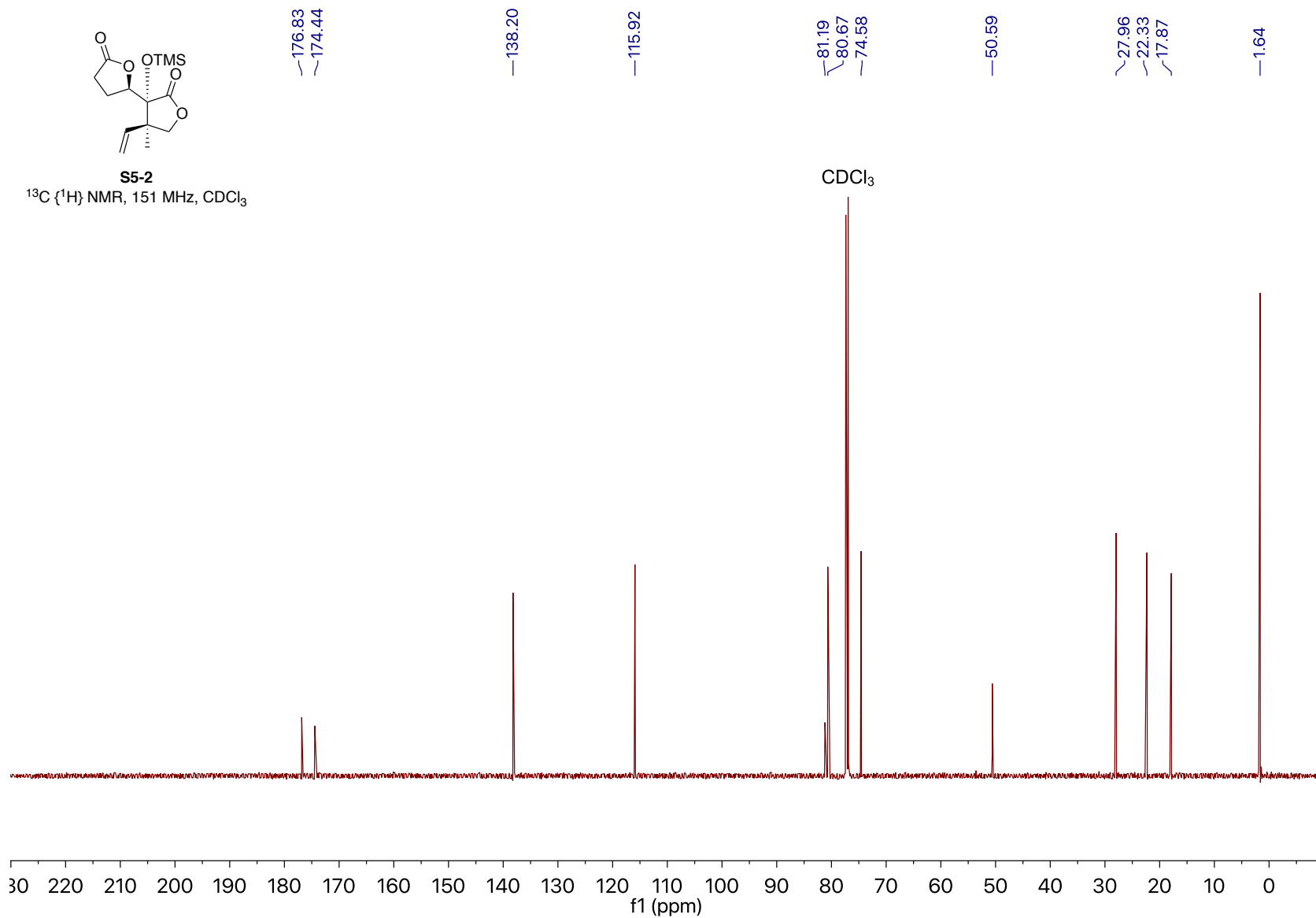
¹H NMR, 600 MHz, CDCl₃

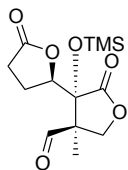




S5-2

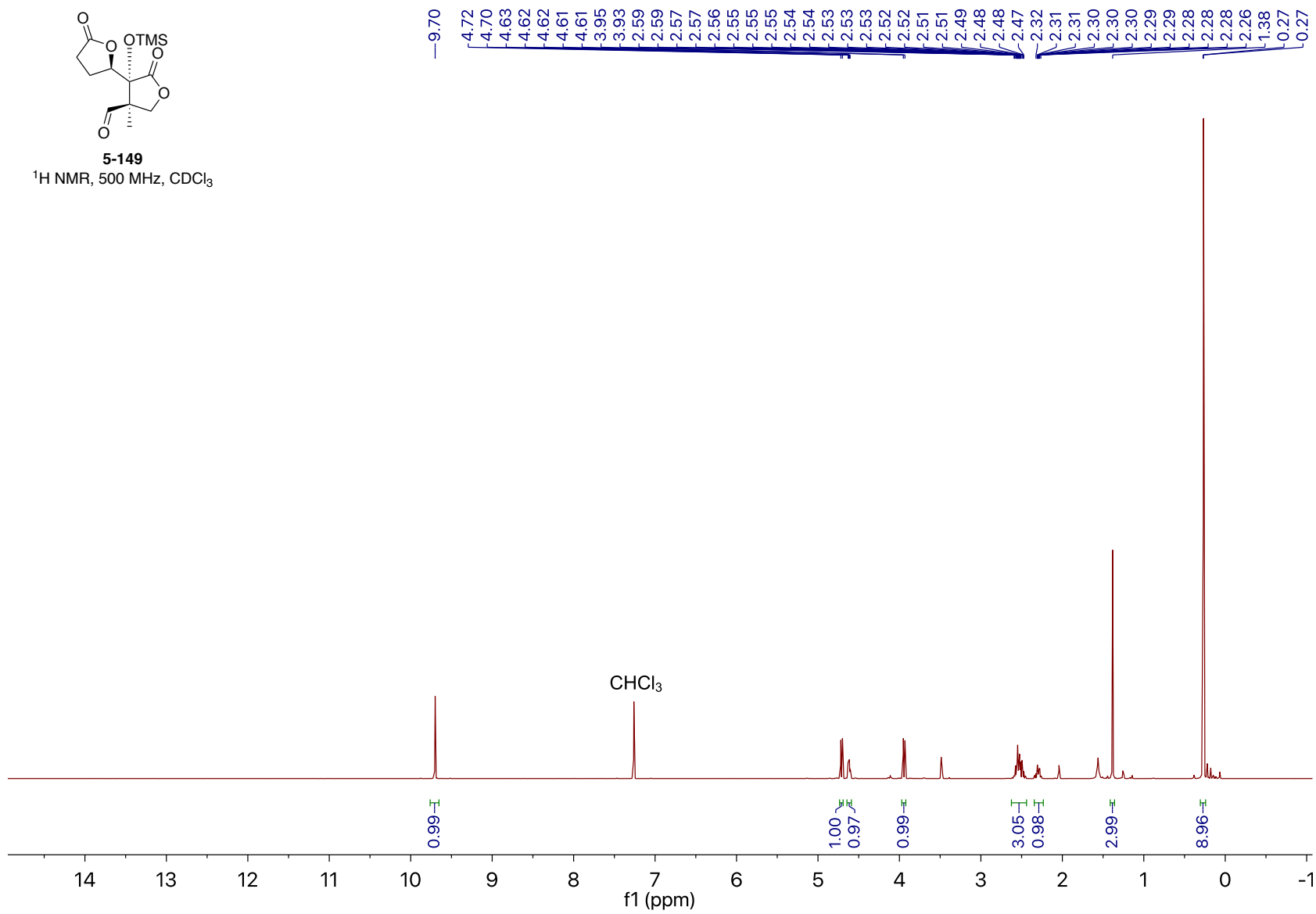
^{13}C { ^1H } NMR, 151 MHz, CDCl_3

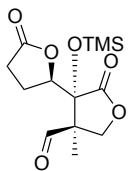




5-149

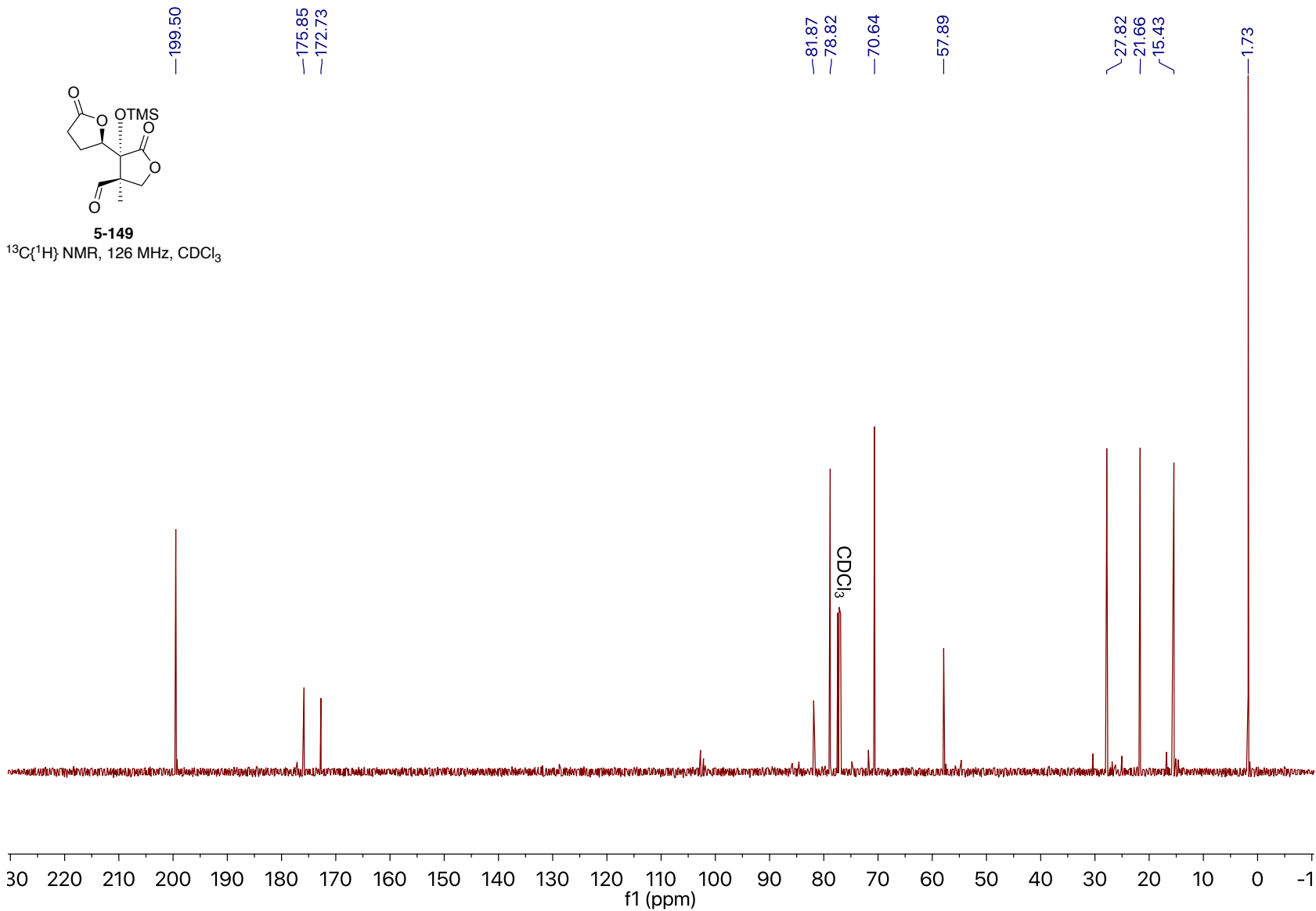
¹H NMR, 500 MHz, CDCl₃

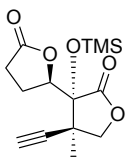




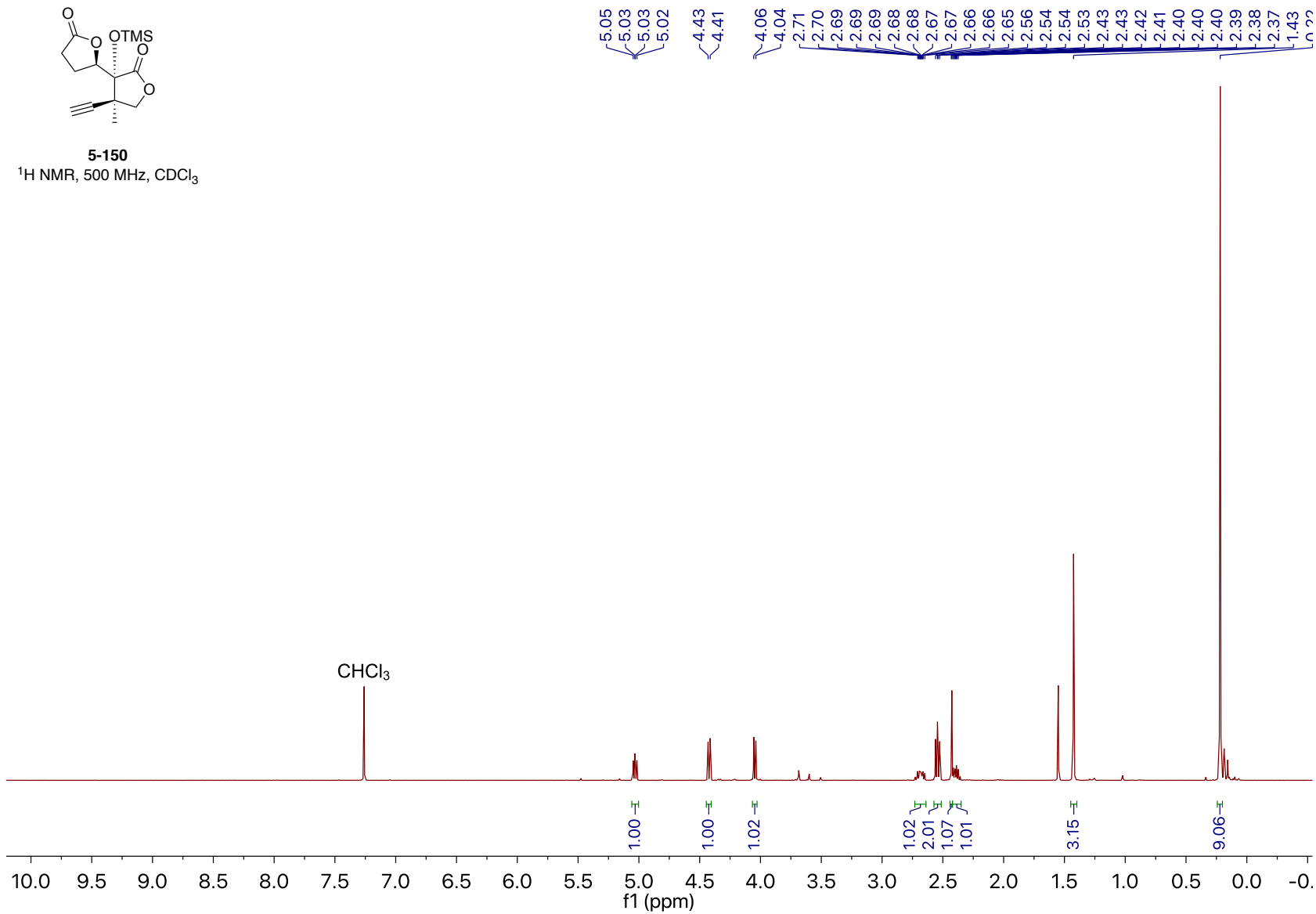
5-149

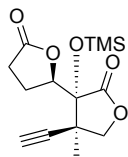
$^{13}\text{C}\{^1\text{H}\}$ NMR, 126 MHz, CDCl_3





5-150
¹H NMR, 500 MHz, CDCl₃





5-150

^{13}C $\{^1\text{H}\}$ NMR, 151 MHz, CDCl_3

~176.63
~174.36

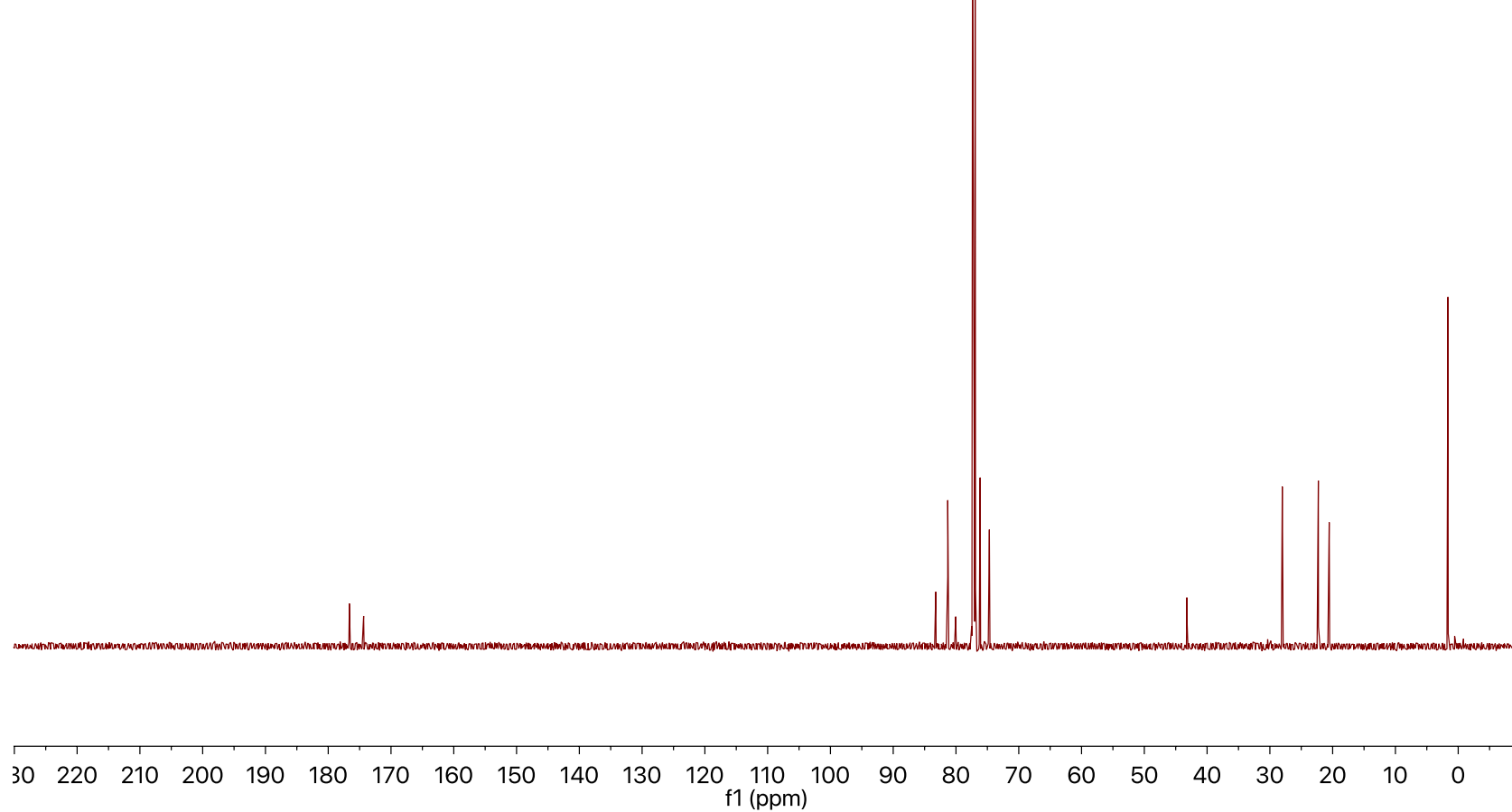
83.22
81.31
80.04
76.15
74.69

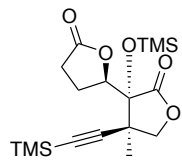
—43.23

~28.02
~22.28
~20.55

—1.64

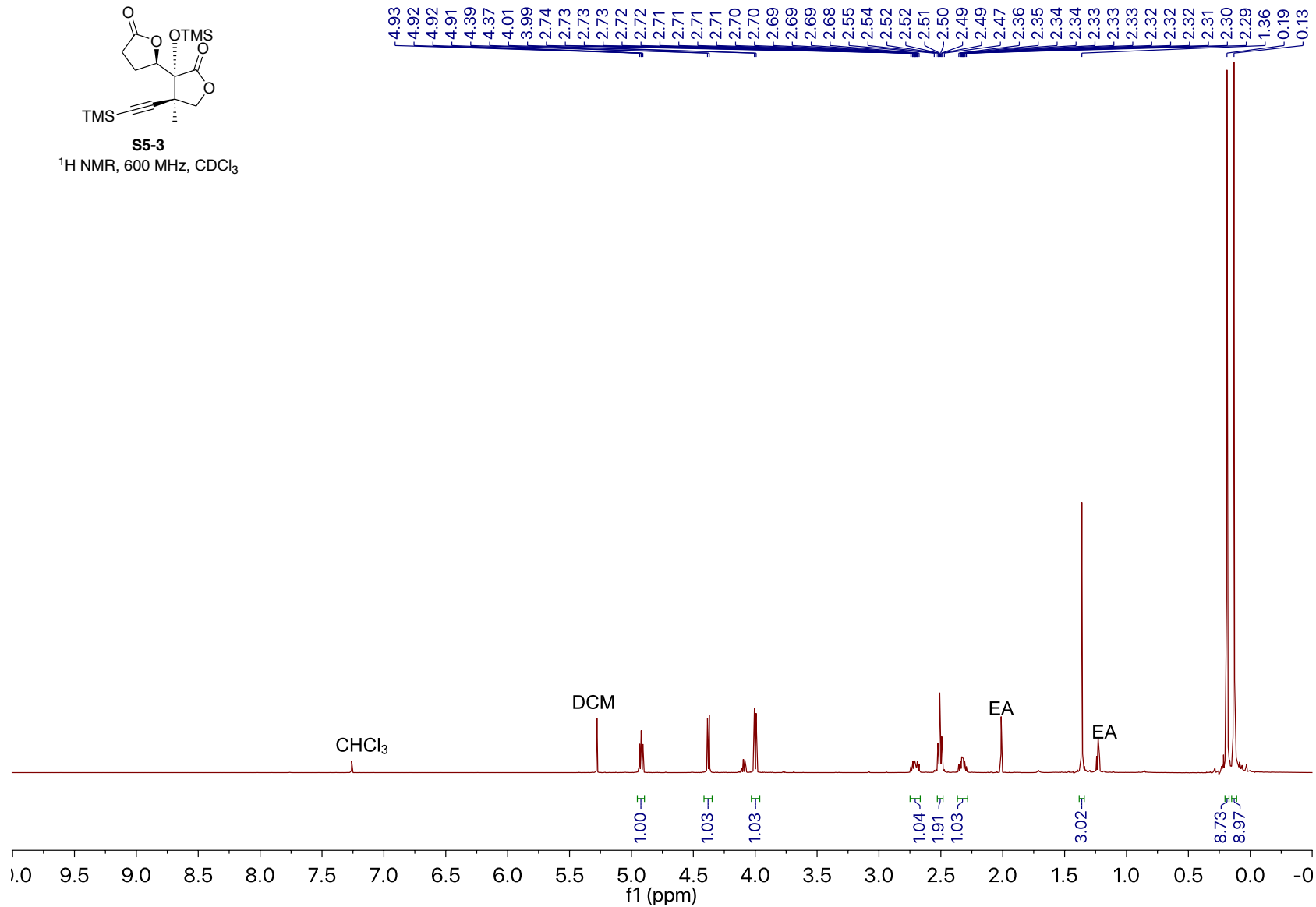
CDCl_3

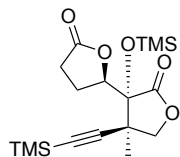




S5-3

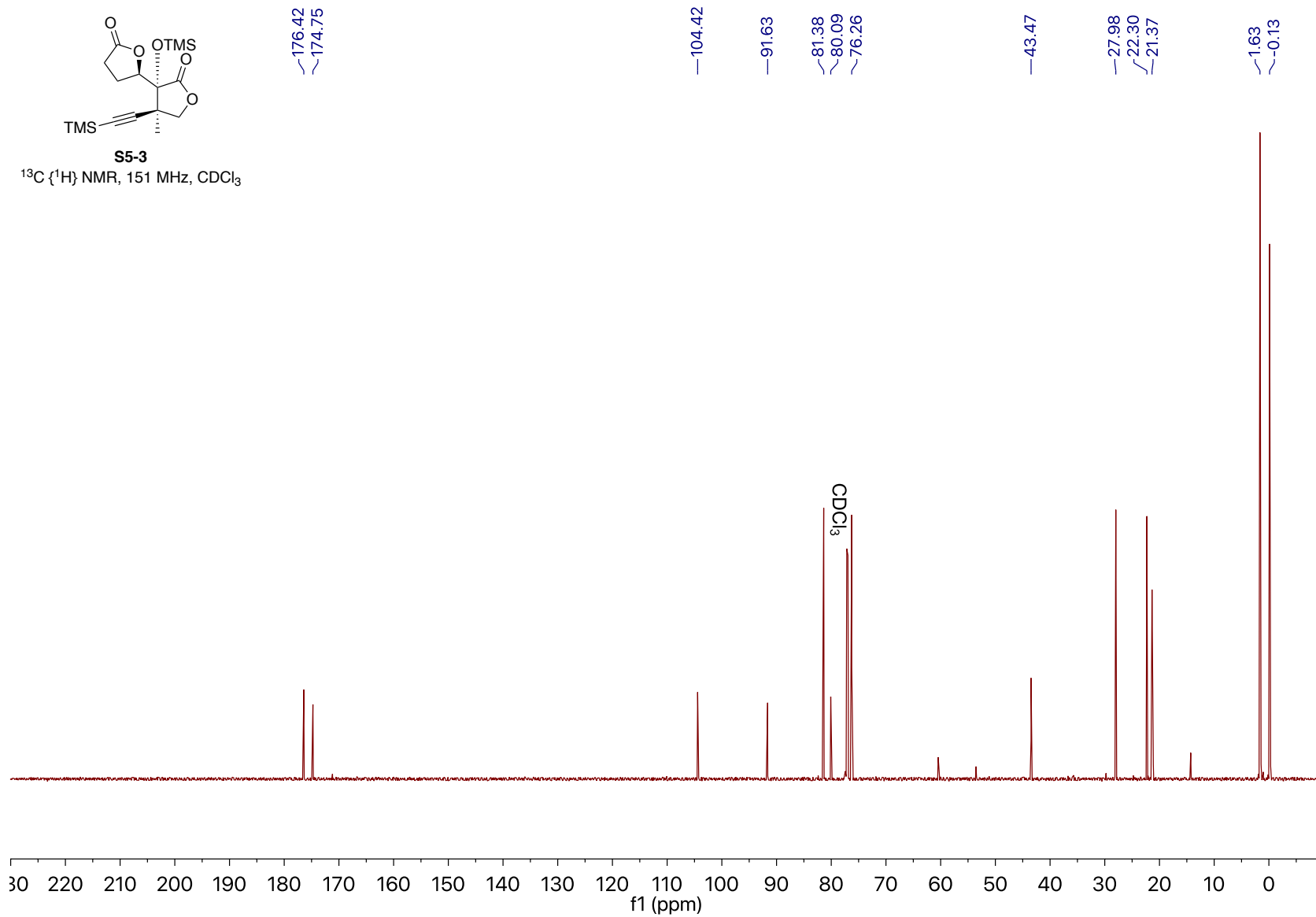
^1H NMR, 600 MHz, CDCl_3

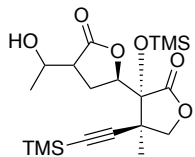




S5-3

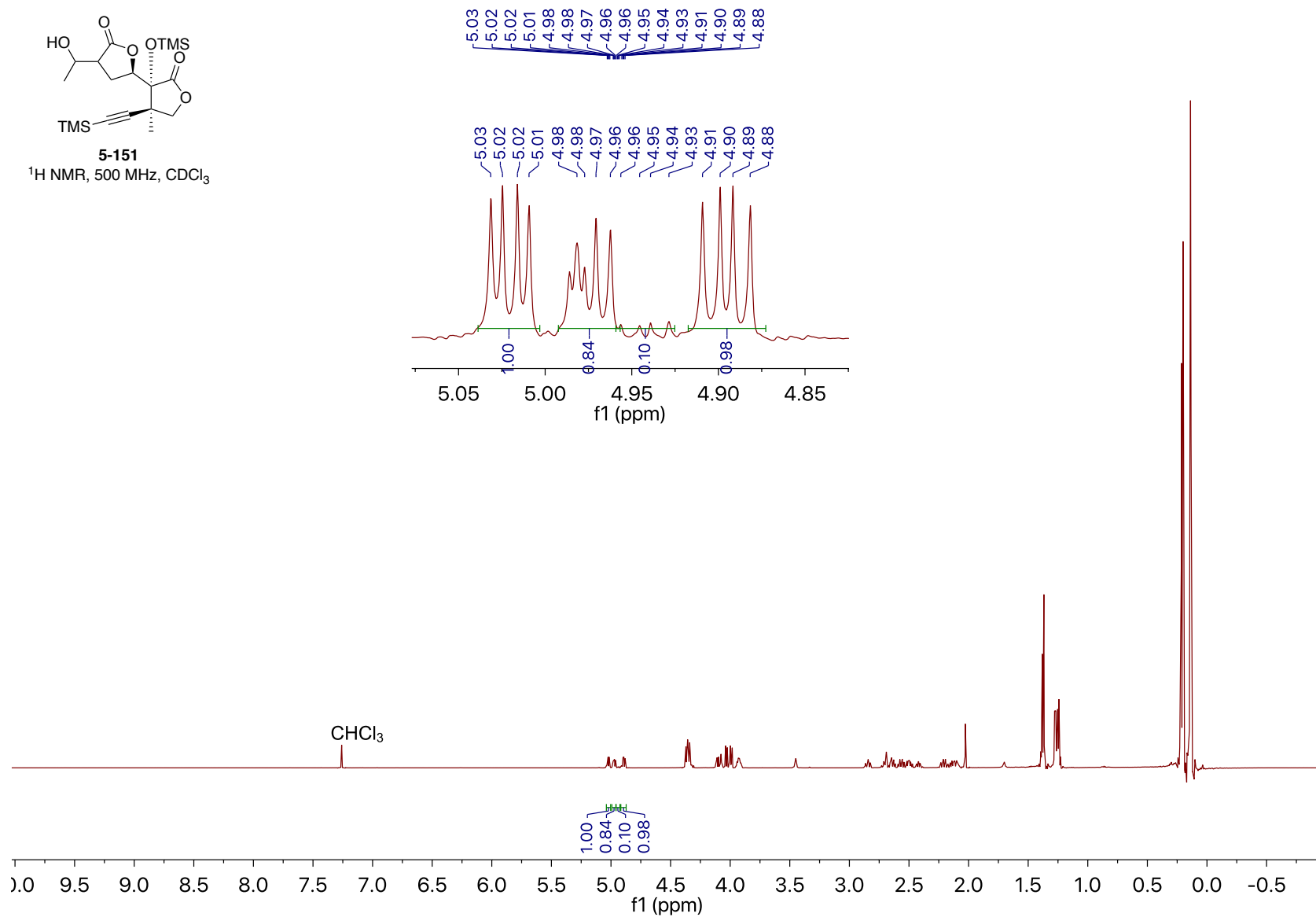
^{13}C (^1H) NMR, 151 MHz, CDCl_3

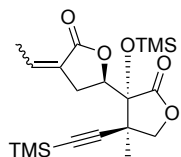




5-151

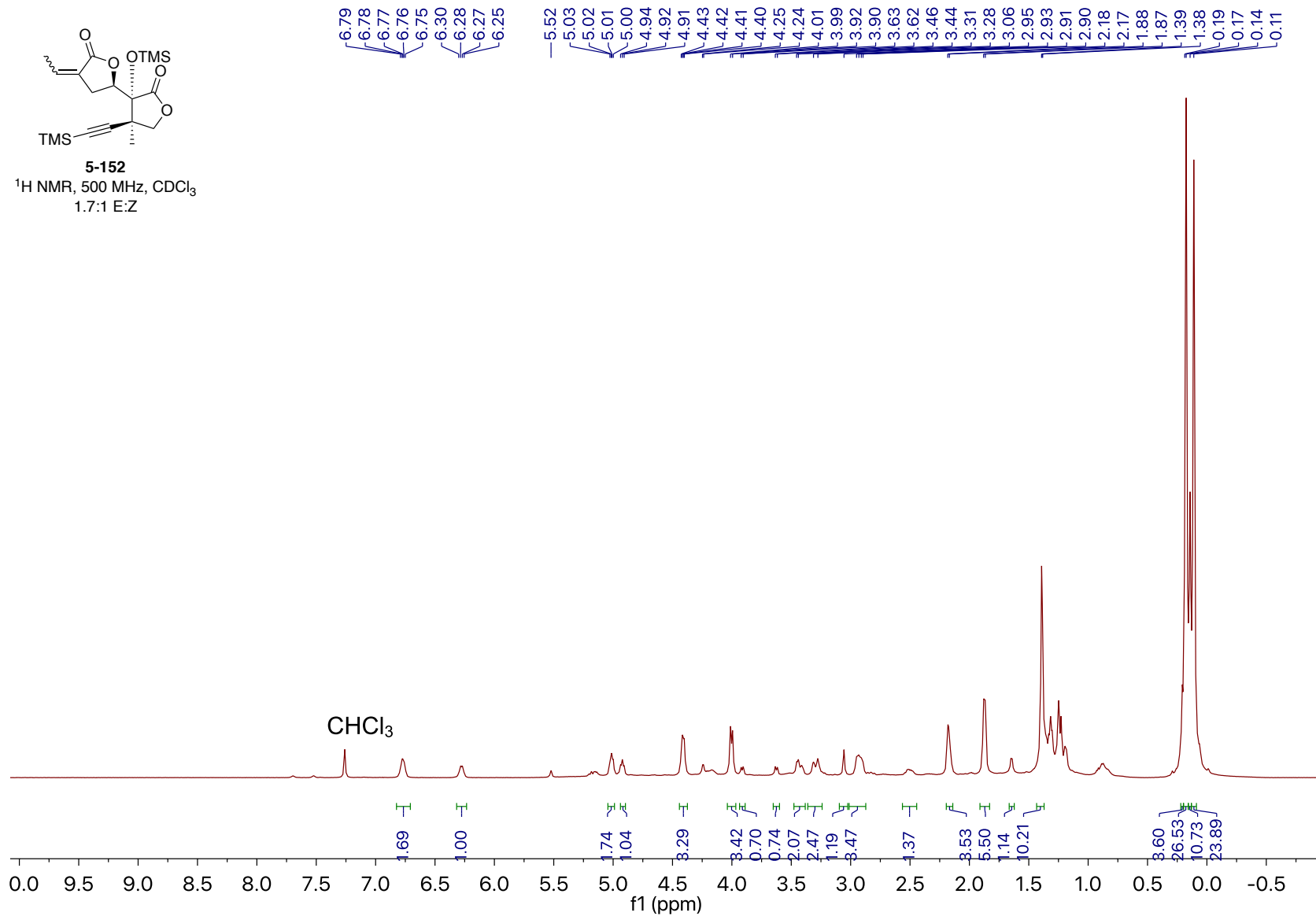
$^1\text{H NMR}$, 500 MHz, CDCl_3

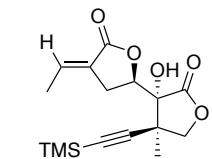




5-152

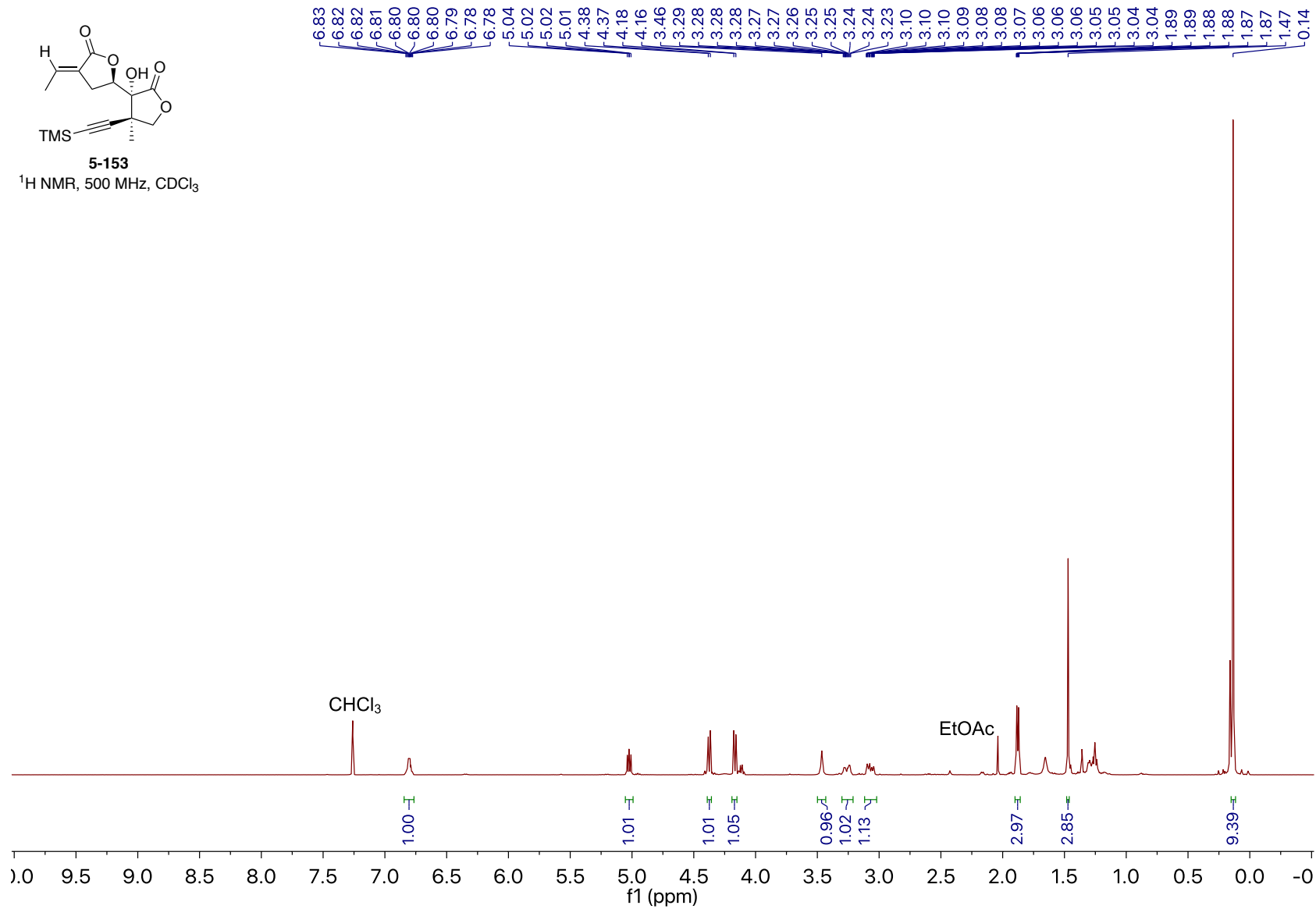
¹H NMR, 500 MHz, CDCl₃
1.7:1 E:Z

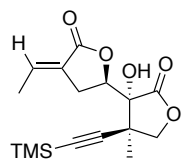




5-153

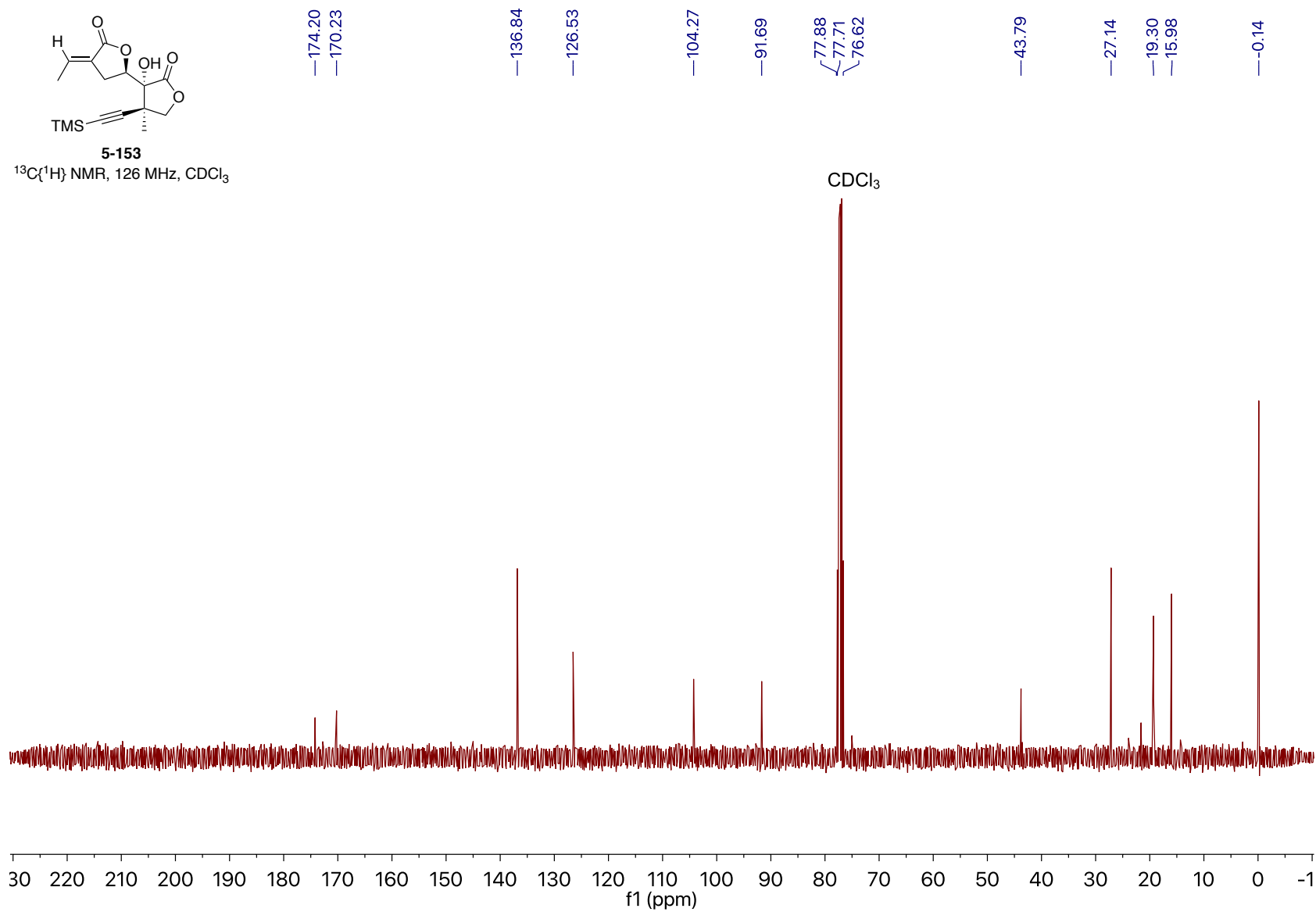
$^1\text{H NMR}$, 500 MHz, CDCl_3

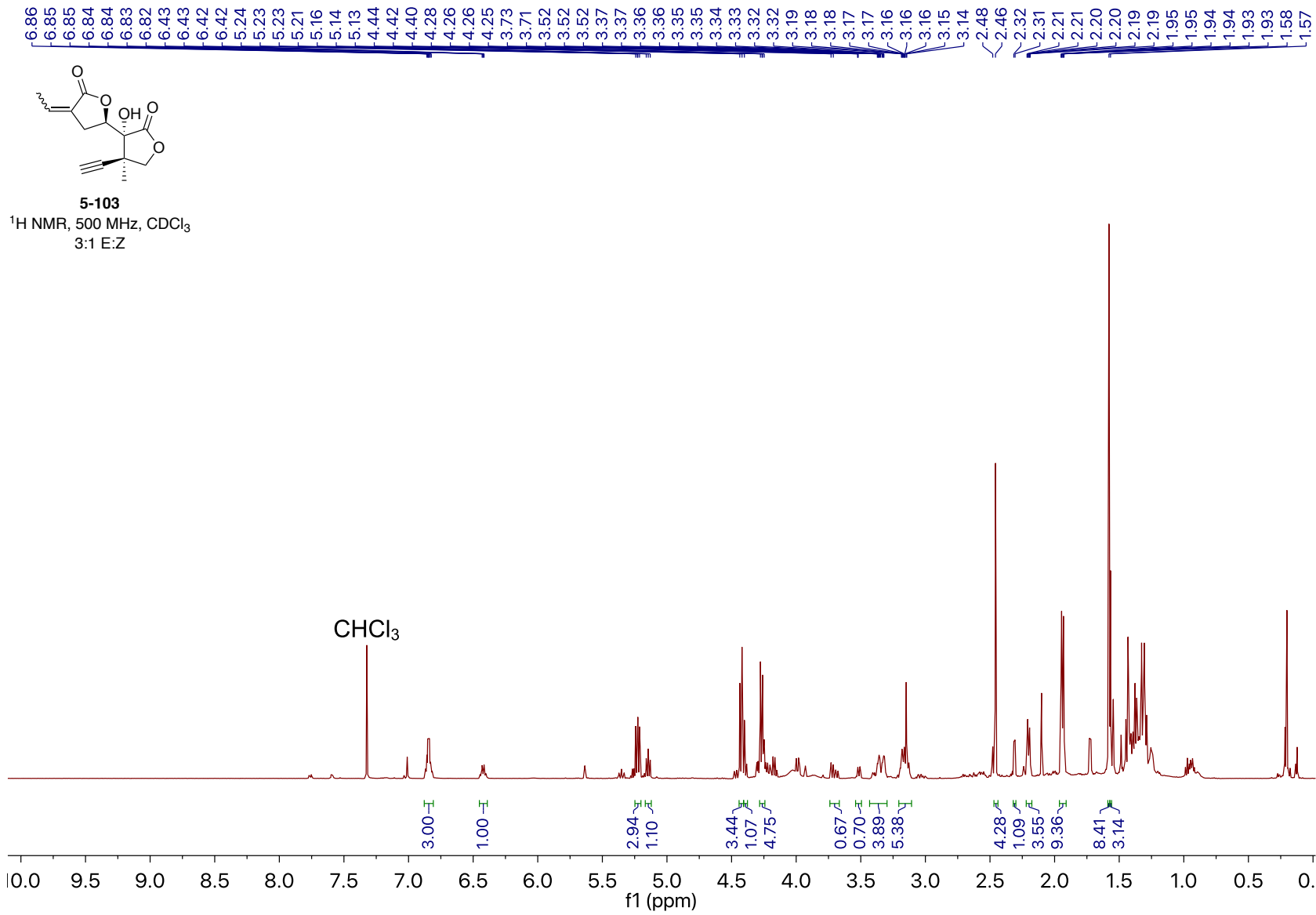


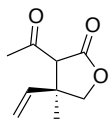


5-153

$^{13}\text{C}\{^1\text{H}\}$ NMR, 126 MHz, CDCl_3

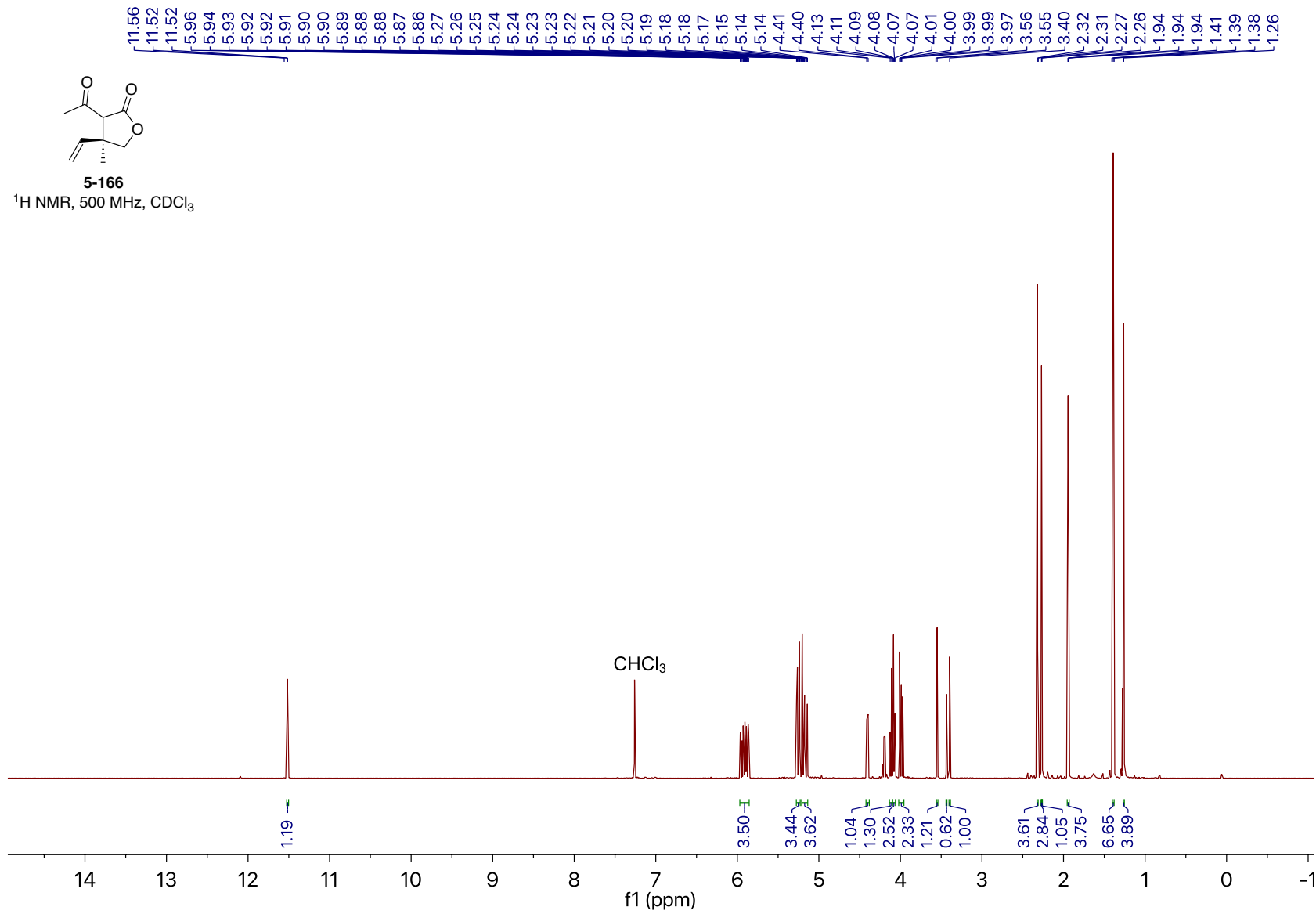


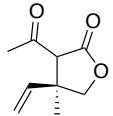




5-166

¹H NMR, 500 MHz, CDCl₃





5-166

$^{13}\text{C}\{^1\text{H}\}$ NMR, 126 MHz, CDCl_3

201.99
201.35

176.36
172.74
172.28
171.02

141.80
140.35
136.94

117.12
115.77
114.52

102.92

79.00
76.54
76.46

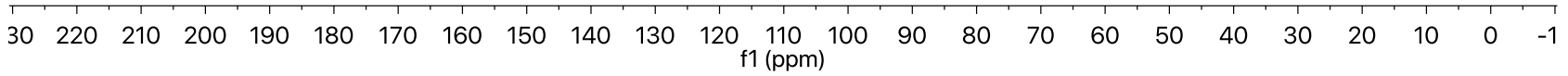
64.54
61.55
61.51

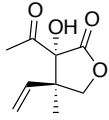
50.28
46.45
46.42
43.49

32.30
32.27

23.78
23.44
18.61
18.43

CDCl_3





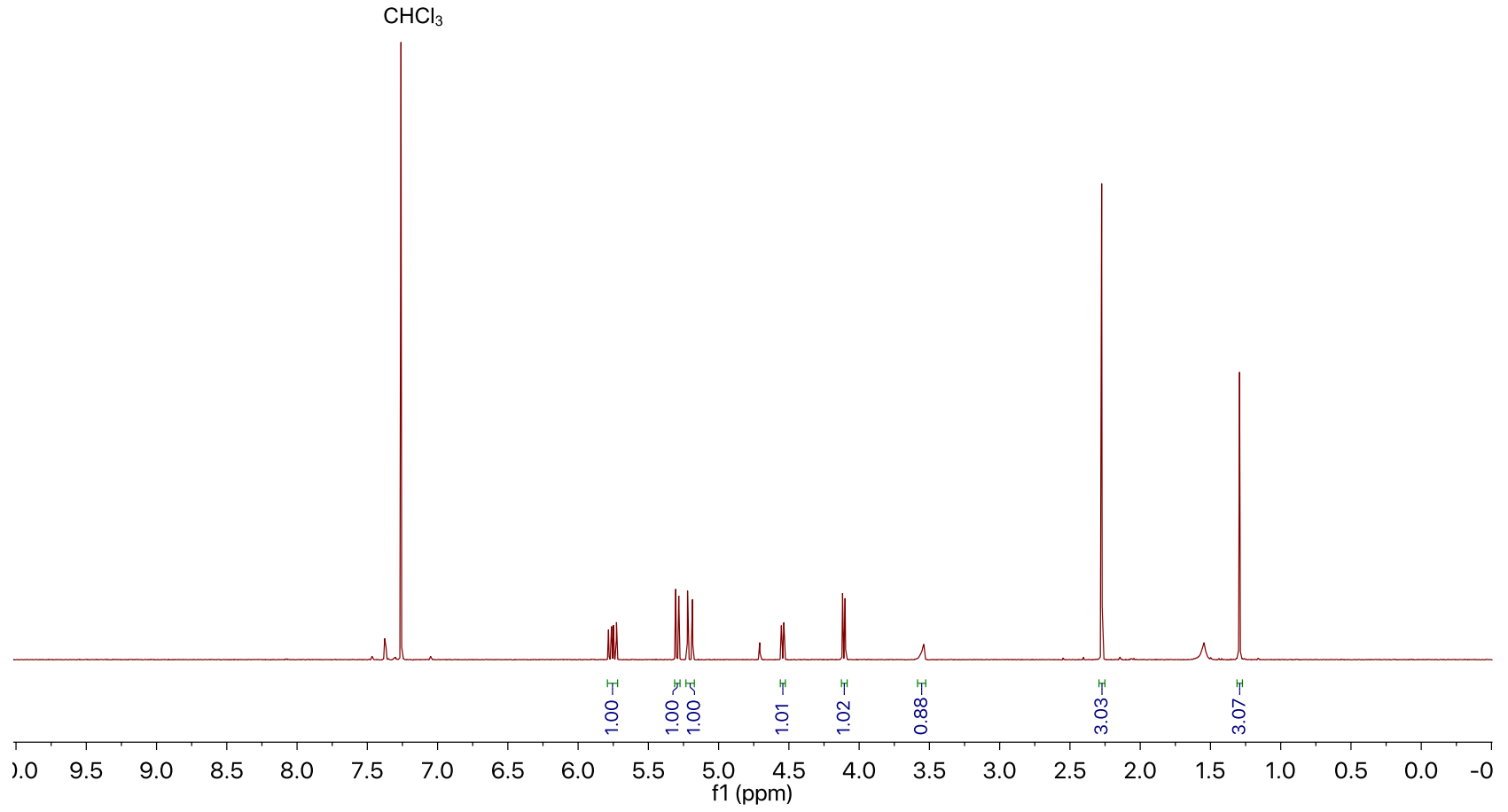
5-167

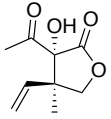
¹H NMR, 500 MHz, CDCl₃

5.78
5.78
5.76
5.76
5.75
5.75
5.73
5.72
5.31
5.30
5.28
5.28
5.22
5.19
4.55
4.55
4.55
4.54
4.54
4.53
4.12
4.11
4.10
4.10
3.54

2.28
2.27
2.27

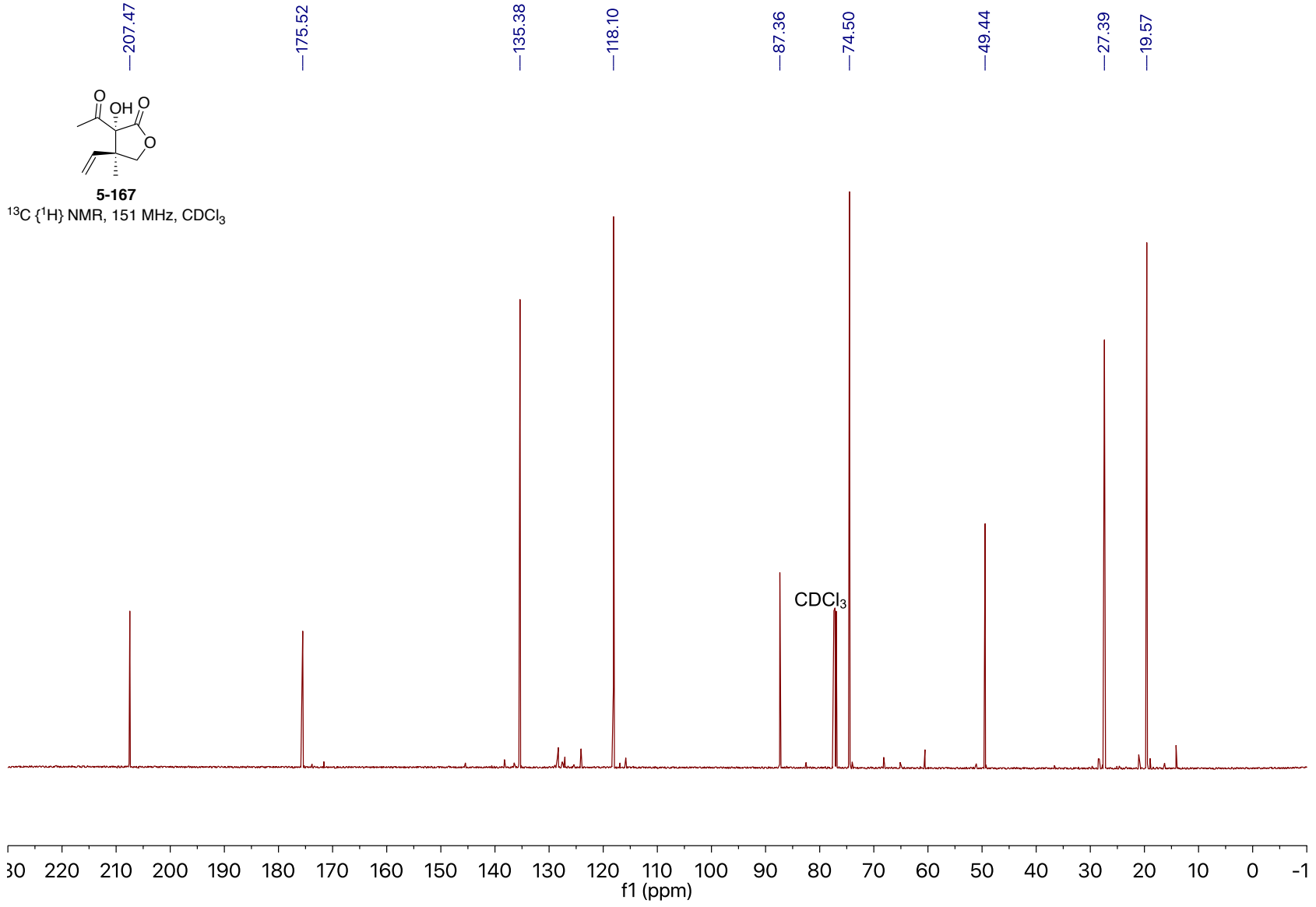
1.29
1.29

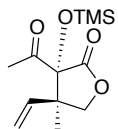




5-167

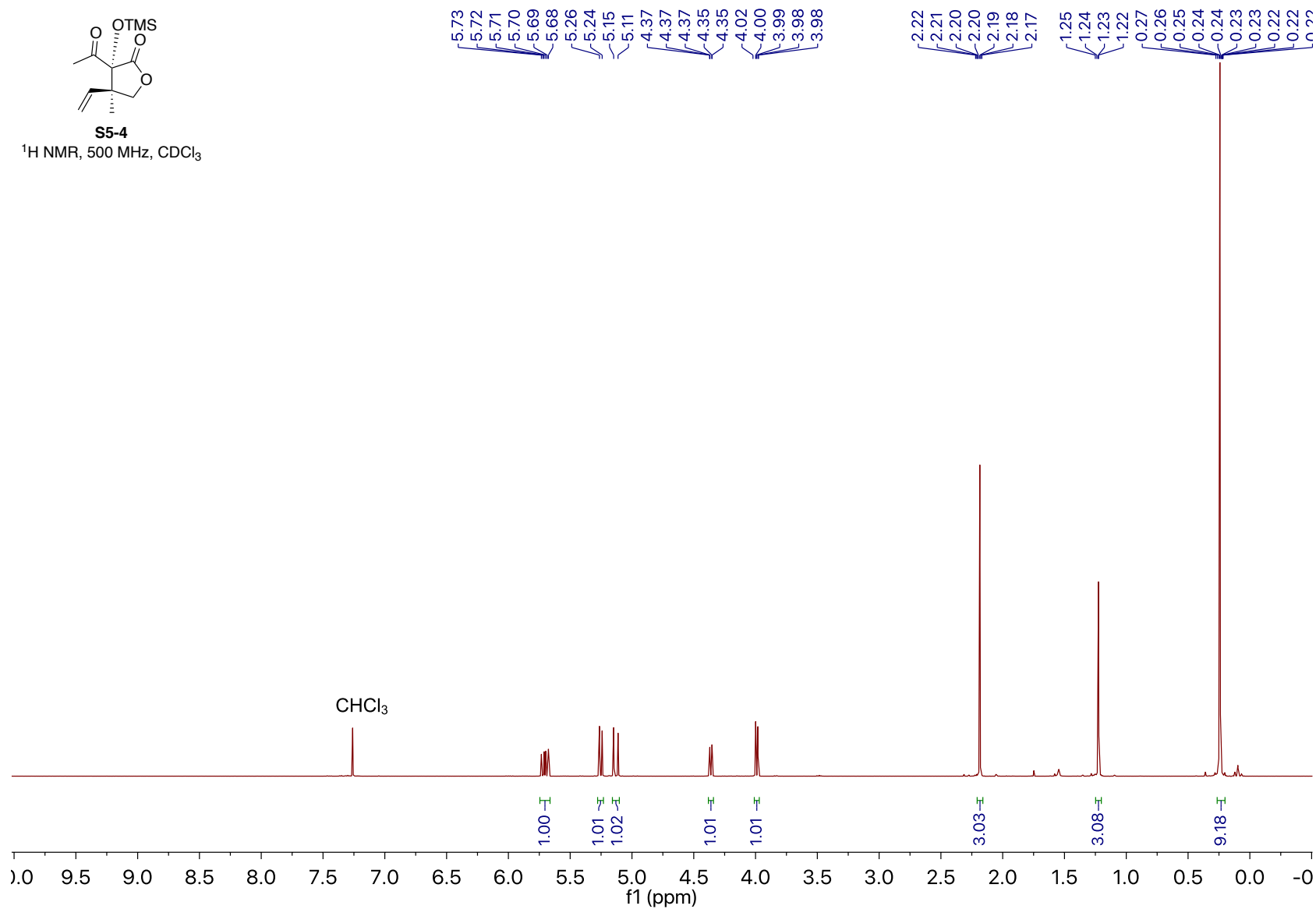
^{13}C { ^1H } NMR, 151 MHz, CDCl_3

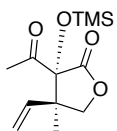




S5-4

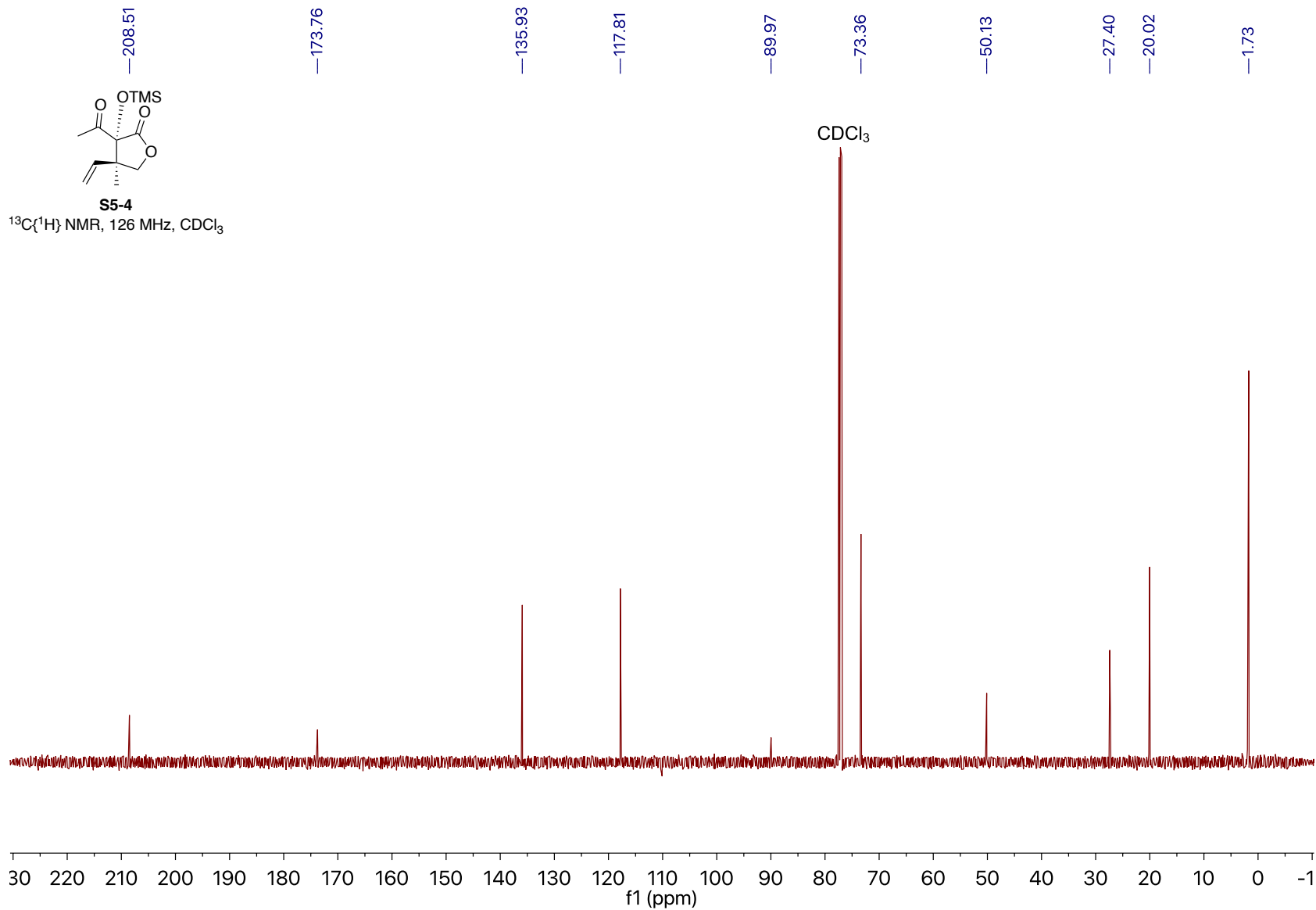
¹H NMR, 500 MHz, CDCl₃

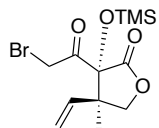




S5-4

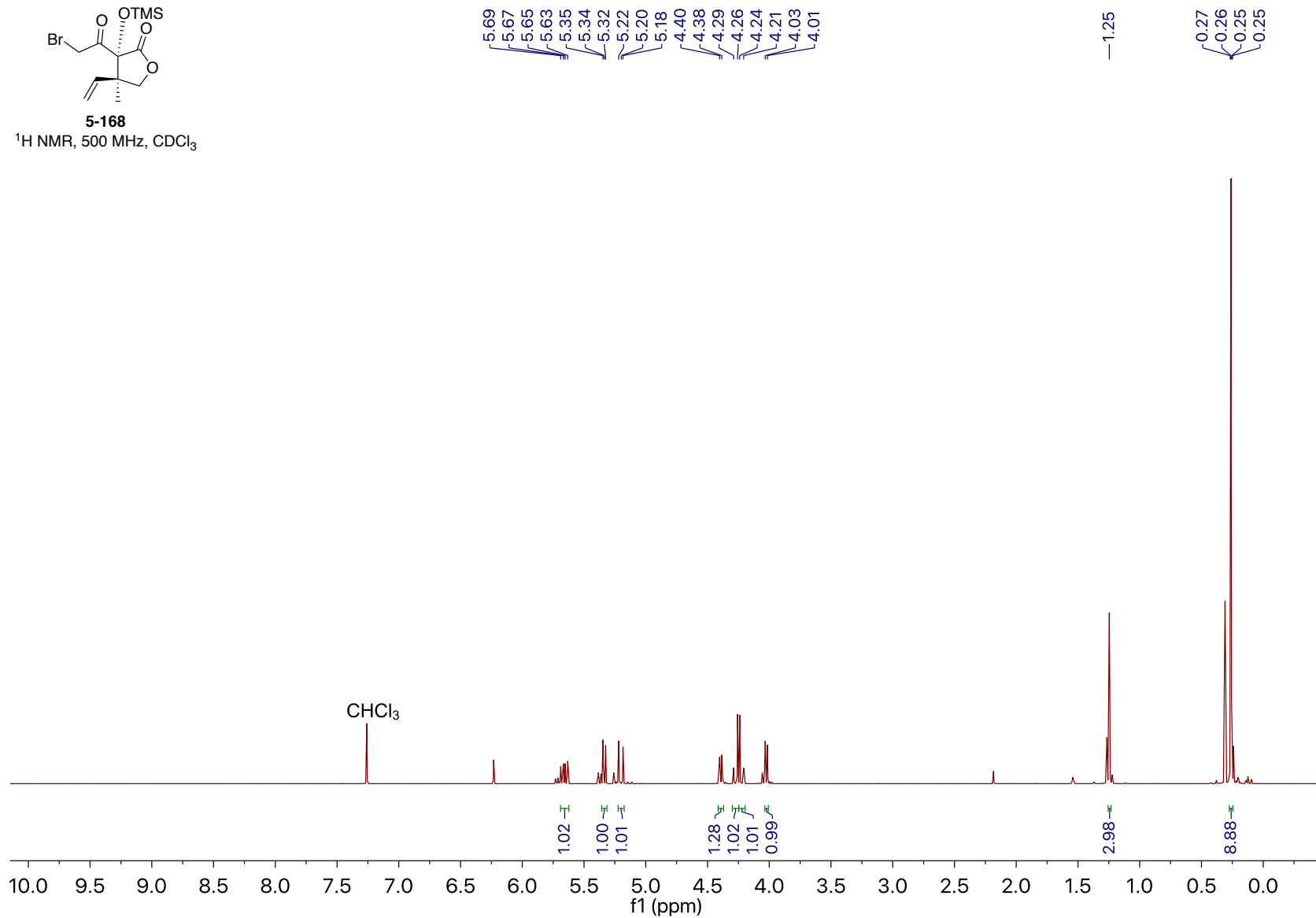
$^{13}\text{C}\{^1\text{H}\}$ NMR, 126 MHz, CDCl_3

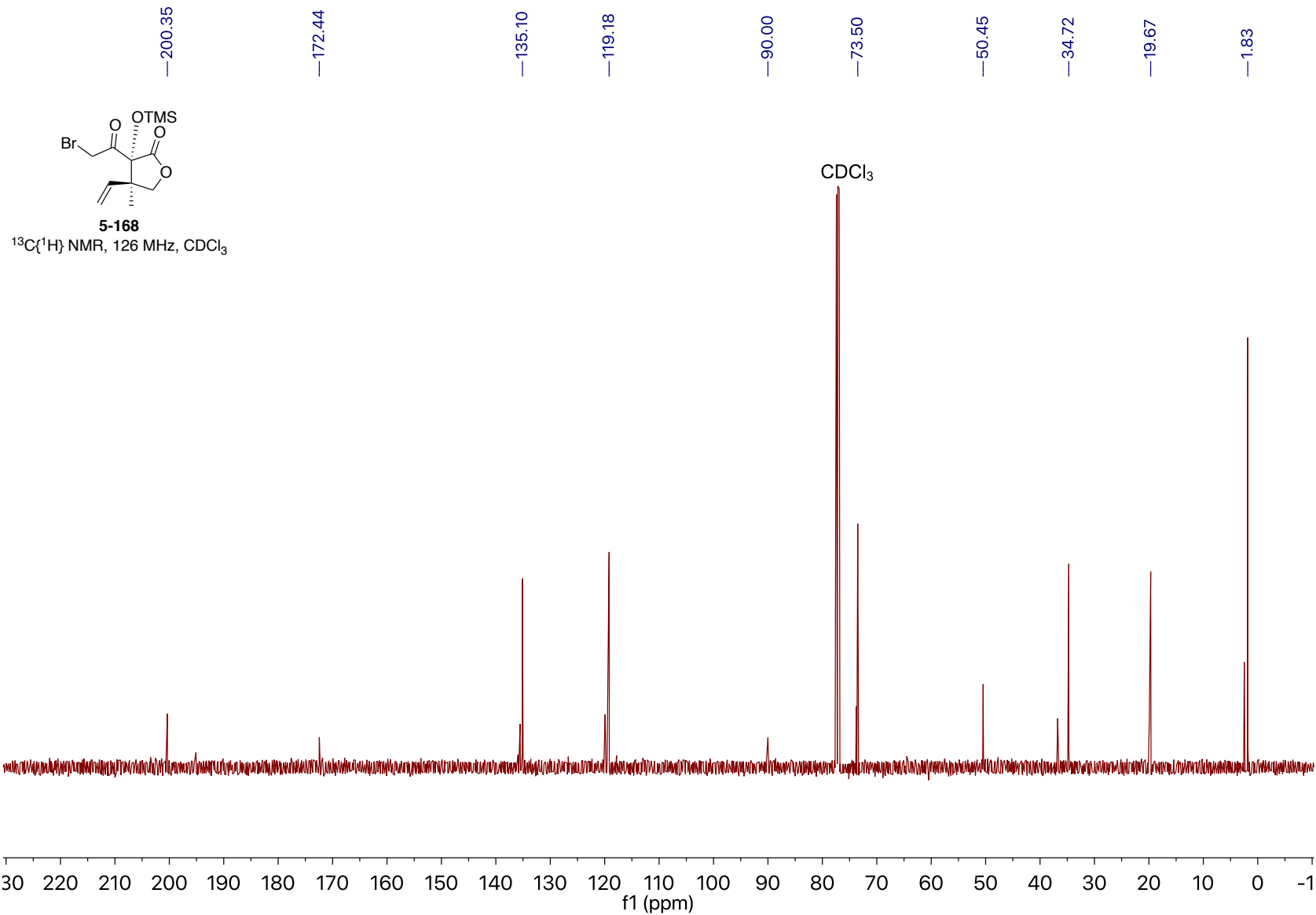


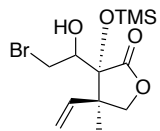


5-168

¹H NMR, 500 MHz, CDCl₃

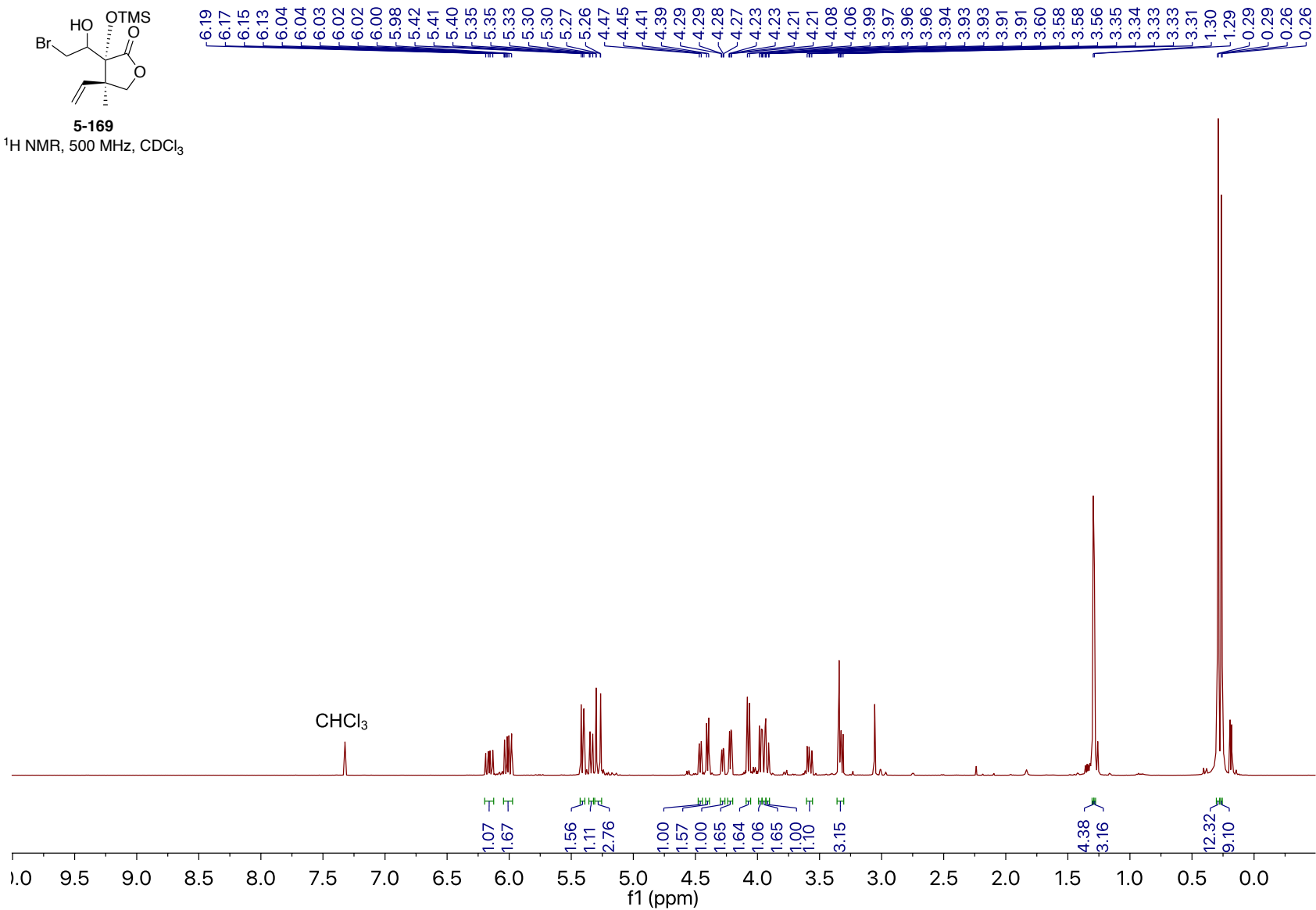


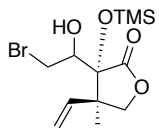




5-169

¹H NMR, 500 MHz, CDCl₃





5-169

$^{13}\text{C}\{^1\text{H}\}$ NMR, 126 MHz, CDCl_3

~178.69
~176.77

~137.59
~136.43

~117.62
~117.20

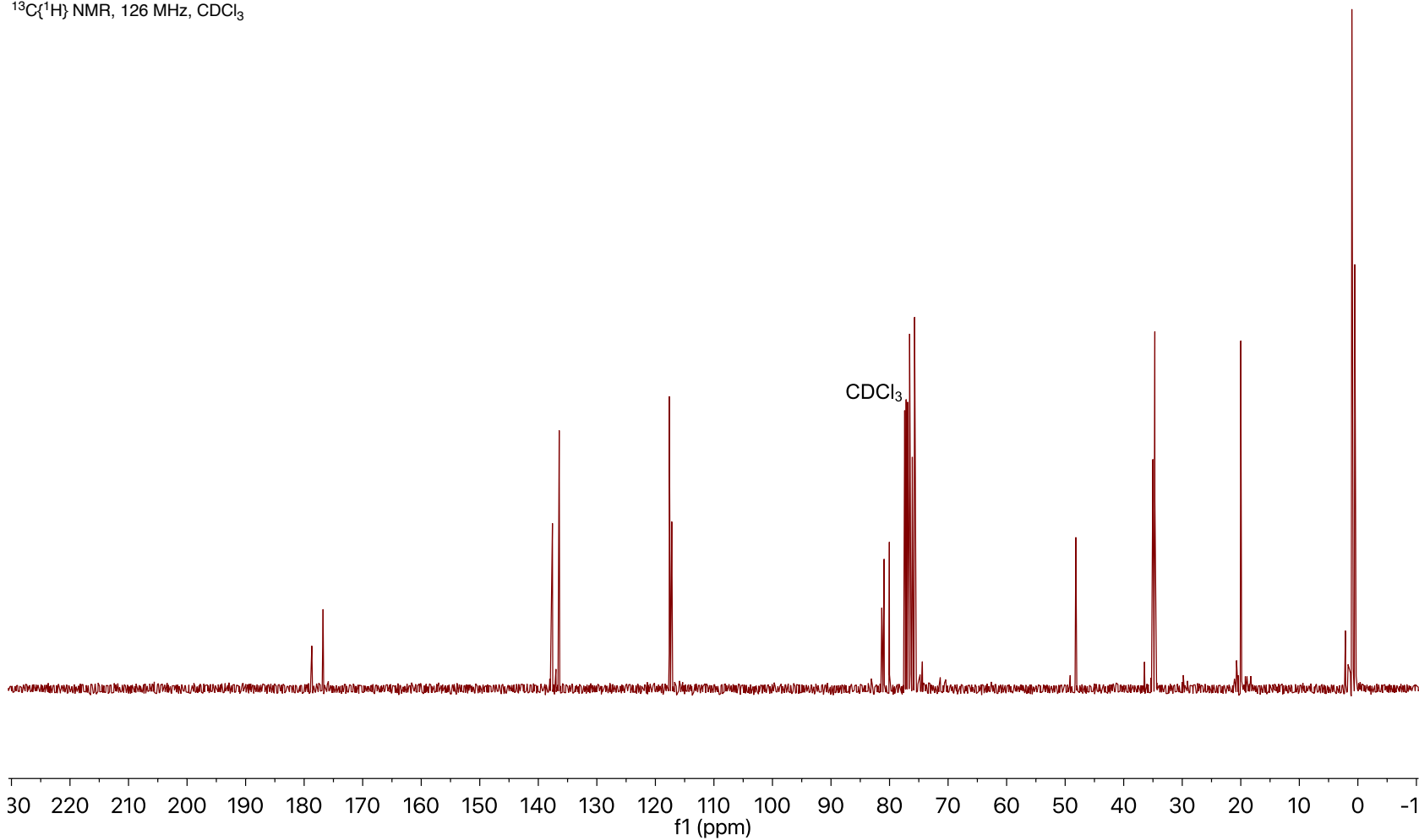
81.32
80.93
80.03
76.57
76.11
75.72

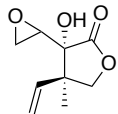
48.17
48.12

35.01
34.68

20.00
19.94

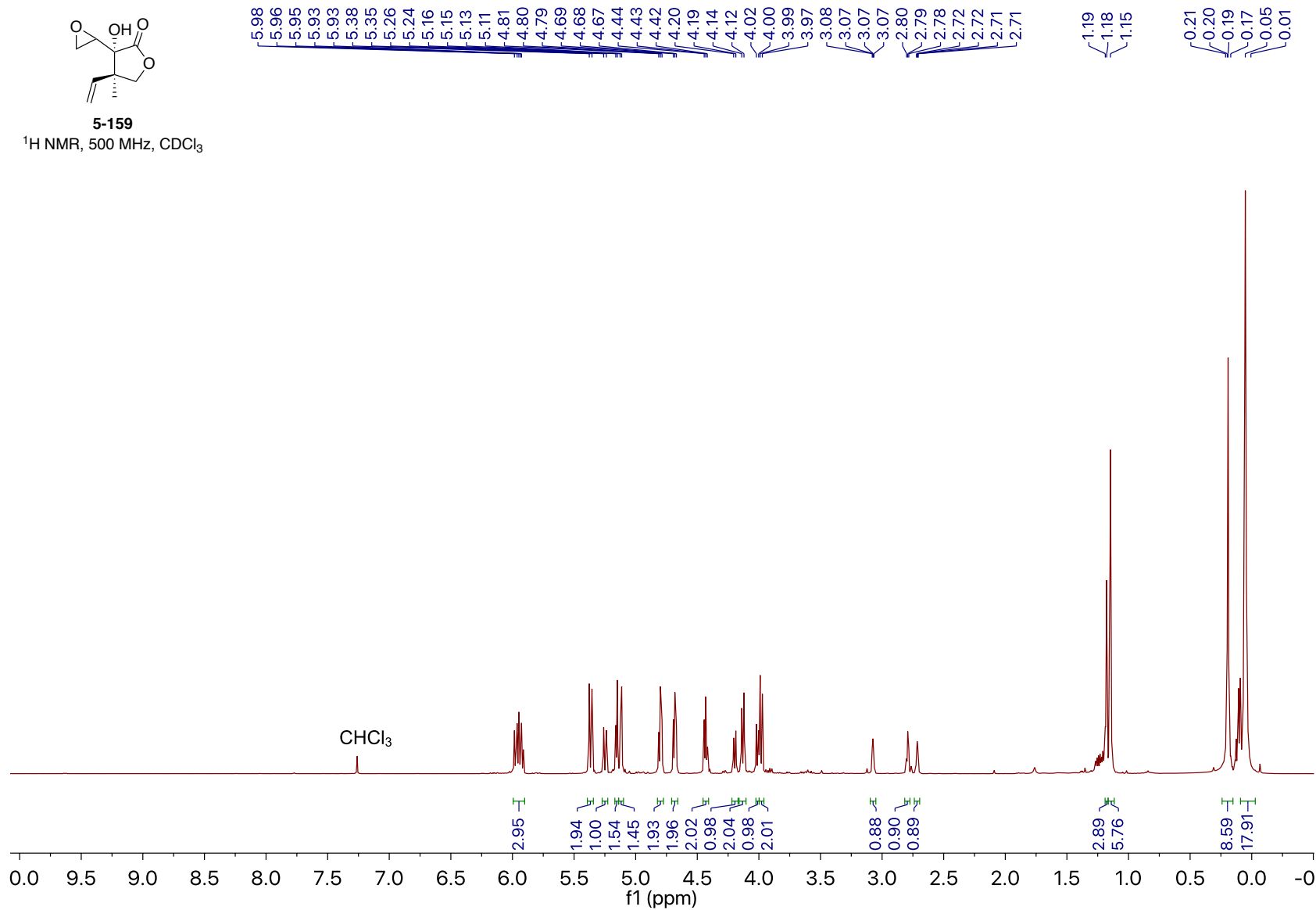
1.02
0.53

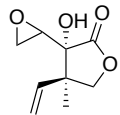




5-159

¹H NMR, 500 MHz, CDCl₃





5-159

$^{13}\text{C}\{^1\text{H}\}$ NMR, 126 MHz, CDCl_3

173.42
173.25

137.08
137.01

117.25
116.42

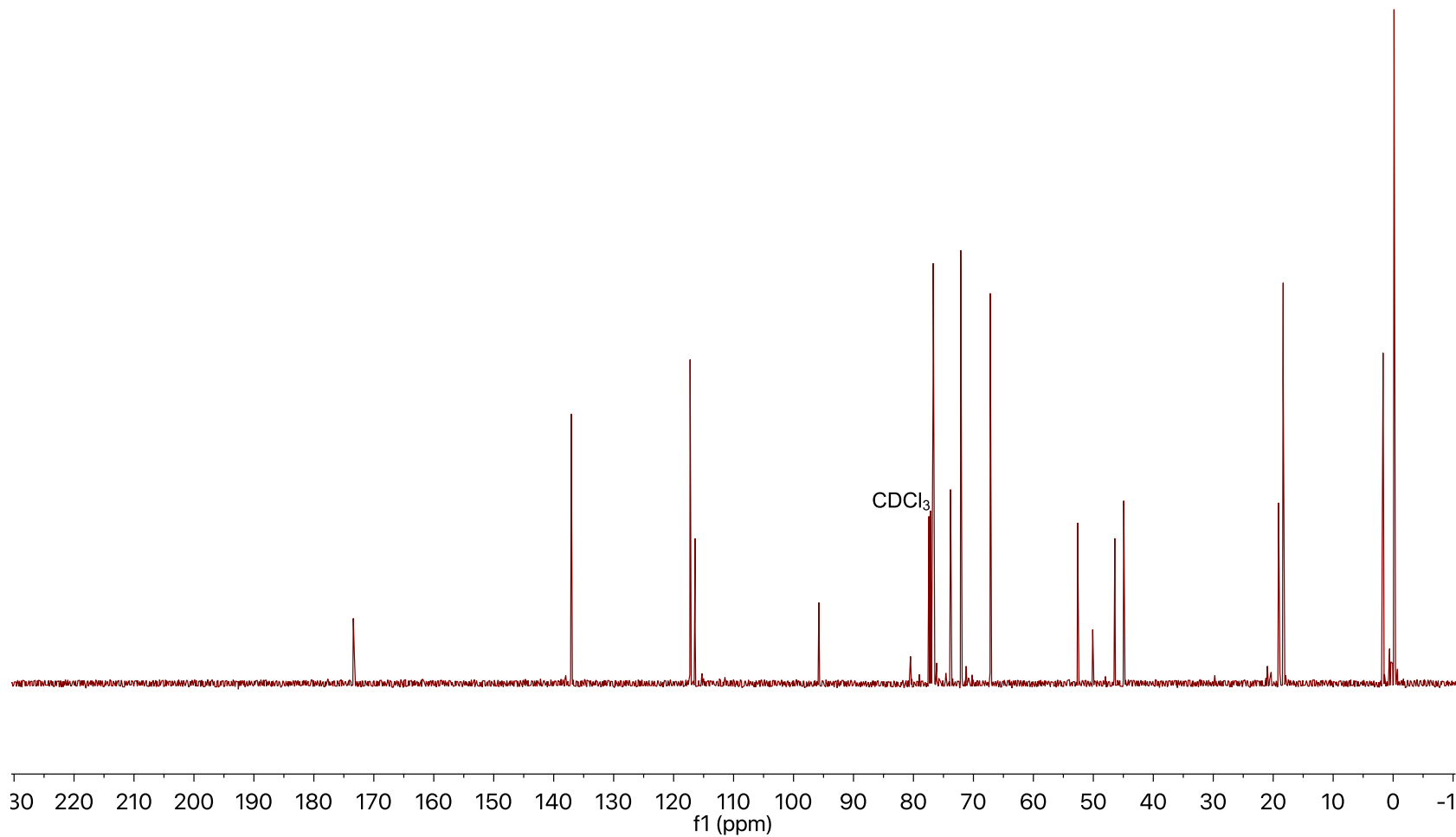
95.78

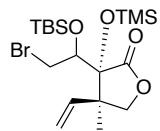
80.50
76.70
73.82
72.12
67.20

52.62
50.10
46.42
44.93

19.10
18.34

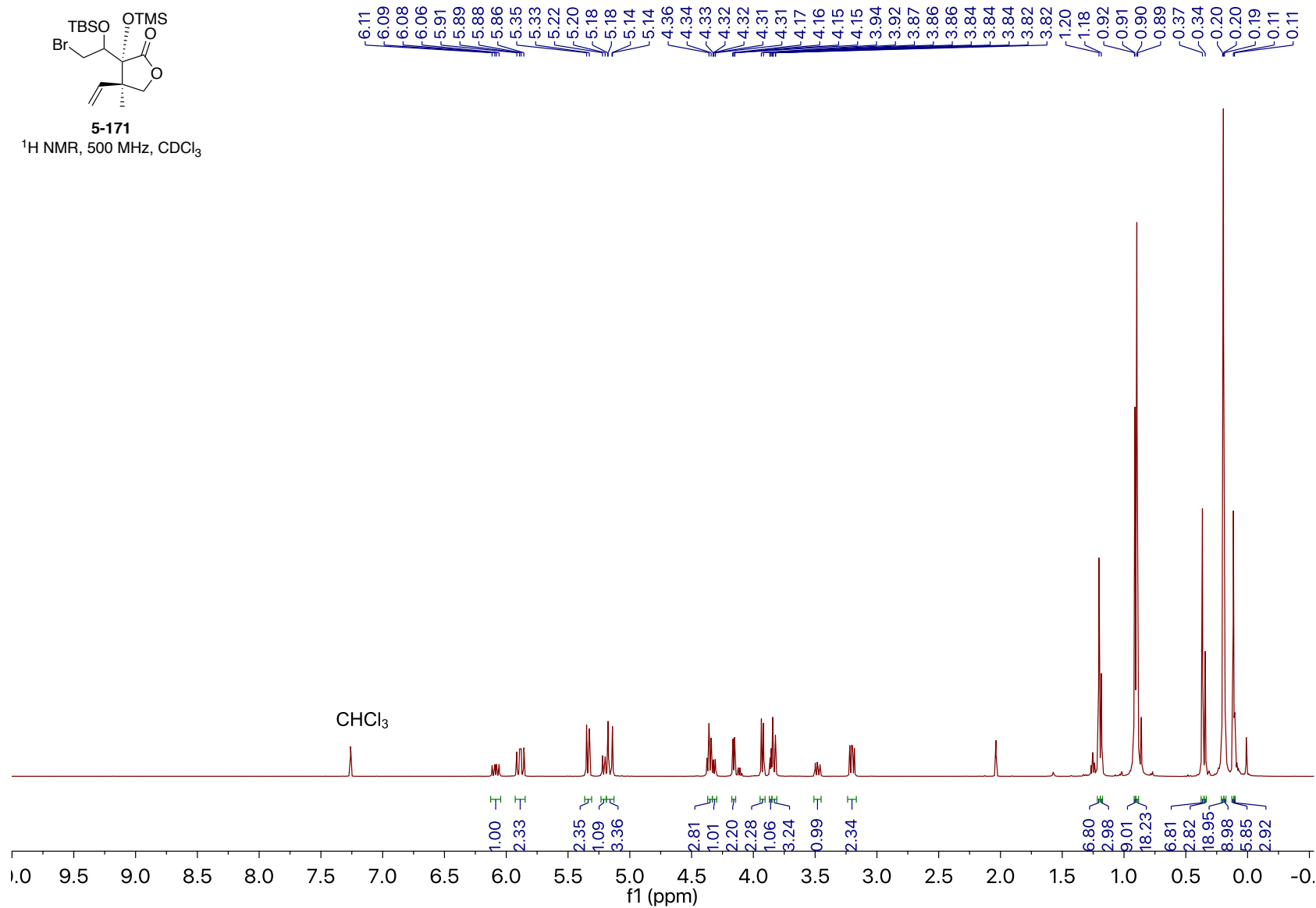
1.68
-0.15

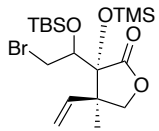




5-171

¹H NMR, 500 MHz, CDCl₃





5-171

$^{13}\text{C}\{^1\text{H}\}$ NMR, 126 MHz, CDCl_3

177.13
174.37

138.37
136.91

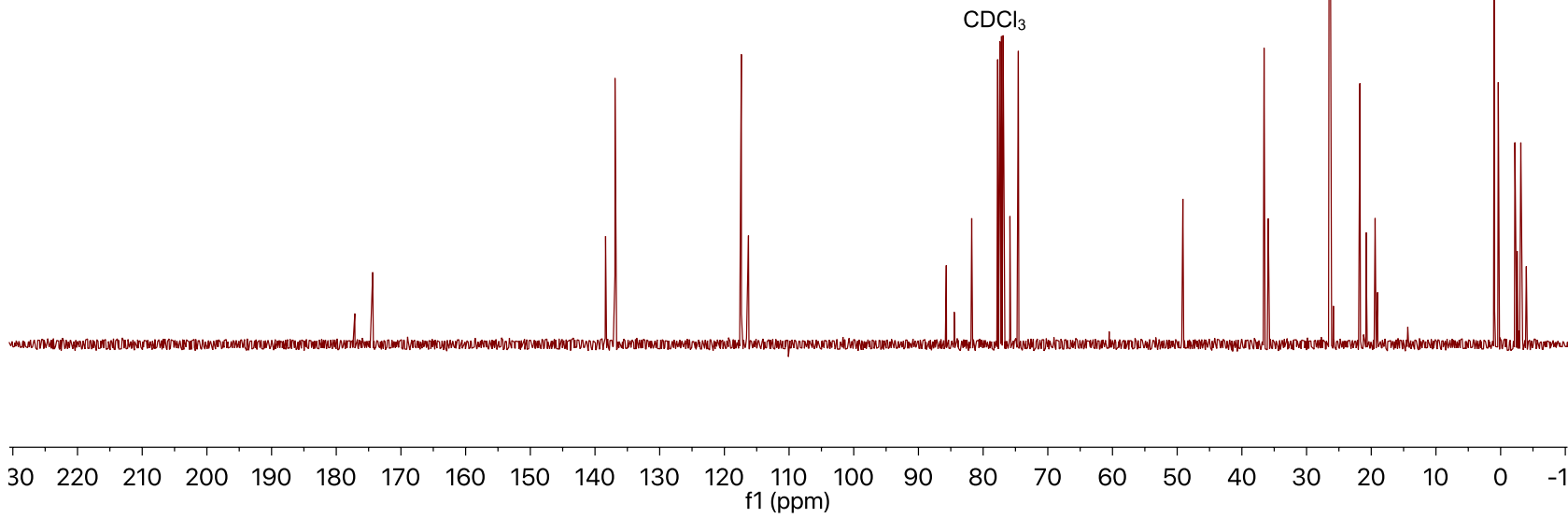
117.38
116.28

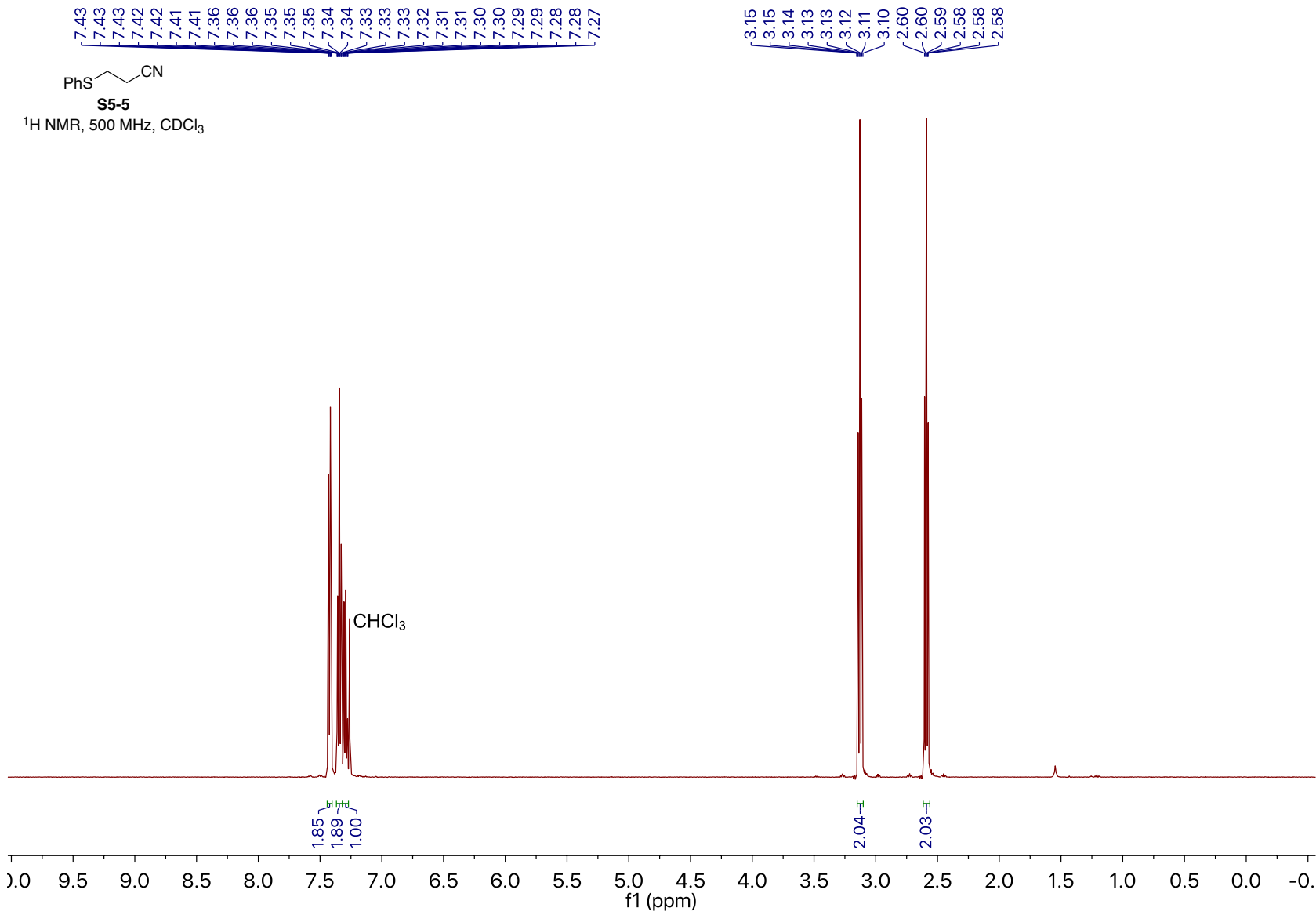
85.69
84.47
81.77
77.75
75.85
74.56

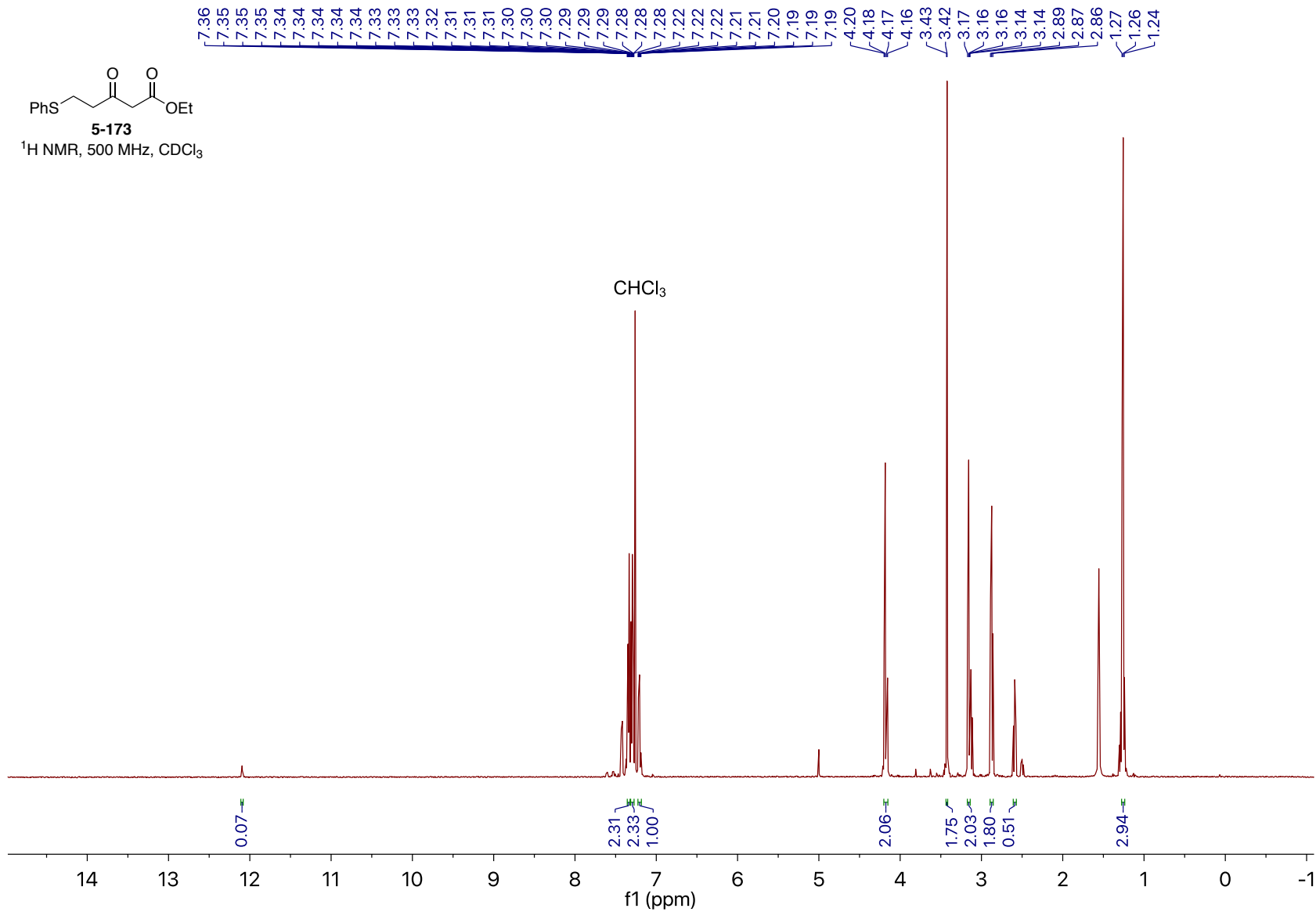
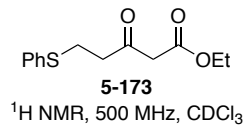
49.12
49.05

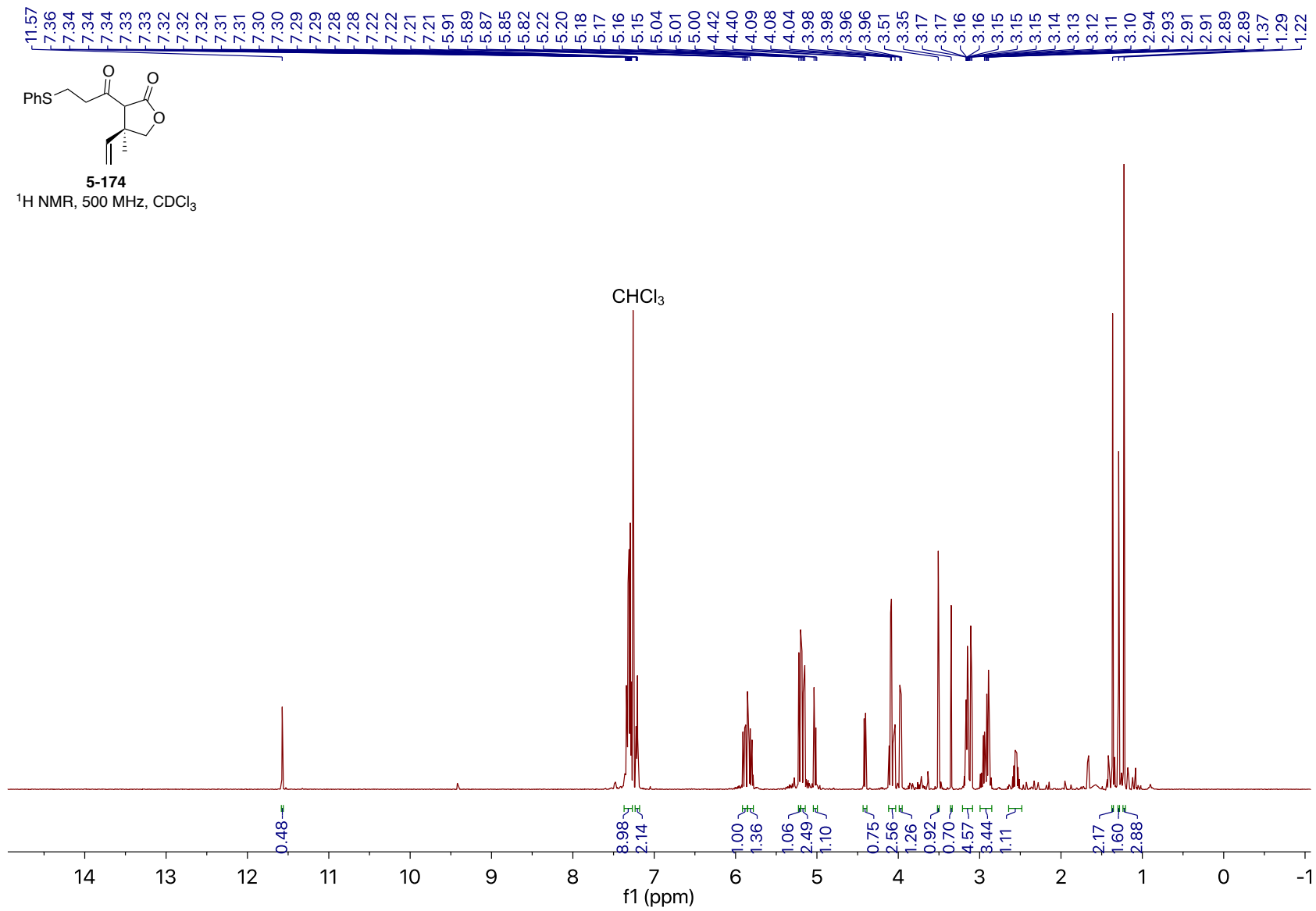
36.57
35.92
26.45
26.28
21.76
20.78
19.40
19.03

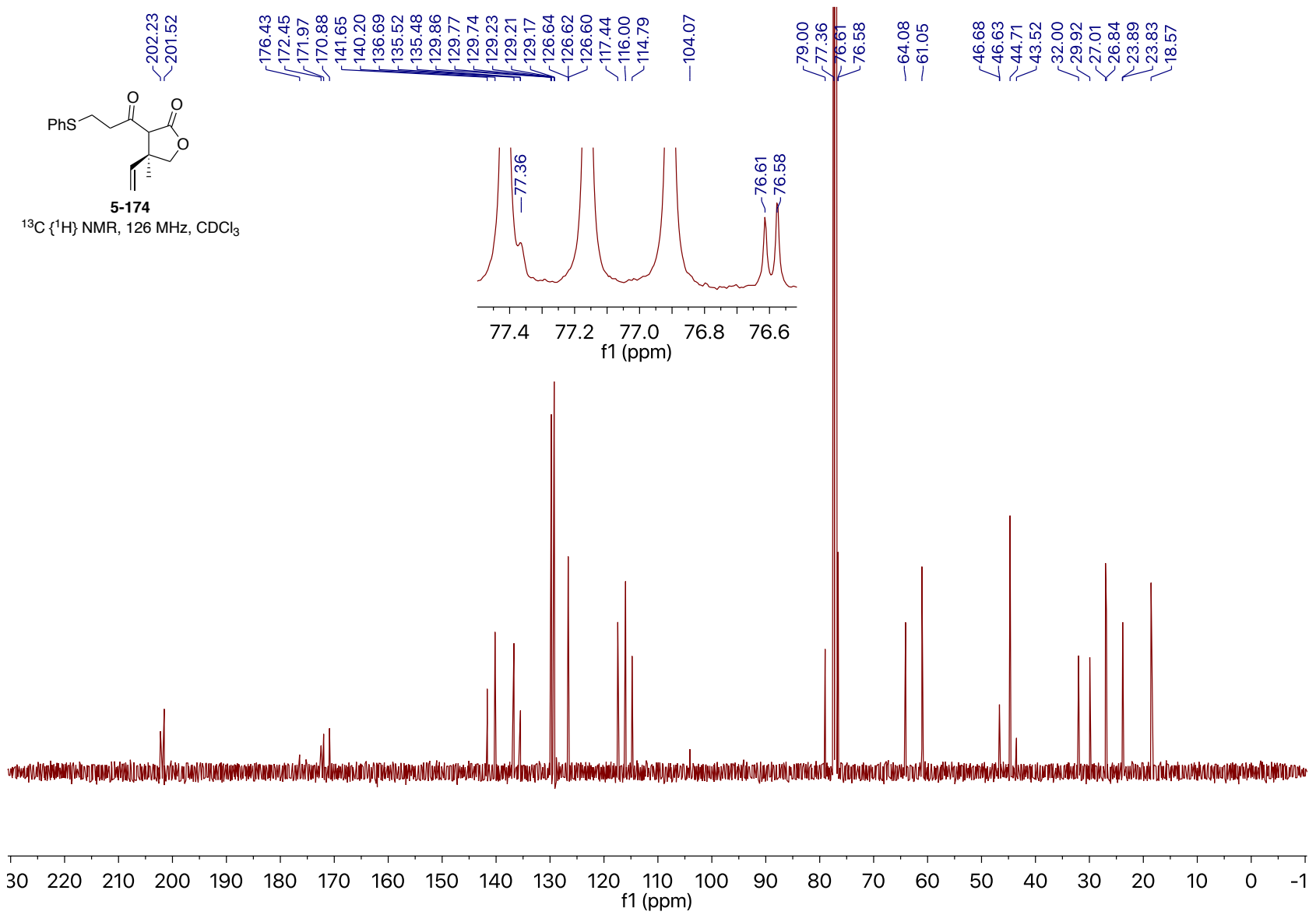
0.94
0.36
-2.21
-3.12

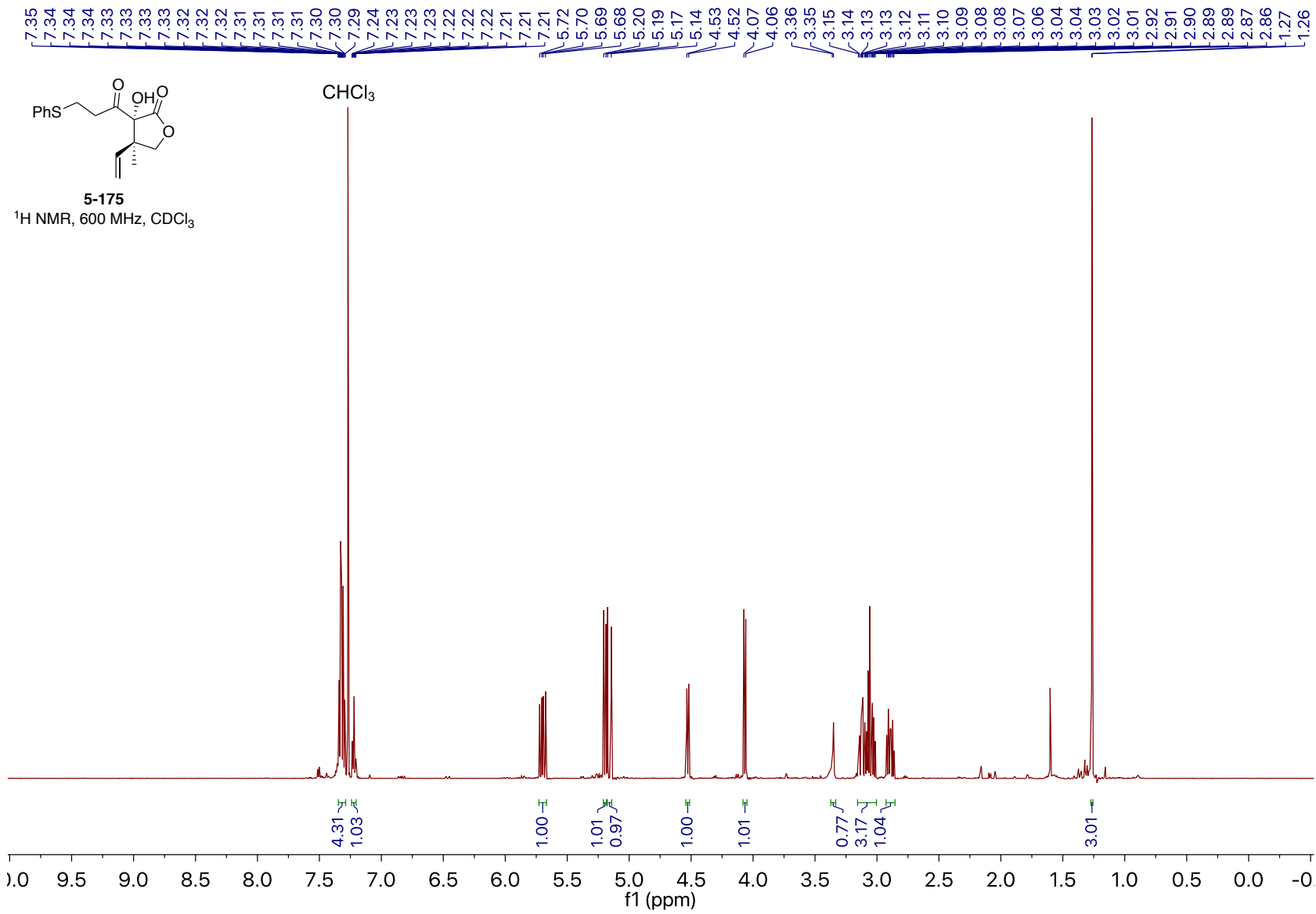


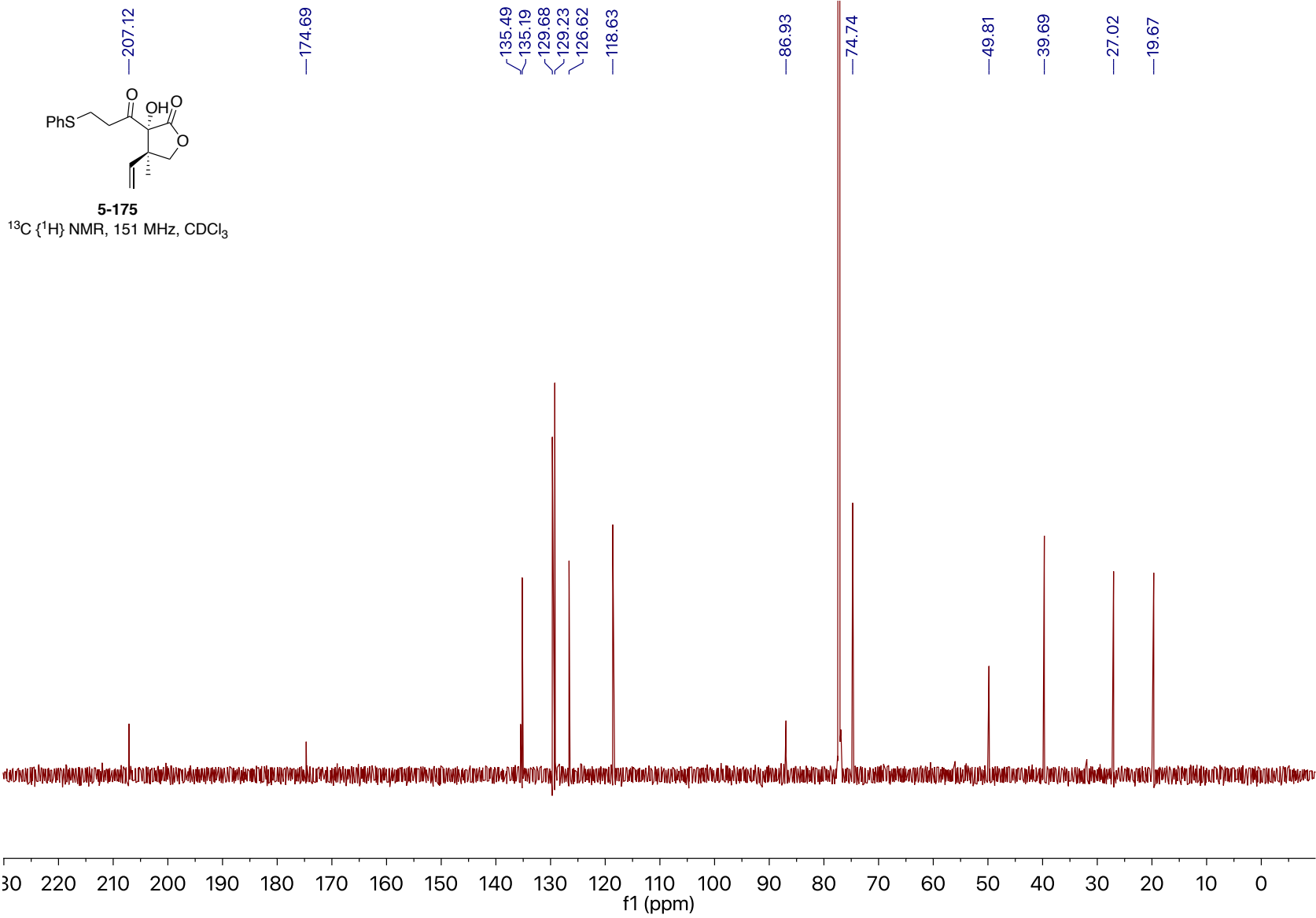


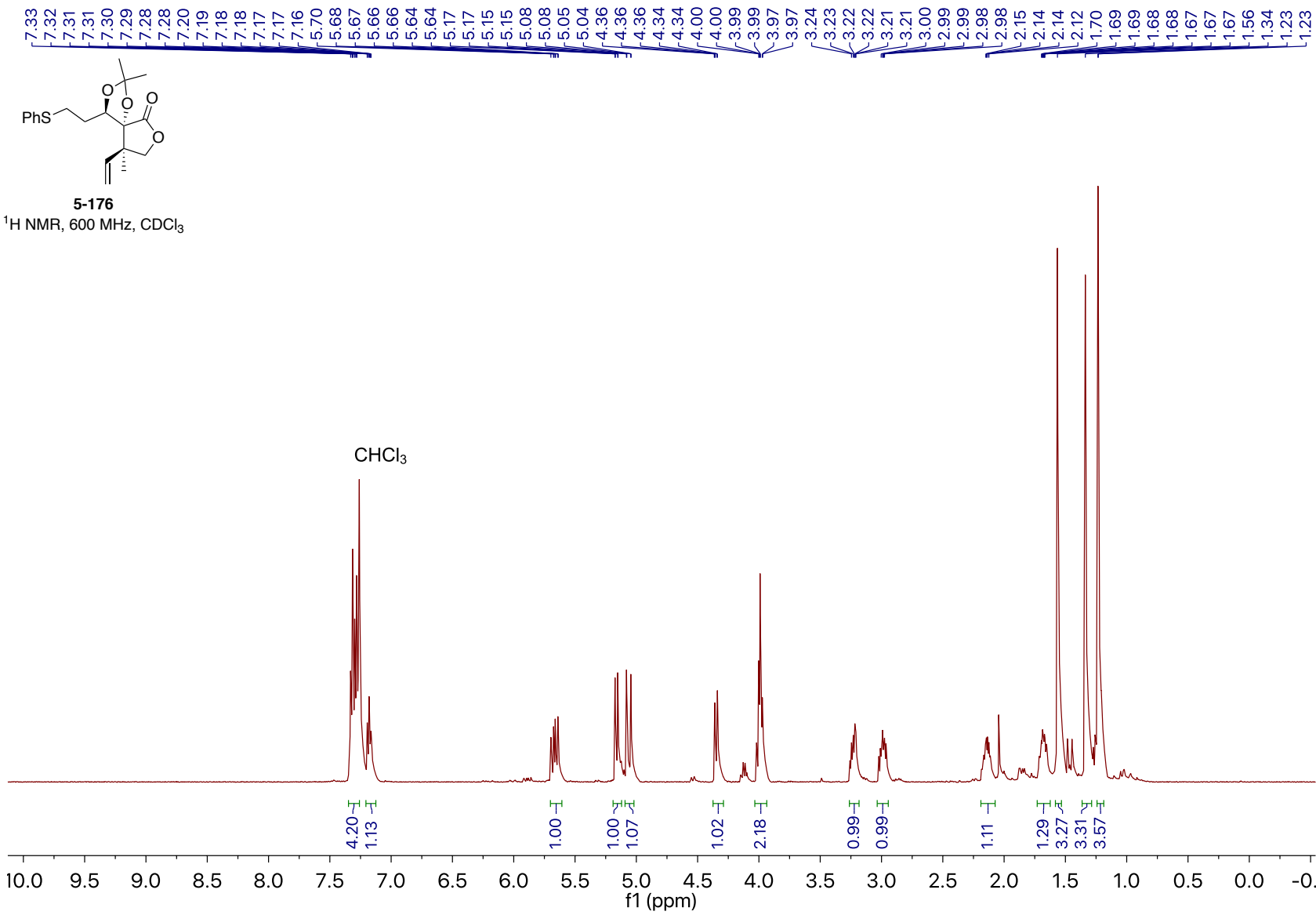


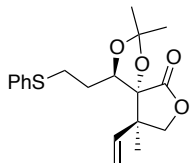






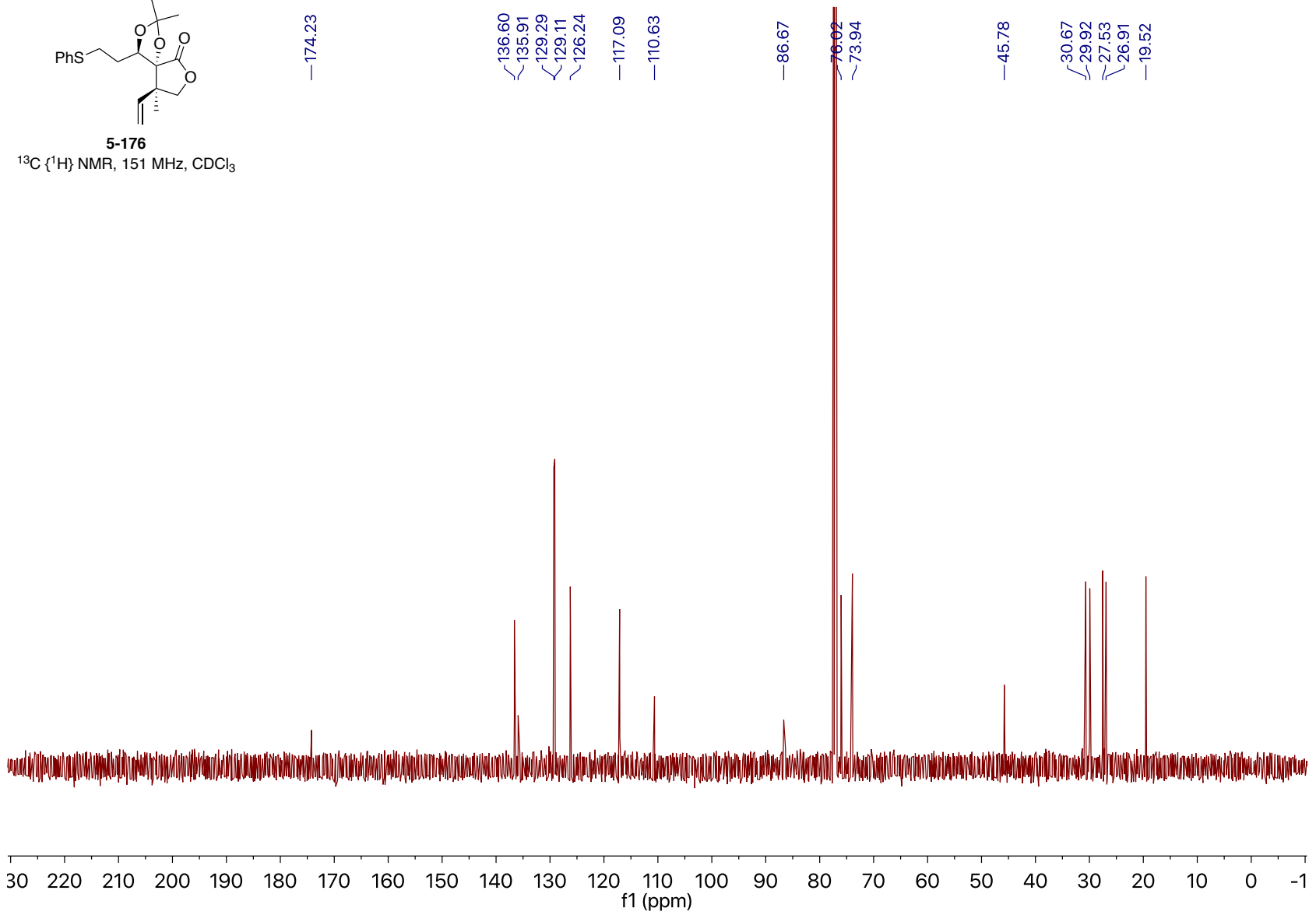


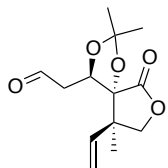




5-176

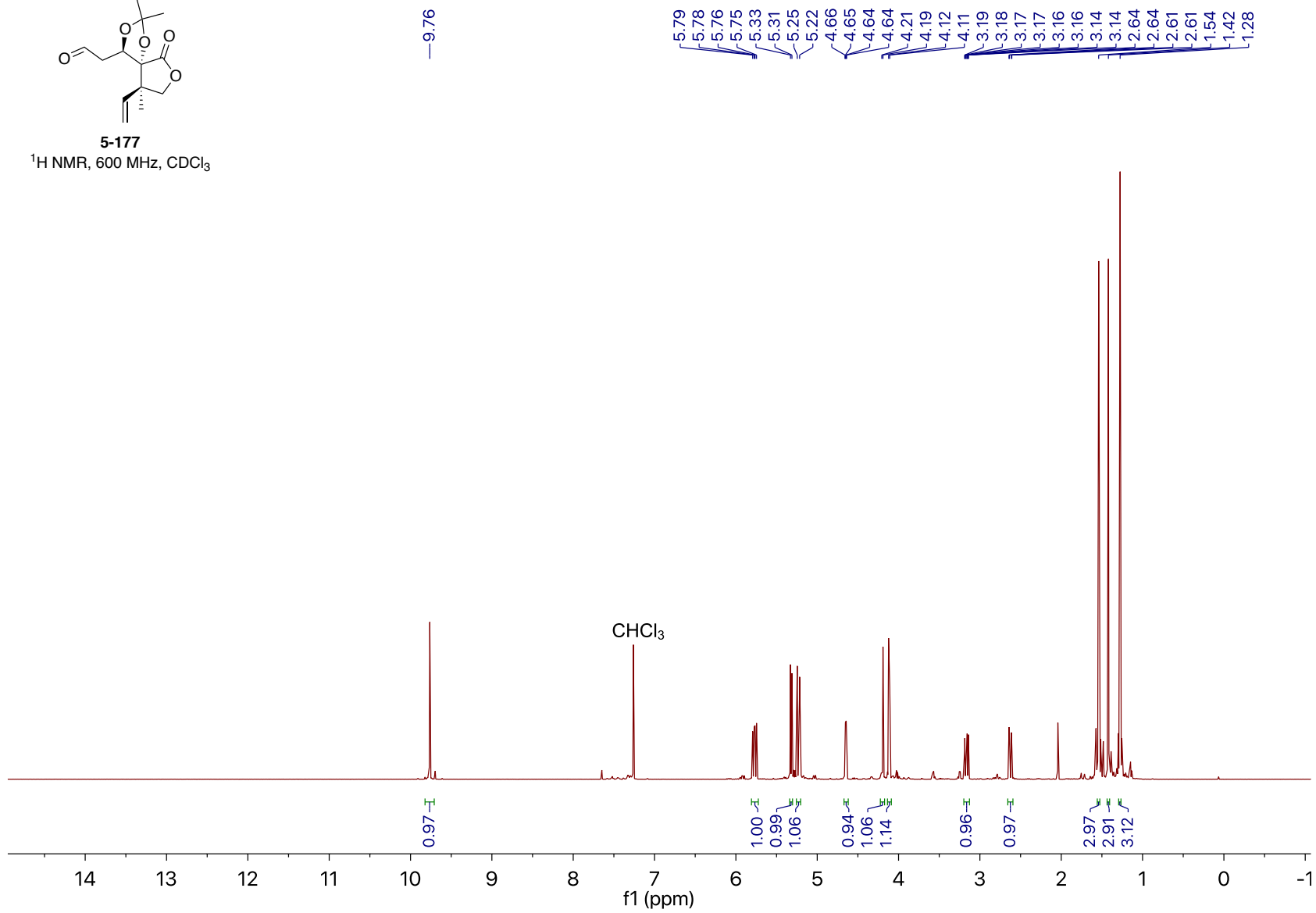
¹³C {¹H} NMR, 151 MHz, CDCl₃

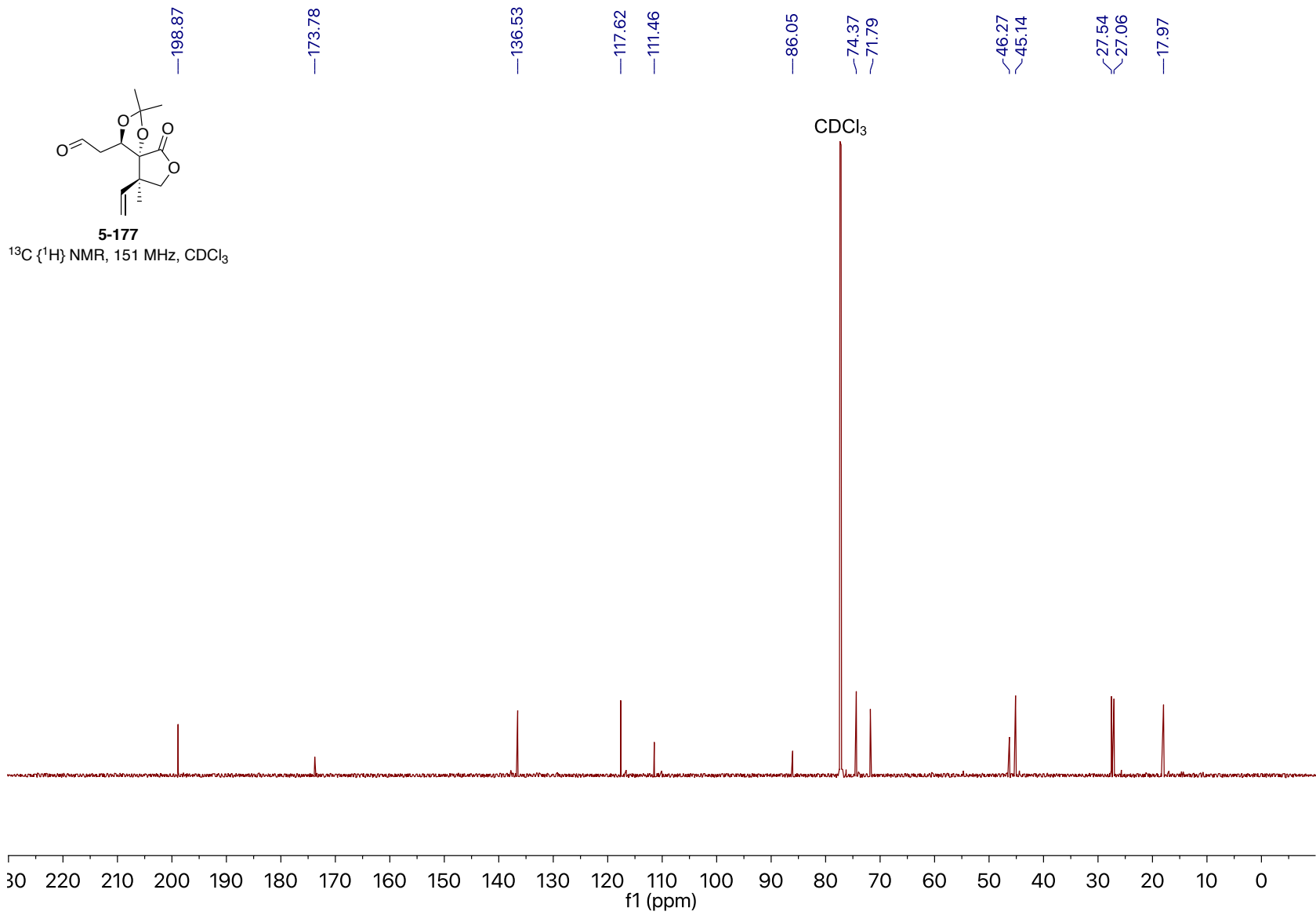


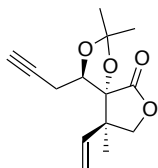


5-177

¹H NMR, 600 MHz, CDCl₃

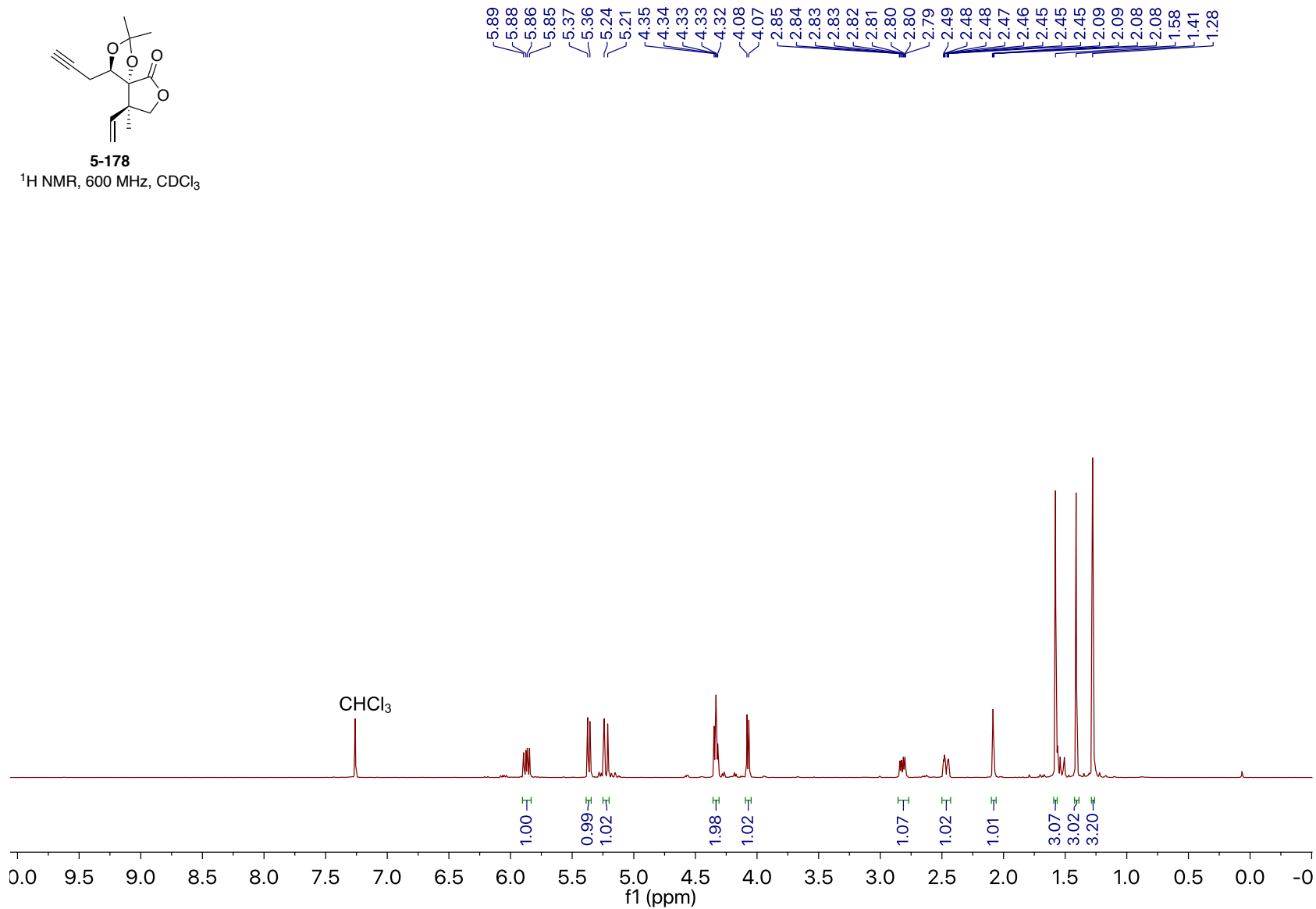


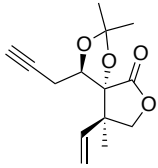




5-178

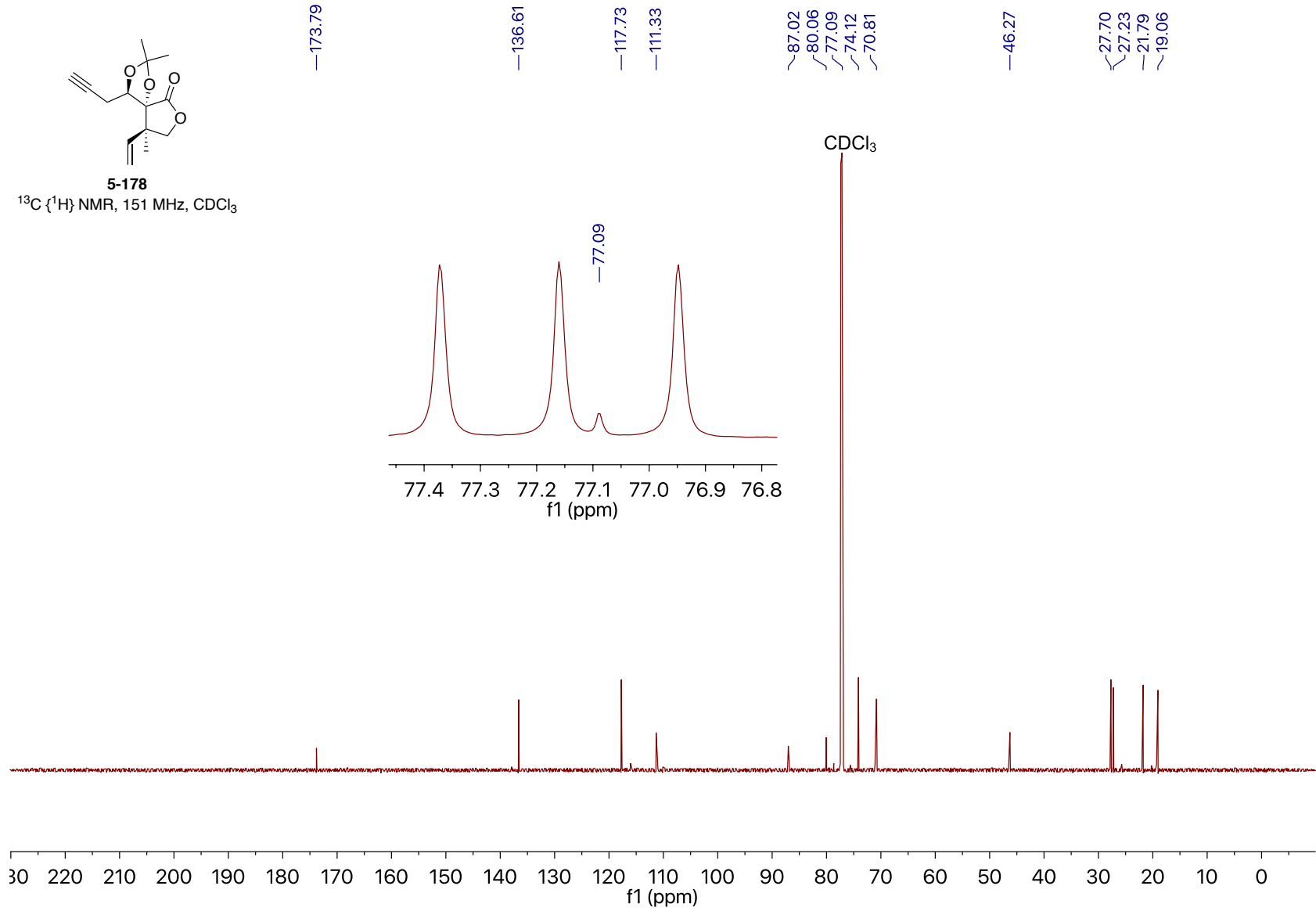
¹H NMR, 600 MHz, CDCl₃

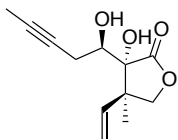




5-178

^{13}C { ^1H } NMR, 151 MHz, CDCl_3

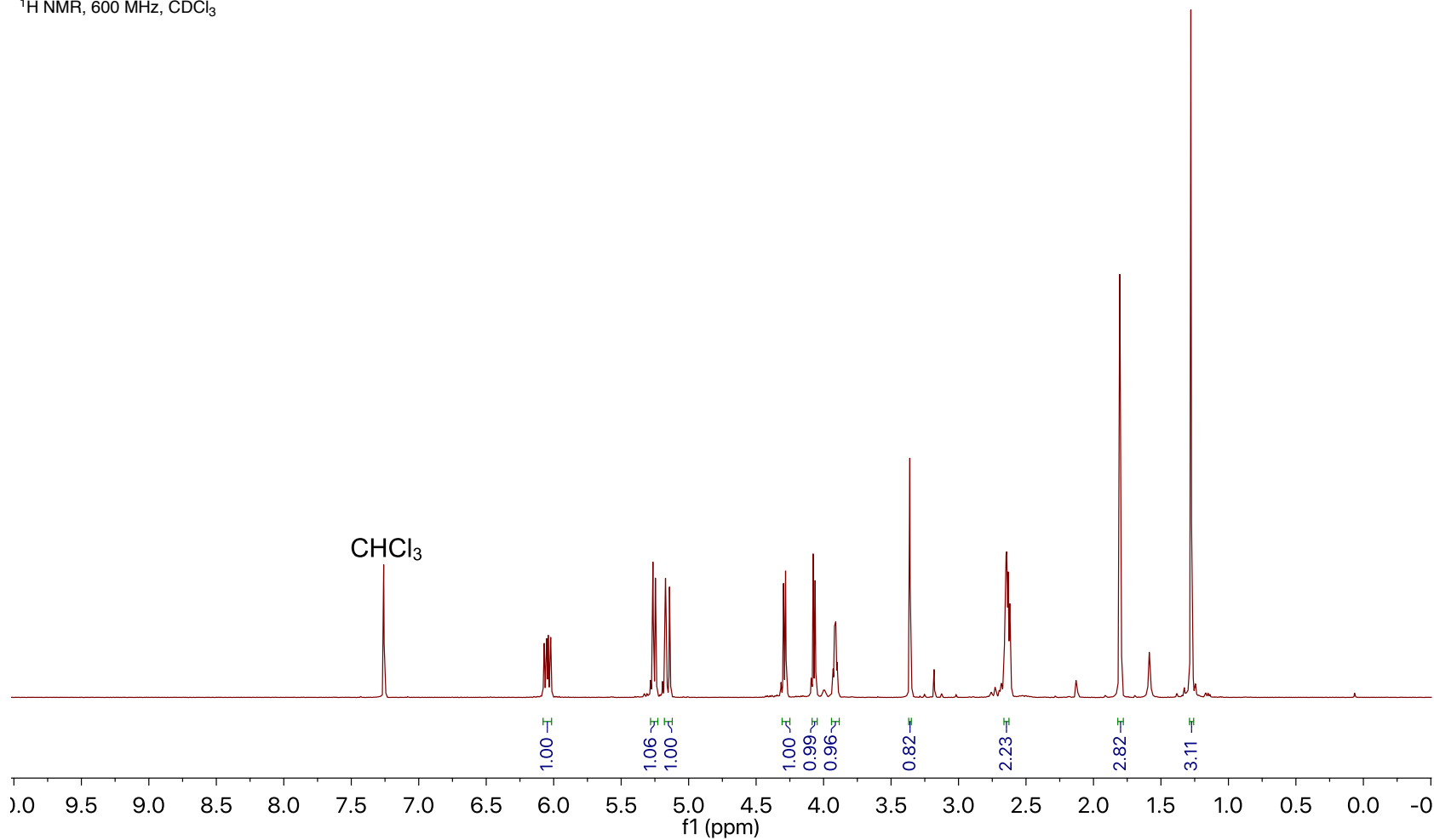


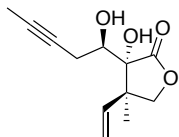


5-156

¹H NMR, 600 MHz, CDCl₃

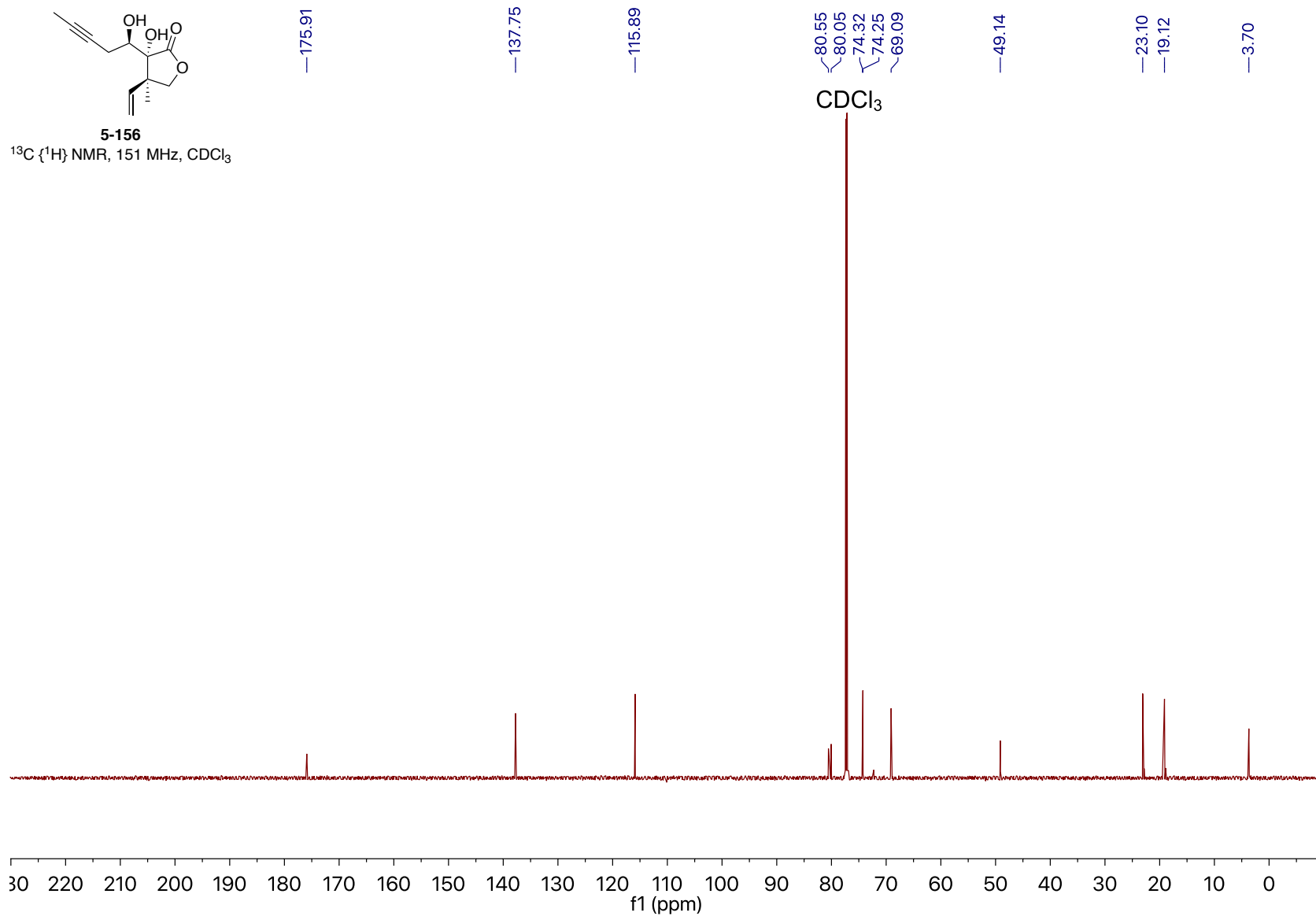
6.07
6.05
6.04
6.02
5.26
5.25
5.17
5.14
4.30
4.28
4.08
4.06
3.93
3.92
3.91
3.90
— 3.36
2.66
2.65
2.65
2.64
2.63
1.81
1.81
1.80
1.79
1.28
1.27
1.26

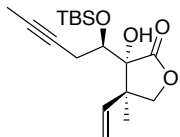




5-156

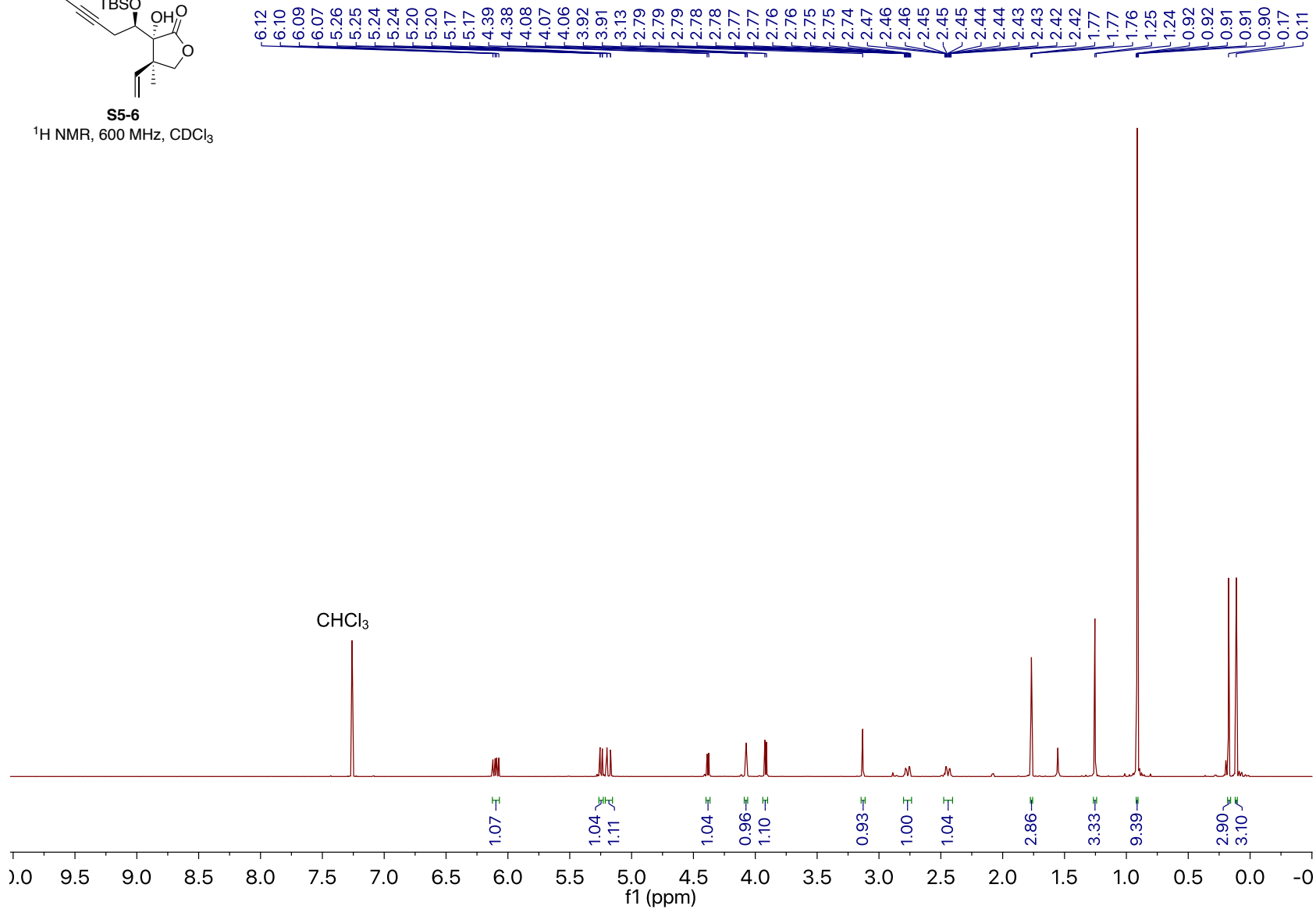
$^{13}\text{C}\{^1\text{H}\}$ NMR, 151 MHz, CDCl_3

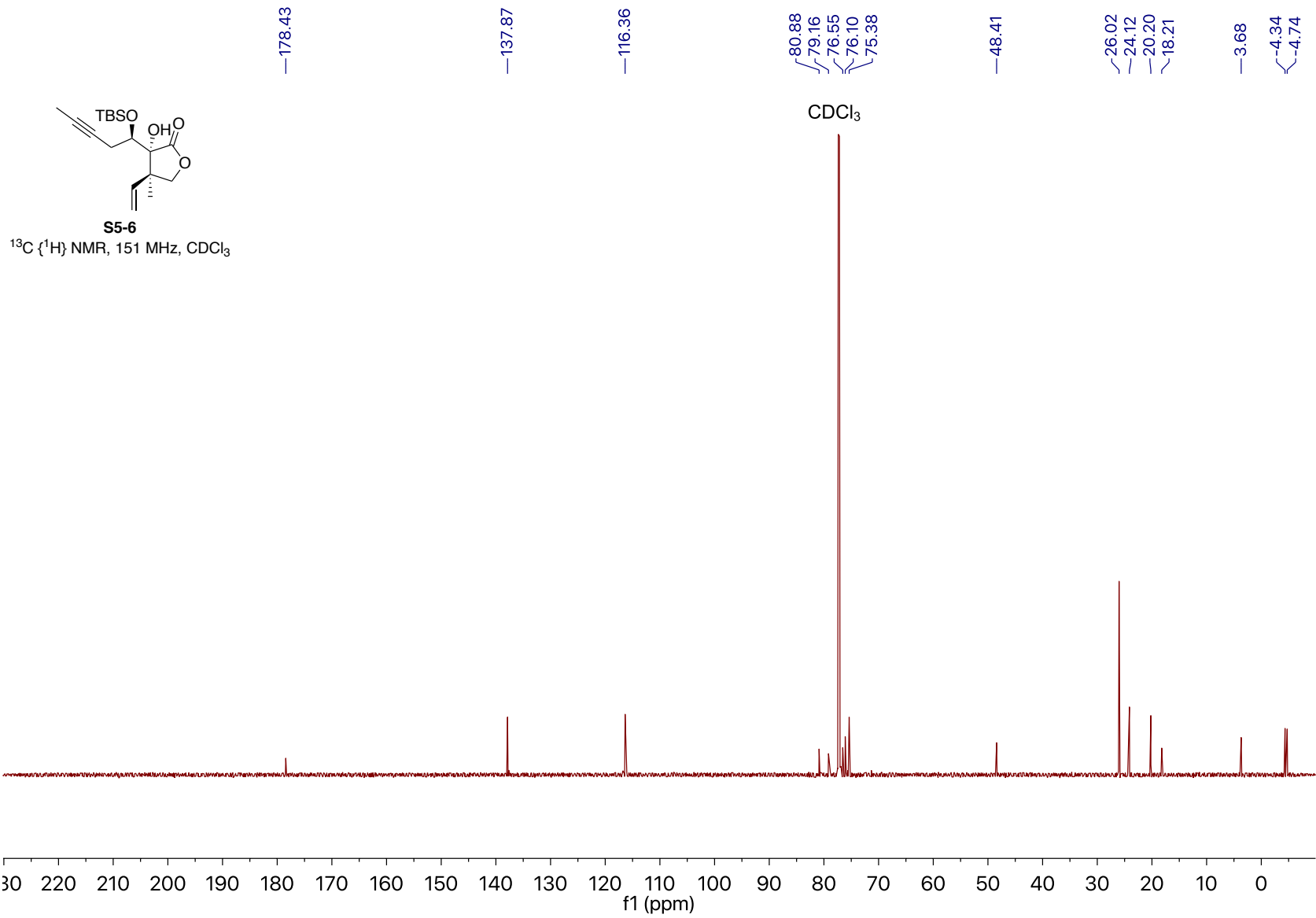


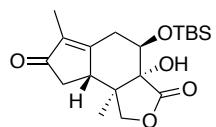


S5-6

¹H NMR, 600 MHz, CDCl₃

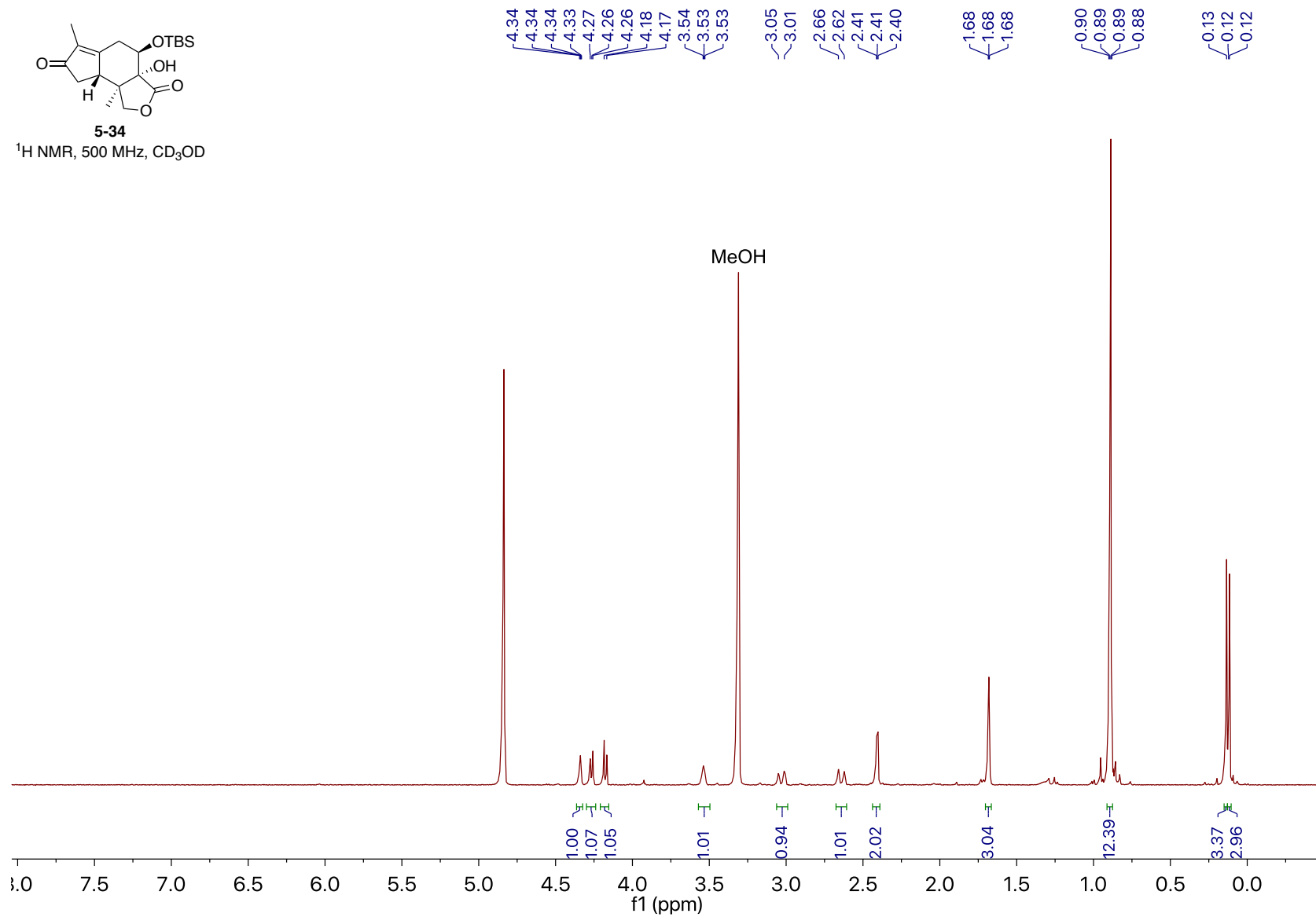


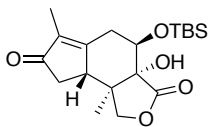




5-34

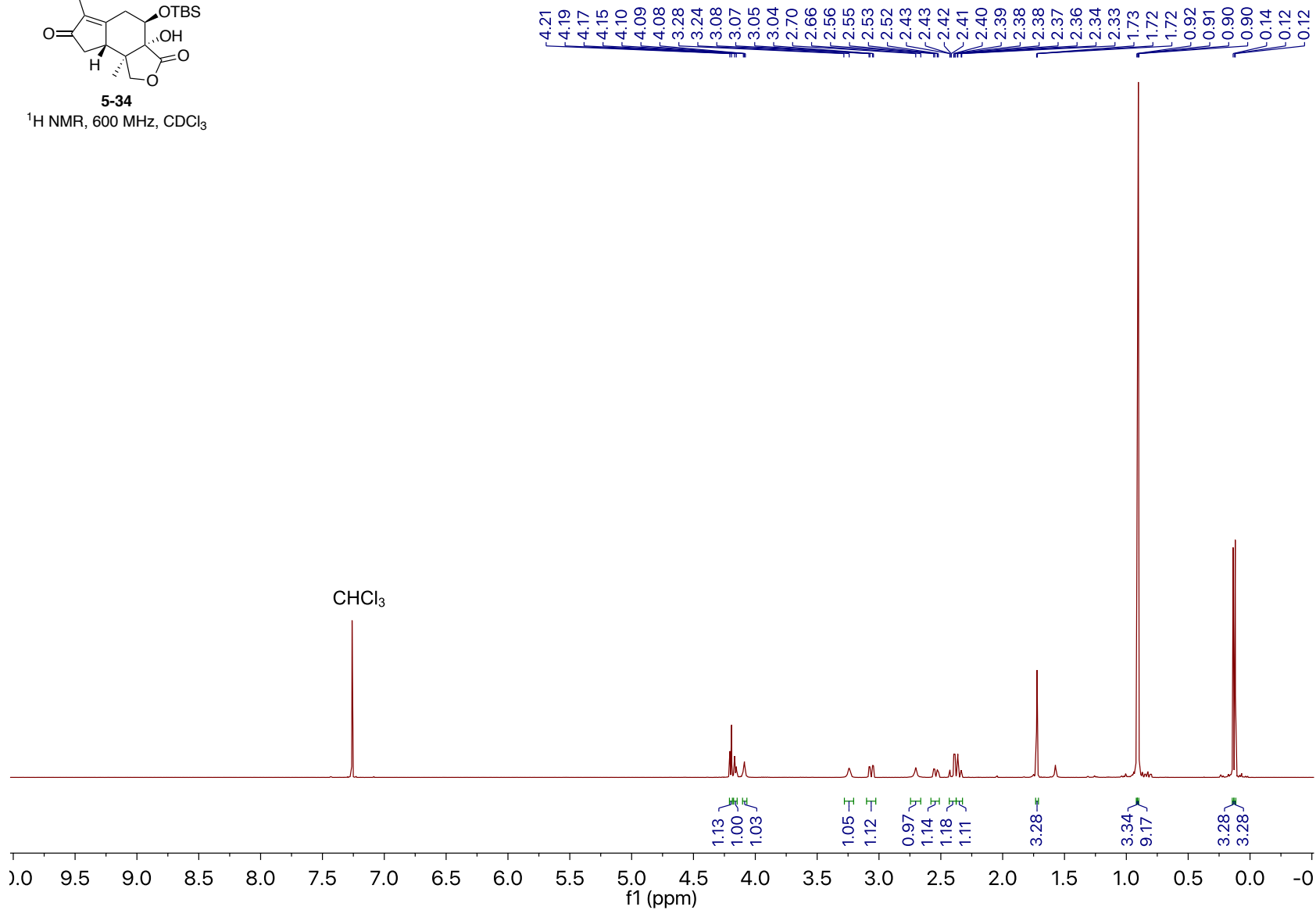
^1H NMR, 500 MHz, CD_3OD

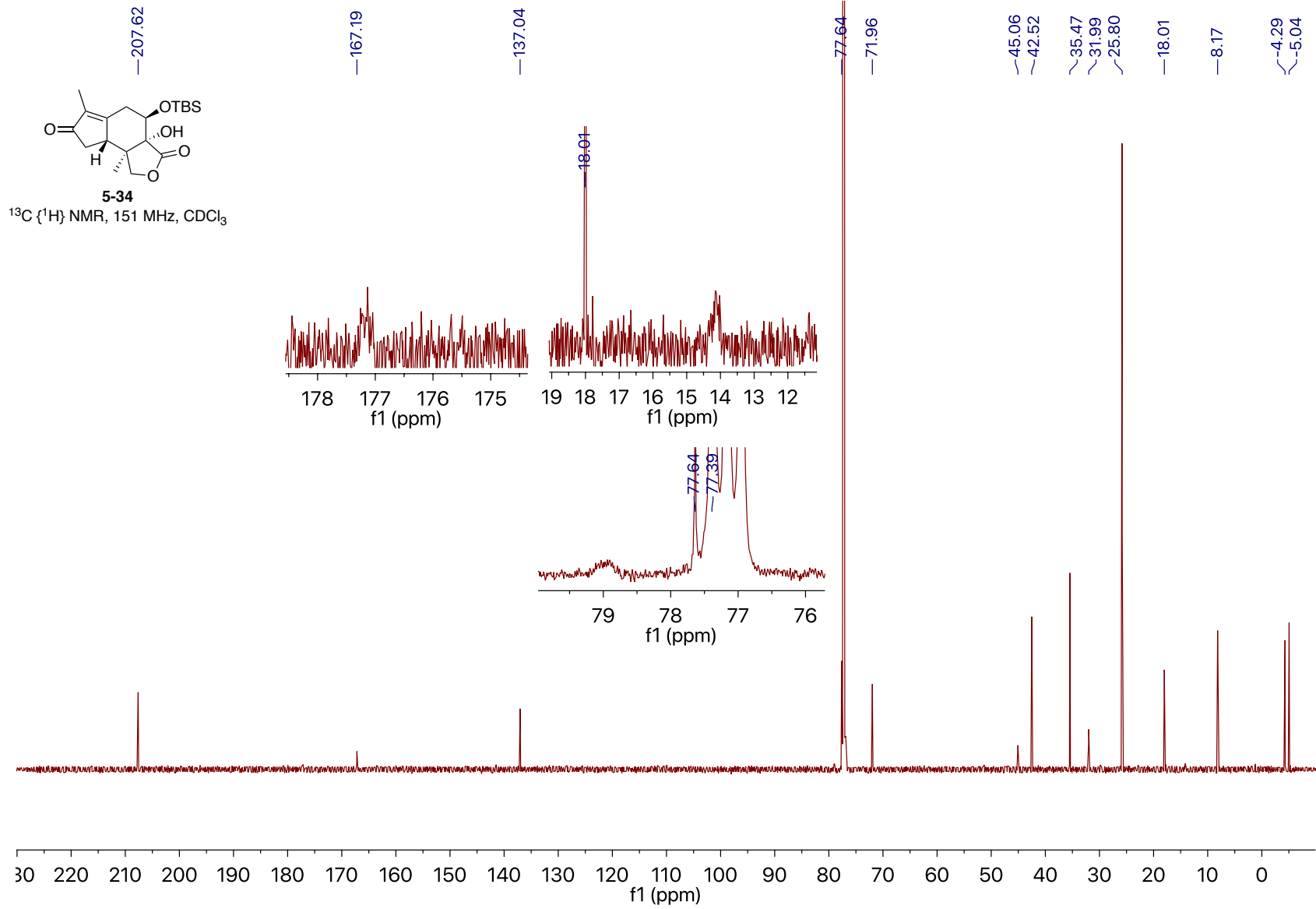


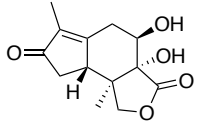


5-34

¹H NMR, 600 MHz, CDCl₃

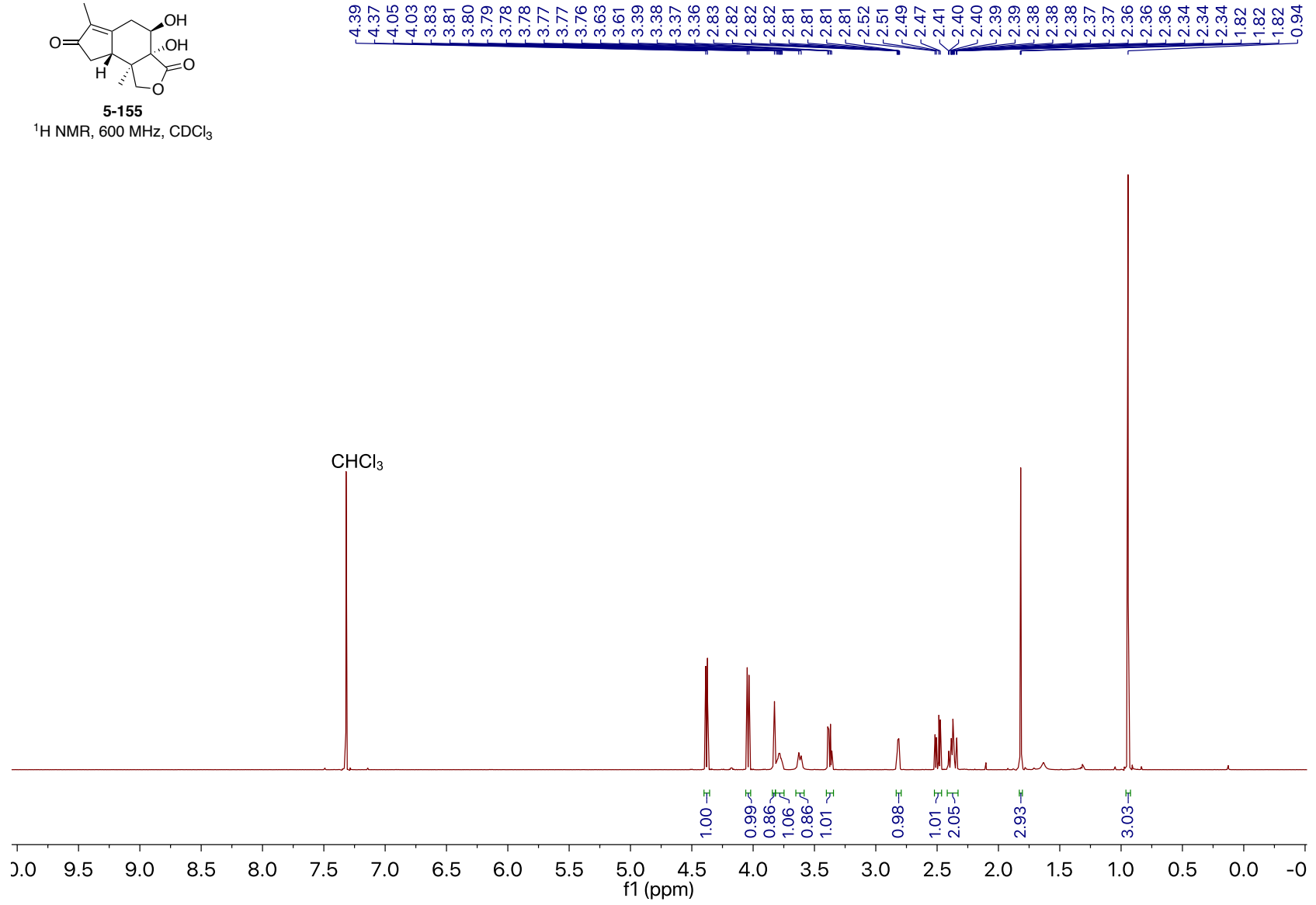


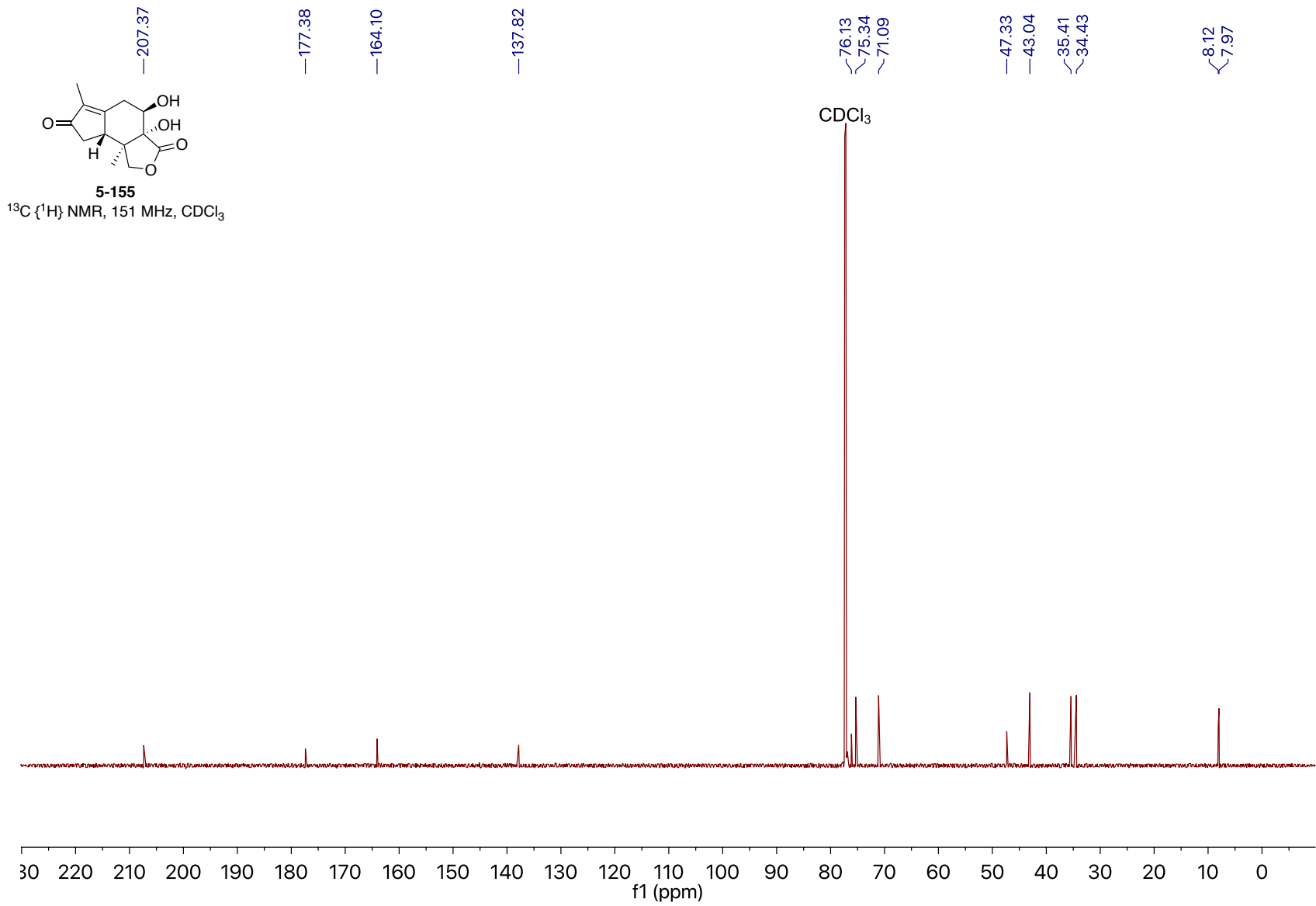


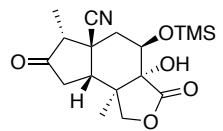


5-155

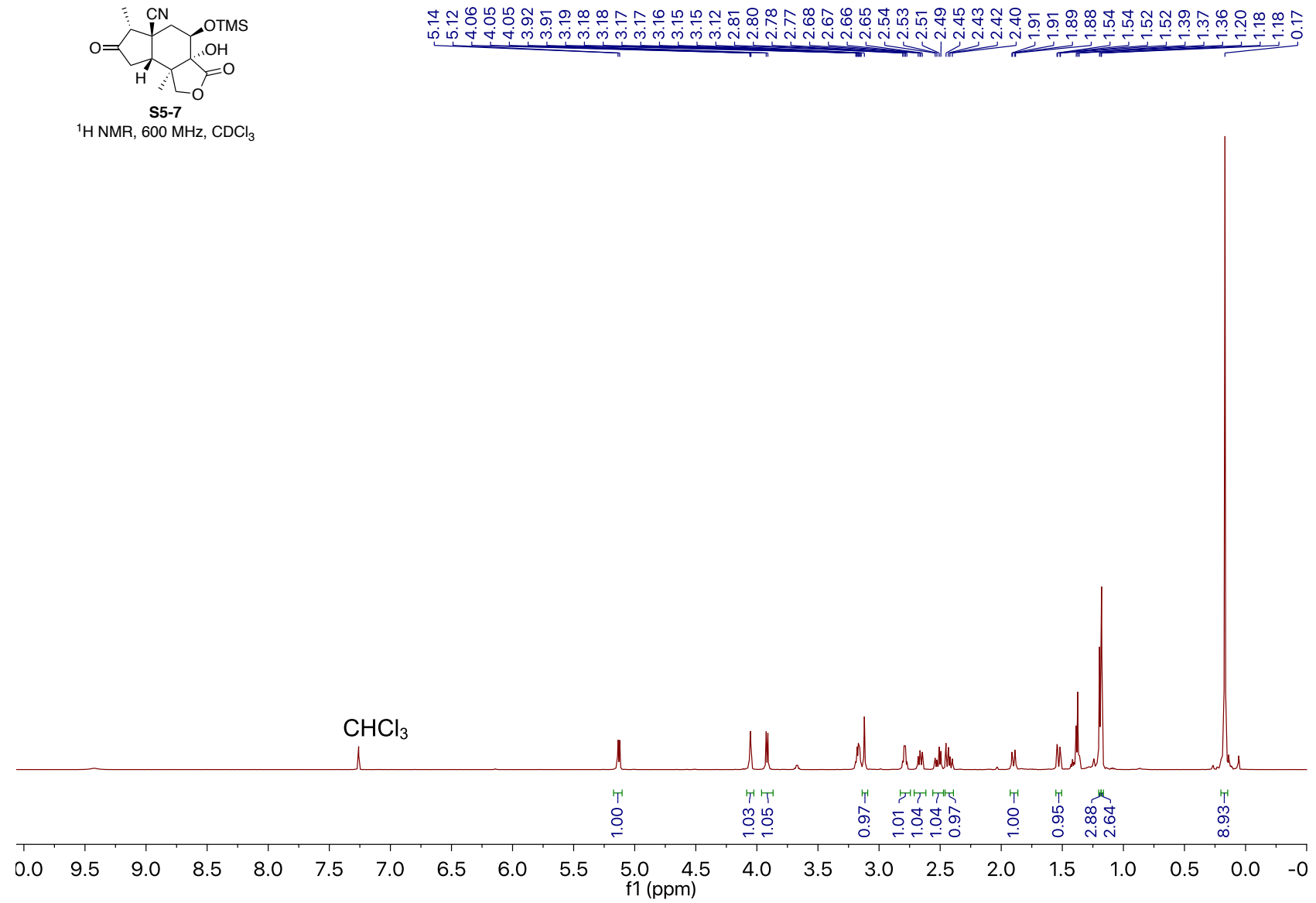
¹H NMR, 600 MHz, CDCl₃

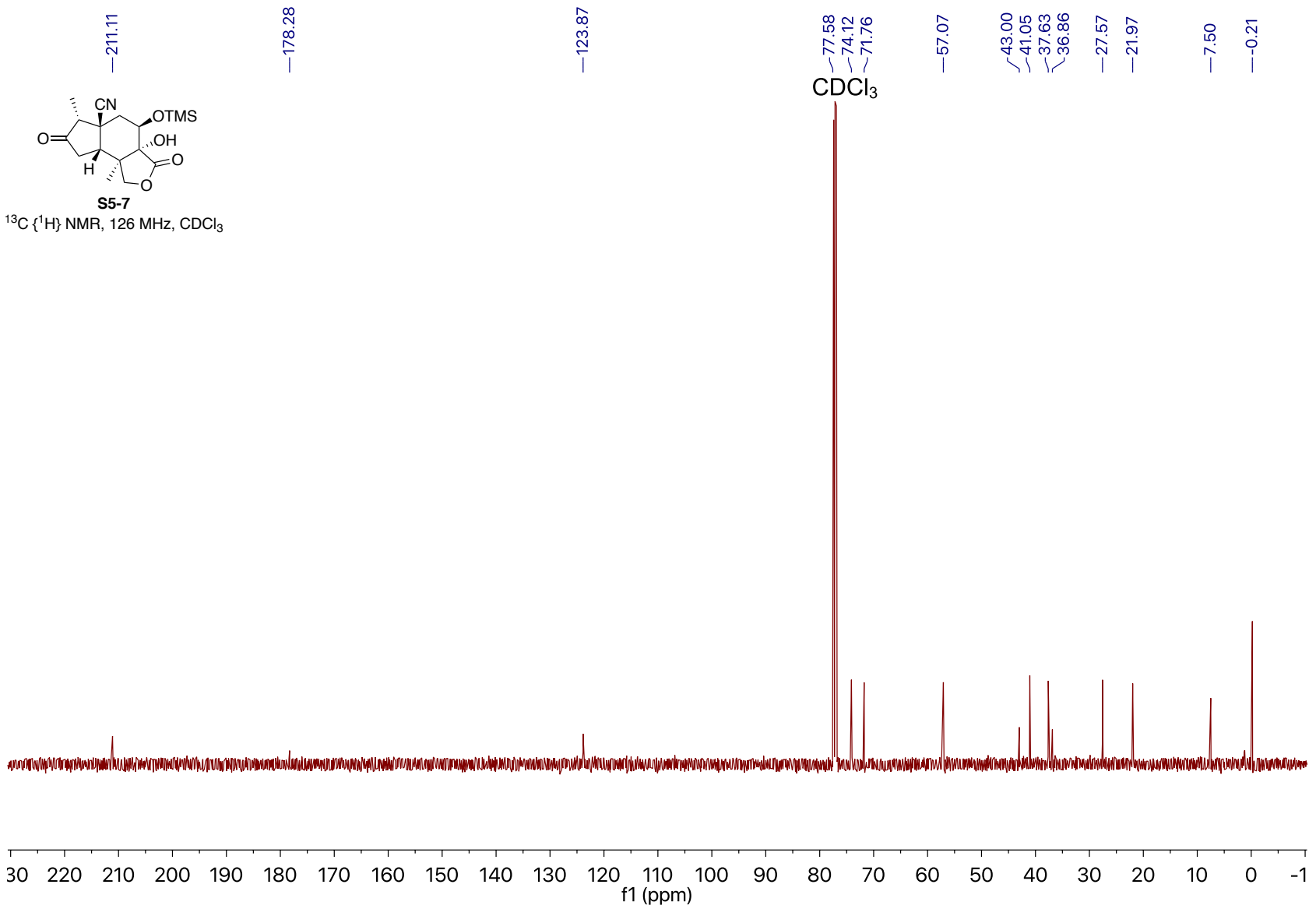


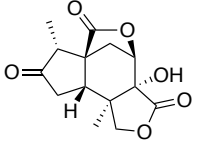




S5-7
¹H NMR, 600 MHz, CDCl₃



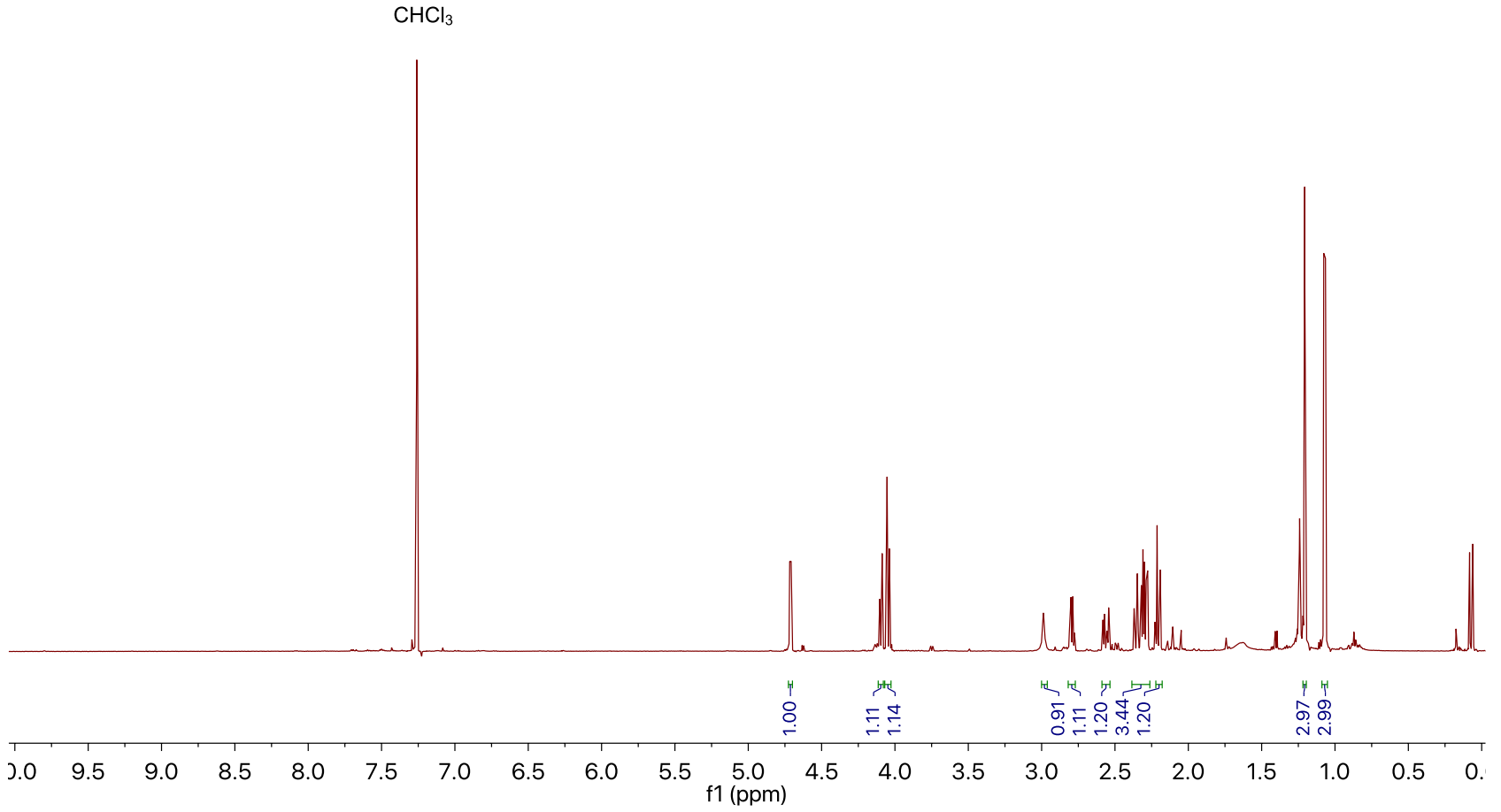


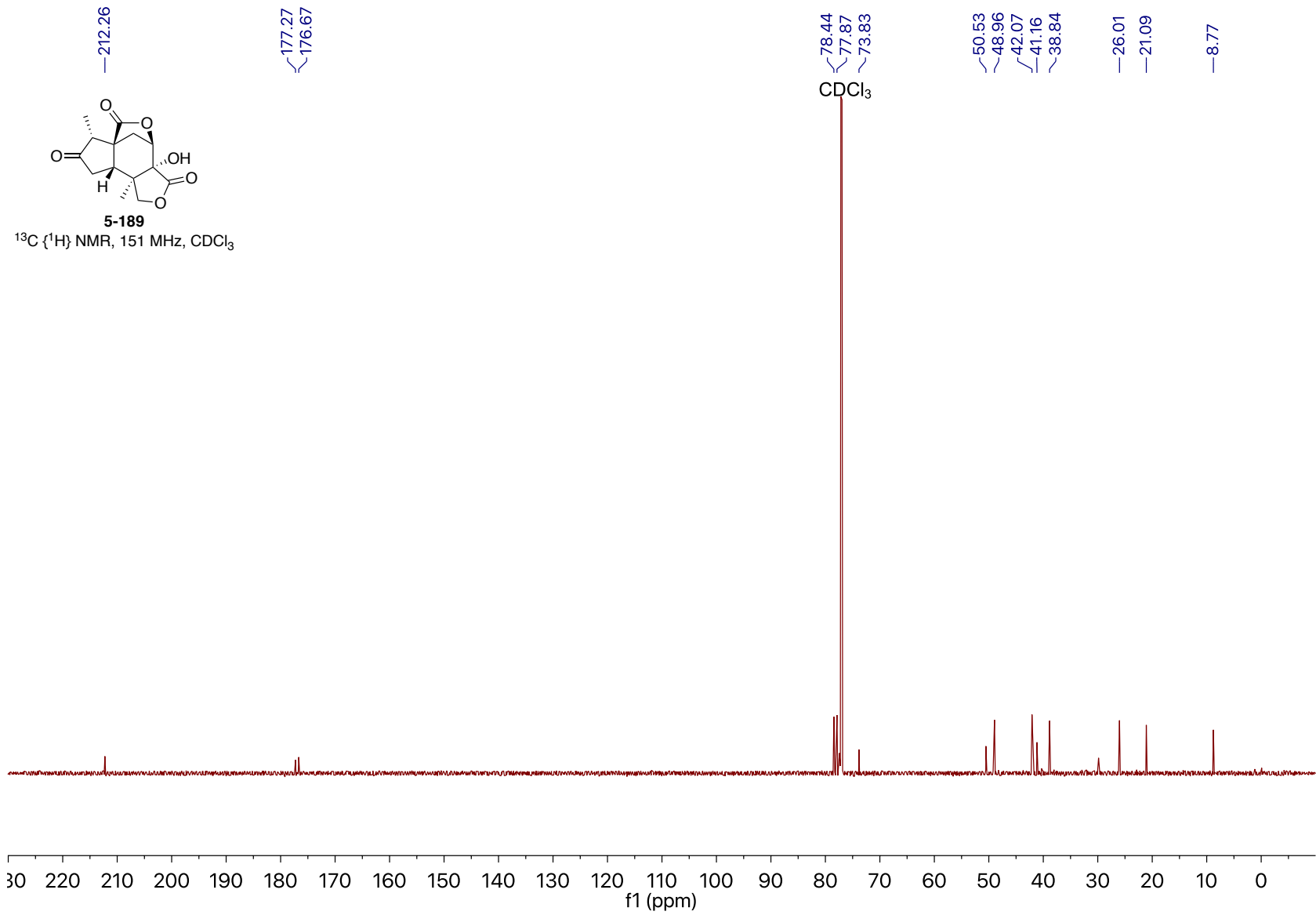
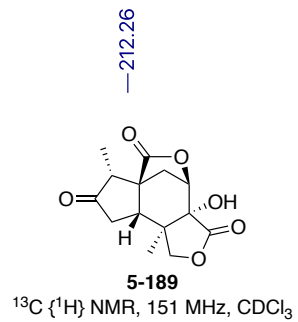


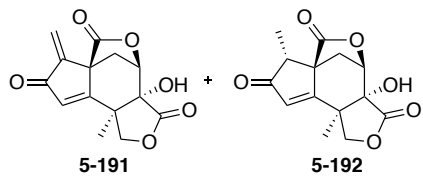
5-189

¹H NMR, 600 MHz, CDCl₃

4.72
4.71
4.10
4.10
4.09
4.09
4.05
4.04
2.99
2.80
2.79
2.58
2.58
2.57
2.57
2.55
2.55
2.54
2.54
2.37
2.35
2.32
2.31
2.30
2.29
2.28
2.21
2.19
1.21
1.21
1.08
1.06

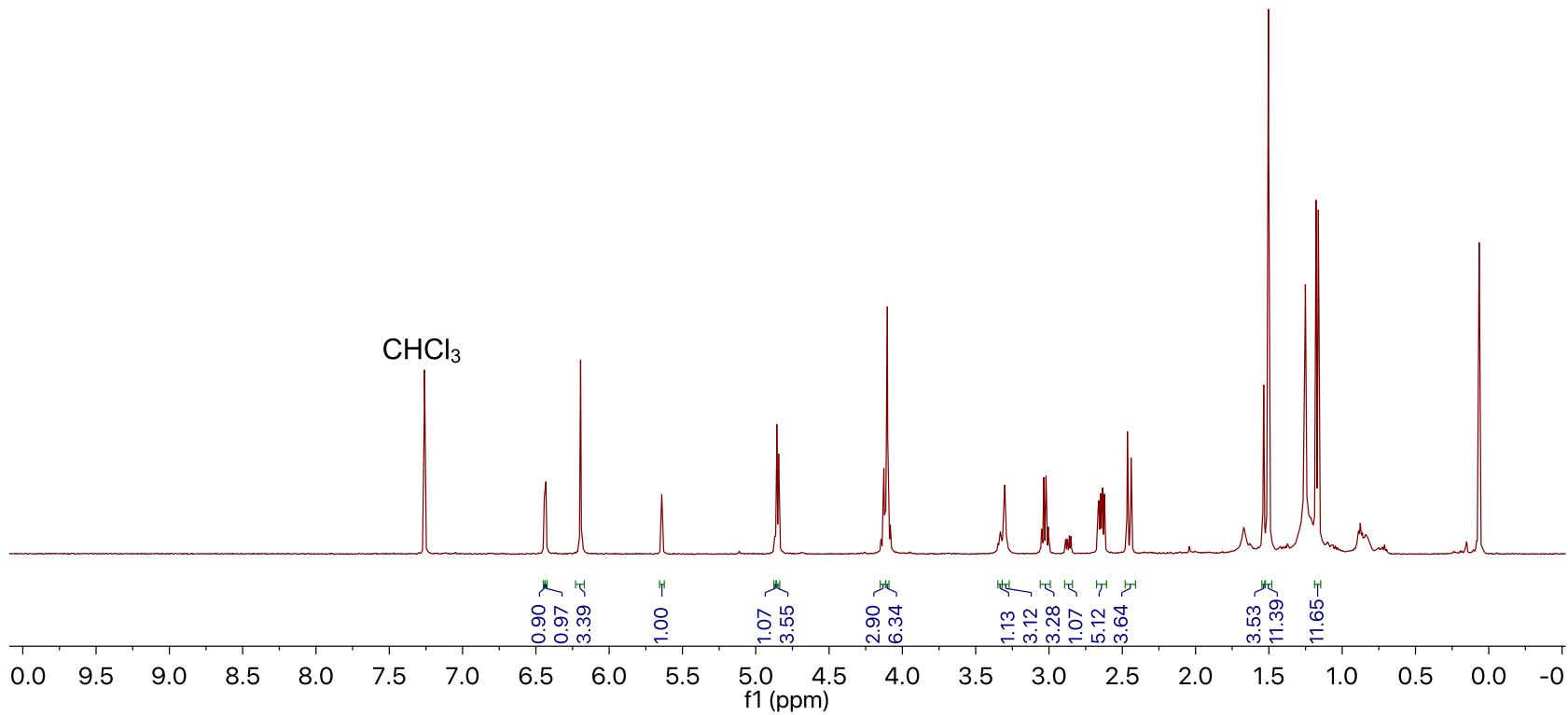


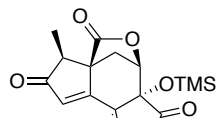




1:3
 $^1\text{H NMR}$, 500 MHz, CDCl_3

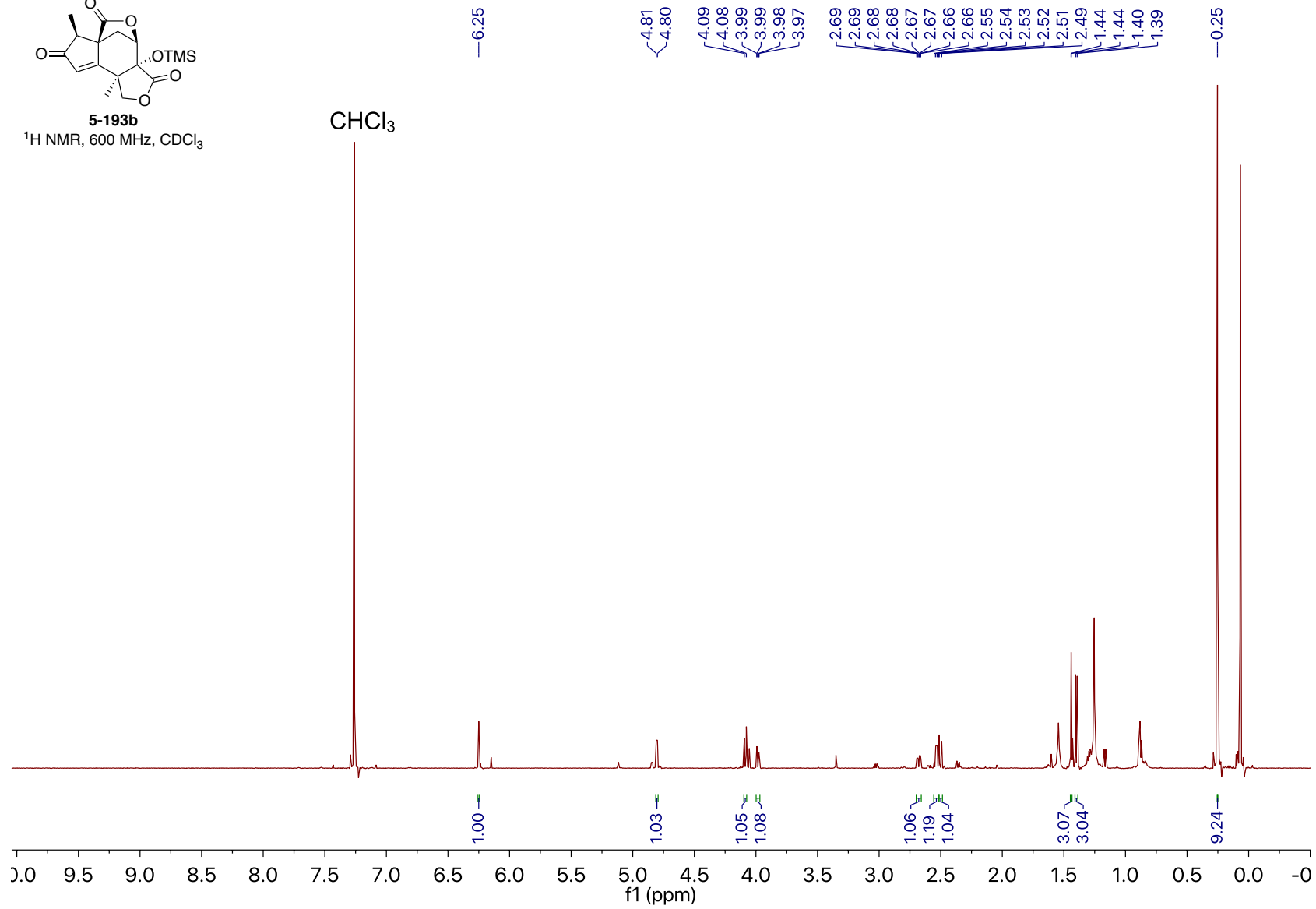
6.44
 6.43
 6.19
 5.64
 4.87
 4.86
 4.84
 4.15
 4.14
 4.13
 4.12
 4.11
 4.10
 4.08
 3.33
 3.30
 3.05
 3.04
 3.02
 3.00
 2.89
 2.87
 2.86
 2.85
 2.66
 2.66
 2.65
 2.65
 2.64
 2.63
 2.62
 2.47
 2.44
 1.54
 1.50
 1.18
 1.16

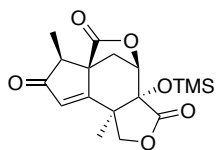




5-193b

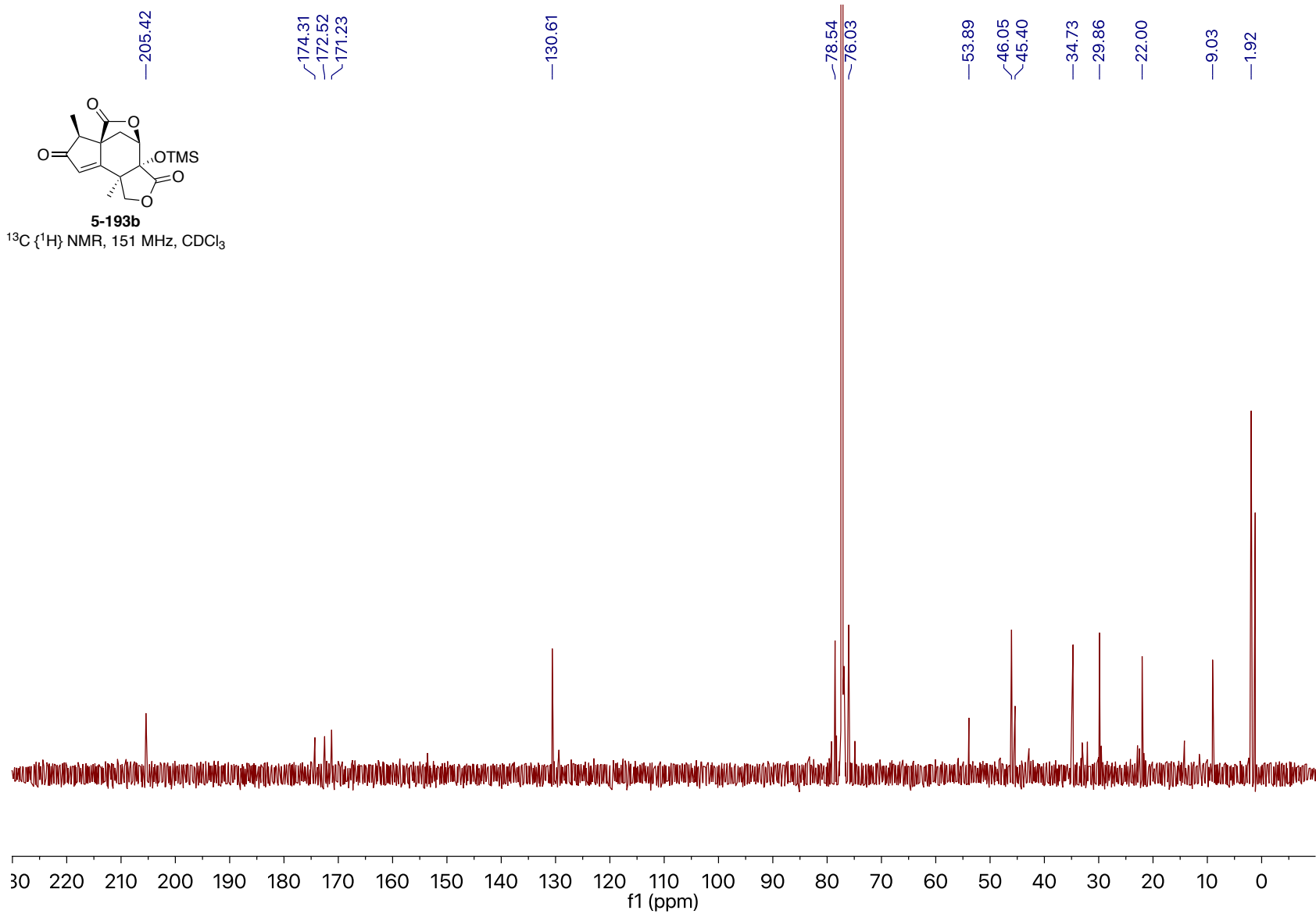
¹H NMR, 600 MHz, CDCl₃

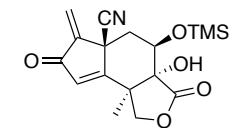




5-193b

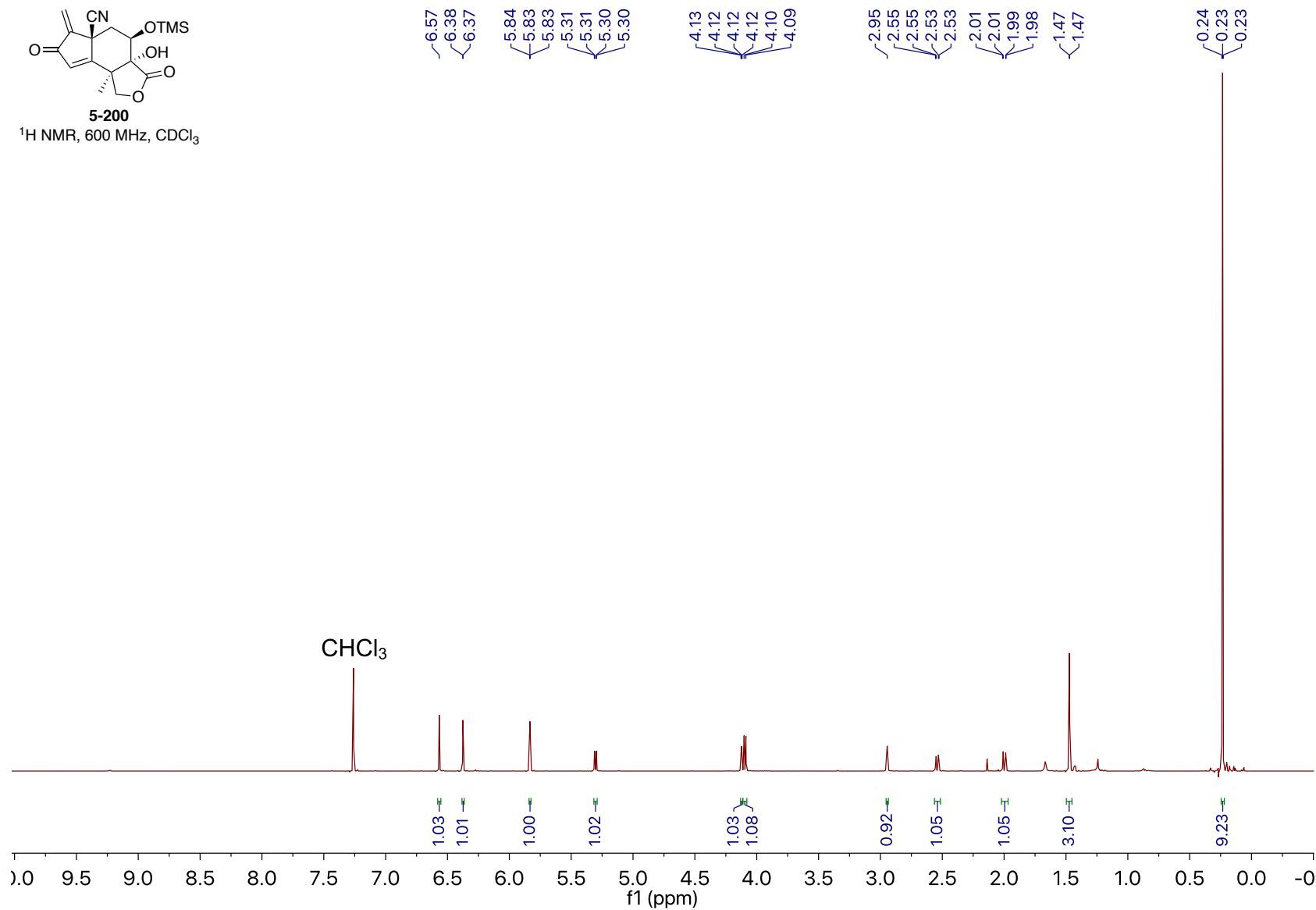
^{13}C $\{^1\text{H}\}$ NMR, 151 MHz, CDCl_3

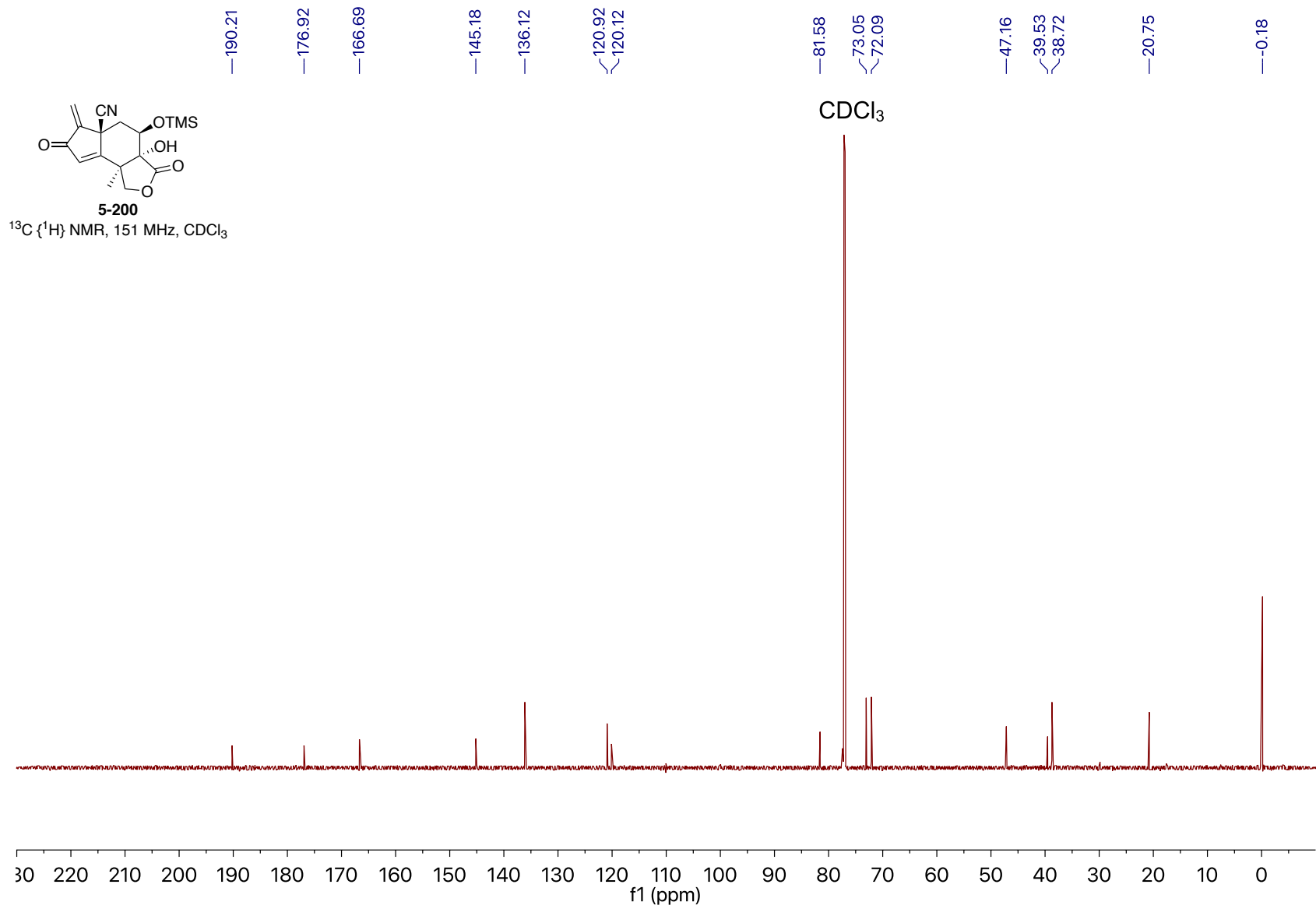


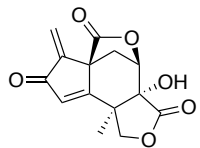


5-200

¹H NMR, 600 MHz, CDCl₃

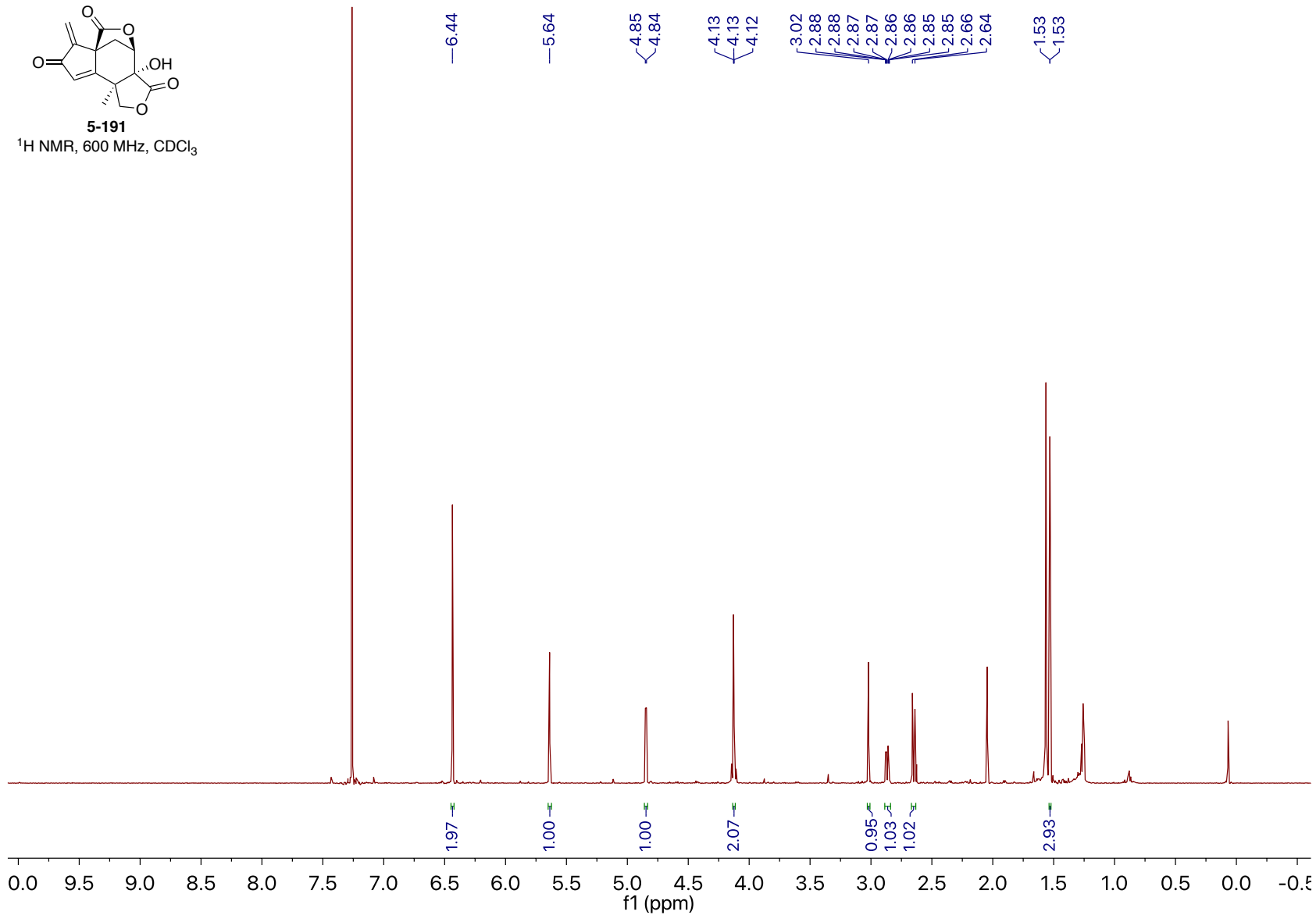


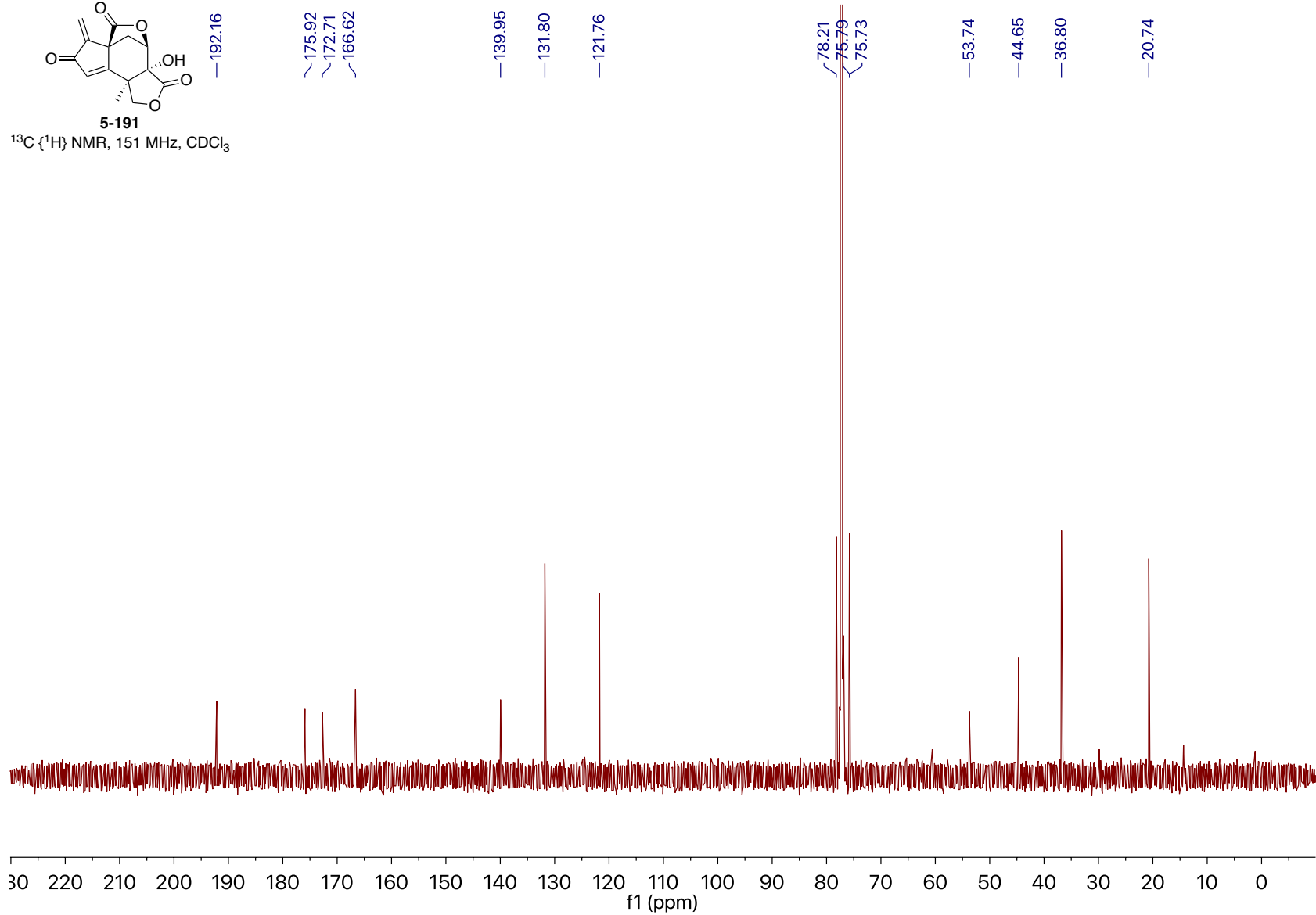
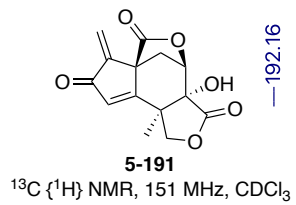


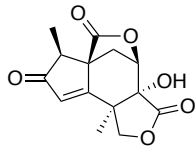


5-191

¹H NMR, 600 MHz, CDCl₃

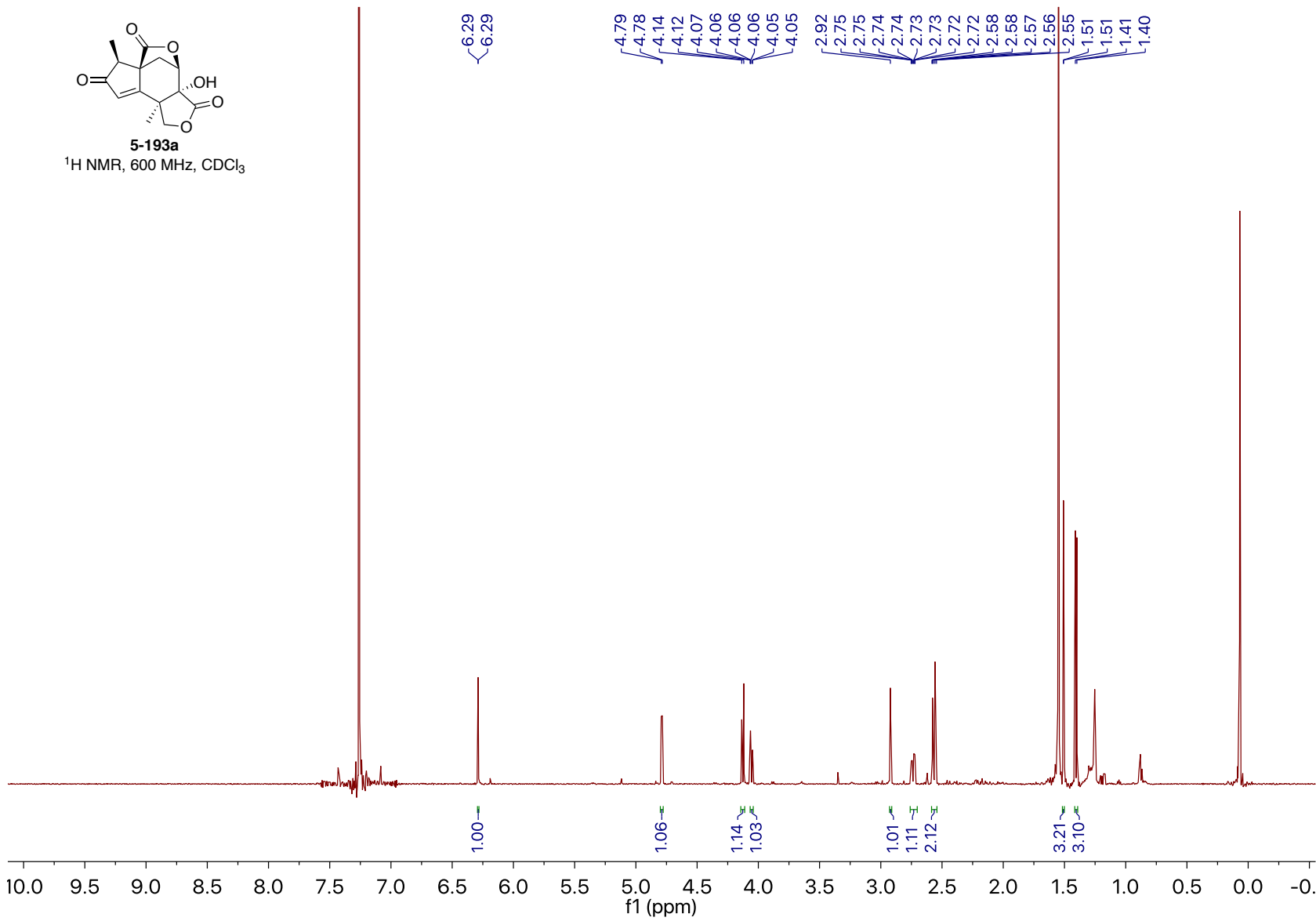


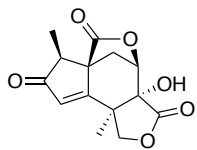




5-193a

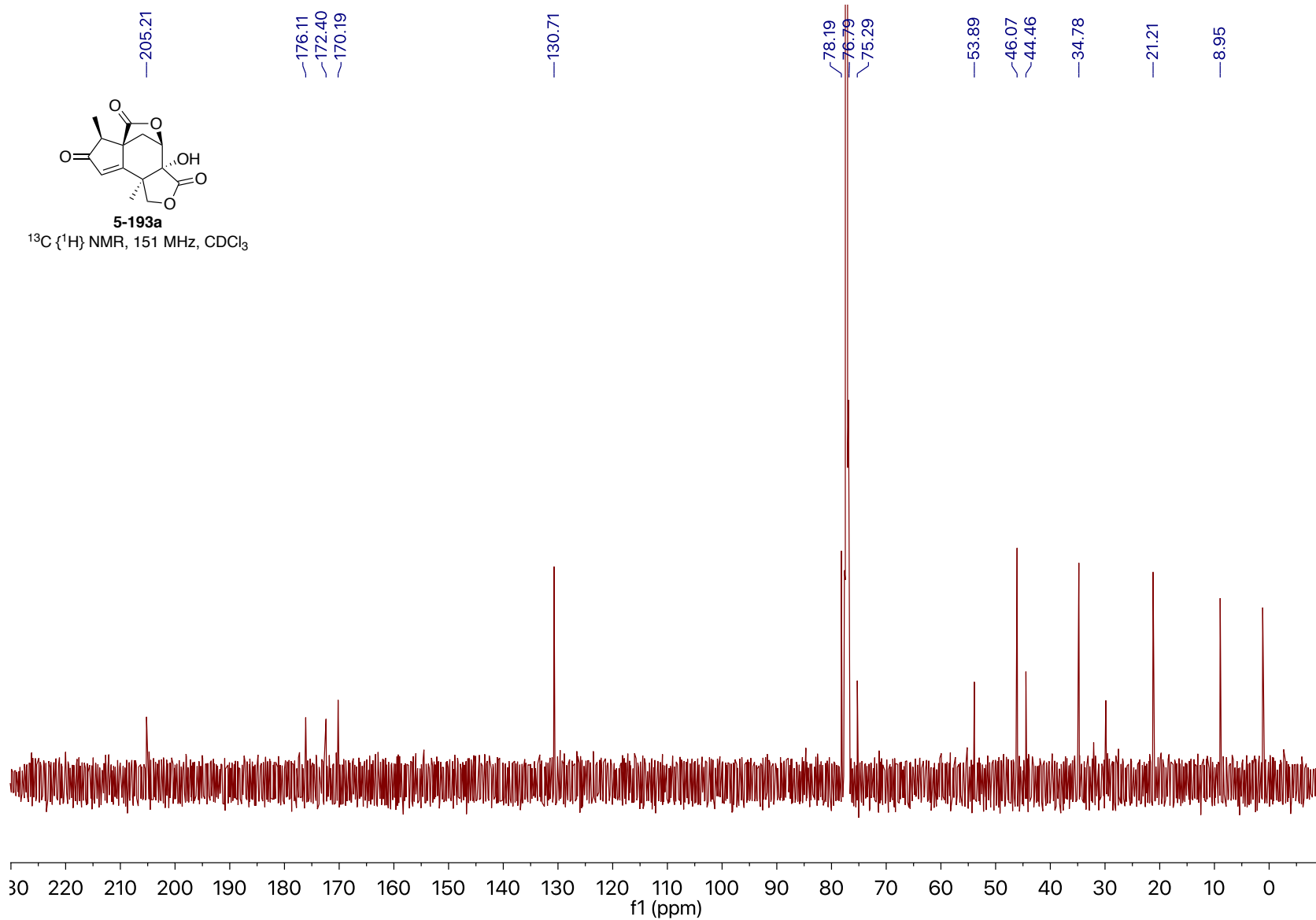
¹H NMR, 600 MHz, CDCl₃

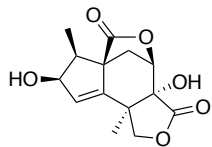




5-193a

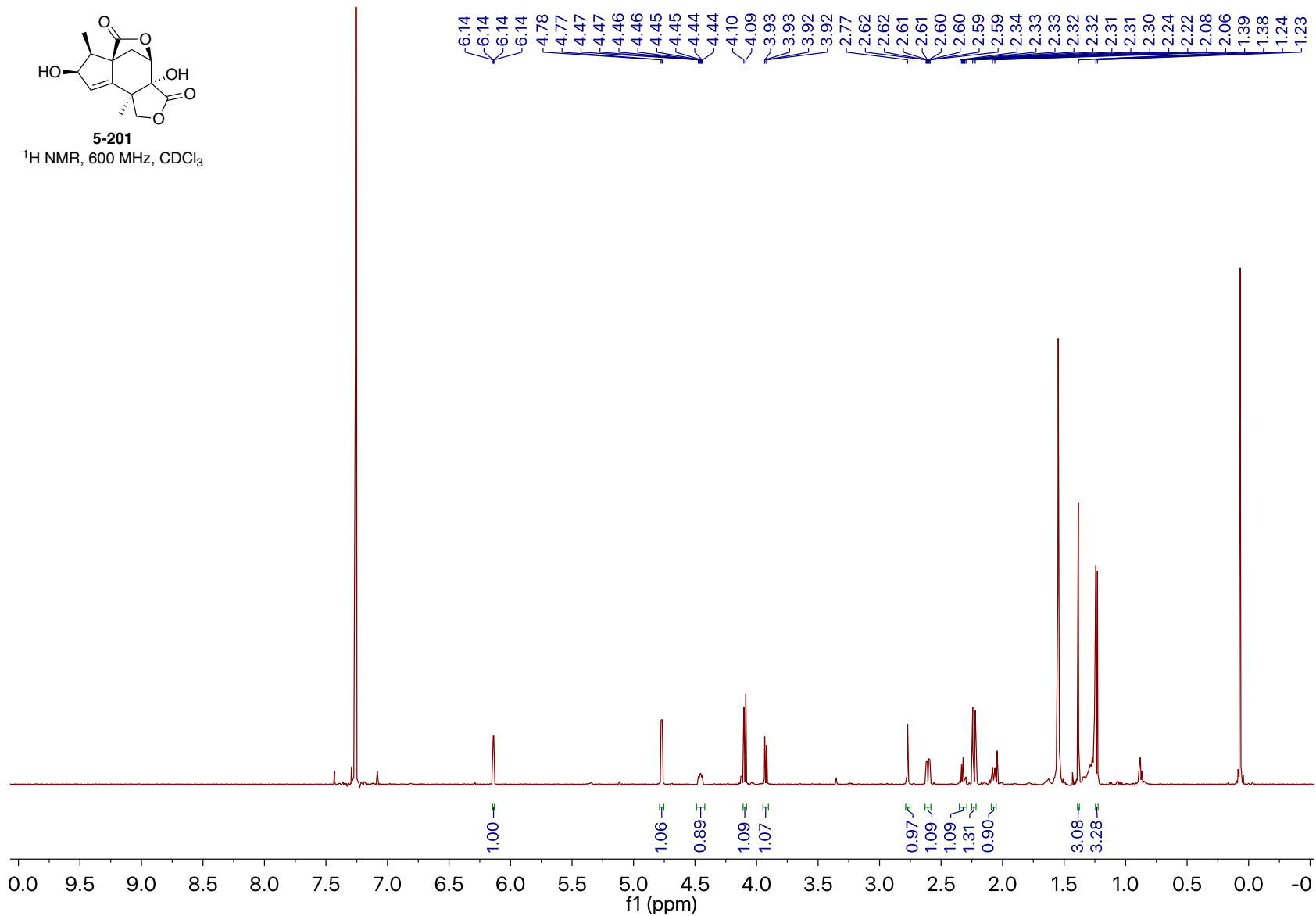
^{13}C $\{^1\text{H}\}$ NMR, 151 MHz, CDCl_3

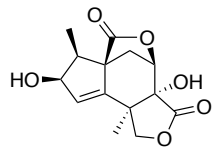




5-201

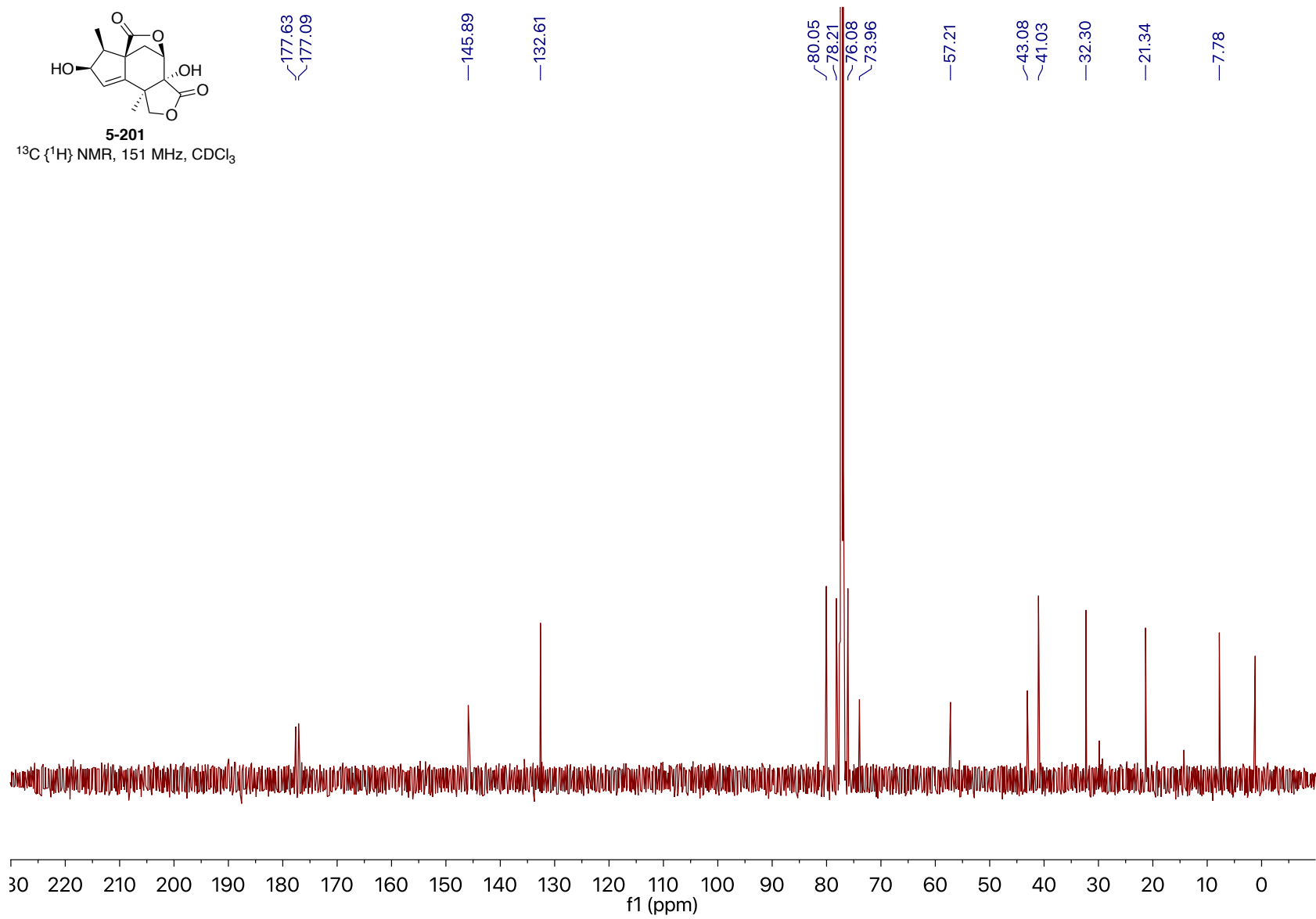
¹H NMR, 600 MHz, CDCl₃

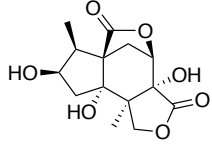




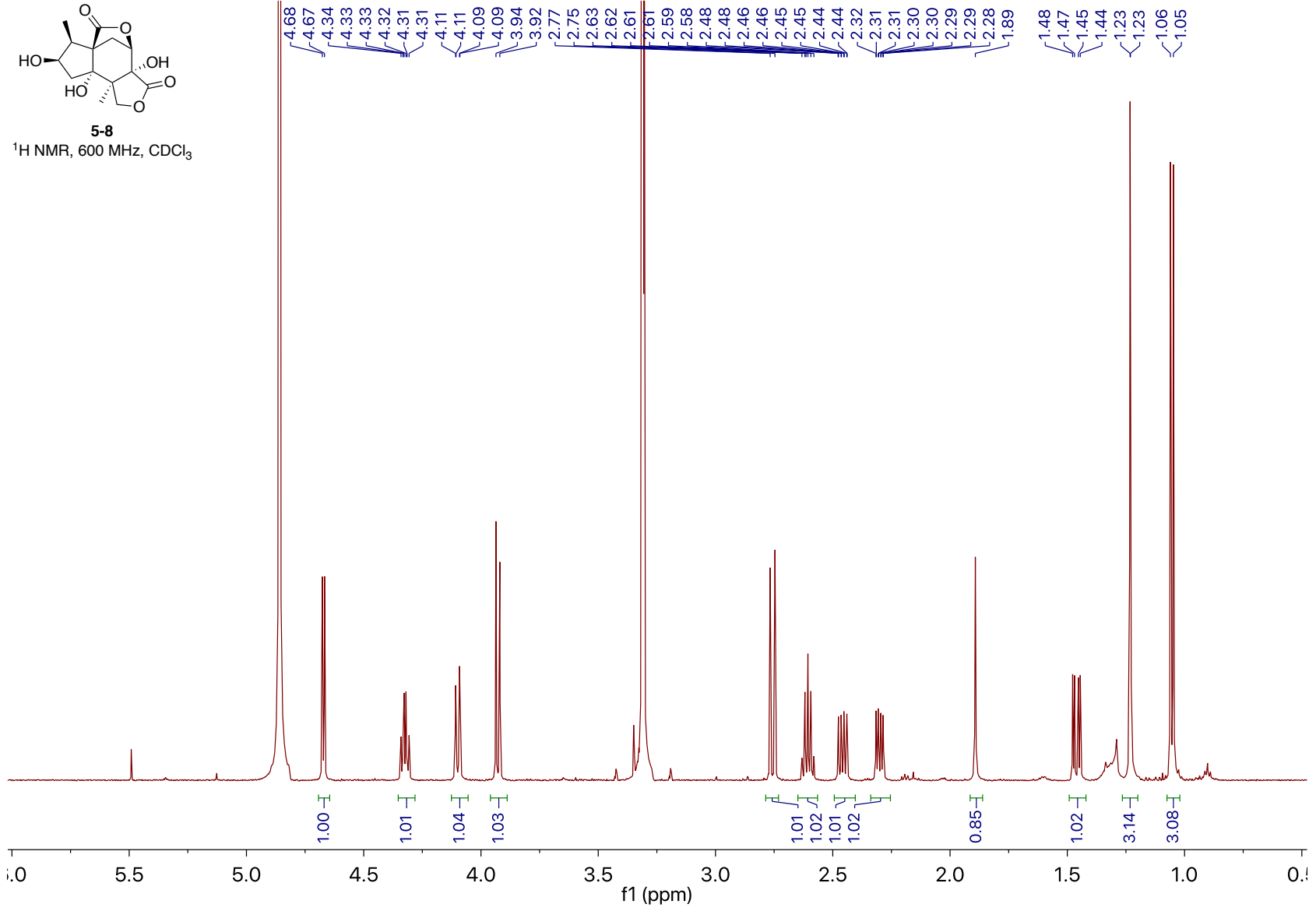
5-201

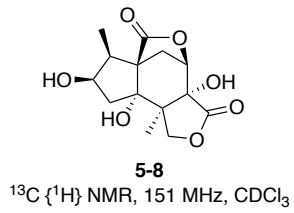
^{13}C $\{^1\text{H}\}$ NMR, 151 MHz, CDCl_3





5-8
¹H NMR, 600 MHz, CDCl₃





~181.03
~178.82

~82.02
~80.21
~76.24
~75.35
~72.99

—60.63

~49.57
~43.65
~38.84

—30.24

—19.93

—7.70

